

# Evaluation of Aluminum Highway Sign Trusses and Standards for Wind and Truck Gust Loadings



**PHYSICAL RESEARCH REPORT NO. 153  
DECEMBER 2006**



**Illinois Department of Transportation**

Bureau of Materials and Physical Research  
126 East Ash Street / Springfield, Illinois / 62704-4766

1. Report No. FHWA/IL/PRR 153	2. Government Accession No.	3. Recipient's Catalog No.	
4. Title and Subtitle  Evaluation of Aluminum Highway Sign Truss Designs and Standards for Wind and Truck Gust Loadings		5. Report Date December 2006	
		6. Performing Organization Code	
		8. Performing Organization Report No.  Physical Research Report No. 153	
7. Author(s) Douglas A. Foutch, S.E.; Jennifer A. Rice; James M. LaFave, P.E.; Schaun Valdovinos; Tae Wan Kim			
9. Performing Organization Name and Address University of Illinois at Urbana-Champaign  801 South Wright Champaign, IL 61820		10. Work Unit ( TRAIS)	
		11. Contract or Grant No. IHR-R37	
12. Sponsoring Agency Name and Address  Illinois Department of Transportation Bureau of Materials and Physical Research 126 East Ash Street Springfield, Illinois 62704-4766		13. Type of Report and Period Covered  Final Report March 2004 – December 2006	
		14. Sponsoring Agency Code	
15. Supplementary Notes			
16. Abstract The use of overhead and cantilever sign structures is quite common throughout Illinois and in the rest of the United States. These structures are used where standard guide signs along the side of the road would be inadequate or otherwise cannot be used. In the year 2000, IDOT changed their standard designs for aluminum highway sign structures. Four new aluminum truss bridges and one cantilever truss were instrumented in the field with anemometers, strain gages and accelerometers to measure their responses to winds and truck gusts. Using the measured responses and analytical studies it was determined that all of the new sign structures satisfied current AASHTO specifications. It was discovered, however, that the AASHTO recommended drag coefficients are significantly smaller than the values recently determined from wind tunnel tests and verified in the field. It was also determined that the currently used wind response equation for estimating fatigue stress ranges is too small by a factor of three or more. The effects of vibration dampers currently installed on all sign truss structures were evaluated through response measurements from the five structures in the field and from individual damper tests in the laboratory. The dampers were found to be ineffective in most cases because the natural period of the damper unit and the sign structure must be almost identical for them to be effective. Vibration tests of individual truss members on older trusses were conducted to determine why fatigue cracking was prevalent for some members. This was most likely due to wind-induced vibration from vortex shedding which should not be a problem with the current designs which have stockier web members.			
17. Key Words Aluminum sign trusses; wind response; AASHTO design specifications; drag coefficients; dampers; fatigue cracks; vortex shedding		18. Distribution Statement No Restrictions. This document is available to the public through the National Technical Information Service, Springfield, Virginia 22161	
19. Security Classif. (of this report) Unclassified	20. Security Classif. (of this page) Unclassified	21. No. of Pages 343	22. Price

# Final Report

## Evaluation of Aluminum Highway Sign Truss Designs and Standards for Wind and Truck Gust Loadings

By:

Douglas A. Foutch, S.E.; Jennifer A. Rice; James M.  
LaFave, P.E.; Schaun Valdovinos; Tae Wan Kim

Department of Civil and Environmental Engineering  
University of Illinois at Urbana-Champaign  
205 N. Mathews  
Urbana, IL 61802

December 2006

## Executive Summary

In the year 2000, IDOT changed their standard designs for aluminum highway sign structures. The design changes included eliminating redundant members, increasing the diameter and thickness of the hollow circular tubes, and installing vibration dampers. These changes were intended to increase the strength, stiffness, and factor of safety for these structures. The design changes were required in part because many cracks had been found at “T”, “Y”, and “K” tube-to-tube welded connections, most likely as a result of wind-induced cyclic loading. Wind damage to overhead and cantilever sign structures is not unique to Illinois; many states have reported damaged and/or collapsed sign structures. The problem has been so broad for cantilevered sign structures that the National Cooperative Highway Research Program (NCHRP) has funded two projects related to their wind response and design for wind loads. Results these studies were used in developing the latest revisions to the AASHTO *Standard Specifications for Structural Supports for Highway Signs, Luminaries and Traffic Signals* (2001).

Initially, there were six research objectives for this IDOT project, as follows:

Objective 1: Develop an analytical model for computing the response of aluminum highway sign truss structures to natural wind and truck-induced wind gust loads.

Objective 2: Based on analysis and testing, determine the AASHTO design load capacity and fatigue resistance of the IDOT sign structures included in the project.

Objective 3: Based on analysis and testing, determine the effectiveness of vibration dampers currently installed on overhead sign structures. If these are found to be ineffective, investigate through analysis the potential effectiveness of other types of dampers currently being used by other highway departments in other states.

Objective 4: Determine the effects of transportation and erection loads on the strength and service life of aluminum overhead sign structures.

Objective 5: Compile data on expected durability of individual truss components and connections to determine the anticipated service life of new truss structures included in this project.

Objective 6: Identify and report potential problem areas of current sign structure design procedures, and recommend detail modifications and/or other corrections where required.

Based on initial tests and analyses, Objective 4 was shown to be unimportant and Objectives 4 and 6 were modified.

Five IDOT aluminum truss sign structures (all representing newer design and construction practices of the last few years) were identified for investigation. This included one cantilever (of Type II-C-A), three simply supported sign bridges (of Types

I-A, II-A, and III-A), and one additional sign bridge (of Type II-A) carrying a variable message sign (VMS). Each sign structure was instrumented with accelerometers, strain gages, and an anemometer. The accelerometers were used to determine the dynamic properties of the structures and to calibrate the analytical model of each. The strain gages were used to determine the axial forces and bending moments in critical members as the structures were subjected to wind loads, truck gusts and manually-induced forces. The anemometer measured the magnitude and direction of the wind at each structure. For a given wind velocity and direction, the axial loads and bending moments determined for critical members were compared to calculated values determined by analysis of the structure using forces determined from code provisions and design assumptions. From these results, the IDOT design procedures were evaluated.

The effectiveness of damping devices installed on IDOT sign structures was also evaluated. The effective damping for each structure (both with and without damping devices) was determined from dynamic response decay initiated by manual-excitation and/or pull-back tests. A series of laboratory tests on as-delivered and modified dampers were also conducted in the laboratory.

Some of the older IDOT sign structures taken out of service were available for inspection and investigation. These had some members that had experienced cracking while in use. Vibration tests were conducted on members with and without cracks to determine their dynamic properties. Analytical studies were used to interpret the measured responses and predict how these members might behave under steady wind of different speeds.

The evaluations of the five structures confirmed that they were in general compliance with the AASHTO Specifications and IDOT standards under which they have been designed. However, in the opinion of the research team, the current AASHTO design provisions are not completely adequate in some areas. The recommendations given are therefore intended to provide guidance if IDOT wishes to amend their designs for future structures to perform better than structures designed to current AASHTO Specifications. Sign structures constructed based on current IDOT designs do not appear to present significant risks for premature damage or failure. In fact, the current IDOT design calculations even make certain simplifications to design procedures that are somewhat more conservative than the AASHTO Specifications.

When field-measured stresses are projected up to the design wind speed of 90 mph, the maximum stresses in some chord members in structures with maximum allowable sign areas will have stresses in the chords approaching 20 ksi, which is the minimum yield stress in the weld heat affected zone. Those projected stresses have a significant bending (stress gradient) component, so the overstress is in a small area of the cross-section. Therefore, although the projected stress may exceed the allowable stress in a small region of the chord member, safety does not appear to be an issue.

The possibility of the aforementioned overstresses is the result of three factors. First, the design drag coefficient for signs, per the current AASHTO Specifications, range from 1.14 to 1.19 for these signs, whereas recent research by Letchford (2001) has shown that, for elevated signs, the average measured drag coefficients were typically in the range of 1.40 to 1.50. As a result, ASCE 7-05 (ASCE, 2006) recently increased their recommended drag coefficients, but these have not yet been adopted by AASHTO. Using the ASCE 7 recommendations, the drag coefficients would range from 1.70 to 1.78 for the IDOT sign structures that were studied. The IDOT designs were based on a value of 1.2, which is larger than the current AASHTO requirements but smaller than recent test values (Letchford, 2001) or ASCE 7-05 recommendations. IDOT design procedures further assume that a 9 psi uniform stress acts on the projected vertical cross section area over regions where the sign is not present. These two factors are the primary reasons why the projected stresses are actually only a little bit larger than the allowable stresses. Two other factors affected the projected stresses, but to a much smaller degree. The current code does not explicitly account for the vibration of a sign structure at ultimate wind loading (although this may have been a factor implicitly considered when the gust factor was developed). At a 90 mph wind speed, the field data suggest that the stress due to dynamic response will only be about 5% larger than the equivalent static design load; this is a mean value, but the coefficient of variation is expected to be small for this wind speed.

Recommendation #1 – Based on the results from this study, IDOT is encouraged to adopt the ASCE 7 recommended drag coefficient (or a reasonable simplification thereof) for design of aluminum sign structures. Given the conservative assumptions used by IDOT for analyzing the wind-induced stresses, the values determined from recent wind tunnel studies referred to above (still larger than current AASHTO values) may also be acceptable. Including a design coefficient of 1.10 in the equation for determining design wind pressure for the 90 mph design wind speed is also recommended to account for vibration of the structure. Alternatively, this effect could be included in one of the other design coefficients.

The AASHTO Specifications require that cantilever sign structures be designed for fatigue loads. However, simply supported trusses are not currently required to be designed for fatigue. This study evaluated fatigue effects in all structures, for consideration by IDOT. The stress ranges experienced by selected truss members were measured under wind loads and truck gusts. The study concluded that the fatigue stress range in each member could be evaluated considering an 11.2 mph wind speed and/or simultaneous truck gust(s). The fatigue stress ranges measured for the chords of all of the structures were considerably lower than the allowable stress range of 1.9 ksi. The fatigue stress ranges measured for the connecting (web) members were almost all smaller than the allowable stress range of 0.44 ksi. If signs with the maximum allowable area were placed on these structures, it is projected that the stress ranges experienced by horizontal and horizontal diagonal members would occasionally exceed the constant amplitude fatigue limit (CAFL). This is most likely to occur under the simultaneous action of moderate wind in conjunction with larger truck gusts, a design loading condition that is not currently mandated by the AASHTO Specifications and is very conservative, since

the peak vibration response to the wind (not the average response) and the peak vibration response to the truck gust would have to occur nearly simultaneously to produce a significant stress range in a member..

Based on the AASHTO Specifications, member stresses calculated using design equations for wind pressure ignore the dynamic response of the structure. For the 90 mph wind speed, the ratio of the maximum stress and the 3-second average stress was only 1.05. On the other hand, for the 11.2 mph wind speed this ratio was about 3.0, on average. In addition, the coefficient of variation was quite large; the mean plus standard deviation exceeded 4.0. This is too significant to be ignored for fatigue design of these sign structures, but the actual maximum stress range observed (for individual cycles) was typically only slightly more than two times the mean value for winds at or near 11.2 mph.

The AASHTO Specifications' design equation for pressure due to truck gusts was modified after the IDOT design standards were completed. The new equation gives smaller design stresses than those determined by IDOT using the previous AASHTO criteria. Therefore, had the new equation been used in design, it is possible that the CAFL would be exceeded in more of the connecting members (which may have been smaller, depending on what design aspect ultimately controlled their sizing). Another factor affecting the calculated design stress range is the area over which the design truck gust pressure is applied. The AASHTO Specifications conservatively require that this pressure be applied over the entire sign area, but the wind gust designs usually control for fatigue design, so truck gusts are actually relatively less important with respect to design.

Recommendation #2 - If IDOT chooses to consider fatigue for design of new simply supported trusses for fatigue (even though this is not required by AASHTO), a reasonable approach for new designs might be to use the current AASHTO design equation along with a dynamic response coefficient of 3.0. This would result in a design pressure about 1½ times that used by IDOT in their current standard designs. However, this may be too conservative, since the allowable stress range would rarely be exceeded in the field, and only under combinations of wind and large truck gusts, a loading that is not mandated by the AASHTO Specifications. In addition, if Recommendation #1 is adopted, it is even less likely that occasional stress ranges in excess of the allowable stress ranges would occur.

Laboratory tests and analytical models of the Stockbridge dampers currently installed on IDOT sign structures were undertaken. Four damper units purchased from the supplier were tested under controlled conditions in the Newmark Structural Engineering Laboratory (NSEL) of the UIUC Department of CEE. Results for the standard dampers mounted on the Types I-A, II-A, and III-A structures studied in this project (in conjunction with field testing) indicate that the dampers offer little protection against fatigue because the damper's natural frequency is much greater than that of any of the sign structures. For a damper to be effective, the ratio of the damper's to the structure's natural frequency should be between about 0.9 and 1.1, with best results when the ratio is around 1.0. The "sloppy" Stockbridge damper has a longer cable, so its natural frequency is indeed lower. However, another important factor is the ratio of

damper weight to structure weight, which is very small for most sign structures. Thus, even the “sloppy” damper will be effective only for the smaller cantilever structures (due to the smaller weight ratios of the damper weight to the structure weight of the larger structures).

Due to these factors, the effectiveness of the dampers at reducing the amplitude of the stress ranges for the sign truss structures, while apparent, is very small. This could be improved by using multiple dampers, but for an impulse load like a truck gust, dampers are generally not effective at reducing the amplitude of the initial cycle. However, if properly designed, dampers can be effective at reducing the number of stress cycles due to wind and/or truck gusts occurring above the CAFL. In other words, a well-designed damper can be quite effective at reducing the response to wind loads that produce a modulated sine wave response in the structure.

Recommendation #3 – Since the projected maximum stress ranges in some of the connecting (web) members in simply supported aluminum trusses designed by current IDOT procedures are larger than the CAFL, IDOT may wish to consider installing more effective dampers on their existing sign structures to reduce the effects of fatigue. However, this would be a very conservative action since the excessive stress ranges are only likely to occur under the simultaneous action of wind and large truck gusts. If IDOT chooses to mitigate the response of existing sign truss structures, a consultant with experience in designing damping systems should be retained (and alternative damper types should be explored). It is not recommended that individual Stockbridge dampers be installed on new structures designed for fatigue resistance because the dampers are ineffective unless multiple units are installed and the natural frequency of each unit is approximately the same as the natural frequency of the structure.

As a part of this study, some of the factors affecting the behavior of the older sign truss designs (with regard to weld cracking) were investigated. Since the weld cracks occurred more often in slender web members, the possibility of vortex shedding causing excessive vibration that exceeded a connection’s fatigue limit was investigated. The results of the investigation suggest that this hypothesis is correct (as a strong contributing cause for certain web members); however, this is probably not the only factor involved. The effect of dynamic response of the structure on the stresses in connecting member welds, as described above, was also a problem for the older structures. The member connections most often damaged were near the ends of the trusses, in situations where web member forces (and possibly even web member moments) would be larger. There were also problems in making quality welds where the multiple connecting members closely approached each other at chord connections, leaving inadequate access for proper welding.

Recommendation #4 – Based on the results reported in Chapter 8.0, then, it is recommended that the slenderness ( $L/r$ ) of truss members (regardless of whether loaded in tension or in compression) should be kept less than about 105 for T-type connections and less than about 115 for K-type connections.



# TABLE OF CONTENTS

Executive Summary .....	i
Table of Contents.....	vii
Disclaimer .....	ix
Acknowledgements.....	ix
List of Figures.....	x
List of Tables.....	xvi
1.0 Introduction.....	1
1.1 Background .....	1
1.2 Research Objectives .....	2
2.0 Sign Structure Descriptions and Locations .....	4
2.1 Introduction.....	4
2.2 Cantilever Structure.....	4
2.3 Type I-A Sign Bridge .....	7
2.4 Type II-A Sign Bridge .....	9
2.5 Type III-A Sign Bridge .....	11
2.6 VMS on Type II-A Sign Bridge .....	12
3.0 Instrumentation, Data Acquisition, and Data Processing .....	15
3.1 Introduction.....	15
3.2 Anemometers .....	16
3.3 Strain Gages .....	18
3.4 Accelerometers .....	21
3.5 Data Processing .....	25
4.0 Analytical Modeling .....	27
4.1 General Information.....	27
4.2 Modeling of the Cantilever Structure .....	27
4.3 Modeling of the Type I-A Sign Bridge.....	33
4.4 Modeling of the Type II-A Sign Bridge.....	40
4.5 Modeling of the Type III-A Sign Bridge.....	43
4.6 Modeling of the Type II-A Sign Bridge with VMS.....	46
5.0 Dynamic Properties of the Sign Structures .....	50
5.1 Background .....	50

5.2	Dynamic Properties of the Cantilever Structure .....	52
5.3	Dynamic Properties of the Type I-A Sign Structure.....	60
5.4	Dynamic Properties of the Type II-A Sign Structure.....	67
5.5	Vibration Characteristics of the Type III-A Sign Structure .....	71
5.6	Dynamic Characteristics of the VMS Sign Structure .....	75
6.0	Response of Sign Structures to Wind Loads and Truck Gusts .....	77
6.1	Background .....	77
6.2	Wind Loads on Structures .....	77
	Natural Wind Gust.....	81
6.3	Response of the Cantilever Sign Structure to Wind Loads and Truck Gusts	86
6.4	Response of Type I-A Sign Structure to Wind Loads and Truck Gusts.....	93
6.5	Response of Type II-A Sign Structure to Wind Loads and Truck Gusts.....	101
6.6	Response of the Type III-A Sign Structure to Wind Loads and Truck Gusts	108
6.7	Response of the VMS Structure to Wind Loads and Truck Gusts.....	113
7.0	Highway Sign Truss Damper.....	119
7.1	Background .....	119
7.2	Current Application .....	120
7.3	Experimental Testing.....	123
7.4	Analytical Modeling with Dampers.....	131
7.5	Damper Recommendations.....	135
8.0	End Connection Effects on Vortex Shedding Susceptibility of Aluminum Truss Tubular Web Members.....	137
8.1	Introduction.....	137
8.2	Web Member Natural Frequency Determination .....	138
8.3	Web Member Critical Wind Speed Estimation.....	143
8.4	Summary and Conclusions .....	149
9.0	Summary and Recommendations .....	150
10.0	References.....	155
	Appendix A.....	157

## DISCLAIMER

The contents of this paper reflect the view of the authors who are responsible for the facts and accuracy of the data presented herein. The contents do not necessarily reflect the official views, or policies, of the Illinois Department of Transportation, or the Federal Highway Administration. This report does not constitute a standard, specification, or regulation.

## ACKNOWLEDGEMENTS

The authors gratefully acknowledge the assistance of Ms. Susan Hale for her work in preparing the final report. The authors also acknowledge the assistance of Chris Mehuys (Traffic Structures and Shop Drawings Engineer, IDOT) for providing important data and background information. The authors would also like to acknowledge the assistance of M. Hodel, J. Edwards and A. Weatherholt (IDOT) for their contributions as members of the Technical Review Panel and for providing traffic control and the test sites. Finally, the authors gratefully acknowledge the assistance and patience of Patty Broers (IDOT).

## LIST OF FIGURES

Figure 1.1-1	Damaged web member-to-chord connections.....	1
Figure 2.2-1	Location of cantilever sign structure .....	5
Figure 2.2-2	Picture of cantilever sign structure looking east .....	5
Figure 2.2-3	Plan and elevation of cantilever truss .....	6
Figure 2.2-4	Isometric view of typical cantilever truss unit.....	7
Figure 2.3-1	Location of the Type I-A sign bridge .....	7
Figure 2.3-2	Pictures of the Type I-A sign bridge.....	8
Figure 2.3-3	Plan and elevation of the Type I-A sign bridge truss and support structure.....	8
Figure 2.3-4	Isometric view of typical Type I-A truss unit.....	9
Figure 2.4-1	Location of the Type II-A sign bridge .....	10
Figure 2.4-2	Picture of the Type II-A sign bridge looking east and west.....	10
Figure 2.5-1	Location of the Type III-A sign bridge .....	11
Figure 2.5-2	Picture of the Type III-A sign bridge looking south .....	12
Figure 2.6-1	Location of the Type II-A sign bridge with VMS.....	13
Figure 2.6-2	Pictures of the Type II-A sign bridge with VMS, located near Shirley, IL.....	13
Figure 2.6-3	Variable message sign (VMS) .....	14
Figure 3.1-1	Picture of cable storage box mounted on support structure .....	16
Figure 3.2-1	Wind monitor mounted on the Type III-A sign bridge .....	17
Figure 3.2-2	Gill Instruments WindMaster mounted on the cantilever structure .....	17
Figure 3.3-1	Typical strain gage placement .....	18
Figure 3.3-2	Strain gage placement for the cantilever structure .....	19
Figure 3.3-3	Location of strain gages on the Type I-A sign bridge .....	19
Figure 3.3-4	Strain gage placement near truss end for Type II-A and Type III-A sign bridges.....	20
Figure 3.3-5	Strain gage and accelerometer placement for the VMS sign structure ...	21
Figure 3.4-1	Location of accelerometers for the Type I-A sign bridge .....	23
Figure 3.4-2	Accelerometer locations for cantilever structure .....	24
Figure 3.4-3	Mounted accelerometers in cases .....	24

Figure 3.4-4	Accelerometer placement for the Type II-A and Type III-A sign trusses.....	25
Figure 3.5-1	Measured strains before and after filtering from the Type II-A sign structure .....	26
Figure 3.5.2	Measured accelerations before and after filtering from the Type II-A sign structure .....	26
Figure 4.2-1	Finite element model of cantilever structure .....	29
Figure 4.2-2	Design wind loading of the cantilever structure .....	30
Figure 4.2-3	Cantilever mode shape 1, plan view – rotation of truss about the column .....	32
Figure 4.2-4	Cantilever mode shape 2, elevation view – vertical motion of truss .....	33
Figure 4.3-1	Connection detail of truss to support frame .....	34
Figure 4.3-2	Detail of truss/support column connection, upper chord/column connection, and lower chord/beam connection .....	34
Figure 4.3-3	End details of model: end release of rigid links connecting top chord/column.....	35
Figure 4.3-4	End details of model: end release of rigid links connecting bottom chords/beam, local axis of beam.....	35
Figure 4.3-5	Foundation detail of median end and shoulder end.....	36
Figure 4.3-6	SAP2000 finite element model of the Type I-A sign bridge .....	36
Figure 4.3-7	Design wind loading.....	37
Figure 4.3-8	(a) First mode, elevation view of longitudinal motion, $T=0.66s$ ; (b) Second mode, plan view of horizontal motion, $T=0.37s$ ; (c) Third mode, elevation view of vertical motion, $T=0.28s$ ; (d) Fourth mode, profile view of twisting motion, $T=0.14s$ .....	39
Figure 4.4-1	SAP2000 model of the Type II-A sign bridge.....	40
Figure 4.5-1	SAP2000 finite element model of Type III-A sign bridge .....	43
Figure 4.6-1	SAP2000 finite element model of the Type II-A structure with VMS.....	47
Figure 5.2-1	Response of cantilever structure to transverse manual excitation .....	52
Figure 5.2-2	Cantilever stresses in selected members due to transverse manual excitation.....	53
Figure 5.2-3	1709-190 15.9-lb. Stockbridge damper .....	54
Figure 5.2-4	Damper mounted on the cantilever truss; disengaged damper .....	54
Figure 5.2-5	Picture of pull-down test being conducted on the cantilever truss.....	55

Figure 5.2-6	Decay of horizontal motion of the truss at the end of the cantilever .....	57
Figure 5.2-7	Decay of vertical motion at the end of the cantilever .....	57
Figure 5.2-8	Cantilever horizontal acceleration at the bottom end of the truss for wind loads.....	59
Figure 5.2-9	FFT – cantilever horizontal bottom acceleration.....	59
Figure 5.2-10	Cantilever vertical acceleration at the bottom end of the truss .....	60
Figure 5.2-11	FFT – Cantilever vertical acceleration at the bottom end of the truss .....	60
Figure 5.3-1	Type I-A horizontal mid-span acceleration due to manual horizontal excitation .....	61
Figure 5.3-2	Type I-A maximum stress in members due to horizontal manual excitation .....	61
Figure 5.3-3	Periodic pull-down test for determining vertical damping in the Type I-A truss.....	62
Figure 5.3-4	Type I-A horizontal and vertical manual excitation without damping .....	63
Figure 5.3-5	Type I-A horizontal and vertical manual excitation with damping .....	63
Figure 5.3-6	Type I-A decay of the horizontal motion with and without the damper ....	67
Figure 5.3-7	Stockbridge-type damper mounted on the Type I-A truss and disengaged damper .....	64
Figure 5.3-8	Type I-A horizontal acceleration at the mid-span of the truss.....	65
Figure 5.3-9	FFT – Type I-A horizontal mid-span acceleration.....	65
Figure 5.3-10	Type I-A vertical acceleration at the mid-span of the truss.....	66
Figure 5.3-11	FFT – Type I-A vertical mid-span acceleration .....	66
Figure 5.4-1	Type II-A horizontal acceleration at mid-span of the truss due to manual excitation.....	67
Figure 5.4-2	Type II-A member stresses due to horizontal manual excitation .....	68
Figure 5.4-3	Type II-A horizontal and vertical manual excitation without damping .....	58
Figure 5.4-4	Type II-A horizontal and vertical manual excitation with damping .....	69
Figure 5.4-5	Type II-A decay of the horizontal motion with and without damper .....	73
Figure 5.4-6	Type II-A horizontal mid-span acceleration and FFT of horizontal mid-span acceleration .....	70
Figure 5.4-7	Type II-A vertical mid-span acceleration and FFT of vertical mid-span acceleration .....	71
Figure 5.5-1	Type III-A horizontal acceleration at the mid-span of the truss due to manual excitation.....	72

Figure 5.5-2	Type III-A stress in each member due to horizontal manual excitation ...	72
Figure 5.5-3	Type III-A horizontal acceleration at the bottom of truss at mid-span.....	74
Figure 5.5-4	Type III-A FFT of bottom horizontal mid-span acceleration.....	74
Figure 5.5-5	Type III-A vertical acceleration at bottom of truss at mid-span.....	75
Figure 5.5-6	Type III-A FFT of vertical mid-span acceleration .....	75
Figure 5.6-1	Measured acceleration responses at the mid-span of the VMS truss for the horizontal and vertical directions .....	76
Figure 5.6-2	Fourier transform of measured horizontal and vertical accelerations at mid-span of the VMS truss .....	76
Figure 6.2-1	Sign panel clearance ratio and length labels .....	79
Figure 6.2-2	Axial stress in cantilever chord member and 3-sec average vs. time.....	83
Figure 6.2-3	Detail of axial stress vs. time compared to 3-sec average .....	83
Figure 6.2-4	Ratio of average peak response to 3-sec average vs. wind speed for four sign trusses .....	84
Figure 6.2-5	Combined plot of mean response ratio for all sign structures and the same plot with one standard deviation experimental error bars .....	85
Figure 6.3-1	Normal wind speed measured for cantilever .....	87
Figure 6.3-2	Average unadjusted strain at various normal wind speeds (cantilever)...	88
Figure 6.3-3	Measurement of cantilever stress in chord members .....	88
Figure 6.3-4	Average stress in the four strain gages on cantilever chord members....	89
Figure 6.3-5	Trucks passing under the cantilever sign structure .....	91
Figure 6.3-6	Acceleration response at end of the cantilever for trucks 1 through 4.....	91
Figure 6.4-1	Type I-A hour-long wind record .....	94
Figure 6.4-2	Type I-A stress values in chord members under normal wind loading ....	95
Figure 6.4-3	Type I-A bending and axial stress in chord member .....	95
Figure 6.4-4	Examples of six truck classes identified for Type I-A sign bridge.....	96
Figure 6.4-5	Gust excitation from typical trailer – horizontal and vertical acceleration .....	97
Figure 6.4-6	Gust excitation from tanker – horizontal and vertical acceleration .....	97
Figure 6.4-7	Gust excitation from flatbed – horizontal and vertical acceleration.....	98
Figure 6.4-8	Gust excitation from cab only – horizontal and vertical acceleration.....	98

Figure 6.4-9	Horizontal response of Type I-A structure to the three largest truck gusts .....	99
Figure 6.5-1	Normal component of wind speed measured at Type II-A truss .....	101
Figure 6.5-2	Type II-A extrapolated stresses in the chord member .....	102
Figure 6.5-3	Type II-A mid-span horizontal and vertical accelerations due to truck gusts .....	104
Figure 6.5-4	Type II-A mid-span horizontal and vertical accelerations from the two largest recorded truck gusts .....	105
Figure 6.5-5	Type II-A chord and horizontal diagonal stresses from the two largest recorded truck gusts. ....	105
Figure 6.5-6	Two additional trucks for the Type II-A included in Table 6.5-2.....	106
Figure 6.6-1	Combined strong wind records recorded for the Type III-A truss on November 3, 2005.....	108
Figure 6.6-2	Type III-A stress in chord members vs. 3-sec average normal wind speed .....	109
Figure 6.6-3	Type III-A horizontal and vertical accelerations from truck gusts .....	111
Figure 6.6-4	Detail of horizontal and vertical accelerations truck 6.....	111
Figure 6.7-1	VMS truss average stress vs. normal wind speed at eight gage locations .....	114
Figure 6.7-2	Pictures taken at one second intervals during truck passing (VMS truss) .....	116
Figure 6.7-3	Measured accelerations for strong wind; original, filtered.....	117
Figure 6.7-4	Measured stresses for strong wind; original, filtered .....	118
Figure 7.2-1	Damper installation for overhead and cantilever sign structures .....	121
Figure 7.2-2	Regular 31-lb. damper installed on a Type II-A truss and <i>sloppy</i> 15.9 damper installed on a Type II-C-A truss.....	121
Figure 7.2-3	Manufacturer's drawing of the Stockbridge highway truss damping device.....	122
Figure 7.2-4	1706 bus vibration damper .....	122
Figure 7.3-1	1708S-17.1 damper .....	124
Figure 7.3-2	1709S-17.1 damper .....	124
Figure 7.3-3	In-tact damper test set-up.....	125
Figure 7.3-4	Example of measured displacement data.....	126
Figure 7.3-5	Frequency response: 1708S-17.1 (31 lb) damper .....	127

Figure 7.3-6	Force vs. frequency: 1708S-17.1 (31 lb) damper .....	127
Figure 7.3-7	Frequency response: 1709S-17.1(34.6 lb) damper .....	128
Figure 7.3-8	Force vs. frequency: 1709S-17.1 (31 lb) damper .....	128
Figure 7.3-9	Dismantled 1708S-17.1 damper and cable lengths tested .....	129
Figure 7.3-10	Dismantled 1709S-17.1 damper and cable lengths tested .....	129
Figure 7.3-11	Test set-up for dismantled dampers .....	129
Figure 7.3-12	1708S-17.1 31 lb. damper natural frequency vs. clamp amplitude .....	130
Figure 7.3-13	1709S-17.1 34.61-lb damper natural frequency vs. clamp amplitude .....	130
Figure 7.4-1	2-DOF model of sign structure with damper .....	131
Figure 7.4-2	Comparison of total structural damping $\zeta_s$ , for different values of damper damping ratios, $\zeta_2$ .....	132
Figure 7.4-3	Total structural damping $\zeta_s$ , in the Type III-A model for different numbers of dampers (with $\zeta_2=33\%$ ) .....	133
Figure 7.4-4	Model of Type III-A truss with six 34.6 lb dampers with 12-inch cables	135
Figure 8.1-1	Newer IDOT aluminum overhead sign structure.....	137
Figure 8.2-1	Rantoul Truss, Type IV-A; Inset: Accelerometer mounted on horizontal member.....	139
Figure 8.2-2	Lincoln Truss, New Type III-A.....	140
Figure 8.2-3	Data analysis of acceleration impulse response for an interior diagonal member in the older Type IV-A truss .....	140
Figure 8.2-4	Web member connection definitions and actual web members framing into a chord .....	142
Figure 8.2-5	Difference in natural frequency of undamaged and damaged interior diagonal members.....	143
Figure 8.3-1	Slenderness limits vs. critical wind speed based on $K_f$ values for T-type end connections and K-type end connections .....	147

## LIST OF TABLES

Table 2.3-1	IDOT design data for Type I-A sign bridges.....	9
Table 2.4-1	IDOT design data for Type II-A sign bridges.....	11
Table 2.5-1	IDOT design data for Type III-A sign bridges.....	12
Table 3.4-1	Type I-A truss accelerometer configuration .....	22
Table 3.4-2	Accelerometer placement for cantilever structure.....	23
Table 4.2-1	Member geometric and material properties of the cantilever structure.....	28
Table 4.2-2	Cantilever drag coefficients and resulting member loads .....	30
Table 4.2-3	Cantilever member stresses from model with applied design wind loading .....	31
Table 4.2-4	Cantilever member stresses from model with dead load and applied design wind loading .....	31
Table 4.2-5	Results of modal analysis for cantilever structure.....	32
Table 4.3-1	Member properties for the Type I-A sign bridge .....	33
Table 4.3-2	Type I-A drag coefficients and resulting member loads.....	37
Table 4.3-3	Type I-A member stresses fro model with applied wind loading.....	38
Table 4.3-4	Type I-A member stresses from model with dead load and applied design wind loading .....	38
Table 4.3-5	Type I-A modal analysis results.....	38
Table 4.4-1	Material and geometric properties for the Type II-A sign bridge.....	40
Table 4.4-2	Type II-A drag coefficients and resulting member loads.....	41
Table 4.4-3	Type II-A member stresses from model with applied design wind loading.....	42
Table 4.4-4	Type II-A member stresses from model with dead load and applied design wind loading .....	42
Table 4.4-5	Modal analysis results for the Type II-A sign bridge .....	42
Table 4.5-1	Geometric and material properties for Type III-A sign bridge .....	43
Table 4.5-2	Type III-A drag coefficients and resulting member loads.....	44
Table 4.5-3	Calculated member stress in the Type III-A structure for applied wind load .....	45
Table 4.5-4	Calculated member stress in the Type III-A structure for dead load plus applied wind load.....	45
Table 4.5-5	Modal analysis results for the Type III-A sign bridge .....	45

Table 4.6-1	Member geometric properties for the VMS sign bridge .....	46
Table 4.6-2	Type II-A with VMS member stresses for applied wind load.....	48
Table 4.6-3	Type II-A with VMS member stresses from model with applied design wind load plus dead load .....	48
Table 4.6-4	Modal analysis results from the VMS sign bridge .....	49
Table 5.2-1	Measured peak stress in selected members for manual transverse excitation of the cantilever .....	53
Table 5.2-2	Comparison of measured and calculated natural periods of vibration for the cantilever truss .....	56
Table 5.3-1	Type I-A member stresses due to horizontal manual excitation .....	62
Table 5.4-1	Type II-A member stresses due to horizontal manual excitation .....	68
Table 5.5-1	Type III-A member stresses due to horizontal manual excitation .....	73
Table 6.2-1	AASHTO (2001) sign panel drag coefficients .....	83
Table 6.2-2	Recommended drag coefficients as a function of aspect and clearance ratios .....	80
Table 6.2-3	Allowable stress for aluminum members .....	80
Table 6.2-4	Constant amplitude fatigue limits (CAFL) for truss members .....	81
Table 6.2-5	Average ratio of peak response to 3-sec average vs. average wind speed .....	86
Table 6.2-6	Statistical properties of response ratios.....	86
Table 6.3-1	Comparison of measured stresses to model stresses .....	89
Table 6.3-2	Cantilever stresses due to measured design wind load + modal dead load.....	92
Table 6.3-3	Estimated stress ranges compared to CAFL values for the cantilever truss.....	93
Table 6.4-1	Comparison of measured stresses to model stresses for Type I-A truss.....	96
Table 6.4-2	Type I-A stresses due to measured design wind load + model dead load.....	100
Table 6.4-3	Type I-A estimated stress ranges compared to CAFL values.....	101
Table 6.5-1	Type II-A stresses calculated from the analytical model and extrapolated from measured stresses .....	103
Table 6.5-2	Summary of Type II-A response to various truck gust types .....	106

Table 6.5-3	TYPE II-A total stress estimated for the design wind speed of 90 mph – measured wind + model dead load stresses .....	107
Table 6.5-4	Type II-A estimated stress ranges compared to CAFL values.....	107
Table 6.6-1	Type III-A comparison of extrapolated measured stresses to model stresses.....	110
Table 6.6-2	Type III-A acceleration and member stresses due to truck gusts .....	112
Table 6.6-3	Type III-A stresses due to measured wind load +model dead load .....	112
Table 6.6-4	Type III-A estimated stress ranges compared to CAFL values.....	113
Table 6.7-1	Comparison of VMS truss measured stresses to model stresses for 90 mph wind .....	115
Table 7.2-1	Highway truss damper selection table .....	122
Table 7.3-1	Field testing results – horizontal vibration.....	123
Table 7.3-2	In-tact damper test summary .....	125
Table 7.4-1	Modeled Type III-A truss with different numbers of tuned Stockbridge dampers .....	134
Table 7.5-1	Estimated dynamic displacement of each sign truss .....	136
Table 8.2-1	$K_r$ values measured for both T- and K-type end connections .....	142
Table 8.3-1	Older IDOT Type IV-A sign truss with 90-ft maximum span and 5-ft panel length.....	144
Table 8.3-2	Older IDOT Type III-A sign truss with 90-ft maximum span and 5-ft panel length.....	144
Table 8.3-4	Older IDOT Type III-C-A cantilever sign truss critical members .....	145
Table 8.3-5	New IDOT Type I-A sign truss with 70-ft maximum span and 5-ft panel length.....	148
Table 8.3-6	New IDOT Type III-A sign truss with 140-ft maximum span and 5-ft 6-in panel length.....	148

## 1.0 Introduction

### 1.1 Background

The use of overhead and cantilever sign structures is quite common throughout Illinois and in the rest of the United States. These structures are used where standard guide signs along the side of the road would be inadequate or otherwise cannot be used. These applications include complicated intersections of highways and roads where high visibility is required, locations with difficult terrain or utility conflicts, etc. Overhead structures are sometimes also used to support signals and lights. Both the American Association of State Highway & Transportation Officials (AASHTO, 2001) and the Illinois Department of Transportation (IDOT, 2001) have specifications for the design of these structures.

In the year 2000, IDOT changed their standard designs for aluminum highway sign structures. The design changes included eliminating redundant members, increasing the diameter and thickness of the hollow circular tubes, and installing vibration dampers. These changes were intended to increase the strength, stiffness, and factor of safety for these structures. The design changes were required in part because many cracks had been found at “T”, “Y”, and “K” tube-to-tube welded connections, most likely as a result of wind-induced cyclic loading. After formation, the cracks would then progress into the base metal. In many cases, the cracks would completely sever web members framing into the chords of the truss at one or both ends. In the most extreme cases these web members dropped onto the highway, causing significant safety problems. In addition, repairing the in-service structure was expensive and sometimes ineffective. In many cases, the structures were simply replaced. Examples of damaged sign structures are shown in Figure 1.1-1



**Figure 1.1-1 Damaged web member-to-chord connections: older IDOT Type III-A truss (left) and older IDOT Type IV-A truss (right)**

Wind damage to overhead and cantilever sign structures is not unique to Illinois; many states have reported damaged and/or collapsed sign structures. The problem has

been so broad for cantilevered sign structures that the National Cooperative Highway Research Program (NCHRP) has funded two projects related to their wind response (Kaczinski et al., 1998) and design for wind loads (Dexter et al., 2002). Results from the report by Dexter et al. (2002) were used in developing the latest revisions to the AASHTO *Standard Specifications for Structural Supports for Highway Signs, Luminaries and Traffic Signals* (2001).

## 1.2 Research Objectives

Initially, there were six research objectives for this IDOT project, as follows:

Objective 1: Develop an analytical model for computing the response of aluminum highway sign truss structures to natural wind and truck-induced wind gust loads.

Objective 2: Based on analysis and testing, determine the AASHTO design load capacity and fatigue resistance of the IDOT sign structures included in the project.

Objective 3: Based on analysis and testing, determine the effectiveness of vibration dampers currently installed on overhead sign structures. If these are found to be ineffective, investigate through analysis the potential effectiveness of other types of dampers currently being used by other highway departments in other states.

Objective 4: Determine the effects of transportation and erection loads on the strength and service life of aluminum overhead sign structures.

Objective 5: Compile data on expected durability of individual truss components and connections to determine the anticipated service life of new truss structures included in this project.

Objective 6: Identify and report potential problem areas of current sign structure design procedures, and recommend detail modifications and/or other corrections where required.

Five IDOT sign structures (all representing newer design and construction practices of the last few years) were identified for investigation. This included one cantilever (of Type II-C-A), three overhead sign bridges (of Types I-A, II-A, and III-A), and one additional sign bridge (of Type II-A) carrying a variable message sign (VMS). These will be described in more detail in Chapter 2 and thereafter. Each sign structure was instrumented with accelerometers, strain gages, and an anemometer. The accelerometers were used to determine the dynamic properties of the structures and to calibrate the analytical model of each. The strain gages were used to determine the axial forces and bending moments in critical members as the structures were subjected to wind loads, truck gusts and manually-induced forces. The anemometer measured the magnitude and direction of the wind at each structure. For a given wind velocity and direction, the axial loads and bending moments determined for critical members can be compared to calculated values determined by analysis of the structure using forces

determined from code provisions and design assumptions. From these results, the IDOT design procedures were evaluated. The instrumentation, test procedures, and analytical modeling procedures will be described in Chapter 3. The modeling procedures and the results of the modeling are then discussed in Chapter 4. Chapter 5 explains the dynamic characteristics of the structures, based on both the experiments and the analyses. Then the AASHTO design specifications and IDOT design procedures are evaluated in Chapter 6.

The effectiveness of damping devices installed on IDOT sign structures was also evaluated. The effective damping for each structure (both with and without damping devices) was determined from dynamic response decay initiated by manual-excitation and/or pull-back tests. A series of laboratory tests on as-delivered and modified dampers were also conducted in the laboratory. The steady state response of each damper to sinusoidal input of varying frequency and amplitude was obtained. A series of analyses using the measured damper properties was also undertaken to determine how effective these devices might be under varying wind conditions. The results of these studies are described in Chapter 7.

Some of the older IDOT sign structures taken out of service were available for inspection and investigation. These had some members that had experienced cracking while in use. Vibration tests were conducted on members with and without cracks to determine their dynamic properties. Analytical studies were used to interpret the measured responses and predict how these members might behave under steady wind of different speeds. Those procedures and results will be discussed in Chapter 8. Finally, a summary and conclusions for the entire project are given in Chapter 9, followed by a list of all the cited references from the entire report in Chapter 10.

## **2.0 Sign Structure Descriptions and Locations**

### **2.1 Introduction**

The current IDOT (2001) design guide identifies four basic sign structure types. These are the cantilever structure (with various sub-types) and then Type I-A, II-A, and III-A overhead sign bridges. The particular sign bridge designations (and therefore their member sizes) are based in part on the span and sign size used. One of each of these four types of structures was studied. An additional overhead sign truss supporting a VMS was also investigated.

All of the structures chosen for this investigation were located on interstate highways. One requirement used in the selection process was the accessibility of the structure. It was necessary to have enough room near the columns of the structure for the instrumentation van to park a safe distance from the traffic lanes. Remote operation of the instrumentation system was not available, so the instrumentation van and the researchers needed to be on-site to collect data. It was also deemed desirable for the signs to be not too distant from the Newmark Civil Engineering Lab at the University of Illinois, to minimize the travel time between the lab and the structures for setting up the tests and subsequently collecting the data. All of the structures tested were within about a one-hour drive from the lab. A brief description of each structure is given here in this chapter, with additional details about the instrumentation used and the analytical models for each provided in subsequent chapters.

### **2.2 Cantilever Structure**

The cantilever sign structure that was tested is located at mile 144 on eastbound Interstate Highway 72, just east of Decatur, Illinois. The structure is perpendicular to the east-west direction and located directly after a bridge as seen in Figure 2.2-1. The sign itself indicates an immediate exit for Illinois 48. A photograph of the structure may be seen in Figure 2.2-2. The topography of the region is fairly flat with an absence of any nearby structures. There is, however, a steep drop-off and lower region to the south of the cantilever where Illinois 48 passes under Highway 72.

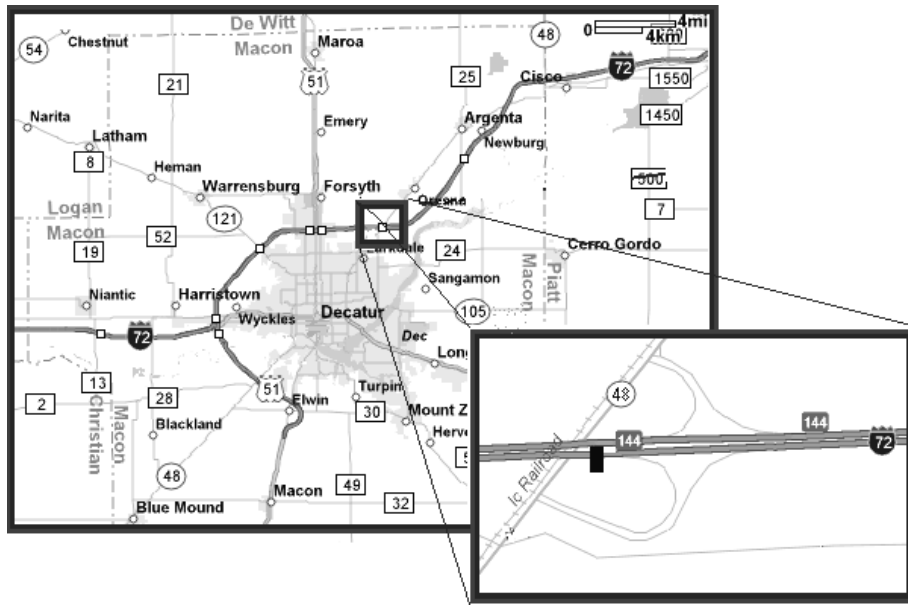


**Figure 2.2-1 Location of cantilever sign structure**



**Figure 2.2-2 Picture of cantilever sign structure looking east**

The IDOT Bureau of Bridges and Structures designates this cantilever sign truss as a Type II-C-A. This type of truss has a maximum cantilever length of 30 ft and a maximum allowed sign area of 340 ft<sup>2</sup>. The truss consists of a number of panels, which can range in length from 42 to 48 in. The maximum allowed length of the column is 30 ft from the column base plate to the centerline of the top chord of the truss.

This particular cantilever consists of a hollow steel column and an aluminum truss comprised of hollow circular tube sections. The column is anchored to a 3.5 ft diameter

drilled shaft concrete foundation. The distance from the top of the foundation to the top of the column is 30 ft. There are seven 48-in. panels along the length of the truss, which measures 66 in. high by 36 in. deep, with a total length of 30 ft from the centerline of the column to its end. The four main chords of the truss have an outside diameter of 6.5 in. and the smaller web members have an outside diameter of 3.25 in. (all wall thicknesses are 5/16 in.) Refer to Figures 2.2-3 and 2.2-4 for drawings of this sign structure. The total weight of the truss is 1860 lbs, and the column weight is 3770 lbs. A 15.9-lb Stockbridge-type damping device is installed towards the end of the cantilever.

The sign itself is a 1/8 in. thick ribbed aluminum sheet that is mounted on a series of 6 in. (or 12 in.) extruded aluminum channels that are bolted together to form a panel that is about 1-1/2 in. thick. The sign measures 175 by 126 in., with a total area of approximately 153 ft<sup>2</sup>, and is mounted to the main chords of the truss with U-bolts. There are also two aluminum grate walkways, one directly below the sign panel running the length of the sign and one along the length of the bottom of the truss.

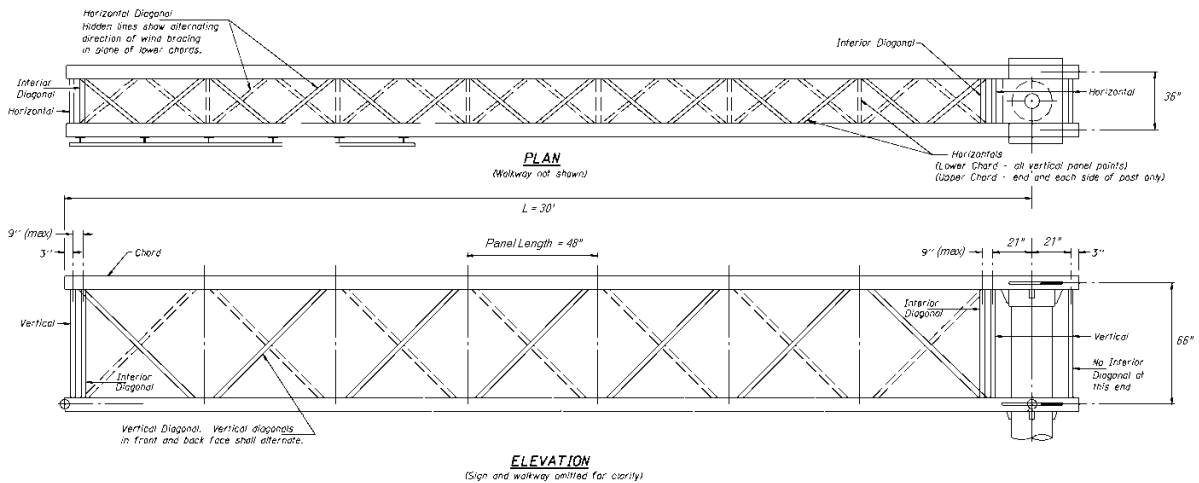


**Figure 2.2-3 Plan and elevation of cantilever truss**

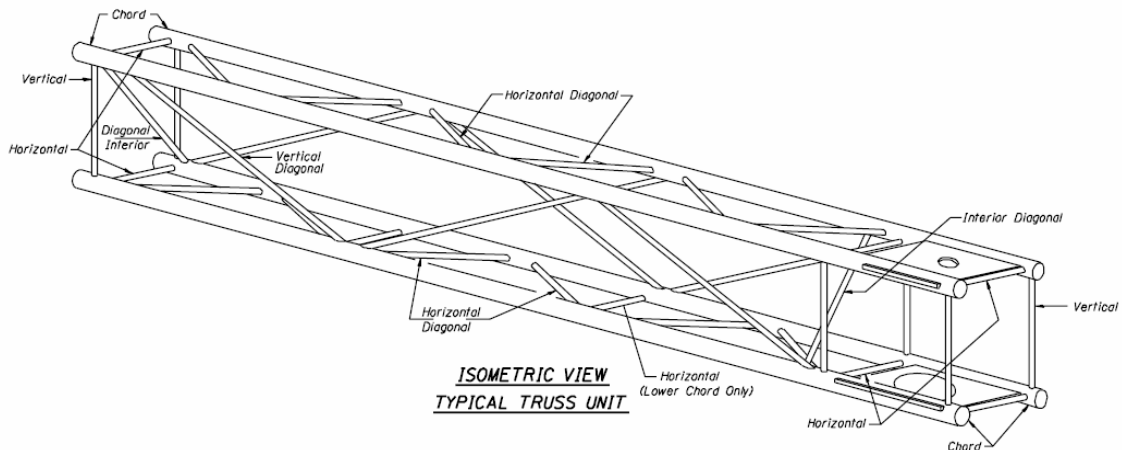


**Figure 2.2-4. Isometric view of typical cantilever truss unit**

### 2.3 Type I-A Sign Bridge

The Type I-A sign structure that was tested is a bridge structure located at mile 134.8 on westbound Interstate Highway 72, just west of Decatur, Illinois. The structure spans this stretch of road, which heads 45-degrees west of south as seen in Figure 2.3-1. The sign itself indicates an exit for Illinois 36 and U.S. 51 one mile down the road. A photograph of the structure may be seen in Figure 2.3-2. The topography of the region is fairly flat with an absence of any nearby structures.

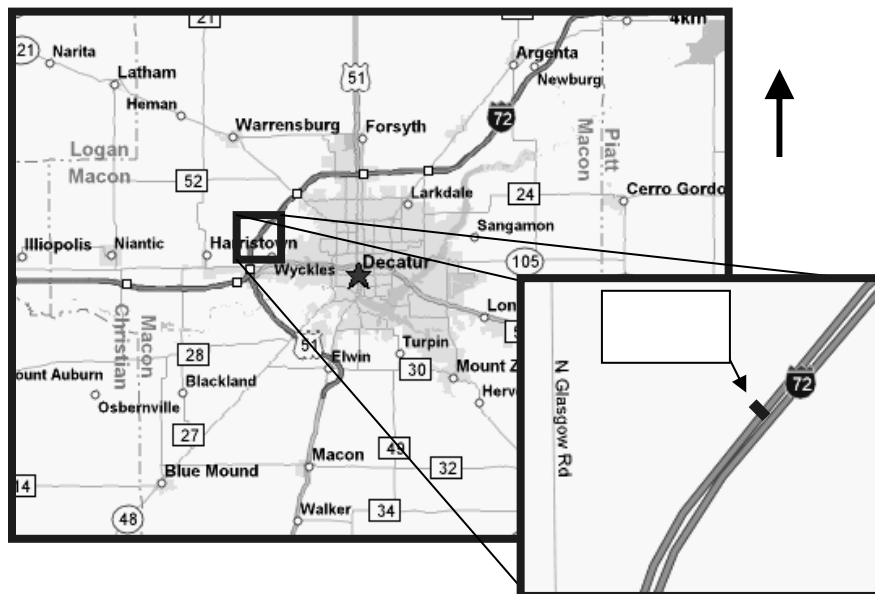


**Figure 2.3-1 Location of the Type I-A sign bridge**



**Figure 2.3-2 Pictures of the Type I-A sign bridge**

This sign bridge is comprised of an aluminum overhead truss with steel support frames at each end. This particular truss is designated by IDOT Bureau of Bridges and Structures as a Type I-A. The truss has a total span of 88.0-ft and a sign area of 352.30 ft<sup>2</sup>.

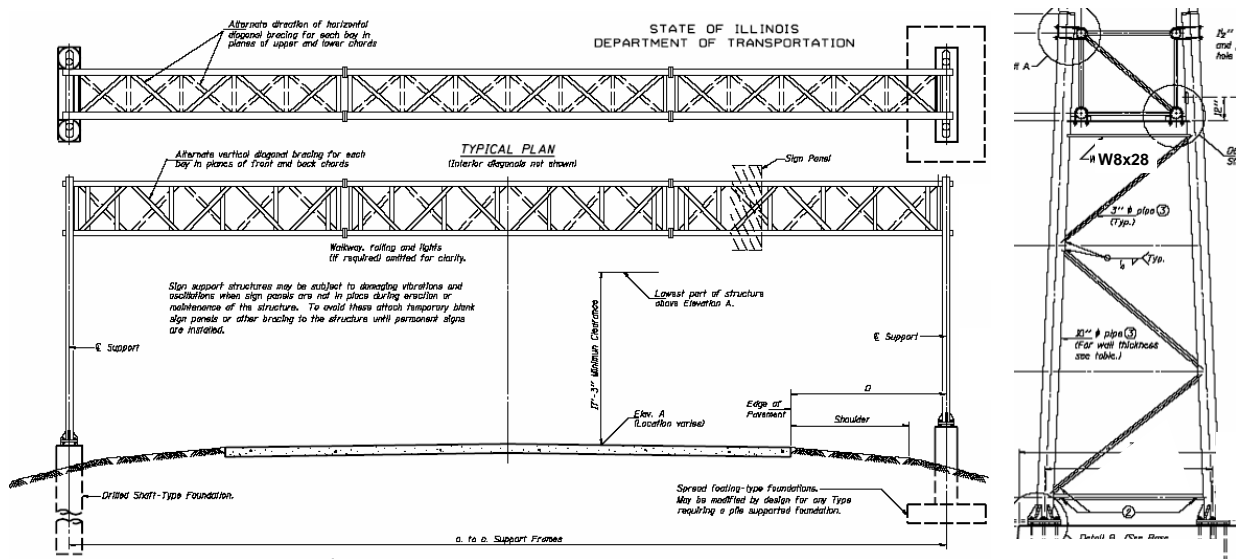


**Figure 2.3-3 Plan and elevation of the Type I-A sign bridge truss (left) and support structure (right)**

The elements of the structure (truss and piers) are hollow tube sections, with the exception of a W8x28 near the top of each support frame that directly supports the end of the truss. The columns are made of 10 in. diameter steel pipe with a wall thickness of 0.365-in. These rise 33 ft – 7½ in. from the top of the concrete foundations, which satisfies the minimum sign clearance of 17 ft – 3 in. above the road surface. Diagonal braces of 3 in. diameter with a wall thickness of 5/16 in. connect the columns at intervals of approximately 8 ft – 13/16 in. The columns slant inward and measure 8 ft – 3 in. between the centerline of the base supports and 5 ft – 6 in. at the top.

This truss was prefabricated and transported to the erection site as three units, which are connected at splicing flanges with six bolts. The two exterior units have a total length of 30 ft – 1½ in., and the single interior unit has a length of 29 ft – 6 in. All units consist of six panels with approximate length of 4 ft – 8½ in. The height and width of truss are 4 ft – 6 in. and 4 ft – 0 in., respectively, between the centerlines of the chords. The four main chords of the truss have an outside diameter of 5-in. and wall thickness of 5/16 in. The smaller vertical, horizontal, and diagonal web members all have an outside diameter of 2½ in. and a wall thickness of 5/16 in. As was the case for all of the overhead (bridge) sign trusses tested, this truss had a 31-lb Stockbridge-type damper located at mid-span.

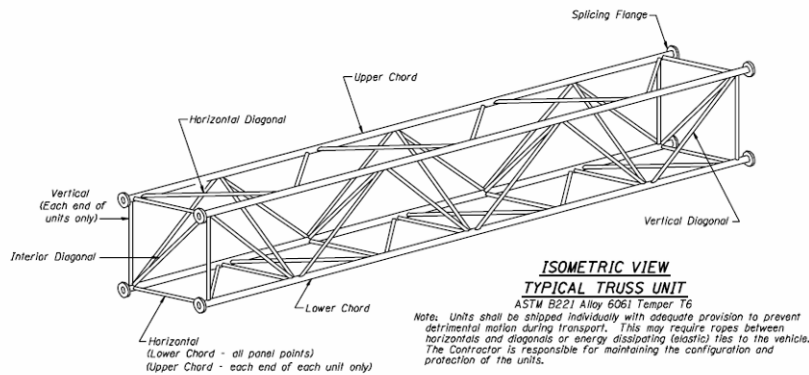


**Figure 2.3-4 Isometric view of typical Type I-A truss unit**

The Type I-A is the smallest truss of the overhead type. It can have a maximum span of 100 ft and a maximum sign area of 610 ft<sup>2</sup>. To provide context as to how the particular Type I-A truss tested as part of this study fits in to this overall category, the general design guidelines for all Type I-A trusses are shown in Table 2.5-1.

**Table 2.3-1 IDOT design data for Type I-A sign bridges**

Max. Span Length (ft)	Max. Sign Area (sf)	Chord Size (in.)	Web Member Size (in.)
70	350	4 ½ x 1/4	2 ¼ x ¼
70	550	5 x 1/4	2 ½ x ¼
80	570	5 x 5/16	2 ½ x 5/16
90	610	5 x 5/16	2 ½ x 5/16
100	610	5 ½ x 5/16	2 ½ x 5/16

## 2.4 Type II-A Sign Bridge

The Type II-A sign structure that was tested is a newer overhead bridge structure (on older existing supports) located at mile 132.8 on eastbound Interstate Highway 72, where the road splits at exits 133A and 133B just west of Decatur, Illinois. The structure

spans this stretch of road, which is aligned 15 degrees north of east as seen in Figure 2.4-1. The sign itself indicates an exit for Illinois 36 East and U.S. 51 South. A photograph of the structure may be seen in Figure 2.4-2. The topography of the region is fairly flat with an absence of any nearby structures.

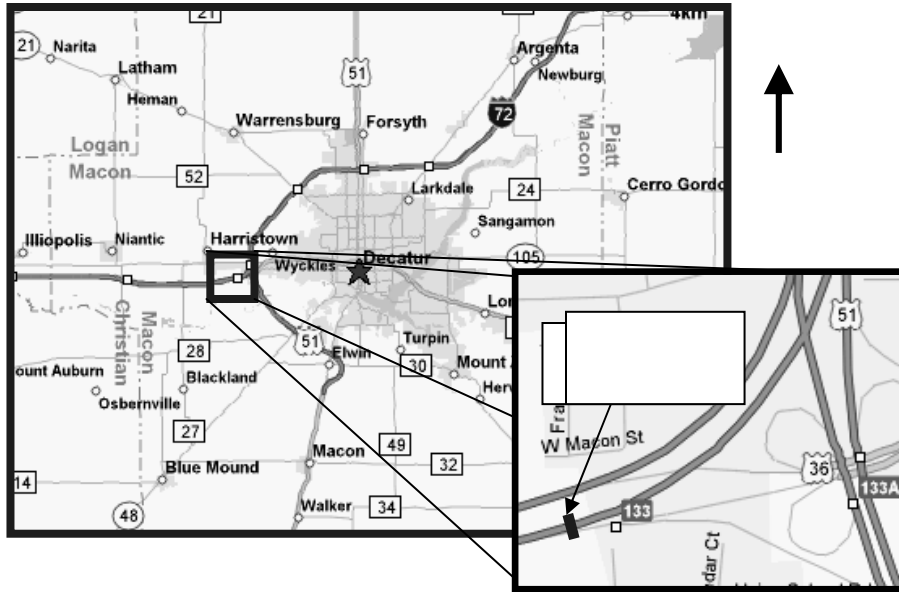


**Figure 2.4-1 Location of the Type II-A sign bridge**



**Figure 2.4-2 Pictures of the Type II-A sign bridge looking east (left) and west (right)**

This Type II-A sign bridge is comprised of an aluminum truss and steel support frames at each end. This particular truss is designated by the IDOT Bureau of Bridges and Structures as a Type II-A. The truss has a total span of 115.0-ft and a sign area of 512.50 ft<sup>2</sup>. The configuration of this structure is the same as that shown in Figure 2.3-4 for the Type I-A sign bridge. This truss type measures 4 ft – 6 in. wide by 5 ft – 3 in. tall. It can have a maximum span of 130 ft and a maximum sign area of 740 ft<sup>2</sup>. The general design guidelines for a Type II-A truss are shown in Table 2.4-1. The chords of this truss have an outside diameter of 5 in and a thickness of 5/16 in. All web members have an outside diameter of 2 1/2 in. and a wall thickness of 5/16 in.

**Table 2.4-1 IDOT design data for Type II-A sign bridges**

<b>Max. Span Length (ft)</b>	<b>Max Sign Area (sq. ft)</b>	<b>Chord Size (in)</b>	<b>Web Member Size (in)</b>
90	740	5 1/2 x 5/16	3 x 5/16
100	740	6 x 5/16	3 x 5/16
110	740	6 1/2 x 5/16	3 x 5/16
120	740	7 x 5/16	3 x 5/16
130	740	7 x 3/8	3 x 5/16

The truss is made up of three units. The two exterior units have a total length of 39 ft – ½ in., and the single interior unit has a length of 38 ft – 5 in. All units consist of eight panels of length 4 ft – 7¾ in., with chord and web member sizes per the table above.

## 2.5 Type III-A Sign Bridge

The largest sign structure that was tested is an overhead sign truss located at mile 0 on southbound Interstate Highway 155 just north of Lincoln, Illinois. The structure is perpendicular to the north-south direction and located where I-155 ends and meets I-55, spanning four lanes of traffic as seen in Figure 2.5-1. A photograph of the structure may be seen in Figure 2.5-2. The topography of the region is fairly flat with an absence of any nearby structures.

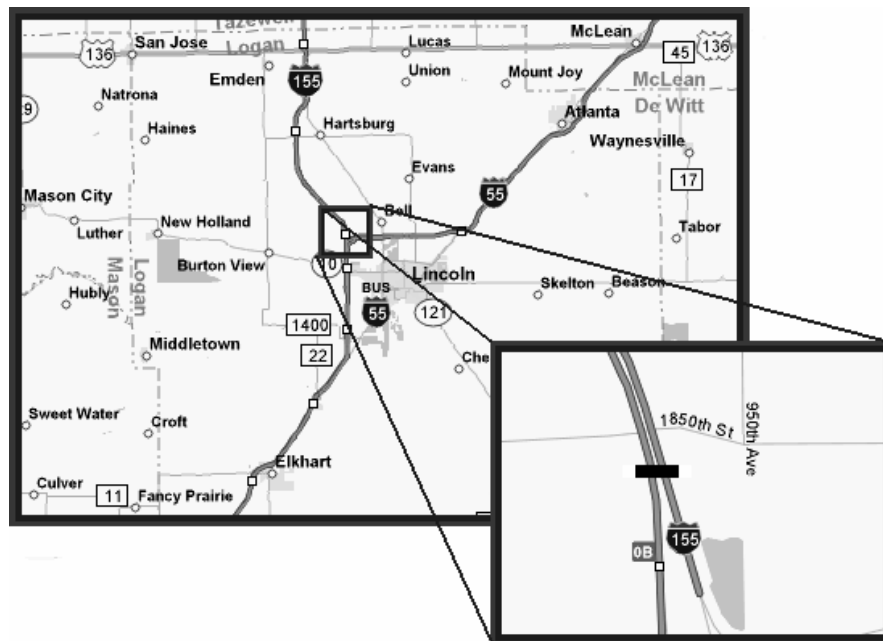


**Figure 2.5-1 Location of the Type III-A sign bridge**



**Figure 2.5-2 Picture of the Type III-A sign bridge looking south**

This truss is designated by the IDOT Bureau of Bridges and Structures as a Type III-A, which is their largest truss of the overhead type, measuring 5-ft wide by 7-ft tall. It can have a maximum span of 160 ft and a maximum sign area of 1200 ft<sup>2</sup>. The general design guidelines for a Type III-A truss are shown in Table 2.5-1.

**Table 2.5-1 IDOT design data for Type III-A sign bridges**

<b>Max. Span Length (ft)</b>	<b>Max Sign Area (sq. ft)</b>	<b>Chord Size (in)</b>	<b>Web Member Size (in)</b>
120	900	7 x 5/16	3 1/4 x 5/16
130	975	7 x 3/8	3 1/4 x 5/16
140	1050	7 x 1/2	3 1/4 x 5/16
150	1125	8.5 x 5/16	3 1/2 x 5/16
160	1200	9 x 1/2	3 1/2 x 5/16

This truss is made up of 4 individual truss units (two exteriors and two interior units). The units, in turn, each consist of a number of panels, all of which measure approximately 5 ft – 3-3/8 in., with seven panels in each of the interior units and six panels in the exterior units. The total centerline-to-centerline span of the truss is 142 ft, and the total area of the three signs is approximately 560 ft<sup>2</sup>. Chord members are 8 1/2 in. by 5/16 in. and the chord members are 3 1/2 in. by 5/16 in.

## **2.6 VMS on Type II-A Sign Bridge**

The final sign structure that was tested in the field was a Type II-A truss with a variable message sign (VMS). The sign bridge structure is located over I-55 near Shirley

interchange (Exit 154) southwest of Bloomington, Illinois. The structure spans this stretch of road which heads in the southwest as seen in Figure 2.6-. This sign structure has a variable VMS mounted at the mid-span of the truss as seen in Figure . The topography of the region is fairly flat with the absence of any nearby structures.



**Figure 2.6-1 Location of the Type II-A sign bridge with VMS**



**Figure 2.6-2 Pictures of the Type II-A sign bridge with VMS, located near Shirley, IL**

This Type II-A structure is comprised of an aluminum truss and steel support frames at each end. This particular truss is designated by the IDOT Bureau of Bridges and Structures, as a Type II-A. The truss has a total span of 94.0-ft. Figure shows the VMS mounted on the truss. The VMS measures 18 ft wide, 7 ft – 9 in. high and 4 ft – 7 in. thick. The weight of the VMS is approximately 2,000 lb. The sign is mounted to sign brackets (W4x3.06) that are connected to the main chords of the truss via U-bolts. Refer to Table 2.4-1 for the general design guidelines for a Type II-A truss.



**Figure 2.6-3 Variable message sign (VMS)**

The truss is prefabricated and transported to the erection site as three units, which are connected at splicing flanges with six bolts. The two exterior units have a total length of 32 ft - 4½ in. and the single interior unit has a length of 31 ft - 9 in. All units consist of six panels with approximate length of 5 ft - 1 in. The height and width of truss are 5 ft - 3 in. and 4 ft - 6 in., respectively, between centerline of chords. The four main chords of the truss have an outside diameter of 6 in. and wall thickness of 5/16 in. The web members all have an outside diameter of 3 in. and wall thickness of 5/16 in.

## 3.0 Instrumentation, Data Acquisition, and Data Processing

### 3.1 Introduction

Three types of field data were required to complete the objectives of this project: wind velocity, member strains, and structure accelerations. The wind velocities and the member strains they produced were required for evaluating the relevant AASHTO and IDOT design specifications and related procedures. The accelerations help to determine the natural frequencies and mode shapes of vibration for each structure. These are useful for comparing with and determining the overall accuracy of the analytical models used to calculate stresses induced by wind pressures.

Based on the desired data to be acquired, three primary components of the instrumentation system were used. These components were an anemometer, accelerometers, and strain gages. The instrumentation system design was based on a range of factors, including analytical model results, expected wind behavior, and the geometry of the structure. This is discussed further in the following sections.

In order to capture the data from each component of the instrumentation system simultaneously, a National Instruments chassis was used in conjunction with LabView software. Each individual instrument was connected into the chassis, which was in turn connected to a laptop computer. A data acquisition card that converted the signals from analog to digital output was used to connect to the computer. With this configuration, communication of all data to the data acquisition program occurs synchronously, with the same time intervals. A sampling rate of 100 Hz was typically used for each test. The length of each test varied depending on what behavior or what types of results were intended to be captured. Some tests required the use of only certain of the instruments, while others engaged all of them.

One of the most challenging aspects of the project was the long time required in order for the wind conditions (both velocity and direction) to be suitable for certain of the tests. It was strongly desired that the average wind speed component normal to the sign be greater than 20 mph. (On the first structure tested, this took almost nine months.) Based on the uncertainty related to when the conditions would be favorable for data acquisition, a system was devised to allow the researchers to keep the structures instrumented for an indefinite period of time. This required that the ends of the instrumentation cables be stored away when the tests were not being conducted. Therefore, a lockable and weather-resistant aluminum box mounted approximately one-third of the way up the height of one of the column supports was used to accomplish this (see Figure 3.1-1). When it was time to collect data, the box was simply accessed with a ladder, and then cables were dropped and connected to the chassis for data acquisition. At the conclusion of a particular period of testing, the cables were once again stored away in the box. It was very important that the cable ends be accessible with a ladder positioned away from the traffic lanes. If the instrumentation cables would have just

been left on the truss structure, this would have required lane closures on each day of testing / data collection.



**Figure 3.1-1 Picture of cable storage box mounted on support structure**

### **3.2 Anemometers**

A single anemometer was installed at the site of each sign structure. The goal of this instrument was to measure the wind speed and direction at the sign truss location. Two different anemometers were used for the project. One of these was a Wind Monitor, a propeller-type anemometer manufactured by R.M. Young. The Wind Monitor has a four-blade propeller that produces an AC sine wave at a frequency directly proportional to the wind velocity. This data is communicated as voltage output, with a range of 0 V to 1 V corresponding to wind speeds from 0 mph to 100 mph. The wind direction is sensed by a potentiometer with an output voltage proportional to the azimuth angle (R.M. Young, 2004).

It was important to obtain the ambient wind characteristics without any interference from the structure or any other outside influence. To accomplish this, the anemometer was always installed 6 ft above the top of the truss (over the support column) with a 1.5-in. diameter steel pipe. Figure 3.2-1 shows the installation of the Wind Monitor mounted on the Type III-A sign structure.



**Figure 3.2-1 Wind Monitor mounted on the Type III-A sign bridge**

The second type of anemometer used was a WindMaster ultrasonic (no moving parts) anemometer, manufactured by Gill Instruments. The WindMaster has sensors that measure pressure variations and resolves these to output the wind magnitude and polar direction in a horizontal plane, as well as the vertical magnitude of the wind. This data is communicated as voltage output, with a range of 0 V to 5 V corresponding to a wind speed range of 0 to 70 m/s. The wind direction ranges from 0° to 540° (Gill Instruments, 2000). Figure 3.2-2 shows this instrument mounted on the cantilever sign structure.



**Figure 3.2-2 Gill Instruments WindMaster mounted on the cantilever structure.**

### 3.3 Strain Gages

To determine the stresses in the truss members resulting from different types of loading, a number of strain gages were mounted on each sign structure. These gages were 350- $\Omega$ , quarter-Wheatstone-bridge gauges with a gage factor,  $K$ , of 2.1. They came from the manufacturer with pre-attached 10-ft lead wires for easier installation in the field. They were installed according to standard gage installation procedures; however, several protective coatings were also added to keep the gages sheltered from the weather and vehicle exhaust. One of the attached gages is pictured below in Figure 3.3-1.



**Figure 3.3-1 Typical strain gage placement**

The locations of the strain gages on each of the instrumented trusses were chosen based on which members were thought to be most critical (highest wind-related stresses) when loading is acting normal to the sign. In the cantilever truss, the most critical web members are those adjacent to the truss-to-column connection, and the highest stress in the chords is also expected to occur near the column. In the overhead trusses, the critical web members are near the truss-support structure connection, along with the upper and lower chords at mid-span. This was verified by results from the computer model.

For the cantilever structure, the members instrumented with strain gages near the support connection are indicated in Figure 3.3-2. Figure 3.3-3 indicates the strain gage placement for the Type I-A structure, and Figure 3.3-4 shows the placement for the Type II-A and Type III-A structures. On each instrumented member, two gages were attached at the mid-span of the member, directly opposite one another. On the Type I-A structure, two gages were mounted at one end of each web member (near the welded connection of the member to the chord) in addition to the gages attached at mid-span of the members.

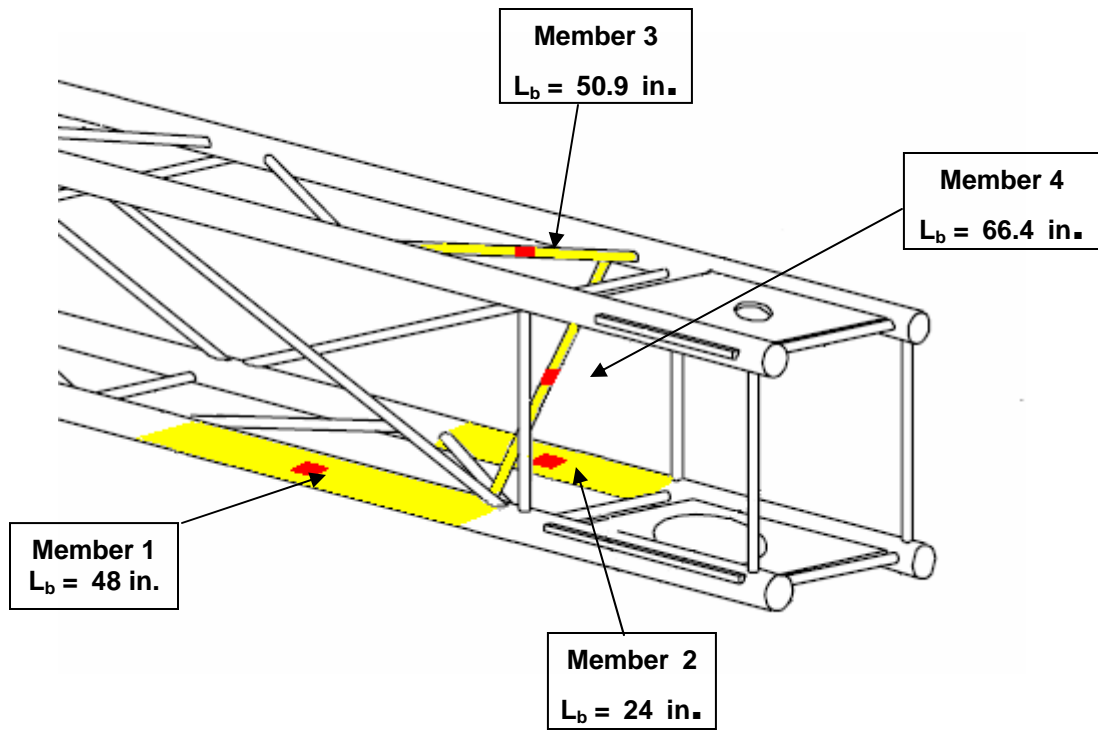


Figure 3.3-2 Strain gage placement for the cantilever structure

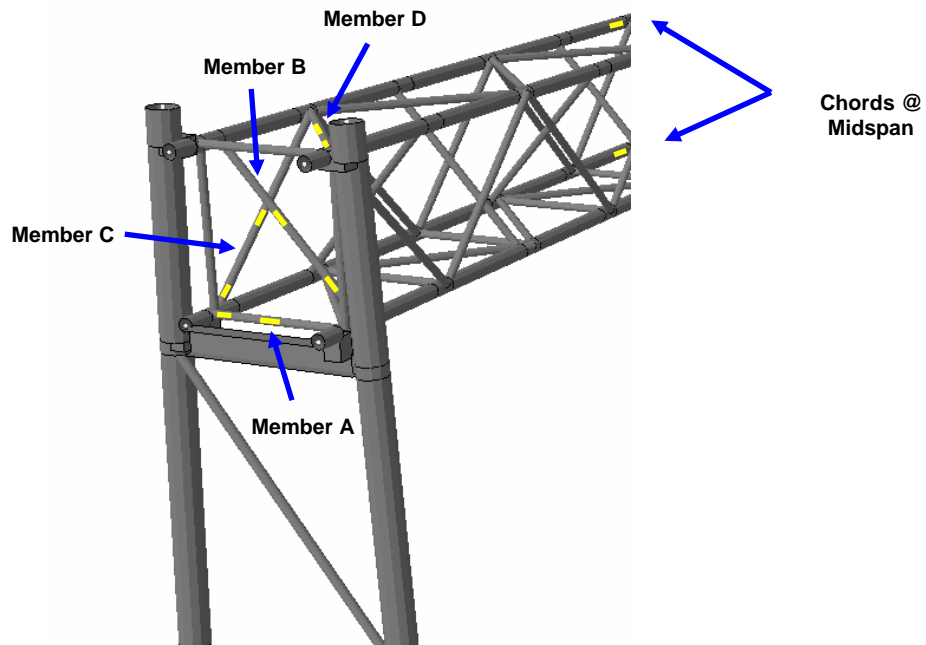
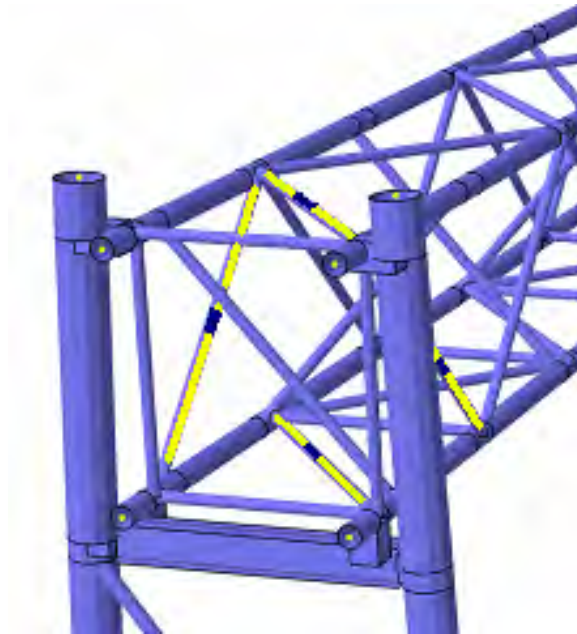
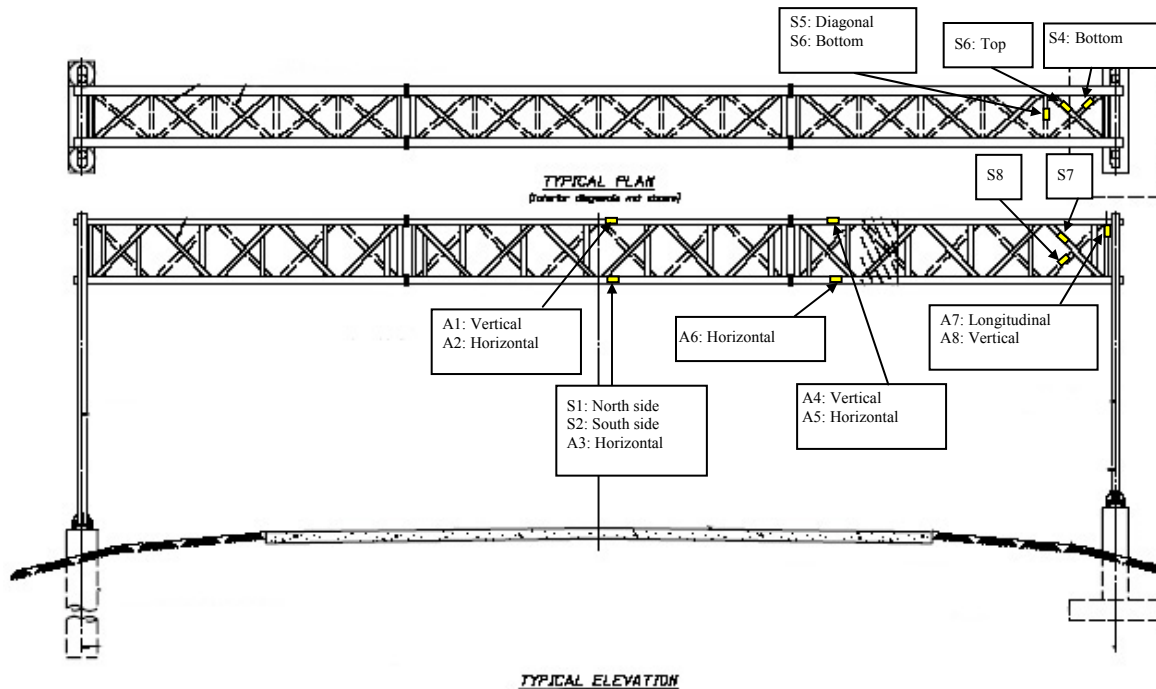


Figure 3.3-3 Location of strain gages on the Type I-A sign bridge



**Figure 3.3-4 Strain gage placement near truss end for Type II-A and Type III-A sign bridges**

The VMS structure was instrumented and data was collected by the private firm of Wiss, Janney, Elstner Associates, Inc. (from Northbrook, Illinois), through a contract with the University of Illinois at Urbana-Champaign (UIUC). Upon completion of the testing of this structure, the data was provided to researchers at UIUC, where it was processed and interpreted. The location of the strain gage placements was again chosen based on which members were thought to be most critical when loading is normal to the sign. In the sign bridge truss, these are some of the web members near the truss-support structure connection, along with the chords at mid-span. Figure 3.3-5 shows the location of these gages (denoted by “S” labels). (The accelerometer locations are also shown (denoted by “A” labels).)



**Figure 3.3-5 Strain gage and accelerometer placement for the VMS sign structure**

In all cases, the reason for placing two gages at each location along each member is that this allows both the axial stresses and bending stresses in the members to be captured. This is accomplished by using the following relationships:

$$\sigma_{bending} = \frac{\sigma_1 - \sigma_2}{2} \quad 3.3-1$$

$$\sigma_{axial} = \frac{\sigma_1 + \sigma_2}{2} \quad 3.3-2$$

### 3.4 Accelerometers

Accelerometers measure the acceleration of the points on the structure to which they are attached. A structure's acceleration allows the dynamic characteristics of the structure to be determined. These characteristics include the predominant (natural) frequencies at which the trusses vibrate, as well as the mode shapes that the structure experiences. The accelerometers were used to determine the response of a structure as it vibrated in its lowest three or four modes of vibration. To accomplish this, accelerometers were placed at joints or ends of members. Accelerometers were not placed at the midpoints of members which could be done to measure the vibration of individual members. Vibration of individual members could be detected from strain gage

measurements, but none was observed for any of the structures. The topic of individual member vibration is addressed in Chapter 8.

The first structure to be instrumented was the Type I-A sign bridge structure. On this truss, the accelerometers were placed at various locations across the entire span of the truss. This helped verify the symmetric and anti-symmetric motion of the structure and also ensured that enough instruments would work properly for sufficient data collection. On subsequent signs, symmetry was utilized to lessen the required number of accelerometers. Twelve accelerometers (manufactured by PCB Piezotronics) were mounted on the truss to capture the movement of the structure in response to wind, truck gusts, and/or manual excitation. These are single-axis accelerometers, they have a frequency range of from 0 to 150 Hz, and they can measure accelerations ranging from  $\pm 0.1$  to  $\pm 5$  g (PCB, 2004). The location and orientation of these accelerometers is summarized in Table 3.4-2 and Figure 3.4-2, with the measurement directions given as they relate to the orientation of the truss.

**Table 3.4-1 Type I-A truss accelerometer configuration**

<b>Accelerometer</b>	<b>Measurement Direction</b>	<b>Top/Bottom</b>	<b>Location</b>
1LE	Longitudinal	Bottom	Over 1 <sup>st</sup> Support
2HE	Horizontal	Bottom	Over 1 <sup>st</sup> Support
3VQ	Vertical	Bottom	Quarter Point
4HQT	Horizontal	Top	Quarter Point
5HQB	Horizontal	Bottom	Quarter Point
6VM	Vertical	Bottom	Mid-Span
7HMT	Horizontal	Top	Mid-Span
8HMB	Horizontal	Bottom	Mid-Span
9VQ	Vertical	Bottom	Three Quarter Point
10HQT	Horizontal	Top Bottom	Three Quarter Point
11HQB	Horizontal		Three Quarter Point
12HE	Horizontal	Bottom	Over 2 <sup>nd</sup> Support

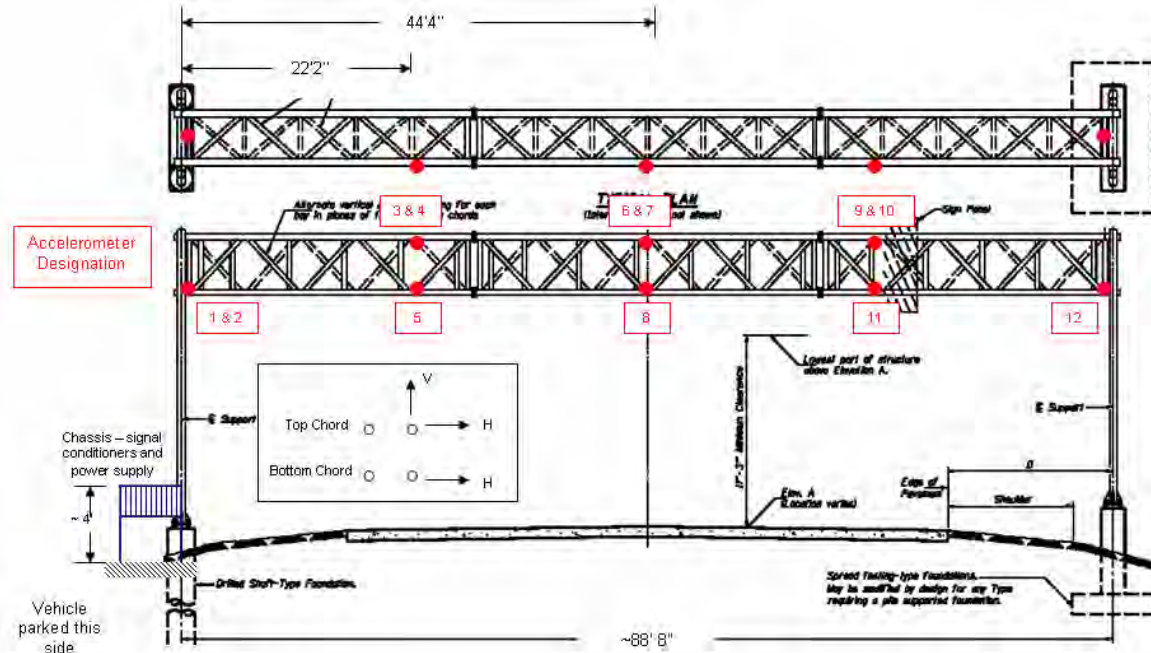


**Figure 3.4-1 Location of accelerometers for the Type I-A sign bridge**

After waiting several months for the wind conditions to be adequate for collecting data on the Type I-A truss, it became clear that it would be necessary to instrument more than one structure at a time. This necessitated the acquisition of additional accelerometers for the instrumentation of the cantilever (Type II-C-A) truss. These were borrowed from the U.S. Army Construction Engineering Research Laboratory in Champaign, Illinois (which is affiliated with UIUC). Five Terra Technology SA-102 accelerometers were mounted on the cantilever truss to capture the movement of the structure in response to wind, truck, and/or manual excitation. These accelerometers have a range of  $\pm 0.1$  to  $\pm 5$  g, where an output of 2.5 V corresponds to 1 g (Terra Technologies, 1988). The location and orientation of these accelerometers is summarized in Table 3.4-2 and Figure 3.4-2, with the measurement directions given as they relate to the orientation of the truss. The accelerometers were mounted to small steel plates that were, in turn, attached to the structure with the desired orientation. To guard against moisture and other elements, the instruments were housed and sealed in plastic boxes, as is shown in Figure 3.4-3.

**Table 3.4-2 Accelerometer placement for cantilever structure**

Accelerometer	Measurement Direction	Location
1185	Horizontal	Top of column
1166	Horizontal	End of Cantilever – Top
1184	Horizontal	End of Cantilever – Bottom
1178	Vertical	End of Cantilever – Bottom
1129	Longitudinal	End of Cantilever – Bottom

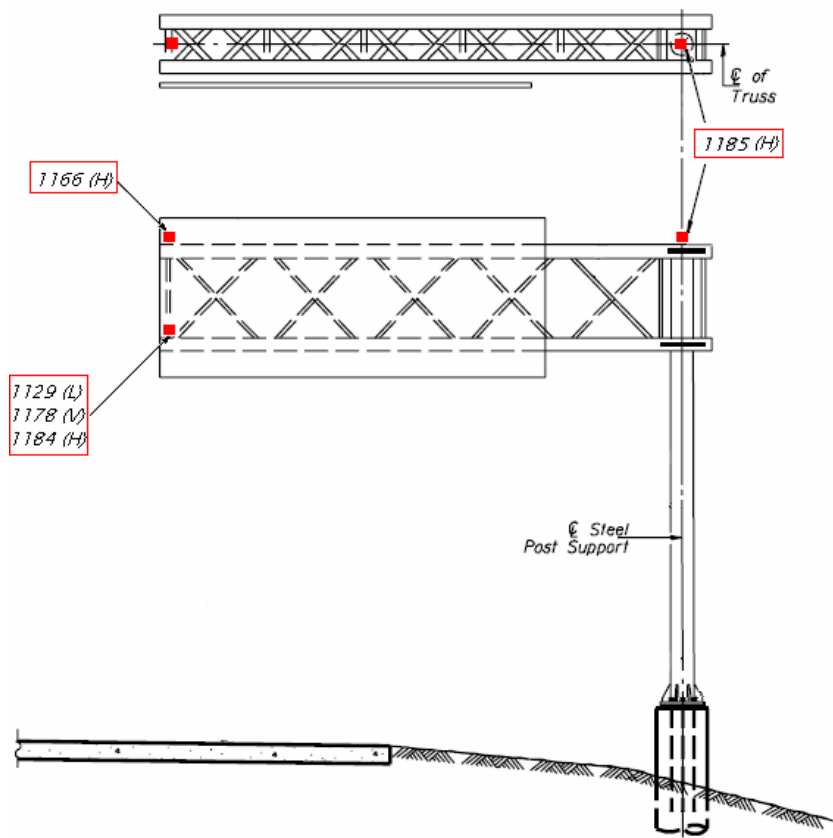


**Figure 3.4-2 Accelerometer locations for cantilever structure**

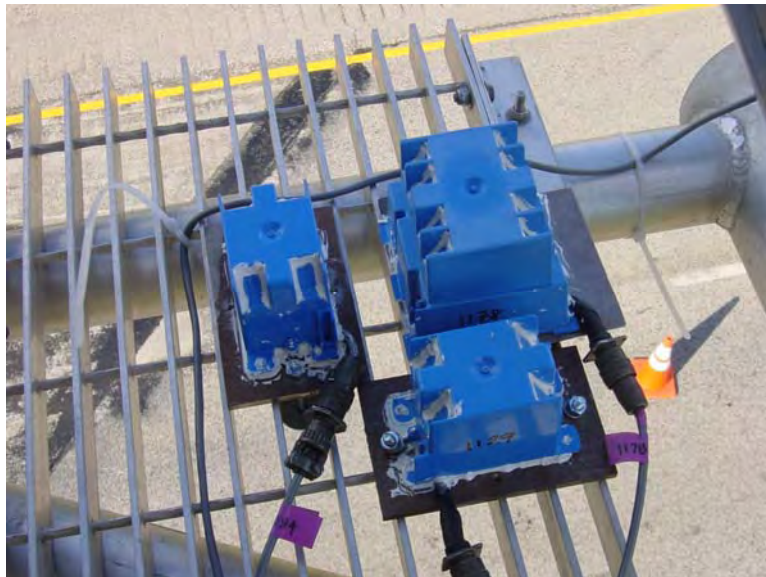


**Figure 3.4-3 Mounted accelerometers in cases**

Once data was successfully collected for the Type I-A and cantilever trusses, the instruments were removed from those structures. The accelerometers were then moved to the Type II-A and III-A trusses, which were instrumented simultaneously. The placements of the accelerometers on these trusses were identical to each other; however, the Type II-A truss utilized the Terra Technologies accelerometers, while the Type III-A truss made use of the PCB accelerometers. As previously mentioned, only one-half of these trusses (for each type) required accelerometers, due to the symmetric nature of the truss motion. This resulted in the placement of eight accelerometers on each truss. The placement of the accelerometers for the Type II-A and Type III-A trusses are shown in Figure 3.4-4.

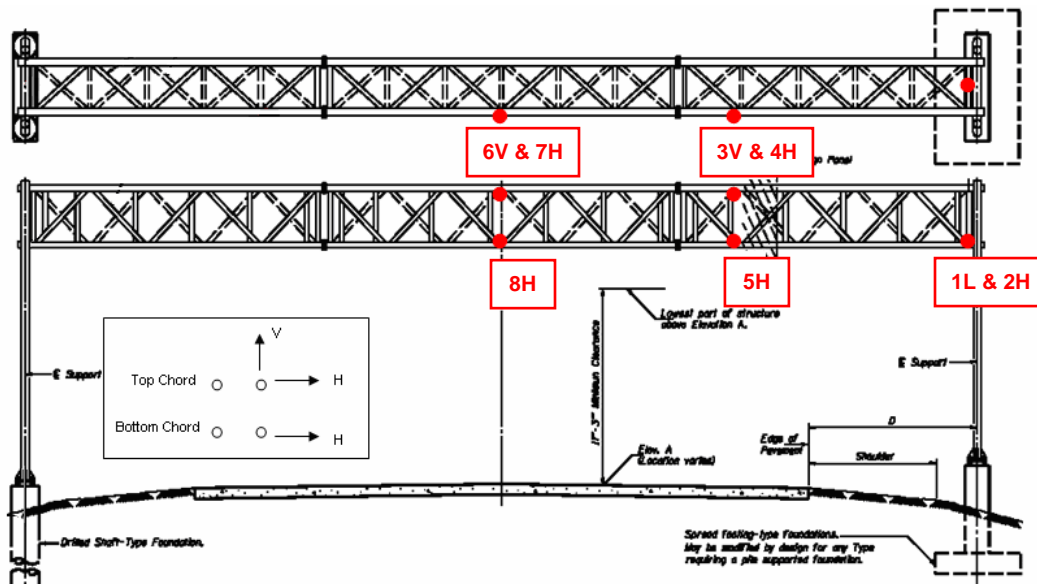


**Figure 3.4-4 Accelerometer placement for the Type II-A and Type III-A sign trusses**

The accelerometer placement for the VMS sign structure is shown in Figure 3.3-5 in the previous section.

### 3.5 Data Processing

The strain gages (and to a lesser degree the accelerometers) had a relatively low signal-to-noise ratio for these instruments and locations, although some sign locations produced noisier data than others due to environmental conditions. As a result, the use of digital low-pass filters facilitated the interpretation of the data. All of the instruments' output voltages are proportional to strain for the strain gages, accelerations for the accelerometers, and wind speed (and direction) for the anemometers. This data is converted into engineering units by the data acquisition system, then filtered, and finally stored. Figure 3.5-1 shows strain data before and after low-pass filtering, and Figure 3.5-

2 shows accelerometer data before and after filtering. Specific data reporting and interpretation is presented in later chapters of this report.

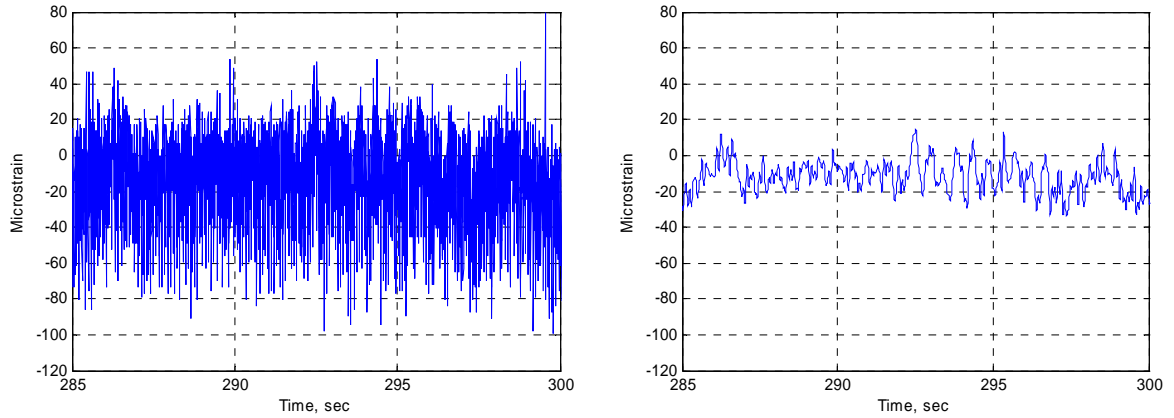


**Figure 3.5-1 Measured strains before (left) and after filtering (right) from the Type II-A sign structure**

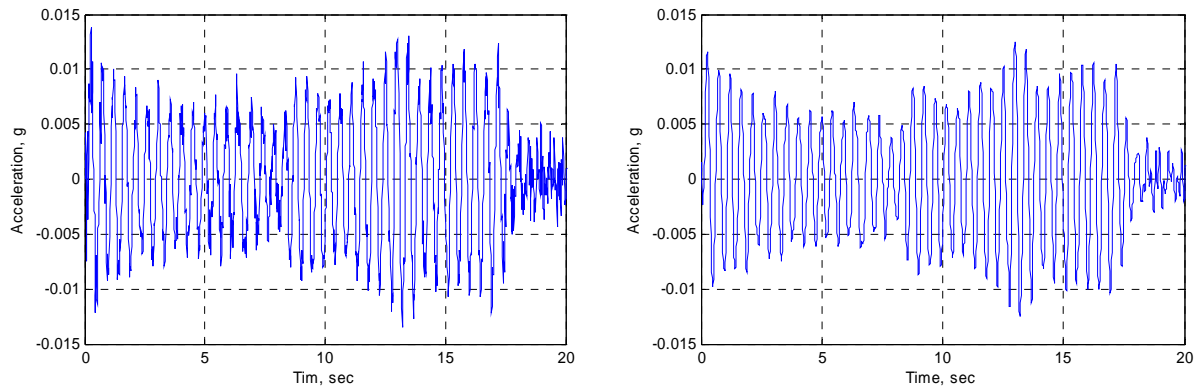


**Figure 3.5-2 Measured accelerations before (left) and after (right) filtering from the Type II-A sign structure**

## **4.0 Analytical Modeling**

### **4.1 General Information**

The commercially available finite element program SAP2000 (CSI, 2004) was used to model and analyze each structure. The dimensions and material properties for the models were taken directly from the design calculations and construction drawings that were provided by IDOT (and the dimensions were later verified by field measurements). The geometric properties of the structures were input via a spreadsheet interface. Using centerline dimensions, coordinates of the nodes were defined first and then associated members were created by inputting the start and end nodes; nodes were placed at every joint or at points where there is a geometric or material change. The members were represented by beam elements that were assigned the appropriate dimensions and material properties (and all of the truss chord-to-chord and web-to-chord connections were assumed to be rigidly framed).

The analytical models and corresponding analyses were used for several purposes. They were initially quite useful for determining the placement of the field instrumentation. The natural frequencies and mode shapes that were calculated were helpful for understanding how each structure behaves relative to the design assumptions. Since the mass of each structure could be calculated very accurately, most of the uncertainties associated with the models were with respect to the stiffness matrices. The main uncertainties in stiffness were related to the accidental eccentricities due to fabrication imperfections, end conditions at each end of the truss (and at the ends of all the truss web members), and end fixity at the bottom of the support frames. The first attempt to model each structure usually resulted in a model that was too stiff, as indicated by the calculated natural frequencies being higher than the measured ones. More discussion of the modeling and calculated properties will be discussed in the following sections of this chapter.

### **4.2 Modeling of the Cantilever Structure**

The geometric and material properties of the cantilever structure are given in Table 4.2-1. These were taken from the design calculations provided by IDOT and verified from field measurements.

**Table 4.2-1 Member geometric and material properties of the cantilever structure**

<b>Member</b>	<b>O.D. (in.)</b>	<b>Wall (in.)</b>	<b>Material</b>	<b>F<sub>y</sub> (ksi)</b>	<b>E (ksi)</b>	<b>L<sub>b</sub> (in.)</b>
Chord	6.50	0.3125	Aluminum	35	10,100	48.00 (24.00)
Vertical	3.25	0.3125	Aluminum	35	10,100	59.50
Horizontal	3.25	0.3125	Aluminum	35	10,100	29.50
Vertical Diagonal	3.25	0.3125	Aluminum	35	10,100	72.54
Horizontal Diagonal	3.25	0.3125	Aluminum	35	10,100	50.92
Interior Diagonal	3.25	0.3125	Aluminum	35	10,100	66.41
Column	24.00	0.5000	Steel	36	29,000	360.00

The truss connects to the column at the top and bottom chords of the truss by 1-in. aluminum plates slotted through the center and welded to the chords. The bottom plate has a hole to accommodate the column and sits atop four welded vertical ribs as well as being bolted with 1¼-in. diameter bolts. The cap plate sits over the top of the column and is bolted to the column via an aluminum collar that is welded to the plate and fit over the top of the column (see Figures 2.2-2 and 2.2-3). This connection is a very rigid one, with the ability to transfer the moments from the truss to the column resulting from wind force normal to the sign and from gravity loads. For this reason, the connection was simplified in the model by using rigid links to connect each of the four chords to the column.

The fixity at the base of the column was modeled by a reinforced concrete pile, representative of the drilled shaft used for the structure. The actual shaft has a total length of 17.75 ft, with about 2.5 to 3 ft exposed above ground and the remainder below ground. This was approximately represented in the model by having the pile fixed at a distance of 6 ft below the bottom of the column. The overall analytical model for the cantilever sign structure is shown in Figure 4.1-2.

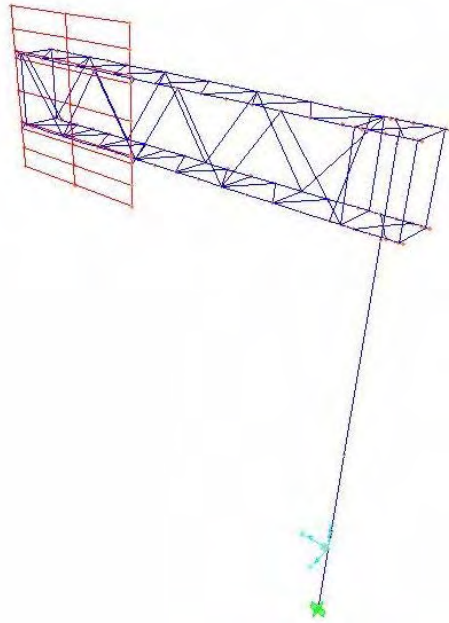


**Figure 4.2-1 Finite element model of cantilever structure**

Besides the dead loads of the sign structure (principally the self-weight of the truss, sign, and walkways), the other significant loading case is the wind load. The wind loads were defined and applied to the model in the same manner as in IDOT's original design of the structure. This resulted in a pressure of 30 psf acting normal to the sign panel. In order to obtain results that will be comparable to the data acquired in the field, the wind pressure was applied to a sign panel with dimensions equal to the actual sign installed on the structure, plus 1 ft of additional height to account for wind loads on brackets, grating edges, handrails, U-bolts, and luminaries. The truss currently has a sign with an approximate area of 152 ft<sup>2</sup>, which is less than 50 percent of the allowed total sign area of 340 ft<sup>2</sup>. For the open truss, it was determined that the design wind load on each member is equivalent to a uniform pressure of 9 psf on a closed surface at the face of the truss. Finally, the wind load on the column was resolved into a uniform load of 0.021 k/ft. This is all illustrated in Figure 4.2-2.

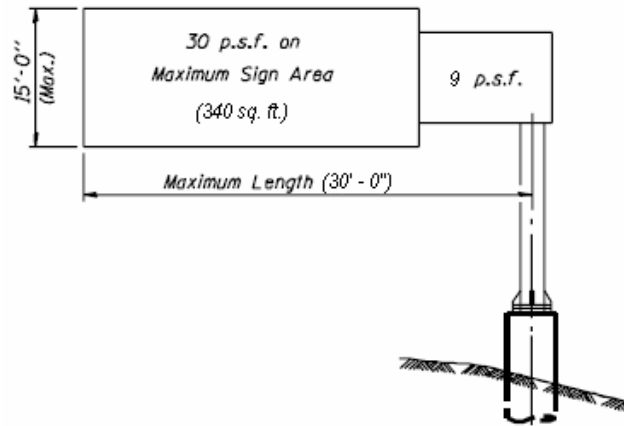


**Figure 4.2-2 Design wind loading of the cantilever structure (IDOT, 2001)**

In order to determine the effect of the loading simplification, the loading in the model was applied in the above manner and also by using loads calculated directly from the drag coefficients for the sign and the truss members. To calculate the load acting on the tube members, a drag coefficient was first determined from Table 4.2-2, as designated in the AASHTO specifications. The pressure was calculated starting from a basic wind speed for Illinois of 90 mph and then converted into a distributed load by multiplying the pressure by the diameter of the member. The results are shown below, without the gust factor. (Comparisons of these loads to actual field measurements will be covered later on in Chapter 6.)

**Table 4.2-2 Cantilever drag coefficients and resulting member loads**

Member	Drag Coefficient	Load
Chord	0.82	9.26 plf
Diagonals	1.10	6.18 plf
Sign	1.20	24.88 psf

It was determined that the simplified IDOT approach for applying the equivalent static wind loads is reasonable and somewhat more conservative than using the drag coefficients based on individual member sizes. In order to have the most accurate comparison with the measured experimental values, the latter approach will be used and discussed from here forward.

Once the model was completed, two types of elastic analysis were performed: 1) linear static analysis for the wind load and gravity load, and 2) modal analysis. The wind load results were examined to determine the maximum stresses in the truss members and which members are the most critical. As expected for a cantilever truss, the maximum stresses occurred in the main chords near the truss to column connection. The highest

stress was found in the bottom chord member closest to the column. This stress was calculated as the sum of the bending stress and axial stress in the member as follows:

$$\sigma_{axial} = \frac{P}{A}$$

$$\sigma_{bending} = \frac{M \cdot y}{I} \quad 4.2-1$$

$$\sigma_{total} = \sigma_{axial} \pm \sigma_{bending}$$

where  $M$  = bending moment  
 $y$  = distance from the neutral axis to the extreme fiber  
 $I$  = moment of inertia about axis of bending  
 $P$  = axial force  
 $A$  = cross-sectional area

Table 4.2-3 provides the stresses in each member that resulted from the application of the design wind loading. The stresses shown in Table 4.2-4 are the result of the design wind load and the dead load applied together. As expected, the axial forces dominate due to truss action. The chord members see the highest stresses; however, they are much smaller than the yield stress of 35 ksi (as well as below the allowable stresses).

**Table 4.2-3 Cantilever member stresses from model with applied design wind loading (excluding the gust factor,  $G$ )**

Member	Axial Stress (ksi)	Bending Stress (ksi)	Max. Total Stress (ksi)	% Axial	% Bending
1. Chord ( $L_b=48''$ )	3.709	0.404	4.112	90	10
2. Chord ( $L_b=24''$ )	4.464	1.060	5.525	81	19
3. Horizontal diag.	0.993	0.145	1.138	87	13
4. Interior diag.	0.556	0.041	0.597	93	7

**Table 4.2-4 Cantilever member stresses from model with dead load and applied design wind loading (excluding  $G$ )**

Member	Axial Stress (ksi)	Bending Stress (ksi)	Max. Total Stress (ksi)	% Axial	% Bending
1. Chord ( $L_b=48''$ )	5.656	0.474	6.130	92	8
2. Chord ( $L_b=24''$ )	7.069	1.064	8.133	87	13
3. Horizontal diag.	1.190	0.200	1.390	86	14
4. Interior diag.	0.895	0.166	1.061	84	16

The modal analysis was performed to determine the primary modes of vibration of the structure and the corresponding natural periods. As expected there were two predominant modes. The results are summarized in Table 4.2-5.

**Table 4.2-5 Results of modal analysis for cantilever structure**

Mode	Mode Description	Period (sec)	Frequency (Hz)
1	Horizontal, about the column end	0.440	2.27
2	Vertical	0.405	2.46
3	Horizontal, about the horizontal midpoint of the truss	0.190	5.26
4	Longitudinal	0.140	7.14
5	Torsional, about the longitudinal axis of the truss	0.114	8.84

The transverse (or horizontal) motion of the truss rotating about the column was the predominant mode; however, the vertical rocking of the truss was also found to be significant. These mode shapes are illustrated below in Figures 4.2-3 and 4.2-4.

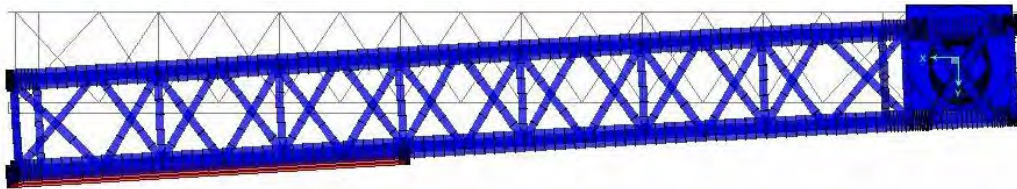


**Figure 4.2-3 Cantilever mode shape 1, plan view – rotation of truss about the column**

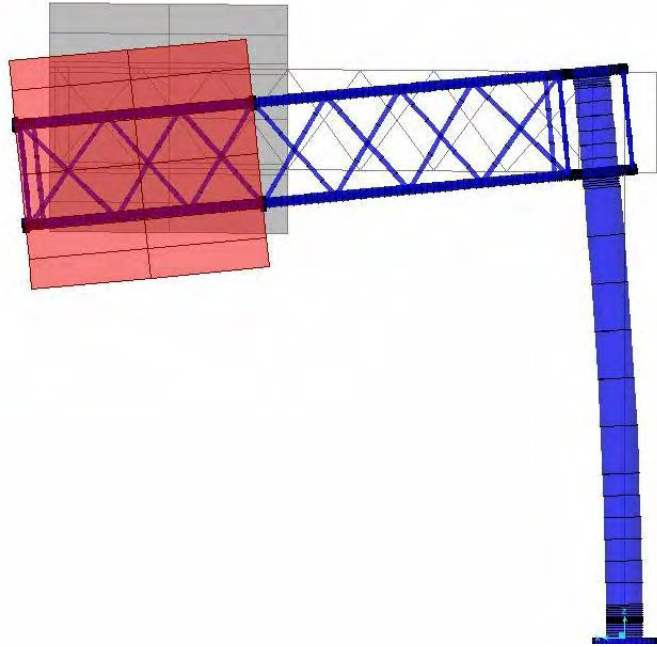


**Figure 4.2-4 Cantilever mode shape 2, elevation view– vertical motion of truss**

### 4.3 Modeling of the Type I-A Sign Bridge

Dimensions and material properties for the model were taken directly from design calculations and drawings that were provided by IDOT (and these dimensions were later verified by field measurements). The member designations and properties are summarized in Table 4.3-1.

**Table 4.3-1 Member properties for the Type I-A sign bridge**

Member	O.D. (in.)	Wall (in.)	Material	F <sub>y</sub> (ksi)	E (ksi)	L <sub>b</sub> (in.)
TRUSS MEMBERS						
Chord	5.00	0.3125	Aluminum	35	10,100	56
Vertical	2.50	0.3125	Aluminum	35	10,100	54
Horizontal	2.50	0.3125	Aluminum	35	10,100	48
Vertical Diagonal	2.50	0.3125	Aluminum	35	10,100	78
Horizontal Diagonal	2.50	0.3125	Aluminum	35	10,100	74
Interior Diagonal	2.50	0.3125	Aluminum	35	10,100	72
SUPPORT STRUCTURE						
Column	10.00	0.365	Steel	>35	29,000	360
Diagonals	3.00	0.3125	Steel	>35	29,000	126-143
I-Beam	W8x28		Steel	>35	29,000	62

The ends of the truss connect to the column support structure through the use of four U-bolts. I-beams of the support structure are utilized as seating for the truss chords, which bear directly on the top flange of the W8x28 members, as shown below.

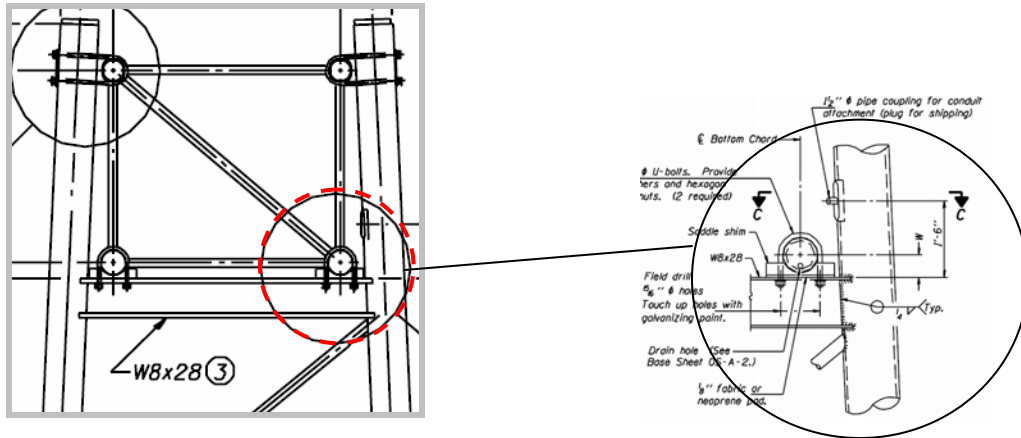


**Figure 4.3-1 Connection detail of truss to support frame**

In describing the discretization of this connection detail in the model, much explanation is warranted because it has considerable influence on the response of the structure. Thus, the connections of the upper chords are represented as primarily pinned and the lower chords as primarily rigid.



**Figure 4.3-2 Detail of truss/support column connection (left), upper chord/column connection (center), and lower chord/beam connection (right)**

The following are images from the SAP2000 model depicting the end region of the sign. Figure 4.3-3 shows the rigid link connecting the top chord to the centerline of the column. The end of the link is released against torsion and moment about both the strong and weak axes. Hence, it models as a true pin, which is physically intuitive from inspection of the center photo of Figure 4.3-2.

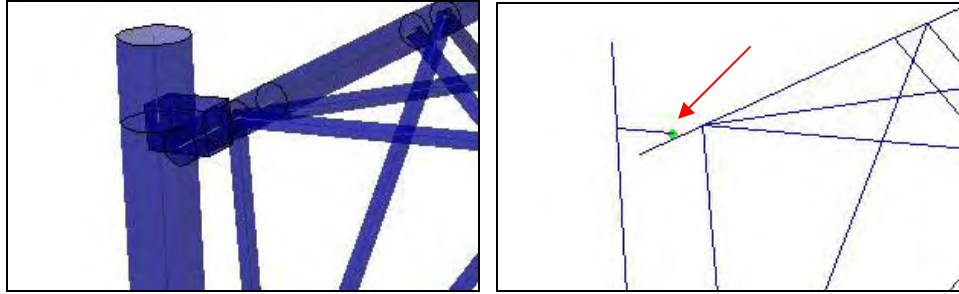


**Figure 4.3-3 End details of model: end release of rigid links connecting top chord/column**

Figure 4.3-4 illustrates the use of rigid links to connect the chords with the beam centerline. From Figure 4.3-2 above, it is seen that two U-bolts are used to connect the chord member to the beam. Physically, this means the beam (see Figure 4.3-4) sees torsion (moment about  $z$ ), and a point moment about its weak axis (about  $y$ ). There is no moment transfer about the beam's strong axis (about  $x$ ) because the circular pipe of the chord can spin about its longitudinal axis. In terms of the rigid links, they carry torsion and moment about their strong axis. They are released from moment about their weak axis. (Variation from exactly these sets of fixity assumptions has little effect on most of the computed stresses, while modestly changing the computed frequencies.)

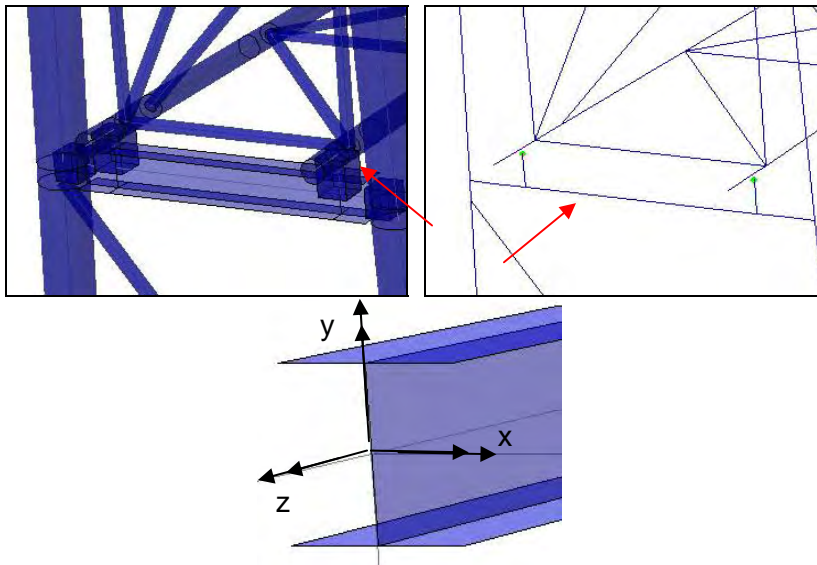


**Figure 4.3-4 End details of model: end release of rigid links connecting bottom chords/beam (left/center), local axis of beam (right)**

Each truss support structure rests on reinforced concrete piles at each end of the bridge. The following picture shows the view of the foundation at both sides of the sign structure. In the median, the slope is steep and the shafts are exposed. On the shoulder side, the slope is gradual and the grass covers the top of foundation. The top of foundation elevations on both ends of the truss are equal.



**Figure 4.3-5 Foundation detail of median end (left) and shoulder end (right)**

Because the stiffness of the foundation is many times greater than the steel pipes, the model is fixed at the top of foundation on both ends. The complete model is shown in Figure 4.3-6.

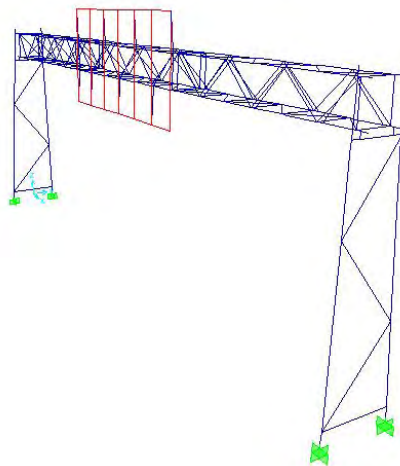


**Figure 4.3-6 SAP2000 finite element model of the Type I-A sign bridge**

Member and sign self-weight were included in the model, and small masses representing the grating were applied at appropriate nodes throughout the structural model, which was an approximate method of representing this extra mass that is mostly important in the calculation of the twisting period of the structure.

IDOT design specifications prescribe that the wind loading be applied to the structure as shown in 4.3-7. This simplifies the way the load is applied to the truss

members by simply considering the exposed truss as a closed region with an applied pressure of 10 psf. A pressure of 30 psf is applied to the sign area.

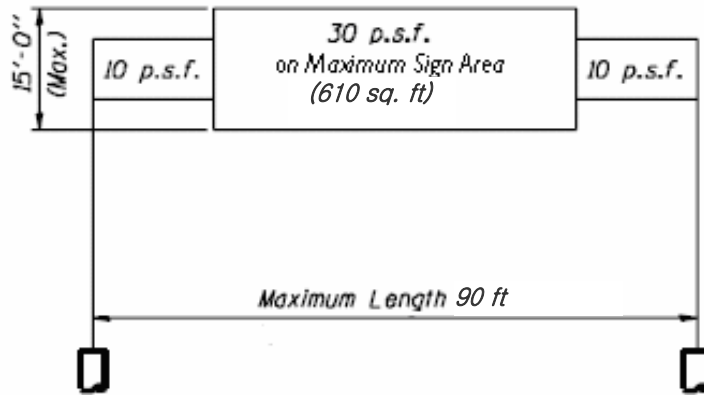


**Figure 4.3-7. Design wind loading (IDOT, 2001)**

In order to determine the effect of this simplification, the loading in the model was applied in this manner and also by using loads calculated directly from the drag coefficients for the sign and the truss members. To calculate the load acting on the tube members, a drag coefficient was first determined from the AASHTO specifications as shown in Table 4.3-2. The pressure (from an assumed 90 mph design wind load) was then converted to a distributed load by multiplying the pressure by the diameter of the member. The results are shown below.

**Table 4.3-2 Type I-A drag coefficients and resulting member loads**

Member	Drag Coefficient	Load
Chord	1.10	9.50 plf
Diagonals	1.10	4.75 plf
Sign	1.20	24.88 psf

It was determined that the simplified approach for applying the equivalent static wind load is reasonable and somewhat more conservative than using the drag coefficients based on individual member size. In order to have the most accurate comparison with the measured values in the field, the latter approach will be used and discussed from here forward.

The signs that are currently mounted on this structure are approximately 13 ft × 18 ft and 13 ft × 10 ft, for a total area of about 352 ft<sup>2</sup>. This is only 58 percent of the allowable sign area for this truss (of 610 ft<sup>2</sup>).

Table 4.3-3 provides the stresses in each member that resulted from the application of the design wind loading (with the gust effect factor,  $G$ , simply taken as

1.0). The stresses shown in Table 4.3-4 are the result of the design wind load and the dead load. As expected, the axial forces dominate due to truss action. The chord members see the highest stresses; however, they are much smaller than the yield stress of 35 ksi (as well as the allowable stresses).

**Table 4.3-3 Type I-A member stresses from model with applied wind loading (excluding G)**

Member	Axial Stress (ksi)	Bending Stress (ksi)	Max. Total Stress (ksi)	% Axial	% Bending
Bottom Chord	4.77	0.65	5.42	88	12
Top Chord	4.31	1.10	5.41	80	20
Horizontal	0.63	0.04	0.68	93	7
Interior Diagonal	0.68	0.15	0.83	82	18
Vertical Diagonal	0.21	0.08	0.29	72	28

**Table 4.3-4 Type I-A member stresses from model with dead load and applied design wind loading (excluding G)**

Member	Axial Stress (ksi)	Bending Stress (ksi)	Max. Total Stress (ksi)	% Axial	% Bending
Bottom Chord	6.18	0.91	7.09	87	13
Top Chord	5.59	1.44	7.02	80	20
Horizontal	0.81	0.06	0.87	93	7
Interior Diagonal	0.74	0.15	0.89	83	17
Vertical Diagonal	1.96	0.06	2.02	97	3

The modal analysis was performed to determine the primary modes of vibration of the structure and the corresponding natural periods. As expected there were two predominant modes. Field tests (see later chapters for further details) revealed the actual natural periods of the structure for its three primary and first twisting modes. The results are summarized below in Table 4.3-5.

**Table 4.3-5 Type I-A Modal analysis results**

Mode	Mode Description	Computer Model		Actual Structure (Measured)	
		Period (sec)	Frequency (Hz)	Period (sec)	Frequency (Hz)
1	Longitudinal	0.66	1.52	0.65	1.54
2	Horizontal	0.364	2.75	0.35	2.84
3	Vertical	0.292	3.42	0.29	3.46
4	Twisting	0.195	5.14	0.20	5.08

Mode 1: Longitudinal motion is developed almost entirely through deformation of the support structures. This mode is not excited to any considerable extent by wind gusts due to the slim profile of the truss in this direction.

Mode 2: The most important mode for the sign structure is transverse horizontal motion, which is most easily excited by wind and truck gust loading on the face of the sign (it is easily seen in the plan view below).

Mode 3: Vertical motion is a combination of bending in the truss and the columns. Both wind and truck gusts can excite this mode.

Mode 4: There is considerable twisting of the structure under wind loading. This mode has a rather high frequency compared to the first three fundamental modes. Differences between predicted and measured periods are due to the lack of model detail for the I-beams and grating in front of the sign (this adds mass at an eccentricity from the truss centerline, resulting in a longer period).

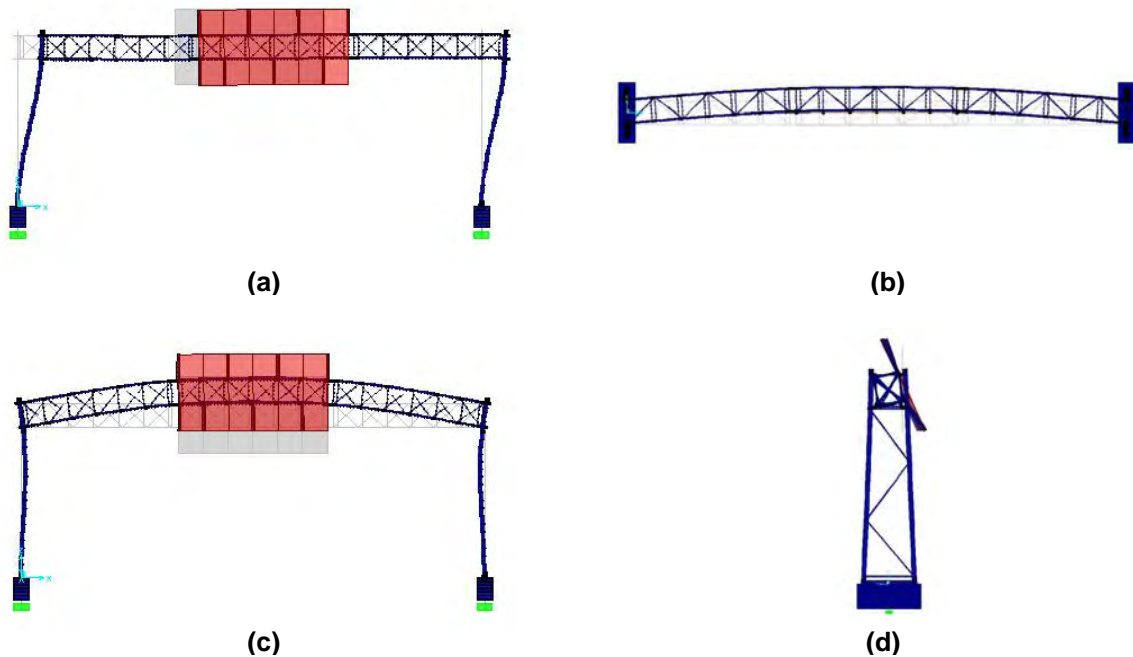


**Figure 4.3-8 (a) First mode, elevation view of longitudinal motion,  $T = 0.66s$ ; (b) Second mode, plan view of horizontal motion,  $T = 0.37s$ ; (c) Third mode, elevation view of vertical motion,  $T = 0.28s$ ; (d) Fourth mode, profile view of twisting motion,  $T = 0.14s$**

#### 4.4 Modeling of the Type II-A Sign Bridge

Dimensions and material properties for the II-A model were taken directly from design calculations and drawings that were provided by IDOT (and these dimensions were later verified by field measurements). The member designations and properties are summarized in Table 4.4-1.

**Table 4.4-1 Material and geometric properties for the Type II-A sign bridge**

Member	O.D. (in.)	Wall (in.)	Material	F <sub>y</sub> (ksi)	E (ksi)	L <sub>b</sub> (in.)
TRUSS MEMBERS						
Chord	7.00	0.3125	Aluminum	35	10,100	56
Vertical	3.00	0.3125	Aluminum	35	10,100	63
Horizontal	3.00	0.3125	Aluminum	35	10,100	54
Vertical Diagonal	3.00	0.3125	Aluminum	35	10,100	84
Horizontal Diagonal	3.00	0.3125	Aluminum	35	10,100	78
Interior Diagonal	3.00	0.3125	Aluminum	35	10,100	83
SUPPORT STRUCTURE						
Column	10.00	0.5000	Steel	>35	29,000	92
Diagonals	3.00	0.3125	Steel	>35	29,000	118- 133
I-Beam	W8x28		Steel	>35	29,000	70

The ends of the truss connect to the column support in the same manner as described above for the Type I-A sign bridge. All of the end conditions and other modeling assumptions used for the Type I-A structure and described in the previous section (including application of the sign and grating masses) were therefore assumed to be the same for the Type II-A sign bridge. A depiction of the analytical model is shown in Figure 4.4-1.

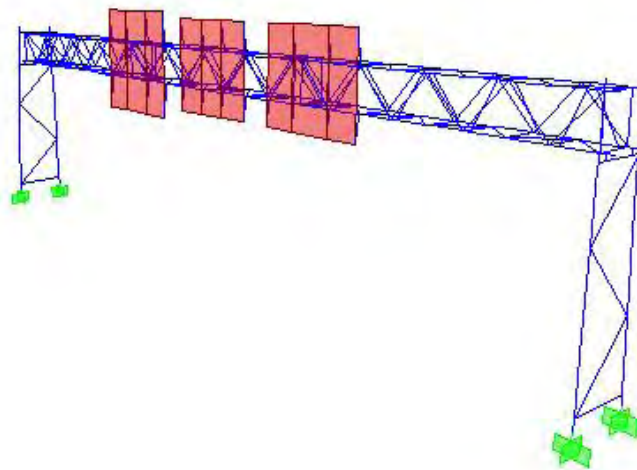


**Figure 4.4-1 SAP2000 model of the Type II-A sign bridge**

The design wind loads were assumed and applied per IDOT as for the Type I-A sign bridge and shown in Figure 4.3-7. In order to determine the effect of this simplification, the loading in the model was applied in this manner and also by using loads calculated directly from the drag coefficients for the sign and the truss members. To calculate the load acting on the tube members, a drag coefficient was first determined (see Table 4.4-2) as designated in the AASHTO specifications. From the assumed design wind speed, the pressure was calculated and then converted to a distributed load by multiplying the pressure by the diameter of the member. The results are shown below, without the gust factor.

**Table 4.4-2 Type II-A drag coefficients and resulting member loads**

Member	Drag Coefficient	Load
Chord	0.75	9.06 plf
Diagonals	1.10	5.70 plf
Sign	1.20	24.88 psf

It was determined that the simplified design approach for applying the equivalent static wind load is reasonable and somewhat more conservative than using the drag coefficients based on individual member size. In order to have the most accurate comparison with the experimentally measured values, the latter approach will be used and discussed from here on forward.

The signs that are currently mounted on the structure are approximately 16 ft × 16 ft, 12 ft × 14 ft, and 13.5 ft × 13.5 ft, for a total area of about 606 ft<sup>2</sup>. This is 82 percent of the maximum allowable sign area for this truss (of 740 ft<sup>2</sup>).

Once the model was completed, two types of elastic analysis were performed: 1) linear static analysis of the wind load and gravity load, and 2) modal analysis. The wind load results were examined to determine the maximum stresses in the truss members and which members are the most critical. As expected, the maximum stresses occurred in the main chords at mid-span. These stresses were calculated as the sum of the bending stress and axial stress in the member.

Per the specific instrumented member designations provided in Chapter 3, Table 4.4-3 provides the stresses in each member that resulted from the application of the wind loading (with a gust effect factor, *G*, of 1.0). The stresses shown in Table 4.4-4 are the result of the wind load and the dead load. As expected, the axial forces dominate due to truss action. The chord members see the highest stresses; however, they are much smaller than the yield stress of 35 ksi (as well as the allowable stresses).

**Table 4.4-3 Type II-A Member Stresses from Model with Applied Design Wind Loading (excluding G)**

<b>Member</b>	<b>Axial Stress (ksi)</b>	<b>Bending Stress (ksi)</b>	<b>Max. Total Stress (ksi)</b>	<b>% Axial</b>	<b>% Bending</b>
Chord 1	6.32	0.95	7.27	87	13
Chord 2	5.86	1.14	7.01	84	16
Horizontal	1.03	0.01	1.04	99	1
Horizontal Diagonal	3.17	0.33	3.49	91	9
Vertical Diagonal 1	0.19	0.27	0.46	42	58
Vertical Diagonal 2	0.13	0.13	0.26	51	49

**Table 4.4-4 Type II-A Member Stresses from Model with Dead Load and Applied Design Wind Loading (excluding G)**

<b>Member</b>	<b>Axial Stress (ksi)</b>	<b>Bending Stress (ksi)</b>	<b>Max. Total Stress (ksi)</b>	<b>% Axial</b>	<b>% Bending</b>
Chord 1	9.79	2.14	11.93	82	18
Chord 2	9.64	2.21	11.85	81	19
Horizontal	1.34	0.19	1.52	88	12
Horizontal Diagonal	3.44	0.36	3.79	91	9
Vertical Diagonal 1	3.04	0.30	3.34	91	9
Vertical Diagonal 2	2.58	0.15	2.74	94	6

The modal analysis was performed to determine the primary modes of vibration of the structure and the corresponding natural periods. As expected, there were two predominant modes. The results are summarized in Table 4.4-5. The mode shapes were similar to those of the Type I-A sign bridge (as shown in Figure 4.3-8).

**Table 4.4-5 Modal analysis results for the Type II-A sign bridge**

<b>Mode</b>	<b>Mode Description</b>	<b>Period (sec)</b>	<b>Frequency (Hz)</b>
1	Longitudinal	0.690	1.45
2	Horizontal	0.488	2.05
3	Vertical	0.395	2.53
4	Torsional, about the longitudinal axis of the truss	0.176	5.69

#### 4.5 Modeling of the Type III-A Sign Bridge

The dimensions and material properties for the Type III-A model were taken directly from design calculations and drawings that were provided by IDOT (and these dimensions were later verified by field measurements). The member designations and properties are summarized in Table 4.5-1.

**Table 4.5-1 Geometric and material properties for Type III-A sign bridge**

Member	O.D. (in.)	Wall (in.)	Material	F <sub>y</sub> (ksi)	E (ksi)	L <sub>b</sub> (in.)
Chord	8.50	0.5	Aluminum	35	10,100	126.75 (63.375)
Vertical	3.50	0.3125	Aluminum	35	10,100	84.00
Horizontal	3.50	0.3125	Aluminum	35	10,100	60.00
Vertical Diagonal	3.50	0.3125	Aluminum	35	10,100	105.22
Horizontal Diagonal	3.50	0.3125	Aluminum	35	10,100	87.27
Interior Diagonal	3.50	0.3125	Aluminum	35	10,100	103.23

The support conditions and modeling assumptions used previously for the Type I-A and II-A structures were used once again for the Type III-A sign bridge. The maximum allowed sign area for the span of this truss is 1125 ft<sup>2</sup>. There are currently three signs mounted on the structure, with a total area of approximately 560 ft<sup>2</sup>; this is just under 50 percent of the maximum allowed sign area. Because the wind acting on the sign faces is by far the most significant contribution to the loading of the structure, it would be expected that the measured stresses will be much lower than the allowable design stresses due to the relatively smaller sign area. A plot of the analytical model is shown in Figure 4.5-1

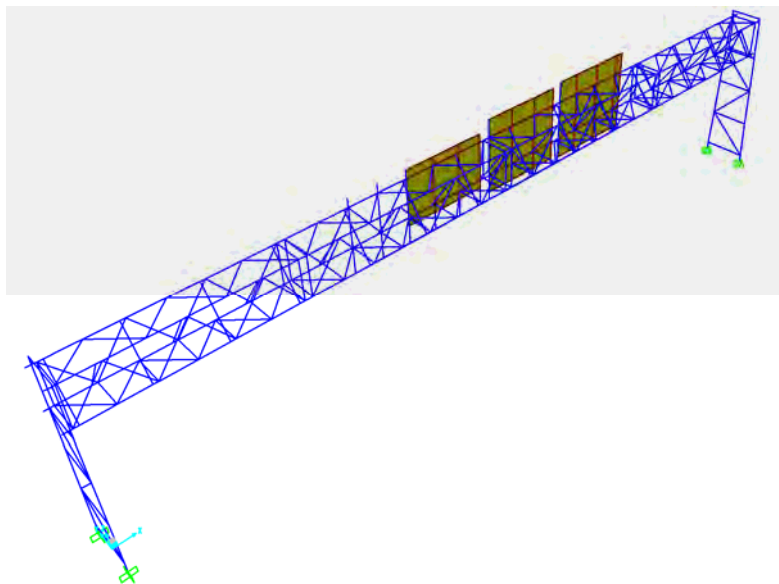


**Figure 4.5-1 SAP2000 finite element model of Type III-A sign bridge**

The design wind loads specified by IDOT are shown in Figure 4.3-7. This simplifies the way the design wind load is applied to the truss members, by considering the exposed truss to be an equivalent closed region with an applied pressure of 10 psf; 30 psf is then applied to the sign panels.

In order to determine the effect of this simplification, the loading in the model was applied in this manner and also by using wind loads calculated directly from the drag coefficients for the sign and the truss members. To calculate the load acting on the tube members, a drag coefficient was first determined from Table 3-6 in the AASHTO specifications. For the assumed design wind speed, the pressure was calculated and then converted to a distributed load by multiplying the pressure by the diameter of the member. The results are shown in Table 4.5-2 below, excluding the gust effect factor.

**Table 4.5-2 Type III-A drag coefficients and resulting member loads**

<b>Member</b>	<b>Drag Coefficient</b>	<b>Load</b>
Chord	0.58	8.55 lb/ft
Diagonals	1.10	6.65 lb/ft
Sign	1.20	24.88 psf

It was determined that the simplified approach for applying the equivalent static wind load is reasonable and somewhat more conservative than using the drag coefficients based on individual member size. However, in order to have the most accurate comparison with the measured experimental values, the latter approach was used in the model and discussed from here forward.

Once the model was completed, two types of elastic analysis were performed: 1) linear static analysis of the wind load and gravity load, and 2) modal analysis. The wind load results were examined to determine the maximum stresses in the truss members and which members are the most critical. As expected, the maximum stresses occurred in the main chords at mid-span.

Table 4.5-3 provides the stresses in each member that resulted from the application of the wind loading. The stresses shown in Table 4.5-4 are the result of the design wind load and the dead load acting together. As expected, the axial forces dominate due to truss action. The chord members see the highest stresses; however, they are much smaller than the yield stress of 35 ksi (as well as the allowable stresses).

**Table 4.5-3 Calculated member stress in the Type III-A structure for applied wind load (excluding G)**

Member	Axial Stress (ksi)	Bending Stress (ksi)	Max. Total Stress (ksi)	% Axial	% Bending
Chord 1	5.17	0.48	5.65	92	8
Chord 2	2.72	0.67	3.39	80	20
H1	0.60	0.09	0.69	87	13
HD	3.13	0.28	3.41	92	8
V1	0.51	0.15	0.65	78	22
V2	0.56	0.27	0.83	67	33

**Table 4.5-4 Calculated member stress in the Type III-A structure for dead load plus applied wind load (excluding G)**

Member	Axial Stress (ksi)	Bending Stress (ksi)	Max. Total Stress (ksi)	% Axial	% Bending
Chord 1	6.43	0.61	7.03	91	9
Chord 2	3.93	0.76	4.69	84	16
H1	0.68	0.09	0.76	88	12
HD	3.23	0.29	3.52	92	8
V1	2.01	0.17	2.18	92	8
V2	2.38	0.27	2.65	90	10

The modal analysis was performed to determine the primary modes of vibration of the structure and the corresponding natural periods. The mode shapes for the Type III-A were similar to those calculated for the Type I-A and II-A structures. The results are summarized in Table 4.5-5.

**Table 4.5-5 Modal analysis results for the Type III-A sign bridge**

Mode	Mode Description	Period (sec)	Frequency (Hz)
1	Longitudinal	0.891	1.122
2	Horizontal	0.568	1.76
3	Vertical	0.383	2.61
4	Torsional, about the longitudinal axis of the truss	0.221	4.52

#### 4.6 Modeling of the Type II-A Sign Bridge with VMS

The dimensions and material properties for the model were taken directly from design calculations and drawings that were provided by IDOT (and these dimensions were later verified by field measurements). The member designations and properties are summarized in Table 4.6-1.

**Table 4.6-1 Member geometric properties for the VMS sign bridge.**

Member	O.D. (in.)	Wall (in.)	Material	F <sub>y</sub> (ksi)	E (ksi)	L <sub>b</sub> (in.)
TRUSS MEMBERS						
Chord	6.0	0.3125	Aluminum	35	10,100	61
Vertical	3.0	0.3125	Aluminum	35	10,100	63
Horizontal	3.0	0.3125	Aluminum	35	10,100	54
Vertical Diagonal	3.0	0.3125	Aluminum	35	10,100	88
Horizontal Diagonal	3.0	0.3125	Aluminum	35	10,100	75
Interior Diagonal	3.0	0.3125	Aluminum	35	10,100	83
SUPPORT STRUCTURE						
Column	10.00	0.3650	Steel	>35	29,000	324
Diagonals	3.00	0.3125	Steel	>35	29,000	114-126
I-Beam	W8x28		Steel	>35	29,000	79
Footing	30 inches diameter		Concrete			36

The support conditions and modeling assumptions used were the same as for the Type I-A, II-A and III-A sign bridges. The maximum allowed sign area for the span of this II-A truss is 740 ft<sup>2</sup>; however, the VMS mounted on the truss has a total area of approximately 139.5 ft<sup>2</sup> (only about 19 percent of the maximum allowed sign area). Because the wind acting on the sign faces is by far the most significant contribution to the loading of the structure, it would be expected that the measured stresses will be much lower than the allowable design stresses due to the smaller sign area. It is further expected that the weight of the VMS is greater than the typical aluminum signs attached to trusses. Due to this additional weight located near the mid-span of the front panel of the truss, eccentric to the longitudinal axis of the truss, it could be expected that the torsional mode of vibration may be more dominant for this structure than those with regular sign panels. As mentioned in Chapter 2, the VMS is not to exceed 20,000 lbs. A plot of the analytical model is shown in Figure 4.6-1.

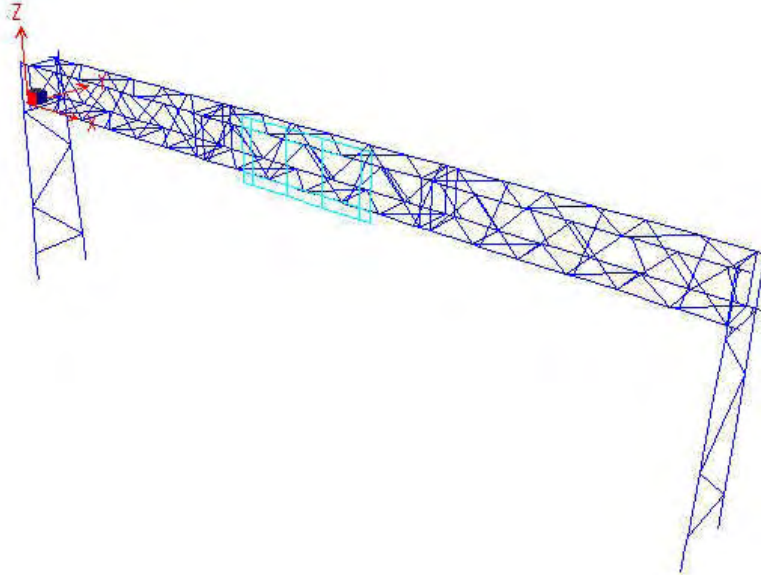


**Figure 4.6-1 SAP2000 finite element model of the Type II-A structure with VMS**

The design wind loads specified by IDOT are shown in Figure 4.3-7. This simplifies the way the wind load is applied to the truss members, by considering the exposed truss a closed region with an applied pressure of 10 psf; 30 psf is then applied to the sign panel.

In order to determine the effect of this simplification, the loading in the model was applied in this manner and also by using wind loads calculated directly from the drag coefficients for the sign and the truss members. To calculate the load acting on the tube members a drag coefficient was first determined from Table 3-6 in the AASHTO specifications. From the design wind speed, the pressure was calculated and then converted to a distributed load by multiplying the pressure by the diameter of the member.

It was determined that the simplified approach for applying the equivalent static wind load is reasonable and somewhat more conservative than using the drag coefficients based on individual member size. However, in order to have the most accurate comparison with the experimentally measured values, the latter approach was used in the model and discussed from here forward.

Once the model was completed, two types of elastic analysis were performed: 1) linear static analysis for the wind load (with and without gravity load), and 2) modal analysis. The wind load results were examined to determine the maximum stresses in the truss members and which members are the most critical. As expected, the maximum stresses occurred in the main chords at mid-span.

Table 4.6-2 provides the stresses in each member that resulted from the application of the wind loading. The stresses shown in Table 4.6-3 are the result of the

design wind load and the dead load. As expected, the axial forces dominate due to truss action. The chord members see the highest stresses; however, they are much smaller than the yield stress of 35 ksi (as well as the allowable stresses).

**Table 4.6-2 Type II-A with VMS member stresses for applied wind load (excluding *G*)**

<b>Member</b>	<b>Axial Stress (ksi)</b>	<b>Bending Stress (ksi)</b>	<b>Max. Total (ksi)</b>	<b>% Axial</b>	<b>% Bending</b>
Chord 1	2.35	1.31	3.66	64	36
Chord 2	2.49	0.41	2.90	86	14
ID - middle	0.64	0.23	0.86	74	26
ID - end	0.64	0.39	1.03	62	38
VD - middle	0.39	0.07	0.46	85	15
VD - end	0.39	0.14	0.53	74	26
Hor. - middle	0.44	0.09	0.53	83	17
Hor - end	0.44	0.14	0.59	75	25
HD - middle	1.44	0.13	1.57	92	8
HD - end	1.44	0.50	1.94	74	26

\* ID: Interior Diagonal, VD: Vertical Diagonal, Hor.: Horizontal, HD: Horizontal Diagonal

**Table 4.6-3 Type II-A with VMS member stresses from model with applied design wind load plus dead load (excluding *G*)**

<b>Member</b>	<b>Axial Stress (ksi)</b>	<b>Bending Stress (ksi)</b>	<b>Max. Total (ksi)</b>	<b>% Axial</b>	<b>% Bending</b>
Chord 1	3.69	1.56	5.25	70	30
Chord 2	3.94	0.68	4.62	85	15
ID - middle	0.65	0.26	0.90	72	28
ID - end	0.65	0.45	1.10	59	41
VD - middle	1.41	0.08	1.49	95	5
VD - end	1.41	0.22	1.63	86	14
Hor. - middle	0.61	0.11	0.73	84	16
Hor. - end	0.61	0.18	0.80	73	27
HD - middle	1.55	0.15	1.70	91	9
HD - end	1.55	0.57	2.12	73	27

\* ID: Interior Diagonal, VD: Vertical Diagonal, Hor.: Horizontal, HD: Horizontal Diagonal

The modal analysis was performed to determine the primary modes of vibration of the structure and the corresponding natural periods. The mode shapes for this structure were similar to those calculated for the Type I-A, II-A, and III-A structures. The results are summarized in Table 4.6-4.

**Table 4.6-4 Modal analysis results for the VMS sign bridge**

<b>Order</b>	<b>Mode Description</b>	<b>Period (sec)</b>	<b>Frequency (Hz)</b>
1	Longitudinal	0.38	2.63
2	Horizontal	0.30	3.33
3	Vertical	0.24	4.17

## 5.0 Dynamic Properties of the Sign Structures

### 5.1 Background

Sign structures can be subjected to wind loads and truck gusts that generate dynamic response. Two basic dynamic properties that are unique for each structure and are important for understanding its behavior under dynamic excitation are the natural frequency and the structural damping. (Mode shapes can be important for some structure-load combinations, but these are not of particular interest for this study.) There are a number of ways to determine these properties, two of which have been used in this study – manual excitation and the natural wind. This chapter, however, will mainly discuss manual excitation. Structural analysis programs are typically capable of computing natural frequencies and mode shapes based on the structural stiffness and mass matrices. One way to evaluate the accuracy of an analytical model is to compare the measured natural frequencies and mode shapes to experimentally determined values. The calculated natural frequencies and mode shapes were given in Chapter 4 for each structure considered in this study.

Manually induced loads were used to check out the instrumentation system prior to measuring truck gust and wind load data. They were also an effective way of determining the natural frequencies and damping of the structures. (The accelerations and stresses determined from manual excitation are not considered for purposes of assessing safety or fatigue because they are one-time only loads and result in stresses in the members that are small compared to the allowable values.)

For a single degree of freedom structure with a mass,  $m$ , and stiffness,  $k$ , the circular natural frequency,  $\omega_n$  in rad/sec, may be calculated as:

$$\omega_n \equiv \sqrt{\frac{k}{m}} \equiv \sqrt{\frac{kg}{W}} \quad 5.1-1$$

where  $g$  is gravitational acceleration and  $W$  is the weight of the structure. The natural frequency in cycles/sec (Hz) is:

$$f_n = \frac{\omega_n}{2\pi} \quad 5.1-2$$

and the natural period (in sec) is:

$$T_n = \frac{1}{f_n} \quad 5.1-3$$

For a multi-degree-of-freedom system (structure), there are a number of natural frequencies and corresponding mode shapes. These were discussed analytically and reported for each sign structure in Chapter 4. However, for a structure that is reasonably symmetric in stiffness and mass, the structure behaves much like a series of single-

degree-of-freedom systems in each of the major directions. This can clearly be seen in the response of any of the sign structures when the wind is normal to the sign – the response is almost entirely in the direction of the wind. If the wind is blowing at an angle to the sign, the structure will vibrate in both the longitudinal and transverse directions, and the response in each direction will almost be independent of the other. Inspecting the mode shapes for the structures reported in Chapter 4 reveals this behavior since each mode shape is defined by motion almost entirely in a single direction. The significance of this is that one can determine the natural frequency of a sign structure in its major directions rather easily, as will be shown in this chapter.

To calculate the natural frequencies and mode shapes from an analytical model of a structure requires a special finite element program that is programmed for this task. However, for symmetric structures the first few natural frequencies and mode shapes can be estimated rather accurately using any structural analysis program, using Equation 5.1-1. The weight,  $W$ , would normally be taken as the weight of the truss and the signs plus half of the weight of the support structure. Since only a small amount of the total weight is usually in the supporting structure, one could include the entire weight of the support structure with only a small error because the natural frequency is then a function of the square root of the weight. This weight can be calculated from the dead load analysis (as can the vertical stiffness) since it will equal the sum of the vertical reactions at the base of the structure. The horizontal stiffness can be estimated from the design wind load analysis (when the wind load is applied normal to the sign). The total force,  $F$ , may be taken as the sum of the horizontal reactions at the base of the structure in the direction of the applied load. The deflection,  $d$ , may be estimated as the average displacement of the top chord of the truss, including the end displacement resulting from the deformation of the support structure. The stiffness,  $k$ , then becomes the force divided by the displacement:

$$k = \frac{F}{d}. \quad 5.1-4$$

The natural frequency in the transverse direction of the sign structure may now be estimated using Equation 5.1-1. One could also estimate the other natural frequencies of the structure in the same manner, although this will probably not be as important. Although the natural frequency is not used in the design of such a sign structure, it can be useful when designing a damper system, which will be discussed later in Chapter 7.

## 5.2 Dynamic Properties of the Cantilever Structure

### *Manual Excitation*

As a point of reference for the response of a sign structure to truck-induced gusts and natural wind gusts, it is beneficial to first examine the results from manual excitation of the structure. These tests serve to verify the results of the modal analysis conducted with the SAP2000 program, as well as to give a relationship between acceleration and strain data. In order to produce dynamic response, a person standing on the truss can hold on to a truss member and then begin moving their body back and forth in one of the principal directions of the structure: longitudinal, transverse, or vertical. While doing this at different frequencies, the body senses the large motion at a particular frequency. Therefore, as the input shaking continues at this sensitive frequency, the amplitude of response increases dramatically because of low damping, and vibration will primarily be in one of the natural modes of vibration of the structure. And as a matter of fact, the motion of the structure at this point was much larger than the response of the structure later to the wind loads that were experienced at the sign structure while wind loads and responses were being recorded. Even without instrumentation, the natural frequency could be estimated very accurately by suddenly stopping the excitation and counting the cycles of response for a few seconds. The natural frequency is just the number of cycles divided by the time required for the cycles to occur. Doing this several times and taking the average value will yield a very accurate estimate of the natural frequency.

Figure 5.2-1 shows the collected acceleration data for the end of the cantilever truss from horizontal (transverse) manual excitation. For this particular test, the maximum acceleration (at about 34 sec) is 0.63 g. Figure 5.2-2 shows the corresponding stress ( $= \text{strain} * E$ ) in each member.

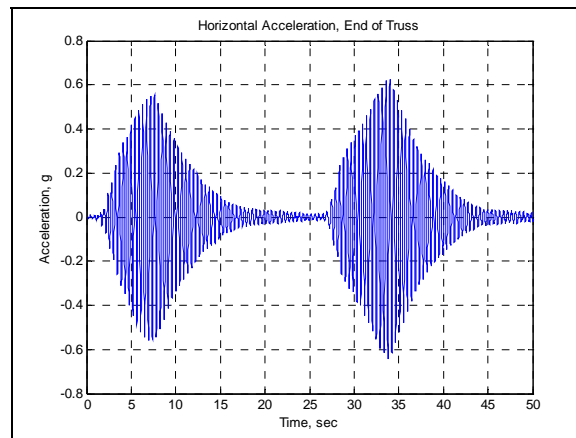


**Figure 5.2-1 Response of cantilever structure to transverse manual excitation**

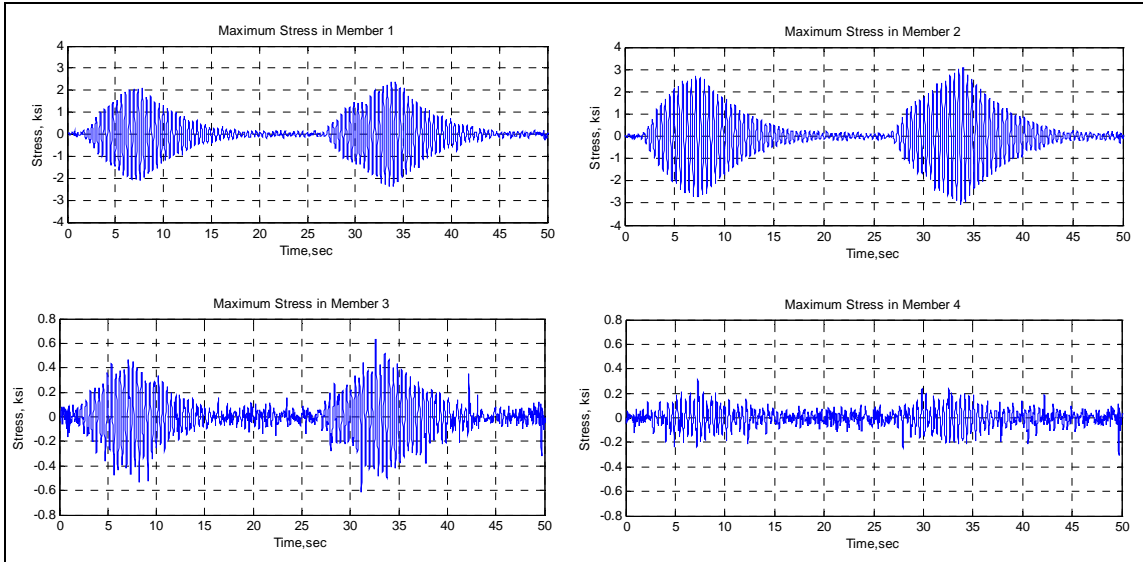


**Figure 5.2-2 Cantilever stresses in selected members due to transverse manual excitation**

**Table 5.2-1 Measured peak stress in selected members for manual transverse excitation of the cantilever**

Member	Peak Stress Corresponding to 0.63 g Peak Horizontal Acceleration
1- Chord ( $L_b = 48$ in.)	2.39 ksi
2 – Chord ( $L_b = 24$ in.)	3.09 ksi
3 – Top Horizontal Diagonal	0.612 ksi
4 – Interior Diagonal	0.243 ksi

The data given in Table 5.2-1 shows the relative amount of stress that each of four instrumented members experienced under this excitation. The chord members felt similar amounts of stress, with the shorter chord member value slightly higher. Member 3, the horizontal diagonal, experienced stresses that are only about 20 percent of those measured in the chord members, while member 4, the interior diagonal, experienced the least stress.

It is interesting to note that, even at fairly high peak accelerations, the members in the cantilever are well below the yield stress of 35 ksi (and even below the traditional AASHTO allowable static stress of 14.63 ksi; see section 6.2 for more details about this). These values are, however, higher than the current AASHTO (2001) allowable fatigue stresses of 1.9 ksi for the chord members and 0.44 ksi for the diagonal web members.

Dampers are installed on sign structures to dissipate vibration (kinetic) energy response due to wind and truck gust forces, thereby decreasing the number and amplitude of gust-induced oscillations. Stockbridge-type dampers consist of two cantilevered and weighted bobs that are intended to limit the amount of vibration of a truss by absorbing

energy with their own oscillation as a mass damper. These types of dampers have traditionally been used on electrical transmission lines and cables to reduce vibration induced fatigue. The damper installed on the cantilever truss is manufactured by Alcoa Conductor Accessories and is designated as a *sloppy* damper to distinguish it from the shorter and stiffer Stockbridge dampers used on transmission lines. The damper is designated as a 1706-190 bus vibration damper (for use in electrical substations). This type of damper has longer cables, with a total length of 29.5 inches. It has a nominal weight of 15.9 lbs. A drawing of the damper is shown in Figure 5.2-3, and it is pictured on the truss in Figure 5.2-4.

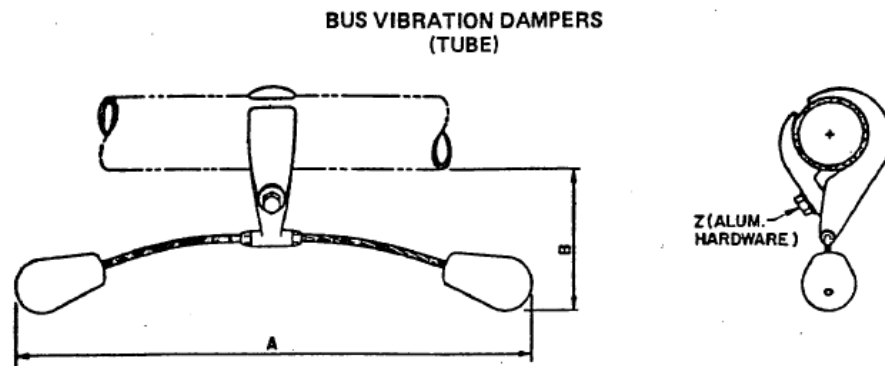


**Figure 5.2-3 1709-190 15.9-lb Stockbridge damper (ACA, 1992)**

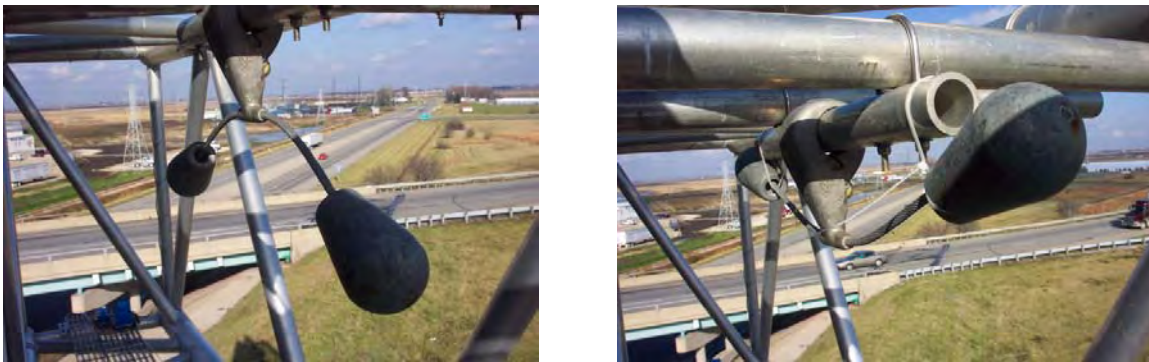


**Figure 5.2-4 Damper mounted on the cantilever truss (left); Disengaged damper (right)**

According to IDOT's current sign structure standards, the damper on this type of sign structure should be located between 1.5 and 2.5 ft from the end of the cantilever. However, the damper on this particular structure was incorrectly mounted at 10.5 ft from the end of the cantilever. It was expected that the damper would be more effective if it was mounted in the location prescribed in the standards, so during the course of testing, the damper was moved such that it was mounted 30 in. from the end of the truss.

In order to test the effectiveness of the damper, several manual excitation tests were conducted. These tests were performed with the damper in its original location, as well as following its move to the end of the truss. Both the horizontal and vertical directions of structural oscillation were examined with and without the damper. To conduct tests “without” the damper, the damper was simply tied up to inhibit the motion of the masses, as seen in the right portion of Figure 5.2-4.

For the horizontal direction, the truss was excited by a person standing on the truss and moving their body back and forth until substantial amplitude of motion was reached. They then ceased to excite the truss and fell into rhythm with the dissipating motion of the truss. This was done several times, both with and without the damper engaged.

The effectiveness of the damper in dissipating vertical motion was investigated with pull-down tests. A pull-down test consisted of a rope attached to the end of the cantilever, which was pulled several times to build up motion. Once the rope was released, the vibration dissipation could be measured. Figure 5.2-5 shows a pull-down test being performed.



**Figure 5.2-5 Picture of pull-down test being conducted on the cantilever truss**

Without any other excitation, and assuming linear viscous damping, the decay of the amplitude of motion should be exponential and of the form:

$$u(t) = A \cdot e^{-\zeta \omega_n t} \quad 5.2-1$$

where

$u(t)$  = displacement in time  
 $A$  = initial amplitude of vibration

$\zeta$  = percent of critical damping  
 $\omega_n$  = natural frequency, rad/sec  
 $t$  = time, sec

To determine the percent of critical damping,  $\zeta$ , in the structure with or without the damper, the acceleration data was plotted and the peaks were isolated. A curve was then fit to the peaks, thereby indicating the rate of decay. The time step between each oscillation cycle (the natural period) was also recorded. Table 5.2-2 shows a comparison of the recorded natural periods with those obtained from the SAP2000 analytical model. It can be seen that the values from the model, although slightly higher, are very close to the actual periods of the structure. For vertical motion, the damper elongated the period slightly; however, the period of the horizontal mode was unchanged when the damper was disengaged (even if a damper is fairly effective at dissipating energy, it would not be expected to have a significant effect on natural frequency).

**Table 5.2-2 Comparison of measured and calculated natural periods of vibration for the cantilever truss**

	Period, $T$ (sec)	
	Horizontal Mode	Vertical Mode
Analytical Model	0.440	0.405
Recorded – Without Damper	0.436	0.404
Recorded – With Damper	0.436	0.405

The cantilever truss damping results are summarized in Figures 5.2-6 and 5.2-7. It can be seen that the damper does have an effect on the rate at which motion is dissipated. For the horizontal motion of the truss, the damper increased the percent of critical damping by an average of 27 percent in its original location and by a substantially increased 64 percent in the new location. For motion in the vertical direction, the damper was successful at increasing the percent of critical damping by 30 percent from the original location and 42 percent in the corrected position.

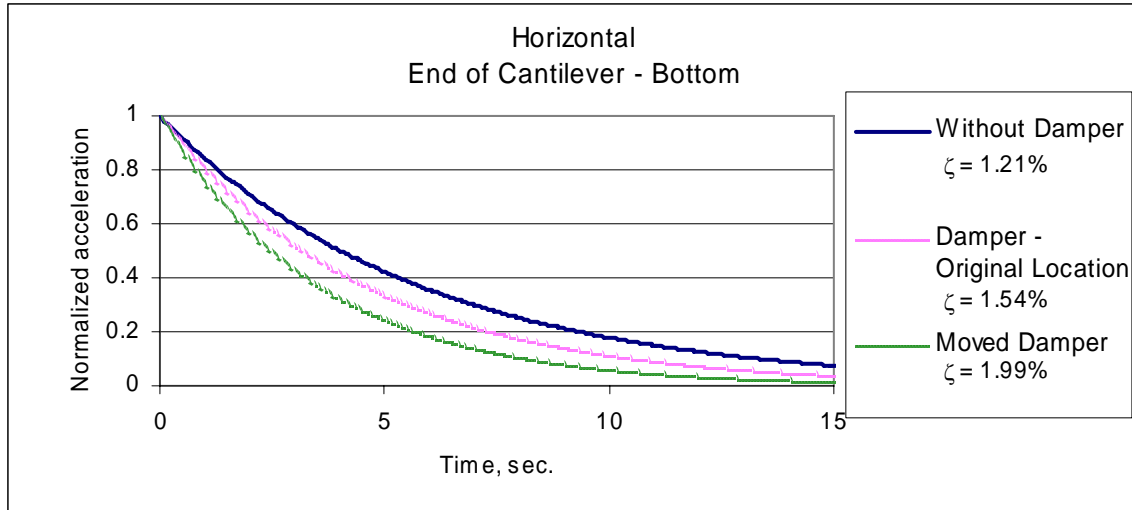


**Figure 5.2-6 Decay of horizontal motion of the truss at the end of the cantilever (with and without the damper)**

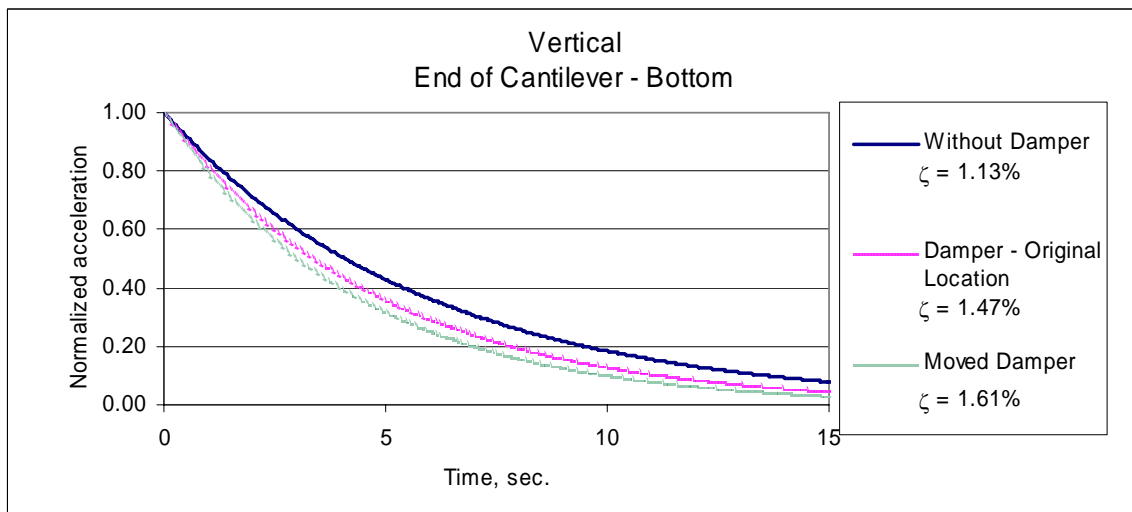


**Figure 5.2-7 Decay of vertical motion at the end of the cantilever (with and without the damper)**

**Wind**

The natural frequency of a sign structure may also be estimated from the response of the structure to wind loads or truck gusts. For truck gusts, this can be done in a crude manner by simply counting the number of observed cycles in a given time period and dividing the number of cycles by the time; this would however only yield an estimate of frequency.

Another way to do this is to calculate the Fourier amplitude spectrum of the recorded response. This can be done using one of a number of commercial software

packages, such as MATLAB (MathWorks, 2005). Although the theory behind this procedure is rather complex, it can be explained in simple terms; it can be thought of as complex curve fitting. It is based on the assumption that the dynamic response can be estimated as the sum of a number of sine and cosine functions. For instance, one can represent the acceleration response as a function of time,  $a(t)$ , as a series:

$$a(t) = \sum_{i=1}^{\infty} a_i \sin(i\Delta f t) + b_i \cos(i\Delta f t) \quad 5.2-2$$

where

- $a_i, b_i$  = coefficients to be determined
- $i$  = an integer that varies from 1 to infinity
- $\Delta f$  = a fixed frequency spacing, say 0.05 cycles per sec

By using some kind of error minimization approach, the values of  $a_i$  and  $b_i$  can be found such that the final values of these coefficients used in Equation 5.2-2 will give a very good representation of the recorded data. The series amplitude function would be the plot of  $A(i\Delta f)$  vs.  $i\Delta f$ , where:

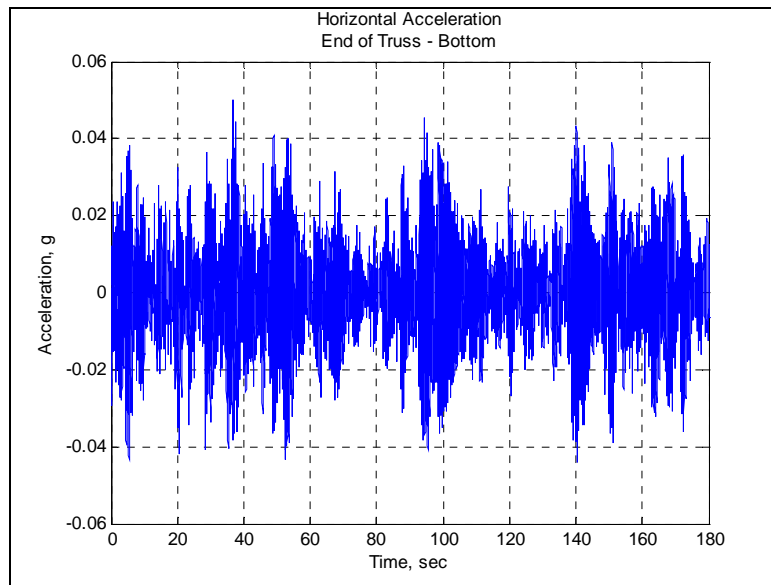
$$A(i\Delta f) = \sqrt{a_i^2 + b_i^2} \quad 5.2-3$$

and the value  $i\Delta f$  is just a frequency. If the original acceleration response record was  $(2g) \cdot \sin(2 \cdot 2\pi t)$ , then this would be a sine wave of frequency 2 cycles per sec (cps) and amplitude of 2g. In this case, if  $\Delta f = .01$  cps, then  $a_{200} = 2g$ ,  $b_{200} = 0g$ ,  $\Delta = 200$ , and all other values of  $a_i$  and  $b_i = 0$ . The amplitude spectrum would be a single point with the value of 2 g plotted at the frequency of 2 cps. Theoretically, this is not exactly a Fourier transform, but it would yield the same function for this example. For this study, MATLAB was used to calculate the Fourier amplitude spectrum through the use of the Fast Fourier Transform (FFT) function.

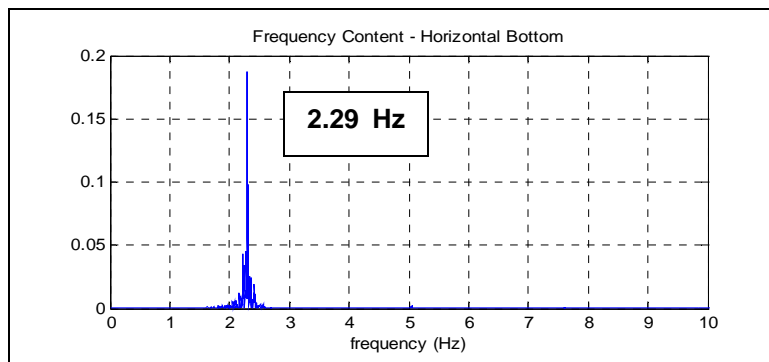
If the response of a sign structure in the direction of the wind loading or truck gust is measured using an accelerometer, the Fourier amplitude spectrum will show the frequency content of the record, making it very easy to identify the natural frequencies of the structure in that direction. This is true even for noisy data where the response cannot be separated from the noise by observation. The reason that this works so well is that the structure can only freely vibrate in its natural frequencies. So, for a long record there are a lot of cycles at these natural frequencies, with noise superimposed on them for low numbers of cycles at a very large number of frequencies. This will be pointed out in the examples for each of the signs discussed below.

Figure 5.2-8 shows the measured horizontal acceleration at the end of the cantilever truss for a 180 sec record of the response to wind loading. Figure 5.2-9 shows the Fourier transform of this record. The first natural frequency of the structure to the wind load is clearly seen. The natural frequency determined from the Fourier transform

is 2.29 cps (Hz). The calculated value from the modal analysis of the analytically modeled structure is 2.27 Hz. This is remarkably good agreement and results from the fact that this is quite a simple structure that can be modeled very accurately. The fact that the natural frequency of the model is slightly smaller than that of the real structure indicates that the model is slightly less stiff than the actual structure. The variations in stiffness between the models and the real structures probably result in part from the differences in the end conditions of the truss at the support(s).



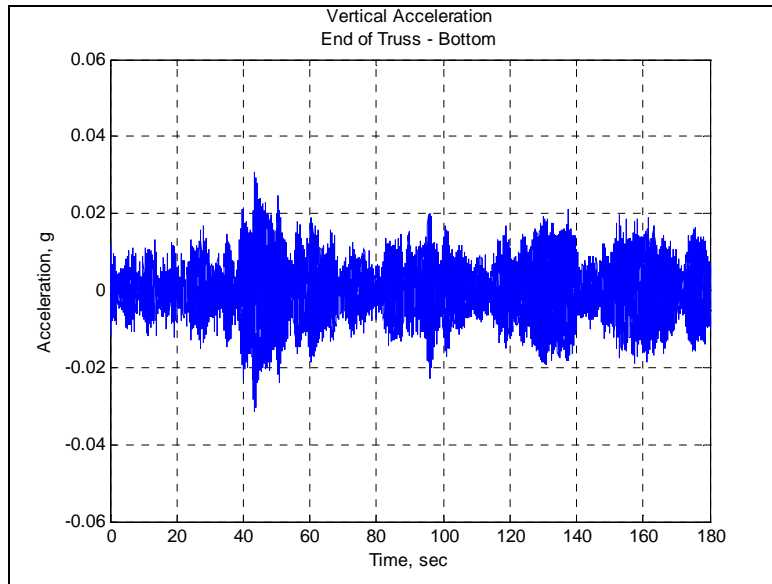
**Figure 5.2-8 Cantilever horizontal acceleration at the bottom end of the truss for wind loads**



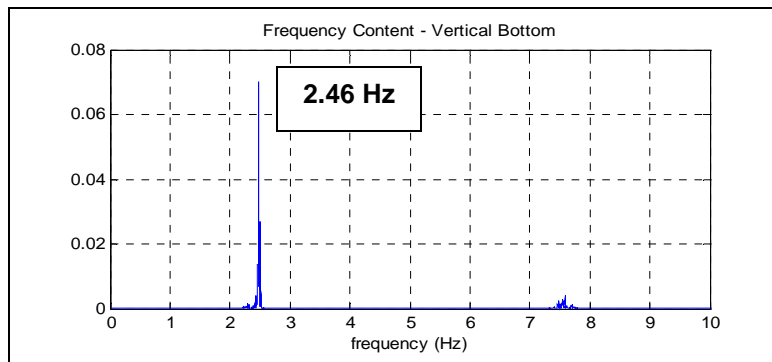
**Figure 5.2-9 FFT – cantilever horizontal bottom acceleration**

Figure 5.2-10 shows the vertical acceleration at the bottom end of the truss, and the Fourier transform of this data is shown in Figure 5.2-11. For the vertical acceleration, the natural frequency is 2.46 Hz, which agrees with the calculated vertical natural frequency. There are very small peaks (perhaps not visible in the figures) in the

horizontal record at 6.2 Hz and 7.6 Hz. A small peak also appears in the vertical record at 7.6 Hz also. Because this frequency shows up in both the horizontal and vertical directions, it could be a torsional mode.



**Figure 5.2-10 Cantilever vertical acceleration at the bottom end of the truss**



**Figure 5.2-11 FFT – Cantilever vertical acceleration at the bottom end of the truss**

### 5.3 Dynamic Properties of the Type I-A Sign Structure

#### *Manual Excitation*

For manual excitation in the horizontal direction, the Type I-A sign truss was excited harmonically by a person standing on the truss and moving back and forth until substantial amplitude of motion was reached. The person then ceased excitation and used their legs as an effective base isolation of their body. As a point of reference for the eventual response of the sign truss to truck-induced gusts and natural wind gusts, it is beneficial to examine the results from manual excitation of the structure. These tests

serve to verify the analytical results from the modal analysis conducted with SAP2000, as well as to give a relationship between acceleration and strain data. The data presented here represent horizontal motion.

Figure 5.3-1 shows the acceleration of the mid-span of the truss due to horizontal manual excitation. For this particular test, the maximum acceleration is 0.37 g. Figure 5.3-2 below shows the corresponding stress in each member type.

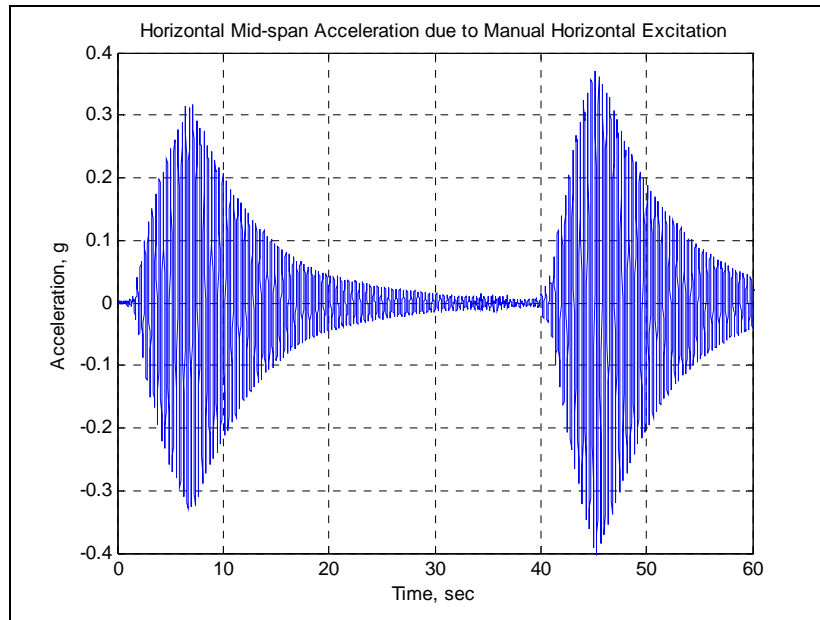


**Figure 5.3-1 Type I-A horizontal mid-span acceleration due to manual horizontal excitation**

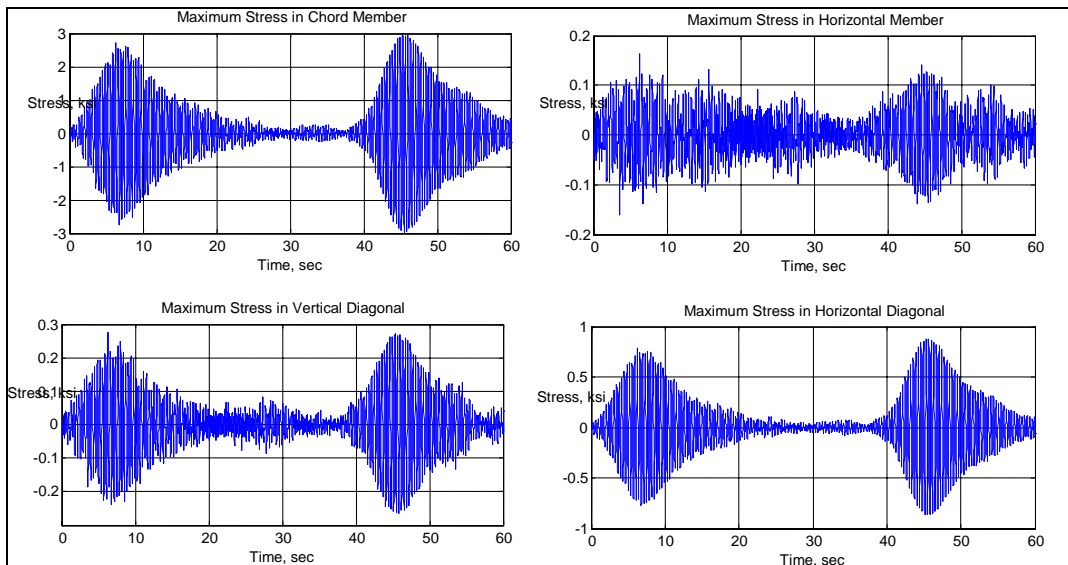


**Figure 5.3-2 Type I-A maximum stress in members due to horizontal manual excitation**

**Table 5.3-1 Type I-A member stresses due to horizontal manual excitation**

Member	Peak Stress for 0.37 g Peak Vertical Acceleration
Chord	2.95 ksi
Horizontal	0.141 ksi
Vertical Diagonal	0.272 ksi
Horizontal Diagonal	0.876 ksi

The stress data given in Table 5.3-1 above shows the relative amount of stress that some of the instrumented member types experienced. The chord members experienced the highest values of stress while the horizontal diagonal member experienced approximately 25 percent of the chord stress. The vertical diagonal is stressed to about 10 percent of the chord stress, and the horizontal member does not experience very much stress.

The natural dissipation of motion by the truss structure was recorded during this free vibration induced by the manual excitation. For each of four types of test (horizontal with damper, horizontal without damper, vertical with damper, and vertical without damper), the mode was excited several times to obtain accurate records.

The effectiveness of the damper in dissipating vertical motion was tested with several pull-down tests. A pull-down test consists of attaching a rope to the sign bridge at mid-span and pulling downward in harmony with the vertical period of the structure until there is sufficient resonance (see Figure 5.3-3). The rope is then released and free vibration takes place. By recording the logarithmic decay of motion, dissipation can be measured. Results from the four manual excitation tests are plotted below in Figures 5.3-4 and 5.3-5.



**Figure 5.3-3 Periodic pull-down test for determining vertical damping in the Type I-A truss**

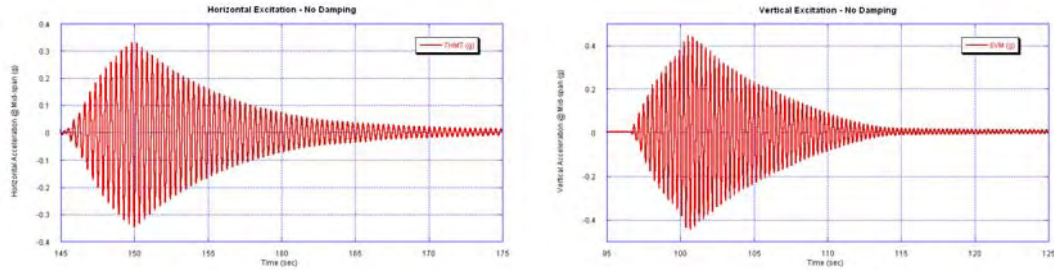


**Figure 5.3-4 Type I-A horizontal (left) and vertical (right) manual excitation without damping**

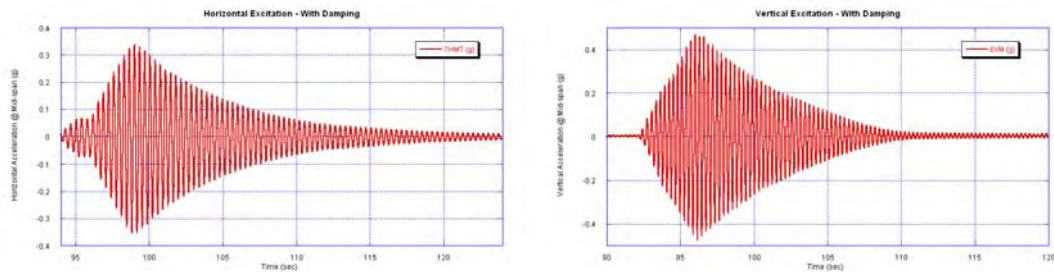


**Figure 5.3-5 Type I-A horizontal (left) and vertical (right) manual excitation with damping**

To determine the percentage of critical damping in the structure with the damper engaged and disengaged, the acceleration data was plotted and the peaks were isolated. A curve was then fit to the peaks, thus indicating the rate of decay. The time step between each oscillation cycle (the natural period) was also recorded. This structure has 0.80% of critical damping without the damper and 0.84% of critical damping with the damper engaged—a minor difference of 5%. Horizontal damping envelopes are plotted in Figure 5.3-6 below.

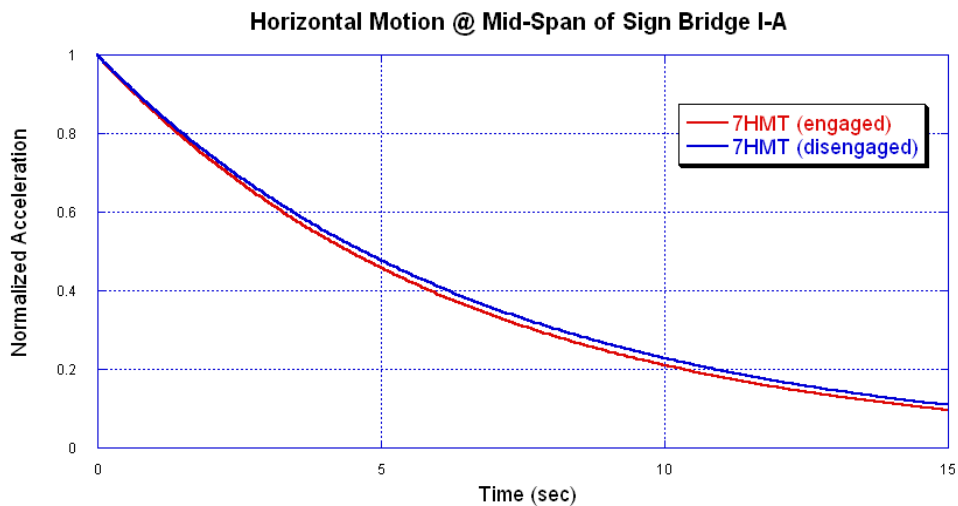


### Figure 5.3-6 Type I-A decay of the horizontal motion with and without the damper

It can be seen that the damper has a negligible impact on the rate of energy dissipation. For greater effect, it is evident that the damper would need to respond to lower frequencies akin to that of the natural frequency of the sign bridge structure. The simplest way to achieve this would probably be by using a longer cable between the bobs. The manufacturer makes a damper like this that is called a *sloppy* damper (which was installed on the cantilever structure described above). It is suggested that this be used in place of the “stiff” dampers currently installed (see Chapter 7 for further details). The stiff damper on the Type I-A structure is pictured in Figure 5.3-7 below. It appears that this style of damper is not effective and therefore should not be used by IDOT.

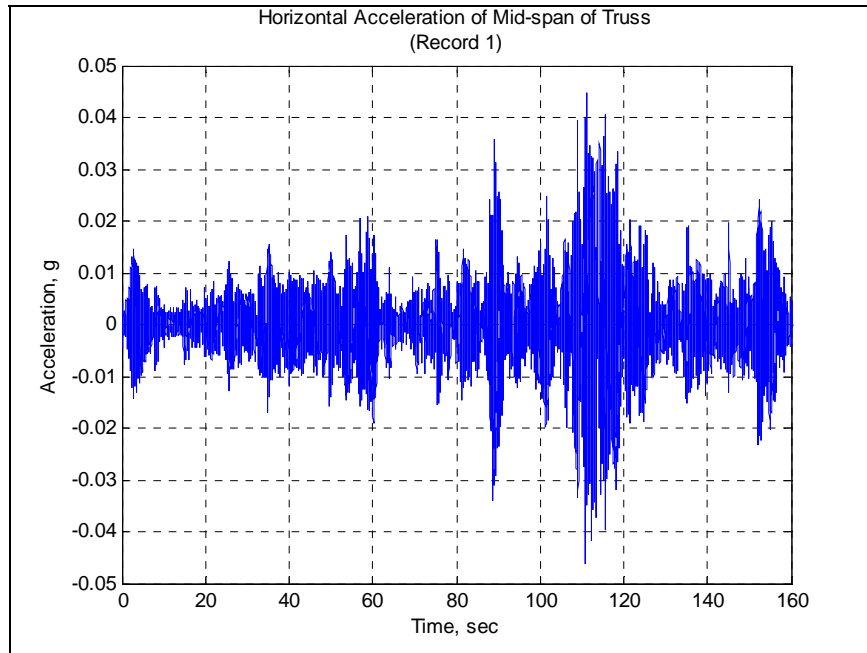


**Figure 5.3-7 Stockbridge-type damper mounted on the Type I-A truss (left), and disengaged damper (right)**

### *Wind Loads*

The response of the Type I-A sign structure to wind loads was recorded on several occasions. The accelerations measured at various locations along the truss serve to describe the motion of the structure in response to wind loading. The acceleration data also aids in the modal analysis of the structure through the use of its Fourier transform. The use of the Fast Fourier Transform (FFT) allows the frequency content of the acceleration to be determined (and thus the structure’s natural frequencies).

Figure 5.3-8 shows the horizontal acceleration at the mid-span of the truss. Below the acceleration plot is a plot (Figure 5.3-9) of the frequency content of the record. For horizontal acceleration, the natural frequency is seen clearly at 2.84 Hz. This experimental value is slightly higher than the calculated horizontal natural frequency of 2.75 Hz.



**5.3-8 Type I-A horizontal acceleration at the mid-span of the truss**

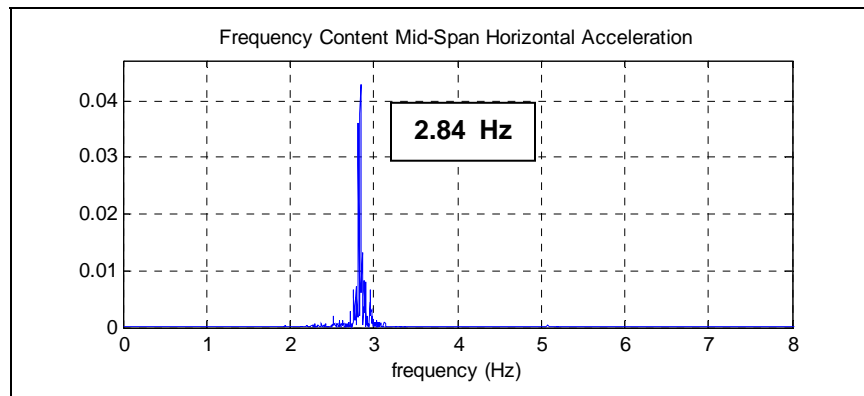


**Figure 5.3-9 FFT – Type I-A horizontal mid-span acceleration**

The vertical acceleration is shown in Figure 5.3-10. The FFT of the vertical acceleration (see Figure 5.3-11) indicates a vertical natural frequency of 3.34 Hz but also includes a higher frequency content corresponding to the torsion of the truss; this smaller peak that also shows up in the FFT plot of the vertical accelerations is at 5.08 Hz. This frequency represents the fourth mode of the structure, the torsional motion of the truss about its longitudinal axis. The measured vertical natural frequency is lower than that calculated by the model (3.42 Hz).

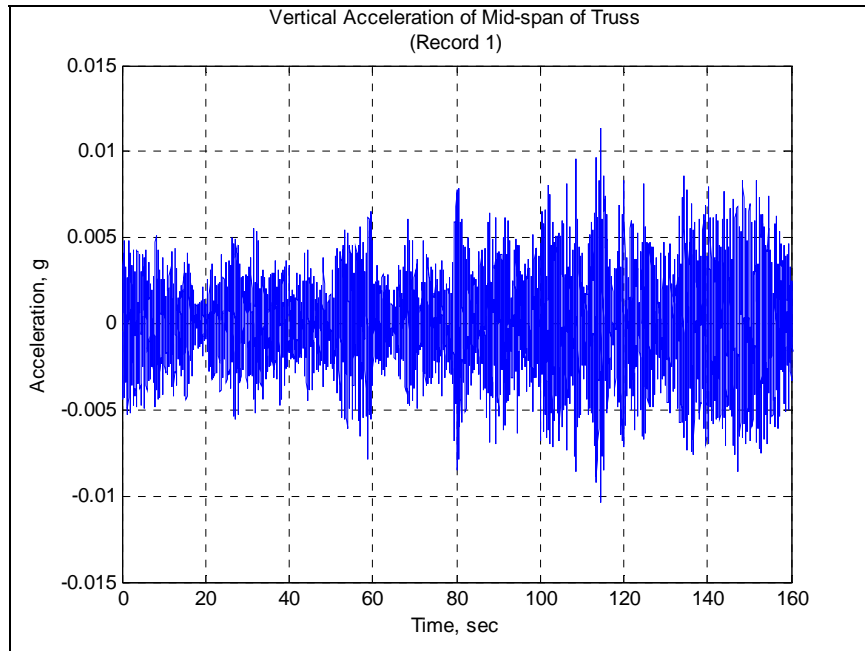


**Figure 5.3-10 Type I-A vertical acceleration at the mid-span of the truss**

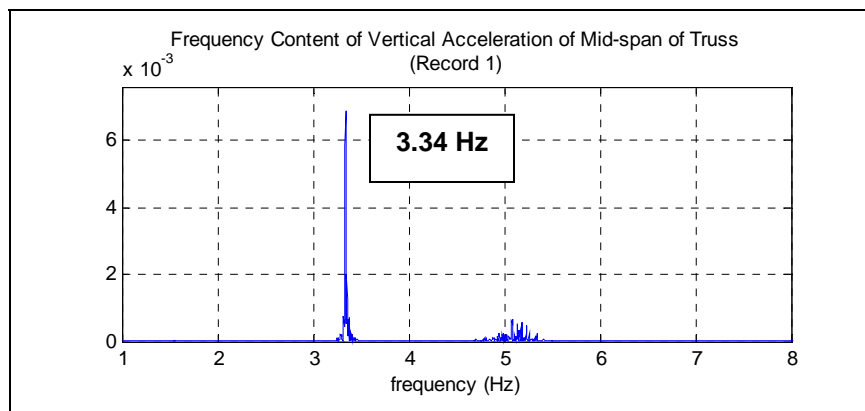


**Figure 5.3-11 FFT – Type I-A vertical mid-span acceleration**

Two important things can be learned from this data. First, the accuracy of the analytical model for this structure is not as high as it was for the cantilever structure. The reason for this is most likely that the boundary conditions are more complicated for the Type I-A sign structure. The U-bolt connections of the truss to the support structure are difficult to model accurately. In fact, there is no guarantee that these connections will even behave the same way all of the time. The model results in a structure that is too flexible in the horizontal direction and too stiff in the vertical direction. The lesson here is that no matter how detailed and complex a model is, it is just an approximate representation of the real structure. Part of the reason that there are factors of safety in design is that our calculations during the design process of a structure are just approximations.

The second interesting facet of these data is that a peak in the Fourier transform of both the horizontal and vertical accelerations occurred at a frequency of 5.08 Hz. The only reasonable explanation for this is that this frequency corresponds to the first torsional mode of vibration. The calculated first torsional mode (from the analytical model) has a frequency of 5.14 Hz, which means that model is stiffer in torsion than the actual structure. Using Equation 5.1-1, the difference in stiffness is approximately a factor of  $(f_m/f_a)^2 = (5.14/5.08)^2 = 1.02$  (assuming that the mass is correct in the analytical model).

## 5.4 Dynamic Properties of the Type II-A Sign Structure

### *Manual Excitation*

The Type II-A sign structure was manually excited in the horizontal and vertical directions in the same manner as described for the Type I-A structure. Each mode was excited several times to obtain accurate records. The acceleration and resulting stress records for the horizontal manual excitation are given below in Figure 5.4-1 and 5.4-2, as well as in Table 5.4-1.

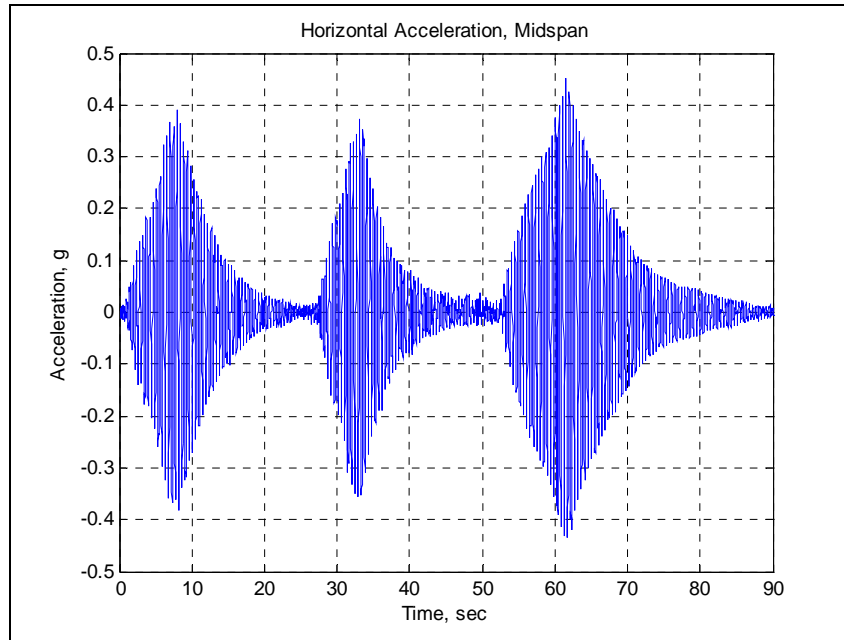


**Figure 5.4-1 Type II-A horizontal acceleration at mid-span of the truss due to manual excitation**

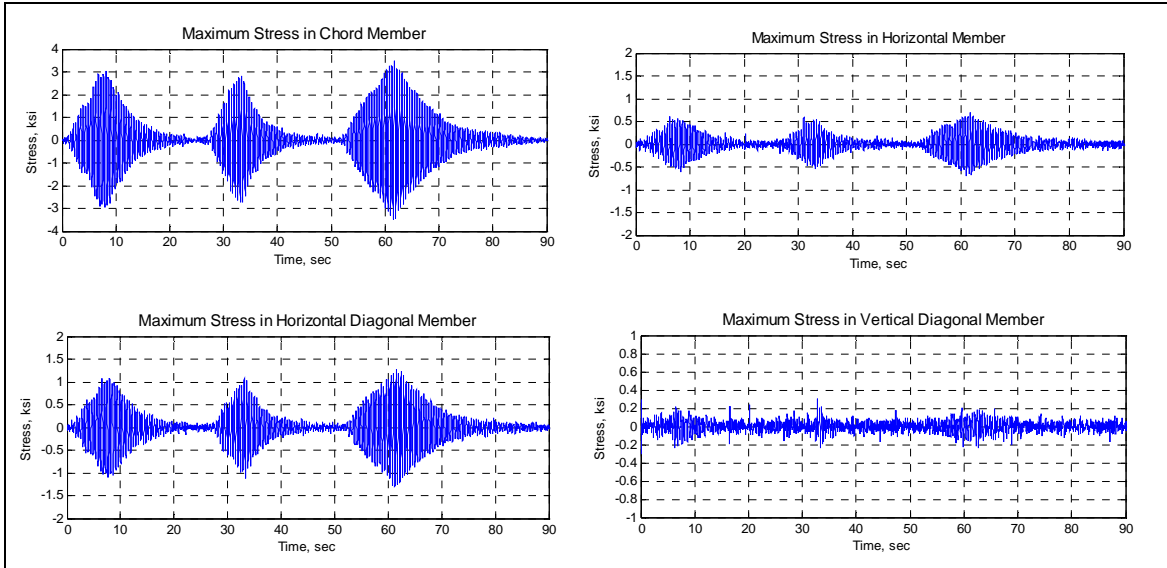


**Figure 5.4-2 Type II-A member stresses due to horizontal manual excitation**

**Table 5.4-1 Type II-A member stresses due to horizontal manual excitation**

Member	Peak Stress Corresponding to 0.45 g Peak Horizontal Acceleration
Chord	3.5 ksi
Horizontal	0.69 ksi
Horizontal Diagonal	1.3 ksi
Vertical Diagonal	0.31 ksi

By measuring the rate of decay in the response over time, the amount of damping can be determined. Results from four of the manual excitation tests are plotted below in Figures 5.4-3 and 5.4-4.

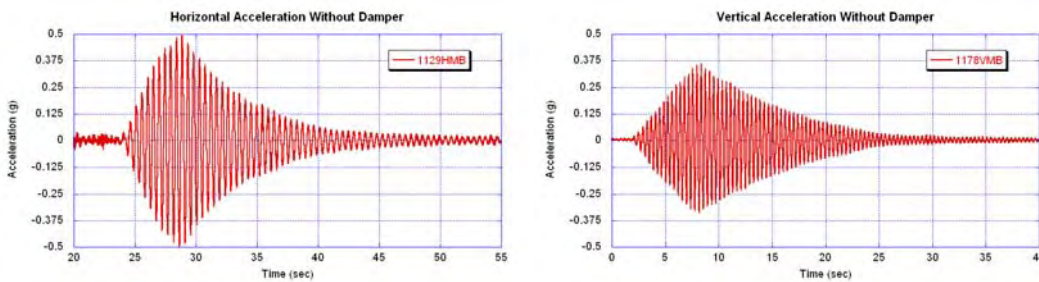


**Figure 5.4-3 Type II-A horizontal (left) and vertical (right) manual excitation without damping**

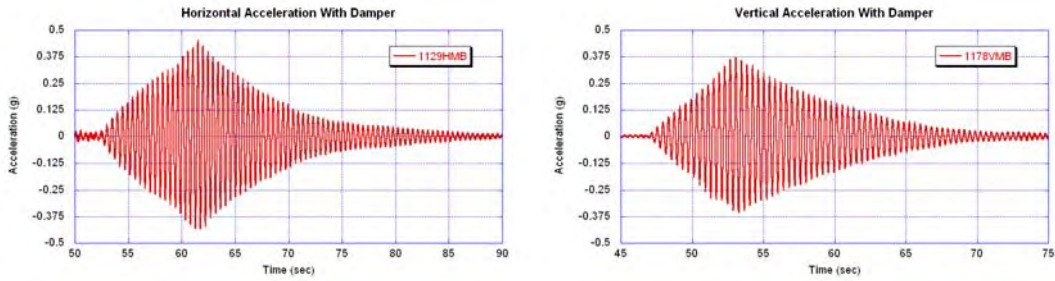


**Figure 5.4-4 Type II-A horizontal (left) and vertical (right) manual excitation with damping**

To determine the percentage of critical damping in the structure with the damper engaged and disengaged, the acceleration data was plotted and the peaks were isolated. An exponential curve was then fit to the peaks, thus indicating the rate of decay. The time step between each oscillation cycle (the natural period) was also recorded. This structure has 1.42% of critical damping without the damper, and 1.61% of critical damping with the damper engaged (which is a 12% increase). This structure had one 31-lb (1708) Stockbridge damper, like the one used on the Type I-A structure. (Recall that when the *sloppy* damper was used on the cantilever structure the damping was increased by 64%.) Horizontal damping envelopes are plotted below in Figure 5.4-5.

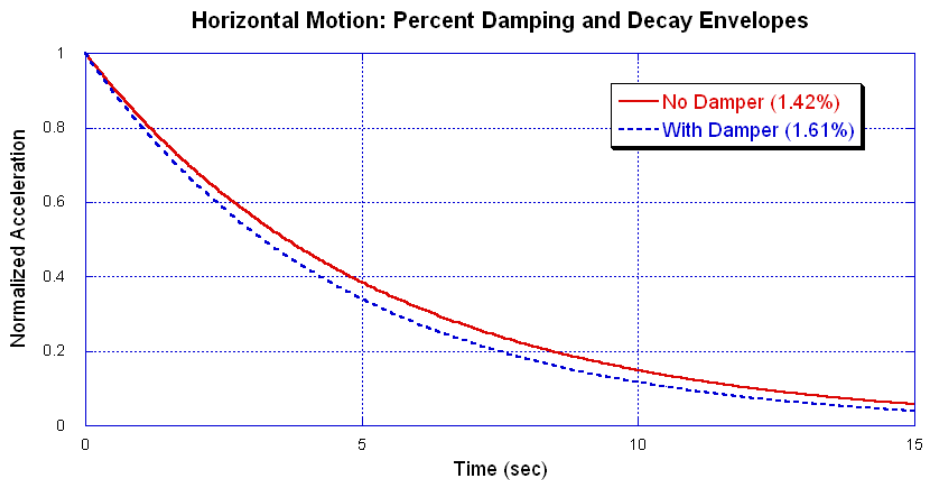


**Figure 5.4-5 Type II-A decay of the horizontal motion with and without the damper**

### ***Wind Excitation***

Accelerations were measured in the horizontal and vertical directions at several locations along the truss during wind excitation. Samples of the horizontal accelerations measured on one of the chords at mid-span are shown in Figure 5.4-6, along with the FFT

of the same record. For horizontal acceleration, the natural frequency is clearly seen at 2.12 Hz.

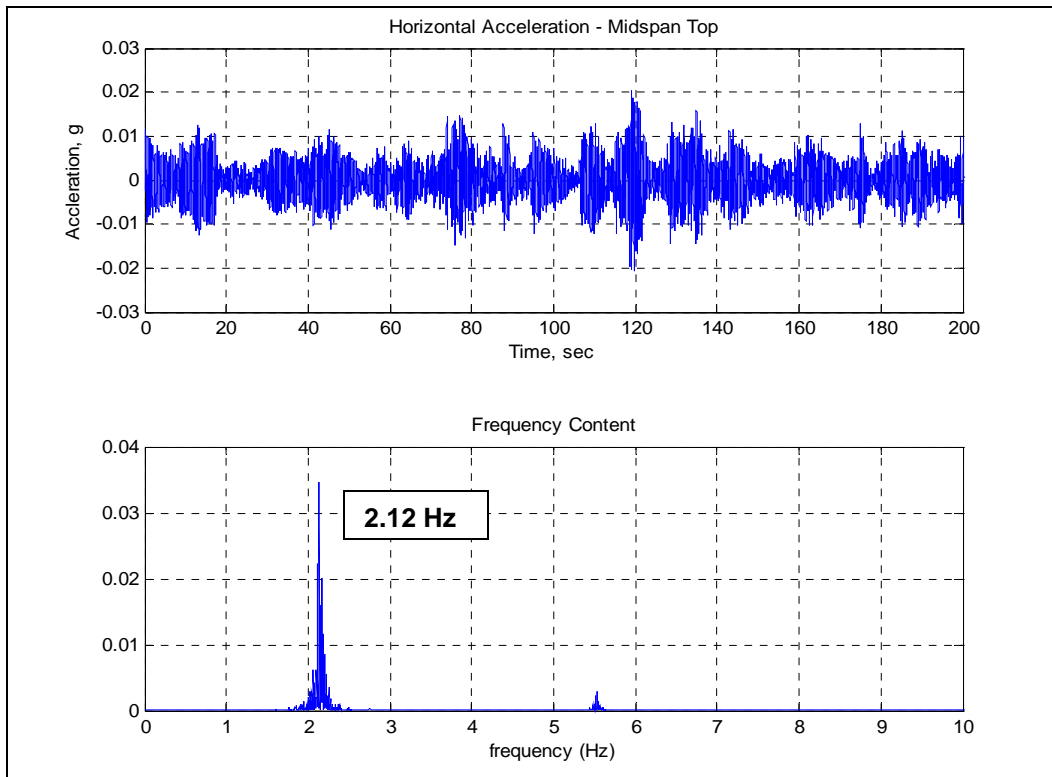


**Figure 5.4-6 Type II-A horizontal mid-span acceleration (top) and FFT of horizontal mid-span acceleration (bottom)**

The vertical acceleration is shown in Figure 5.4-7. The FFT of the vertical acceleration indicates a vertical natural frequency of 2.59 Hz, but also includes a higher frequency content at 5.53 Hz (similar to that also seen horizontally) corresponding to torsion of the truss.

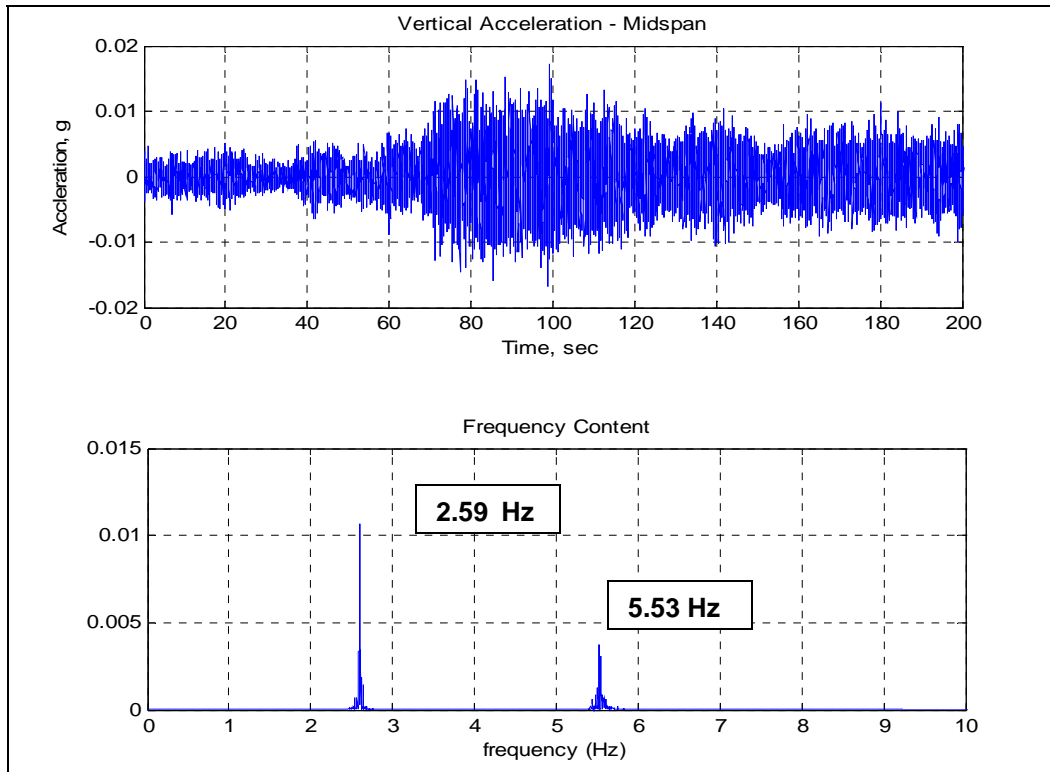


**Figure 5.4-7 Type II-A vertical mid-span acceleration (top) and FFT of vertical mid-span acceleration (bottom)**

## 5.5 Vibration Characteristics of the Type III-A Sign Structure

### *Manual Excitation*

Manual excitation of this structure was accomplished in the same manner as described previously. These tests serve to verify the results of the modal analysis conducted using SAP2000, as well as to give a relationship between acceleration and strain data. The data presented here represents horizontal and vertical motion separately. Figure 5.5-1 shows the acceleration at mid-span of the truss from horizontal manual excitation. For this particular test, the maximum acceleration is 0.26 g. Figure 5.5-2 below shows the corresponding stress in each member type.

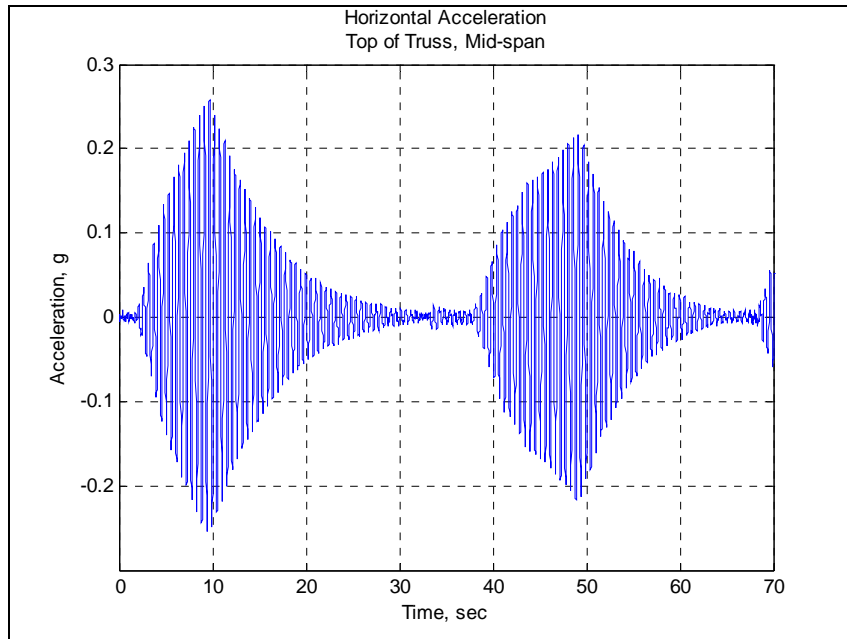


**Figure 5.5-1 Type III-A horizontal acceleration at the mid-span of the truss due to manual excitation**

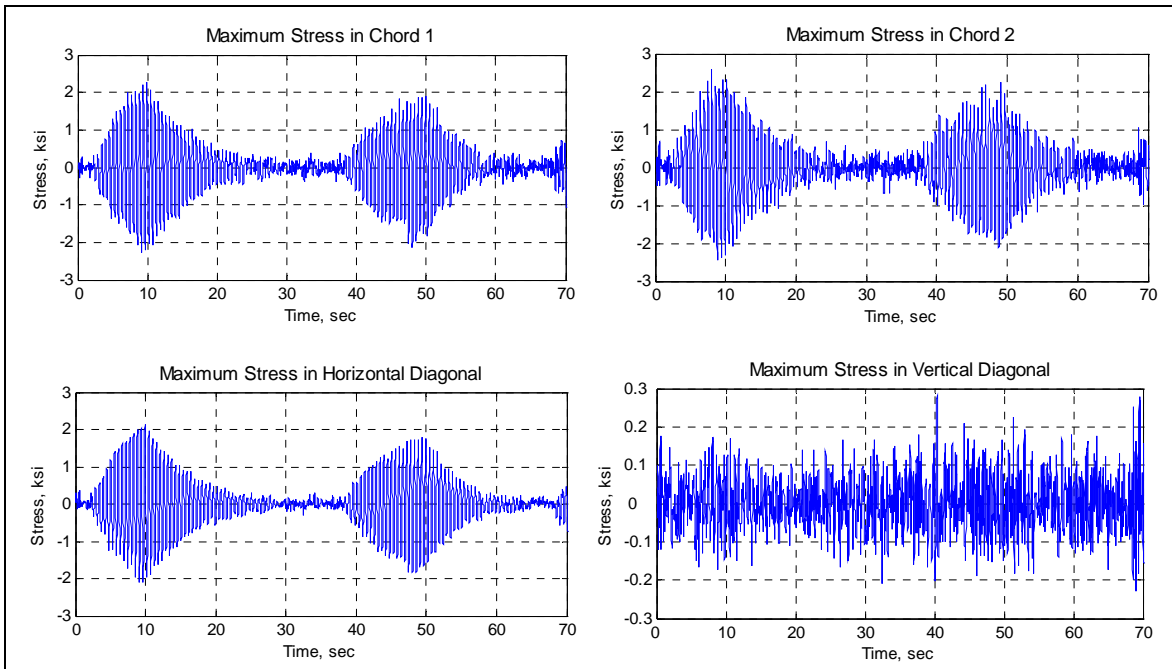


**Figure 5.5-2 Type III-A stress in each member due to horizontal manual excitation**

**Table 5.5-1 Type III-A Member stresses due to horizontal manual excitation**

<b>Member</b>	<b>Peak Stress for 0.26 g Peak Horizontal Acceleration</b>
Chord 1	2.28 ksi
Chord 2	2.69 ksi
Horizontal Diagonal	2.13 ksi
Vertical Diagonal	0.314 ksi

The data given in Table 5.5-1 above show the relative amount of stress that each of four instrumented member types will experience due to horizontal motion of the truss. The chord members both experience similar amounts of stress. The horizontal diagonal member experiences almost as much stress as the chord members, while the vertical diagonal is stressed to a much lower level.

Manual tests were also performed on the Type III-A truss to determine the effectiveness of the currently installed 31-lb Stockbridge damper. These tests were conducted in the same way as for the other trusses. It was determined that the structure without the damper and with the damper exhibit the same amount of damping (0.8% of critical). This is not surprising considering that this truss is the heaviest of the four tested yet has the same damper as the Type I-A and II-A trusses. These damping issues will be discussed further in Chapter 7.

### ***Wind Excitation***

Figure 5.5-3 shows an example of the horizontal acceleration of the top chord at the mid-span of this truss. Below the acceleration plot (in Figure 5.5-4) is a plot of the Fourier transform of the record. For horizontal acceleration, the natural frequency is clearly seen at 1.85 Hz, which is close to the calculated value (from the analytical model) of 1.76 Hz.

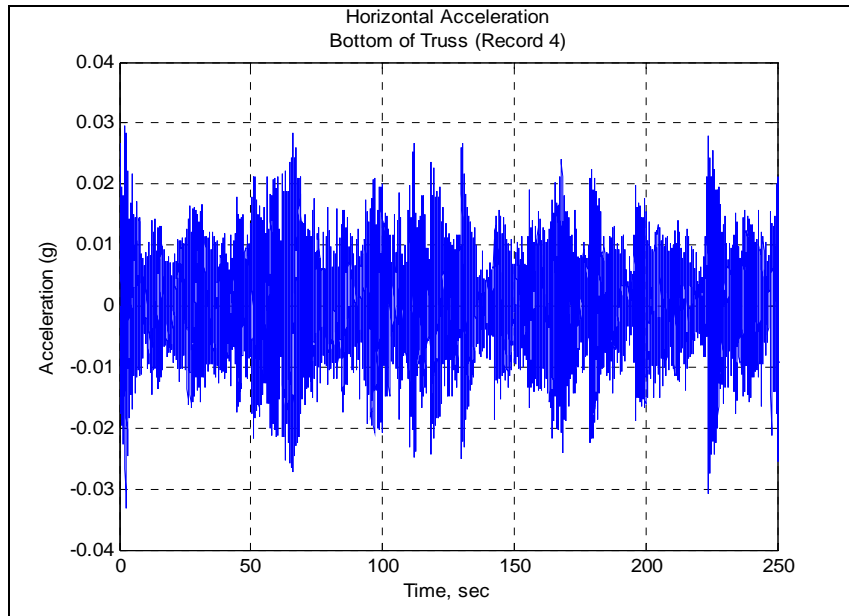


**Figure 5.5-3 Type III-A horizontal acceleration at the bottom of truss at mid-span**

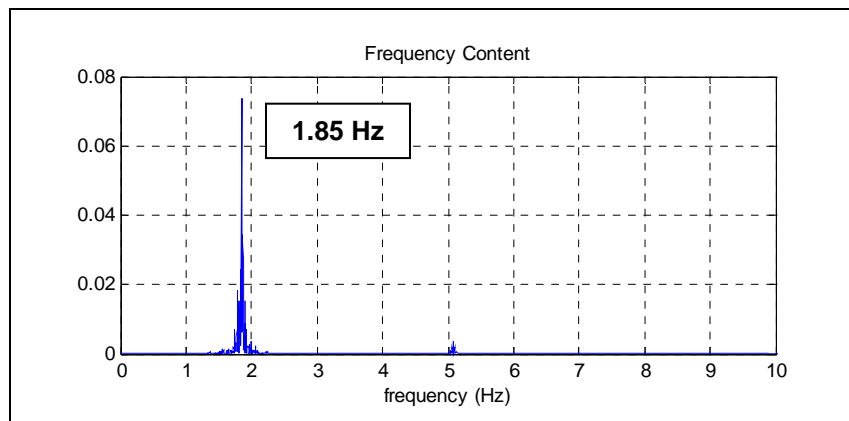


**Figure 5.5-4 Type III-A FFT of bottom horizontal mid-span acceleration**

Figure 5.5-5 shows a plot of the vertical acceleration of the top chord at the mid-span of the truss; Figure 5.5-6 shows a plot of the Fourier transform of this record. The natural frequency in the vertical direction is seen to be 2.55 Hz (the calculated value is 2.61 Hz). The other peak that shows up in the FFTs (particularly of the vertical accelerations) is at 5.09 Hz. This frequency represents the fourth mode of the structure, the torsional motion of the truss about its longitudinal axis. The calculated natural frequency of the torsional mode for the model is 4.52 Hz; again, this indicates that the model is somewhat stiffer than the real structure (at least with respect to this particular mode of vibration).

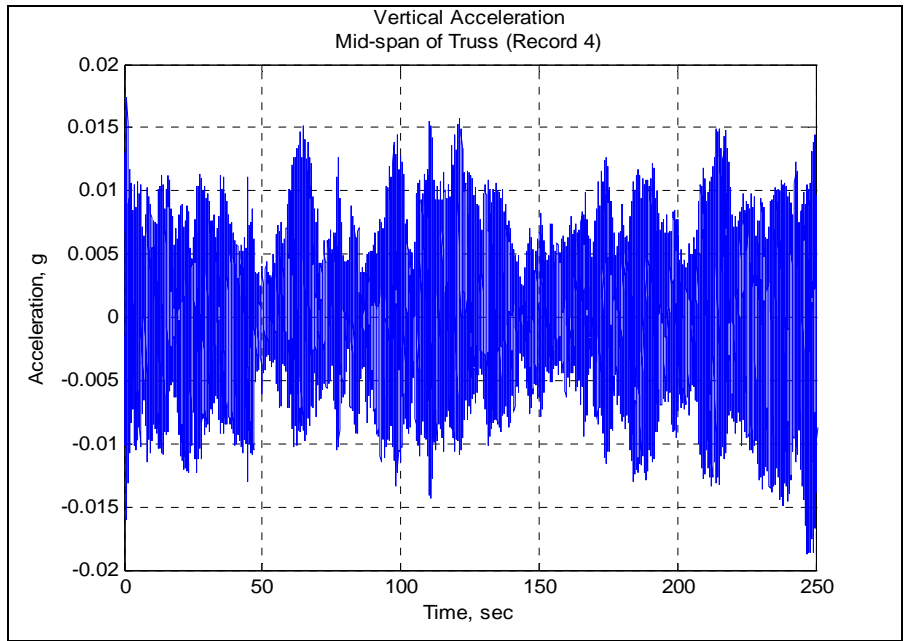


**Figure 5.5-5 Type III-A vertical acceleration at bottom of truss at mid-span**

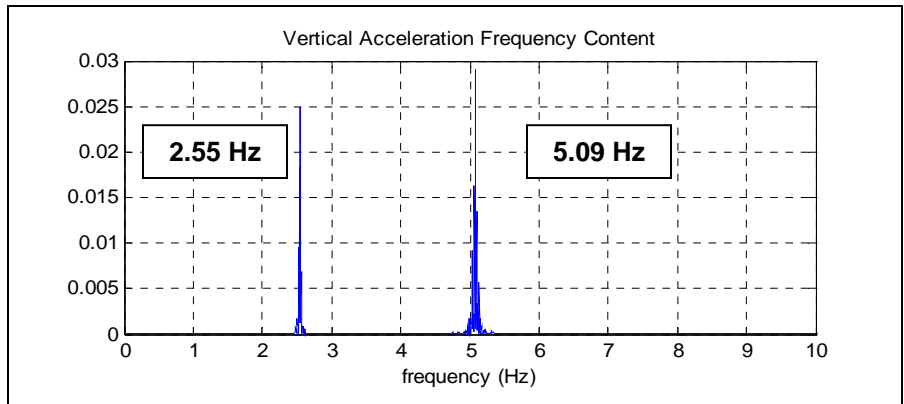


**Figure 5.5-6 Type III-A FFT of vertical mid-span acceleration**

## 5.6 Dynamic Characteristics of the VMS Sign Structure

### *Wind Excitation*

The response of this structure to wind excitation was recorded on several days. Some of the horizontal and vertical accelerations measured at mid-span of the structure are shown in Figure 5.6-1; the Fourier transforms of these records are shown in Figure 5.6-2. The results indicate that the natural frequencies in the horizontal and vertical directions are 2.88 Hz and 3.38 Hz, respectively. The calculated natural frequencies from the model are 3.33 Hz in the horizontal direction and 4.17 Hz in the vertical direction. Several unsuccessful attempts were made to better match the measured and calculated

natural frequencies by changing the analytical model end conditions for the connections of the truss to the support structure. The source of the discrepancy is therefore most likely the assumed support condition at the base of the structure. It is possible to have the horizontal natural frequencies match by assuming a point of fixity in the foundation at some location below the ground. The discrepancy in the vertical direction is a bit more problematic to resolve.

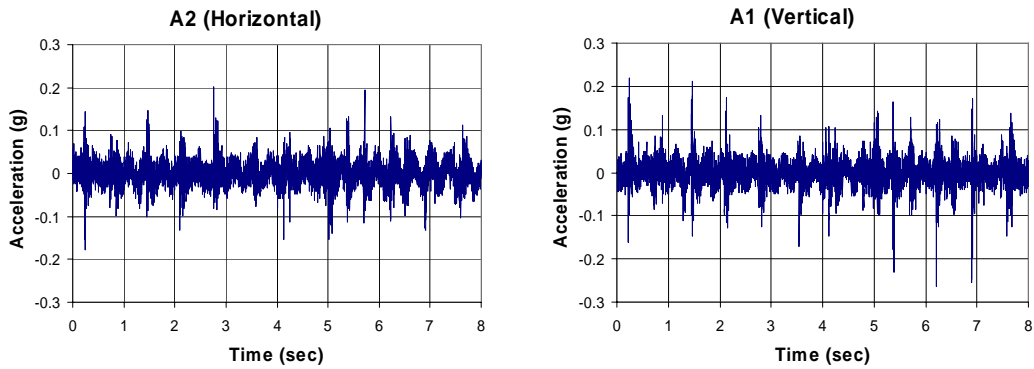


**Figure 5.6-1 Measured acceleration responses at the mid-span of the VMS truss for the horizontal (left) and vertical (right) directions**

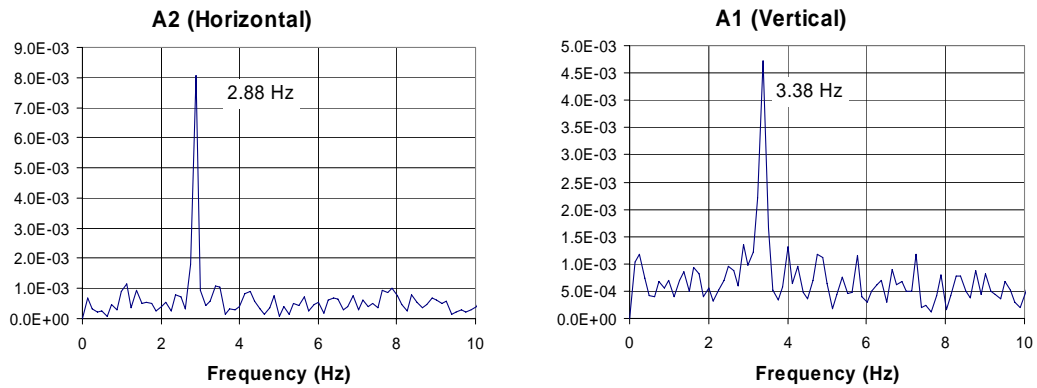


**Figure 5.6-2 Fourier transform of measured horizontal (left) and vertical (right) accelerations at mid-span of the VMS truss**

## 6.0 Response of Sign Structures to Wind Loads and Truck Gusts

### 6.1 Background

This chapter provides a general discussion of the response of sign structures to wind loads and truck gusts. The relationships between these loadings and structural response and current design specifications will be explored. The measured responses of the particular sign structures being studied to varying wind speeds will be presented. Based on these measured wind loads and structural responses, the design procedures and specifications will be evaluated.

### 6.2 Wind Loads on Structures

#### *Background*

The design wind loads for sign structures are currently calculated according to the *Standard Specifications for Structural Supports for Highway Signs, Luminaires and Traffic Signals* (AASHTO, 2001). The wind loading is considered as a static pressure acting horizontally on the sign and on the rest of the structure. The pressure is calculated using an ASCE 7-95 design wind loading formula:

$$P = 0.00256K_zGV^2I_rC_d \quad 6.2-1$$

where  $P$  = design pressure, psf  
 $K_z$  = velocity pressure exposure coefficient  
 $G$  = gust effect factor  
 $V$  = basic wind speed, mph  
 $I$  = importance factor  
 $C_d$  = drag coefficient

The basic wind speed,  $V$ , is defined as the 3-sec gust wind speed at a height of 32.8 ft above ground. This is a regional value corresponding to a mean return period of 50 years. For Illinois, the basic wind speed is 90 mph.

The gust effect factor,  $G$ , used in the pressure formula actually accounts for two phenomena. One is the anticipated spatial variation of the wind pressure acting on a structure. The other is in fact the gustiness of the wind with respect to the 3-sec basic wind speed. The dynamic response of a structure is not explicitly accounted for, although the specifications may include some of this effect in the values of various terms (which are sometimes arrived at in part simply through the experience of the specification committee). The response that is calculated when using the design code wind is the static response to the 3-sec average wind speed, increased to account for gust magnitudes through the use of the gust effect factor. In a flexible and relatively small structure, such

as a highway sign truss, the spatial variation of the wind pressure is of little effect, whereas the dynamic effects will be shown to be significant. Since these structures have very short periods of vibration relative to the periods that contain the significant energy in the wind spectrum, such structures are assumed to have relatively little dynamic response. In this case, the gust effect factor adjusts the effective wind pressure to account for the interaction between the structure and the wind gusts. Actually calculating  $G$  can be quite a complicated process, so design specifications have traditionally adopted a value, based on historical research and results, which has performed well. This value ( $G = 1.14$ ) is used in conjunction with the basic wind speed (3-sec gust) to yield an effective velocity pressure for use in design calculations (AASHTO, 2001). The gust effect factor will be examined further later on in this report. It should also be noted here that the gust effect factor is actually the square root of the so-called gust factor that is often discussed in standard texts on the subject.

The pressures that might be measured on the surface of a structural body are the result of the wind velocity directly outside the boundary layer. For the same wind velocity, different bodies will experience different pressures due to geometry and their Reynolds numbers. The introduction of a non-dimensional drag coefficient,  $C_d$ , accounts for differences in force, as defined by:

$$C_d = \frac{F_D}{\frac{1}{2} \rho V^2 B} \quad 6.2-2$$

where  $\rho$  = air density

$F_D$  = drag force

$V$  = mean speed value for the reference wind

$B$  = typical reference dimension of the body

The pressure,  $P$ , is then calculated according to the formula:

$$P = \frac{1}{2} \rho V^2 C_d \quad 6.2-3$$

which is essentially the same formula as Equation 6.2-1, excluding the importance factor, exposure coefficient, and gust effect factor (as well as the constant out front that simply accounts for the use of inconsistent units).

Because of the difficulty in quantifying the wind pressures that actually result from turbulent wind flow across a variety of structures and components, large amounts of experimental data should be generated and utilized to adequately determine drag coefficients acting on various types of structures. These experiments are typically conducted via full-scale testing, modeling, and wind tunnel tests (Simiu and Scanlan, 1996).

The first work that was done to accurately determine drag coefficients on wall panels mounted on the ground was conducted in the 1930s by Flachsbar. Drag or force coefficients were determined as a function of the aspect ratio (width/height) of the panels. This research became the basis of many design codes, but it did not consider turbulent flow or the effects of panels raised above ground level (as is the case for sign panels) (Simiu and Scanlan, 1996).

When a sign panel is a significant distance from the ground, the wake flow is dominated by separating horizontal shear layers above and below the sign. This separating shear layer interaction increases the drag coefficient (Letchford, 2001). Therefore, the appropriate drag coefficient to be used for a solid rectangular sign has recently been examined by Letchford (2001). The results of wind tunnel tests show that the drag or force coefficient is not only a function of the aspect ratio,  $B/s$ , but also the “clearance ratio,”  $s/h$  (see Figure 6.2-1). The ASCE 7-05 (2006) general loading design standard has been updated to reflect this.

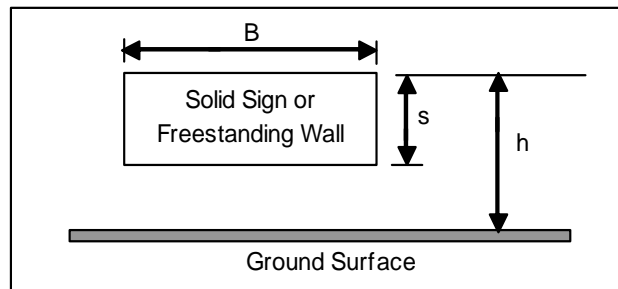


**Figure 6.2-1 Sign panel clearance ratio and length labels**

The wind drag coefficients used in the *Standard Specifications for Structural Supports for Highway Signs, Luminaires and Traffic Signals* (AASHTO, 2001) for rectangular signs are shown in Table 6.2-1 below (regardless of the clearance ratio).

**Table 6.2-1 AASHTO (2001) sign panel drag coefficients**

Aspect Ratio, $B/s$	Drag Coefficient, $C_d$
1.0	1.12
2.0	1.19
5.0	1.20
15.0	1.23
20.0	1.30

The aspect ratios for the IDOT overhead highway signs are in the range of 1.0 to 1.50. For this range, the drag coefficients would vary between 1.12 and 1.16 according to the AASHTO specifications (2001). The IDOT design calculations show that a constant drag coefficient value of 1.20 was used in their sign truss designs. In response to the new

data, ASCE has changed their values of drag coefficients for sign structures (these are more conservative than those suggested by Letchford). According to that updated standard, the drag coefficients that should be used for the IDOT signs that are part of this project are in the range of 1.75 to 1.80 (ASCE, 2006). These are approximately 56 percent higher than those given by the 2001 AASHTO specifications. Drag coefficients from the current AASHTO (2001) specification, Letchford's (2001) tests, and ASCE 7-05 (2006) are shown in Table 6.2-2.

**Table 6.2-2 Recommended drag coefficients as a function of aspect and clearance ratios**

Sign Truss	Clearance Ratio <i>s/h</i>	Aspect Ratio <i>B/s</i>	<i>C<sub>d</sub></i>		
			AASHTO (2001)	Letchford (2001)	ASCE 7-05 (2006)
Cantilever	0.36	1.04	1.12	1.39	1.78
Type I-A	0.49	1.59	1.16	1.40	1.72
Type II-A	0.50	2.53	1.19	1.43	1.70
Type III-A	0.38	3.47	1.19	1.47	1.76
Single Sign	0.30-0.50	1.0-1.5	1.12-1.16	1.39-1.44	1.75-1.80

The other values used in determining the design wind loads for these sign structures, with a maximum sign area of 340 sf, are:

$$K_z = 1.0 \text{ (for Wind Exposure Category C (open terrain with scattered structures) and maximum sign mounting height of 32.8 ft)}$$

$$I = 1.00 \text{ (for 50 year design life)}$$

The allowable stresses for this type of sign structure are determined according to Section 6 of the AASHTO design specifications (2001). The applicable results of the allowable stress calculations are shown in Table 6.2-3 below. The code increases the allowable stress by 33 percent for certain load combinations including wind; these increased values are also given in the table. Aluminum has a yield strength of 35 ksi. The allowable stresses given in Table 6.2-3 may seem low because the effective yield strength of the material within an inch of the connections is reduced due to welding (Kissell and Ferry, 2002).

**Table 6.2-3 Allowable stress for aluminum members**

	Allowable Stress (ksi)	Allowable Stress * 1.33 (ksi)
Tension	11.0	14.63
Compression	12.0	15.96

## ***Fatigue Loads***

Fatigue is defined in the AASHTO (2001) design specifications as "...the damage that may result in fracture after a sufficient number of stress fluctuations." When a structure or component is subjected repeatedly to stresses that are below the allowable stress of the material, small cracks may form. With continued cyclic loading, these cracks may propagate, leading to the failure of the structure. These fatigue cracks tend to form in regions of stress concentration, such as at notches, holes, welds, or other discontinuities.

The AASHTO design specifications are based in part on NCHRP Report 412, *Fatigue Resistant Design of Cantilevered Signal, Sign and Light Supports* (Kaczinski et al., 1998). The components of a sign structure should be designed for fatigue to resist equivalent static loading due to galloping, natural wind gusts and truck-induced gusts. The stresses must not be greater than the Constant Amplitude Fatigue Limit (CAFL) listed for each detail category in Table 11.3 of the specification (AASHTO, 2001). The CAFL values that are applicable to the members tested in these sign structures are listed in Table 6.2-4. Detail categories E and ET refer to chords and fillet welded T-, Y-, and K-tube-to-tube (web-to-chord) connections, respectively. AASHTO specifications require design for fatigue for cantilever sign structures but not for span-type structures.

**Table 6.2-4 Constant amplitude fatigue limits (CAFL) for truss members**

<b>Member</b>	<b>Detail Category</b>	<b>CAFL (ksi)</b>
Chord	E	1.9
Vertical Diagonal Horizontal Diagonal Vertical Horizontal Interior Diagonal	ET	0.44

## ***Natural Wind Gust***

A sign truss is designed with respect to fatigue to resist the following equivalent static natural wind pressure:

$$P_{NW} = 5.2C_dI_F \text{ (psf)} \quad 6.2-4$$

where

$C_d$  = drag coefficient

$I_F$  = applicable importance factor (1.0 for Fatigue Category I)

This formula is based on a yearly mean wind speed of 11.2 mph, with a 0.01 percent probability of exceedence (Kaczinski et al., 1998).

### ***Truck-Induced Gust***

The equivalent static truck pressure for fatigue design is given by:

$$P_{TG} = 18.8C_dI_F \text{ (psf)} \quad 6.2-5$$

where

$C_d$  = drag coefficient

$I_F$  = applicable importance factor (1.0 for Fatigue Category I)

This pressure is to be applied in the vertical direction to the truss, as well as to all portions of the structure projected onto a horizontal plane. The above equation is the result of the wind pressure formula given in Equation 6.2-1 with a velocity of 65 mph, set to coincide with the posted traffic speed limit.

It should be noted that the formula for static truck pressure that was used to produce the current IDOT truss designs is the original truck gust formula of  $P_{TG} = 36.6C_dI_F$ , from the 2001 AASTHO specifications. The 2002 AASHTO Interim (AASTHO, 2002) reduced this formula down to the one found in Equation 6.2-5. The result is that, for members that are controlled by truck gusts, the designs are conservative according to the latest AASHTO guidelines.

### ***Dynamic Response of a Sign***

It was mentioned above that the response of a sign to wind gusts is nearly static in nature, with little or no dynamic component. A plot of the axial stress in a chord member of the cantilever structure, along with the 3-sec moving average of the axial stress, is shown in Figure 6.2-2 (recall that the 3-sec average wind speed is used for calculating the design loads). Since the structure is linear, the member strain (and therefore stress) is proportional to the square of the wind velocity. A region in Figure 6.2-2 is expanded in time in Figure 6.3-3 to show better detail of the two curves. This figure clearly shows that the dynamic component of the response is very significant and indeed is not negligible. It should further be expected that the ratio of the peak dynamic response divided by the 3-sec average would tend to be quite small as the wind velocity gets large and would become very large as the 3-second average approaches zero.

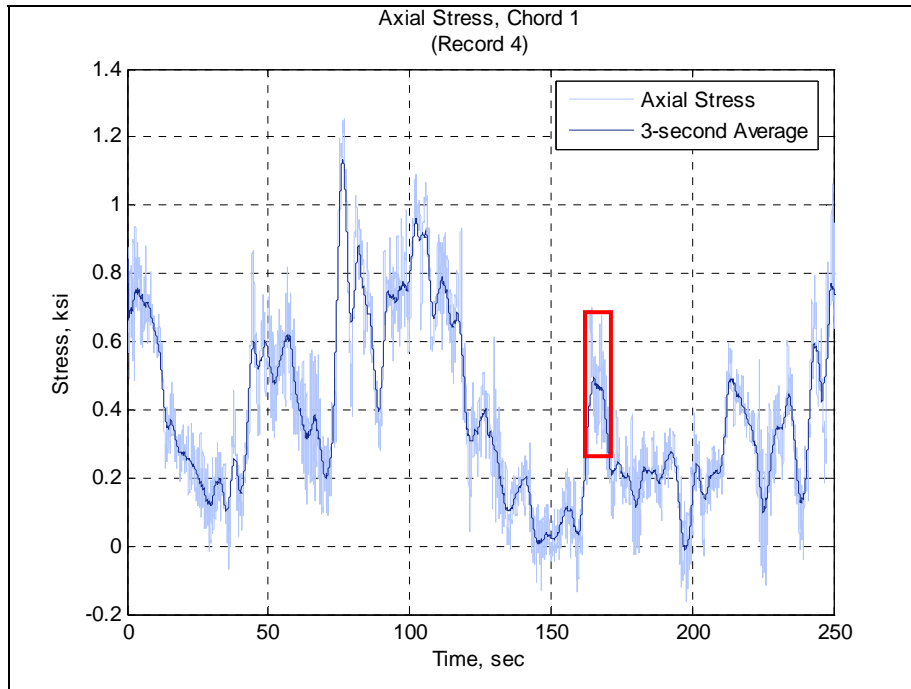


**Figure 6.2-2 Axial stress in cantilever chord member, and 3-sec average, vs. time**

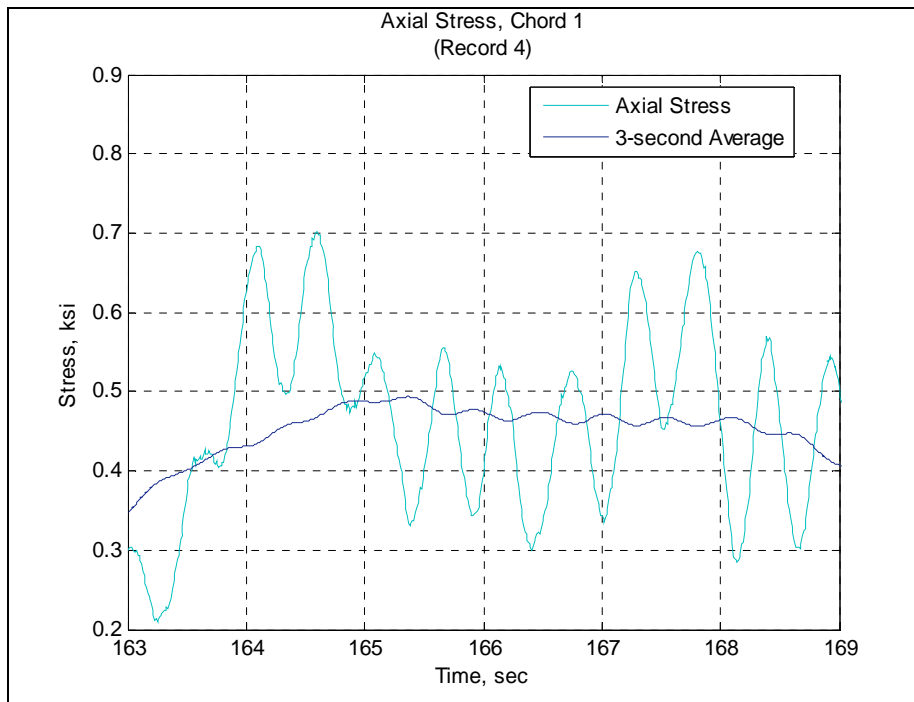


**Figure 6.2-3 Detail of axial stress vs. time compared to 3-sec average**

Figure 6.2-4 shows the ratio of average peak response to the three-second average response vs. the three-second average wind speed for a large number of points (for four of the sign structures). The values of the peak to average ratios for five wind speeds on each of the four signs are given in Table 6.2-5. If these ratios are extrapolated up to a 90 mph wind speed, the average ratio would be about 1.05. This is not large, but it is on the same order of magnitude as the gust effect factor that is used for design. This value will be used for extrapolating measured stresses to those expected for a 90 mph wind speed for the purpose of evaluating the response of the sign structures for code design checks of each structure, as given below.

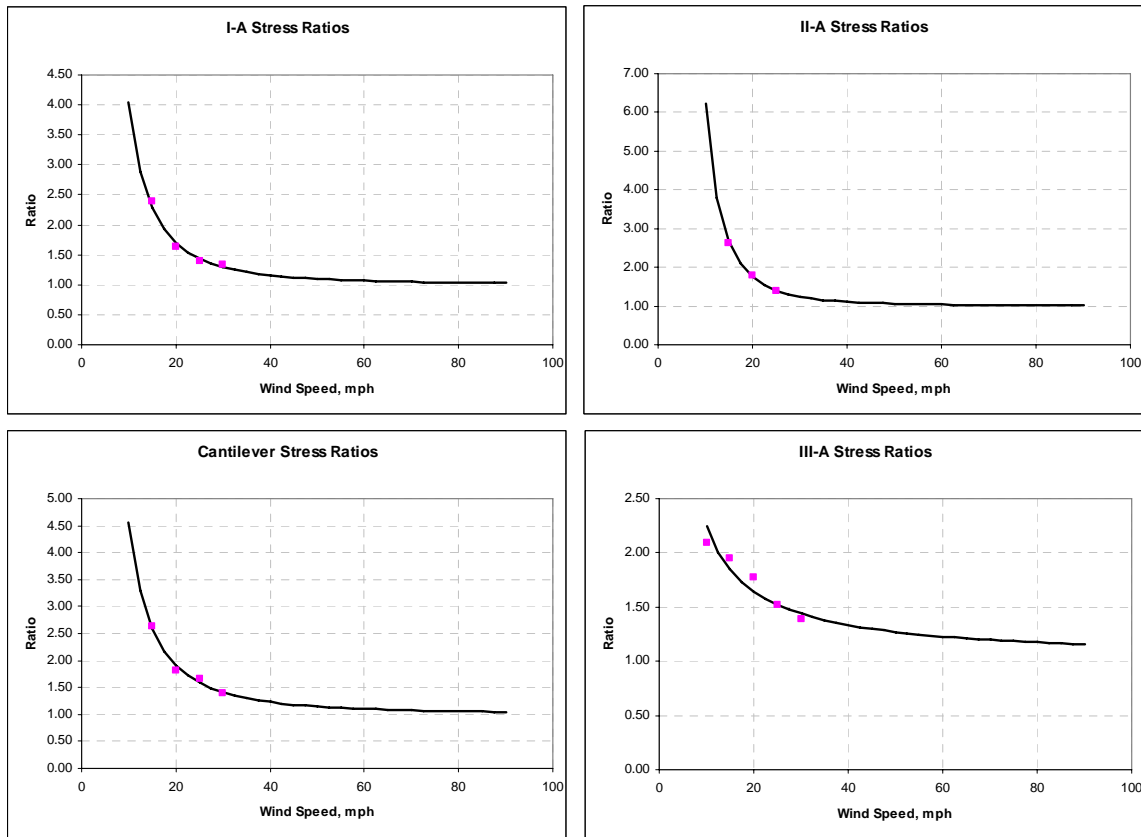


**Figure 6.2-4 Ratio of average peak response to 3-sec average vs. wind speed for four sign trusses**

All of the data was combined into a single relationship for assessing the design of all structures. The resulting curve of response ratio vs. wind speed is shown in Figure 6.2-5 (top). Also shown in this figure is the ratio value of 3.1 at 11.2 mph; this is of great significance for fatigue design. A curve showing one standard deviation bounds (based on the experimental results) is given in Figure 6.2-5 (bottom). The statistical properties of the response ratio data are given in Table 6.2-6. Notice that the coefficient of variation becomes small for higher wind speeds, but large for lower wind speeds. As a result, the

use of the average value for strength design is quite acceptable; however, the use of the average value for fatigue evaluation needs some further consideration.

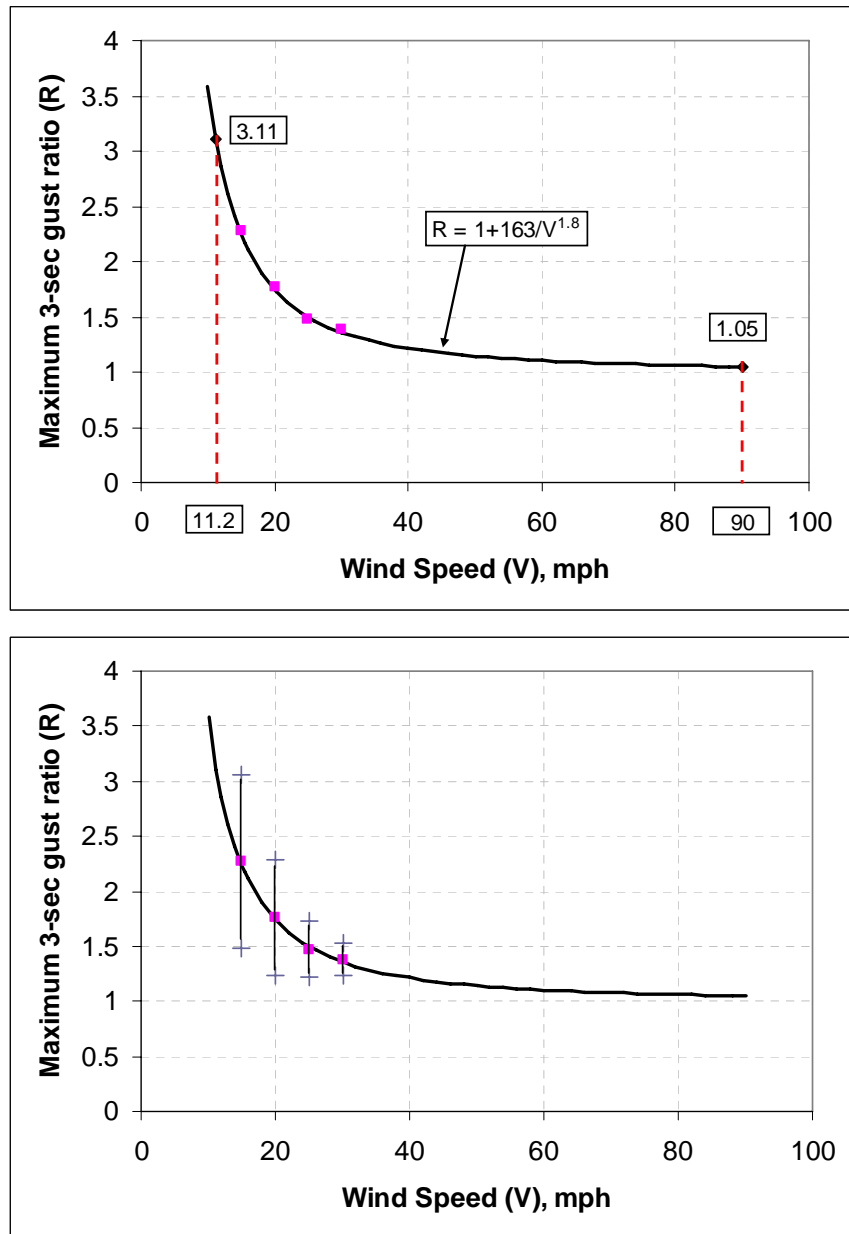


Figure 6.2-5 Combined plot of mean response ratio for all sign structures (top) and the same plot with one standard deviation experimental error bars (bottom)

**Table 6.2-5 Average ratio of peak response to 3-sec average vs. average wind speed**

Sign Truss	Wind Speed (mph)				
	10	15	20	25	30
Cantilever	--	2.63	1.82	1.66	1.39
Type I-A	--	2.39	1.63	1.40	1.33
Type II-A	--	2.61	1.80	1.38	--
Type III-A	2.10	1.95	1.77	1.52	1.38

**Table 6.2-6 Statistical properties of response ratios**

Wind Speed (mph)	Mean	Standard Deviation	Mean – Std. Dev	Mean + Std. Dev	Coefficient of Variation
	$\mu$	$\sigma$	$\mu - \sigma$	$\mu + \sigma$	$c_v = \sigma / \mu$
15	2.27	0.784	1.49	3.06	0.3449
20	1.76	0.526	1.24	2.29	0.2981
25	1.47	0.251	1.22	1.72	0.1709
30	1.38	0.146	1.23	1.53	0.1055

### 6.3 Response of the Cantilever Sign Structure to Wind Loads and Truck Gusts

#### *Wind Loads*

To determine the cantilever's response to strong wind events, acceleration, strain, and wind data were collected on March 11, 2005, when the winds were gusting to over 30 mph (see Figure 6.3-1).

#### *Average Stress*

The structure responds to the wind in two ways: 1) the long period response that can be considered as an almost static behavior, and 2) the shorter-period, fluctuating response of the structure that is superimposed on top of the "static" response. One of the challenges associated with acquiring strain data on a windy day is that it is difficult to identify a point of zero strain. The strain gage is "zeroed" out at the beginning of the test, but due to the constant wind / vibration movement and stress on the structure, this does not represent a true state of zero stress. This results in the record being offset from actual zero by an unknown value. To overcome this issue and to ensure that accurate strain measurements were obtained, several records were evaluated. Since wind force, and therefore resulting strain, is proportional to the square of the wind speed, a relationship between the strain and the wind speed could be developed by using regression analysis. From this relationship, the offset value (from zero) for each record was then determined.

First, the average value of recorded strain was determined for a given wind speed. This was done by finding the values of recorded strain that corresponded to a range of wind speed  $\pm 0.5$  mph from the velocity in question. These strain values were then averaged. This process was repeated for specific wind speeds ranging from 10 to 30 mph, in increments of 2.5 mph. To determine the offset, the average recorded strain values were plotted versus their corresponding normal wind speeds. A quadratic curve was then fit to these points. The intercept of this curve then became the value by which to adjust the record. This procedure is illustrated in Figure 6.3-2 for a single stress record.

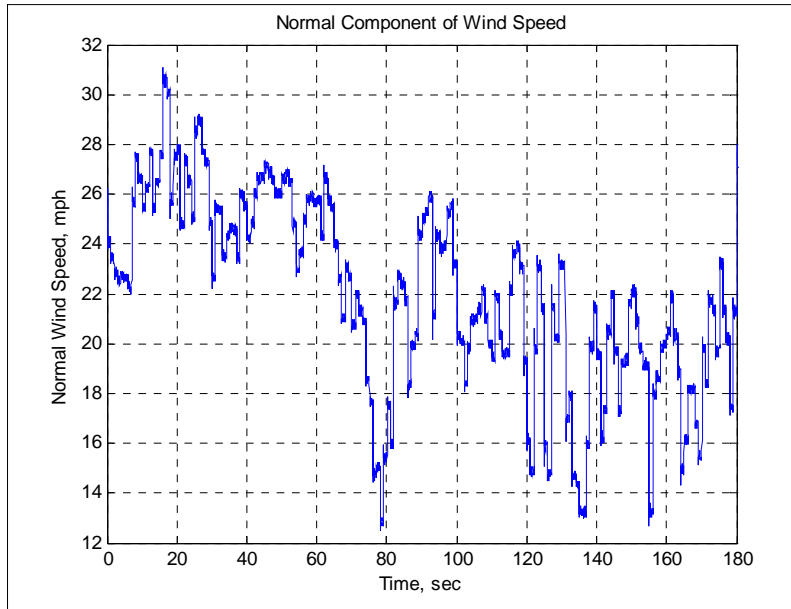


**Figure 6.3-1. Normal wind speed measured for cantilever**

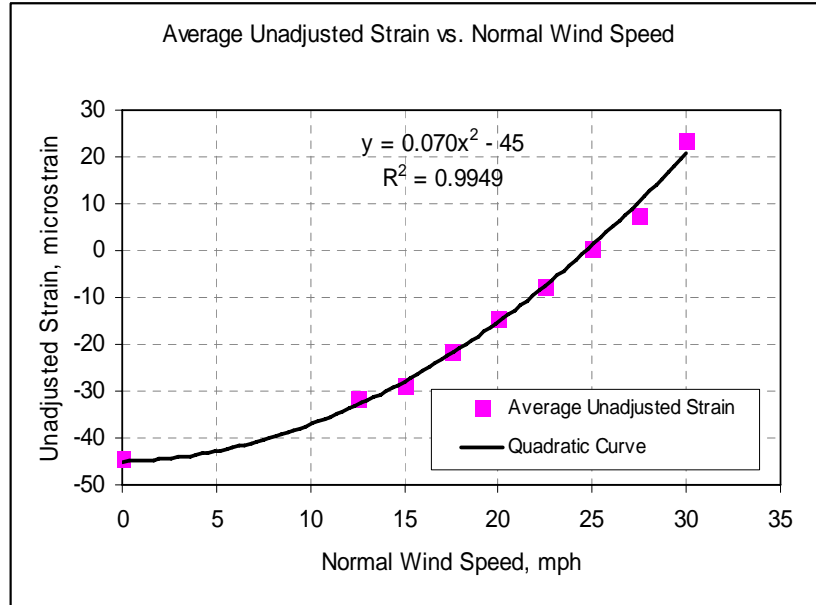


**Figure 6.3-2 Average unadjusted strain at various normal wind speeds (cantilever)**

From the figure above, it can be seen that this particular record needs to be adjusted (for zeroing) by adding 45 microstrain. This type of strain adjustment process was completed for all of the strain records (for each gage). The overall results then provided a good idea of the average strain in each of the instrumented members corresponding to a given average wind speed. This also allowed for extrapolation of the results to higher wind speeds, such as the design wind speed of 90 mph.

Figure 6.3-3 illustrates where the strains (and therefore stresses) were measured on the chords of the cantilever. Figure 6.3-4 then shows the curves of the average stresses in each chord member due to particular normal wind speeds (including expected average stress values extrapolated out to a 90 mph wind). Similar curves were also developed for web Members 3 and 4.

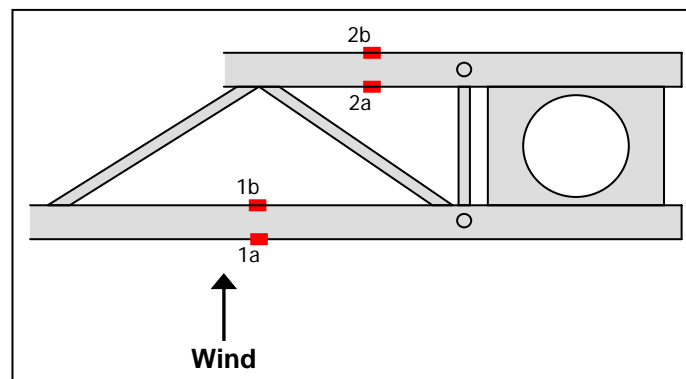


**Figure 6.3-3 Measurement of cantilever stress in chord members (plan view of the bottom chords)**

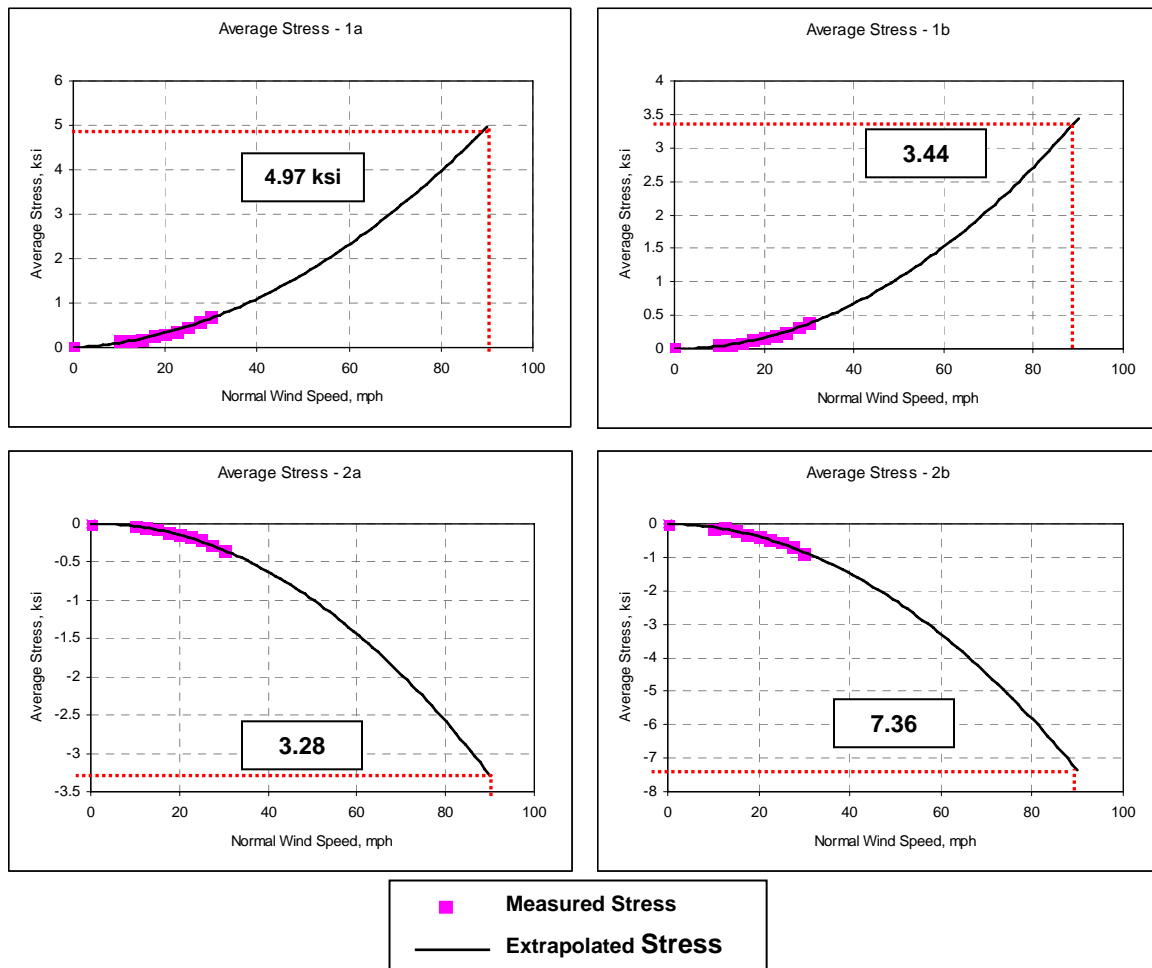


**Figure 6.3-4 Average stress in the four strain gages on cantilever chord members**

At the basic design wind speed of 90 mph, then, the stresses in each of these members would be as follows:

**Table 6.3-1 Comparison of measured stresses to model stresses (cantilever)**

Member	Model – Wind Loads Only (Excluding G)			Extrapolated from Measured Stresses		
	Axial Stress (ksi)	Bending Stress (ksi)	Max. Total Stress (ksi)	Axial Stress (ksi)	Bending Stress (ksi)	Max. Total Stress (ksi)
1	3.61	0.49	4.10	4.21	0.77	4.98
2	4.28	0.76	5.04	5.32	2.04	7.36
3	0.82	0.16	0.98	0.99	0.16	1.15
4	0.52	0.04	0.55	0.37	0.07	0.44

### ***Truck Gusts***

The effect of truck-induced gusts on the cantilever structure was also examined. Overall, the truck gusts did not seem to be much of an issue for this particular sign due to location specific factors. As seen back in Figure 2.2-2, the sign is located directly over an exit with a posted speed limit of 35 mph. Therefore, the trucks are either not exiting (and thus not traveling under the cantilever), or they are exiting and traveling under the cantilever but slowing down fairly rapidly. It would be rare to encounter a truck passing under this sign at normal highway speeds.

In order to verify that truck-induced gusts are not a critical factor for this structure, the strain and acceleration data was acquired on a calm day. As a truck passed under the sign, the type was recorded and its picture was taken. Pictured below in Figure 6.3-5 are the four trucks that correspond to the 72-sec acceleration record shown in Figure 6.3-6. Trucks 1, 3, and 4 have deflectors of some type. Truck 2 does not have a deflector and is the only truck in this record to pass directly under the sign as it exits. Also note that Truck 4 follows quite closely behind Truck 3, as seen in the picture of Truck 3.

Truck 2 causes the greatest horizontal vibration, with a peak response of 0.039 g. Trucks 1, 3, and 4 induce horizontal excitation similar to one another, with peaks in the range of 0.026 g. This shows that a truck passing more directly under this sign will have a greater effect, even at a reduced speed, than a truck not passing directly under the sign. The vertical acceleration also reaches its peak of 0.015 g shortly after Truck 2 passes under the sign. In relation to the accelerations achieved during the manual excitation test, these are quite small. To put them into perspective, the largest strain experienced by a chord for all four trucks was only about 0.2 ksi, with a maximum stress range of about 0.4 ksi.

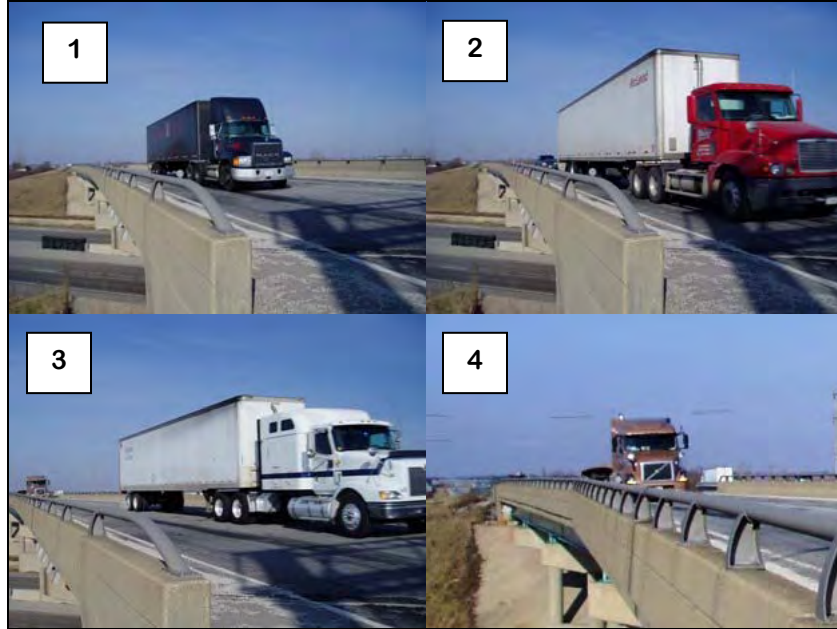


**Figure 6.3-5 Trucks passing under the cantilever sign structure: 1 upper left; 2 upper right; 3 lower left; 4 lower right**

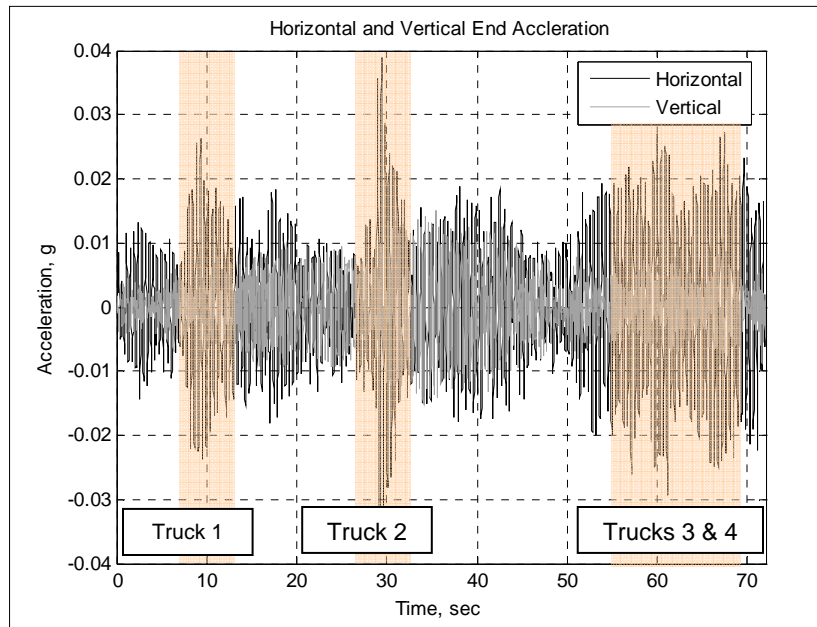


**Figure 6.3-6 Acceleration response at end of the cantilever for trucks 1 through 4**

## Code Check

### Design Wind Load

To verify the design calculations for wind loading, the results of the analytical model and field measurements for the cantilever were examined and compared to allowable stress values. The values calculated for the dead load from the model plus the values extrapolated from measured stresses due to the wind are shown in Table 6.3-2.

**Table 6.3-2 Cantilever stresses due to measured (extrapolated) design wind load + model dead load**

<b>Member</b>	<b>Max. Total Stress (ksi)</b>
1	6.68
2	9.51
3	1.31
4	0.87

Included in the table then are stresses that represent the expected average stress in a 90 mph wind event. These values are well below the allowable stress values of 14.63 ksi (tension) and 15.96 ksi (compression). One reason that the stresses are low compared to the design values is that the demand on this design here is lower than the demand level for which it was designed. The truss currently has a sign with an approximate area of 152 ft<sup>2</sup>, which is less than half of the allowed total sign area of 340 ft<sup>2</sup>.

### Fatigue

The fatigue design specifications (AASHTO, 2001) are based on a yearly mean wind speed of 11.2 mph. In order to compare the results that were obtained in the field to the AASHTO design formulas, the maximum value of stress in each member was determined for wind speeds ranging from 10.9 mph to 11.5 mph acting normal to the truss. These values were then compared to the Constant Amplitude Fatigue Limits (CAFL) for each member. To show the combined effect of a mean wind speed of 11.2 mph and truck gusts, the stresses from each event were superimposed.

Table 6.3-3 shows the combination of the response to the 11.2 mph wind and the truck gust for each member.

**Table 6.3-3 Measured stresses compared to CAFL values for the cantilever truss**

<b>Member</b>	<b>Max. Response to 11.2 mph Wind (ksi)</b>	<b>Max. Response to Truck Gust (ksi)</b>	<b>11.2 mph Wind + Truck Gust (ksi)</b>	<b>CAFL (ksi)</b>
1	0.97	0.36	1.33	1.9
2	0.47	0.46	0.93	1.9
3	0.59	0.33	0.92	0.44
4	0.30	0.21	0.51	0.44

The response values given above were measured when the damper was in the original location at the mid-span of the truss. From the results of the damping tests, it can be assumed that the response would be somewhat higher without the damper. For members 1 and 2 (which are chords), the stress ranges are well below the CAFL. Member 3 is a horizontal diagonal and member 4 is an interior diagonal. These members experience stress ranges above the CAFL even though the sign area is smaller than allowed and the truck speeds are less than 65 mph (and in one case even just the wind load alone is sufficient to exceed the CAFL).

#### **6.4 Response of Type I-A Sign Structure to Wind Loads and Truck Gusts**

##### ***Wind Loads***

Strong wind data was collected for this sign structure on two separate days. On March 18, 2005, the normal component of the wind speeds ranged between 10 and 32 mph. This resulted in excellent wind, strain, and acceleration data. A total of six records were logged, with durations close to 6 minutes each. Data was collected again on April 7, 2005, when continuous records were taken back-to-back for 40 minutes and then 20 minutes. Later, these were combined to form a 1-hour long record. There were significant stretches where wind speeds were in excess of 20-mph, and several peaks above 30-mph. This full wind record is plotted in Figure 6.4-1.

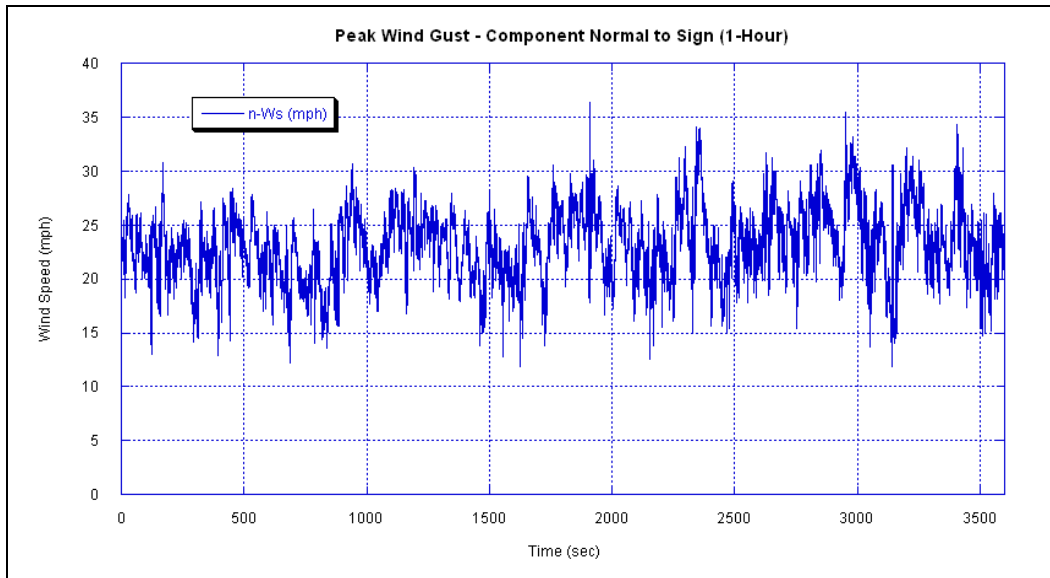


**Figure 6.4-1 Type I-A hour-long wind record**

The measured stresses in the members were processed in the same manner as described above for the cantilever structure. The extrapolated stresses measured in the two chords are shown in Figure 6.4-2. Measured axial and bending stress for one chord member are shown in Figure 6.4-3. A comparison of member stresses calculated (using the analytical model) for the design wind loads with the extrapolated measured member stresses is shown in Table 6.4-1. The extrapolated measured stresses are substantially larger than the calculated values. This mainly results from the drag coefficient that is used for design being too small. Also, the dynamic response of the structure is not considered in design. The results indicate that the percentage of the total stress contributed from bending is larger for the measured values than for the calculated ones. This is probably the result of small member eccentricities resulting from the fabrication of the truss that are not included in the analytical model.

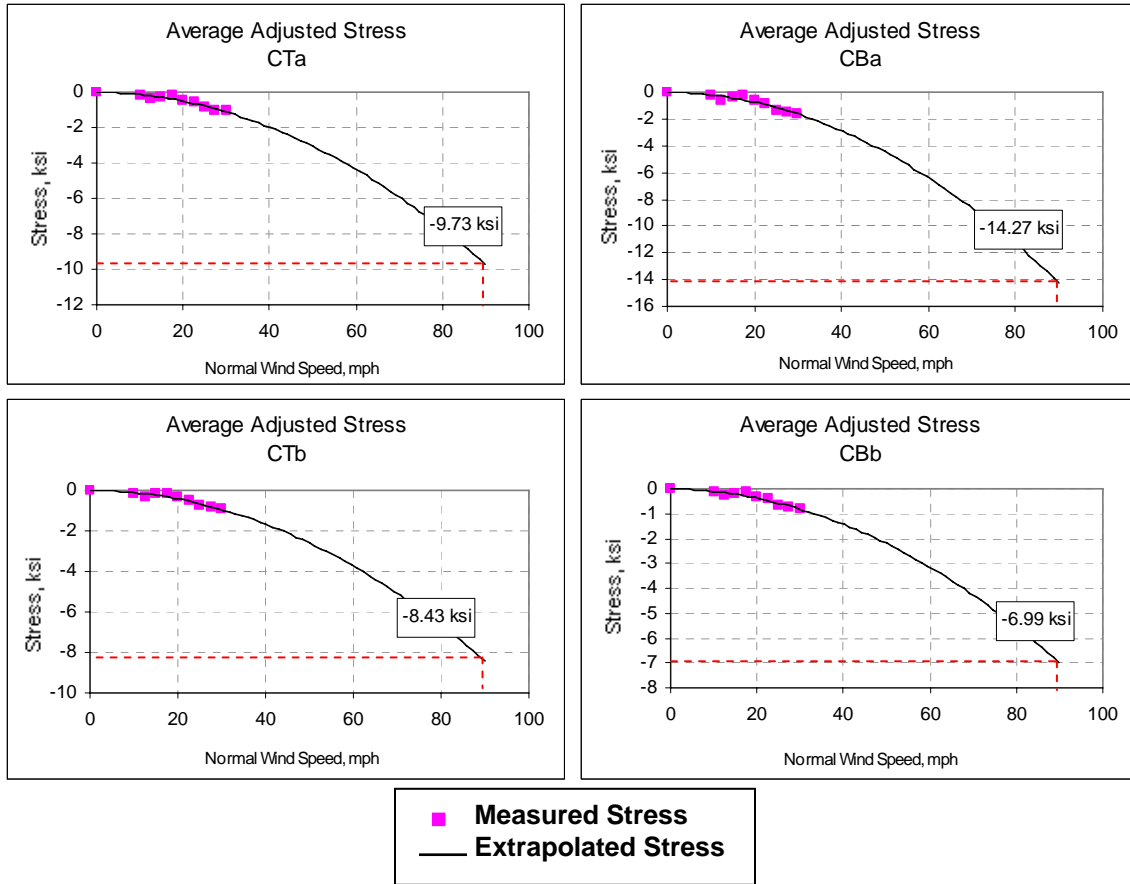


**Figure 6.4-2 Type I-A stress values in chord members under normal wind loading**

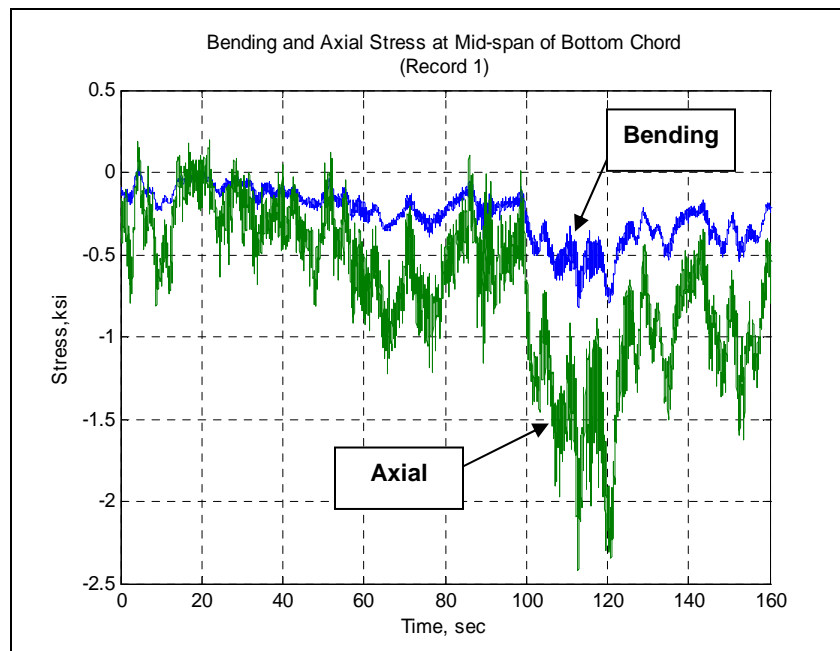


**Figure 6.4-3 Type I-A bending and axial stress in chord member**

**Table 6.4-1 Comparison of measured stresses to model stresses for Type I-A truss**

Member	Analytical Model – Wind Loads Only					Extrapolated from Measured Stresses				
	Axial Stress (ksi)	Bending Stress (ksi)	Max. Total Stress (ksi)	% Axial	% Bending	Axial Stress (ksi)	Bending Stress (ksi)	Max. Total Stress (ksi)	% Axial	% Bending
Chord Bottom	5.09	0.74	5.83	88	12	10.63	4.19	14.82	71.7	28.3
Chord Top	4.91	1.25	6.16	80	20	9.08	0.75	9.83	92.4	7.6
Horizontal	0.72	0.05	0.77	93	7	2.84	0.50	3.34	85.0	15.0
Interior Diagonal	0.76	0.71	1.47	82	18	0.66	1.25	1.91	35.0	65.0
Vertical Diagonal	0.24	0.09	0.33	72	28	0.94	0.49	1.43	65.7	34.3

***Truck Gusts***

As part of this research, truck gust excitation was studied to understand its affect on the IDOT sign structures. The subject raises concern on busy highways where high-cycles of low-stress could lead to fatigue. To approach this issue, trucks were divided into several categories. The six main categories of trucks investigated in this study are summarized in Figure 6.4-4 below.



**Figure 6.4-4 Examples of six truck classes identified for Type I-A sign bridge**

Qualitative data was collected while instrumenting the signs and it was concluded that the worst truck gusts seemed to come from oversized loads such as prefabricated homes, boxy trailers, and cabs without any trailer in tow. Tankers and flat beds seemed to be the most streamlined. Coal trailers created large turbulence observed roadside, while the gusts above them were quite small—these trucks have a small impact on the sign structures.

The process of obtaining truck gust data began with logging data continuously for 10 minute to half-hour intervals. The time and type of each truck passing under the sign structure was noted, and photos were taken. The individual gusts were later isolated from

the longer records back in the lab. These were then reassembled in files dedicated to each of four main types of trucks: 1) typical boxy trailer (with deflector, without deflector, tandem trailers), 2) tankers, 3) flat bed trailers, and 4) cabs without trailers in tow. These new files are plotted in Figures 6.4-5 through 6.4-8 for comparison of the horizontal and vertical excitation created by each respective truck type.



**Figure 6.4-5 Gust excitation from typical trailer – horizontal (left) and vertical (right) acceleration**

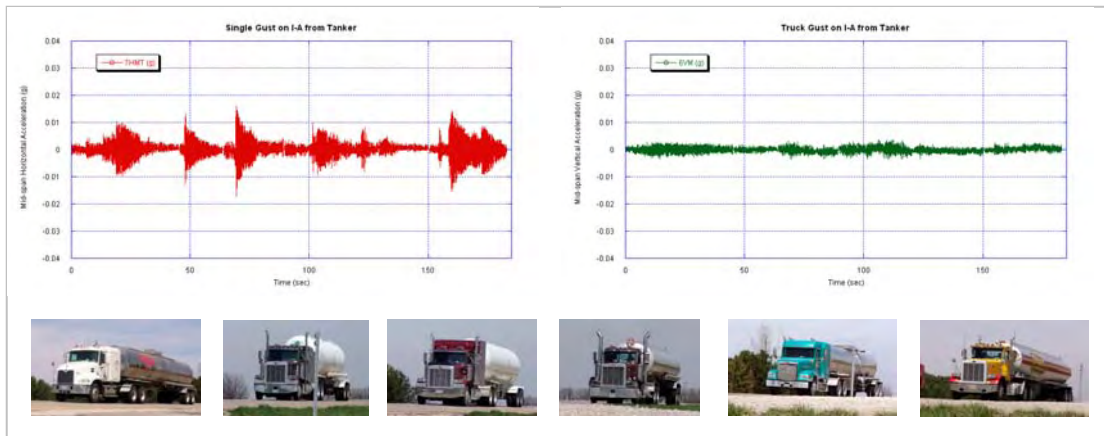


**Figure 6.4-6 Gust excitation from tanker – horizontal (left) and vertical (right) acceleration**

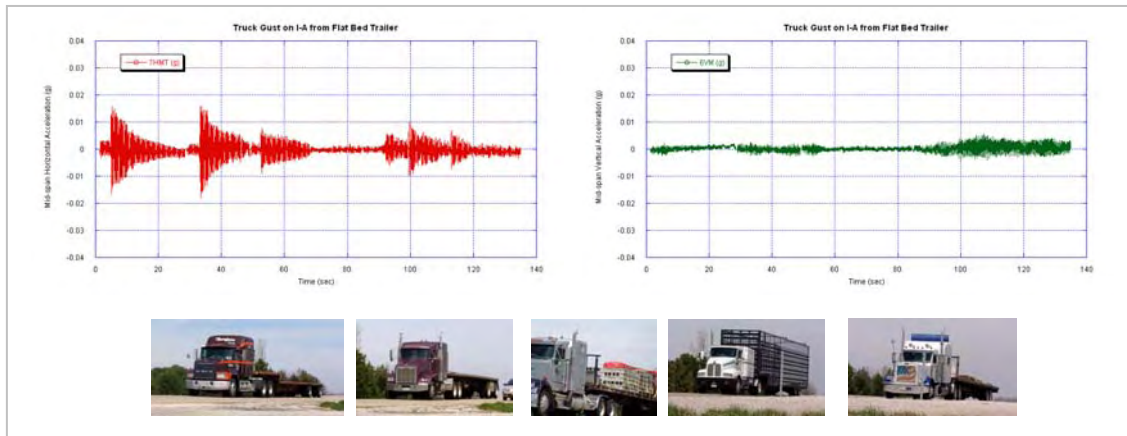


**Figure 6.4-7 Gust excitation from flatbed – horizontal (left) and vertical (right) acceleration**

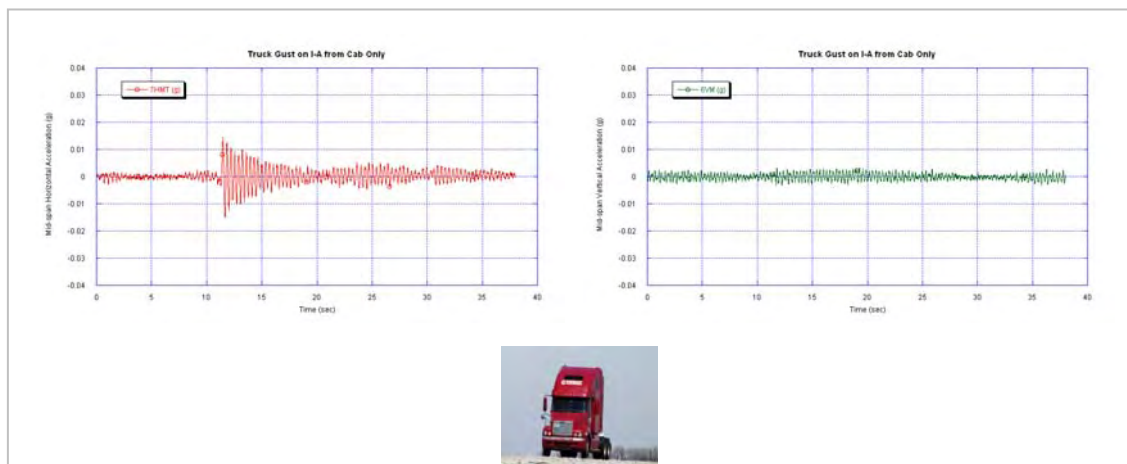


**Figure 6.4-8 Gust excitation from cab only – horizontal (left) and vertical (right) acceleration**

The above plots have been produced on a consistent scale for both horizontal and vertical acceleration. One feature of the complementary horizontal and vertical graphs is that it may be seen that sometimes when the horizontal component of acceleration is large, the vertical component is small (and vice versa). Peak horizontal accelerations reach a maximum of a little above 0.03 g.

Examining the response to the first category of trucks (typical boxy trailers), there are three notable gusts toward the end of the record. These are enlarged in Figure 6.4-9 below (for horizontal acceleration), next to a photo of the respective truck responsible for the gust.

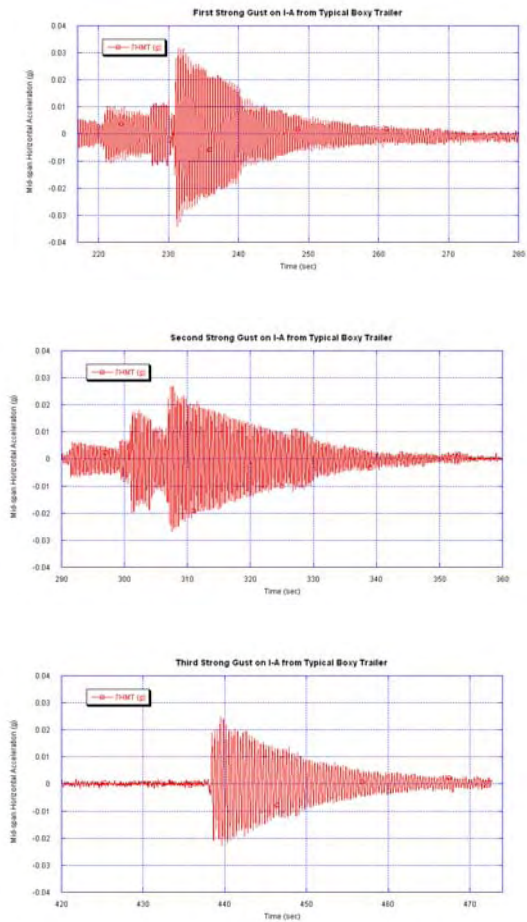


**Figure 6.4-9 Horizontal response of Type I-A structure to the three largest truck gusts**

- 1) In the top two graphs, there appear to be several gusts present in the excitation record. It is possible that this comes from the turbulent air over the cab. The first jump corresponds to the grill and windshield, the second to the gap between the cab and the trailer (the second truck had an exaggerated gap between the cab and trailer, which is reflected in the acceleration plot), and the third (primary gust) to the end of the trailer.
- 2) The influence of the deflector on the tandem truck (third truck gust) is apparently effective in smoothing out the airflow over the cab.

Aside from infrequent oversized loads, the strongest gusts come from typical boxy trailers, as can be seen from the plots above. The highest recorded horizontal acceleration due to truck gusts was 0.032 g, as seen in the top plot of Figure 6.4-9. The estimated member stresses from this are discussed below in the code check section.

## *Code Check*

### Design Wind Load

The following table (6.4-2) represents extrapolated measured stresses due to wind, plus the dead load calculated from the model.

**Table 6.4-2 Type I-A stresses due to measured (extrapolated) design wind load + model dead load**

<b>Member</b>	<b>Total Stress (ksi)</b>
Chord Bottom	16.7
Chord Top	12.2
Horizontal	3.27
Interior Diagonal	1.22
Vertical Diagonal	4.03

The stress in the bottom chord member here is not below the allowable stress values of 14.63 ksi (tension) and 15.96 ksi (compression). However, they are still well below the yield stress, so there is no significant cause for concern. The original design stresses were calculated using the gust effect factor from the code, which is substantially smaller than the newly proposed values as described above. The dynamic response is also not included in design calculations.

### Fatigue

The fatigue design specifications (AASHTO, 2001) are based on a yearly mean wind speed of 11.2 mph. In order to compare the results that were obtained in the field to the AASHTO design formulas, the maximum value of stress range in each member was determined for wind speeds ranging from 10.9 mph to 11.5 mph (acting normal to the sign). These values were then compared to the Constant Amplitude Fatigue Limits (CAFL) for each member. To show the combined effect of a mean wind speed of 11.2 mph and truck gusts, the stresses from each event were superimposed. Table 6.4-3 shows that the combination of the response to the 11.2 mph wind and the truck gust is below the CAFL for each member. It should be noted that the AASHTO specifications do not require that fatigue be checked for a sign bridge but only for cantilever structures

**Table 6.4-3 Type I-A measured stresses compared to CAFL values**

<b>Member</b>	<b>Max. Response to 11.2 mph Wind (ksi)</b>	<b>Estimated Max. Response to Truck Gust (ksi)</b>	<b>11.2 mph Wind + Truck Gust (ksi)</b>	<b>CAFL (ksi)</b>
Chord Bottom	0.51	0.33	0.84	1.9
Chord Top	0.35	0.23	0.58	1.9
Horizontal	0.11	0.32	0.43	0.44
Interior Diagonal	0.06	0.02	0.08	0.44
Vertical Diagonal	0.15	0.21	0.36	0.44

**6.5 Response of Type II-A Sign Structure to Wind Loads and Truck Gusts**

**Wind Loads**

Strong wind data for this structure was recorded on a single day, March 31, 2005. The component of the wind velocity acting normal to the sign ranged between 8 and 29 mph during data collection. Figure 6.5-1 is a plot of one record of the normal component of the wind velocity acting on the truss. It represents 200 sec of data and will be used to illustrate the process of determining the stresses in the members due to various normal wind speeds.

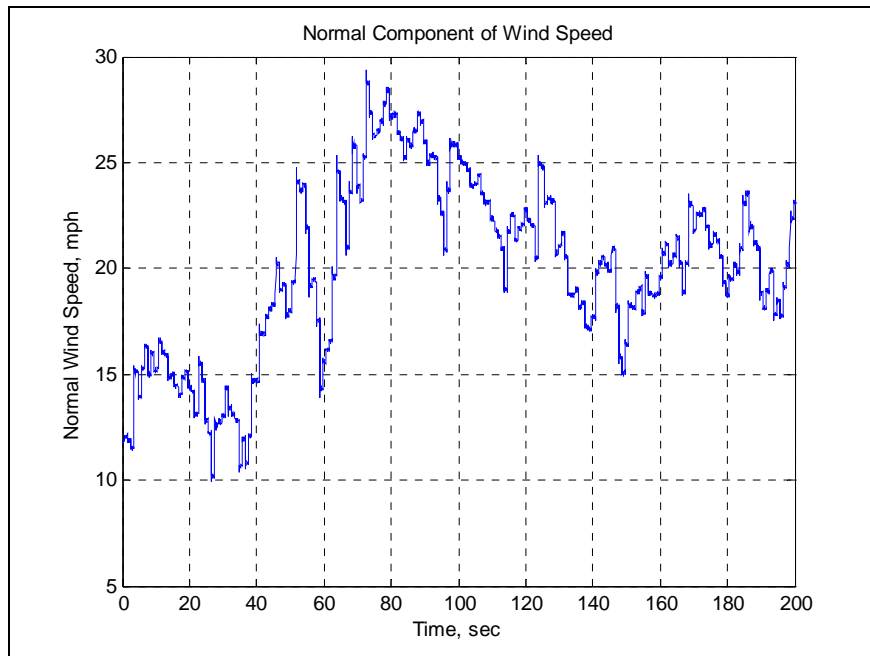


**Figure 6.5-1 Normal component of wind speed measured at Type II-A truss**

The data was collected and processed in the same manner as that described for the other structures. The zero-adjusted and extrapolated stresses for the two bottom chords are shown in Figure 6.5-2.

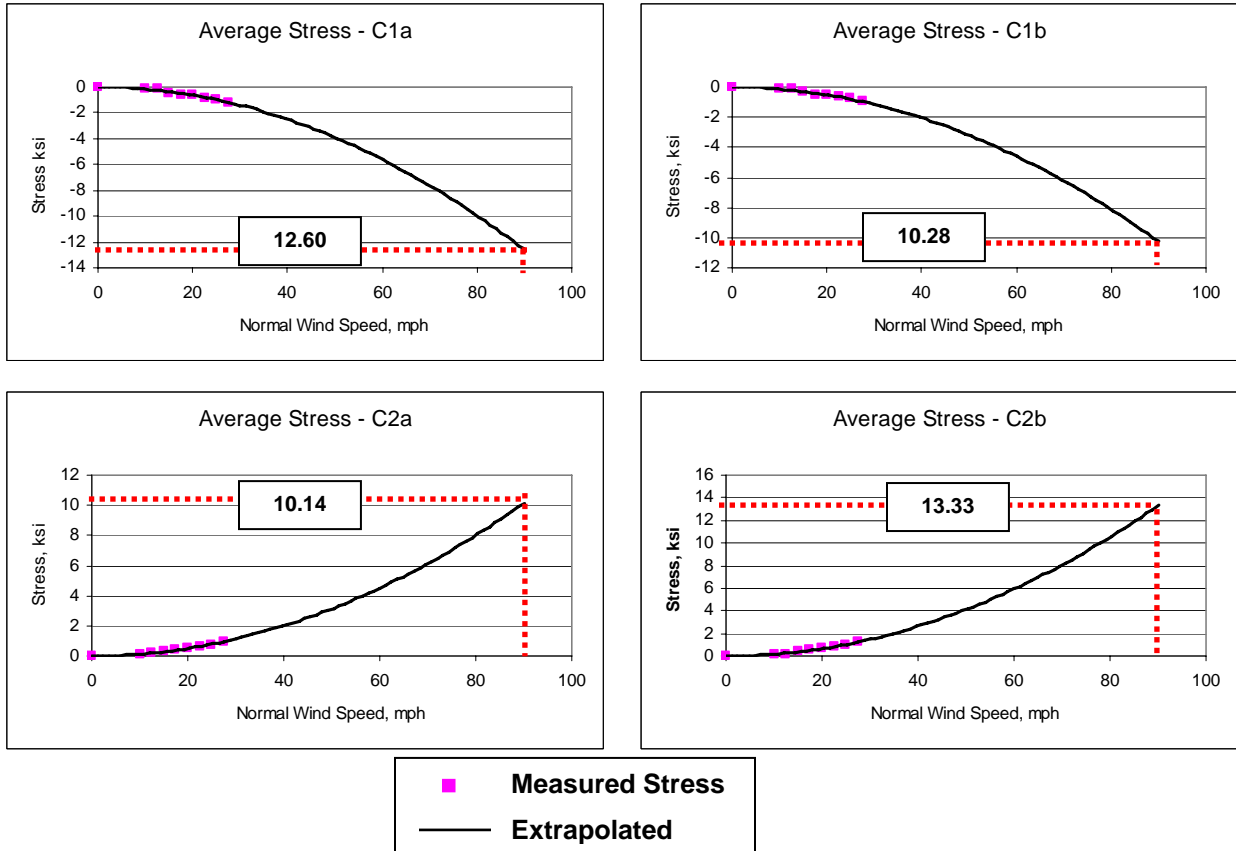


**Figure 6.5-2 Type II-A extrapolated stresses in the chord members**

Analytical model member stresses calculated using design equations are compared to measured and extrapolated values for wind load only in Table 6.5-1. These values correspond to one of the largest wind speeds recorded. The comparisons are made for stress at a point where the strain gage was located, which is not the point of maximum stress for some members. It can be seen that the estimated values for the chord stresses at the 90 mph design wind velocity are just below twice the values predicted by the model, which is about equal to the effect that would be predicted using the proposed gust factor multiplied by the dynamic effect factor.

**Table 6.5-1 Type II-A stresses calculated from the analytical model and extrapolated from measured stresses (for wind loads only)**

Member	Model – Wind Loads Only					Extrapolated from Measured Stresses				
	Axial Stress (ksi)	Bending Stress (ksi)	Max. Total Stress (ksi)	% Axial	% Bending	Axial Stress (ksi)	Bending Stress (ksi)	Max. Total Stress (ksi)	% Axial	% Bending
Chord 1	7.20	1.08	8.28	86.9	13.1	11.44	1.16	12.60	90.8	9.2
Chord 2	6.68	1.30	7.98	83.7	16.3	11.74	1.60	13.34	88.0	12.0
Horizontal	1.17	0.01	1.04	1.18	1.0	2.01	0.63	2.63	76.4	23.6
Horizontal Diag.	3.61	0.38	3.99	90.7	9.3	3.28	0.82	4.11	79.8	20.2
Vertical Diag 1	0.25	0.31	0.56	41.5	58.5	1.34	0.02	1.37	97.8	2.2
Vertical Diag 2	0.13	0.13	0.26	50.7	49.3	0.90	0.47	1.37	65.7	34.3

***Truck Gusts***

The process of obtaining truck gust data for the Type II-A truss was similar to that for the Type I-A truss. The time and type of each truck passing under the sign structure was noted and photos were taken. Individual truck gust records were identified by truck type and then isolated. These were then reassembled into files dedicated to containing gusts from trucks with specific typical trailer types (with deflector, without deflector, tandem trailers). Some representative examples of trucks with regular deflectors are shown below in Figure 6.5-3.

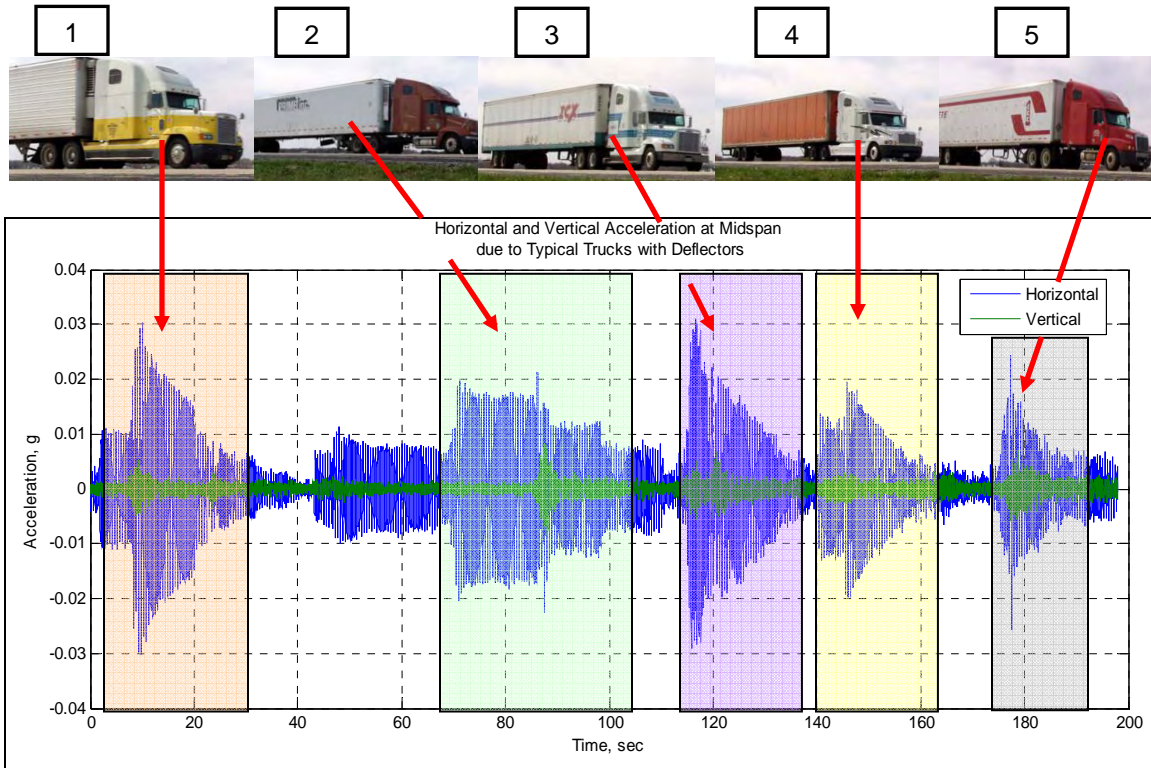


**Figure 6.5-3 Type II-A mid-span horizontal and vertical accelerations due to truck gusts**

Two of the highest truck gust responses are shown below in Figures 6.5-4 (acceleration) and 6.5-5 (resulting stresses). Truck 6 has a deflector although its slim profile can be contrasted to the typical curved deflectors seen on Trucks 1 to 5. For this reason it is referred to as a “plate deflector.” Two additional trucks for which data was also collected are shown in Figure 6.5-6. Trucks similar to Truck 9 (coal trucks) are common at the location of the II-A sign structure and are operated by Curry Ice & Coal (Carlinville, IL).

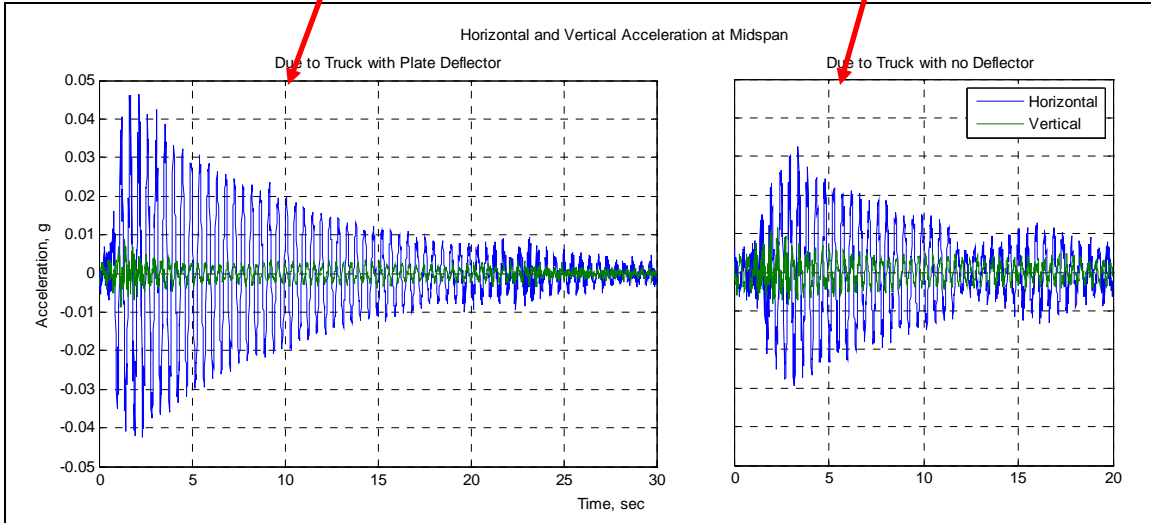


**Figure 6.5-4 Type II-A mid-span horizontal and vertical accelerations from the two largest recorded truck gusts**

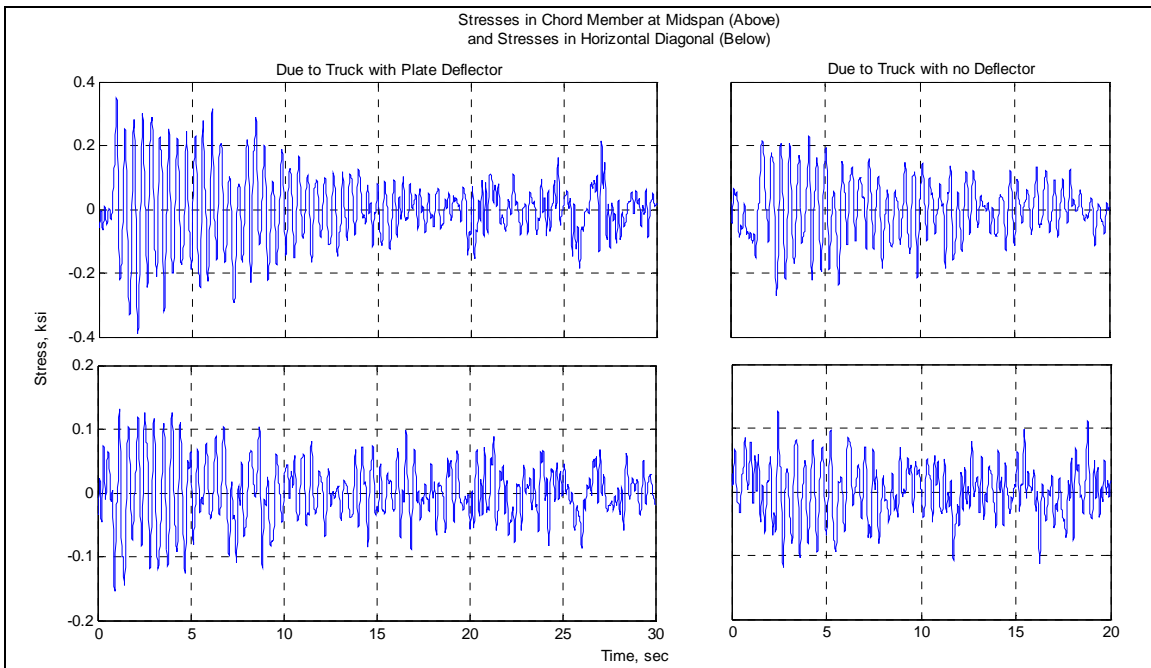


**Figure 6.5-5 Type II-A chord (top) and horizontal diagonal (bottom) stresses from the two largest recorded truck gusts**

Table 6.5-2 below gives a summary of the response of this truss to various truck types. For a typical truck with a deflector (by far the most common, trucks 1 through 5) the average maximum horizontal acceleration was about 0.25 g, with an average maximum stress in the chord of approximately 0.266 ksi. The vertical accelerations were about one-fourth the magnitude of the horizontal accelerations. The stresses in the horizontal diagonal member were fairly negligible although they were the highest measured of all of the instrumented end members.

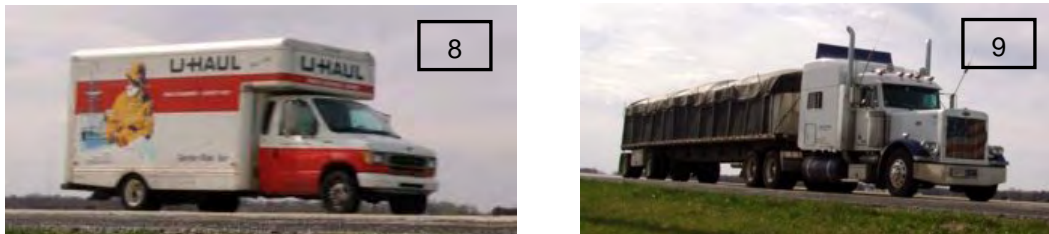


**Figure 6.5-6 Two additional trucks for the Type II-A included in Table 6.5-2**

**Table 6.5-2 Summary of Type II-A response to various truck gust types**

Truck Designation	Max. Acceleration (g)		Max. Stress (ksi)	
	Horizontal	Vertical	Chord	Horizontal Diagonal
1. Deflector, Yellow & White	0.0303	0.0053	0.294	0.176
2. Deflector, Brown	0.0213	0.0083	0.255	0.123
3. Deflector, White	0.0311	0.0069	0.278	0.137
4. Deflector, Orange Trailer	0.0195	0.0034	0.224	0.128
5. Deflector, Red	0.0243	0.0071	0.281	0.105
6. Plate Deflector	0.0464	0.0087	0.351	0.132
7 No Deflector, White	0.0327	0.0120	0.229	0.127
8. Short, U-Haul	0.0269	0.0050	0.274	0.124
9. Coal Trucks	0.0225	0.0062	0.209	0.117

**Code Check**

Design Wind Load

The following table (6.5-3) represents measured stresses in the Type II-A truss extrapolated to the 90 mph wind plus the dead load calculated from the model.

**Table 6.5-3 Type II-A total stress estimated for the design wind speed of 90 mph – measured (extrapolated) wind + model dead load stresses**

<b>Member</b>	<b>Total Stress, (ksi)</b>
Chord 1	16.5
Chord 2	17.4
Horizontal	2.97
Horizontal Diag.	3.82
Vertical Diag. 1	4.06
Vertical Diag. 2	3.68

The values in the chord members are not below the allowable stress values of 14.63 ksi (tension) and 15.96 ksi (compression), although this scenario does represent just about the absolute worst-case situation.

Fatigue

The fatigue design specifications (AASHTO, 2001) are based on a yearly mean wind speed of 11.2 mph. In order to compare the results that were obtained in the field to the AASHTO design formulas, the maximum value of stress in each member was determined for wind speeds ranging from 10.9 mph to 11.5 mph acting normal to the truss. These values were then compared to the Constant Amplitude Fatigue Limits (CAFL) for each member. To show the combined effect of a mean wind speed of 11.2 mph and truck gusts, the stresses from each event were superimposed. Table 6.5-4 shows that the combination of the stress range response to the 11.2 mph wind and the truck gust is larger than the CAFL in each of the non-chord members evaluated. As mentioned above, AASHTO does not require that sign bridges be designed for fatigue.

**Table 6.5-4 Type II-A measured fatigue stresses compared to CAFL values**

<b>Member</b>	<b>Max. Response to 11.2 mph Wind (ksi)</b>	<b>Max. Response to Truck Gust (ksi)</b>	<b>11.2 mph Wind + Truck Gust (ksi)</b>	<b>CAFL (ksi)</b>
Chord 1	0.52	0.70	1.22	1.9
Chord 2	0.44	0.82	1.26	1.9
Horizontal	0.12	0.40	0.52	0.44
Horizontal Diag.	0.19	0.53	0.72	0.44
Vertical Diag. 1	0.08	0.40	0.48	0.44
Vertical Diag. 2	0.09	0.38	0.47	0.44

The code check for strength under the 90 mph wind revealed that both chords will likely be overstressed (vs. allowable values), one by 24% and the other by 18%. This should not be too large of a concern because these expected stresses are still well within the elastic stress range of the material. It is not likely, but still possible, that an extra large gust could cause minor yielding in the heat affected zones near the welds (especially in light of the expected residual stresses), but this is a ductile material so collapse of the truss is very unlikely. All of the connecting (web) members between the chords are not likely to approach the yield condition. Contrary to the strength limit state, it is the connecting members that are the most problematic with regard to fatigue. All of the non-chord members will experience stress ranges larger than the CAFL under a combination of 11.2 mph wind and truck gusts. The horizontal diagonal may have stress reversals larger than the CAFL under truck gusts alone. It may be feasible to add dampers to reduce the response of the structure under truck gusts. This solution will be addressed in the next chapter of this report.

## 6.6 Response of the Type III-A Sign Structure to Wind Loads and Truck Gusts

### *Wind Loads*

To determine the Type III-A truss response to strong wind events, acceleration, strain, and wind data were collected on a day when the wind speed acting normal to the truss exceeded 30 mph. Almost an hour of data was collected on November 3, 2005, when the recorded normal wind speed reached as high as 38.2 mph. The combined wind records for that time period are shown in Figure 6.6-1.

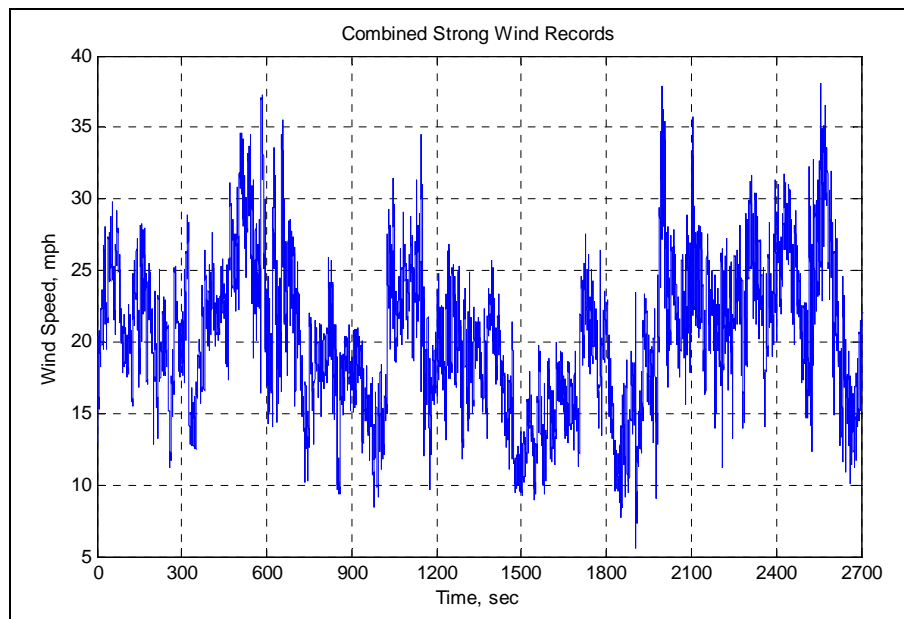


**Figure 6.6-1 Combined strong wind records recorded for the Type III-A truss on November 3, 2005**

The data was processed in the same manner as already described for the other structures. Figure 6.6-2 shows the curves of the 3-sec average stresses in each chord member as a function of normal wind speeds. The curves were generated by fitting a quadratic function to the data such that the curve goes to zero at zero wind speed. The boxed-in numerical values indicate the expected average stress value for a 90 mph wind. Similar curves were also developed for the web members.

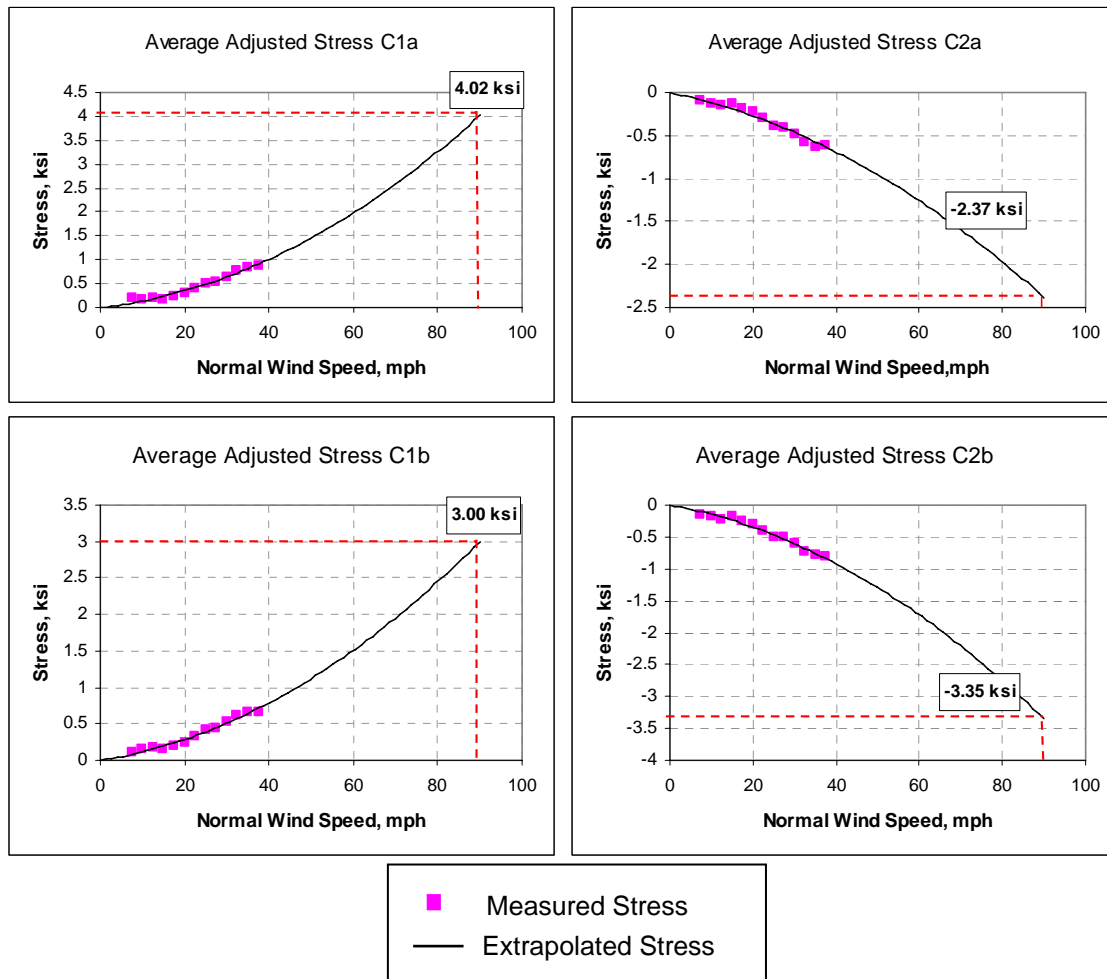


**Figure 6.6-2 Type III-A stress in chord members vs. 3-sec average normal wind speed**

Measured and calculated stresses in several truss members are compared in Table 6.6-1. The comparisons are made for sign structure response to one of the largest wind speeds recorded. The comparisons are made for each member at the location of the strain gages, which in some cases is not the point where the maximum strain occurred. Unlike for the previous structures, these stresses are comparable in magnitude for both estimates.

**Table 6.6-1 Type III-A comparison of extrapolated measured stresses to model stresses.**

Member	Model – Wind Loads Only					Extrapolated from Measured Stresses		
	Axial Stress (ksi)	Bending Stress (ksi)	Max. Total Stress (ksi)	% Axial	% Bending	Axial Stress (ksi)	Bending Stress (ksi)	Max. Total Stress (ksi)
Chord 1	4.00	0.58	4.58	87.3	12.7	5.17	0.48	5.65
Chord 2	3.26	0.57	3.83	85.4	14.6	2.72	0.67	3.39
HD	3.44	0.84	4.28	80.4	19.6	3.13	0.28	3.41
VD1	1.19	0.38	1.57	75.5	24.5	0.51	0.15	0.65
VD2	0.46	0.21	0.67	68.6	31.4	0.56	0.27	0.83

***Truck Gusts***

Accelerations and strains due to truck gusts were obtained on two separate days when the ambient wind conditions were calm (less than about 10 mph). Over the course of the two days, 200 trucks passing under the truss were recorded. During the tests, the type of truck was recorded in order to determine which types, if any, induced the greatest structural response.

The type of trucks that were recorded include: typical trucks with single trailers, typical trucks with flow deflectors on the cab, trucks with shorter boxy trailers, flatbed trailers, and tankers. Over the two days and for the 200 trucks that were observed, there were none with multiple trailers.

There is not conclusive data on which truck type causes the highest response in this truss. The response is not only dependent on the truck type but also its travel speed, whether multiple vehicles are passing underneath, whether many vehicles in a row are passing underneath and what the wind conditions are at that particular time. The horizontal motion of the truss dominates the response to the truck gusts.

Figure 6.6-3 shows the measured acceleration at the center of the structure for a 500 sec period of testing. Figure 6.6-4 shows an expanded part of this record during the time of maximum response. Table 6.6-2 then gives the maximum acceleration and maximum stress recorded in a chord member and a horizontal diagonal; note that these are peak stresses and not stress ranges.

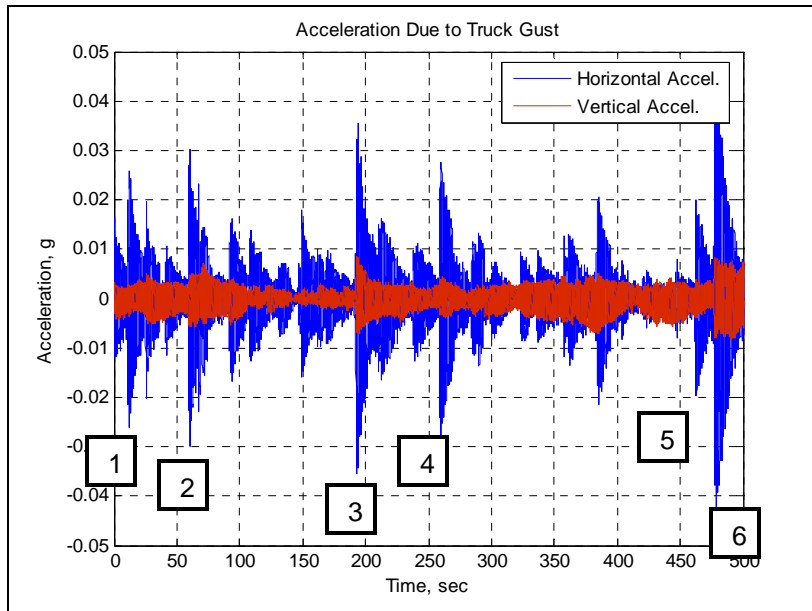


**Figure 6.6-3 Type III-A horizontal and vertical accelerations from truck gusts**

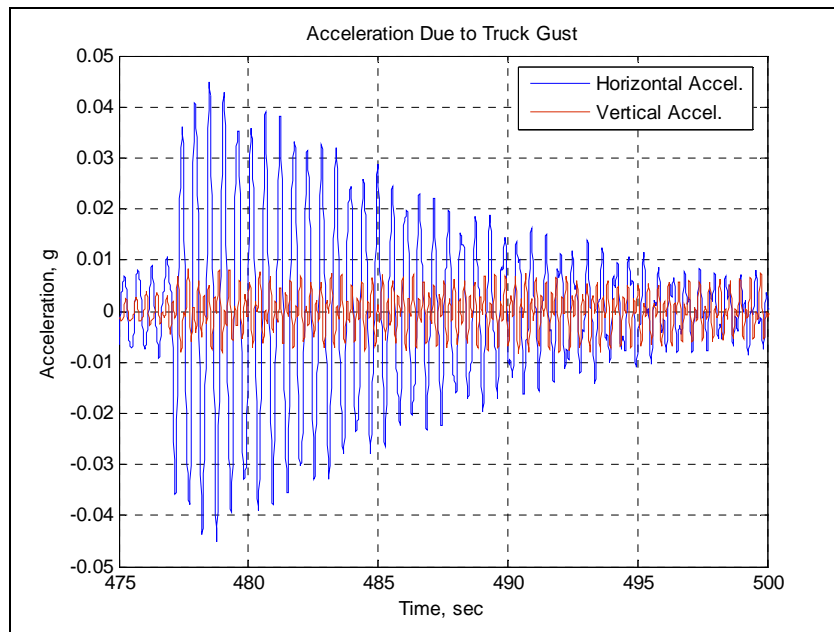


**Figure 6.6-4 Detail of horizontal and vertical accelerations - Truck 6**

**Table 6.6-2 Type III-A acceleration and member stresses due to truck gusts**

Truck Number	Truck Type	Peak Values		
		Horizontal Acceleration (g)	Chord Stress (ksi)	Horizontal Diagonal Stress (ksi)
1	Typical with deflector	0.0267	0.167	0.155
2	Typical with deflector	0.0303	0.216	0.168
3	Typical w/o deflector	0.0355	0.275	0.170
4	Typical w/o deflector	0.0276	0.257	0.201
5	Typical w/o deflector	0.0200	0.162	0.131
6	Typical with deflector	0.0453	0.381	0.280

**Code Check**Wind Loads

To verify the design calculations for wind loading, the results from the analytical model and field measurements were examined and compared to allowable stress values. The values calculated for the dead load from the model plus the values extrapolated (to 90 mph) from measured stresses due to the wind are shown in Table 6.6-3.

**Table 6.6-3 Type III-A stresses due to measured (extrapolated) wind load + model dead load**

Member	Total Stress (ksi)
Chord 1	5.60
Chord 2	5.10
Horizontal Diagonal 1	5.46
Vertical Diagonal 1	4.14
Vertical Diagonal 2	3.47

Included in the table are stresses that represent the expected average peak stress in a 90 mph wind event. These values are well below the allowable stress values of 14.63 ksi (tension) and 15.96 ksi (compression). One reason that the stresses are low compared to the design values is that the demand on the design is lower than the demand it was designed for. The total sign area currently installed on the truss is less than 50-percent of the maximum allowed, and the length of the truss is 8-ft less than the allowed 150-ft span.

Fatigue

The fatigue design specifications (AASHTO, 2001) are based on a yearly mean wind speed of 11.2 mph. In order to compare the results that were obtained in the field to

the AASHTO design formulas, the value of stress in each member was determined for wind speed of 11.2 mph acting normal to the truss. These values were then compared to the Constant Amplitude Fatigue Limits (CAFL) for each member. To show the combined effect of a mean wind speed of 11.2 mph and truck gusts, the stresses from each event were superimposed. Table 6.6-4 shows that the combination of the response to the 11.2 mph wind and the truck gust is below the CAFL for each member.

**Table 6.6-4 Measured stress ranges compared to CAFL values**

<b>Member</b>	<b>Max. Response to 11.2 mph Wind (ksi)</b>	<b>Max. Response to Truck Gust (ksi)</b>	<b>11.2 mph Wind + Truck Gust (ksi)</b>	<b>CAFL (ksi)</b>
Chord 1	0.37	0.66	1.03	1.9
Chord 2	0.38	0.88	1.26	1.9
Horizontal Diagonal 1	0.47	0.84	1.31	0.44
Vertical Diagonal 1	0.29	0.08	0.37	0.44
Vertical Diagonal 2	0.15	0.04	0.19	0.44

For this truss, only the horizontal diagonal member experienced a stress range larger than the CAFL. Unlike the previous structure, the CAFL was exceeded under both an 11.2 mph wind speed and truck gusts acting separately. It should be noted that AASHTO does not require that fatigue be checked for span type structures, only cantilever structures.

## **6.7 Response of the VMS Structure to Wind Loads and Truck Gusts**

To determine the VMS truss response to strong wind events, acceleration, strain and wind data were collected on a number of windy days. Unlike for the other signs, the VMS sign instrumentation could be monitored remotely; the recording devices could be triggered to begin recording data when the wind speed exceeded a certain threshold value. Almost an hour of data was collected on November 3, 2005 where the recorded normal wind speed reached 38.15 mph. The maximum wind speed measured normal to the sign was about 25 mph, which was above the minimum of 20 mph that was established at the beginning of the study. One point that can be noticed in Figure 6.7-1 is that the stresses are quite small compared to the other structures. The reason for this is that the VMS sign area is considerably smaller than could be allowed on this structure.

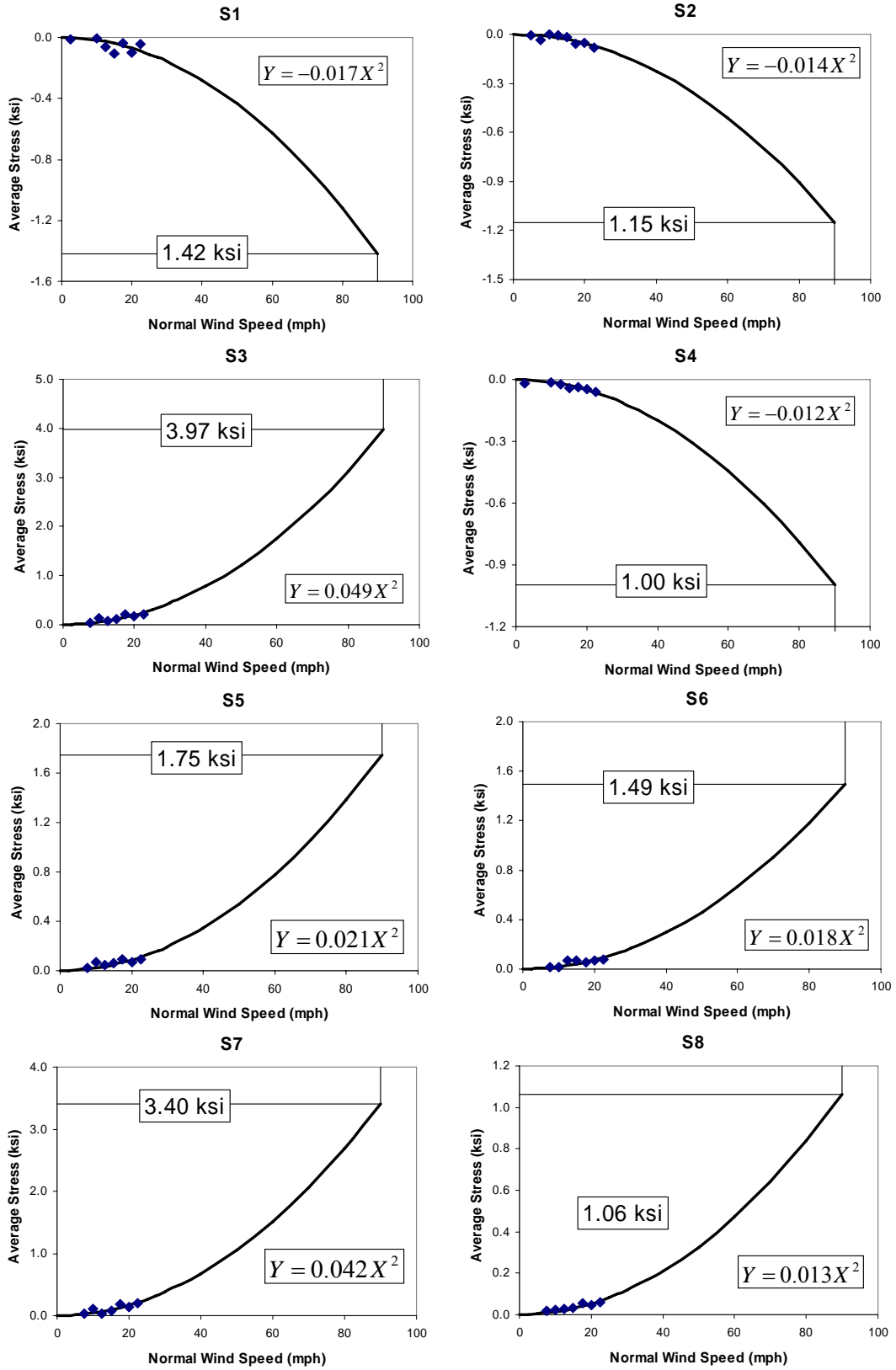


Figure 6.7-1 VMS truss average stress vs. normal wind speed at eight gage locations

**Table 6.7-1 Comparison of VMS truss measured stresses to model stresses (ksi) for 90 mph wind**

Gage	Member	Measured	Model
S1	Chord	1.42	2.60
S2	Chord	1.15	1.38
S3	Interior Diag.	3.97	0.39
S4	Horizontal Diag.	1.00	1.11
S5	Horizontal	1.75	0.25
S6	Horizontal Diag.	1.49	1.25
S7	Vertical Diag.	3.40	0.39
S8	Vertical Diag.	1.60	0.50

Table 6.7-1 gives a comparison of the measured (extrapolated) and calculated (model) 3-sec average stress in selected member locations for a 90 mph wind. As pointed out in Chapter 4, the stresses are small compared to the other structures because the area of the VMS is relatively small compared to the maximum allowable sign area for this structure. Unlike all of the other structures, the chord stresses are not larger than those in the connecting (web) members. Also, the model stresses are larger than the measured ones for the chords, but substantially smaller for the connecting members. The measured strains for this sign were considerably noisier than for the other signs; this may have resulted from an unforeseen and undetected grounding problem. Strong conclusions should probably not be drawn from this data.

#### *Truck Gusts*

A camera located at the top of the VMS truss took eight pictures (one every second) when trucks passed under the sign structure. Some events included two trucks passing under the structure almost simultaneously and created the maximum recorded response to truck gusts. In order to verify the truck-induced gusts, data was typically selected when the wind speed was very low. Figure 6.7-2 shows a group of eight pictures taken when two trucks passed. Figures 6.7-3 and 6.7-4 show the measured accelerations and strains, respectively, which correspond to the pictures in Figure 6.7-2 (the numbers in the box at each picture indicate the time in seconds for Figures 6.7-3 and 6.7-4). During this period, the average wind speed was essentially zero.

The largest acceleration was measured between four and five seconds when trucks passed by the sign structure. The maximum acceleration was 0.054 g, and the typical value was about 0.029 g for single trucks. The measured accelerations for truck gust showed that they contain high frequencies less than those for strong wind.

A comparison of the horizontal acceleration and the stress records show that they correlate very well. The maximum horizontal acceleration and chord stress occurred between 4 and 5 seconds as shown in Figure 6.7-3 and Figure 6.7-4. The maximum vertical acceleration occurred around 4 seconds, which is a little earlier than the other

values. As can be seen in Figure 6.7-2, the two trucks just passed the sign structure at between 4 and 5 seconds. The maximum stress range in the chord member (average of S1 and S2) was 0.50 ksi, which is much smaller than the fatigue stress limit of 1.9 ksi for the chord member given in the AASHTO specifications. The maximum stress range in the interior diagonal (S5) was 0.14 ksi and the maximum stress in the front diagonal (S7) was 0.20 ksi. These values are also smaller than the allowable fatigue stress range of 0.44 ksi for the diagonal truss members. Like the data for strong wind, measured strains at S7 were almost entirely noise. In the filtered record, they showed meaningless values.



**Figure 6.7-2 Pictures taken at one second intervals during truck passing (VMS truss)**

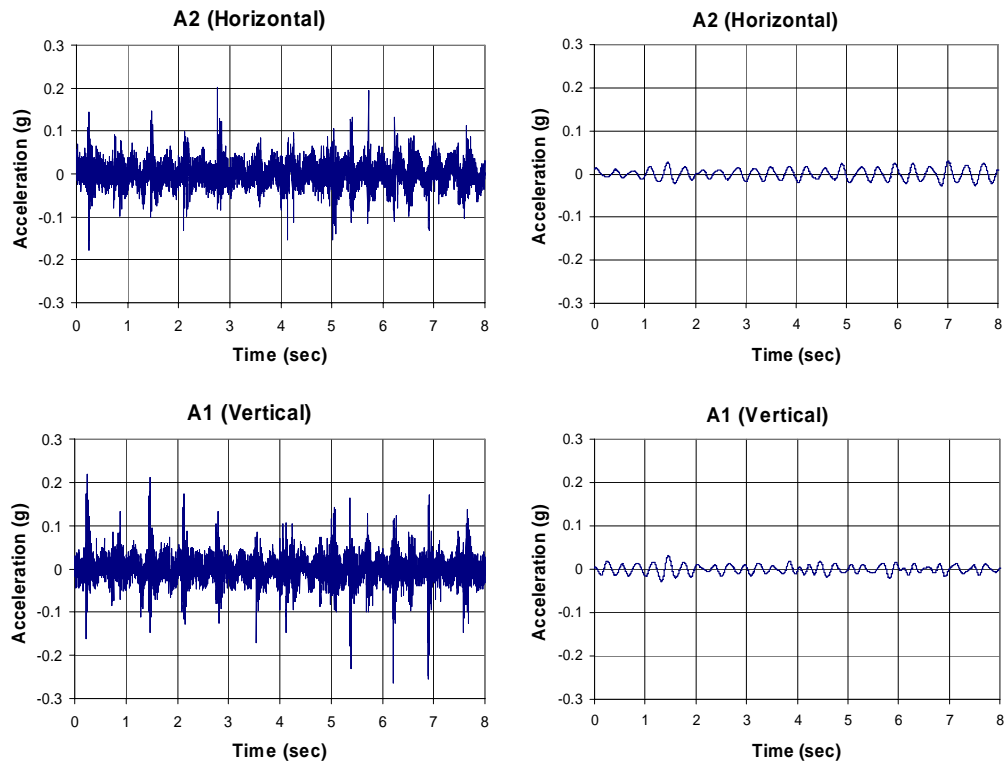


**Figure 6.7-3 Measured accelerations for strong wind; original (left), filtered (right)**

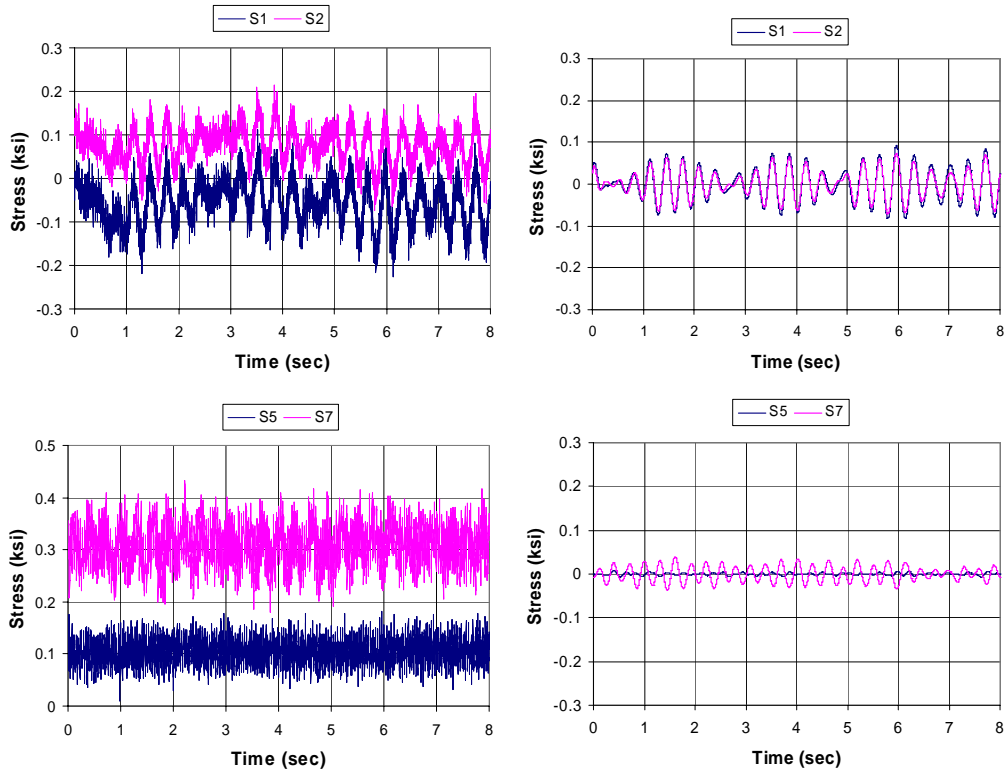


**Figure 6.7-4 Measured stresses for strong wind; original (left), filtered (right)**

### *Code Check*

Even though some of the data was corrupted, it is clear from the remaining data that the projected maximum stresses in all of the truss members will be significantly smaller than the allowable stresses. Likewise for the truck gusts, the maximum stress ranges that the members will experience will be significantly smaller than the CAFL values. In both cases, this results from the VMS sign area being much smaller than would be allowed for this structure.

## 7.0 Highway Sign Truss Damper

### 7.1 Background

In the year 2000, IDOT sought to improve the fatigue performance of their aluminum highway sign structures by implementing new standard designs for both overhead and cantilever sign trusses. These designs include the installation of vibration dampers, with the hope that they will limit the amplitude and frequency of potentially damaging truss vibrations. The dampers installed on the sign structures are a type of passive tuned mass damper (TMD) called Stockbridge-type dampers. These dampers consist of two cantilevered weights suspended by multi-stranded twisted cables extending from either side of a clamp that attaches to the structure. The weights (inertial masses) and damper cables are intended to limit the amount of vibration of the truss by absorbing energy with their own oscillations. Stockbridge dampers can be an attractive retrofit solution for highway sign structure vibrations due to their relatively low cost, ease of installation, durability, and lack of sensitivity to temperature and environmental conditions.

Stockbridge-type dampers have traditionally been used on electrical transmission lines to reduce the vortex shedding induced vibration of the lines. For that application, the dampers dissipate energy in their cables via the inter-strand friction that occurs as the cables undergo flexural deformation. The effectiveness of the damper is estimated according to an energy balance method where the total power dissipated by the damper is determined and is compared to the power introduced to the line by the wind (Bahtovska, 2000). The power dissipated by the damper is a function of its impedance, which for nonlinear systems such as the Stockbridge damper depends on both the frequency and the amplitude of the clamp vibration (Sauter and Hagedorn, 2002).

The application of Stockbridge dampers to aluminum highway sign structures can be traced back to work conducted by Lengel and Sharp (1969). The motivation for their research was excessive vibration of such structures observed after they were erected but prior to the installation of the sign panels. In some cases, cracking due to fatigue occurred in a truss before the signs were ever installed in normal wind speeds between 7 and 12 mph. In this state, the structures (or more specifically the chord members) are susceptible to vortex-shedding because the sign panels are not present to diffuse the wind flow. In fact, this vibration was only seen in the vertical mode, consistent with vortex shedding induced vibration (Lengel and Sharp, 1969).

Practical measures were sought out to reduce the wind-induced vibration in these trusses prior to sign installation. Stockbridge dampers were tested on aluminum highway sign structures by Lengel and Sharp. Similar to transmission line applications, the effectiveness of the dampers was determined in terms of the power they could dissipate relative to the power input to the structure from the wind. They were proven to be effective in mitigating the vortex-shedding induced vibration of the trusses and thus became the method of choice for vibration reduction (Sharp, 1993).

The current study aims to evaluate the effectiveness of these dampers on the structures once they are in service (with the sign panels attached). In this case, the predominant source of vibration is wind and truck gusts acting horizontally on the sign panels, causing vibration of the truss. Unlike global vortex-shedding, the response of the structure to these forces is primarily in the horizontal mode. The resulting amplitudes of vibration that are observed with the signs in place are much lower (0.01 to 0.08 in.) than those seen by Lengel and Sharp without signs (0.1 to 0.6 in.). The natural frequency of the structure also decreases upon installation of the signs (due to the increase in total mass). In the case of the IDOT structures tested, the natural frequencies in the horizontal mode range from 1.85 to 2.85 Hz, quite a bit less than for the trusses that Lengel and Sharp evaluated (4 to 11 Hz). Due to the non-linear nature of the Stockbridge dampers, both the natural frequency of the truss and also the expected amplitude of vibration must be considered when selecting effective dampers. Also, in order for the dampers to be most effective, the weight of the structure must be taken into account when selecting the weight of the damper. Modifications to currently available dampers are also explored to determine if their effectiveness can be increased.

## **7.2 Current Application**

IDOT's new sign truss designs are broken into two main groups, overhead and cantilever structures. There are three types of overhead trusses and three types of cantilever trusses, classified by their truss and member dimensions, maximum spans, and maximum total sign areas. This study focuses on four specific structures – overhead Types I-A, II-A, and III-A, and a cantilever Type II-C-A.

The drawings of the various types of IDOT sign structures show generic figures for the dampers and give mounting instructions. They are typically designated as 31-lb Stockbridge-type aluminum dampers for both overhead and cantilever structures (regardless of the span and weight of the structure). These drawings are shown in Figure 7.2-1 below.

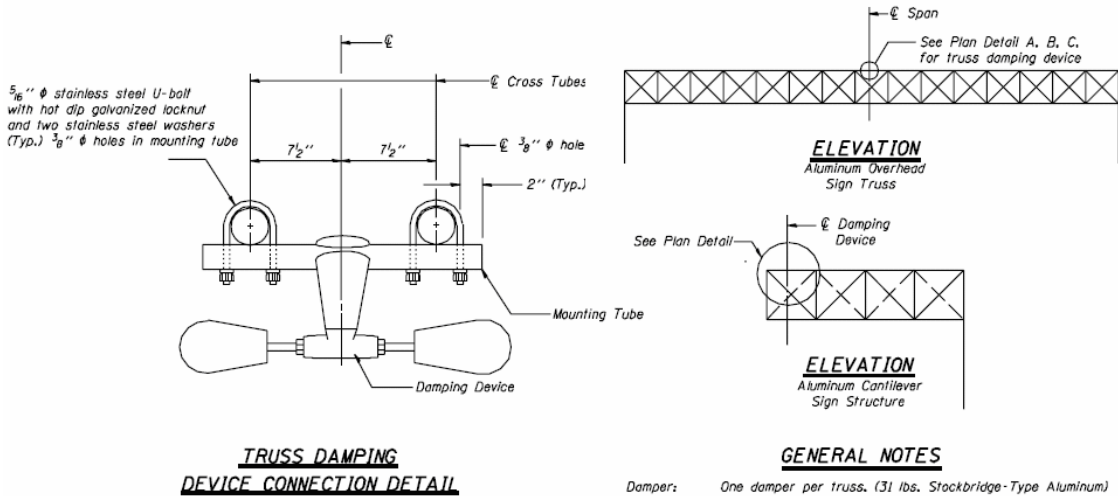


**Figure 7.2-1 Damper installation for overhead and cantilever sign structures**

Field investigations revealed that there are two distinct types of dampers actually being used by IDOT, regular dampers and *sloppy* dampers. The difference is evident in Figure 7.2-2. The manufacturer makes the distinction between these types with the term *sloppy* damper. The *sloppy* dampers refer to those whose weights are suspended by much longer cables, thereby decreasing the natural frequency of vibration of the damper. The models available from the manufacturer are shown in Table 7.2-1, and the drawings included in the damper specifications are shown in Figure 7.2-3 below



**Figure 7.2-2 Regular 31-lb damper installed on a Type II-A truss (left) and *sloppy* 15.9-lb damper installed on a Type II-C-A truss (right)**

**Table 7.2-1 Highway truss damper selection table**

Catalog Number	Total Weight (kg)	Total Weight (lbs)	Total Length, A (in.)
1706-17.1	6.8	15.0	15.75
1708-17.1	14.1	31.0	22.50
1709-17.1	15.6	34.4	24.50
1709S*-17.1	15.7	34.6	29.62

\*Note: S means the damper is *sloppy*

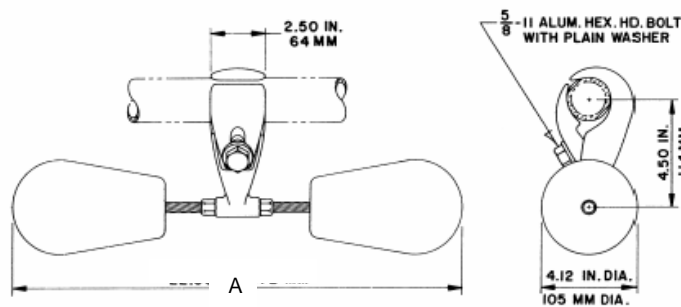


**Figure 7.2-3 Manufacturer's drawing of the Stockbridge highway truss damping device**

The damper on the cantilever truss does not appear to be any one of the recommended dampers given in Table 7.2-1. According to discussions with the manufacturer, this damper is actually a 1706-190 bus vibration damper (for use in electrical substations). This type of damper has much longer cables, with a total length of 29.5 inches, and has a nominal weight of only 15.9 lb (7.21 kg). This damper is shown in Figure 7.2-4.

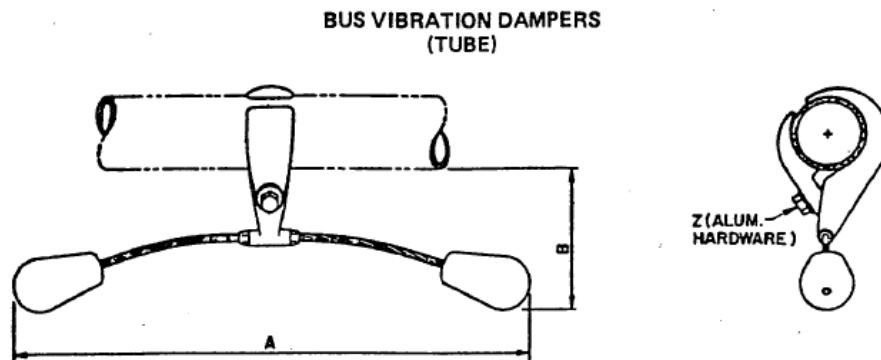


**Figure 7.2-4 1706 bus vibration damper**

The manufacturer’s website states that the 31-lb 1708-17.1 damper is the size most commonly used for highway truss applications. The dampers actually installed on the overhead trusses are indeed the regular 31-lb 1708-17.1. It is stated that a “single damper located at the mid-point of the truss will provide vibration protection for lengths between 60 and 140 ft” (AFL Tele, 2003). This statement is drawn directly from the research of Lengel and Sharp (1969), and while accurate in some cases, it is perhaps not a general rule. Typical TMDs are most effective when their own natural frequency matches the frequency of vibration to be damped, which will be discussed in more detail below in Section 7.4.

### 7.3 Experimental Testing

#### *Field Testing*

The field testing of the dampers when installed on the structures was discussed back in Chapter 5. Results from the field testing showed that the damper was moderately effective on the cantilever structure. On the overhead structures, however, there was only a slight increase in damping for the Type I-A truss, while the other trusses showed no measurable difference between their damped and undamped cases. A summary of the results for the manual field tests in the horizontal direction are shown in Table 7.3-1.

**Table 7.3-1 Field testing results – horizontal vibration**

<b>Sign Truss</b>	<b>Peak disp. (in.)</b>	<b><math>\zeta</math> without damper (%)</b>	<b><math>\zeta</math> with damper (%)</b>	<b>Horizontal <math>f_n</math> (Hz)</b>
Cantilever	1.1	1.21	1.66	2.29
Type I-A	0.4	0.80	0.84	2.84
Type II-A	0.9	1.42	1.61	2.12
Type III-A	0.7	0.80	0.80	1.85

The tests conducted on the trusses with their currently installed dampers demonstrated that the dampers are not providing a desirable level of vibration mitigation for the overhead truss structures, especially as the size (and therefore mass) of the structures increases. It seems that the only damper providing any noticeable damping was the *sloppy* type damper on the cantilever structure, presumably because it possesses a natural frequency in the range of the cantilever’s natural frequency and also because the weight of the cantilever structure is significantly smaller than the weight of any of the other sign structures. There was a small amount of additional damping measured on the Type II-A truss.

## Laboratory Testing

The purpose of the laboratory testing was to determine the frequency responses of two types of the *sloppy* dampers available from the manufacturer. Additional tests were also conducted to determine if modifications could be made to improve the dampers' effectiveness.

The dampers tested were the 1708S-17.1 and the 1709S-17.1 models. These types were chosen because it was clear that in order to more closely match the dynamic characteristics of the structures, the dampers with the lower natural frequencies would be the most effective. The geometric characteristics of these dampers are shown in the two figures below.

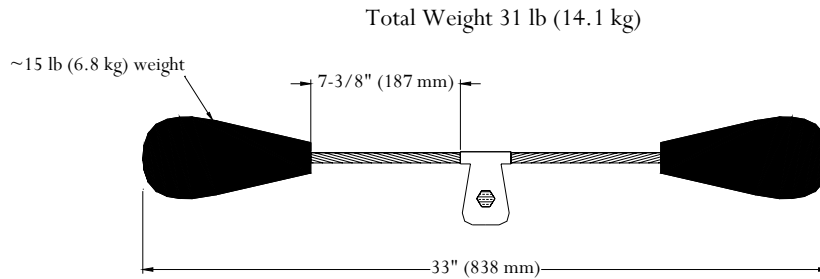


**Figure 7.3-1 1708S-17.1 damper**

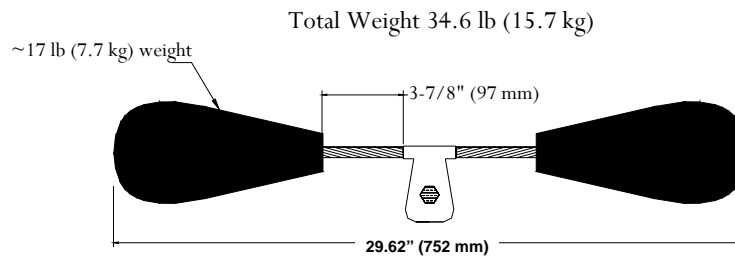


**Figure 7.3-2 1709S-17.1 damper**

## Test Method

Two sets of tests were conducted on the dampers. The first set of tests aimed to characterize the dynamic response of each damper type in their original configuration. The second set of tests involved deconstructing the dampers so that only the cable and one weight remained. This allowed the unbraced length of the cable (from clamp to weight) to be changed throughout the testing.

The tests were conducted on an MTS Universal uniaxial testing frame with a 5-k load cell. The actuator was controlled by an Instron 8500 Plus controller, and the data

was collected with a LabView-based data collector. The dampers were attached to the actuator at the clamp location to simulate attachment to the moving structure, as can be seen in Figure 7.3-3. The actuator then moved vertically with a position-controlled sinusoidal waveform while the actuator displacement and force were measured. Each step of the test was conducted for a prescribed amplitude of motion (peak-to-peak) and a prescribed frequency (there were upper limits on the maximum frequency the actuator could achieve for each amplitude). Table 7.3-2 gives a summary of each of the tests conducted for the intact dampers.

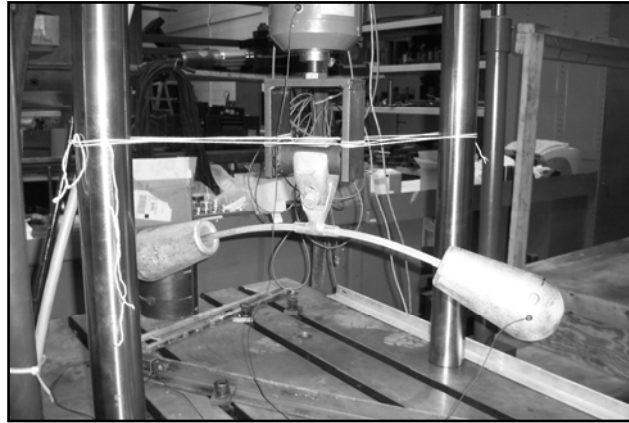


**Figure 7.3-3 In-tact damper test set-up.**

**Table 7.3-2. In-tact damper test summary**

<b>1708S-17.1 (31 lb)</b>		<b>1709S-17.1 (34.6 lb)</b>	
<b>Amplitude (in.)</b>	<b>Frequency Range (Hz)</b>	<b>Amplitude (in.)</b>	<b>Frequency Range (Hz)</b>
0.01	1.00 - 6.00	0.01	1.00 - 6.00
0.03	1.00 - 6.00	0.03	1.00 - 6.00
0.05	1.00 - 6.00	0.05	1.00 - 6.00
0.10	1.00 - 6.00	0.10	1.00 - 6.00
0.20	1.00 - 4.50	0.20	1.00 - 4.00
0.30	1.00 - 3.25	0.30	1.00 - 2.75
0.40	1.00 - 2.50	0.40	1.00 - 2.50
0.50	1.00 - 2.00	0.50	1.00 - 2.00

To determine the frequency response of the dampers, the displacements of the weights were measured throughout the tests. This was accomplished using the Krypton DMM system, which is a 3-dimensional dynamic non-contact coordinate measurement system. The Krypton DMM camera contains three linear CCD cameras consisting of 2048 elements each. The cameras triangulate the position of infrared light emitting diode (LED) targets. The system can measure the position of the LED targets to an accuracy of  $\pm 7.9 \times 10^{-4}$  in. (0.02 mm).

The tests were performed on two dampers of each type. Because each damper has two identical sides, there were four resulting sets of data for each amplitude/frequency scenario. Although the dampers are manufactured to standard specifications, there are inherently slight differences in each product. This was taken into account by averaging the four data sets to determine the overall response of each damper type.

### ***Damper Response***

Once the tests were completed, the response curves could be constructed. Figure 7.3-4 shows an example of an individual test record. The input from the actuator is represented by a dashed line, and the vertical displacement of the weight is shown as a solid line. For each of these records, the ratio of the amplitude of the response to the amplitude of the input is recorded. The process is repeated for all tests with the data points comprising the frequency response curves. There is a separate curve for each amplitude of input displacement, which then shows the ratio of the vertical displacement response to the input as a function of frequency. The maximum response, and thus the natural frequency of the damper, is characterized by the peak in the curve.

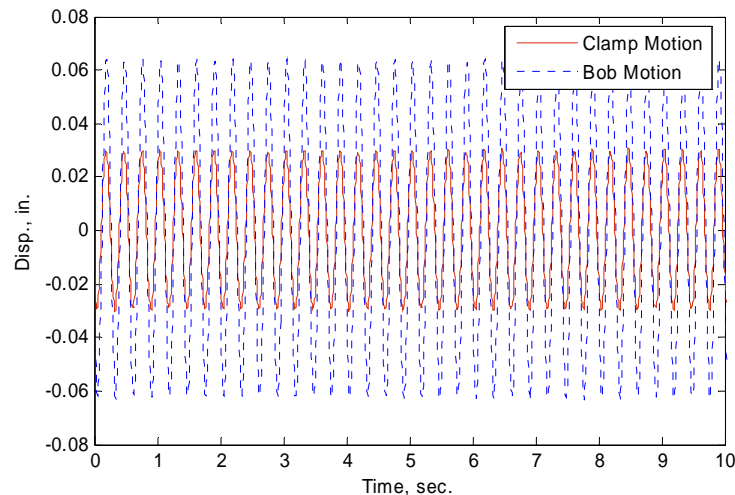


**Figure 7.3-4 Example of measured displacement data.**

The averaged frequency response curves for both damper types are given below (in Figure 7.3-5 and Figure 7.3-6). It can be seen that the natural frequency of the damper is highly dependent on both the excitation frequency and also the amplitude of vibration. Figure 7.3-7 and Figure 7.3-8 show the actuator force as a function of the actuator displacement frequency. The force response shows that even beyond the natural frequency of the damper, the damper clamp force will continue to increase, especially for larger amplitudes of clamp displacement.

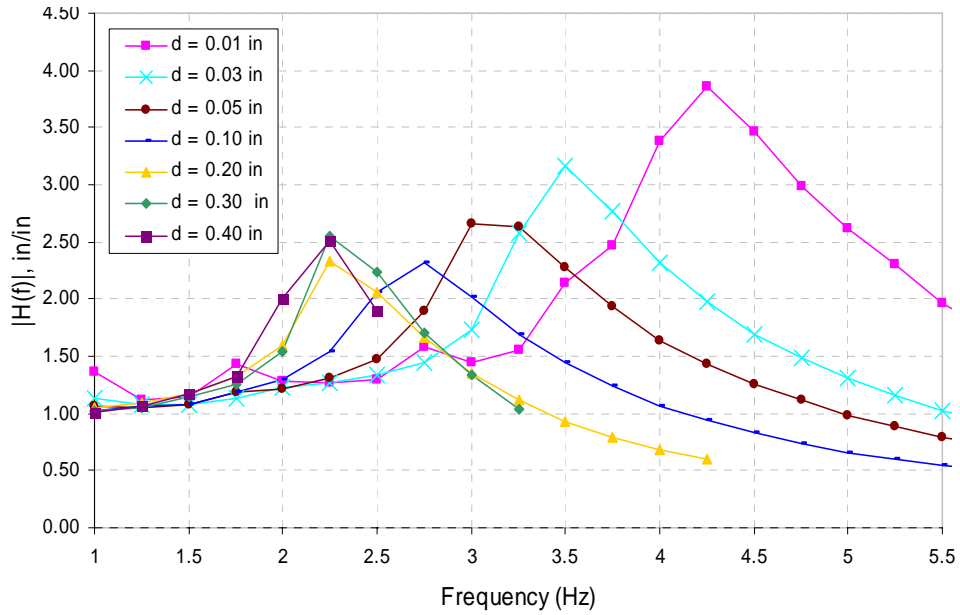


**Figure 7.3-5 Frequency response: 1708S-17.1 (31 lb) damper**

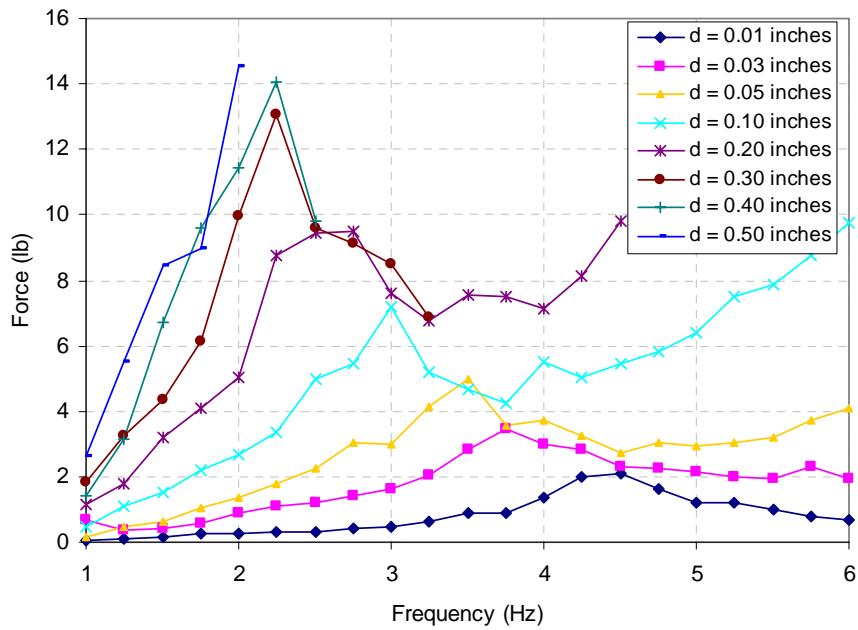


**Figure 7.3-6 Force vs. frequency: 1708S-17.1 (31 lb) damper**

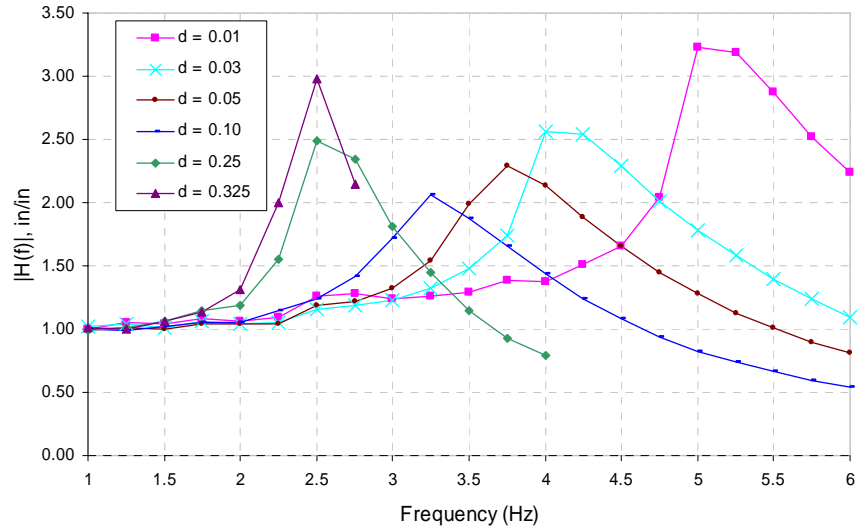


**Figure 7.3-7 Frequency response: 1709S-17.1(34.6 lb) damper**

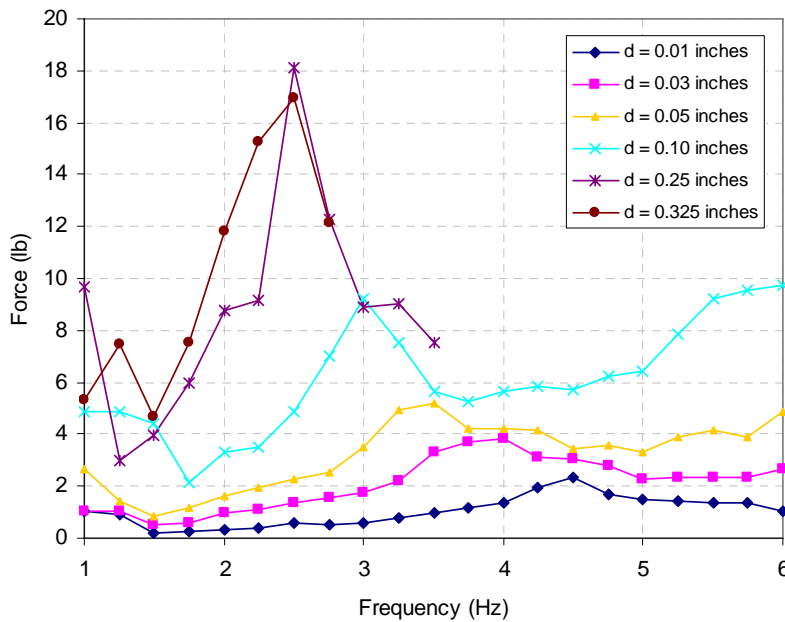


**Figure 7.3-8 Force vs. frequency: 1709S-17.1 (31 lb) damper**

The range of natural frequencies of the IDOT structures tested is between 1.85 and 2.85 Hz. The displacements due to truck gusts and the average yearly wind speed of 11.2 mph (AASHTO, 2001) reach up to about 0.08 in. Once it was confirmed that the dampers in their original configuration do not exhibit natural frequencies in the required range, further tests were conducted to determine whether longer cables could shift the response into the correct frequency range. This was accomplished through dismantling of the dampers by removing the center clamp and one of the weights. The remaining portion of the damper was then tested by clamping the cable at various lengths and repeating the tests performed for the in-tact dampers. Figures 7.3-9 and 7.3-10 show the

dampers with the cable lengths that were tested (with the shortest of each being the original length). Figure 7.3-11 shows the test set-up.

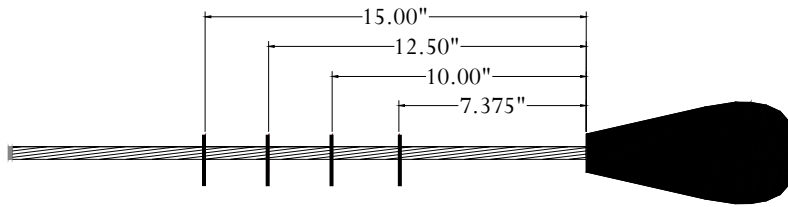


**Figure 7.3-9 Dismantled 1708S-17.1 damper and cable lengths tested**

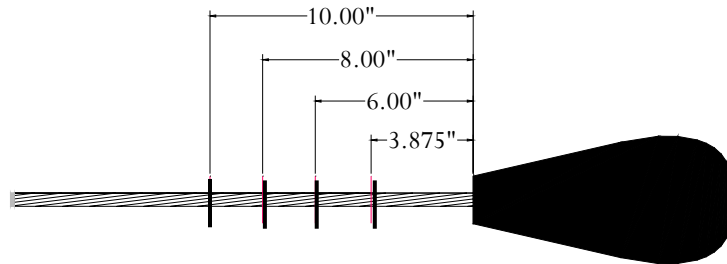


**Figure 7.3-10 Dismantled 1709S-17.1 damper and cable lengths tested**

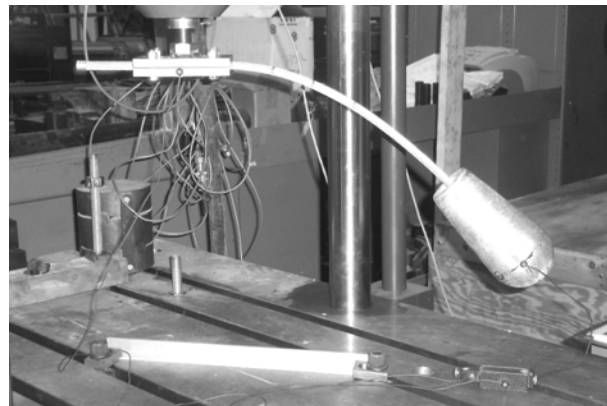


**Figure 7.3-11 Test set-up for dismantled dampers**

Similar frequency response curves as before were constructed from the results of the tests on the dismantled dampers. As expected, lengthening the cables served to decrease the natural frequencies for each amplitude of excitation. The nonlinearity of the dampers can be captured by expressing the natural frequency of each damper as a function of the input amplitude for each cable length tested (see Figure 7.3-12 and Figure 7.3-13). This data is very well fit by logarithmic curves. Therefore, once the

relationships were established between the cable length and the frequency response (from the experimental data), similar relationships could be estimated for cases that were not tested.

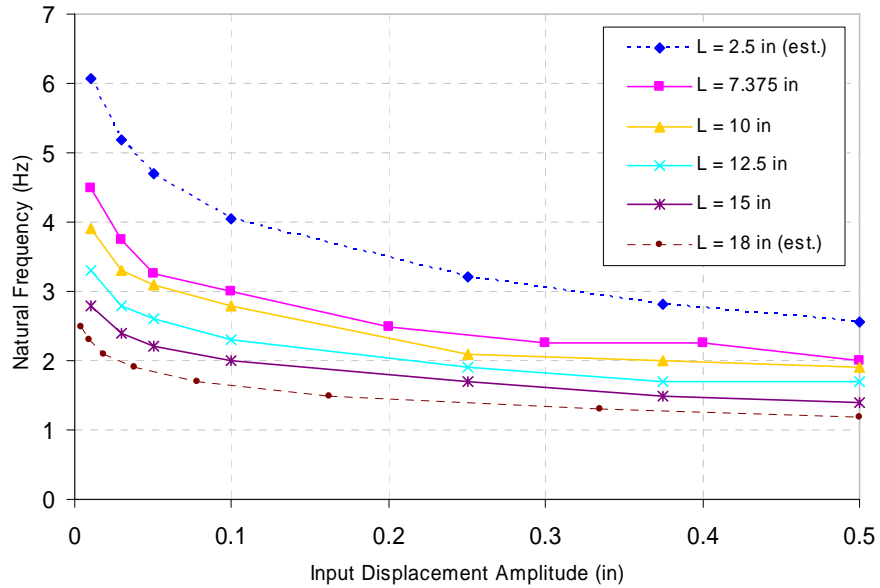


**Figure 7.3-12 1708S-17.1 31-lb damper natural frequency vs. clamp amplitude**

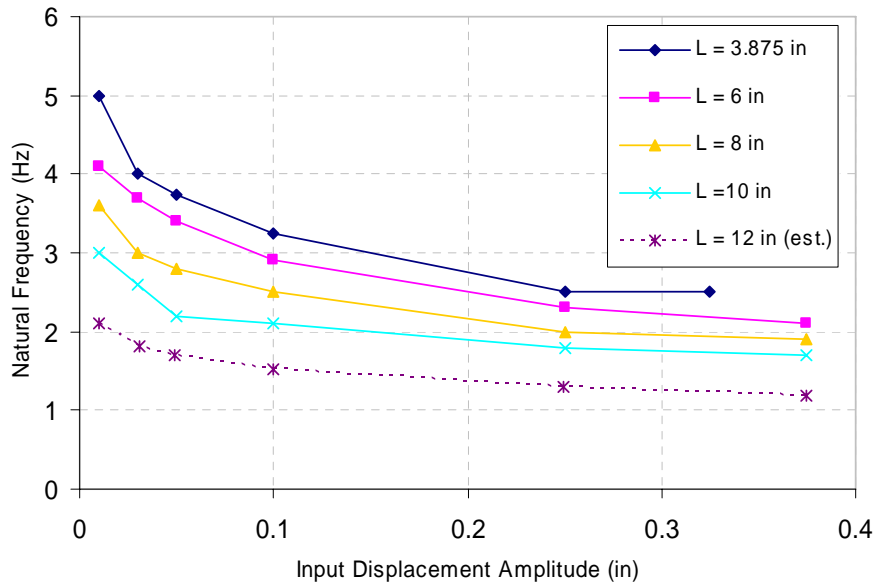


**Figure 7.3-13 1709S-17.1 34.61-lb damper natural frequency vs. clamp amplitude**

## 7.4 Analytical Modeling with Dampers

The results of the laboratory experiments revealed that the natural frequency (and therefore the stiffness) of the damper depends on both the input (clamp) vibration amplitude and the frequency of the vibration. To add to the complexity of the damper behavior, the length of the damper cable may also be changed to obtain a desired response. With so many variables to consider, a parametric analysis was required to evaluate how the damper affects the structure under various conditions. A simple 2 degree-of-freedom (DOF) model was constructed in which the first DOF represents the IDOT sign structures tested in the field and the second DOF represents the Stockbridge damper with constant stiffness,  $k_2$ , and damping,  $c_2$ , terms. A representation of the model is shown in Figure 7.4-.

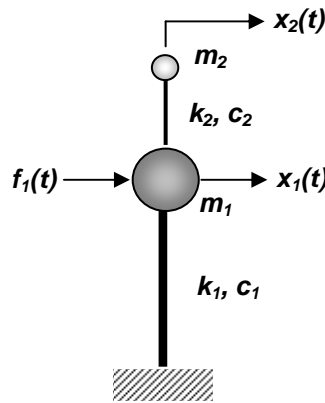


**Figure 7.4-1 2-DOF model of sign structure with damper**

The equation of motion for this model is given by:

$$\begin{bmatrix} m_1 & 0 \\ 0 & m_2 \end{bmatrix} \begin{Bmatrix} \ddot{x}_1 \\ \ddot{x}_2 \end{Bmatrix} + \begin{bmatrix} c_1 + c_2 & -c_2 \\ -c_2 & c_2 \end{bmatrix} \begin{Bmatrix} \dot{x}_1 \\ \dot{x}_2 \end{Bmatrix} + \begin{bmatrix} k_1 + k_2 & -k_2 \\ -k_2 & k_2 \end{bmatrix} \begin{Bmatrix} x_1 \\ x_2 \end{Bmatrix} = \begin{Bmatrix} f_1(t) \\ 0 \end{Bmatrix} \quad 7.4-1$$

where:  $m_1$  = total mass of the sign truss (including sign panels, grating, etc.)

$m_2$  = total mass of the two damper weights

$k_1$  = horizontal mode stiffness of the sign truss structures

$f_1(t)$  = input force to the sign structure (i.e. truck gusts or natural wind gusts)

$c_1$  = truss damping term

The damping terms,  $c_i$ , are determined by  $c_i = 2\zeta_i\omega_{ni}m_i$ , where  $\omega_{ni}$  are the coupled natural frequencies of the 2-DOF system and  $\zeta_i$  are the equivalent viscous damping ratios determined separately for the sign structure and the damper from experimental free vibration tests. The structure alone is lightly damped with  $\zeta_1 \approx 0.8\%$  (of critical); however, the damper itself has a very high damping ratio,  $\zeta_2$ , of approximately 33% of critical damping. There has been extensive research on how Stockbridge dampers dissipate energy. The damper cables consist of twisted cable strands that absorb energy

through Coulomb frictional damping. There are more sophisticated models for this behavior (Sauter and Hagedorn, 2002); however, for simplicity, the damping in this model is considered to be equivalent viscous damping.

To explore how changes in the parameters ( $m_2$ ,  $c_2$ , and  $k_2$ ) of the modeled Stockbridge damper can affect the overall structure, the impulse response of each sign structure with its respective damper is compared to the impulse response without the damper. The total damping in the structure,  $\zeta_s$ , is determined from the decay of the free vibration of the “damped” structure. As seen from the experimental results above, the natural frequencies of the tested 1708 (31-lb) damper and the 1709 (34.6-lb) damper can range from 1.2 Hz to above 6 Hz depending on the chosen cable length and the frequency and amplitude of the sign truss vibration. For example, in the case of the Type III-A sign truss, the natural frequency in the horizontal mode is 1.85 Hz ( $\omega_1 = 11.6$  rad/s). The potential damper frequency range corresponds to an uncoupled frequency ratio ( $\omega_r = \omega_2/\omega_1$ ) range of from 0.65 to 3.3. The total damping in the structure can therefore be expressed as a function of this uncoupled frequency ratio.

In a typical TMD system, the design goal is to closely match the uncoupled natural frequencies of the structure and the damper (i.e.  $\omega_r \approx 1.0$ ). When the natural frequency of the damper is not tuned to the range of that of the structure, it becomes ineffective. The damping in the TMD also plays a large role in the overall system behavior. For small values of  $\zeta_2$ , the TMD is effective only when  $\omega_r = 1.0$ . As  $\zeta_2$  increases, the effective range of  $\omega_r$  also increases (Ginsberg, 2001). Figure 7.4- illustrates that, for  $\zeta_2 = 33\%$ , the effective frequency ratio range is broadened but the amount of damping that is added to the structure is minimal. According to the linear model, the most effective uncoupled frequency ratio is approximately 0.9 for this level of damping in the damper cables.

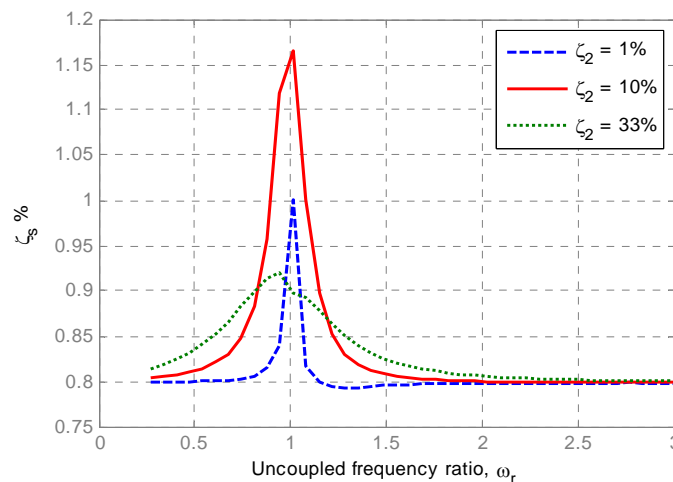


**Figure 7.4-2 Comparison of total structural damping,  $\zeta_s$ , for different values of damper damping ratios,  $\zeta_2$**

The mass ratio,  $m_r = m_2/m_1$ , also contributes to the effectiveness of the TMD. For example, the mass ratio of the current 31-lb damper on the Type III-A overhead truss is approximately 0.0015. With this low value of  $m_r$ , there is a limit as to how effective the damper can be. Additional dampers may be added to increase the mass ratio and therefore the total damping in the structure, as shown in Figure 7.4-. Although added dampers will improve the damping in the structure, it remains to be seen what level of damping is truly required for each truss and if the levels can be achieved with a reasonable number of dampers.

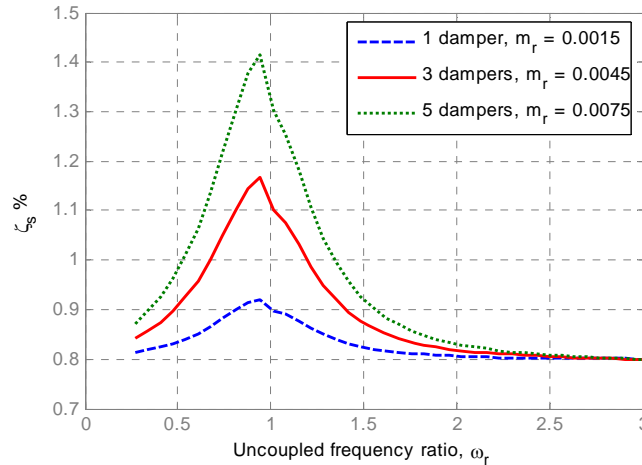


**Figure 7.4-3 Total structural damping,  $\zeta_s$ , in the Type III-A model for different numbers of dampers (with  $\zeta_2 = 33\%$ )**

One way to determine the level of damping that each sign truss requires is to compare the measured stresses with the constant amplitude fatigue limit (CAFL) values. Using the simple 2-DOF model, the impulse response of the structure can be examined both with a damper or dampers present (with prescribed characteristics) and also without a damper present. The impulse response of the structure, which is the decaying vibration of the truss due to an impulse load, is a good representation of how the sign structures respond to truck gusts. The acceleration impulse response is proportional to the (elastic) stress impulse responses experienced by each member. The number of stress cycles in the stress impulse response above the CAFL can be calculated both with and without the damper present for each critical member.

For all of the structures tested, the web members (with ET type connection details) were the only members that experienced stresses due to truck gusts and the 11.2 mph average yearly wind speed that were above the CAFL of 0.44 ksi (AASHTO, 2001). For example, in the Type III-A truss, the estimated maximum stress cycle magnitude in response to a strong truck gust is 0.56 ksi (this occurs in the horizontal diagonal at the end of the truss). The CAFL is 78.6 percent of this value. During the impulse response of the modeled Type III-A truss without any damper present, there are 5 cycles above the CAFL. Then a damper may be added to the model, representing the heaviest available

damper, the 1709 (34.6-lbs). To most closely match the natural frequency of the structure (1.85 Hz) at the expected truss displacement levels ( $d \approx 0.05$  in.), a cable length of 12 in. is chosen. From experimental testing, the estimated natural frequency of this damper is 1.7 Hz ( $\omega_r = 0.92$ ). Table 7.4-1 shows how the number of these dampers adds to the total damping of the structure,  $\zeta_s$ . For instance, with four 34.6-lb dampers, each with 12-in. cables, the number of cycles above the CAFL can be cut from five cycles to three.

**Table 7.4-1 Modeled Type III-A truss with different numbers of tuned Stockbridge dampers**

Damper	Weight (lbs)	Cable Length (in.)	Est. Damper $f_n$ (Hz)	Number of dampers	$m_r$	$\zeta_s$ (%)	# of cycles above CAFL
1709	34.6	12	1.7	1	0.001647	0.93	5
1709	34.6	12	1.7	2	0.003295	1.07	4
1709	34.6	12	1.7	4	0.006589	1.34	3

Figure 7.4-4 below illustrates the normalized impulse response of the structure with and without the dampers present. It is clear how the addition of the dampers would reduce the number of stress cycles exceeding the CAFL stress range. By reducing the number of stress cycles above the CAFL, the life of the structure may be increased. While the dampers can limit the number of cycles above the threshold, it is not possible to completely eliminate peak responses outside of the desired range (due to the initial effect of the impulse). To reduce the peak stress values, larger members would be required.

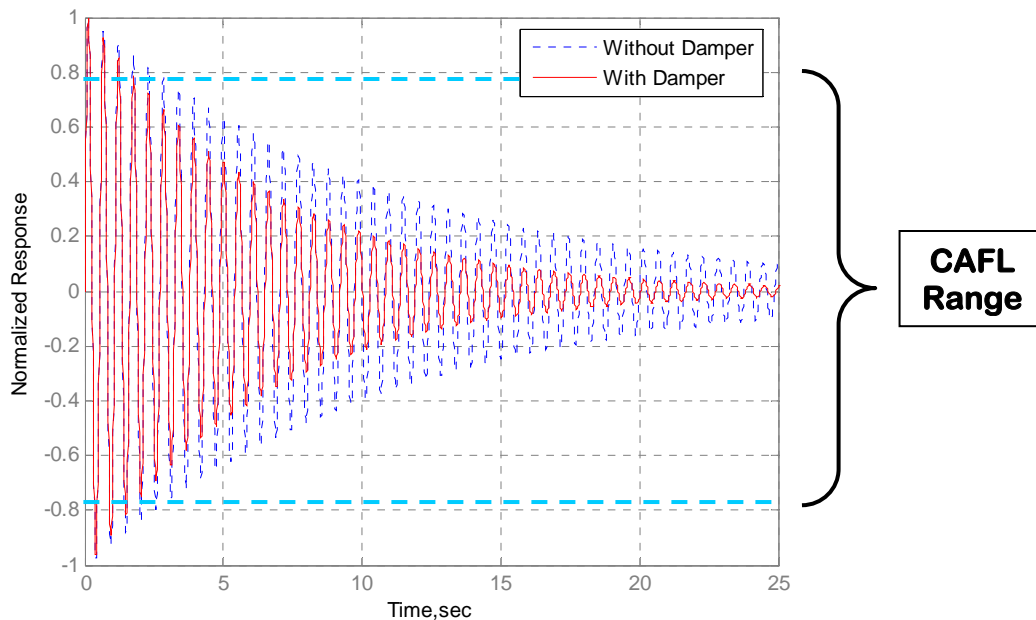


**Figure 7.4-4 Model of Type III-A truss with six 34.6-lb dampers with 12-inch cables ( $f_d = 1.82$  Hz)**

The simplified model utilized above assumes that the stiffness and damping in the damper remains constant during the impulse response of the structure. In actuality, the stiffness and damping properties of the dampers possess strong amplitude dependence and will therefore not remain completely constant as the amplitude decays. Therefore, the simplified model should be viewed as illustrating the basic behavior; more detailed modeling could be required to fully understand the behavior of the system.

## 7.5 Damper Recommendations

Stockbridge dampers are an effective way to provide lightly damped aluminum highway sign structures with additional damping. The increase in energy dissipation provided by the damping devices may prolong the (fatigue) life of the structures by decreasing the amplitude and number of stress cycles experienced by the truss members. These dampers are not only recommended for new structures but may provide a simple solution for the retrofit of structures currently in service.

Several factors should be considered when properly designing the most appropriate damping strategy for each structure. The weight of the truss and sign panels determines the natural period of vibration of the structure and dictates the total mass or number of dampers required to reach the target damping level. The estimated amplitude of vibration of the structure in response to truck gust loading and the average yearly wind speed must also be taken into account. Table 7.5-1 shows estimated dynamic displacement ranges of each sign structure along with their horizontal natural frequencies. These values are

estimated from field measured acceleration responses during times when the wind speed ranged between 10 and 30 mph and trucks were passing underneath. This does not take into account any “static” displacement due to the low frequency gusting of the wind. The dampers would not be excited by the long period variations in the wind speed, but rather by the dynamic vibrations of the truss.

**Table 7.5-1 Estimated dynamic displacement of each sign truss**

<b>Truss Type</b>	<b>Displacement Range (in.)</b>	<b>Horizontal Natural Frequency (Hz)</b>
Cantilever	0.02 – 0.08	2.29
Type I-A	0.01 – 0.05	2.84
Type II-A	0.01 – 0.045	2.12
Type III-A	0.02 – 0.08	1.85

According to the simple model presented, optimal damping is achieved when the natural frequency of the Stockbridge damper at the expected levels of truss vibration is between 90 and 110 percent of the horizontal natural frequency of the sign support structure. Also, the mass ratio,  $m_r$  should be maximized. This can be done by installing the heaviest dampers available from the manufacturer and/or installing multiple dampers. The test and model results presented in this report serve to illustrate that the effectiveness of the Stockbridge-type damping devices is highly dependent on the dynamic characteristics of both the damper and the structure. By choosing a damper or number of dampers with the correct weight and cable length, the vibrations of the structure may be most effectively reduced. It is possible that the nonlinearities of the damper will make the dampers effective over a wider range of frequencies; however, simply implementing the recommendations given in this report would be a clear improvement over the currently installed dampers. It is clear that only the *sloppy* dampers offer any improvement in response of the sign structures. Before implementing a damping plan for all of the IDOT structures, simple field tests with modified dampers and/or multiple dampers (using a single accelerometer at mid-span and manual excitation) are suggested to confirm the results of the laboratory tests and analysis.

## 8.0 End Connection Effects on Vortex Shedding Susceptibility of Aluminum Truss Tubular Web Members

### 8.1 Introduction

IDOT has had some difficulty in recent years with their older aluminum truss overhead sign structure (OSS) designs that has manifested itself in the formation of cracks at “T”, “Y”, and “K” web-to-chord welded connections of hollow circular tube members. Based on field observations by IDOT inspectors, the damage usually seemed to be localized at the welded end connections of some of the most slender web members to the main chords of the trusses. Many of these cracks propagated into the base metal, some even resulting in complete failure of the connection. Similar weld cracking has been observed in aluminum sign structures in other states throughout the country (Ginal, 2003; Zalewski & Huckelbridge, 2005), including in New York where efforts have been made to implement a repair program (Pantelides et al., 2003). For IDOT, the solution has primarily been to implement new standard designs for both overhead and cantilevered structures that are intended to improve the structures through the use of fewer and larger members, along with the elimination of very slender, low-force web members. Fig. 8.1-1 shows an example of a newer IDOT OSS.

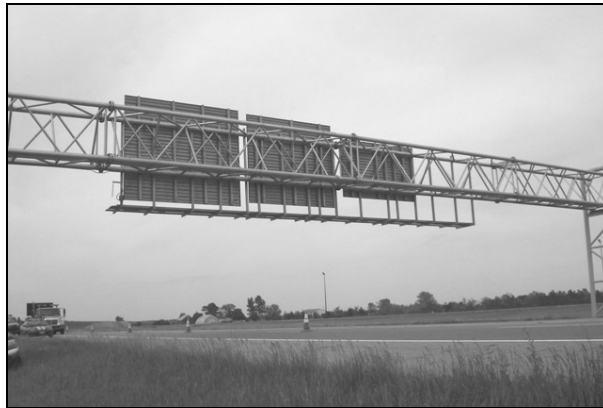


**Figure 8.1-1 Newer IDOT aluminum overhead sign structure**

In general, cyclic loading of any sort, even at fairly low amplitudes, can cause fatigue of structural members and connections. Cracks in welds at truss connections tend to occur due to fatigue stresses induced by wind loading on a truss (Ocel et al., 2006). The wind primarily acts on the sign panels, resulting in global deformation of the truss and thereby causing varying stresses in the members that may eventually lead to fatigue damage. Fairly strict stress range limits are found in AASHTO (2001) for evaluating that sort of fatigue at welded connections. This portion of the current study, however, focuses on fatigue caused by the local phenomenon of vortex shedding induced vibration of individual web members. When it is possible, this vibration occurs at a much higher frequency than overall (global) vibration of the truss and could therefore more quickly lead to weld cracks and connection failures. For these reasons, local web member

behavior should be well understood and appropriate design measures should be undertaken to ensure avoiding resonant vibration of individual members.

A series of experiments and analyses were therefore conducted in order to assess the vulnerability of individual hollow circular aluminum web members in IDOT sign truss structures to severe wind-induced resonant vibrations that might eventually lead to fatigue failures at their welded end connections (to chord members). The likelihood of such vibrations is in part a function of the member natural frequency in bending, so the first step in the assessment was to develop a reliable (and somewhat conservative) method for estimating the fundamental natural frequency of vibration for various categories of truss web members. This method, based on field results from simple non-destructive tests on web members of trusses representing both older and newer IDOT sign truss designs, was then applied to estimate the natural frequencies of key web members for all types of IDOT aluminum overhead and cantilever sign trusses currently in use. These natural frequencies for each type, size, and length of web member were then related to the computed vortex-shedding frequencies of such circular cylinders in an assumed laminar flow, to estimate the critical oncoming wind speeds necessary to generate resonant vibration. The relative magnitudes of critical uniform wind speed for different web members can serve as a comparative indicator of their vulnerability to wind-induced resonant flexural vibrations (which can also be correlated to actual observed damage), while their absolute magnitudes may be compared to actual field wind data to ascertain the likelihood of such vibrations occurring (or having occurred).

## 8.2 Web Member Natural Frequency Determination

It is well known that the fundamental (first-mode) natural frequency of vibration for a beam-type oscillator (of constant flexural stiffness and with uniformly distributed mass) is proportional to the square root of the flexural modulus ( $EI$ ), inversely proportional to the square root of the distributed mass ( $\rho$ ), and inversely proportional to the square of the length of the member ( $L$ ) (Thomson & Dahleh, 1998). For instance, assuming simple (pinned) end supports, the fundamental natural frequency of vibration ( $f_{s.s.}$ ) in Hz for a member of length  $L$ , flexural modulus  $EI$ , and mass per unit length  $\rho$  is:

$$f_{s.s.} = \frac{\pi}{2} \cdot \left( \frac{1}{L^2} \right) \cdot \sqrt{\frac{EI}{\rho}} \quad 8.2-1$$

If the same member instead had fixed (rigidly clamped) end supports, the fundamental natural frequency ( $f_{f.f.}$ ) would be the value from Equation 8.2-1 times an appropriate “boundary condition adjustment factor”, which turns out to be about 2.25 for the case of two fixed ends.

Alternatively, the “correction” to account for end boundary conditions in between simple-simple and fixed-fixed can be directly incorporated into Eq. 8.2-1, by adjusting the value of  $L$  used to reflect the particular boundary conditions (in effect treating all boundary condition cases as equivalent to a simple-simple member, only of a somewhat

shorter length  $K_f * L$ ). In this approach, the “equivalent length factor” for natural frequency calculation ( $K_f$ ) ranges from about 0.67 for the fixed-fixed support case on up to 1.00 for the simple-simple support case. (While this approach is conceptually similar to determining and using an effective length factor  $K$  to evaluate the buckling compressive strength of slender axially loaded compression members with different end conditions, the value of  $K_f$  is only equal to  $K$  for the pinned end case, when both are unity.)

### ***Field Testing of Undamaged Web Members***

Actual aluminum sign truss web members that are fillet welded at their ends to larger chord members have end conditions somewhere in between simple and fixed ( $0.67 < K_f < 1.00$ ). In order to determine appropriate equivalent length factors for various types of hollow circular web members, a field testing program was undertaken. Forty-five undamaged web members (including verticals, horizontals, interior diagonals, vertical diagonals, and horizontal diagonals) from three different overhead trusses were evaluated. The three trusses investigated included truss units from an older Type I-A truss (with interior diagonals not offset) located in the IDOT District 6 storage yard in Springfield, assembled truss units from an older Type IV-A truss (with offset interior diagonals) located at UIUC-ATREL in Rantoul (Figure 8.2-1), and a newer Type III-A truss in service near Lincoln (Figure 8.2-2). The web members in these trusses ranged in size from 1-3/4 in. outside diameter (O.D.) by 3/16 in. wall thickness (1-3/4” x 3/16”) on up to 3-1/2” x 5/16”, and they were fillet welded all around at their ends (typically with 5/16 in. welds) to chord members ranging in O.D. from 4-3/4 in. to 8-1/2 in. (the web members were never more than half as big around as the corresponding chords). The slenderness ratios,  $L/r$  (where  $r$  is the radius of gyration (square root of moment-of-inertia over area) and  $L$  is the face-to-face length of the member), of the tested web members ranged from 59 to 138.

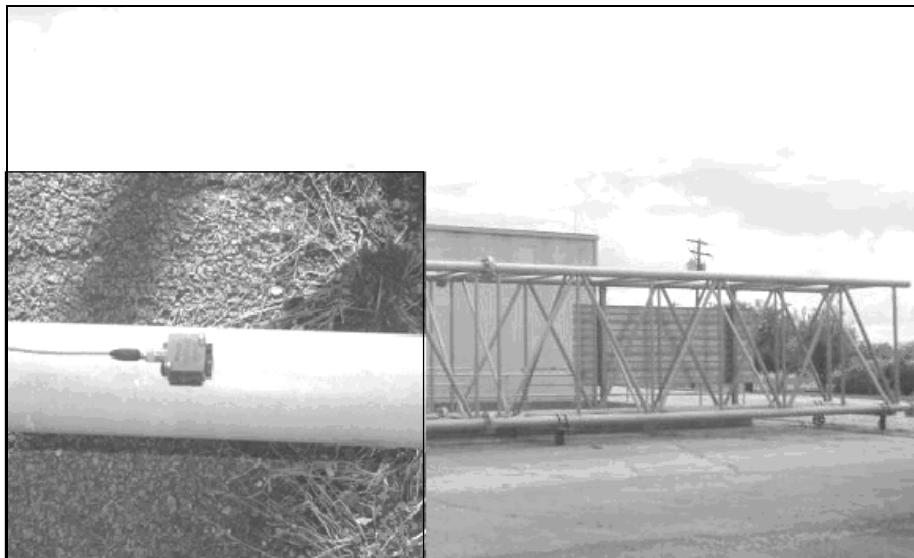


**Figure 8.2-1 Rantoul Truss, Type IV-A; Inset: Accelerometer mounted on horizontal member**



**Figure 8.2-2 Lincoln Truss, New Type III-A**

The non-destructive field testing procedure simply consisted of tapping on a web member (near mid-length) normal to its longitudinal axis with a plastic mallet and recording the member's response (parallel to the direction of excitation) using an accelerometer (mounted near mid-length of the member; see Figure 8.2-1 inset) connected to a computer data acquisition system. (In the early stages of testing, input excitations from a rubber mallet and a metal hammer were also explored; results were similar to those obtained using the plastic mallet.) The impact test imparted an impulse that caused damped free vibration of the member. The recorded signal was then processed in the frequency domain using a Fast Fourier Transform (FFT) to determine the first-mode natural frequency of vibration. This test method was primarily concerned with modal analysis of the element, and therefore the actual amplitude of vibration was neglected (although the behavior was certainly in the elastic range). The data analysis process is illustrated in Figure 8.2-3 for an interior diagonal member from the older Type IV-A truss in Rantoul (2-1/2" x 3/16").

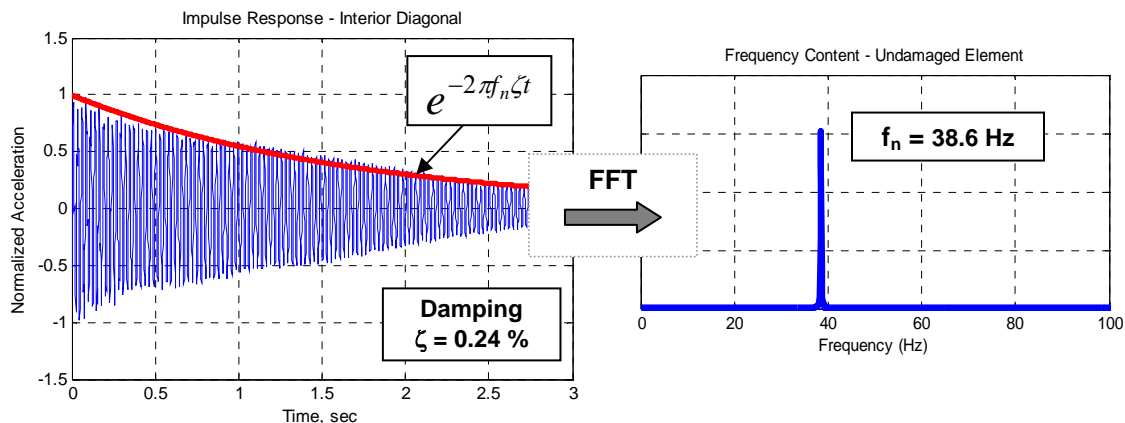


**Figure 8.2-3 Data analysis of acceleration impulse response for an interior diagonal member in the older Type IV-A truss**

The critical damping ratio of the web members was determined by fitting a curve to the envelope of the acceleration impulse response. The envelope ( $A$ ) of the response as a function of time ( $t$ ) is given by:

$$A(t) = e^{-2\pi f_n \zeta t} \quad 8.2-2$$

where  $f_n$  is the natural frequency of the member in Hz and  $\zeta$  is the damping ratio of the member.

Each web member was tested twice – once normal to the longitudinal direction of the truss and a second time parallel to the longitudinal direction of the truss. The direction normal to the truss span typically exhibited frequencies about 5% to 15% lower than in the direction parallel to the truss span, owing in part to the way in which the web-to-chord connection of two circular members leads to slightly different face-to-face dimensions in the two perpendicular directions. In a couple of cases, tests were also conducted along an axis half-way in between the truss normal and truss parallel directions; those results never yielded a lower frequency than that in the truss normal direction.

Since the likelihood of wind-induced web member vibrations is typically greater when the member frequency is lower, the remainder of this section will focus on the lesser natural frequencies recorded for each of the web members tested. This natural frequency was compared in each case to that computed using Equation 8.2-1, assuming  $E$  and the density of the ASTM Alloy 6061 Temper T6 aluminum to be 10,100 ksi and 169 pcf, respectively, and taking  $L$  to be the least chord-to-chord (face-to-face) dimension of the web member in question.

From the standpoint of end fixity, there appear to be two distinct categories of web members – those with T-type end connections (verticals, horizontals, and interior diagonals) and those with K-type end connections that have an angle between the longitudinal axes of the web and chord that is significantly less than 90 degrees (vertical diagonals and horizontal diagonals) as seen in Figure 8.2-4. A summary of the results from the tests conducted on each connection type are given in Table 8.2-1.

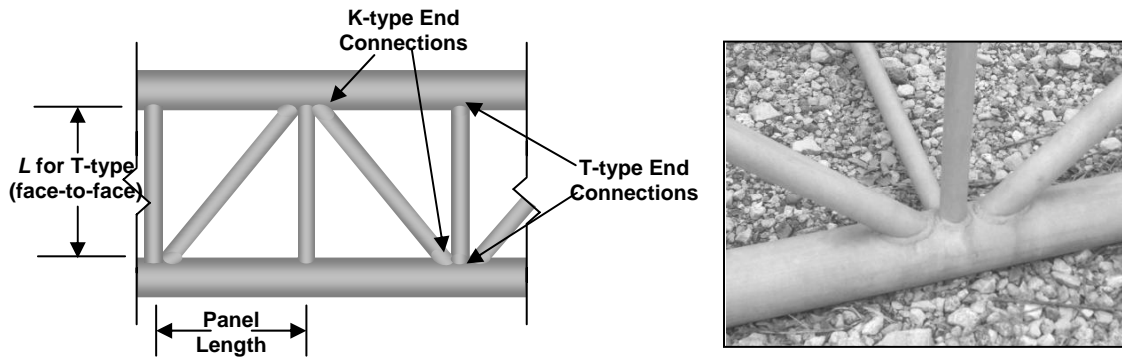


**Figure 8.2-4 Web member connection definitions (left) and actual web members framing into a chord (right)**

**Table 8.2-1  $K_f$  values measured for both T- and K-type end connections**

Category	Number Tested	Average $K_f$	Sample Std. Dev.	Abs. Max $K_f$
T-type	35	0.79	0.05	0.89
K-type	10	0.74	0.02	0.77

In addition to the clear differences in end-fixity between T-type and K-type web members, there were also some other more subtle trends observed – it appears that interior (non-end) web members and very slender web members typically have slightly more fixity (slightly lower  $K_f$ ) than their non-interior and less slender counterparts.

Therefore, for obtaining a simple “best estimate” of the actual natural frequency for a given hollow circular web member with welded ends, it appears reasonable to use “average”  $K_f$  values of about 0.8 and 0.75 for T-type and K-type web members, respectively. If, on the other hand, a “worst-case” estimate of the natural frequency is desired, then using  $K_f$  values of 0.9 and 0.8 for T-type and K-type web members, respectively, might be more appropriate (each of these values is at least two standard deviations above the recommended corresponding mean value and exceeds all actual test values).

### ***Field Testing of Damaged Web Members***

An additional seven tests were conducted on some damaged web members found in the Rantoul truss units. All of the damaged web members observed were either verticals or interior diagonals, typically with small (but visible) weld or member cracks at one T-type end connection (around one-fourth to three-fourths of the member perimeter). There was no pattern to these cracks from the standpoint of joint congestion (isolated single web member joints were just as likely to be cracked as were joints with three web members coming together in one plane at a connection). The crack locations, however,

usually seemed to correspond to the web member extreme fibers for bending in the truss normal direction. (Similar fatigue cracks have also been observed in aluminum overhead sign truss structures in other states as well, and these have even included some cases of cracking at the connection of K-type diagonal web members (Ginal, 2003; Pantelides et al., 2003; Ocel et al., 2006).) On average, the damaged web members tested had natural frequencies about 15% lower than for corresponding members without any cracks, which effectively corresponds to an increase in  $K_f$  of about 0.05. And, even in the least-damaged of these cracked web members, there was still always some distinct reduction in the natural frequency from that of a comparable undamaged member. Figure 8.2-5 shows an example of the variation in natural frequency between a damaged and undamaged interior diagonal member on the older Type IV-A truss in Rantoul.

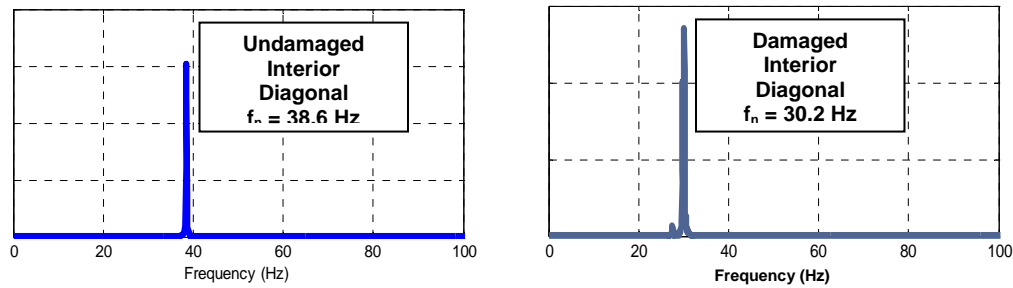


**Figure 8.2-5 Difference in natural frequency of undamaged (left) and damaged (right) interior diagonal members**

### 8.3 Web Member Critical Wind Speed Estimation

For the type of hollow circular web members under consideration, the relationship between the uniform wind speed that will cause transverse vibration of the member and the natural frequency of the member has been well established (Simiu & Scanlan, 1996). The following expression is based on an assumption that the source of web member bending vibrations as wind flows across the member (of diameter  $D$ ) at a velocity (speed)  $V$  is from the periodic impulses (perpendicular to the wind direction) on the member due to vortex shedding at a frequency near that of the member ( $f$ ):

$$V = \frac{f \cdot D}{S} \tag{8.3-1}$$

where  $S$  is the Strouhal number (typically taken as approximately 0.2 for a circular cylinder). This expression can then be used for different web member types, sizes, lengths, and  $K_f$  values to estimate critical uniform wind speeds ( $V_c$ ) for various web member situations that can occur per both the older and the newer IDOT aluminum sign truss design standards.

*Aluminum Sign Trusses per Older IDOT Design Standards (IDOT, 1982)*

In older Type IV-A (6 ft deep and 8 ft high) overhead sign trusses, the smallest web members occur when used to span no more than 100 ft. For this type of truss (for large signs), the absolute worst case with respect to slender web members occurs with span lengths of less than about 90 ft (chord diameters of 5-1/2 in.) and with the maximum panel length of 5 ft. The results for this case are given in Table 8.3-2.

**Table 8.3-1 Older IDOT Type IV-A sign truss with 90-ft maximum span and 5-ft panel length**

Member	Connection Type	O.D. (in.)	Wall (in.)	$L/r$	$V_c$ from average $K_f$ (mph)	$V_c$ from worst-case $K_f$ (mph)	$V_c$ from $K_{f(s,s)} = 1.0$ (mph)
Interior diag. (non-end)	T-type	2-1/2	3/16	143	22	17	14
Vertical (non-end)	T-type	2-1/4	3/16	124	28	22	18
Vertical diag.	K-type	3-1/4	1/4	100	48	42	27
Interior diag. (end)	T-type	3-1/4	1/4	110	40	31	26

Similarly, in older Type III-A (5 ft deep and 7 ft high) overhead trusses the smallest web members occur when the span is not more than 90 ft (again with 5-1/2 in. diameter chords and a maximum panel length of 5 ft). Key values for this situation are shown in Table 8.3-2.

**Table 8.3-2 Older IDOT Type III-A sign truss with 90-ft maximum span and 5-ft panel length**

Member	Connection Type	O.D. (in.)	Wall (in.)	$L/r$	$V_c$ from average $K_f$ (mph)	$V_c$ from worst-case $K_f$ (mph)	$V_c$ from $K_{f(s,s)} = 1.0$ (mph)
Interior diag. (non end)	T-type	2-1/4	3/16	147	24	19	15
Vertical (non end)	T-type	2	3/16	122	29	23	19
Vertical diag.	K-type	3	3/16	97	51	45	29

In older Type I-A and II-A overhead trusses, all of the web member critical wind speeds determined using the *average*  $K_f$  values are at least 40 mph, and even the *worst-case* critical wind speeds are always greater than 30 mph. However, if web member end fixity was completely neglected ( $K_f = 1.0$ ), some of these computed critical wind speeds could even be as low as about 25 mph.

In older Type III-C-A cantilever sign trusses, which are 7 ft high and as deep as 3 ft, the most slender interior diagonal and vertical web members occur in conjunction with the smallest chord (5 in. diameter), whereas the most slender vertical diagonals occur when the maximum panel length of about 6 ft – 7 in. is used (in conjunction with 5-1/2 in. diameter chords). The critical wind speeds for these cases are given in Table 8.3-4.

**Table 8.3-4 Older IDOT Type III-C-A cantilever sign truss critical members**

Member	Connection Type	O.D. (in.)	Wall (in.)	$L/r$	$V_c$ from average $K_f$ (mph)	$V_c$ from worst-case $K_f$ (mph)	$V_c$ from $K_{f(s,s)} = 1.0$ (mph)
Interior diag.	T-type	2-1/4	3/16	121	31	24	20
Vertical	T-type	2-1/4	3/16	107	37	29	24
Vertical diag.	K-type	3	3/16	108	41	36	23

The most critical cases that can occur in older Type I-C-A and II-C-A cantilever trusses for verticals, interior diagonals, and vertical diagonals give wind speeds similar to those cited above for older Type III-C-A trusses. The absolute lowest critical wind speeds of any older cantilever truss web member would be for a 1-3/4" x 3/16" interior diagonal of a 5 ft – 6 in. high and 3 ft deep (Type II-C-A) truss with 3-1/2 in. diameter chords (27 mph with the *average*  $K_f$  and 22 mph with the *worst-case*  $K_f$ ;  $L/r = 128$ ), which is the only cantilever truss case where the critical wind speed is less than 30 mph when the *average*  $K_f$  is used.

The bulk of the problems that IDOT has noted with respect to cracked welds and fractured members in existing older aluminum sign trusses have occurred in very lightly loaded vertical and interior diagonal web members of Type III-A and IV-A overhead sign trusses, and occasionally in cantilever trusses. (The only exception to this has apparently been a few cases of cracks at the ends of vertical diagonals that were specifically attributed to a poor weld profile that had sometimes been used to make this K-type connection; ever since this type of connection has been made carefully following AWS recommendations about cutting back the member at the toe edge to facilitate achieving the prescribed weld throat thickness, this type of problem has no longer been observed.) Furthermore, it seems quite reasonable that many of these trusses could have in fact often been subjected to uniform wind speeds in the range of 15 mph on up to about 30 mph, while not nearly as often to wind speeds of much more than about 30 mph (Ginal, 2003).

And, as a matter of fact, given the typically turbulent nature of winds more than about 35 mph, it is much less likely in such a case for vortex shedding to even be able to occur (Dexter & Ricker, 2002).

Given that almost all welded web member connections to chords likely have very small defects resulting from their initial fabrication, transportation, and installation, any sustained period of time in which such slender members are subjected to winds in the range of the critical speed could grow small fatigue cracks (which could be made even worse by other stress variations due to global truss vibration). The natural frequencies of the most vulnerable web members are in the range of 30 to 50 Hz, which means that just one hour of fairly uniform wind near the critical value can produce well over 100,000 vibration cycles (that are probably even sustainable through some small wind speed variation (Dexter & Ricker, 2002) given the very low system and member damping in such aluminum sign trusses). And while the stresses generated during such vibrations are likely to be fairly small, it has been shown from fatigue strength tests on welded tubular trusses and other fillet welded aluminum connections that their life when subjected to stress ranges of even just a couple ksi may only be on the order of 1,000,000 to 10,000,000 cycles, or even less than that (Sharp et al., 1996; Kissell & Ferry, 2002; Zalewski & Huckelbridge, 2005). This is in general agreement with another observation made elsewhere that typical tubular connections are less fatigue-resistant than connections between angles (Dexter & Ricker, 2002), as further reflected in a recent standard specification that prescribes a constant amplitude fatigue threshold design stress range of less than 1 ksi for this type of detail (AASHTO, 2001). And, of course, as any damage does grow at an end of such a vulnerable web member, the natural frequency will drop a bit, making the member susceptible to resonant vibrations at even lower (and therefore more likely) wind speeds.

Beyond the assessment procedures provided above, there are also some limited published design recommendations intended to minimize the vulnerability of aluminum sign truss members to wind induced vibrations (Sharp, 1993). These consist of suggested maximum permissible slenderness ratios ( $L/r$ ) for circular members that could be susceptible to flexural vibrations. For most locations having rolling terrain with some trees and other vegetation, they recommend that  $L/r$  should be kept to no more than 95 (supposedly based on an assumed maximum sustained uniform wind speed of approximately 20 mph). The only web members in existing IDOT older-design sign trusses that can ever have  $L/r$  significantly in excess of 95 (by more than 10%) are precisely the verticals ( $L/r$  as much as 125) and interior diagonals ( $L/r$  as much as 140) in Type III-A and IV-A overhead sign trusses, as well as some cantilever truss interior diagonals ( $L/r$  also up to about 125). And, as a matter of fact, the damaged interior diagonals found in the Rantoul truss had  $L/r$  of 138 (and computed critical wind speeds in the range of 18 to 22 mph), while the damaged vertical web members in the Rantoul truss had  $L/r$  of 109 (and computed critical wind speeds of about 28 to 35 mph). (Similar calculations, where sufficient design information was available, have indicated that the aluminum sign truss fatigue cracking reported by some other states was not attributable to vortex shedding induced vibrations since the members and connections in those cases that experienced cracking were not nearly as slender as those in Illinois.) As a side note, the

2001 AASTHO code limits  $L/r$  to 200 for the design of tension members. This value, of course, is much too high when designing against vortex-shedding susceptibility.

Based on the experimentally determined  $K_f$  values for T- and K-type end connections, curves can be constructed that relate the critical wind speed to the  $L/r$  values of hollow circular web members (Figure 8.3-1). The upper and lower bounds on each plot indicate the extreme cases of fixed-fixed (upper bound) and simple-simple (lower bound) end conditions, while the intermediate curves represent the *average* and *worst-case*  $K_f$  values determined for each connection type. Considering that vortex shedding is unlikely to occur when wind speeds are above about 35 mph (Dexter & Ricker, 2002), one possible guideline for selecting maximum  $L/r$  limits would be to use values corresponding to a critical wind speed of 35 mph along with the *average*  $K_f$  values. This approach would yield limiting  $L/r$  values of 110 for T-type connections and 117 for K-type connections. Alternatively, one could use a critical wind speed of 30 mph (nearly three times the average yearly wind speed of 11.2 mph for Illinois used in fatigue design (AASTHO, 2001)) paired with the *worst-case*  $K_f$  values. This would yield maximum  $L/r$  limits of 106 for T-type connections and 119 for K-type connections. For other critical wind speeds (perhaps based on specific knowledge of the surrounding terrain and local wind speed data), the curves given in Figure 8.3-1 may be used to determine appropriate  $L/r$  limits for the design of truss web members.

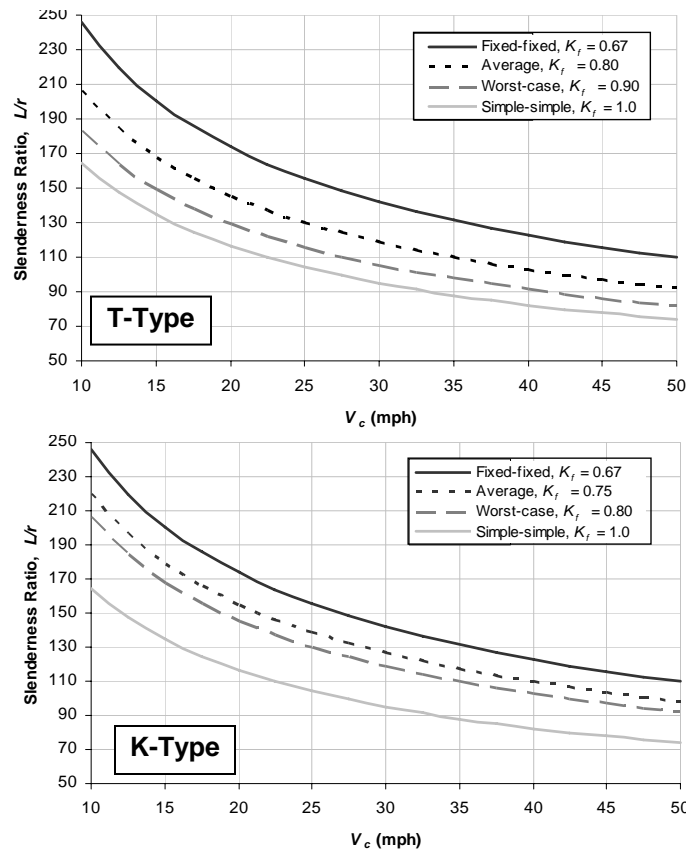


**Figure 8.3-1 Slenderness limits vs. critical wind speed based on  $K_f$  values for T-type end connections (top) and K-type end connections (bottom)**

**Aluminum Sign Trusses per Newer IDOT Design Standards (IDOT, 2001)**

In accordance with current newer IDOT overhead aluminum sign truss design standards, it turns out that the most slender possible web members that can occur are in the new Type I-A and III-A trusses. In new Type I-A sign trusses, which are 4 ft deep and 4 ft – 6 in. high (center-to-center of the chords), the smallest web members occur in trusses with span lengths of no more than 70 ft, as summarized in Table 8.3-5.

**Table 8.3-5 New IDOT Type I-A sign truss with 70-ft maximum span and 5-ft panel length**

Member	Connection Type	O.D. (in.)	Wall (in.)	$L/r$	$V_c$ from average $K_f$ (mph)	$V_c$ from worst-case $K_f$ (mph)	$V_c$ from $K_{f(s,s)} = 1.0$ (mph)
Interior diag.	T-type	2-1/4	1/4	97	49	38	31
Vertical diag.	K-type	2-1/4	1/4	104	46	41	26

Similarly, in newer Type III-A trusses, which are 5 ft deep and 7 ft high, the smallest and most slender web members can occur when used to span up to 140 ft (with 7 in. diameter chords and the maximum panel length of 5 ft – 6 in.) as summarized in Table 8.3-6.

**Table 8.3-6 New IDOT Type III-A sign truss with 140-ft maximum span and 5-ft 6-in. panel length**

Member	Connection Type	O.D. (in.)	Wall (in.)	$L/r$	$V_c$ from average $K_f$ (mph)	$V_c$ from worst-case $K_f$ (mph)	$V_c$ from $K_{f(s,s)} = 1.0$ (mph)
Interior diag.	T-type	3-1/4	5/16	96	51	40	33
Vertical diag.	K-type	3-1/4	5/16	93	56	49	32

For the case of newer design cantilever sign truss web members, even the most slender members (using the *worst-case*  $K_f$ ) have computed critical uniform wind speeds of greater than 50 mph.

The greatest web member slenderness ratios ( $L/r$ ) that can possibly occur in these newer sign trusses are less than 105 for K-type connections in overhead trusses, less than 100 for T-type connections in overhead trusses, and less than 90 for cantilever trusses. In the above tables, it can also be seen that the critical wind speeds calculated just assuming

the very conservative simply-supported end conditions ( $K_{f(s,s)} = 1.0$ ) are all in the range of 25 to 35 mph and might therefore be expected to occur with some frequency, thus possibly leading a designer to decrease the slenderness of the members. This approach would however likely yield unnecessarily conservative designs, illustrating the benefit of properly accounting for the true level of end fixity in web member design. All in all, after consideration of the experiments, analyses, and field observations reported above, it appears that  $L/r$  should be kept less than about 105 for T-type connections and less than about 115 for K-type connections of hollow circular web members.

#### **8.4 Summary and Conclusions**

Using a combined experimental and analytical approach, it has been determined which hollow circular web members in existing IDOT aluminum sign truss structures are the most vulnerable to wind-induced flexural vibrations. These web members (mainly lightly loaded interior diagonals and verticals in older Type III-A and IV-A overhead trusses, as well as some interior diagonals in older Type II-C-A cantilever trusses) are exactly the ones that have experienced some end cracking in service over the years, which indicates that resonant member vibration (rather than poor welding at the joints or stress variations due to global vibration) has most likely been the primary cause of the observed fatigue cracking. Finally, additional calculations indicate that even the most slender possible web members of the newer IDOT standard design sign trusses should be substantially less vulnerable to wind-induced resonant flexural vibrations than were the members from older trusses that have experienced cracking. Results and concepts presented here may be used in the design of aluminum hollow tube web members, without the need for excess conservatism (and they could be extended, with appropriate additional experimental backup, to other types of web members and end connections). By ensuring that these members are designed with appropriate  $L/r$  values, fatigue caused by vortex shedding induced resonant vibration may be avoided.

## 9.0 Summary and Recommendations

This project was conducted by researchers from the Department of Civil and Environmental Engineering (CEE) at the University of Illinois at Urbana-Champaign (UIUC) for the Illinois Department of Transportation (IDOT). Five aluminum sign truss structures were the focus of this study – one cantilever and four simple spans. The simple spans comprised one Type I-A, one Type II-A, and one Type III-A (all structures with normal signage), as well as a Type II-A with a Variable Message Sign (VMS). The main objective was to evaluate the behavior of each sign structure through field testing and analytical modeling to ensure that IDOT's 2001 sign structure designs are satisfactory with respect to both strength and fatigue criteria, as specified in the 2001 AASHTO Standard Specifications for Structural Supports for Highway Signs, Luminaires and Traffic Signals (AASHTO Specifications). Another objective was to determine if the damper devices IDOT currently requires on sign truss structures indeed provide benefits commensurate with their cost. Finally, in addition to these objectives, insight was desired as to why some of the older design sign structures experienced weld cracking (and even complete member fracture) in certain situations.

The evaluations of the five structures confirmed that they were in general compliance with the AASHTO Specifications and IDOT standards under which they have been designed. However, in the opinion of the research team, the current AASHTO design provisions are not completely adequate in some areas, as discussed in detail below. The recommendations given are therefore intended to provide guidance if IDOT wishes to amend their designs for future structures to perform better than structures designed to current AASHTO Specifications. Sign structures constructed based on current IDOT designs do not appear to present significant risks for premature damage or failure. In fact, the current IDOT design calculations even make certain simplifications to design procedures that are somewhat more conservative than the AASHTO Specifications.

When field-measured stresses were projected up to the design wind speed of 90 mph, two of the sign structures (the Types I-A and II-A) had members that did not satisfy a pure axial allowable tension stress limit. The cantilever structure, the Type III-A structure, and the Type II-A structure with the VMS all had projected stresses below the allowable stress limits (but all of these structures had considerably smaller sign areas than allowed by IDOT design tables). The Type I-A and Type II-A structures with close to the maximum allowable sign areas have projected stresses in the chords approaching 20 ksi, which is the minimum yield stress in the weld heat affected zone. Those projected stresses have a significant bending (stress gradient) component, so the overstress is in a small area of the cross-section. Therefore, although the projected stress may exceed the allowable stress in a small region of the chord member, safety does not appear to be an issue.

The possibility of the aforementioned overstresses is the result of three factors. First, the design drag coefficient for signs, per the current AASHTO Specifications, range from 1.14 to 1.19 for these signs, whereas recent research by Letchford (2001) has shown

that, for elevated signs, the average measured drag coefficients were typically in the range of 1.40 to 1.50. As a result, ASCE 7-05 (ASCE, 2006) recently increased their recommended drag coefficients, but these have not yet been adopted by AASHTO. Using the ASCE 7 recommendations, the drag coefficients would range from 1.70 to 1.78 for the IDOT sign structures that were studied. The IDOT designs were based on a value of 1.2, which is larger than the current AASHTO requirements but smaller than recent test values (Letchford, 2001) or ASCE 7-05 recommendations. IDOT design procedures further assume that a 9 psi uniform stress acts on the projected vertical cross section area over regions where the sign is not present. These two factors are the primary reasons why the projected stresses are actually only a little bit larger than the allowable stresses. Two other factors affected the projected stresses, but to a much smaller degree. The current code does not explicitly account for the vibration of a sign structure at ultimate wind loading (although this may have been a factor implicitly considered when the gust factor was developed). At a 90 mph wind speed, the field data suggest that the stress due to dynamic response will only be about 5% larger than the equivalent static design load; this is a mean value, but the coefficient of variation is expected to be small for this wind speed.

Finally, a comparison of measured and calculated bending stresses indicates that the measured bending stress is almost always larger than the calculated one. This is not entirely unexpected because an analytical model is based on idealized behavior and an assumption that the constructed structure is identical to the one on the drawings, which is not the case. The calculations' underestimates were typically larger for bending than for axial stress, and larger for the connecting (web) members than the chords. This has little effect on the expected behavior of the connecting members since they were universally under-stressed (compared to the allowable stress). Part of the factor of safety assumed in design is to account for such omissions and/or simplifications in the analysis.

Recommendation #1 – Based on the results from this study, IDOT is encouraged to adopt the ASCE 7 recommended drag coefficient (or a reasonable simplification thereof) for design of aluminum sign structures. Given the conservative assumptions used by IDOT for analyzing the wind-induced stresses, the values determined from recent wind tunnel studies (still larger than current AASHTO values) may also be acceptable. Including a design coefficient of 1.10 in the equation for determining design wind pressure for the 90 mph design wind speed is also recommended to account for vibration of the structure. Alternatively, this effect could be included in one of the other design coefficients.

The AASHTO Specifications require that cantilever sign structures be designed for fatigue loads. However, simply supported trusses are not currently required to be designed for fatigue. This study evaluated fatigue effects in all structures, for consideration by IDOT. The stress ranges experienced by selected truss members were measured under wind loads and truck gusts. The study concluded that the fatigue stress range in each member could be evaluated considering an 11.2 mph wind speed and/or simultaneous truck gust(s). The fatigue stress ranges measured for the chords of all of the structures were considerably lower than the allowable stress range of 1.9 ksi. The fatigue

stress ranges measured for the connecting (web) members were almost all smaller than the allowable stress range of 0.44 ksi. If signs with the maximum allowable area were placed on these structures, it is projected that the stress ranges experienced by horizontal and horizontal diagonal members would occasionally exceed the constant amplitude fatigue limit (CAFL). This is most likely to occur under the simultaneous action of moderate wind in conjunction with larger truck gusts, a design loading condition that is not currently mandated by the AASHTO Specifications and is very conservative, since the peak vibration response to the wind (not the average response) and the peak vibration response to the truck gust would have to occur nearly simultaneously to produce a significant stress range in a member..

Based on the AASHTO Specifications, member stresses calculated using design equations for wind pressure ignore the dynamic response of the structure. For the 90 mph wind speed, the ratio of the maximum stress and the 3-second average stress was only 1.05. On the other hand, for the 11.2 mph wind speed this ratio was about 3.0, on average. In addition, the coefficient of variation was quite large; the mean plus standard deviation exceeded 4.0. This is too significant to be ignored for fatigue design of these sign structures, but the actual maximum stress range observed (for individual cycles) was typically only slightly more than two times the mean value for winds at or near 11.2 mph.

Although measured stresses exceeded those calculated, with only a small affect on the strength design, this could have a more significant impact on the fatigue of the web members in a truss. For a given bending moment increase where connecting members attach to a chord, the stress increases in the chord will be relatively small because it has a much larger section modulus than any of the connecting members. However, the typical connecting members have a much smaller section modulus, so the stress increase can be greater. For the members where the design stress range was exceeded, all but one had bending as the largest stress component. Another factor that makes the fatigue situation more significant for the connecting members is their very restrictive prescribed allowable stress range of 0.44 ksi (as opposed to 1.9 ksi for chord members). For this reason, no chord members experienced stress ranges even close to their allowable values. Connection details and member sizes should consider these restrictions.

As mentioned in this report, the AASHTO Specifications' design equation for pressure due to truck gusts was modified after the IDOT design standards were completed. The new equation gives smaller design stresses than those determined by IDOT using the previous AASHTO criteria. Therefore, had the new equation been used in design, it is possible that the CAFL would be exceeded in more of the connecting members (which may have been smaller, depending on what design aspect ultimately controlled their sizing). Another factor affecting the calculated design stress range is the area over which the design truck gust pressure is applied. The AASHTO Specifications conservatively require that this pressure be applied over the entire sign area, but the wind gust designs usually control for fatigue design, so truck gusts are actually relatively less important with respect to design.

Given all of the factors that affect the design (and actual) stresses in sign truss members (and their corresponding measured stress ranges), it is not practical to provide an accurate and consistent design equation for fatigue stresses. However, from the empirical data gathered in this study, some important final observations can be made. The sign structure designs developed and currently used by IDOT may be slightly under-designed with respect to fatigue in the horizontal and horizontal diagonal members even though they were designed for twice the truck gust pressure required by the current AASHTO Specifications. Recall also that AASHTO does not require that simply supported trusses be designed for fatigue.

Recommendation #2 - If IDOT chooses to consider fatigue for design of new simply supported trusses for fatigue (even though this is not required by AASHTO), a reasonable approach for new designs might be to use the current AASHTO design equation along with a dynamic response coefficient of 3.0. This would result in a design pressure about 1½ times that used by IDOT in their current standard designs. However, this may be too conservative, since the allowable stress range would rarely be exceeded in the field, and only under combinations of wind and large truck gusts, a loading that is not mandated by the AASHTO Specifications. In addition, if Recommendation #1 is adopted, it is even less likely that occasional stress ranges in excess of the allowable stress ranges would occur.

Laboratory tests and analytical models of the Stockbridge dampers currently installed on IDOT sign structures were undertaken. Four damper units purchased from the supplier were tested under controlled conditions in the Newmark Structural Engineering Laboratory (NSEL) of the UIUC Department of CEE. Results for the standard dampers mounted on the Types I-A, II-A, and III-A structures studied in this project (in conjunction with field testing) indicate that the dampers offer little protection against fatigue because the damper's natural frequency is much greater than that of any of the sign structures. For a damper to be effective, the ratio of the damper's to the structure's natural frequency should be between about 0.9 and 1.1, with best results when the ratio is around 1.0. The "sloppy" Stockbridge damper has a longer cable, so its natural frequency is indeed lower. However, another important factor is the ratio of damper weight to structure weight, which is very small for most sign structures. Thus, even the "sloppy" damper will be effective only for the smaller cantilever structures (due to the smaller weight ratios of the damper weight to the structure weight of the larger structures).

Due to these factors, the effectiveness of the dampers at reducing the amplitude of the stress ranges for the sign truss structures, while apparent, is very small. This could be improved by using multiple dampers, but for an impulse load like a truck gust, dampers are generally not effective at reducing the amplitude of the initial cycle. However, if properly designed, dampers can be effective at reducing the number of stress cycles due to wind and/or truck gusts occurring above the CAFL. In other words, a well-designed damper can be quite effective at reducing the response to wind loads that produce a modulated sine wave response in the structure.

Recommendation #3 – Since the projected maximum stress ranges in some of the connecting (web) members in simply supported aluminum trusses designed by current IDOT procedures are larger than the CAFL, IDOT may wish to consider installing more effective dampers on their existing sign structures to reduce the effects of fatigue. However, this would be a very conservative action since the excessive stress ranges are only likely to occur under the simultaneous action of wind and large truck gusts. If IDOT chooses to mitigate the response of existing sign truss structures, a consultant with experience in designing damping systems should be retained (and alternative damper types should be explored). It is not recommended that individual Stockbridge dampers be installed on new structures designed for fatigue resistance because the dampers are ineffective unless multiple units are installed and the natural frequency of each unit is approximately the same as the natural frequency of the structure.

As a part of this study, some of the factors affecting the behavior of the older sign truss designs (with regard to weld cracking) were investigated. Since the weld cracks occurred more often in slender web members, the possibility of vortex shedding causing excessive vibration that exceeded a connection's fatigue limit was investigated. The results of the investigation suggest that this hypothesis is correct (as a strong contributing cause for certain web members); however, this is probably not the only factor involved. The effect of dynamic response of the structure on the stresses in connecting member welds, as described above, was also a problem for the older structures. The member connections most often damaged were near the ends of the trusses, in situations where web member forces (and possibly even web member moments) would be larger. There were also problems in making quality welds where the multiple connecting members closely approached each other at chord connections, leaving inadequate access for proper welding.

Recommendation #4 – Based on the results reported in Chapter 8.0, then, it is recommended that the slenderness ( $L/r$ ) of truss members (regardless of whether loaded in tension or in compression) should be kept less than about 105 for T-type connections and less than about 115 for K-type connections.

## 10.0 References

- AASHTO (2001). *Standard Specifications for Structural Supports for Highway Signs, Luminaires, and Traffic Signals*, 4<sup>th</sup> Ed., American Association of State Highway and Transportation Officials, Washington D.C.
- AFL Telecommunications (2003). *Highway Truss Vibration Dampers Specifications*, <[http://www.alcoa.com/afl\\_tele/aca/catalog/pdf/specifications/Highway\\_Truss\\_Damper.pdf](http://www.alcoa.com/afl_tele/aca/catalog/pdf/specifications/Highway_Truss_Damper.pdf)> (April 8, 2005).
- Alcoa Conductor Accessories (1992). *Substation Accessories Section ACA20*.
- ASCE/SEI (2006), *Minimum Design Loads for Buildings and Other Structures (ASCE 7-05)*, American Society of Civil Engineers, Washington, D.C.
- Bahtovska, E. (2000). "The Energy Balance for Damped Wind-Excited Vibrations," *Facta Universitatis, Mechanical Engineering*, 1(7) 769-773.
- Cook, R.A., Bloomquist, D., Richard, D.S., and Kalajian, M.A. (2001). "Damping of Cantilevered Traffic Signal Structures," *ASCE Journal of Structural Engineering*, 127(12), 1476-1483.
- Dexter, R.J., and Ricker, M. J. (2002). *NCHRP Report 469: Fatigue-Resistant Design of Cantilevered Signal, Sign, and Light Supports*, Transportation Research Board, National Research Council, Washington, D.C.
- Gill Instruments (2000). *WindMaster Ultrasonic Anemometer User Manual*, Hampshire, England.
- Ginal, S. (2003). *Fatigue Performance of Full-Span Sign Support Structures Considering Truck-Induced Gust and Natural Wind Pressures*, Marquette University (M.S. Thesis), Milwaukee, WI.
- Hamilton III, H.R., Riggs, G.S., and Puckett, J.A. (2000). "Increased Damping in Cantilevered Traffic Signal Structures," *ASCE Journal of Structural Engineering*, 126(4), 530-537.
- Illinois Department of Transportation (1982). *Sign Structures Manual*, Bureau of Bridges and Structures, Springfield, IL.
- Illinois Department of Transportation (2001). *Sign Structures Manual*, Bureau of Bridges and Structures, Springfield, IL.
- Kaczinski, M.R., Dexter, R.J., and Van Dien, J.P. (1998). "Fatigue-Resistant Design of Cantilevered Signal, Sign and Light Supports," *NCHRP Report 412*, Transportation Research Board, National Research Council, Washington, D.C.
- Kissell, J.R., and Ferry, R.L. (2002). *Aluminum Structures: A Guide to Their Specifications and Design*, 2<sup>nd</sup> Ed., John Wiley & Sons, New York, NY.

- Lengel, J.S., and Sharp, M.L. (1969). "Vibration and Damping of Aluminum Overhead Sign Structures," *Highway Research Record*, No. 259, 51-60.
- Letchford, C.W. (2001). "Wind Loads on Rectangular Signboards and Hoardings," *Journal of Wind Engineering and Industrial Aerodynamics*, 89(2), 135-151.
- MATLAB 7.0 (2004). The MathWorks, Natick, MA.
- Ocel, J.M., Dexter, R.J., and Hajjar, J.F. (2006). "Fatigue-Resistant Design For Overhead Signs, Mast Arm Signal Poles, and Lighting Standards", Minnesota Department of Transportation, St. Paul, MN.
- Pantelides, C., Nadauld, J., and Cercone, L. (2003). "Repair of Cracked Aluminum Overhead Sign Structures with Glass Fiber Reinforced Polymer Composites," *ASCE Journal of Composites for Construction*, 7(2) 118-126.
- PCB Piezotronics, Inc. (2004). Depew, NY.
- R.M. Young Company, (2003). Traverse City, MI.
- SAP2000<sup>®</sup>, v.9 (2004). Computer and Structures, Inc. (CSI), Berkeley, California.
- Sauter, D., and Hagedorn, P. (2002). "On the Hysteresis of Wire Cables in Stockbridge Dampers," *International Journal of Non-Linear Mechanics*, 37(8), 1453-1459.
- Sharp, M.L. (1993). *Behavior and Design of Aluminum Structures*, McGraw-Hill, New York, NY.
- Sharp, M.L., Nordmark, G.E., and Menzemer, C.C. (1996). *Fatigue Design of Aluminum Components and Structures*, McGraw-Hill, New York, NY.
- Simiu, E., and Scanlan, R.H. (1996). *Wind Effects on Structures: Fundamentals and Applications to Design*, 3<sup>rd</sup> Ed., John Wiley & Sons, New York, NY.
- Terra Technology Corp. (1988). Redwood, Washington.
- Thomson, W.T., and Dahleh, M.T. (1998). *Theory of Vibration with Applications*, 5<sup>th</sup> Ed., Prentice-Hall, Upper Saddle River, NJ.
- Wen, Y.K. (2005). "Probabilistic Loads and Design," *CEE 574 Class Notes*, Spring 2005, UIUC, Urbana, IL.
- Zalewski, B., and Huckelbridge, A. (2005). *Dynamic Load Environment of Bridge-Mounted Sign Support Structures*, Ohio Department of Transportation, Columbus, OH.

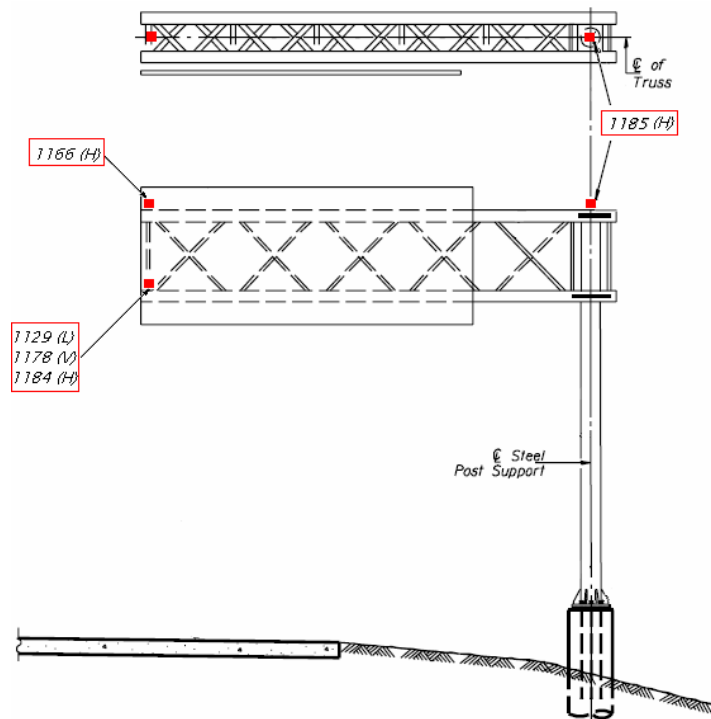
## Appendix A Recorded Data

### A1.0 Type II-C-A Sign Structure Data

#### A1.1 Sensor names and locations

##### *Accelerometers*

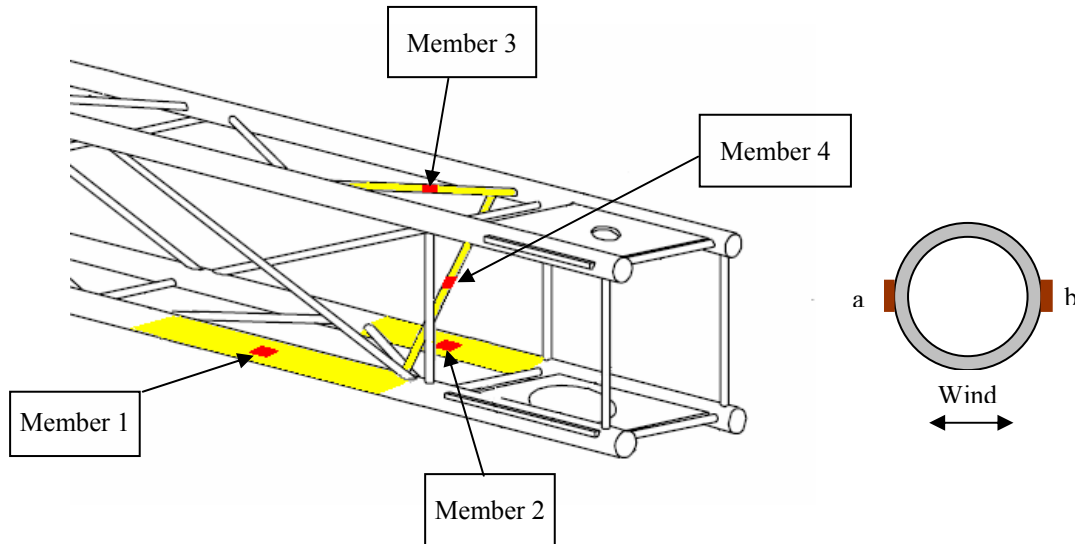
The figure below shows the placement of the accelerometers on the Type II-C-A cantilever sign structure. The table following gives a detailed description of the sensor labels and locations.



Accelerometer	Location	Measurement Direction
1185	Top of column	Horizontal
1166	End of Cantilever – Top	Horizontal
1184	End of Cantilever – Bottom	Horizontal
1178	End of Cantilever – Bottom	Vertical
1129	End of Cantilever – Bottom	Longitudinal

### Strain gages

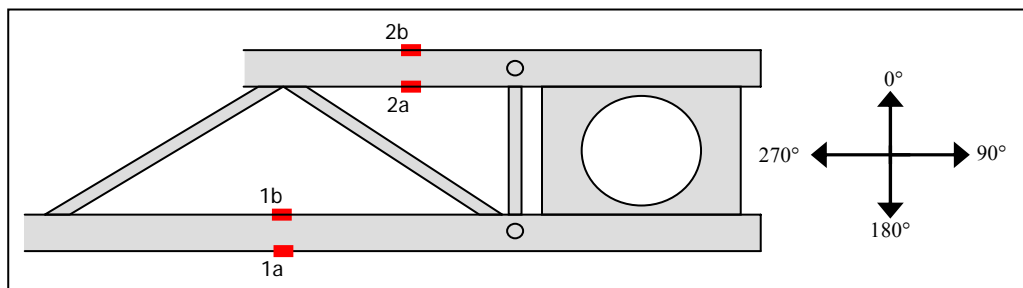
Eight strain gages were installed on the C-II-A sign structure. The locations of the strain gages are indicated in the figure below. The table below details the locations and labeling of each gage.



Strain Gage	Location
1a 1b	Bottom Chord – front plane, $L_b = 48$ in.
2a 2b	Bottom Chord – back plane, $L_b = 24$ in.
3a 3b	Horizontal Diagonal – top plane
4a 4b	Interior Diagonal

### Anemometer

The wind velocity and direction measured by the anemometer relative to the sign is shown in the figure below.



## A1.2 Data Description

The data contained in the appendix files and plotted below is the filtered data acquired for the Type II-C-A cantilever sign structure. A link to a text file of each test is included with the plots of the data. To import the data into Excel follow the steps given below:

1. Click on the link to open a text file of the data
2. Click Edit → Select All
3. Click Edit → Copy
4. Open Excel
5. Once in Excel, click Edit → Paste

Test descriptions:

- W1-W6 are tests that were taken under strong wind conditions. Note that when the wind direction is equal to 0 degrees, the wind is blowing perpendicular to the sign face. This data was taken on March 11, 2005 when the wind was primarily blowing perpendicular to the sign face and ranged in speed from about.
- TG1 was a test taken during calm conditions to record the response of the sign to truck gusts. This data was collected on March 21, 2005. Although other tests were taken at the same time, the instrumentation was not functioning correctly.
- M1-M8 are tests that were taken during calm conditions while the structure was manually excited in either the horizontal or vertical direction. Tests M1-M4 were taken on December 2, 2004 when the damper was located near the mid-span of the truss. Tests M5-M8 were taken on March 21, 2005 after the damper was moved to the end of the truss.

## A1.3 Wind Data

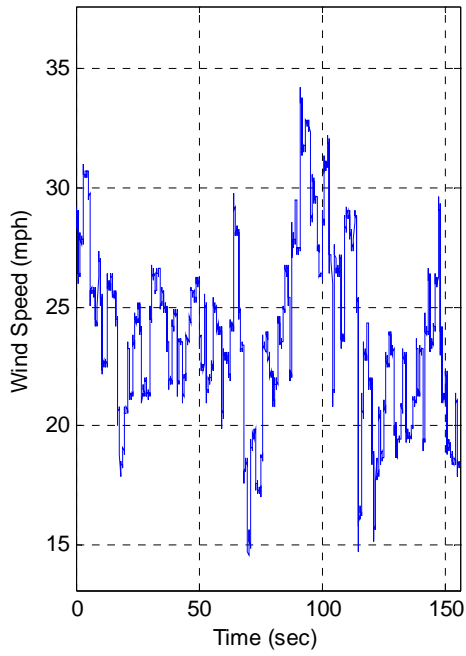
The data structure for the wind data is as follows:

Time(sec), 1a, 1b, 2a, 2b, 3a, 4b, a1185, a1166, a1184, a1178, a1129, WS(mph),  
WD(deg)

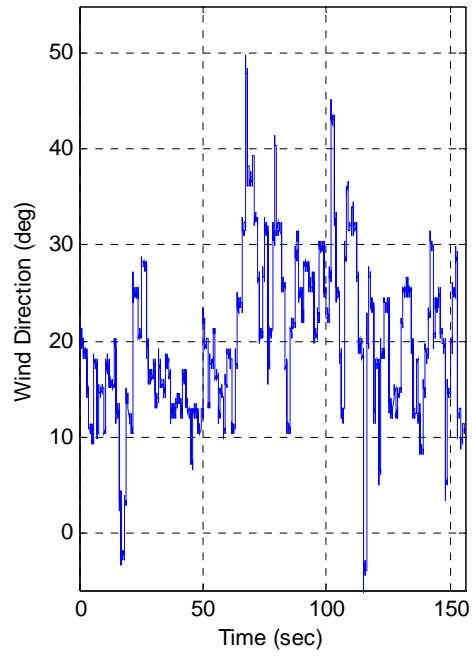
To determine the wind velocity acting perpendicular to the sign face the following calculation must be made:

$$WS_{\text{perpendicular}} = WS * \cos(WD)$$

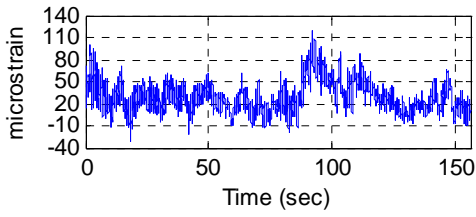
**Test W1**  
Data\II-C-A\II-C-A W1.txt



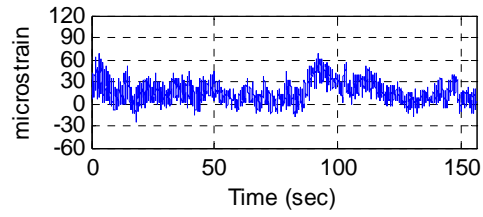
1a



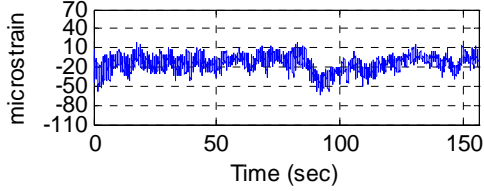
1b



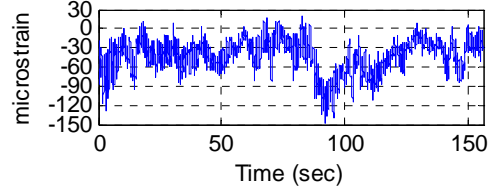
2a



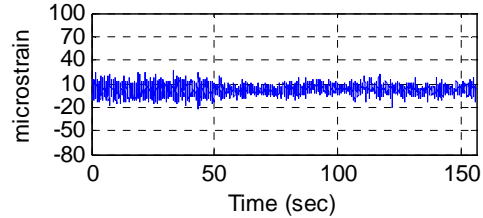
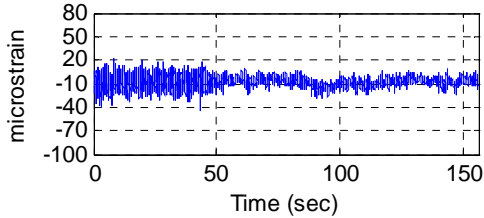
2b

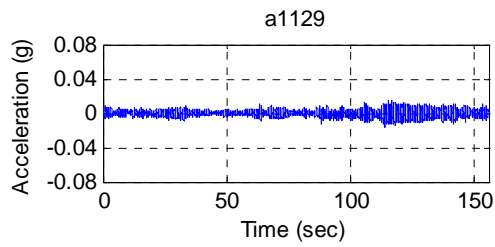
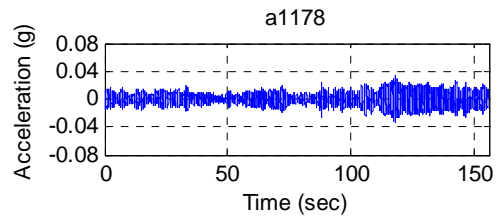
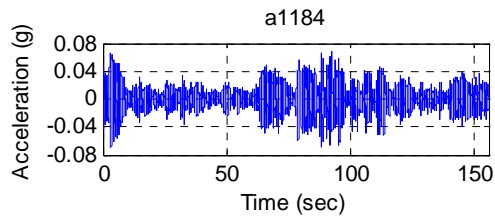
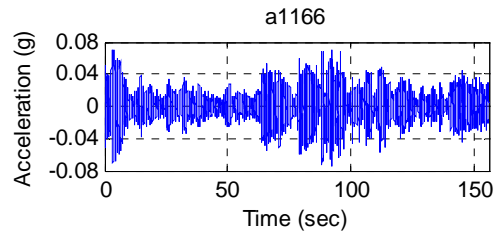
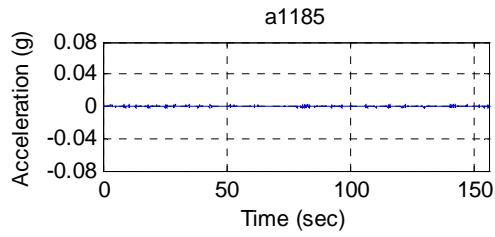


3a

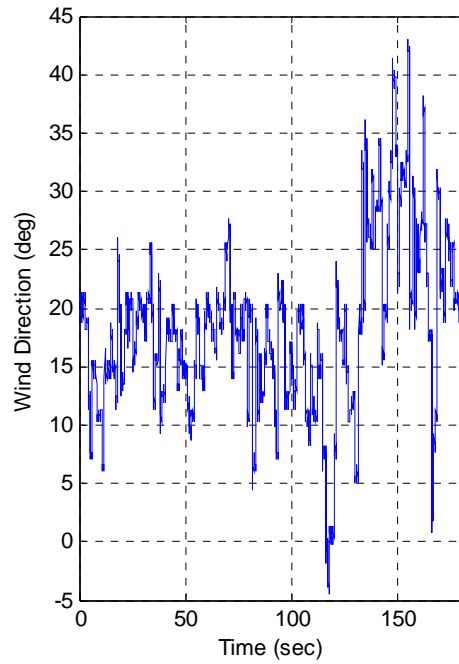
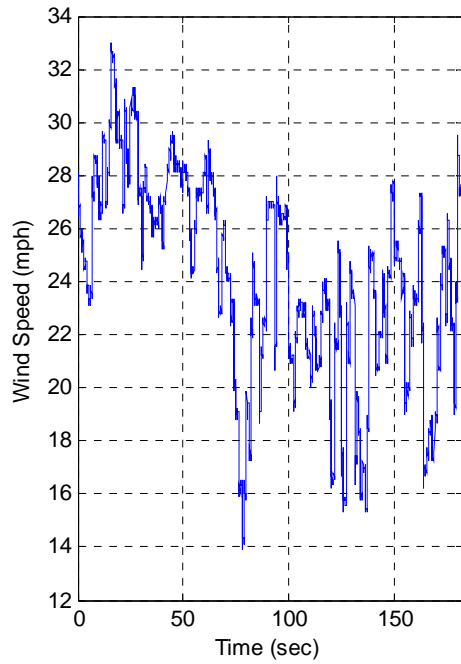


4b

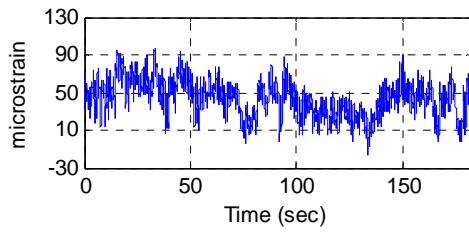




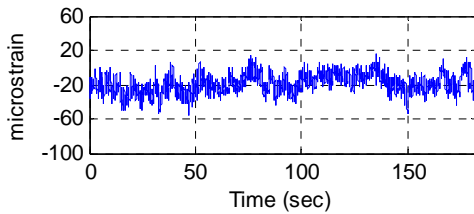
**Test W2**  
Data\II-C-A\II-C-A W2.txt



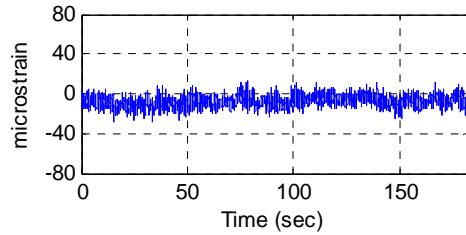
1a



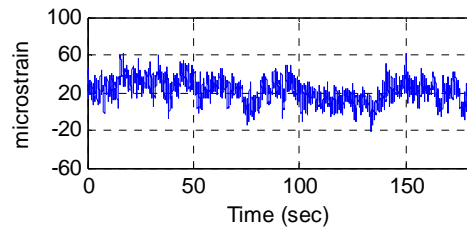
2a



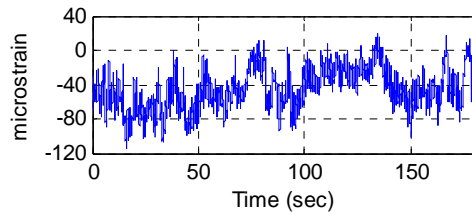
3a



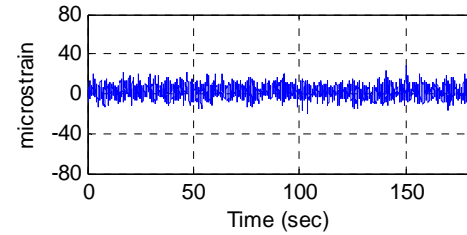
1b

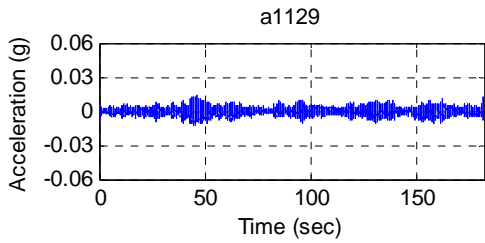
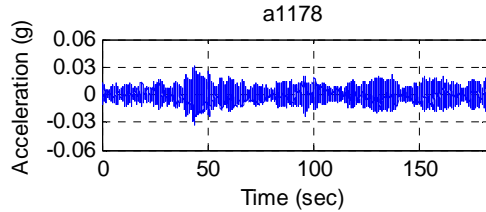
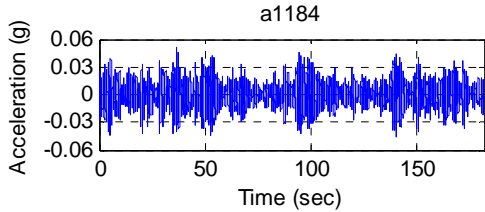
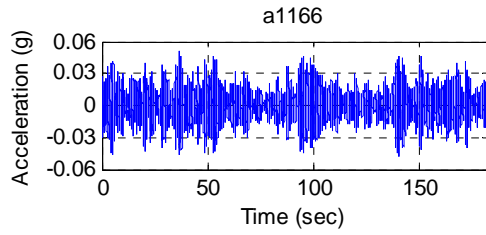
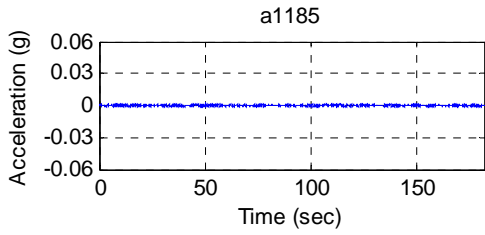


2b

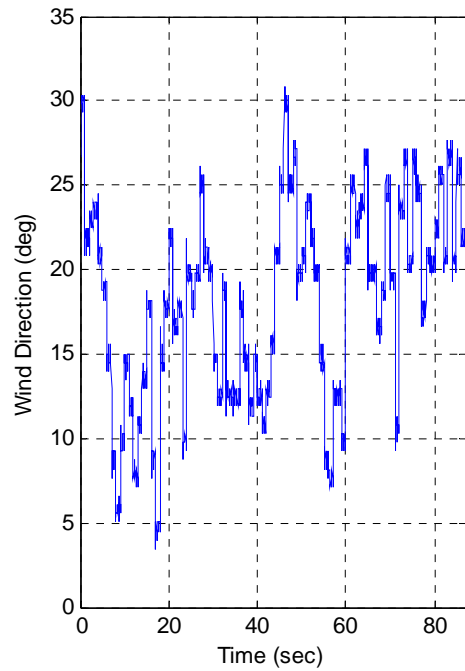
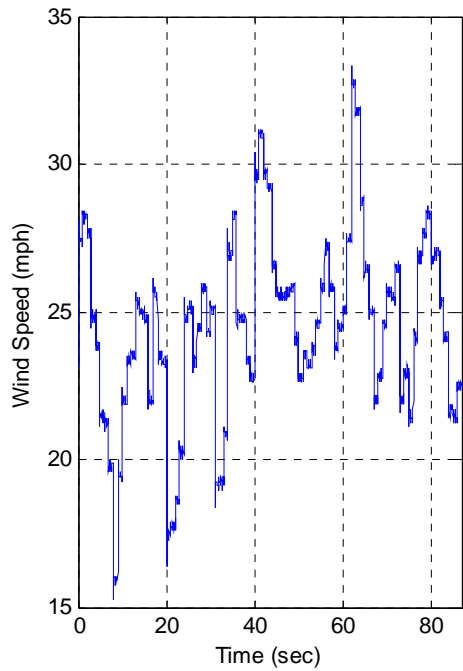


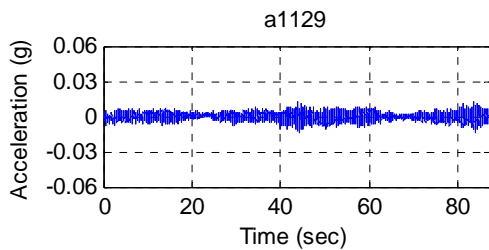
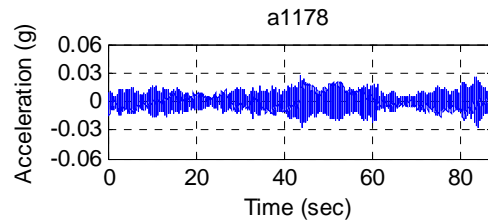
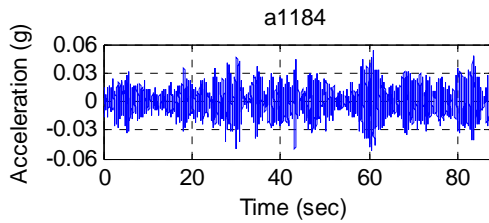
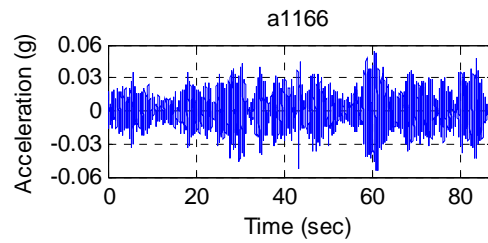
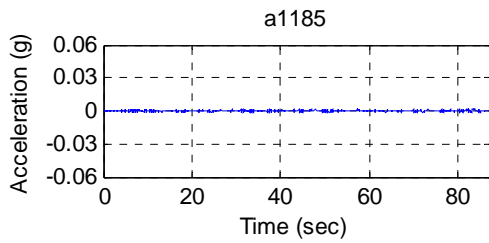
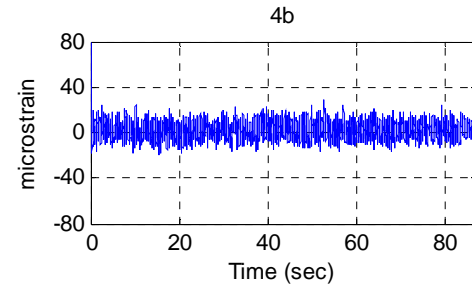
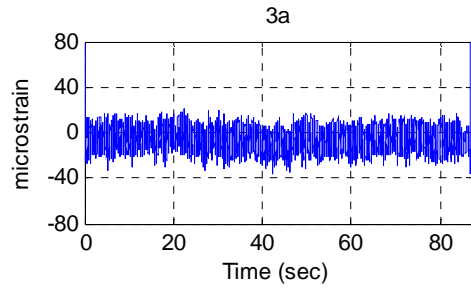
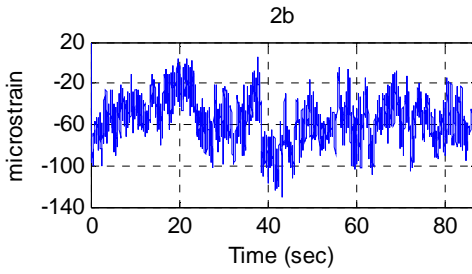
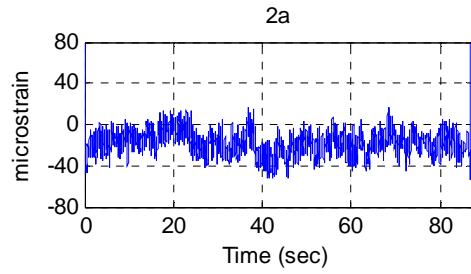
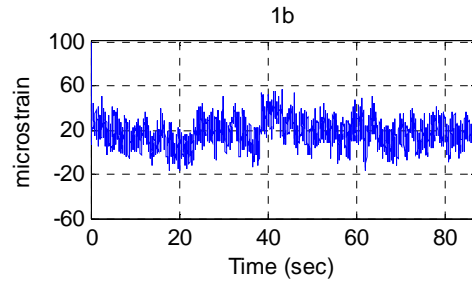
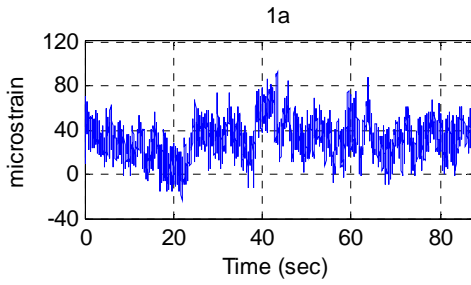
4b



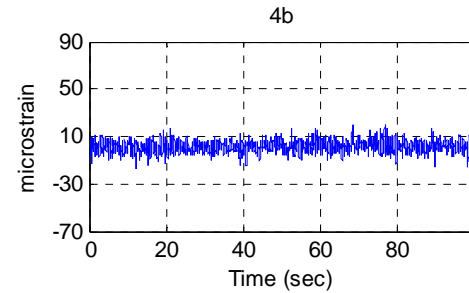
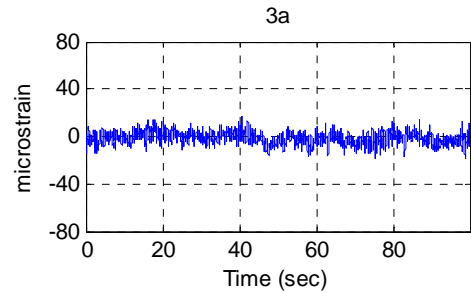
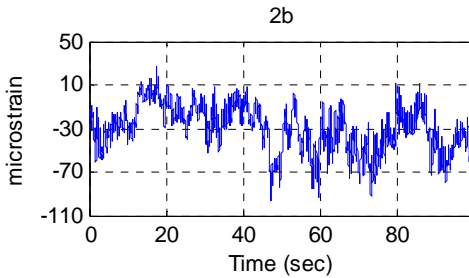
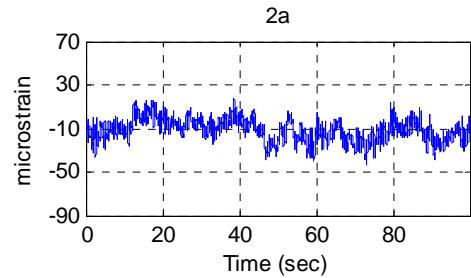
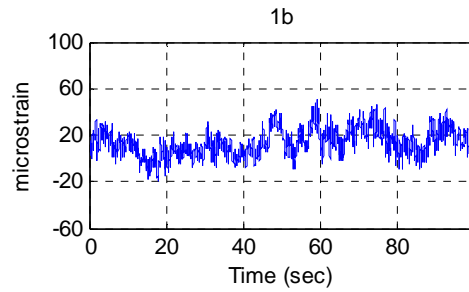
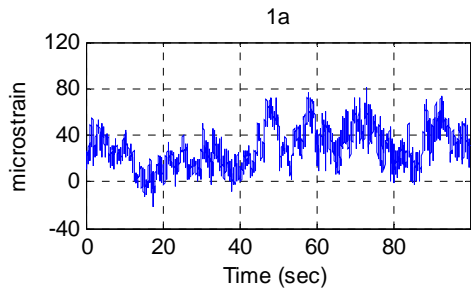
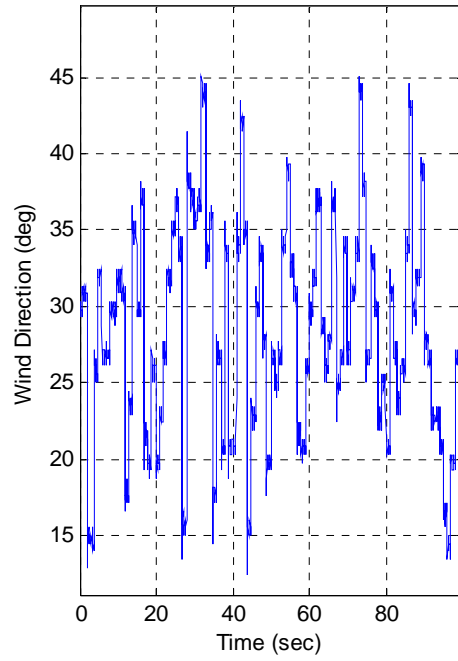
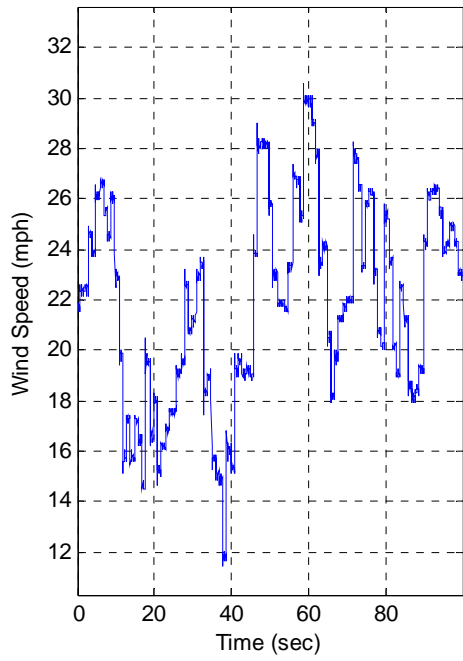


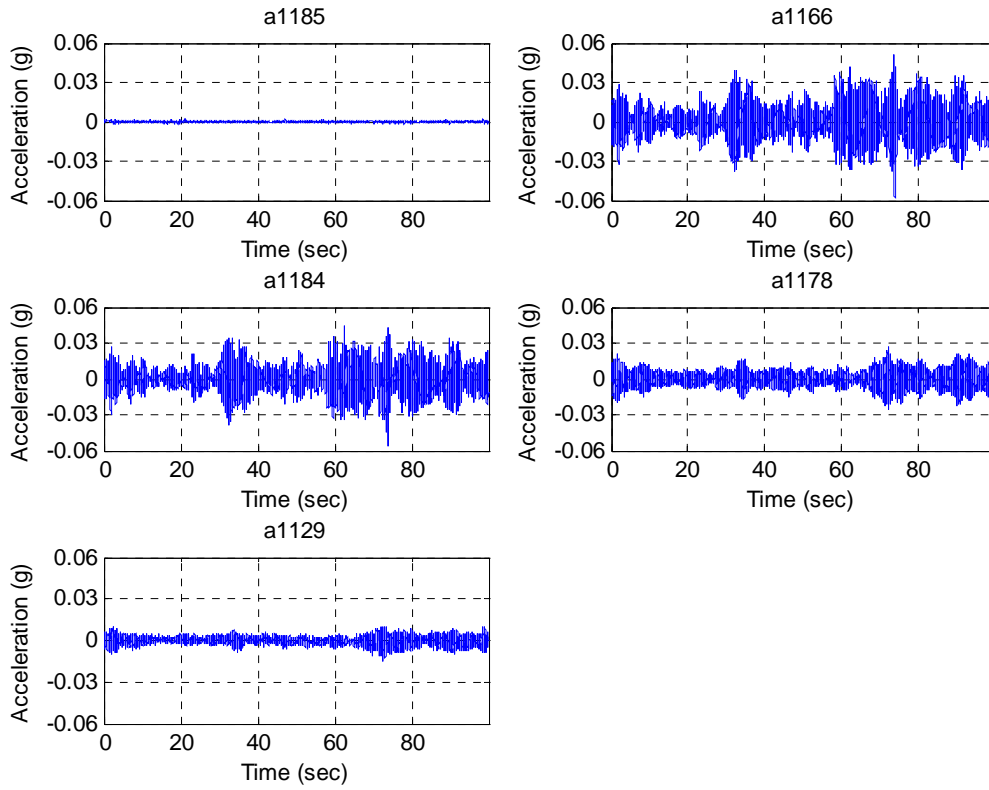
**Test W3**  
[Data\II-C-A\II-C-A\\_W3.txt](#)





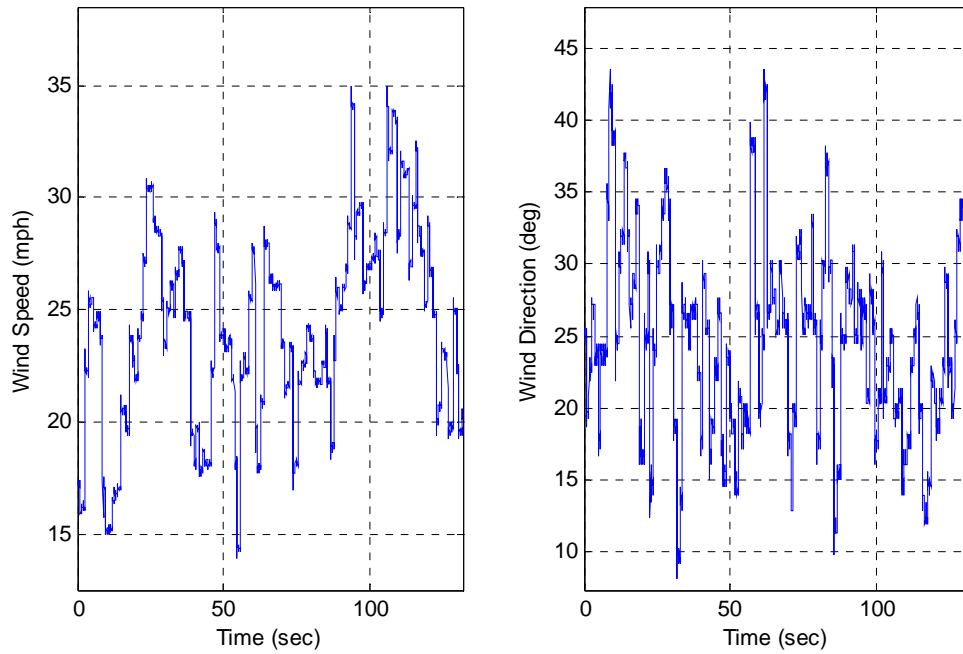
**Test W4**  
Data\II-C-A\II-C-A W4.txt

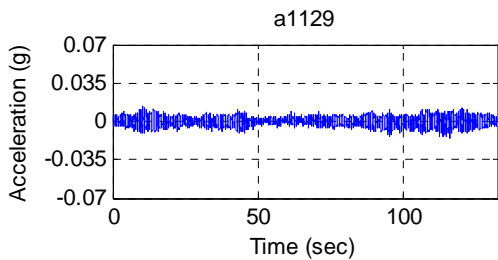
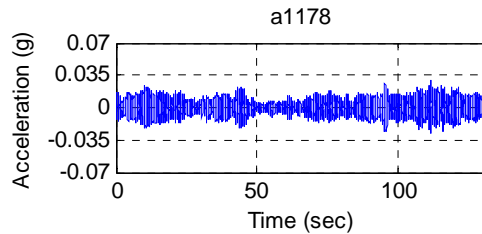
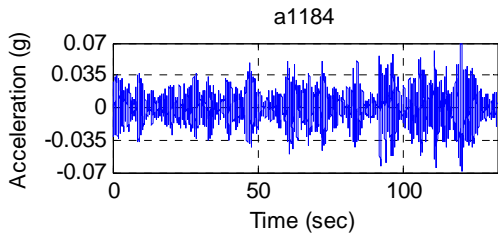
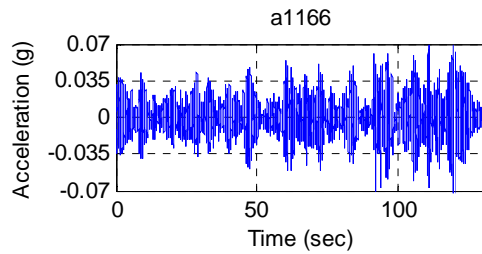
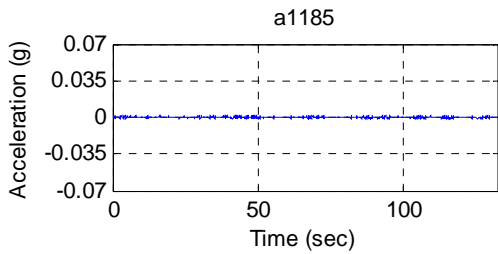
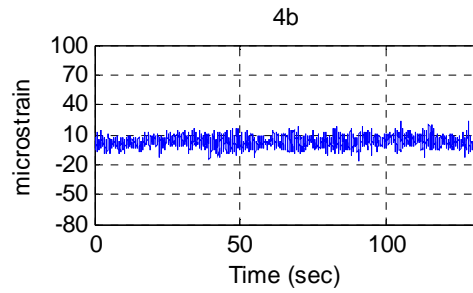
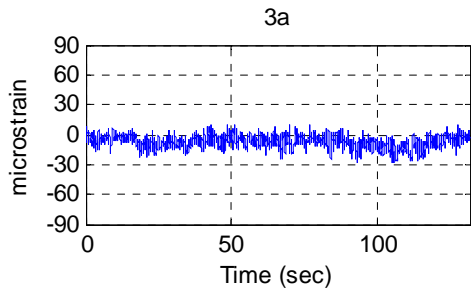
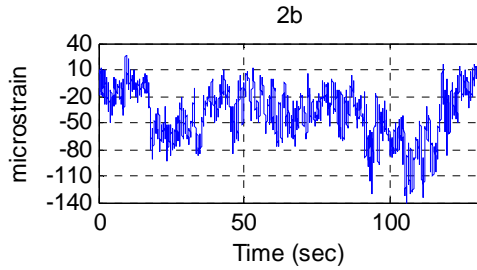
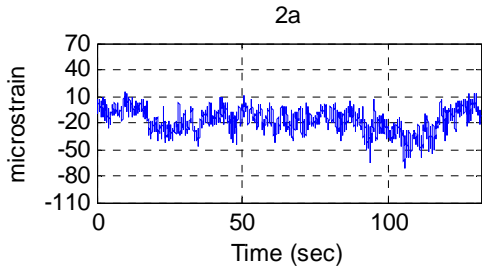
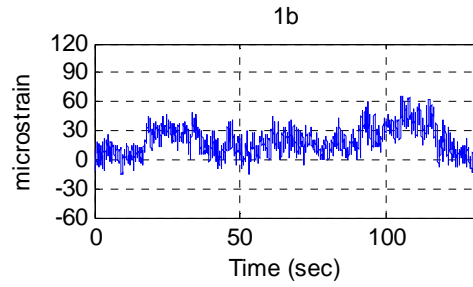
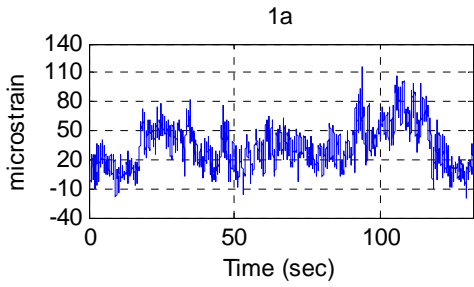




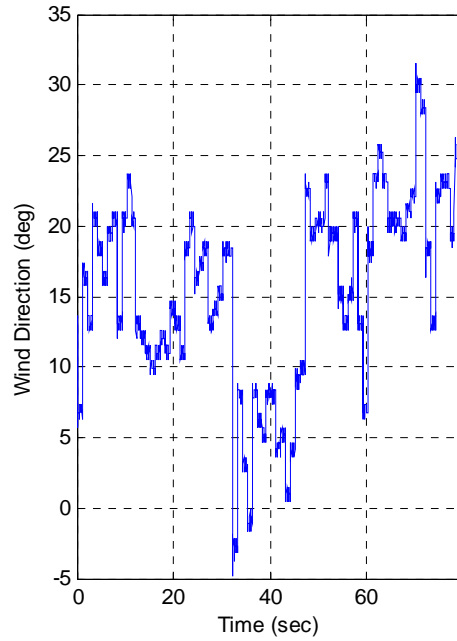
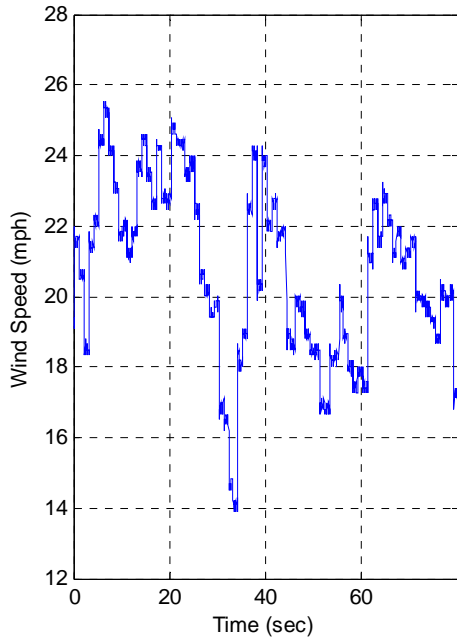
**Test W5**

[Data\II-C-A\II-C-A\\_W5.txt](#)

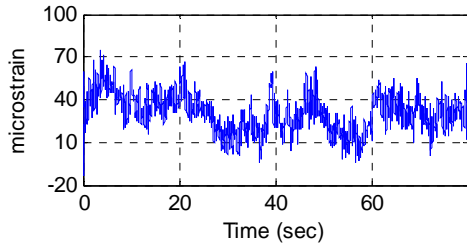




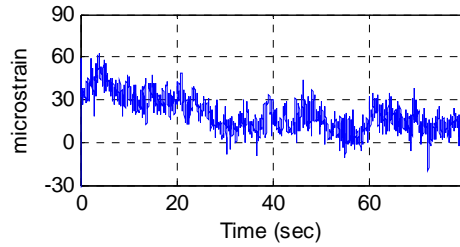
**Test W6**  
**Data\II-C-A\II-C-A W6.txt**



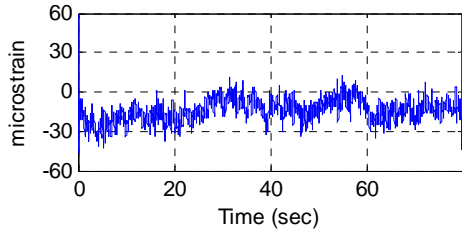
1a



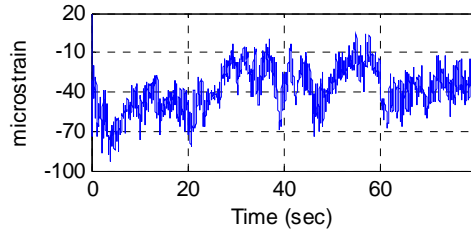
1b



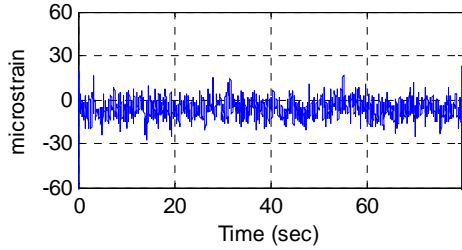
2a



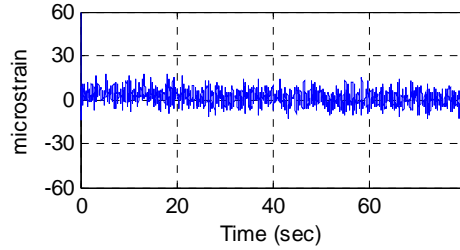
2b

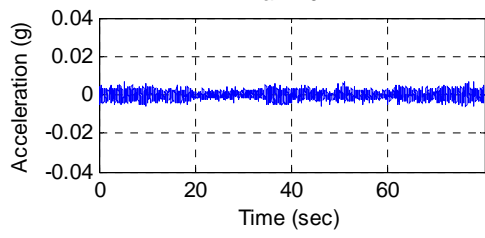
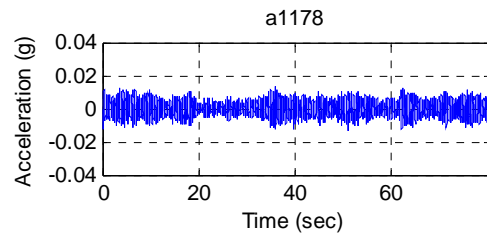
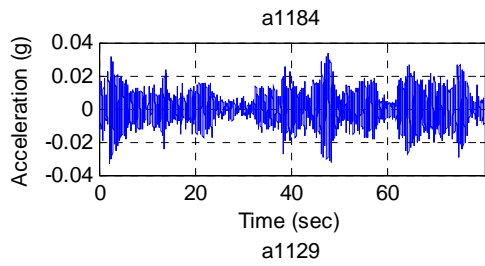
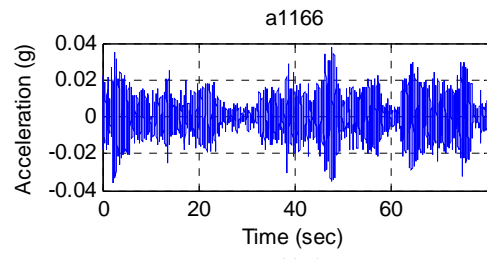
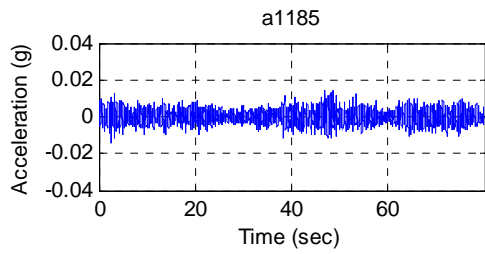


3a



4b





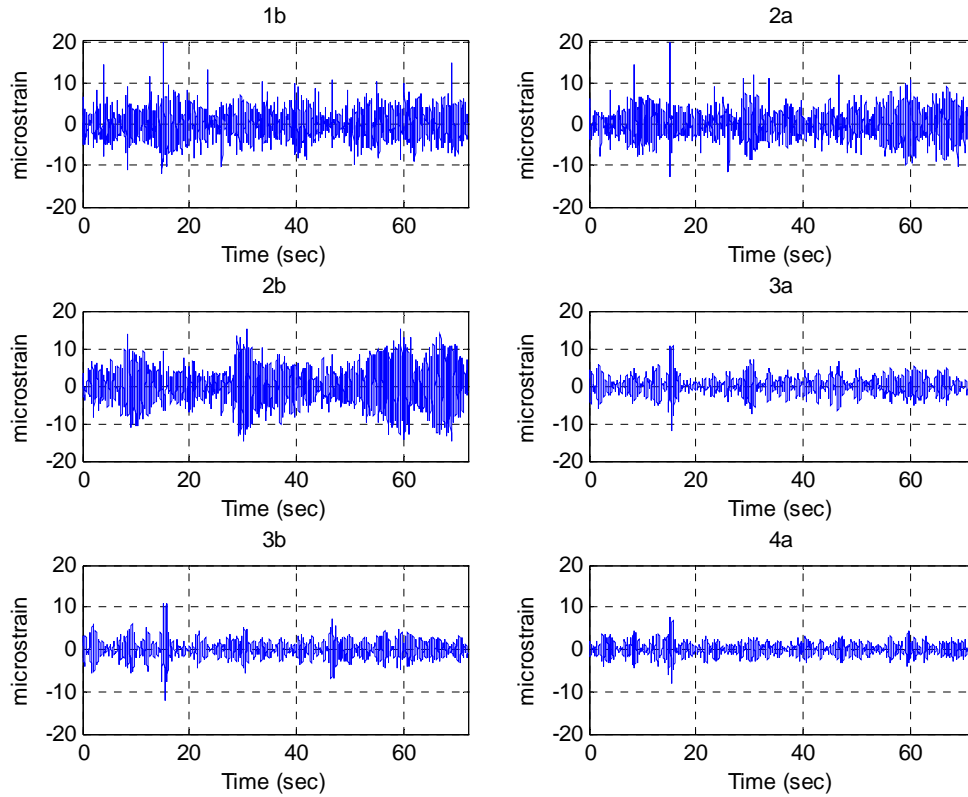
## A1.4 Truck Gust Data

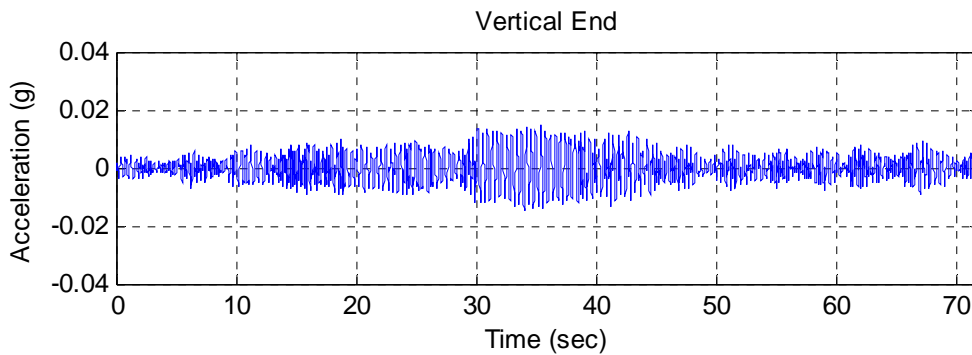
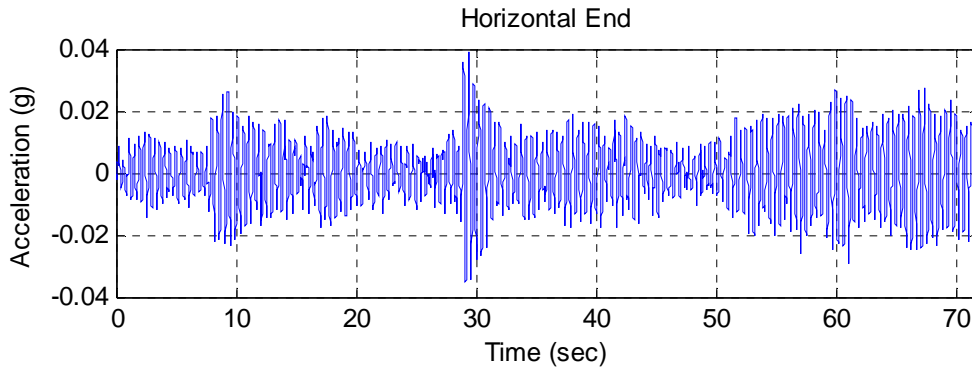
The data structure for the truck gust data is as follows:

Time(sec), 1b, 2a, 2b, 3a, 3b, 4a, a1184, a1178

### Test TG1

[Data\II-C-A\II-C-A\\_TG1.txt](#)





### A1.5 Manual Excitation Data

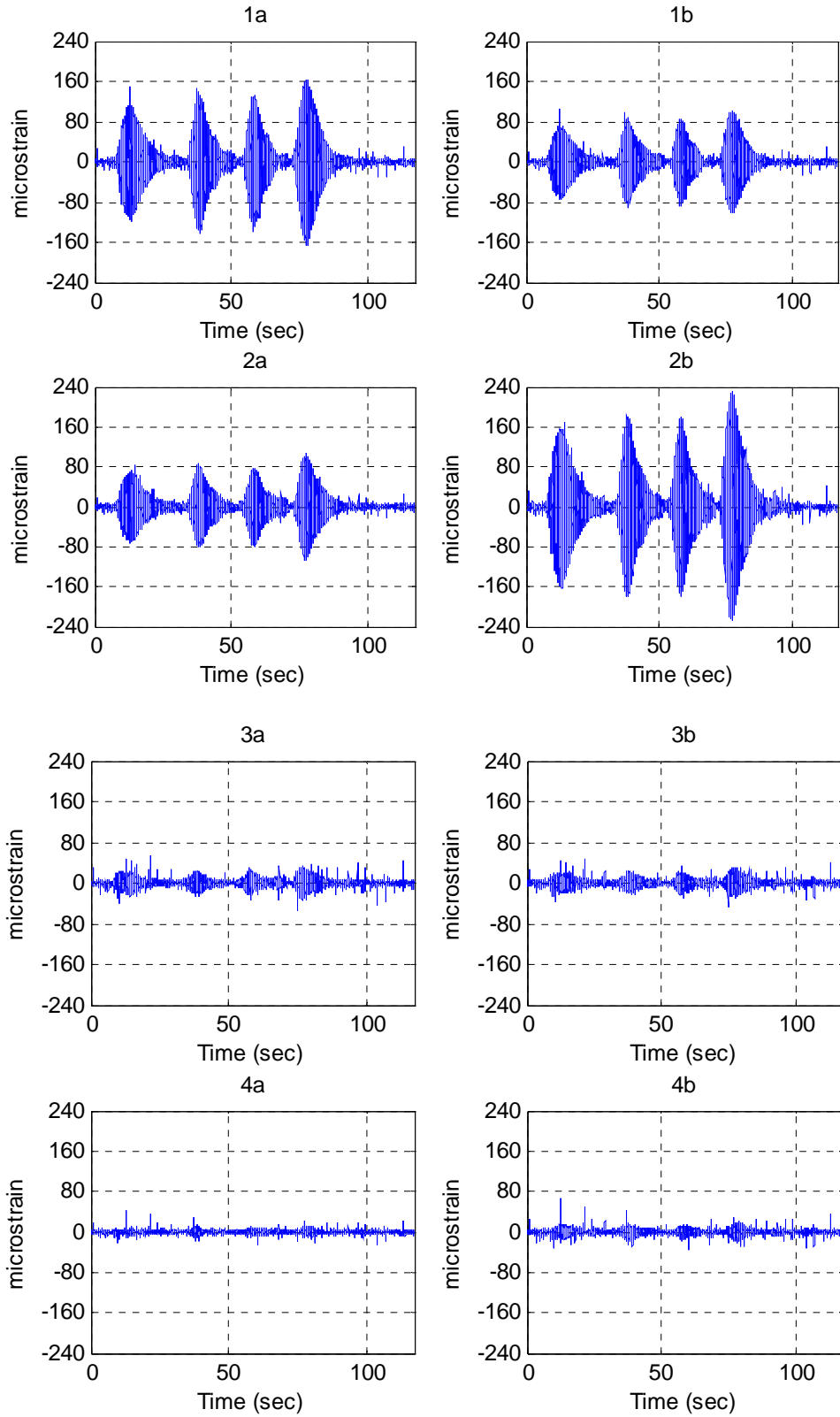
The data structure for the manual excitation data is as follows:

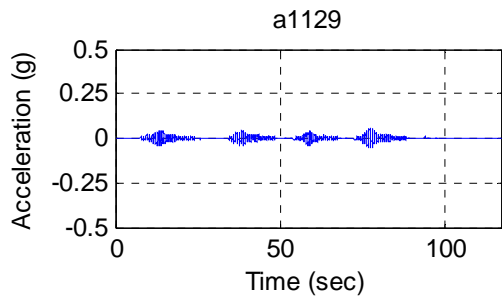
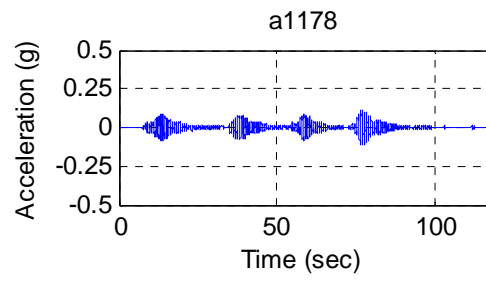
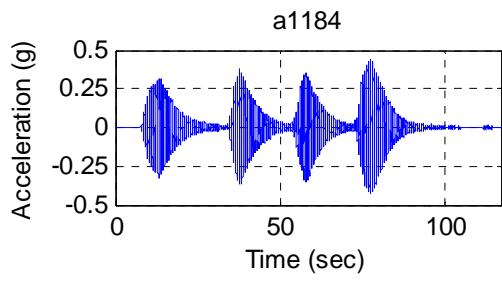
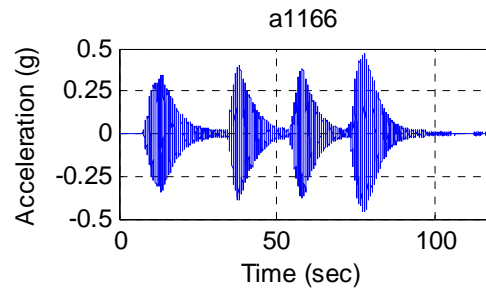
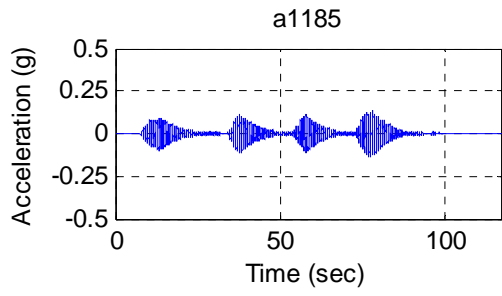
Time(sec), 1a, 1b, 2a, 2b, 3a, 3b, 4a, 4b, a1185, a1166, a1184, a1178, a1129

Test descriptions:

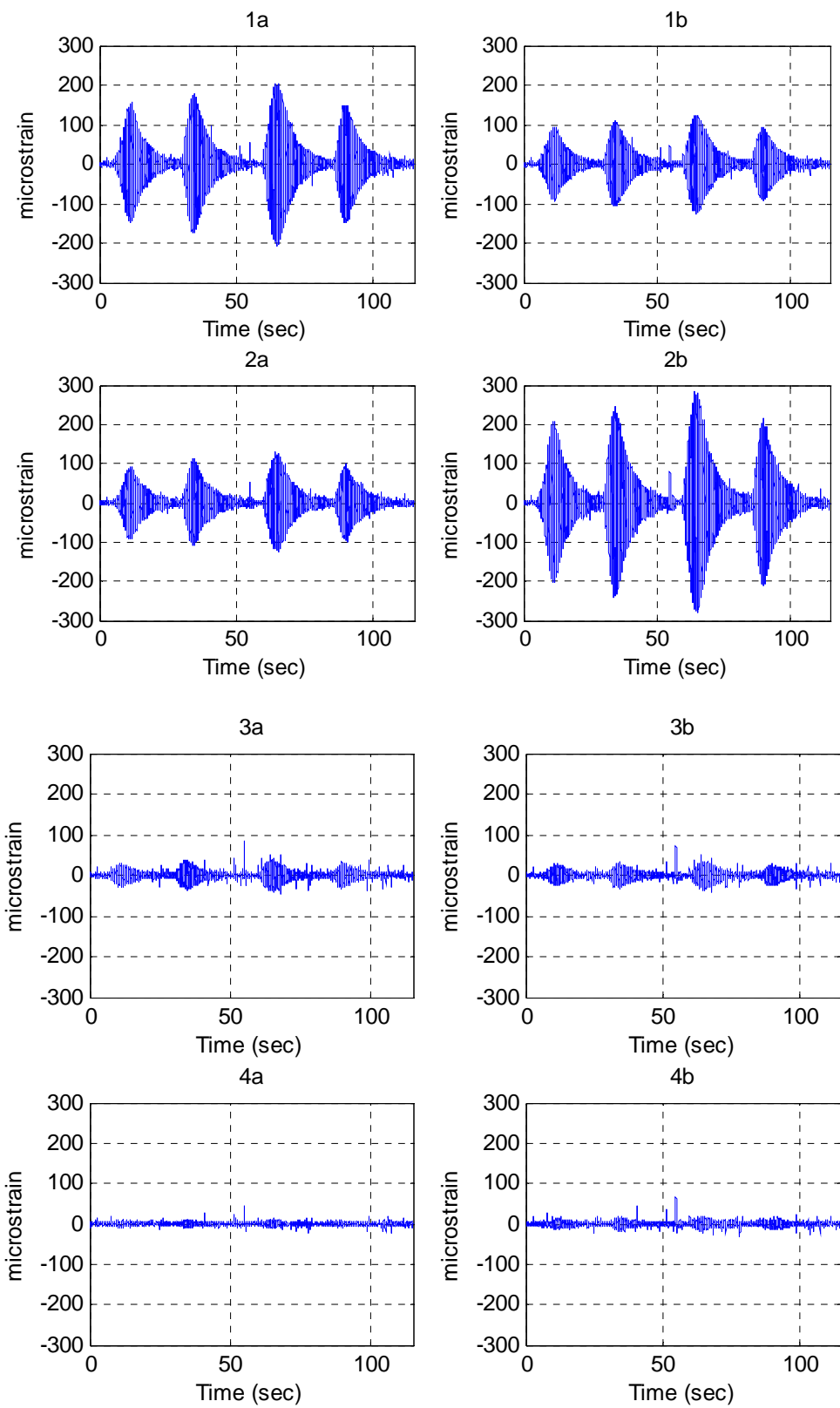
- M1 – horizontal with damper in middle
- M2 – horizontal without damper
- M3 – vertical with damper in middle
- M4 – vertical without damper
- M5 – horizontal with damper at end
- M6 – horizontal without damper
- M7 – vertical with damper at end
- M8 – vertical without damper

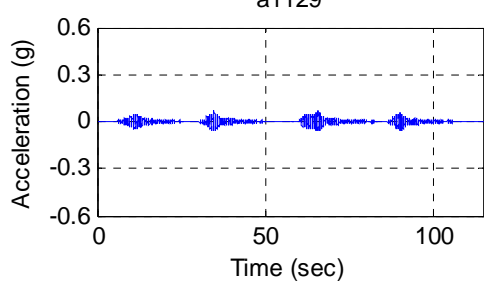
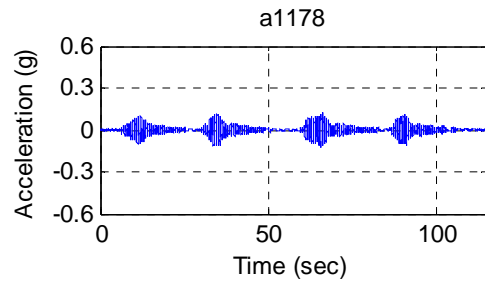
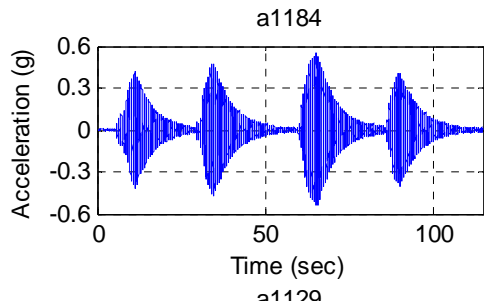
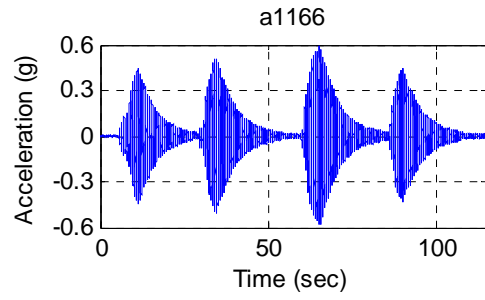
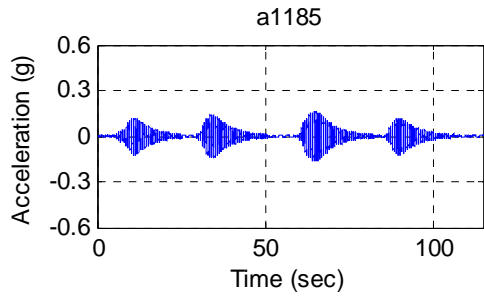
**Test M1**  
Data\II-C-A\II-C-A M1.txt



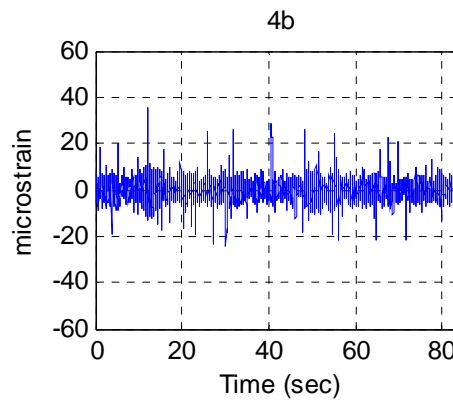
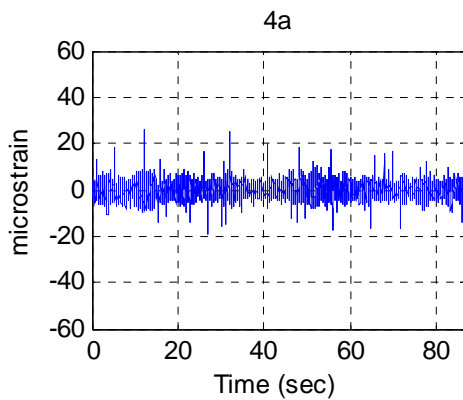
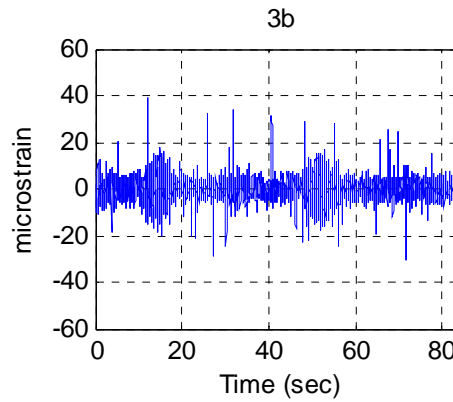
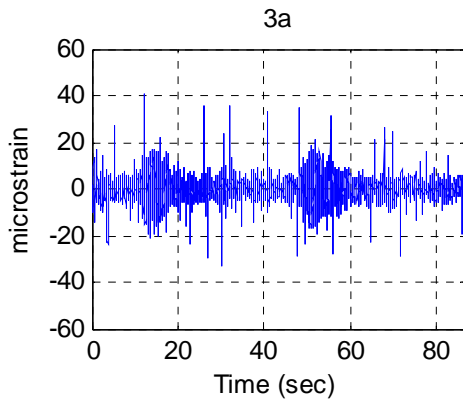
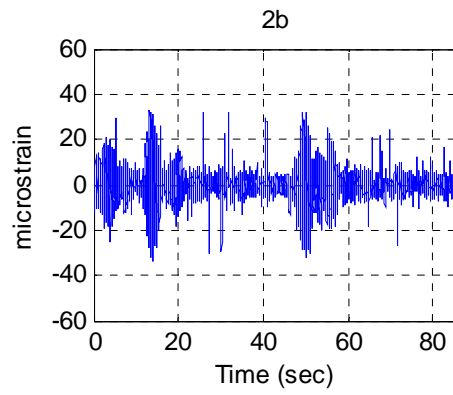
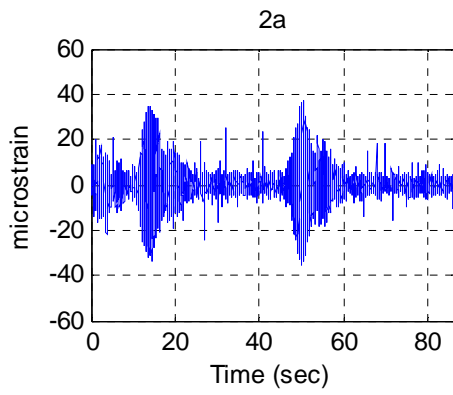
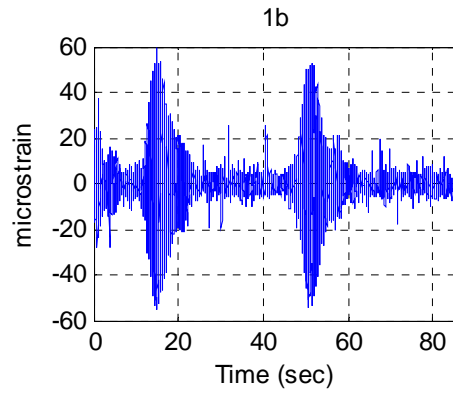
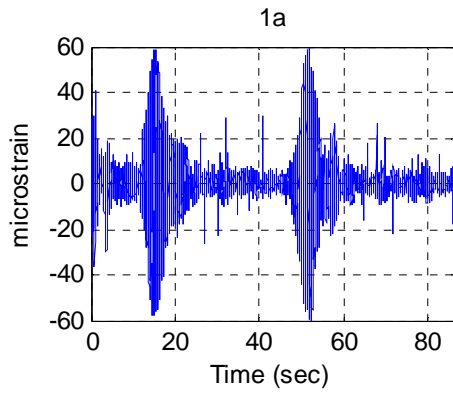


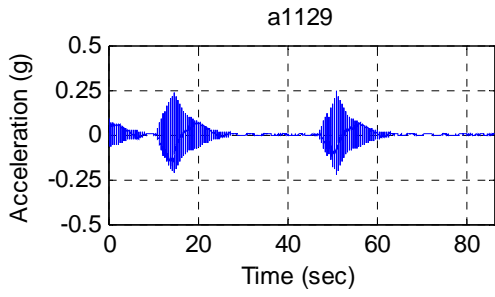
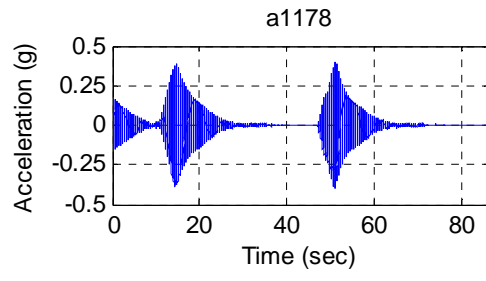
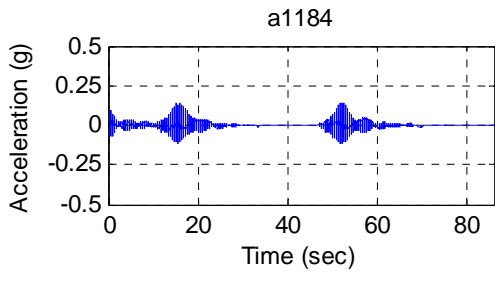
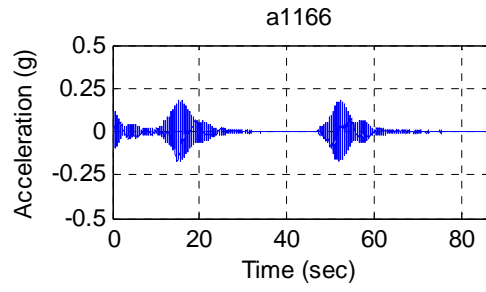
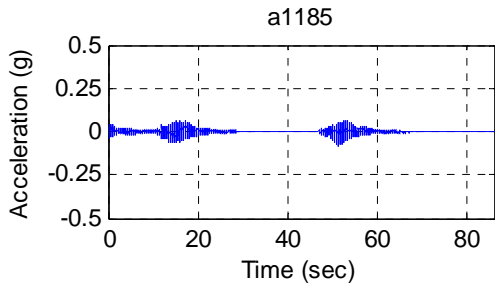
**Test M2**  
Data\II-C-A\II-C-A M2.txt



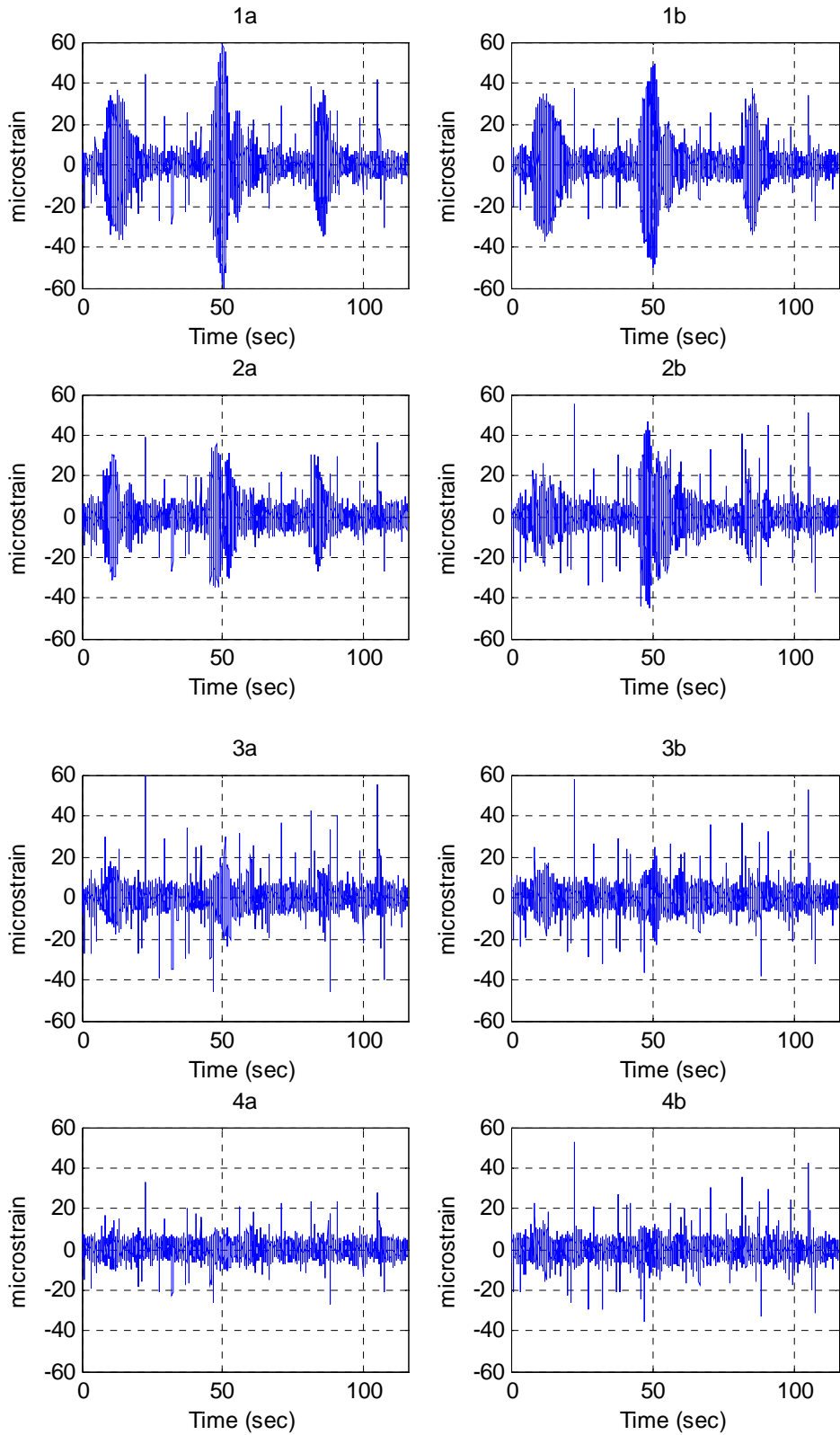


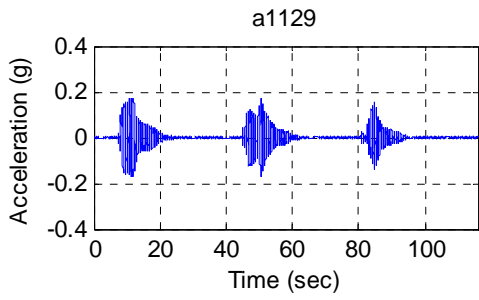
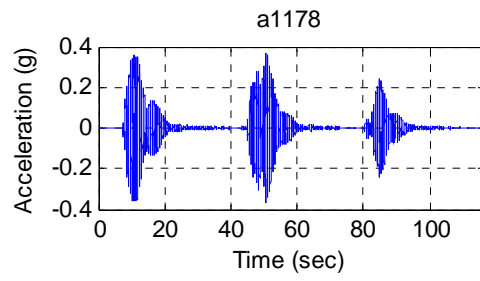
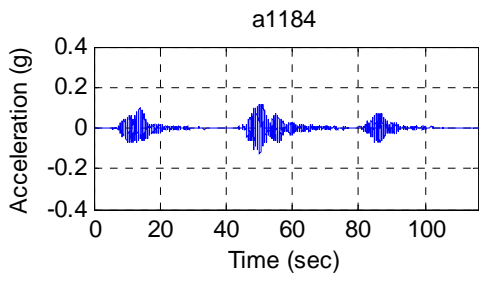
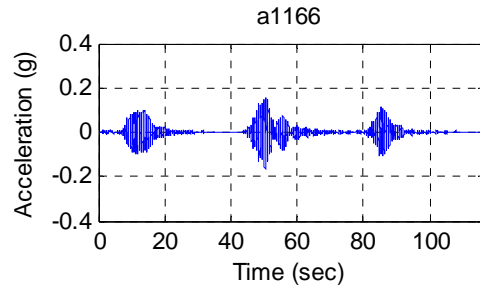
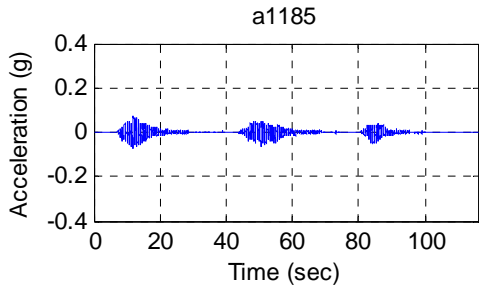
**Test M3**  
Data\II-C-A\II-C-A M3.txt



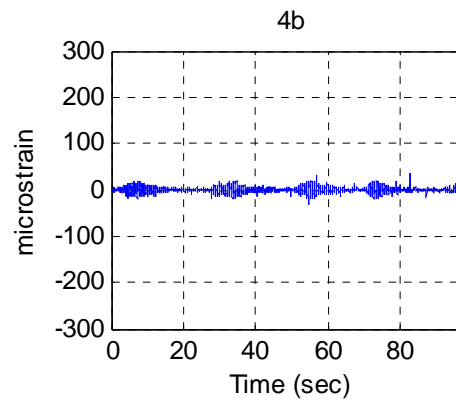
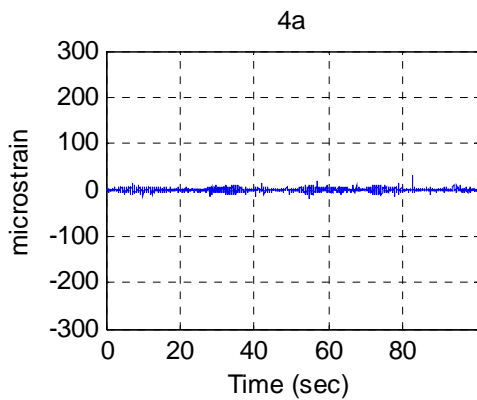
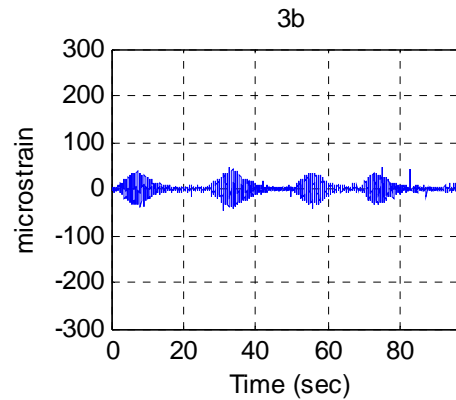
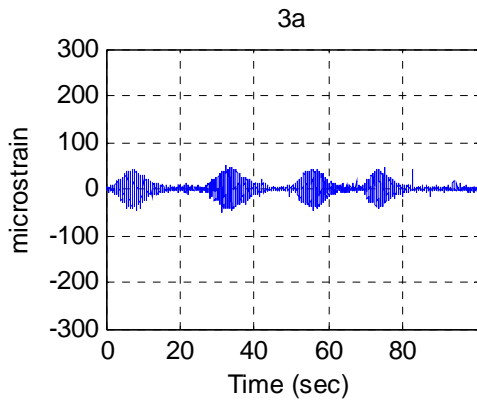
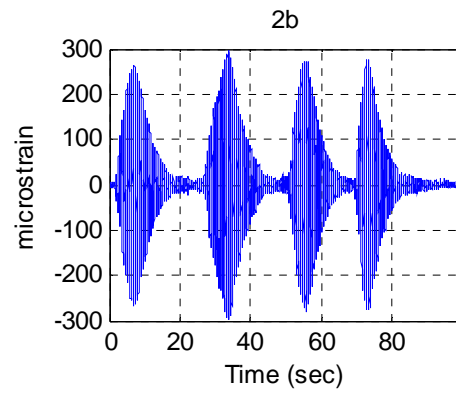
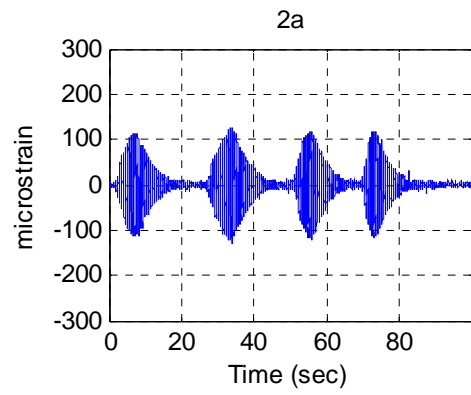
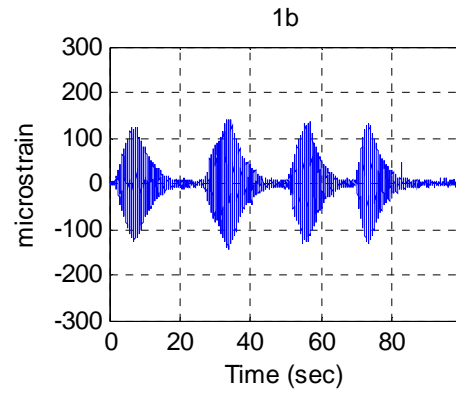
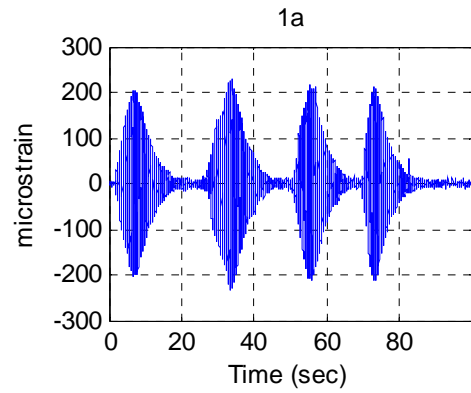


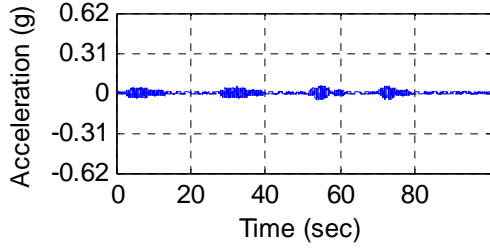
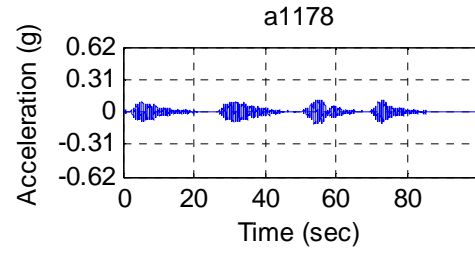
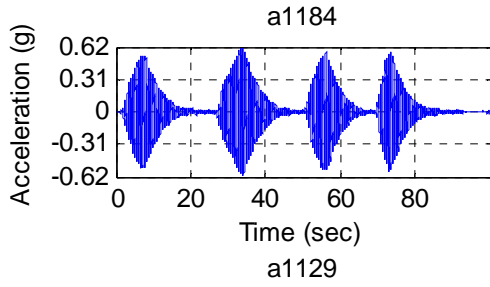
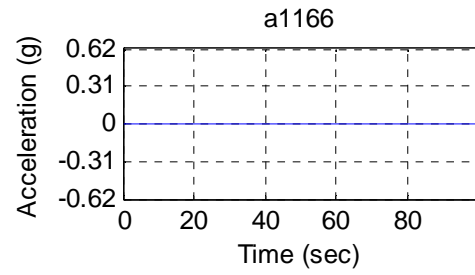
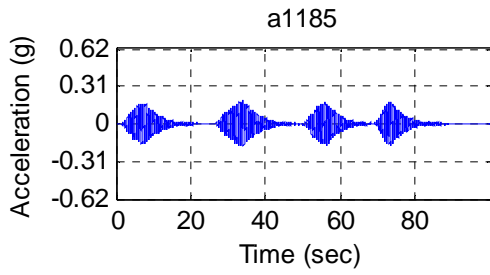
**Test M4**  
Data\II-C-A\II-C-A M4.txt



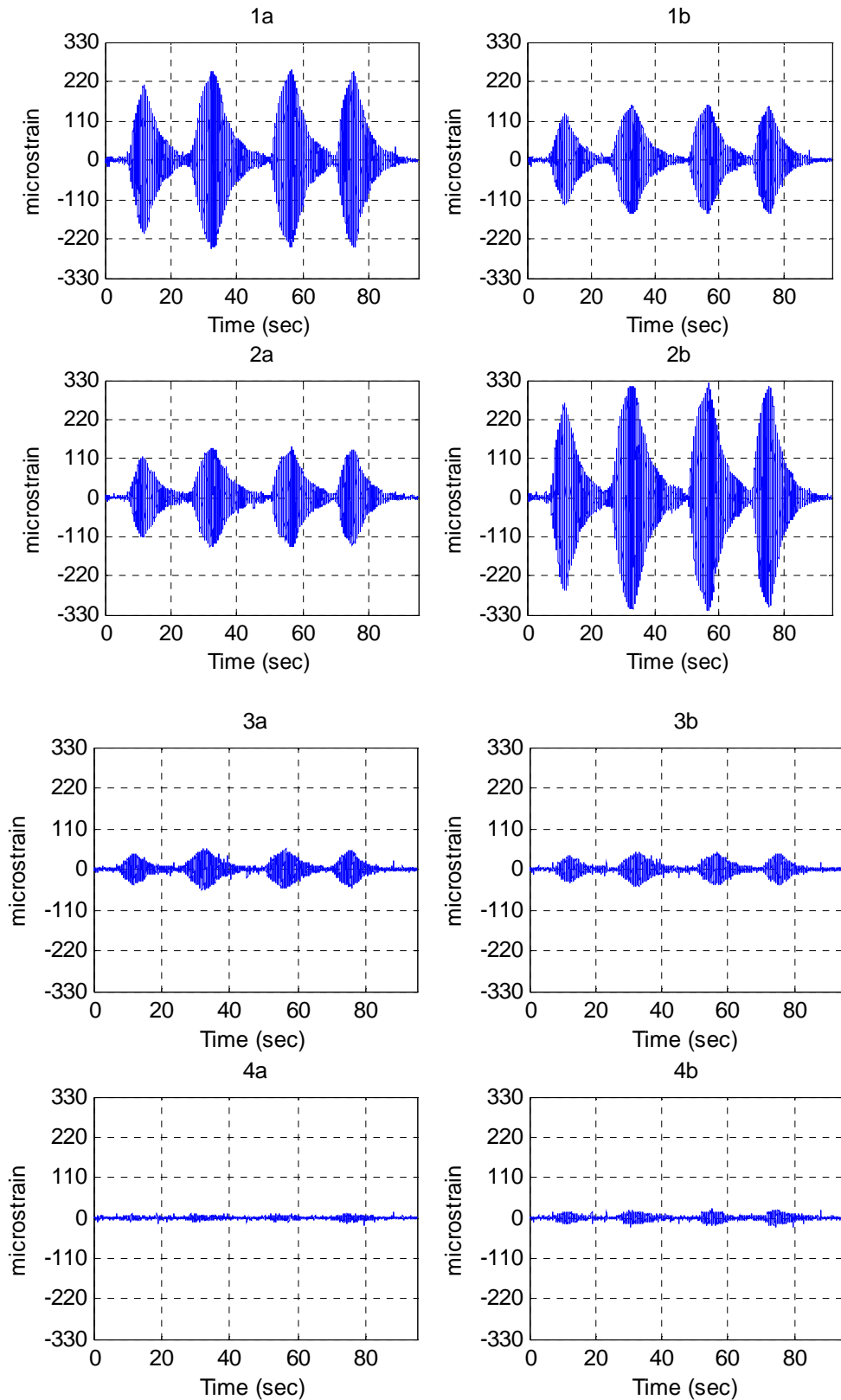


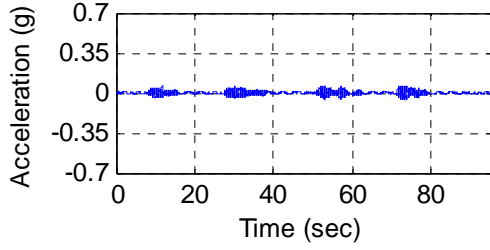
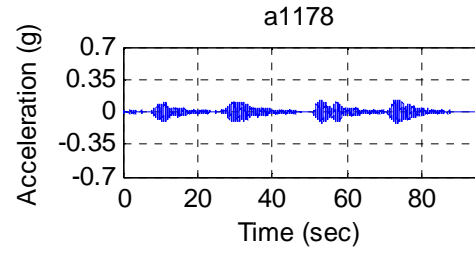
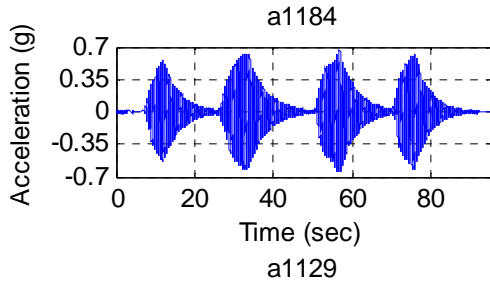
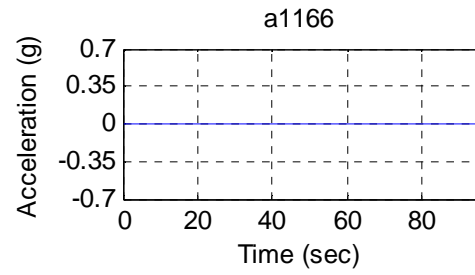
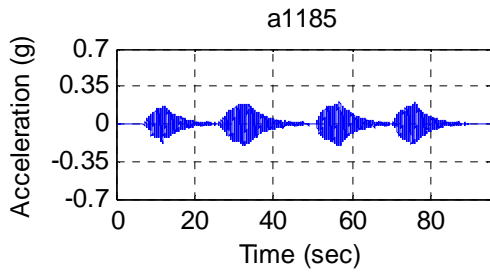
**Test M5**  
**Data\II-C-A\II-C-A M5.txt**



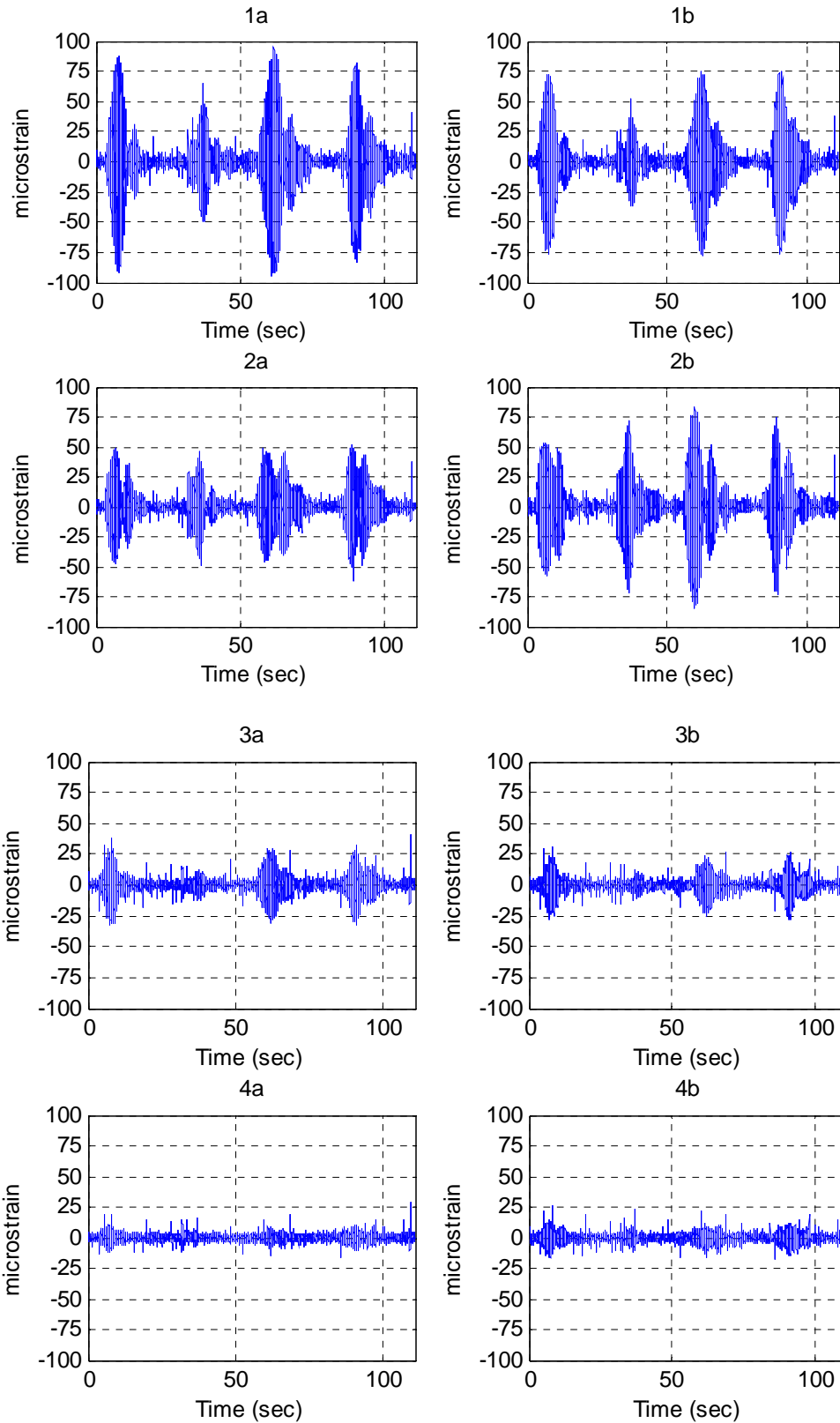


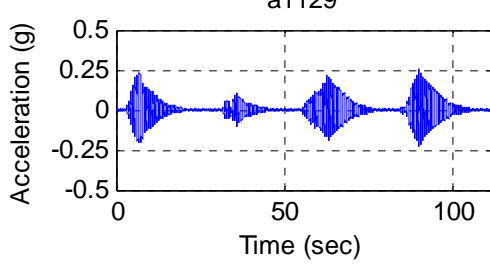
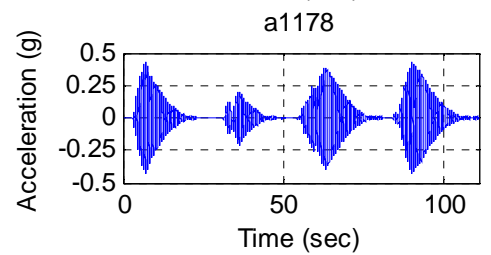
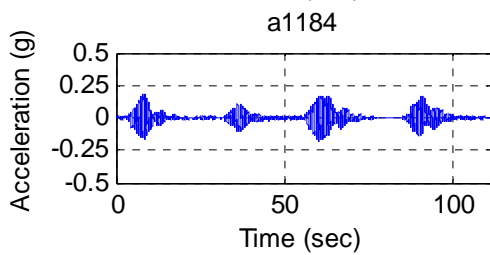
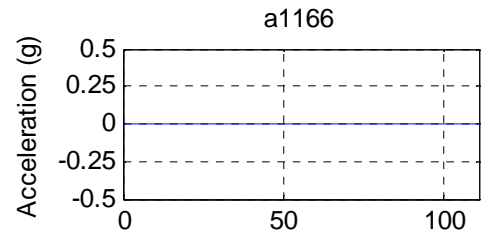
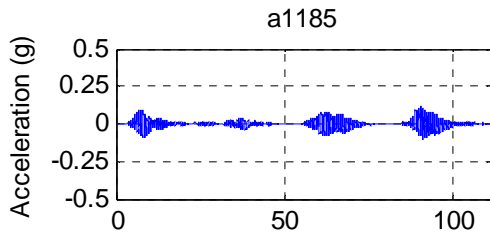
**Test M6**  
Data\II-C-A\II-C-A M6.txt



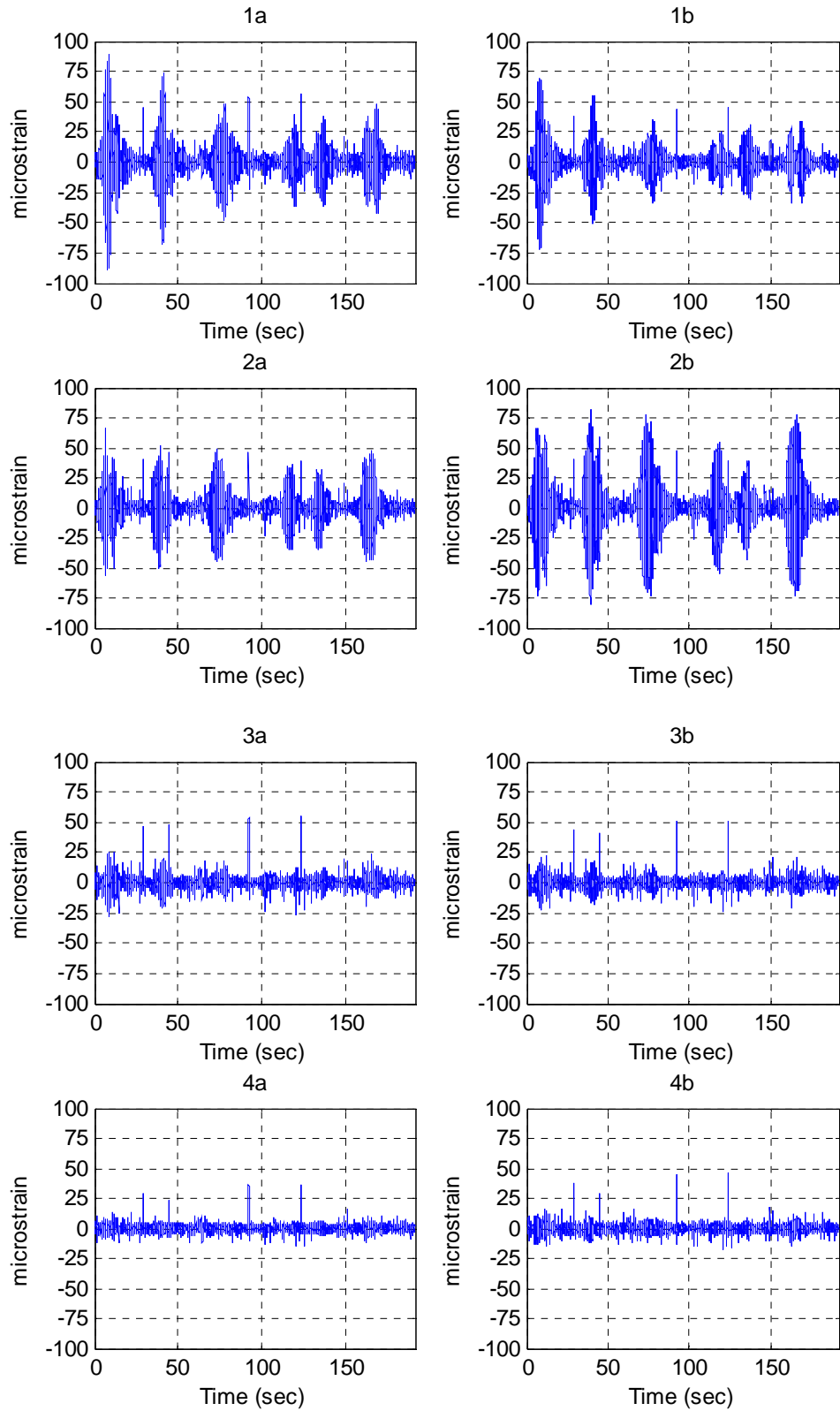


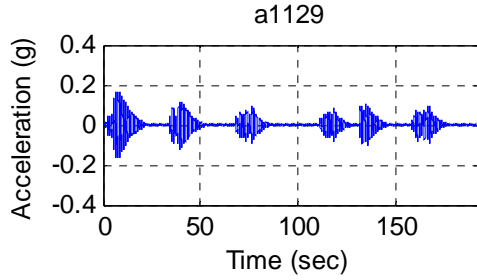
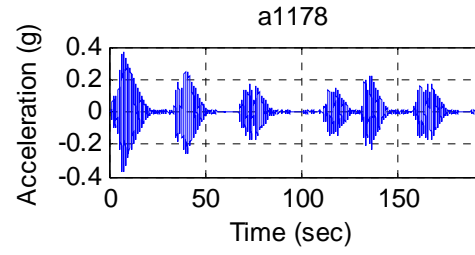
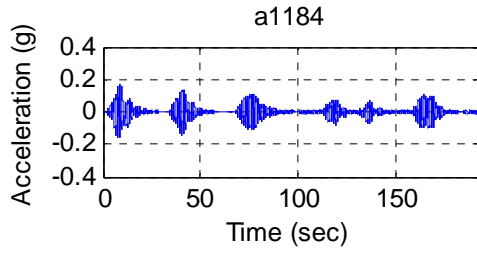
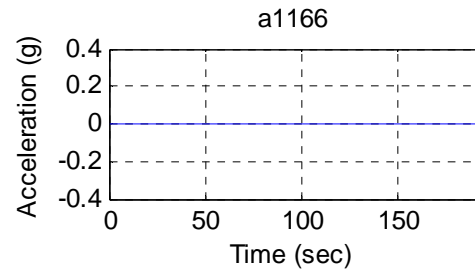
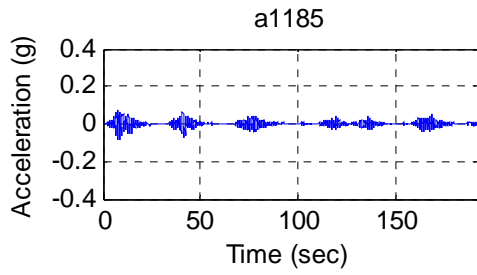
**Test M7**  
**Data\II-C-A\II-C-A M7.txt**





**Test M8**  
Data\II-C-A\II-C-A M8.txt



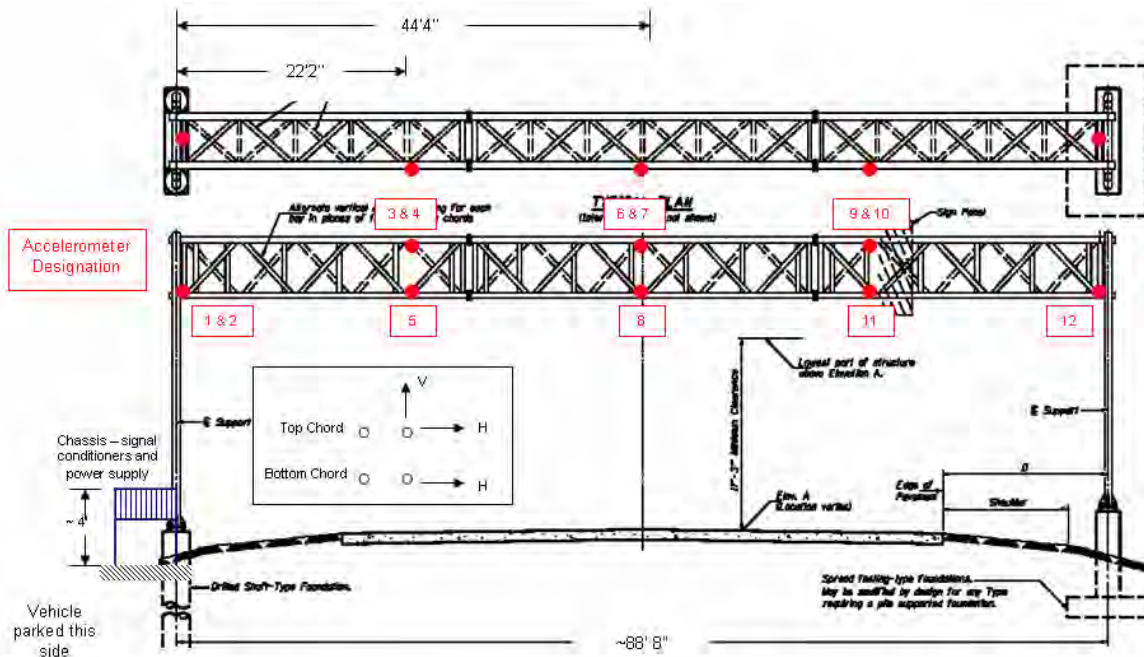


## A2.0 Type I -A Sign Structure Data

### A2.1 Sensor names and locations

#### Accelerometers

The figure below shows the placement of the accelerometers on the Type I-A sign structure. The following table gives a detailed description of the sensor labels and locations.

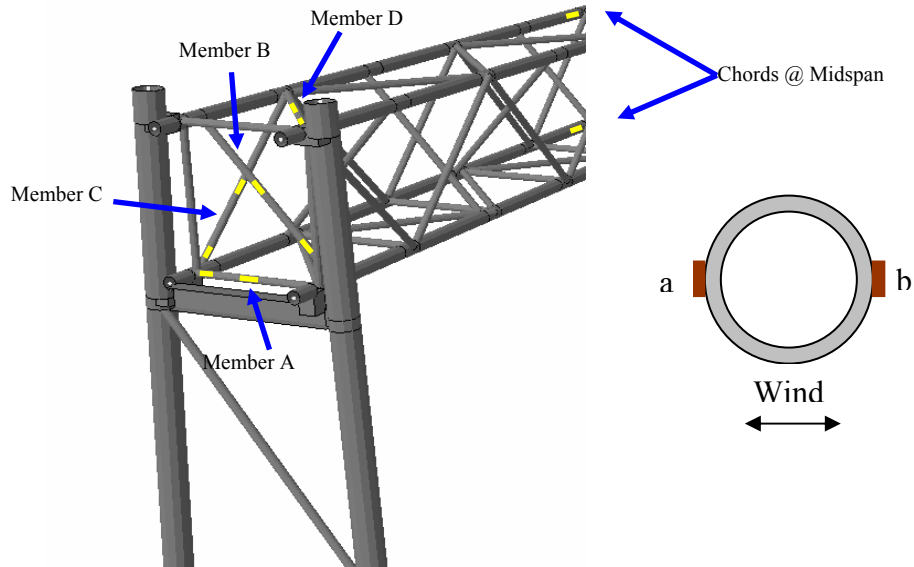


Accelerometer	Measurement Direction	Top/Bottom	Location
a1	Longitudinal	Bottom	Over 1 <sup>st</sup> Support
a2	Horizontal	Bottom	Over 1 <sup>st</sup> Support
a3	Vertical	Bottom	Quarter Point
a4	Horizontal	Top	Quarter Point
a5	Horizontal	Bottom	Quarter Point
a6*	Vertical	Bottom	Mid-Span
a7	Horizontal	Top	Mid-Span
a8*	Horizontal	Bottom	Mid-Span
a9	Vertical	Bottom	Three Quarter Point
a10	Horizontal	Top	Three Quarter Point
a11	Horizontal	Bottom	Three Quarter Point
a12	Horizontal	Bottom	Over 2 <sup>nd</sup> Support

\*These were bad accelerometer channels

## Strain gages

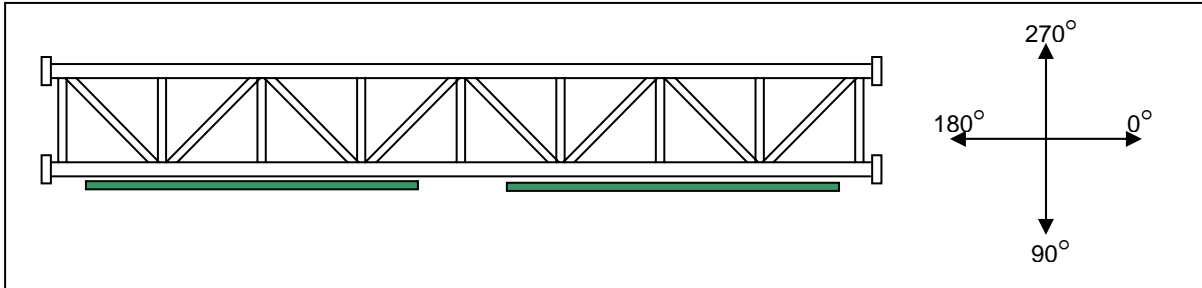
Twelve strain gages were installed on the I-A sign structure. Four gages were located on two chord members at the mid-span of the truss as well as web members at one end of the truss. The locations of the strain gages at the end of the truss are indicated in the figure below. The table below details the locations and labeling of each gage.



Strain Gage	Location
CBF CBB	Chord Bottom
CTF CTB	Chord Top
A1a A1b	Horizontal End
A2a A2b	Horizontal Middle
B1a B1b	Interior Diagonal End
B2a B2b	Interior Diagonal Middle
C1a C1b	Vertical Diagonal End
C2a C2b	Vertical Diagonal Middle
D1a D1b	Horizontal Diagonal End
D2a D2b	Horizontal Diagonal Middle

## Anemometer

The wind velocity and direction measured by the anemometer relative to the sign is shown in the figure below. When the wind is blowing perpendicular to the face of the sign, the instrument will read a direction of 270 degrees.



### A2.2 Data Description

The data contained in the appendix files and plotted below is the filtered data acquired for the Type I-A sign structure. A link to a text file of each test is included with the plots of the data. To import the data into Excel follow the steps given below:

1. Click on the link to open a text file of the data
2. Click Edit → Select All
3. Click Edit → Copy
4. Open Excel
5. Once in Excel, click Edit → Paste

Test descriptions:

- W1-W4 are tests that were taken under strong wind conditions. Note that when the wind direction is equal to 90 degrees, the wind is blowing perpendicular to the back side of the sign face. Tests W1-W3 were taken on March 18, 2005. Test W4 was taken on April 7, 2005 and is an hour long record.
- TG1-TG18 are tests that were taken under calm wind conditions to measure the response of the truss to truck gust excitation. These tests were taken on April 9, 2005. Each record represents an individual truck gust.
- M1-M4 are manual tests that were taken on April 15, 2005 when the structure was subjected to horizontal and vertical manual excitation

### A2.3 Wind Data

The data structure for tests W1-W3 is as follows:

Time(sec), CBB, CFB, CBT, CFT, A1a, A1b, A2a, A2b, B1b, B2a, B2b, C1a, C1b, C2a, C2b, a1, a2, a3, a4, a5, a7, a9, a10, a11, a12, WS(mph), WD(deg)

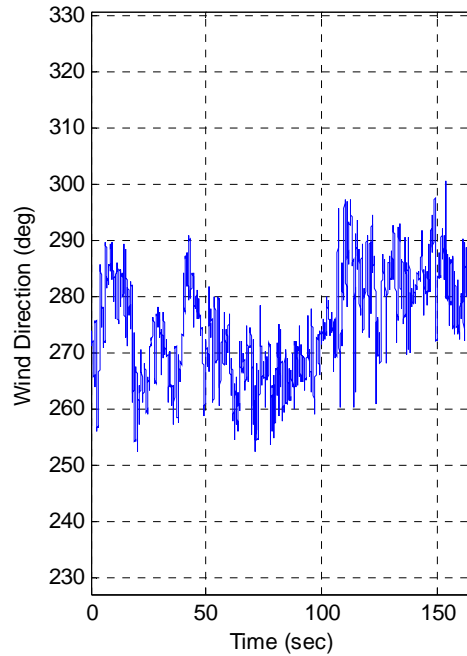
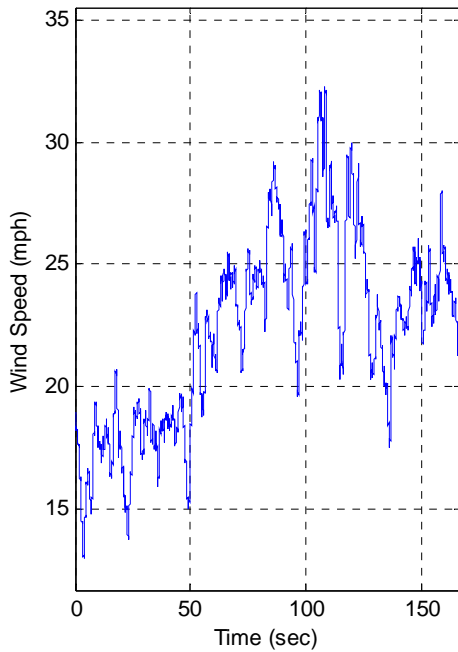
The data structure for test W4 is as follows:

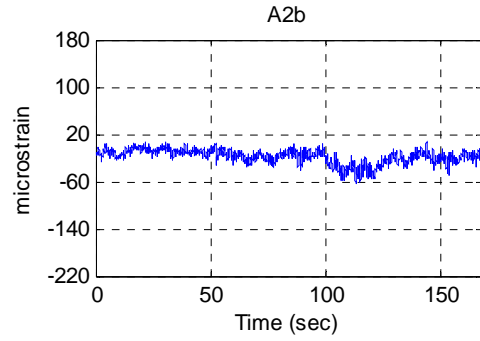
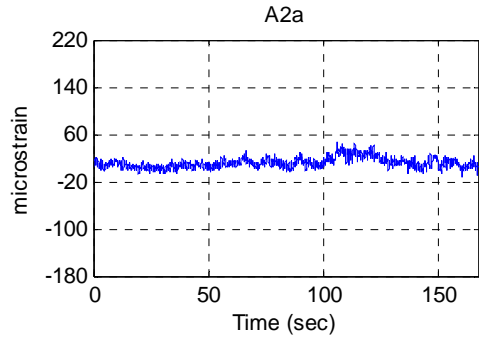
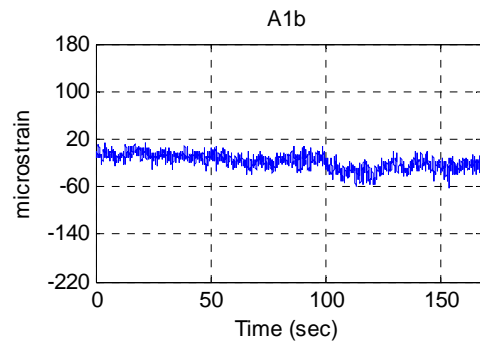
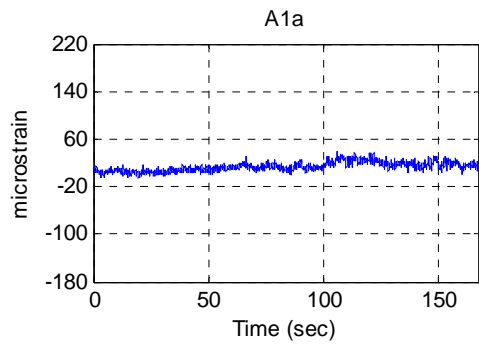
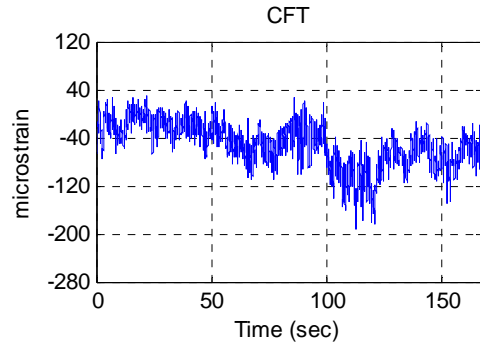
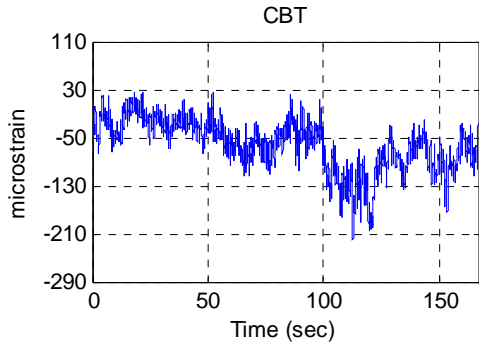
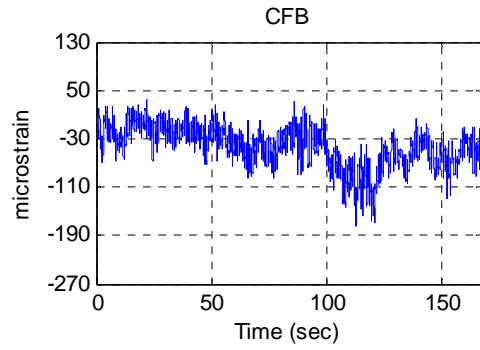
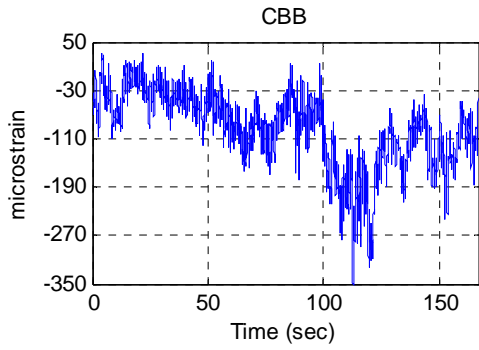
Time(sec), CBB, CFB, CBT, CFT, A1a, A1b, B1a, B1b, C1a, C1b, C2a, C2b, D1a, D1b, D2a, D2b, a1, a2, a3, a4, a5, a7, a9, a10, a11, a12, WS(mph), WD(deg)

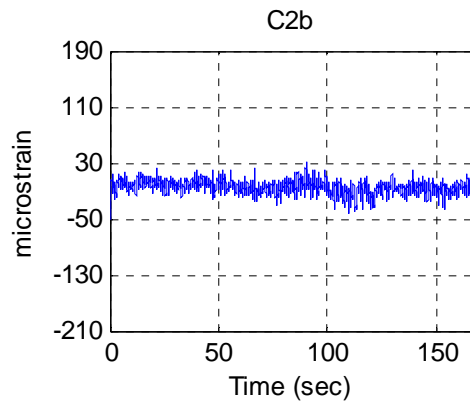
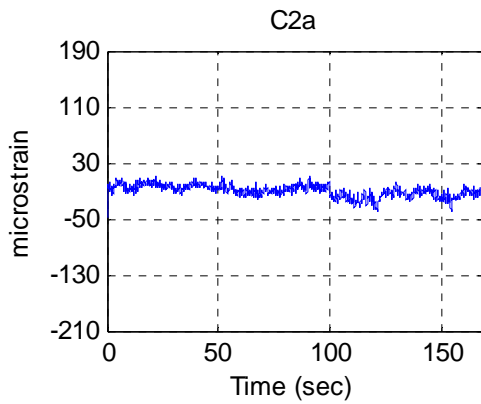
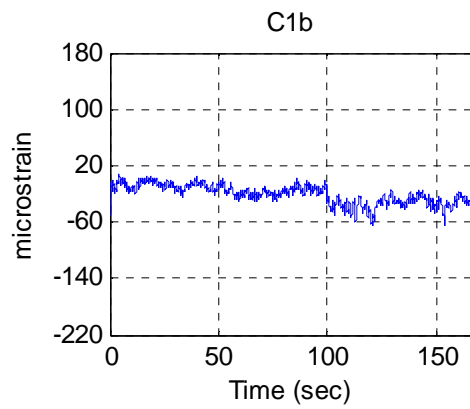
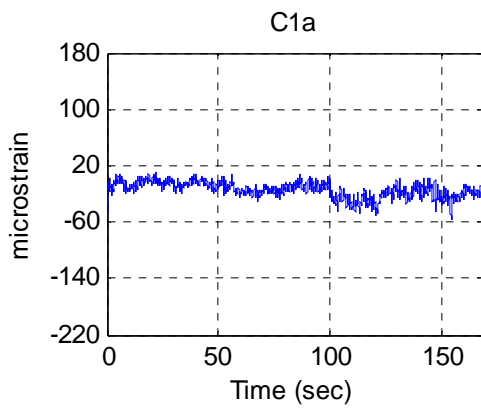
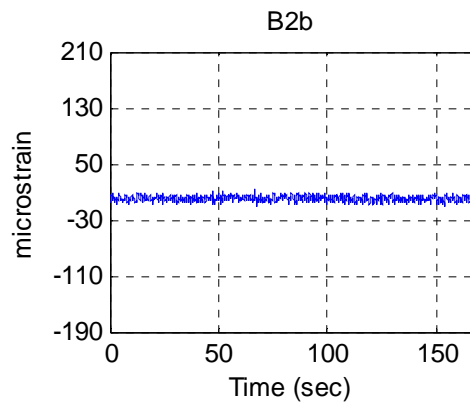
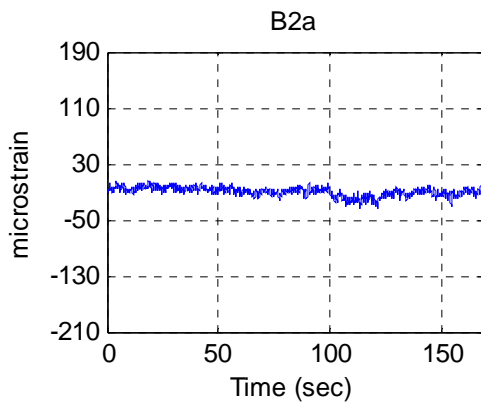
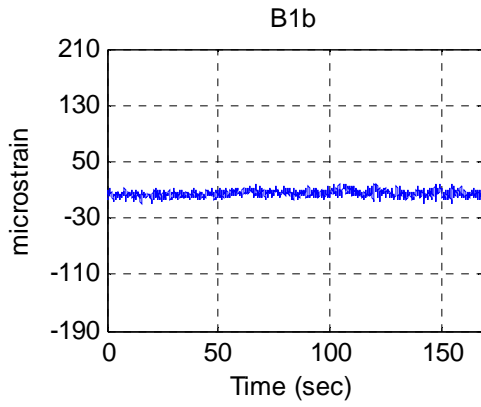
To determine the wind velocity acting perpendicular to the sign face the following calculation must be made:

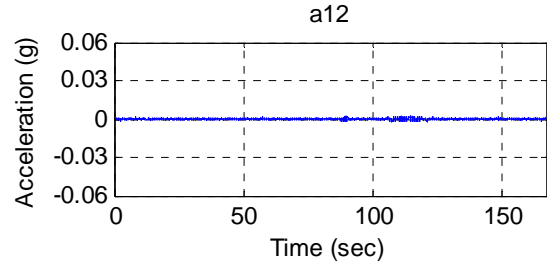
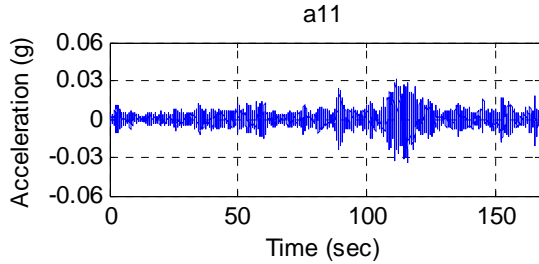
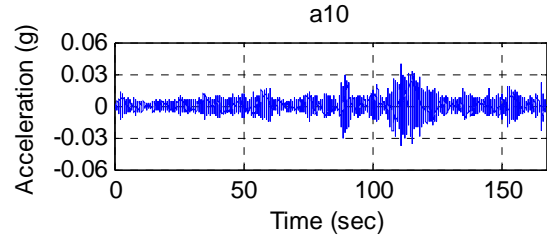
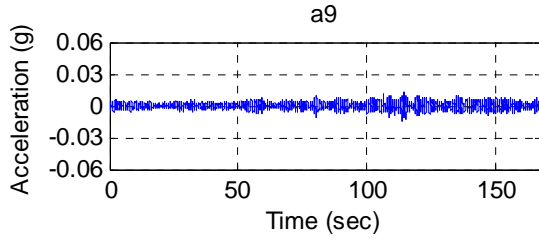
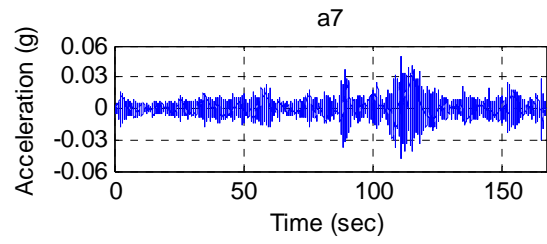
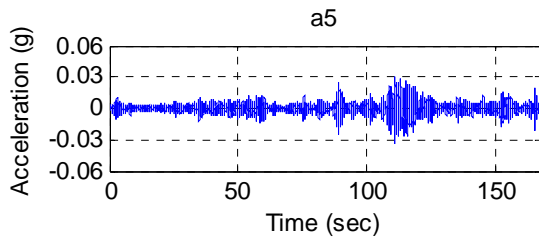
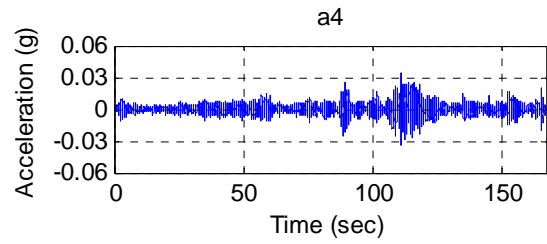
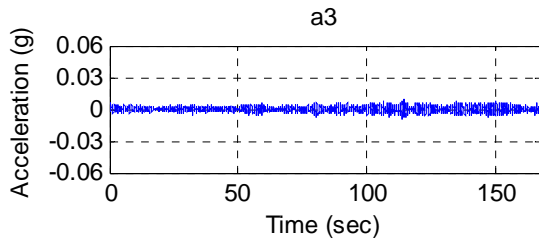
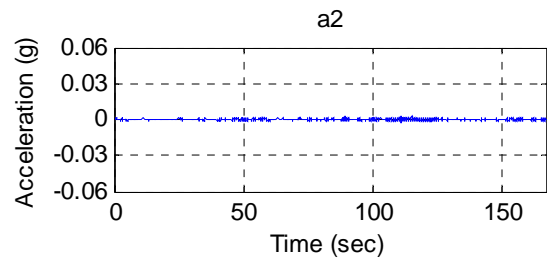
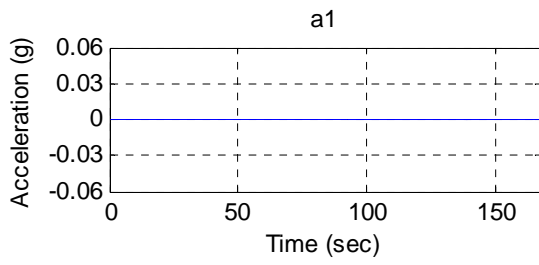
$$WS_{\text{perpendicular}} = WS * \sin(WD)$$

**Test W1**  
[Data\I-A\I-A\\_W1.txt](#)

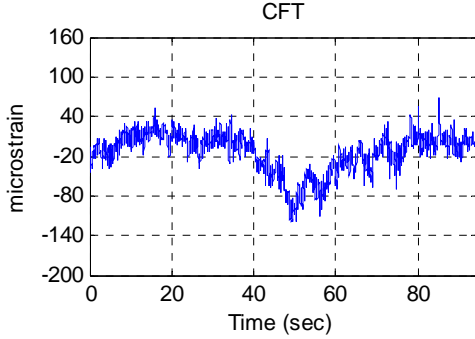
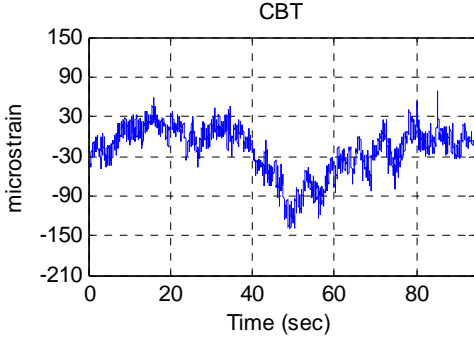
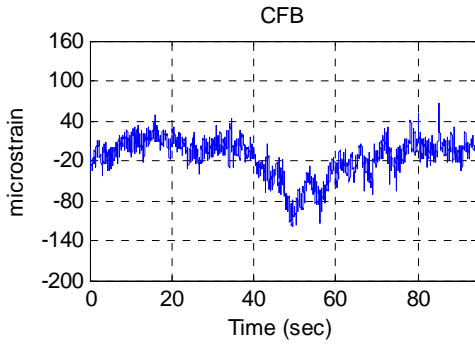
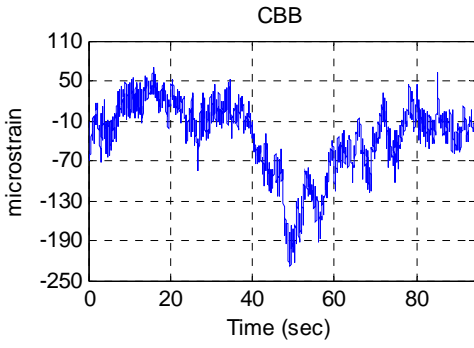
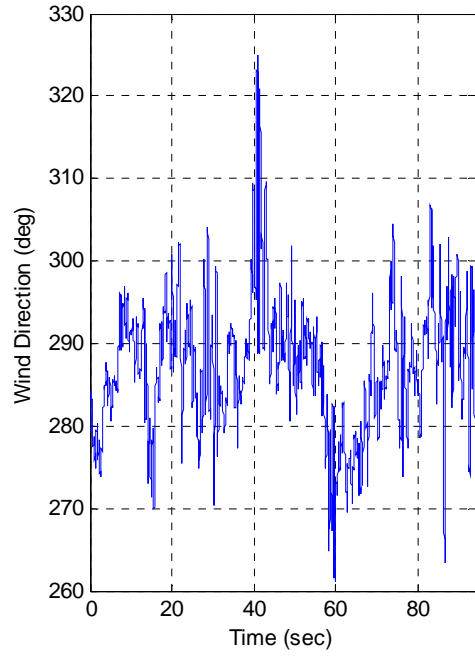
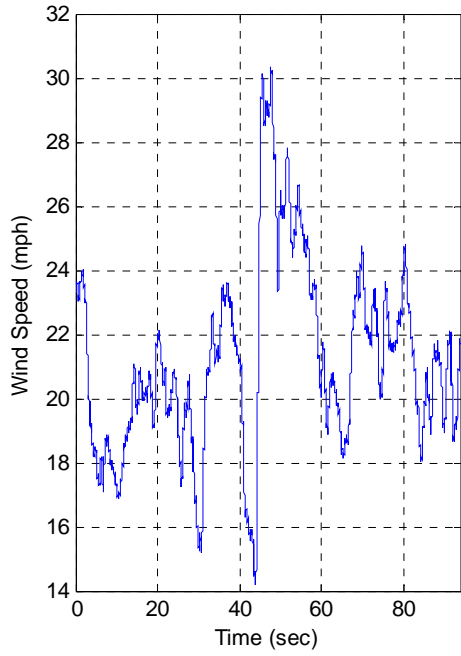


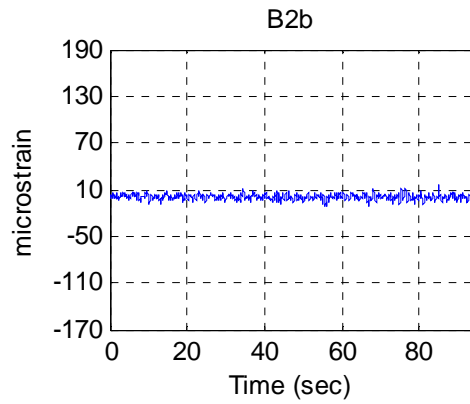
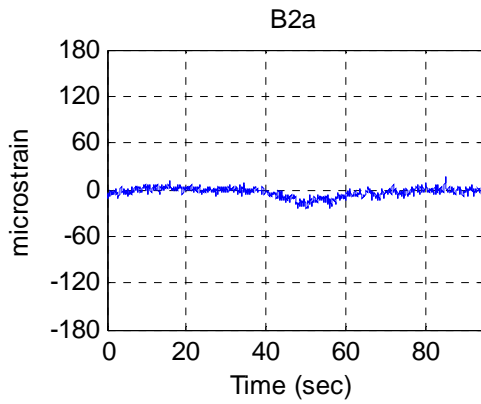
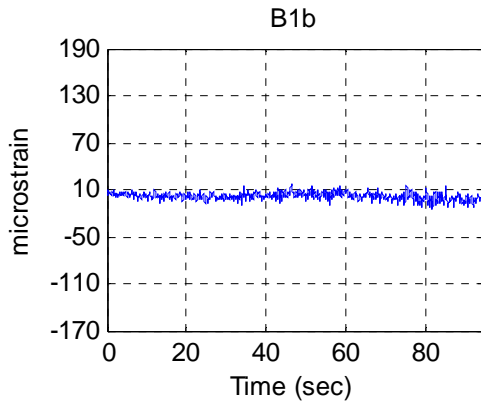
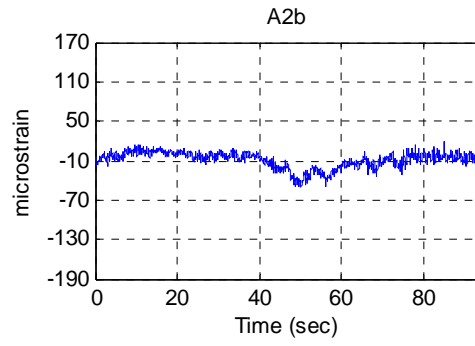
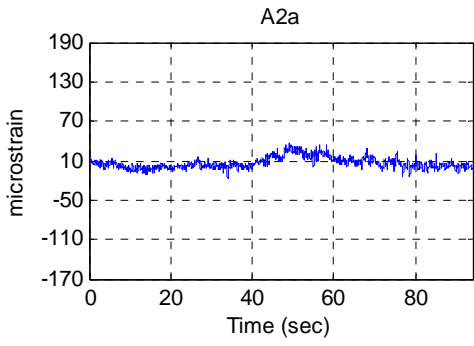
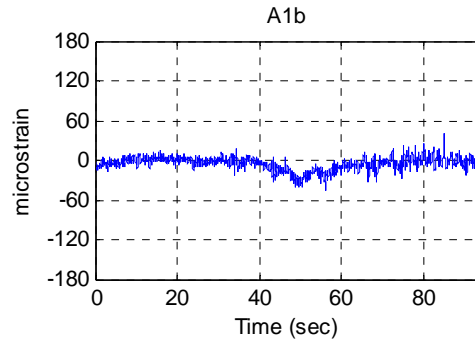
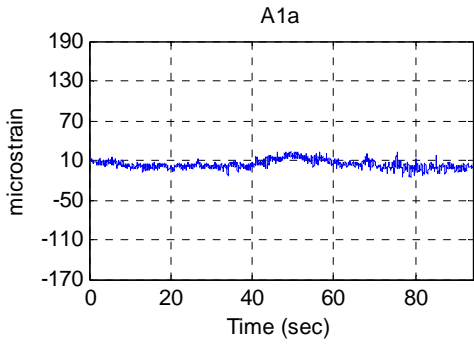


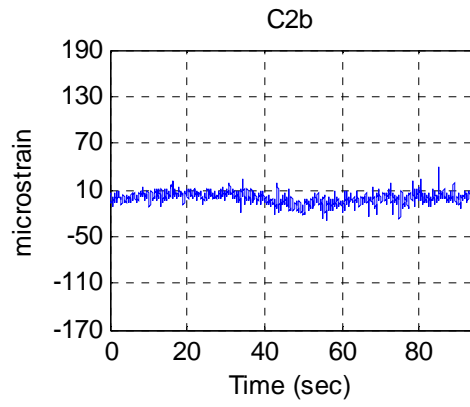
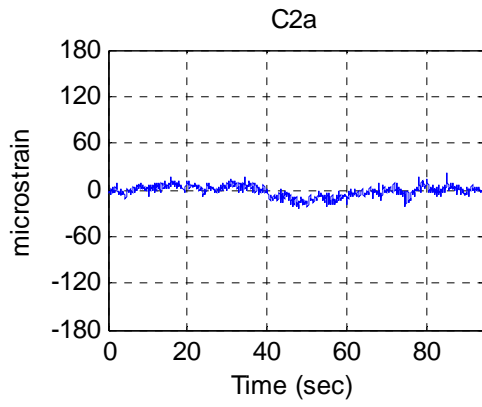
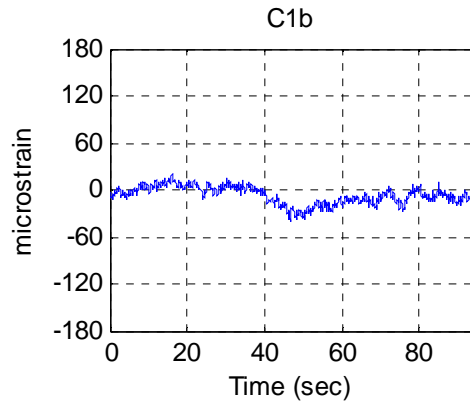
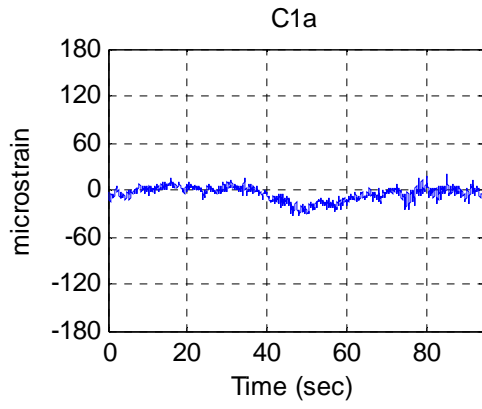


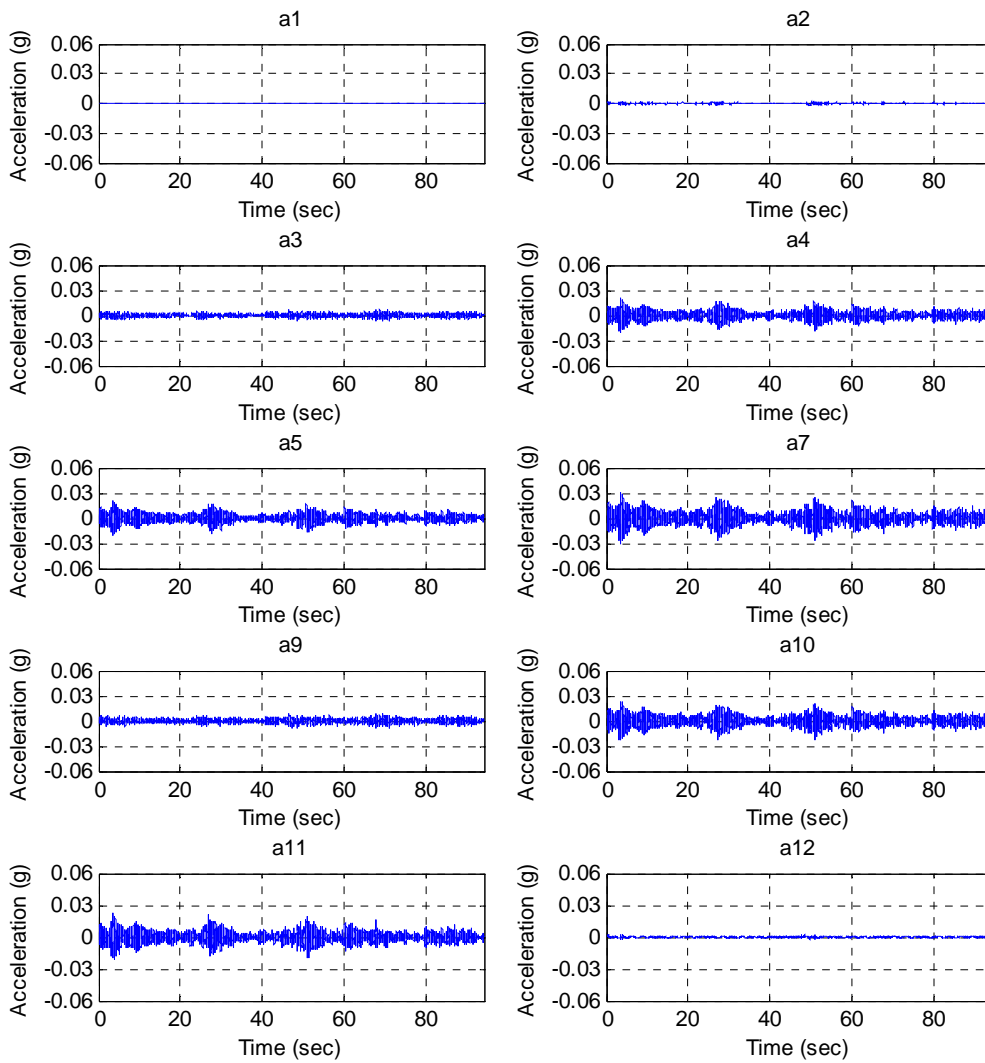


**Test W1**  
**Data\I-A\I-A W2.txt**

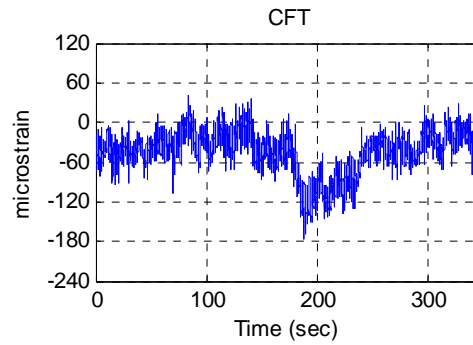
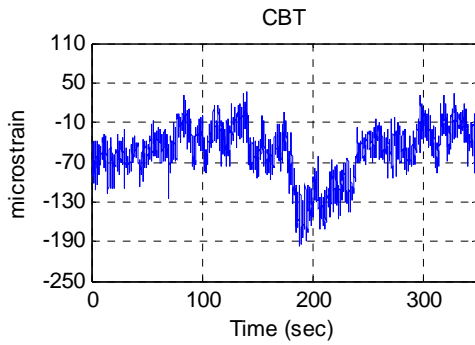
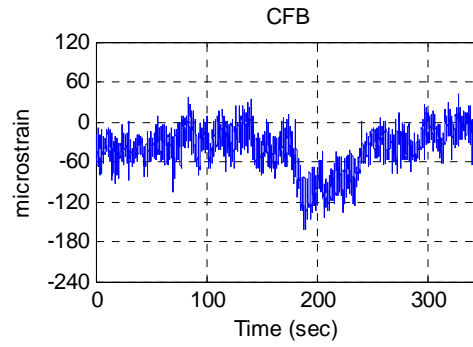
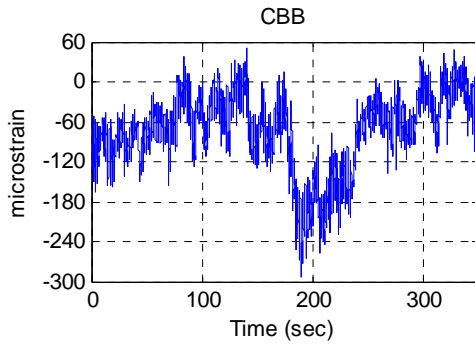
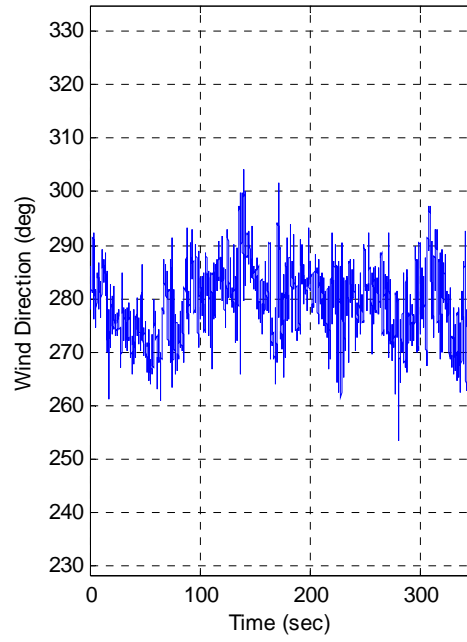
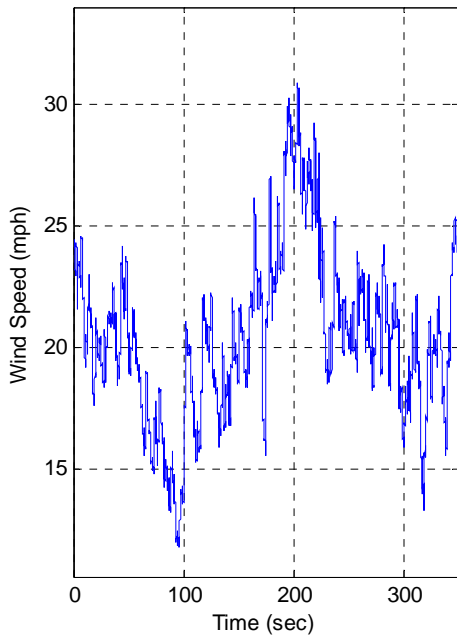


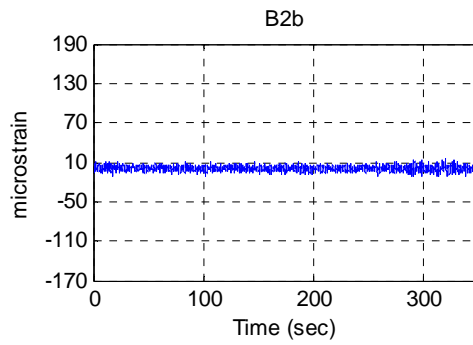
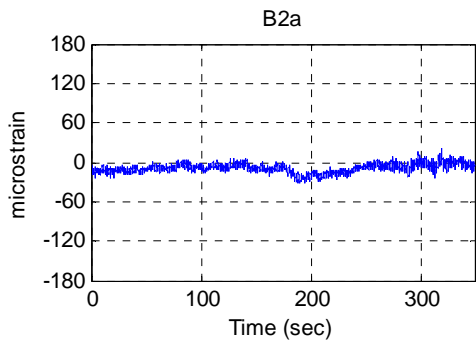
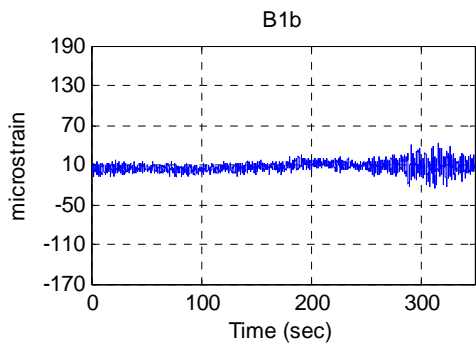
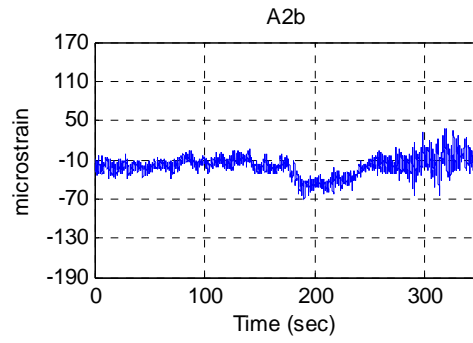
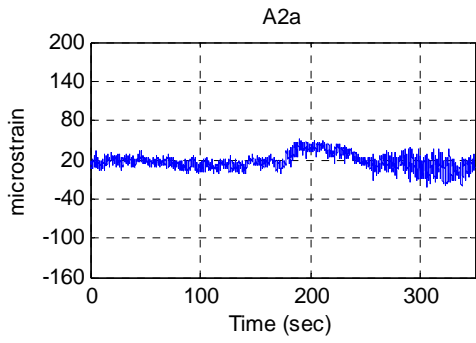
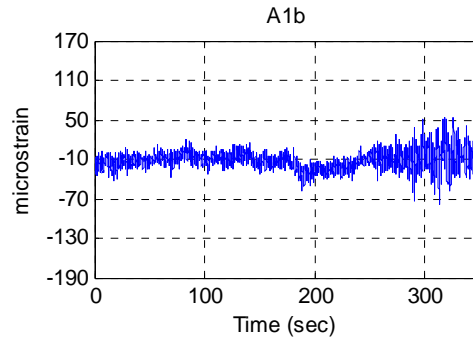
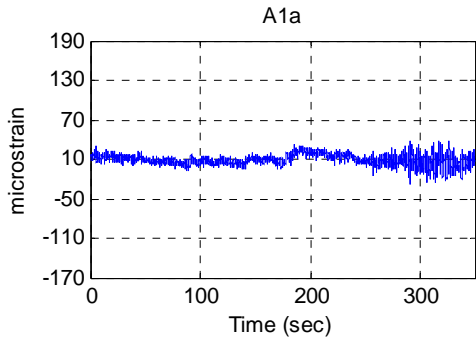


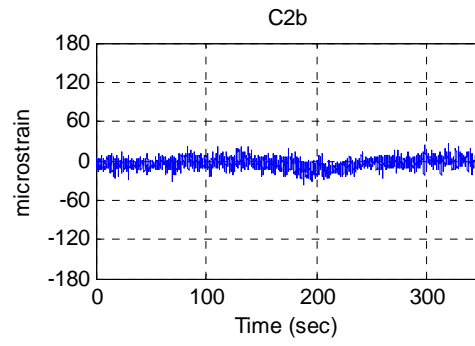
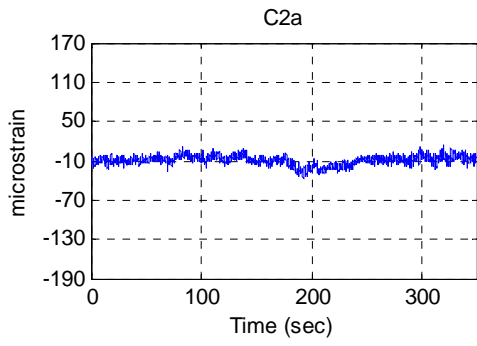
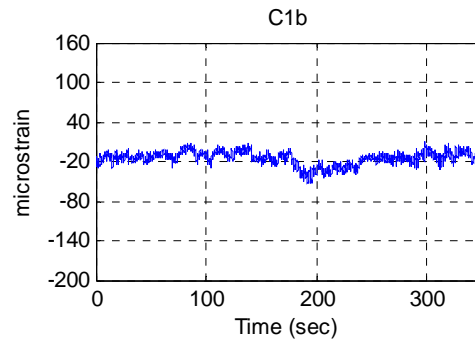
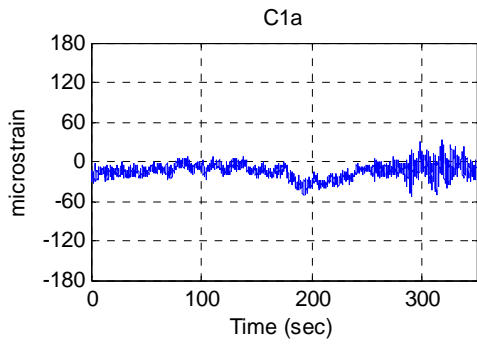


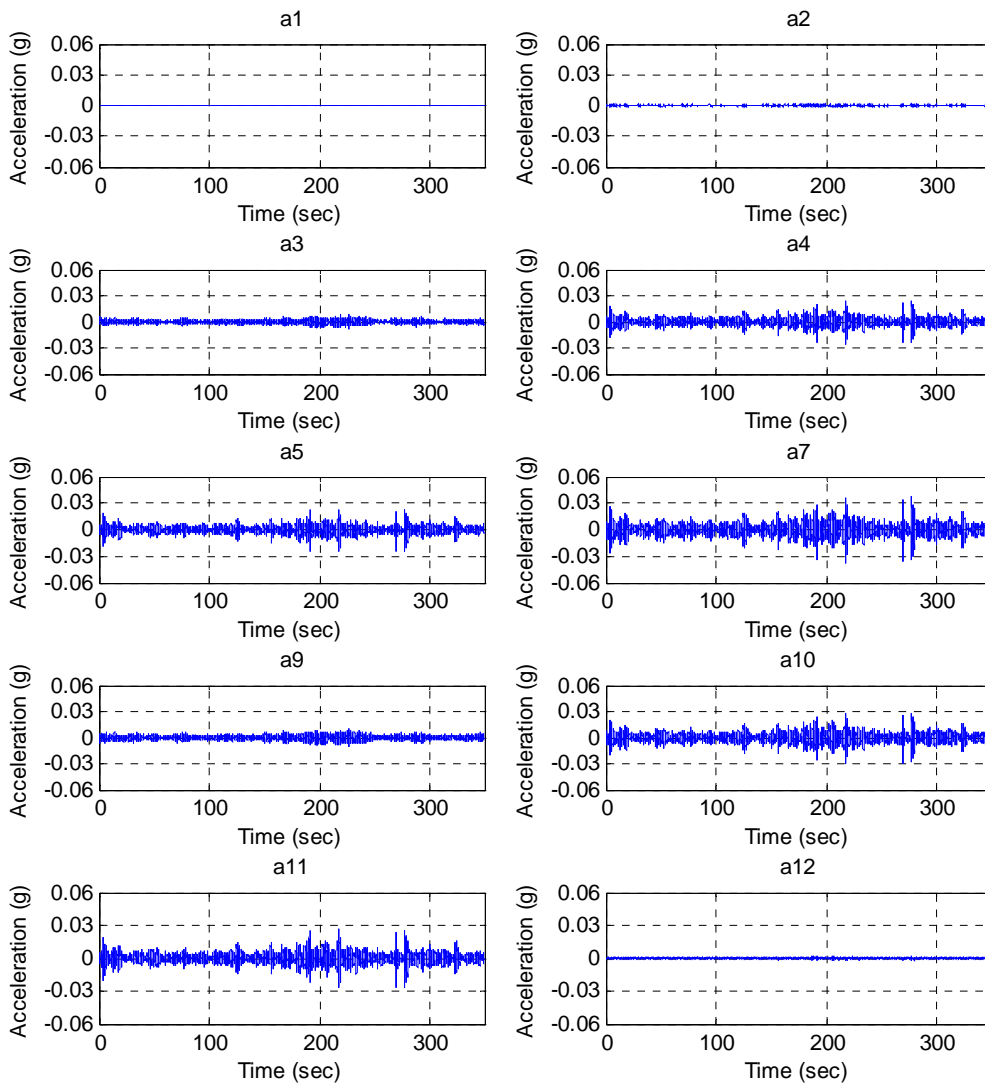


**Test W3**  
Data\I-A\I-A\_W3.txt

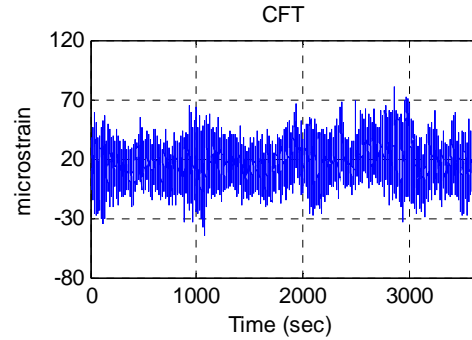
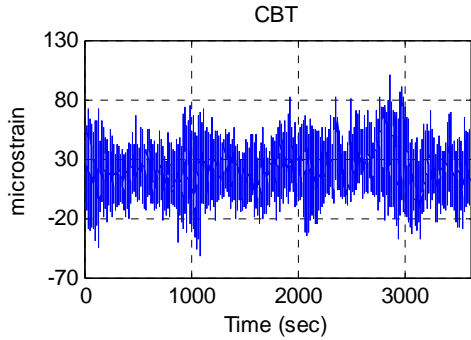
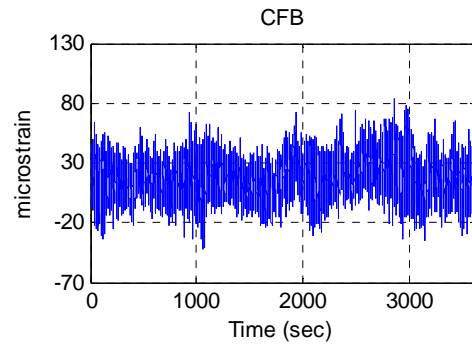
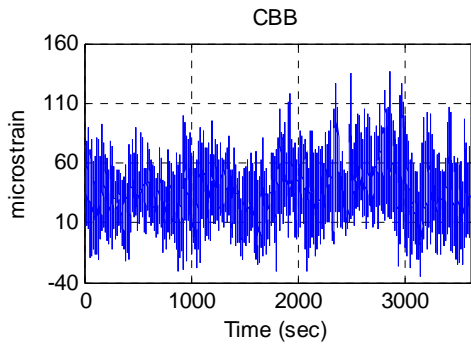
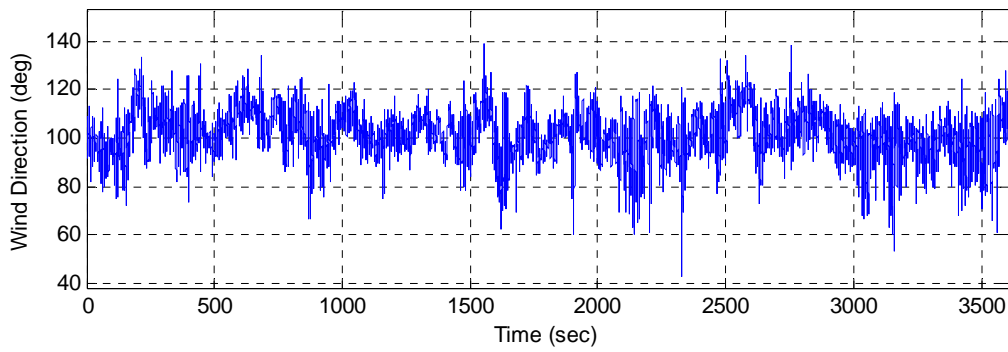
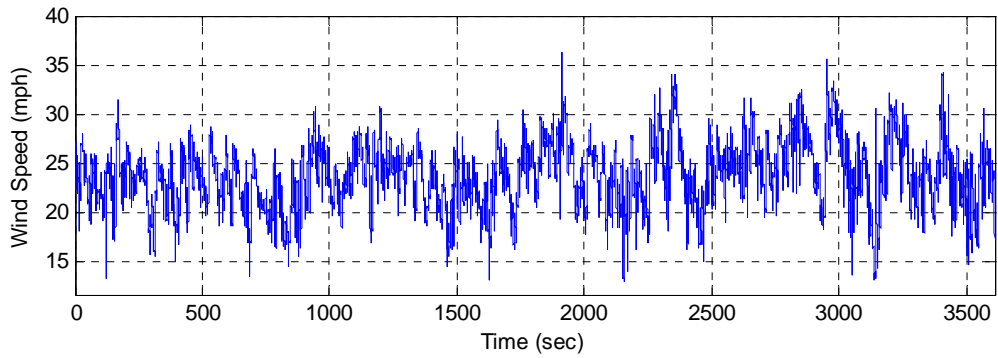


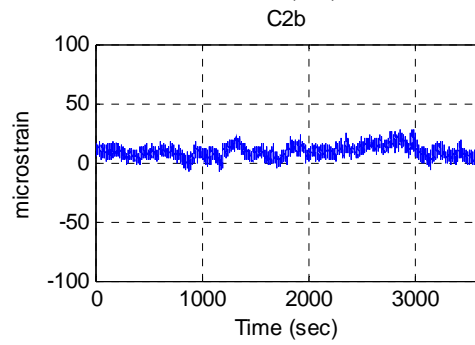
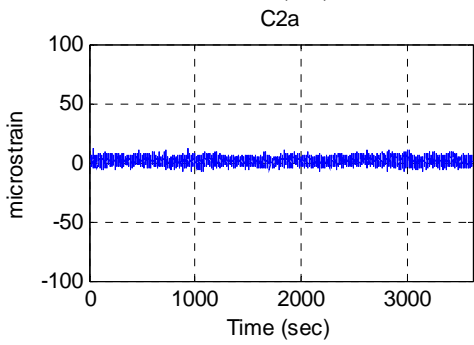
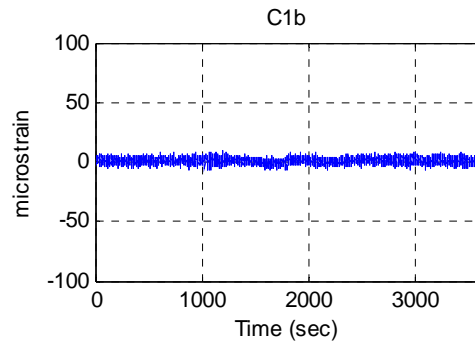
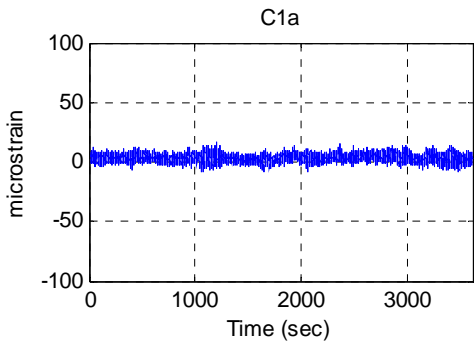
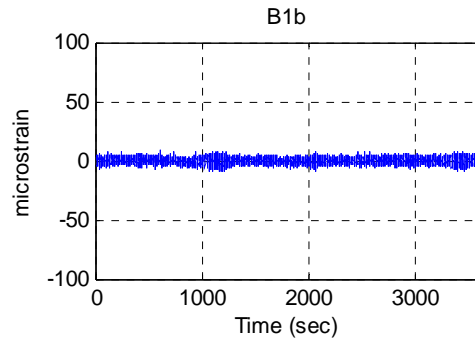
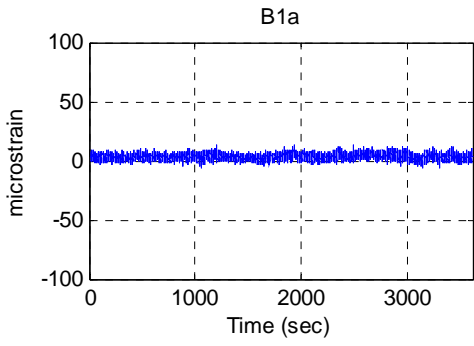
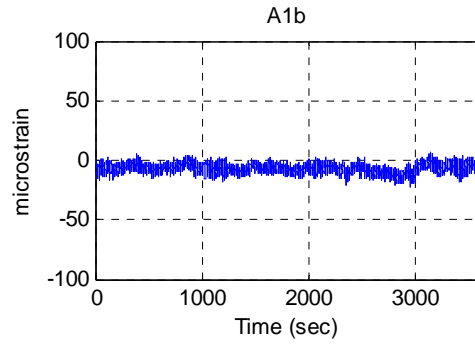
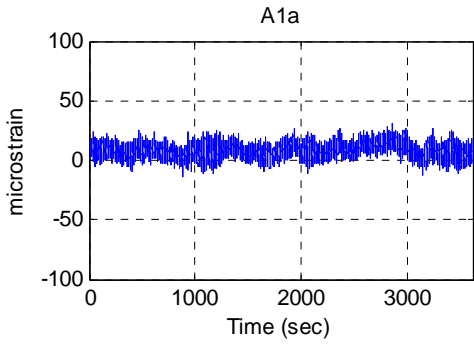


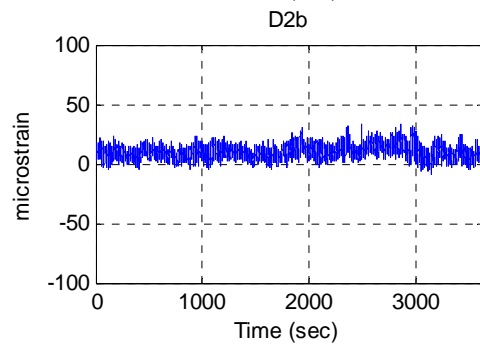
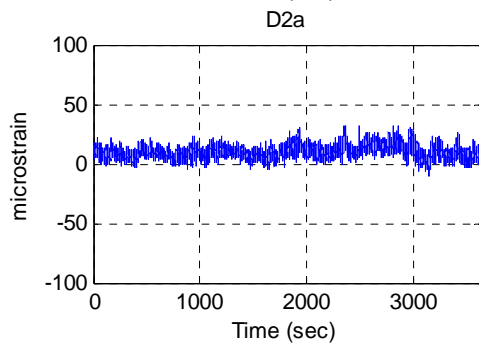
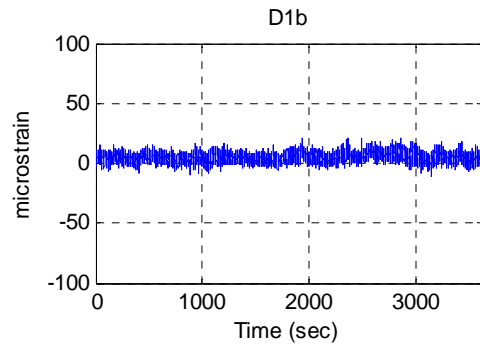
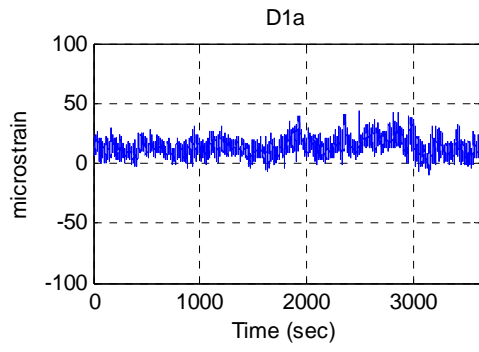


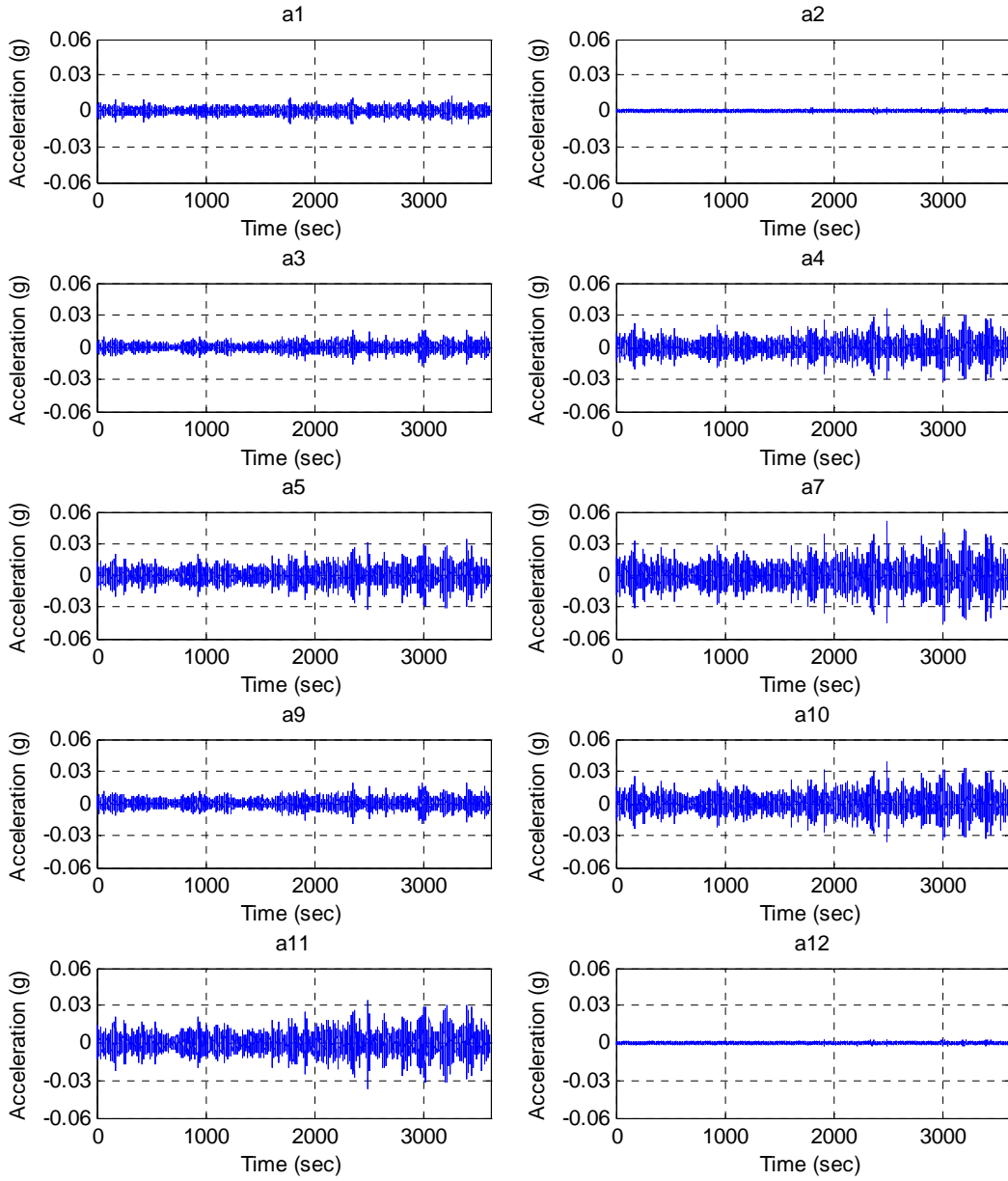


**Test W4**  
Data\I-A\I-A\_W4.txt







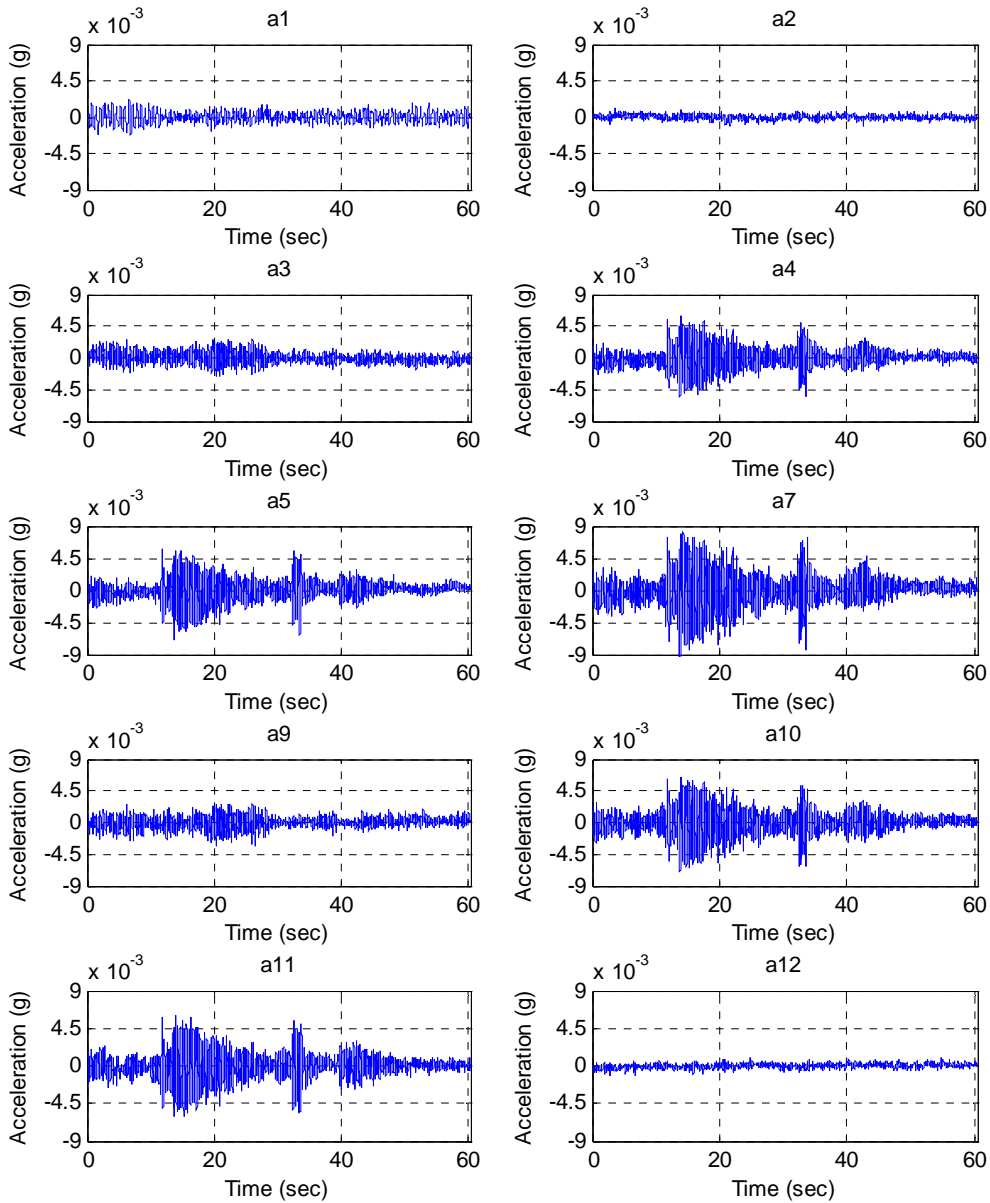


## A2.4 Truck Gust Data

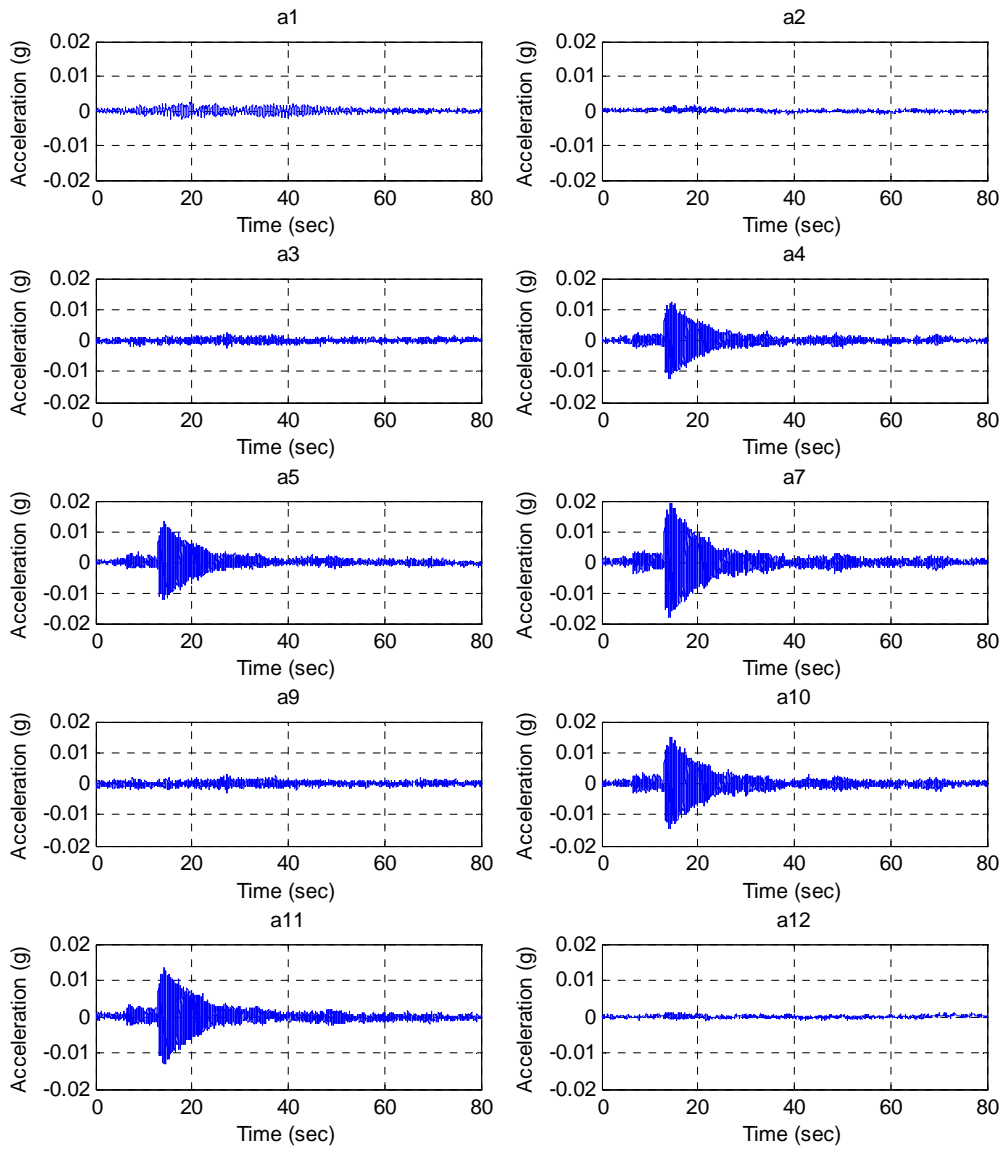
The truck gust data does not include strain measurements. The data structure for the truck gust data is as follows:

Time(sec), a1, a2, a3, a4, a5, a7, a9, a10, a11, a12

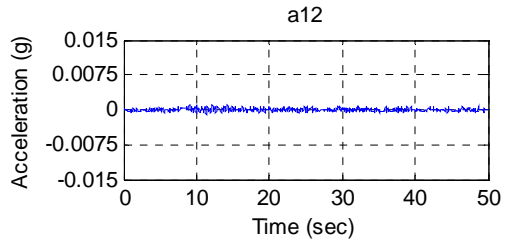
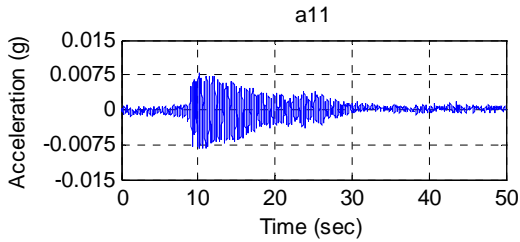
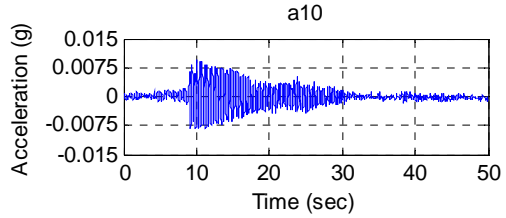
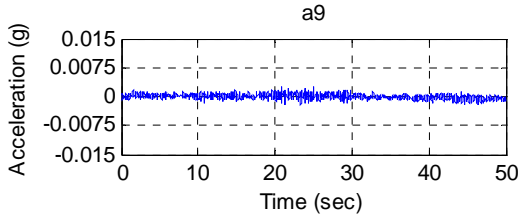
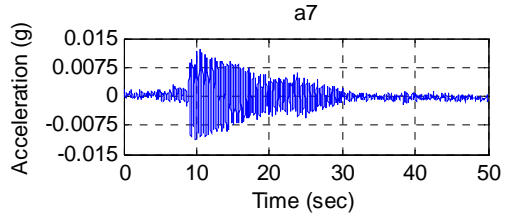
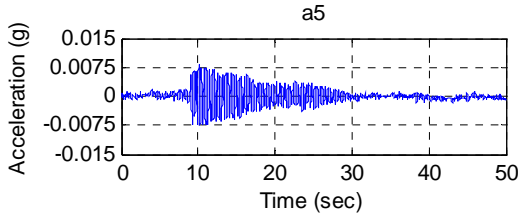
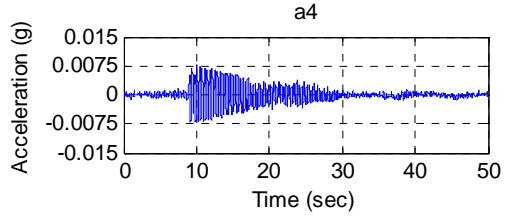
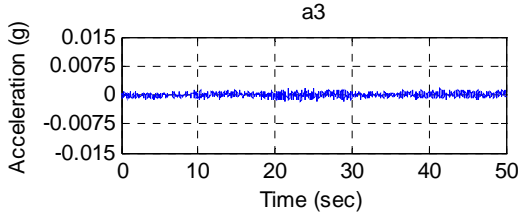
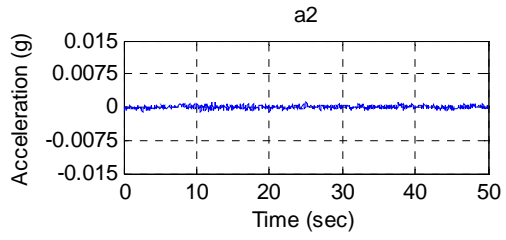
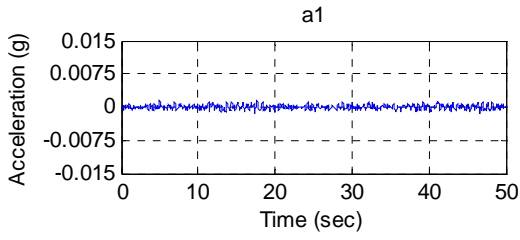
### Test TG1 [Data\I-A\I-A\\_TG1.txt](#)



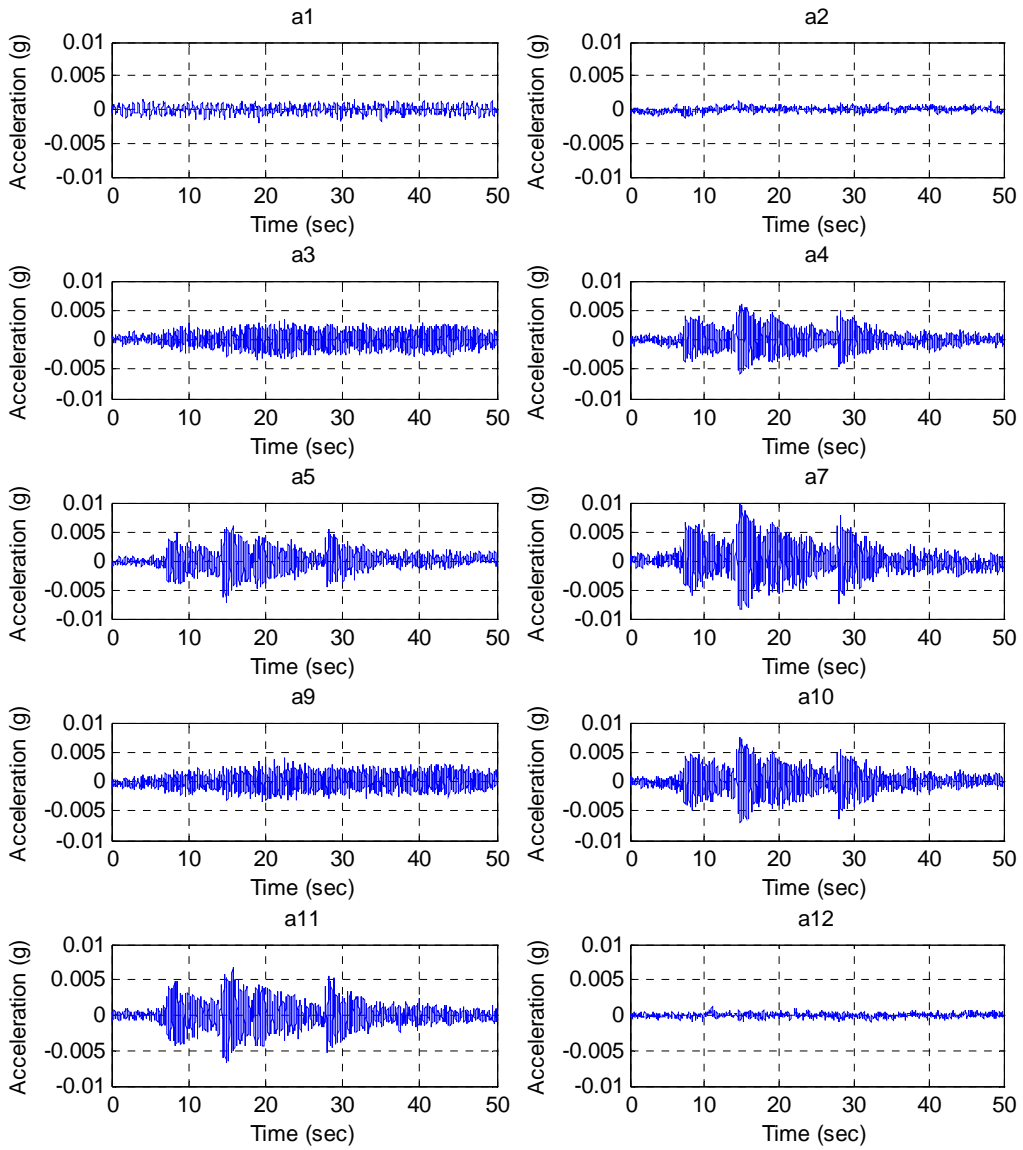
**Test TG2**  
Data\I-A\I-A TG2.txt



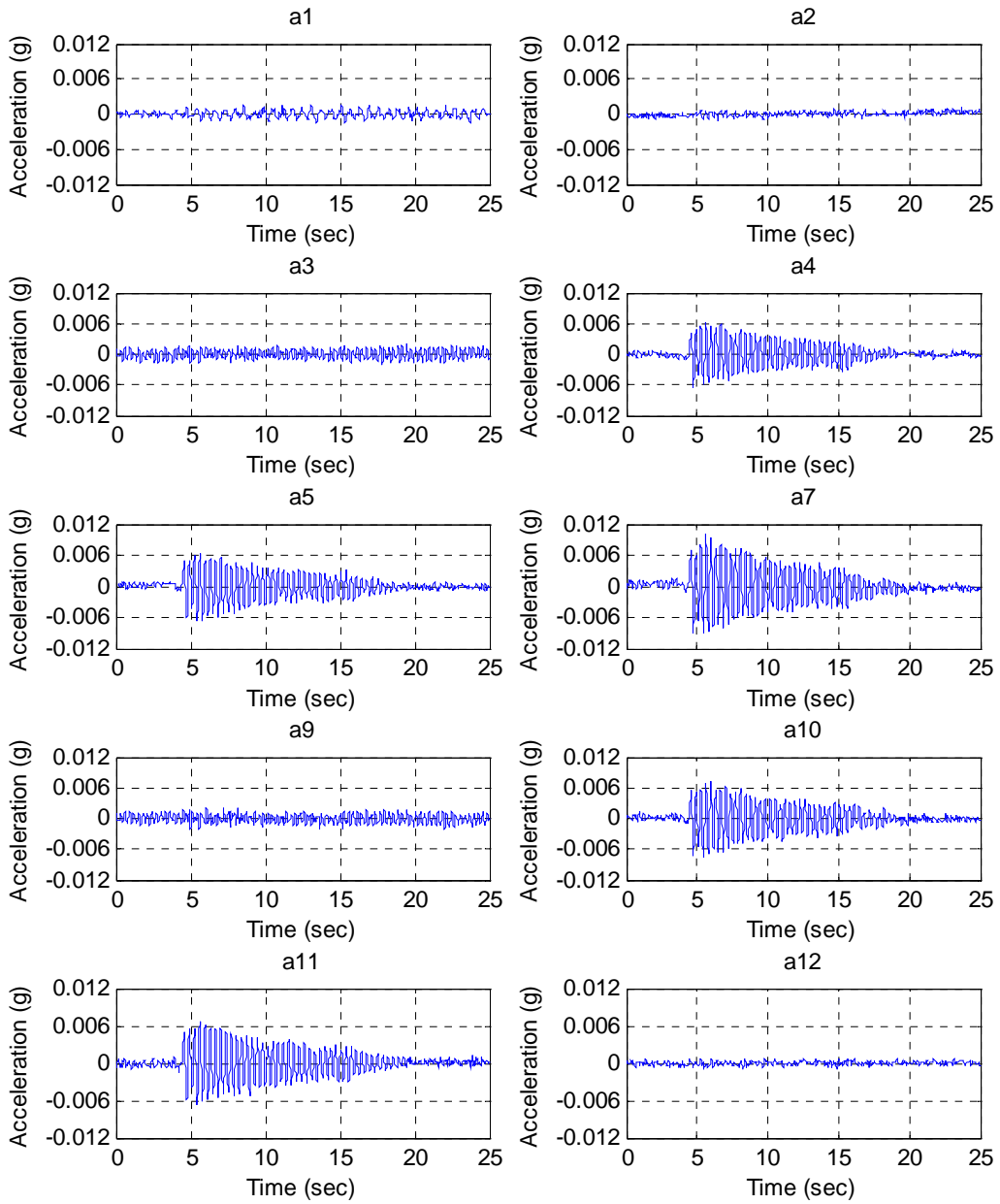
**Test TG3**  
Data\I-A\I-A TG3.txt



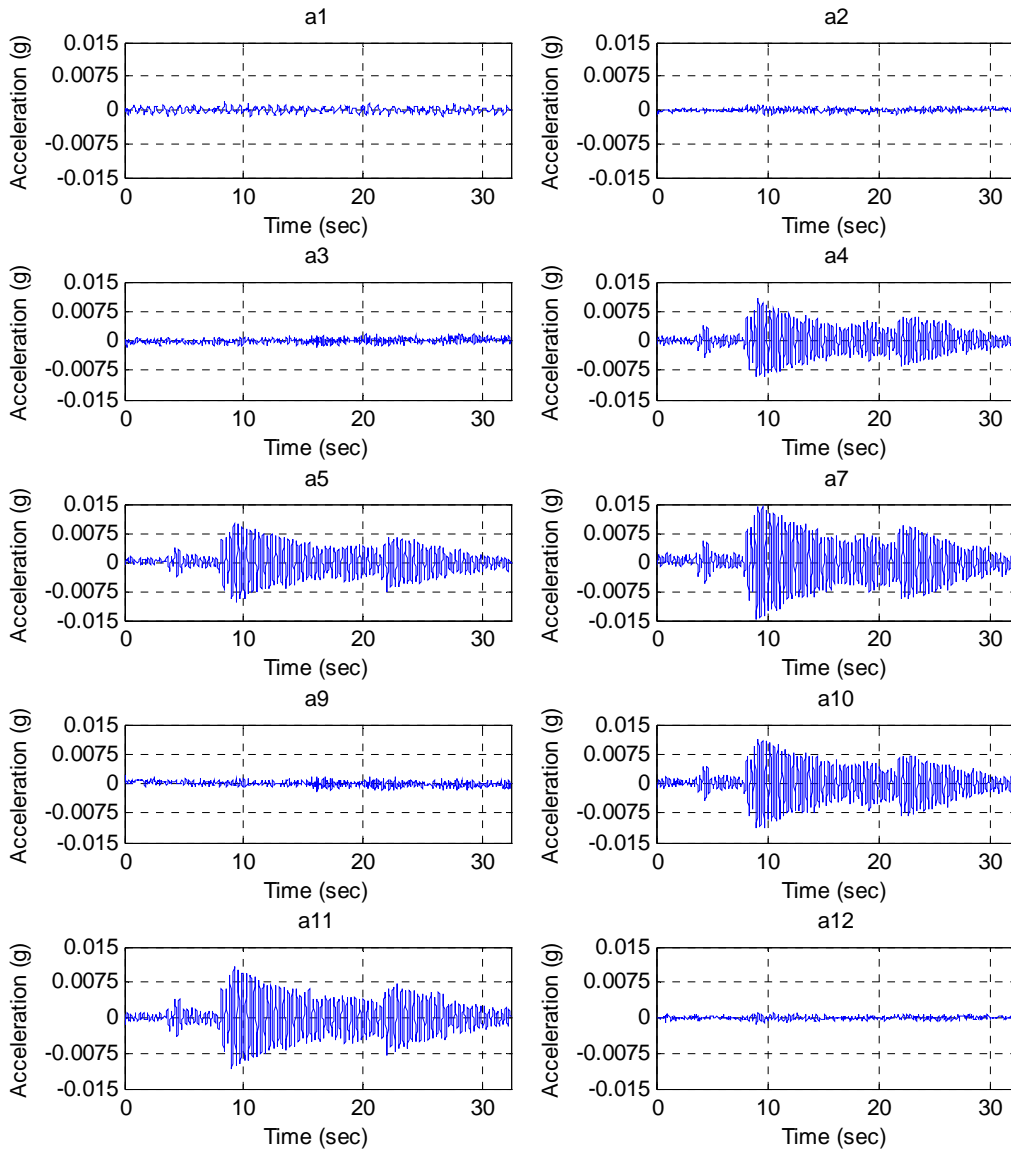
**Test TG4**  
**Data\I-A\I-A TG4.txt**



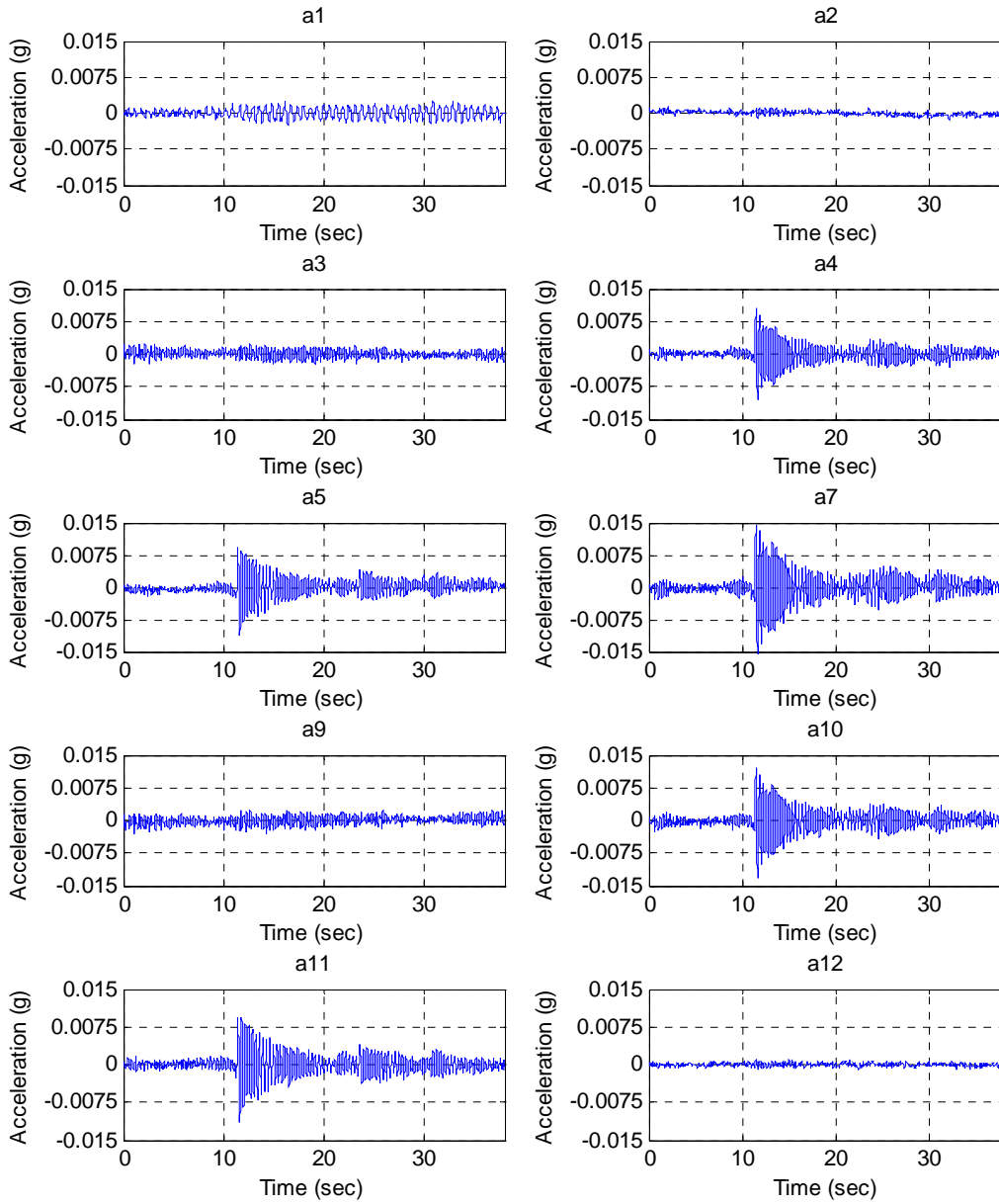
**Test TG5**  
[Data\I-A\I-A TG5.txt](#)



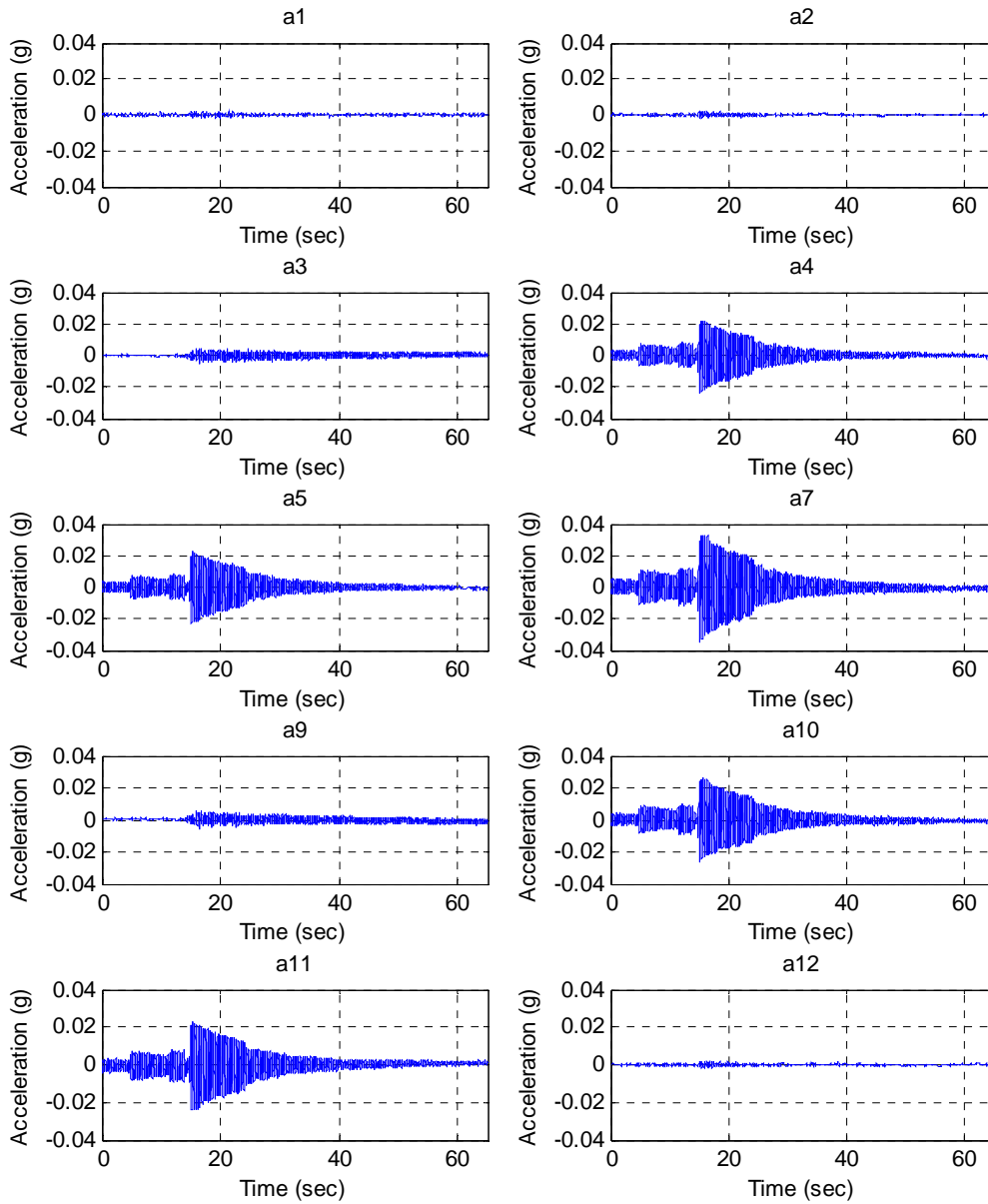
**Test TG6**  
Data\I-A\I-A TG6.txt



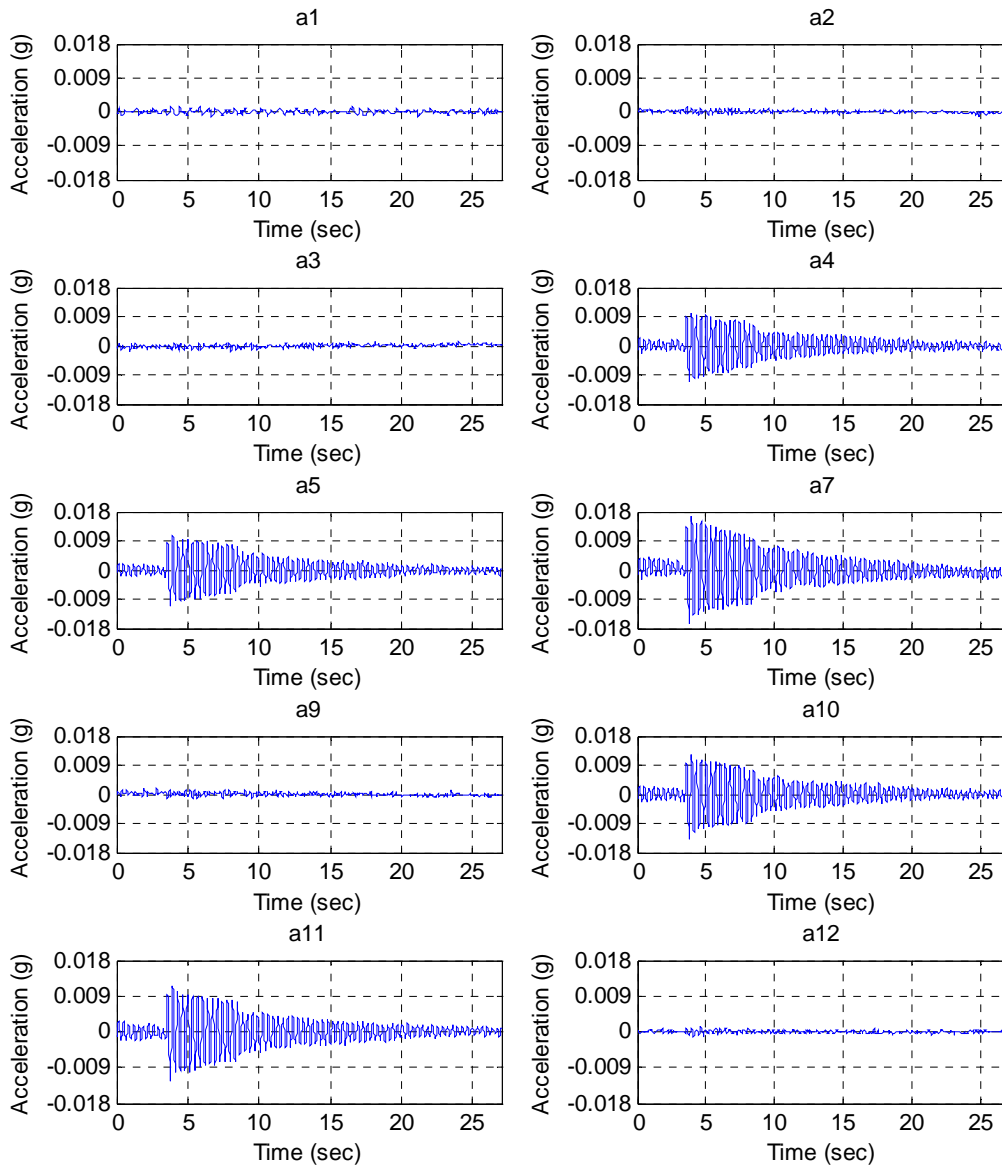
**Test TG7**  
[Data\I-A\I-A TG7.txt](#)



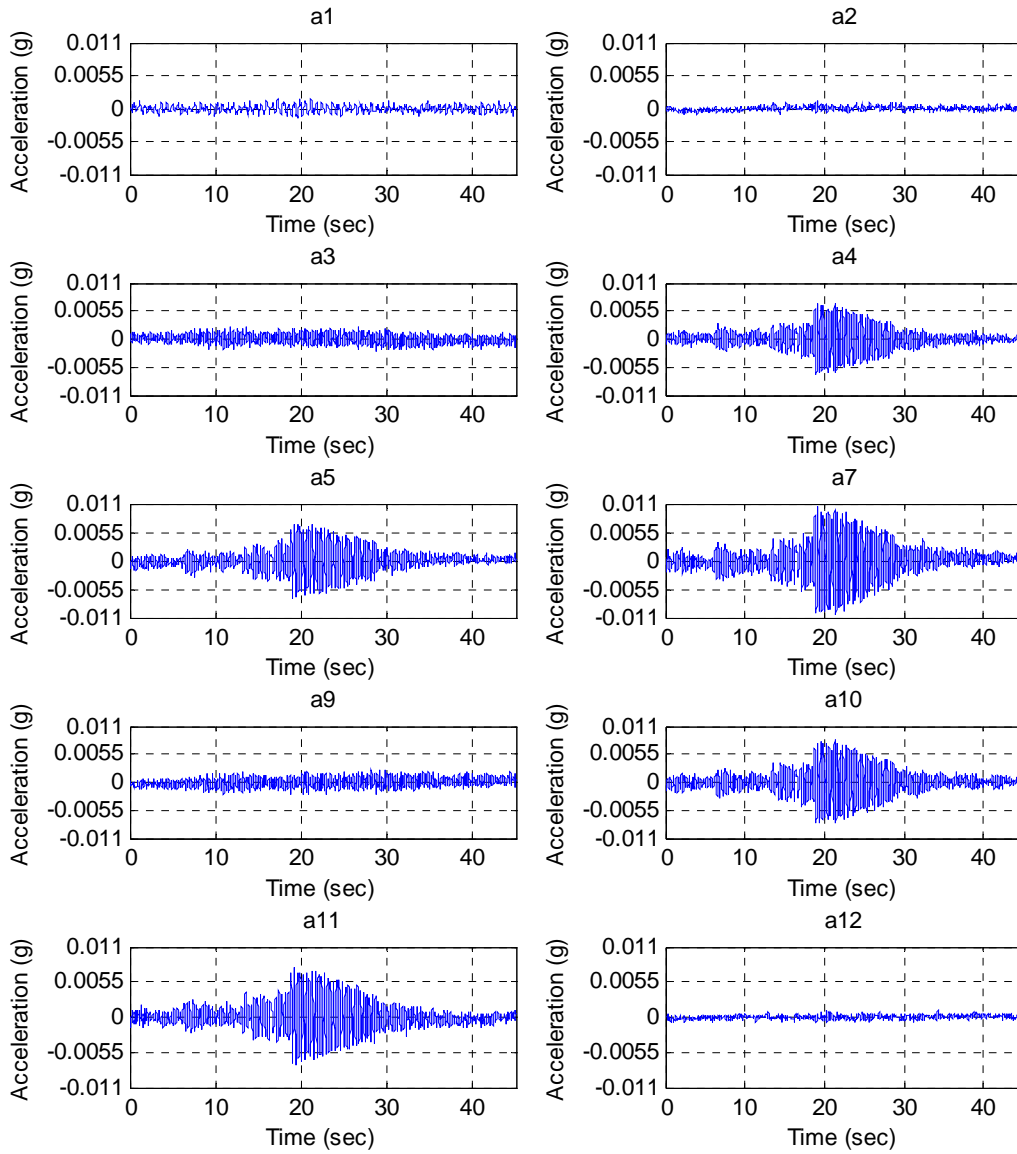
**Test TG8**  
Data\I-A\I-A TG8.txt



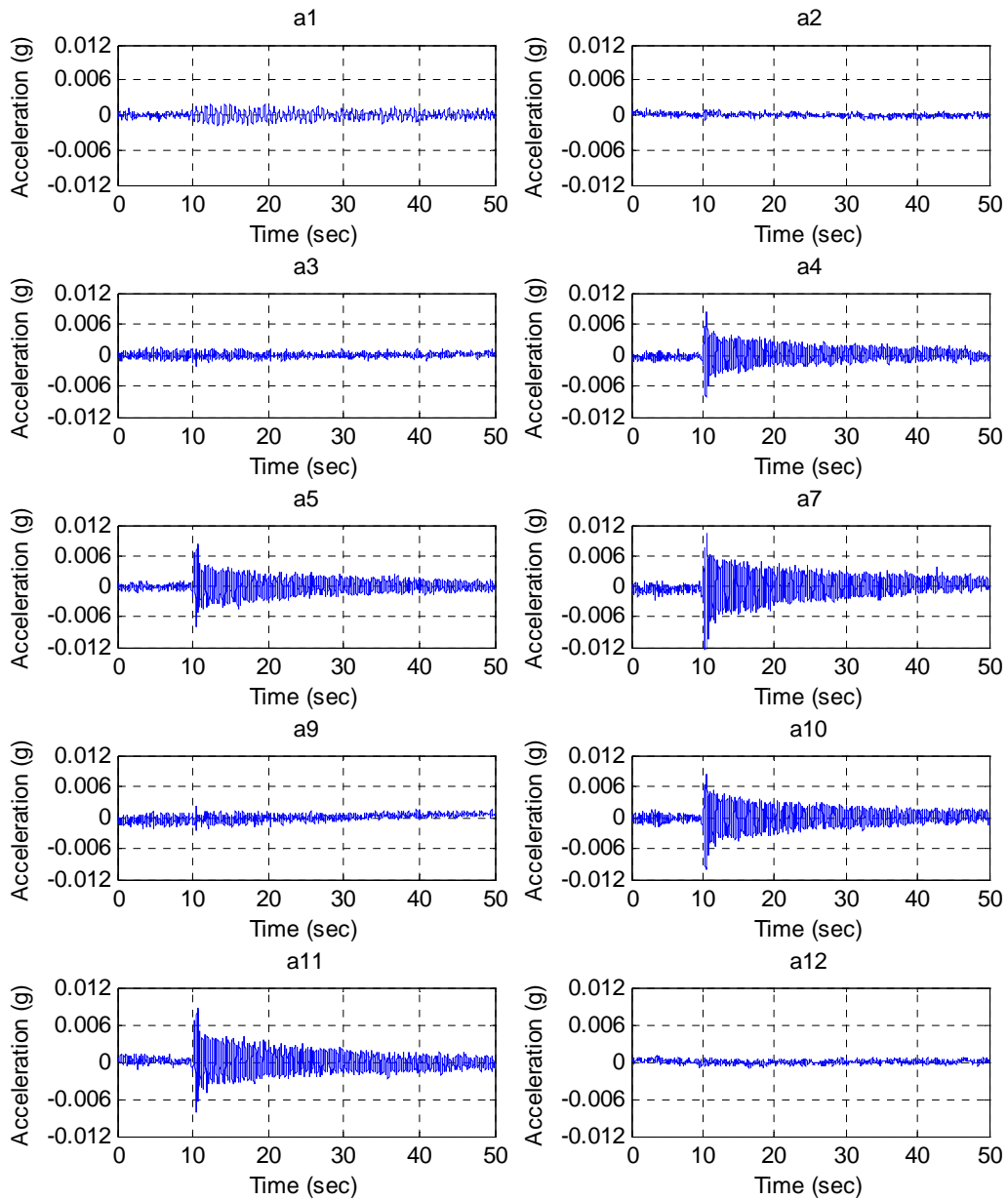
**Test TG9**  
Data\I-A\I-A TG9.txt



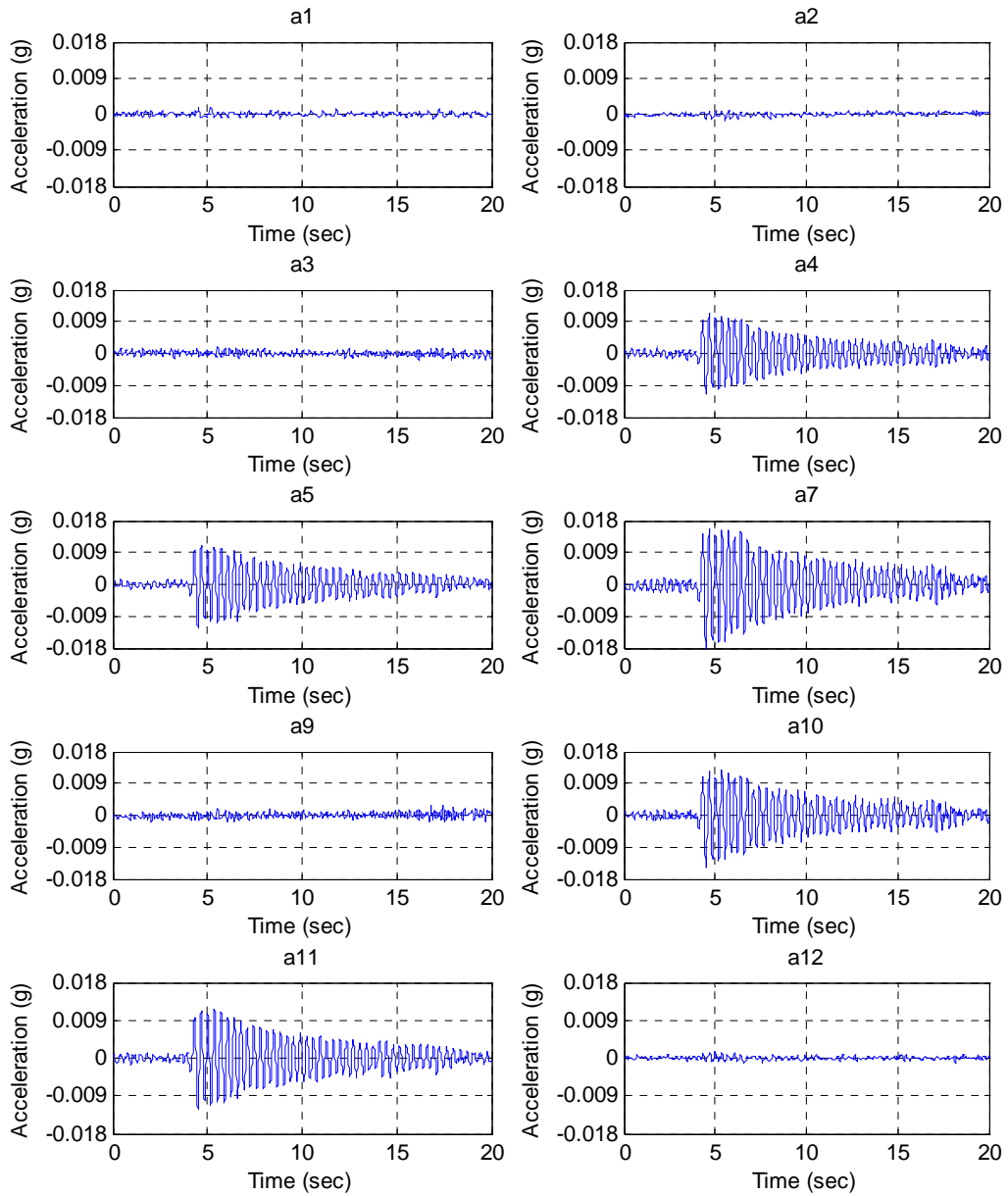
**Test TG10**  
**Data\I-A\I-A TG10.txt**



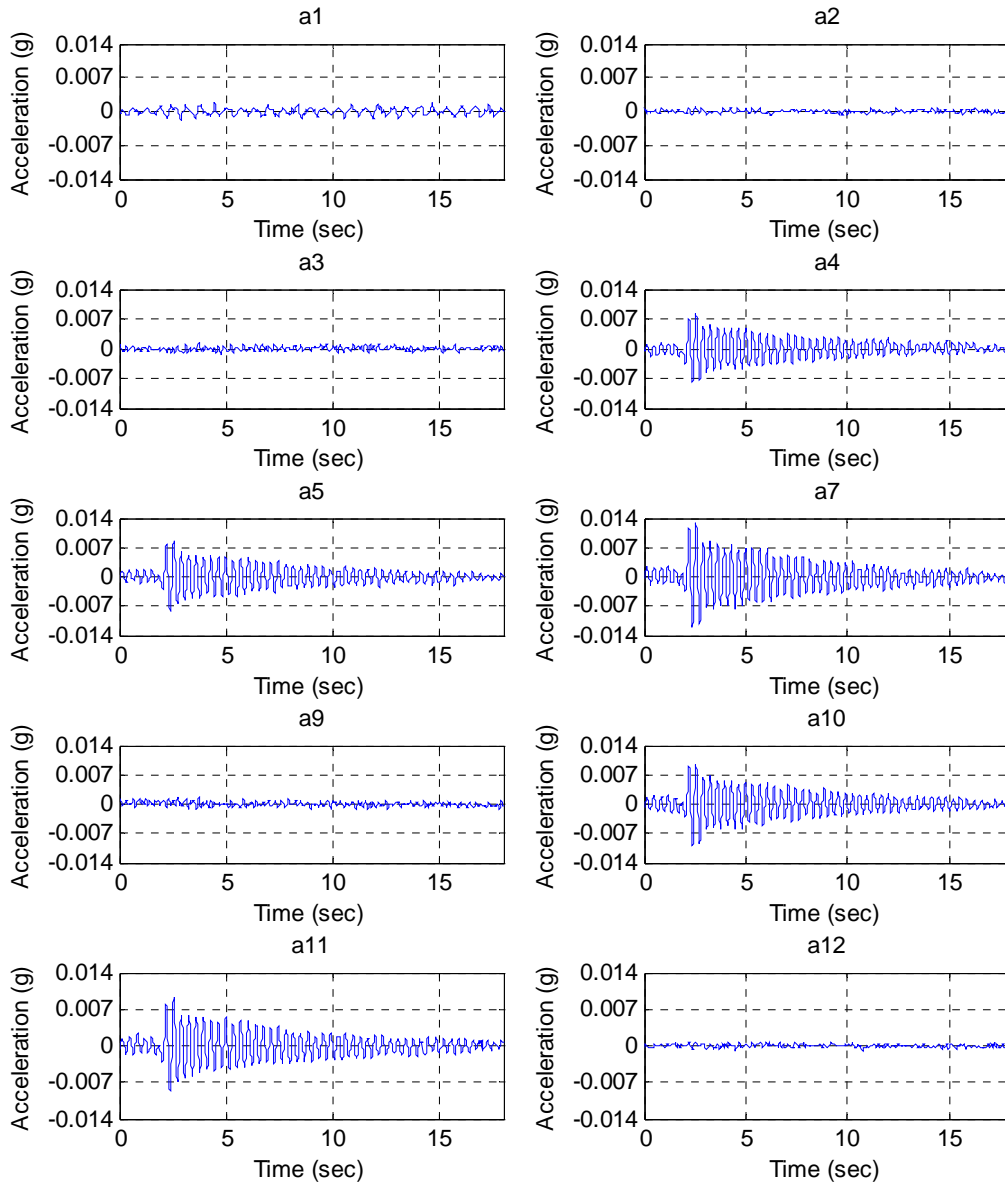
**Test TG11**  
**Data\I-A\I-A TG11.txt**



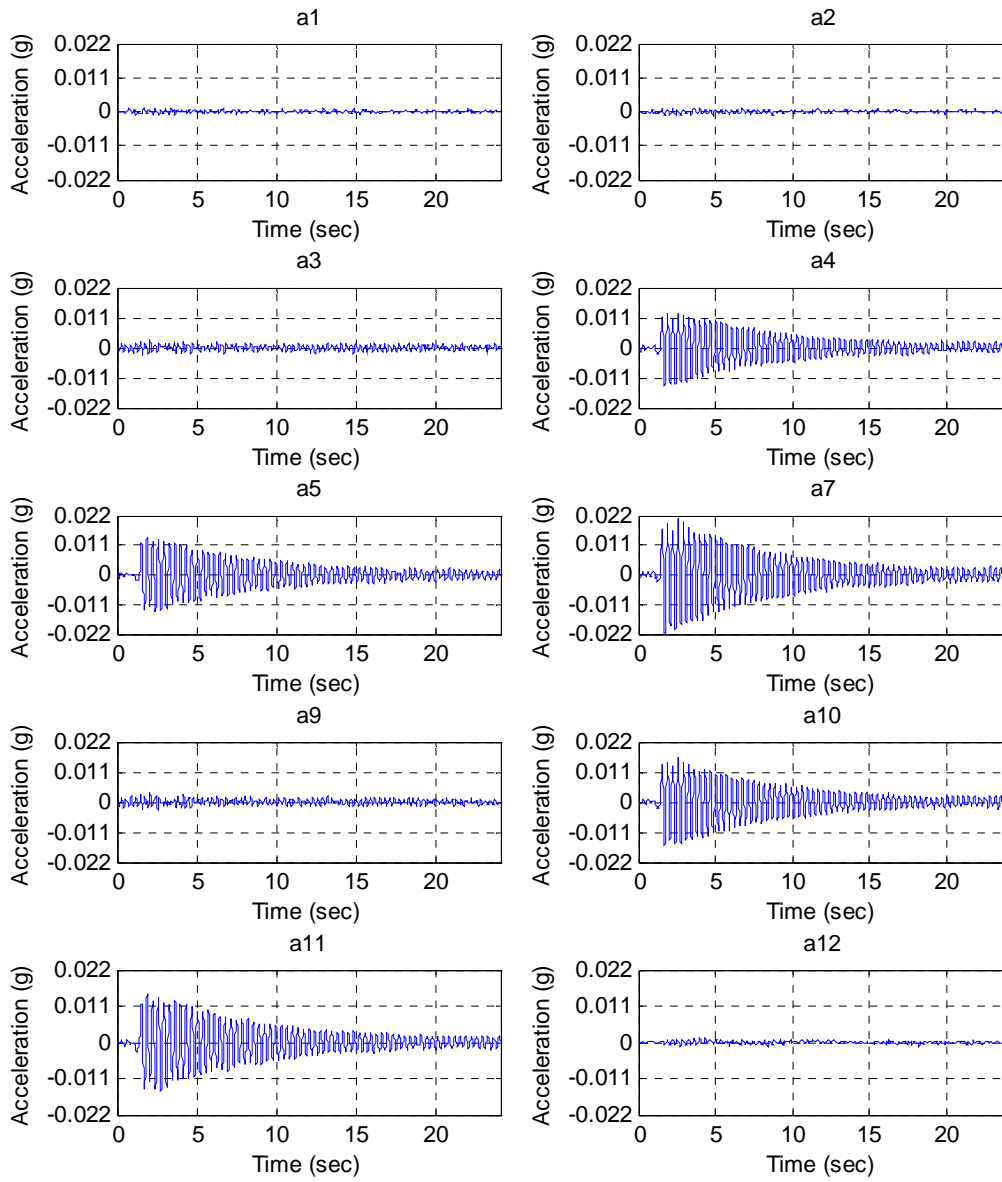
**Test TG12**  
**Data\I-A\I-A TG12.txt**



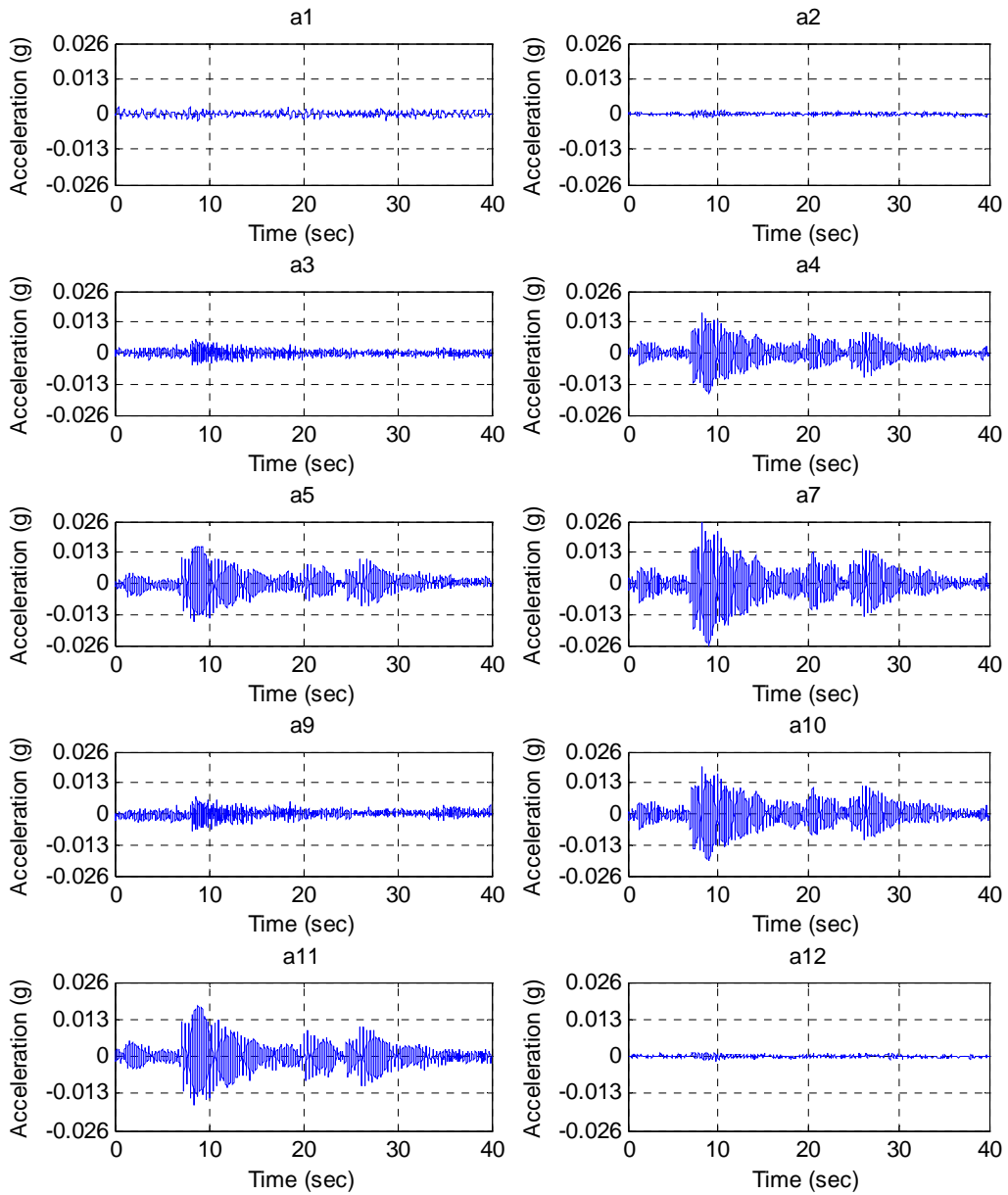
**Test TG13**  
**Data\I-A\I-A TG13.txt**



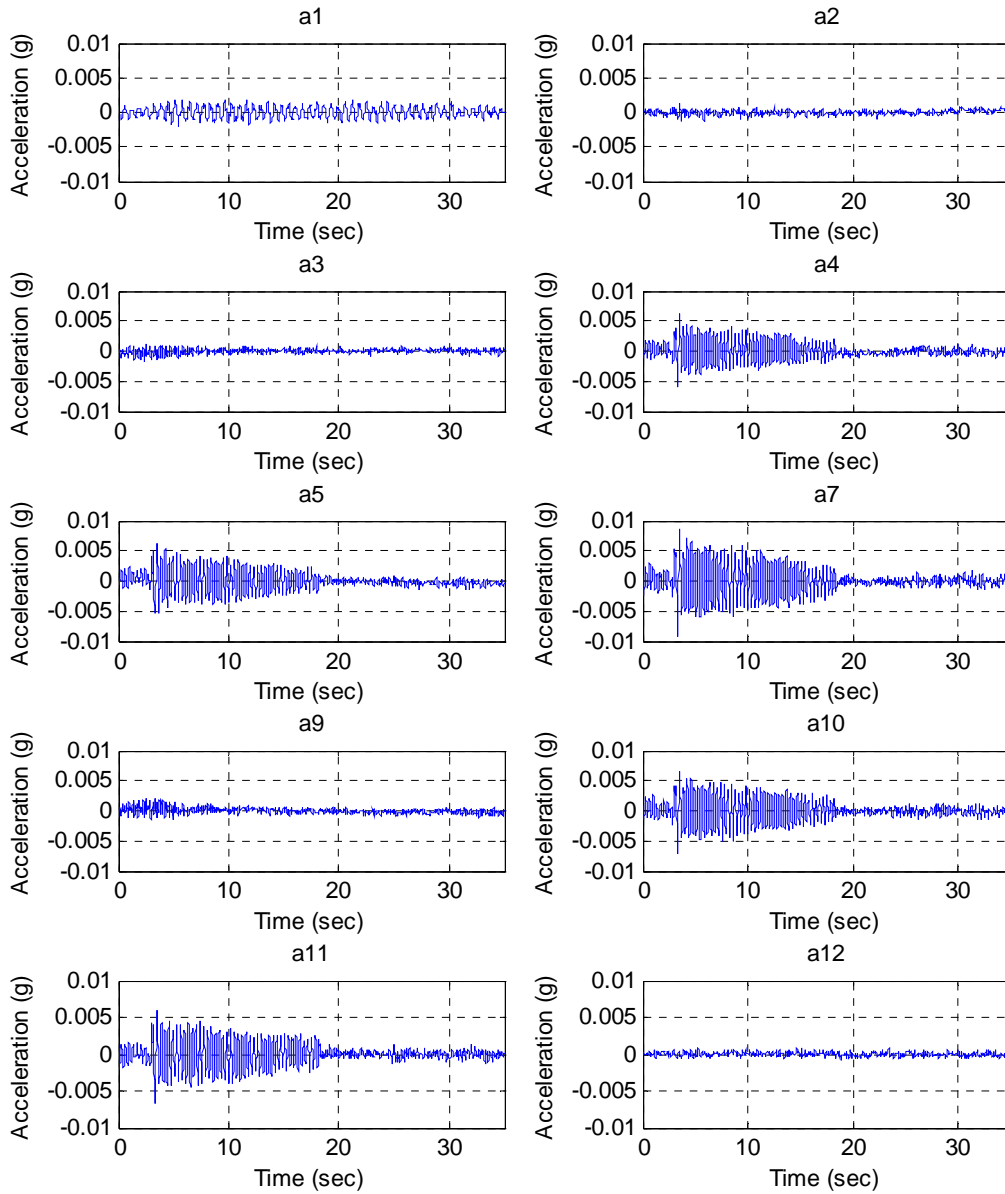
**Test TG14**  
**Data\I-A\I-A TG14.txt**



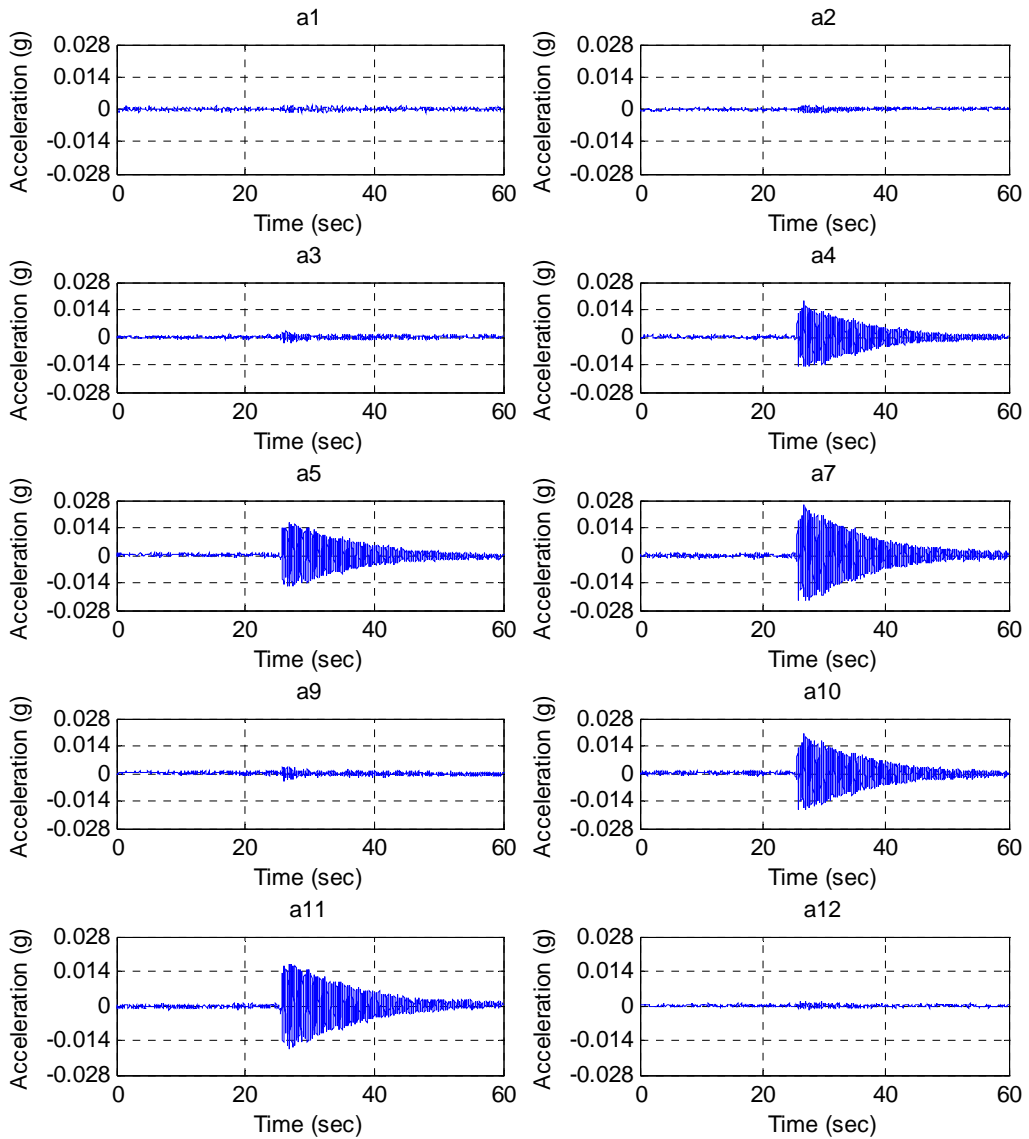
**Test TG15**  
**Data\I-A\I-A TG15.txt**



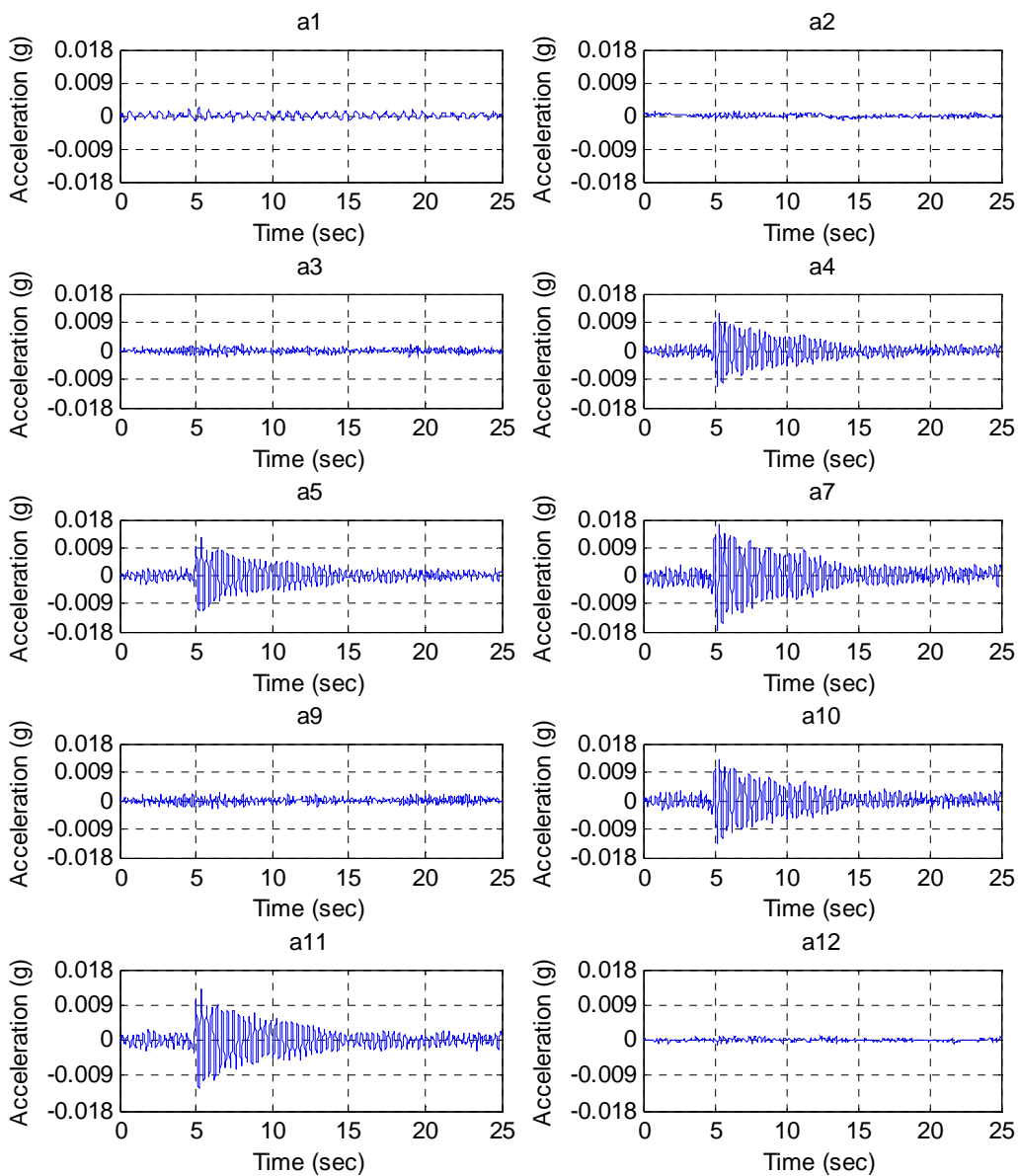
**Test TG16**  
**Data\I-A\I-A TG16.txt**



**Test TG17**  
**Data\I-A\I-A TG17.txt**



**Test TG18**  
**Data\I-A\I-A TG18.txt**



## A2.5 Manual Excitation Data

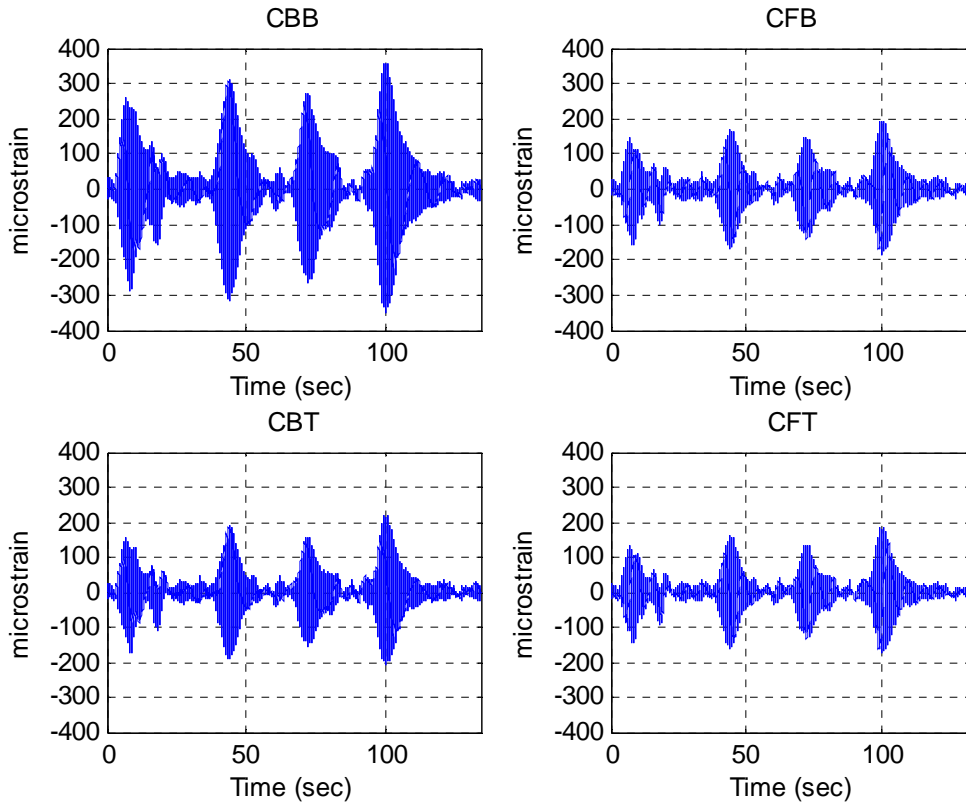
The data structure for tests M1-M4 is as follows:

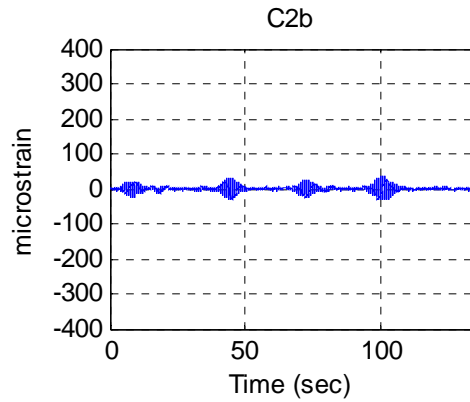
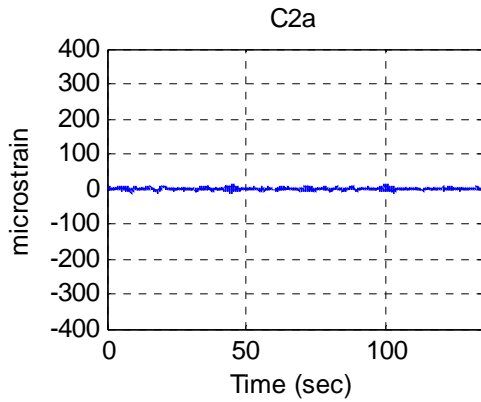
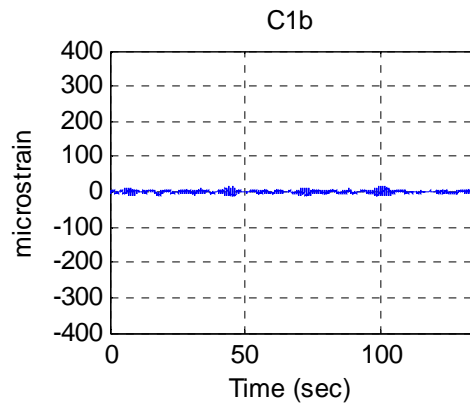
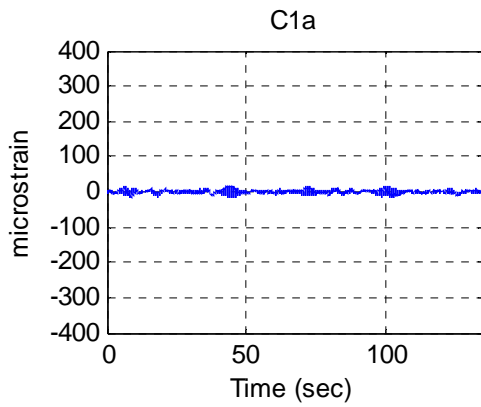
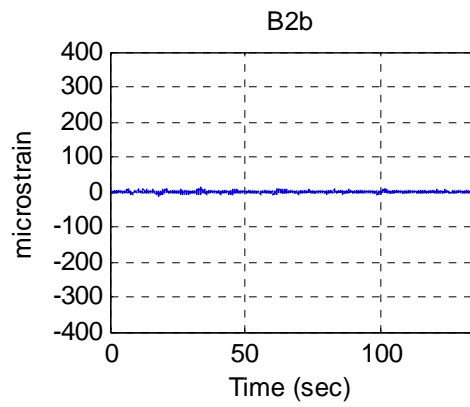
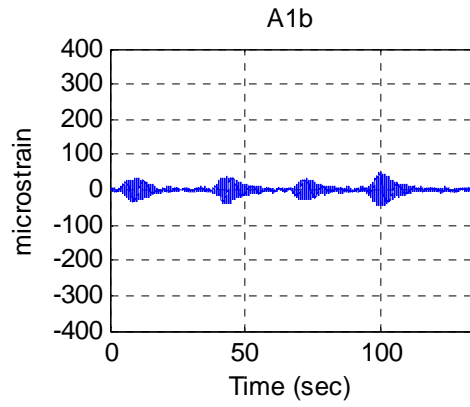
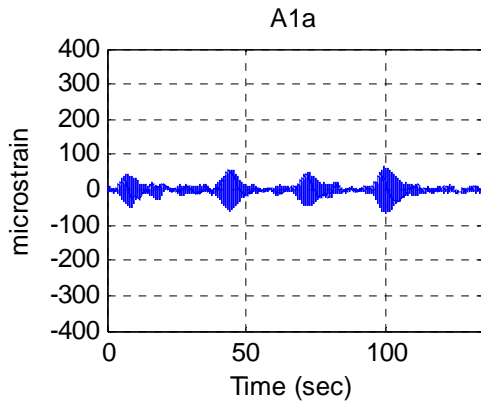
Time(sec), CBB, CFB, CBT, CFT, A1a, A1b, B2b, C1a, C1b, C2a, C2b, D1a, D1b, D2a, D2b, a1, a2, a3, a4, a5, a7, a9, a10, a11, a12

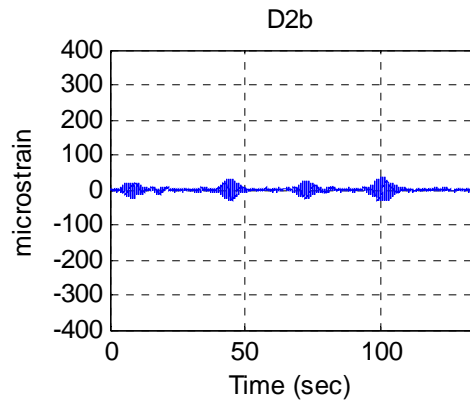
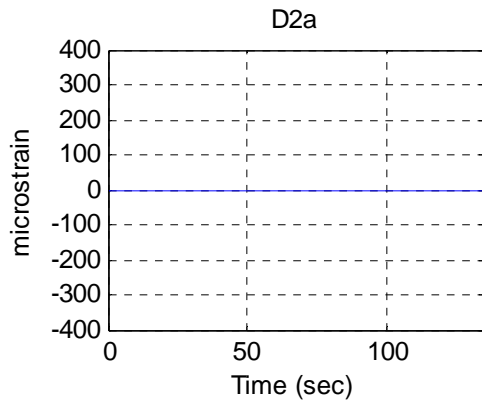
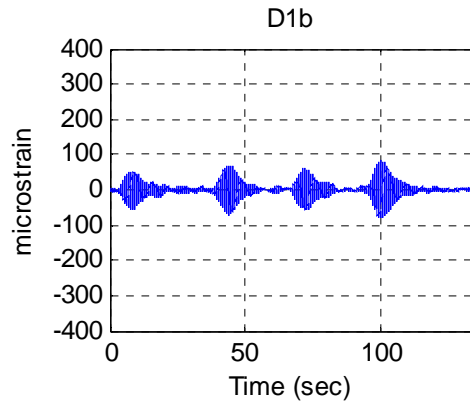
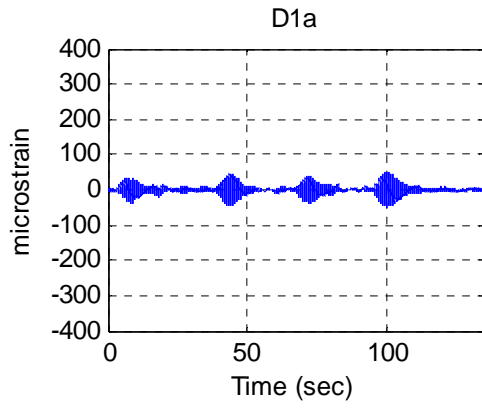
Test descriptions:

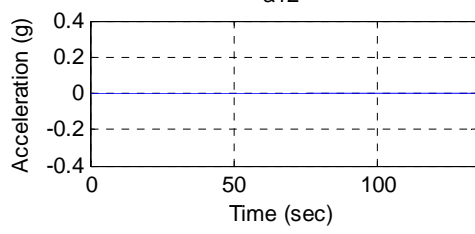
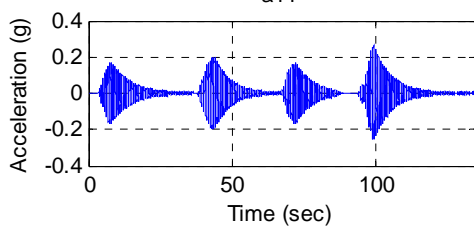
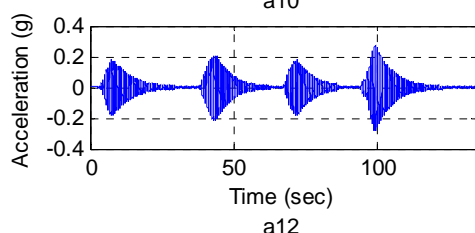
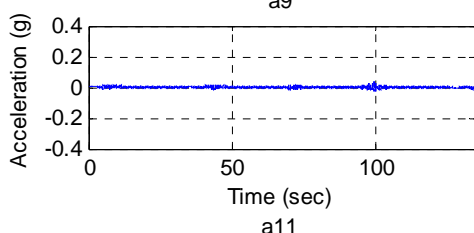
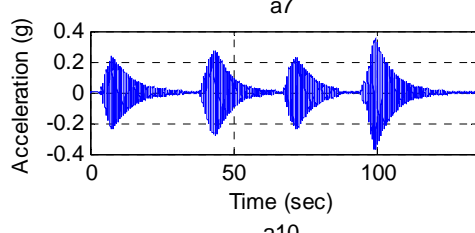
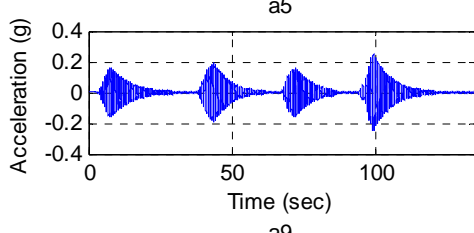
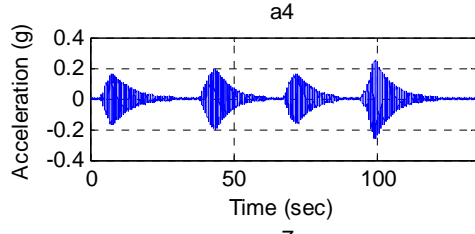
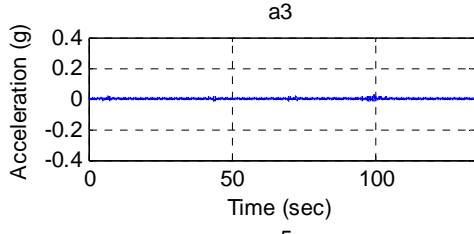
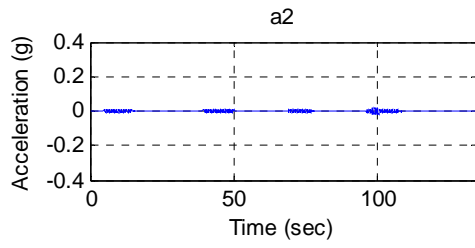
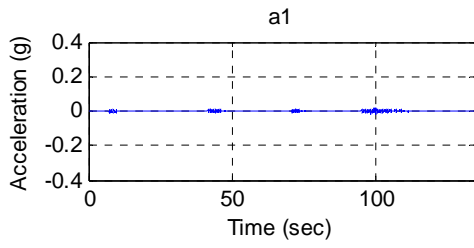
- M1 – horizontal excitation, damper engaged
- M2 – horizontal excitation, damper disengaged
- M3 – vertical excitation, damper engaged
- M4 – vertical excitation, damper disengaged

### Test M1 [Data\I-A\I-A M1.txt](#)

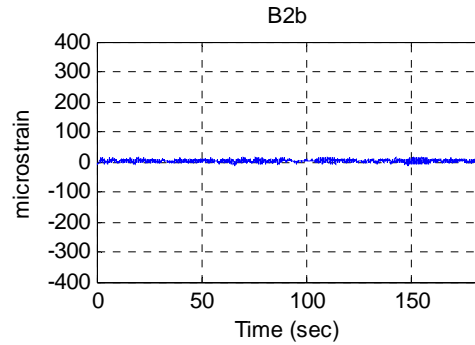
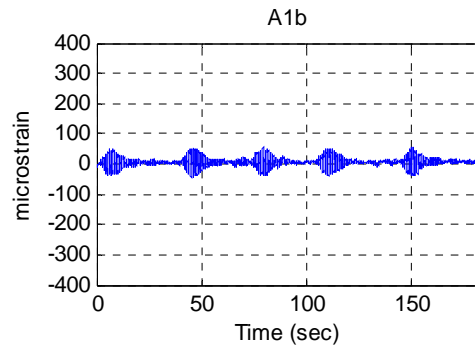
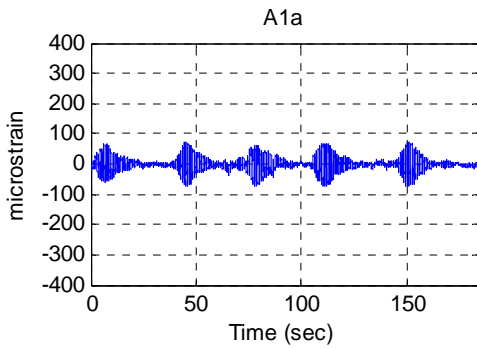
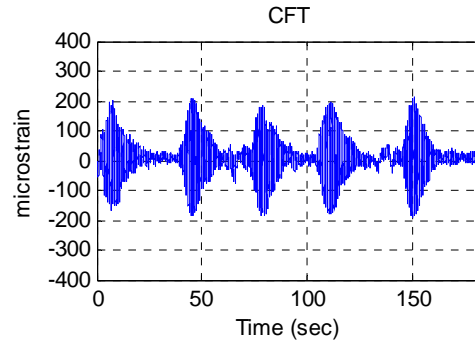
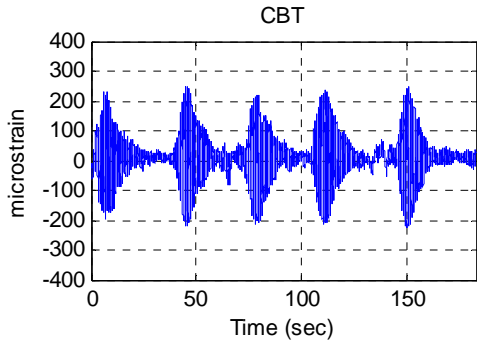
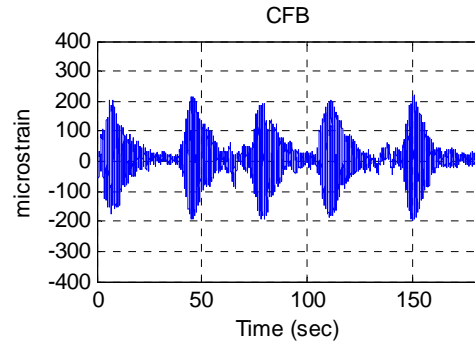
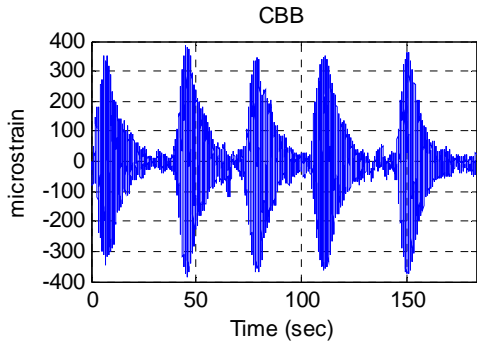


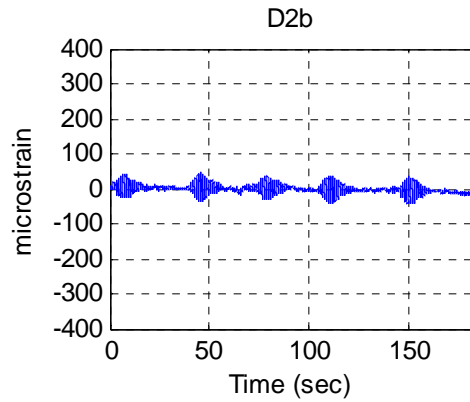
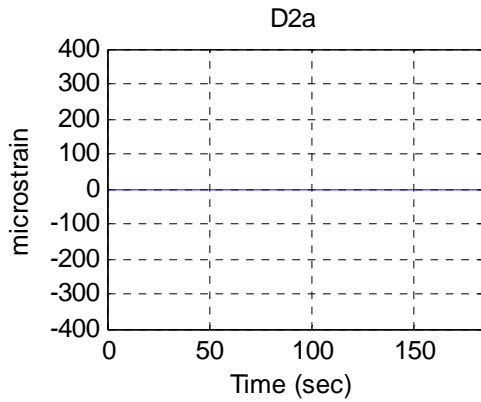
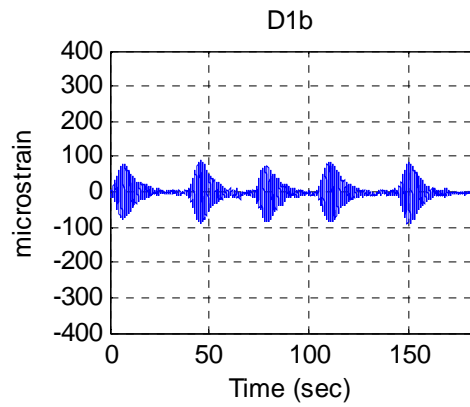
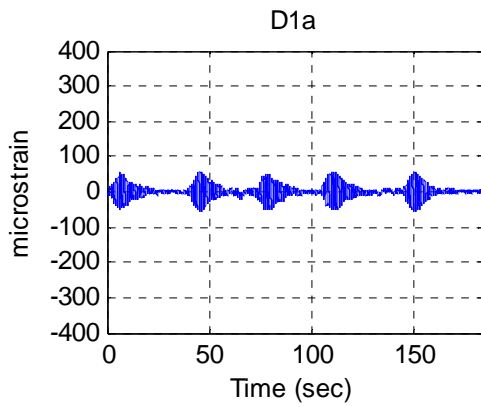
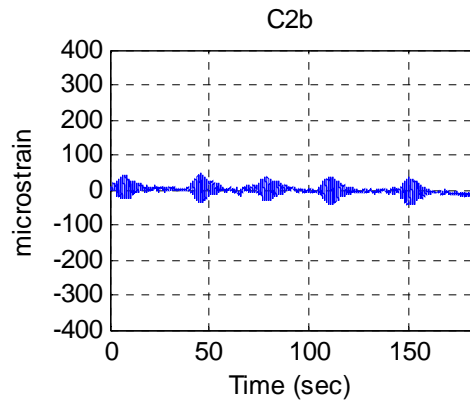
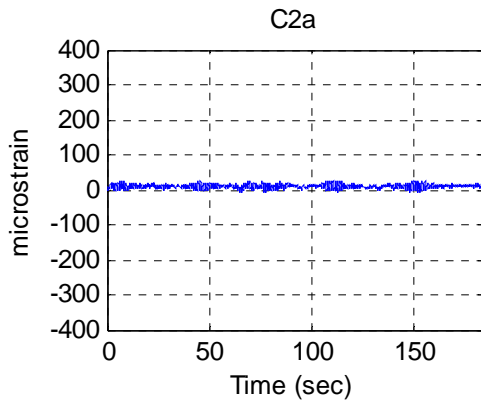
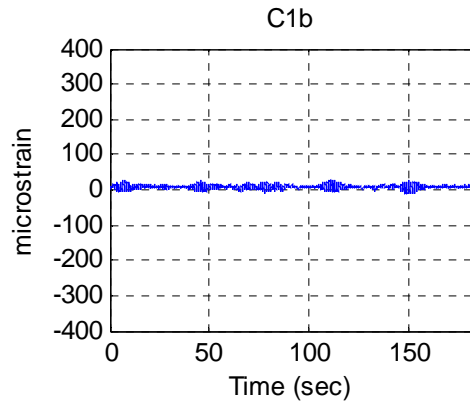
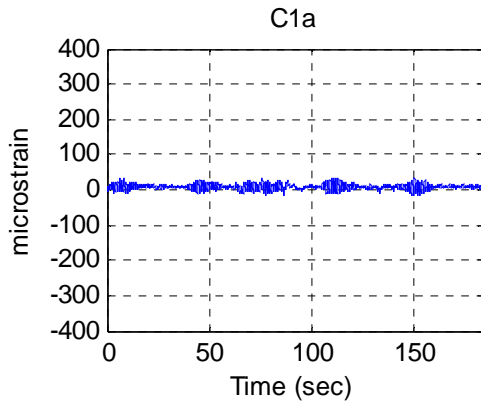


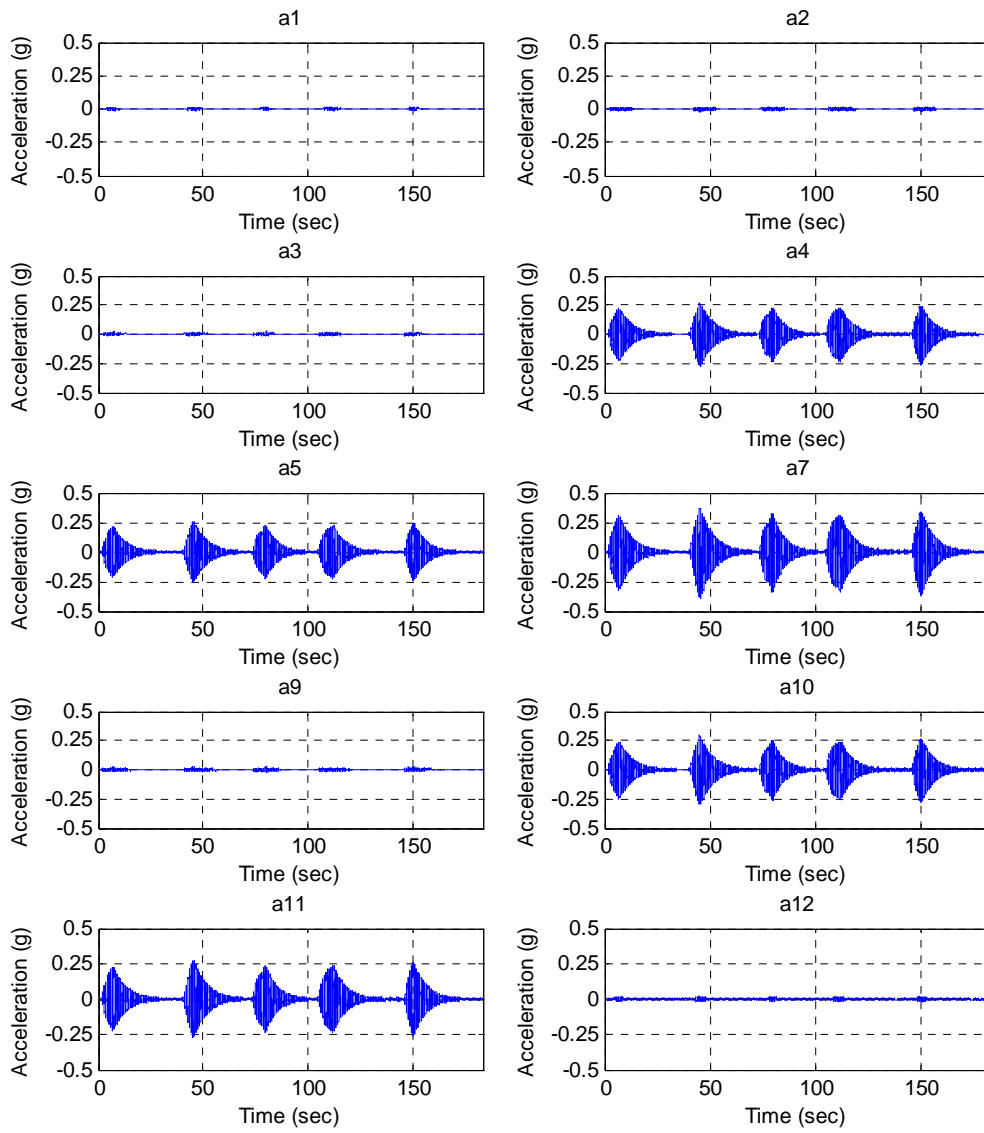




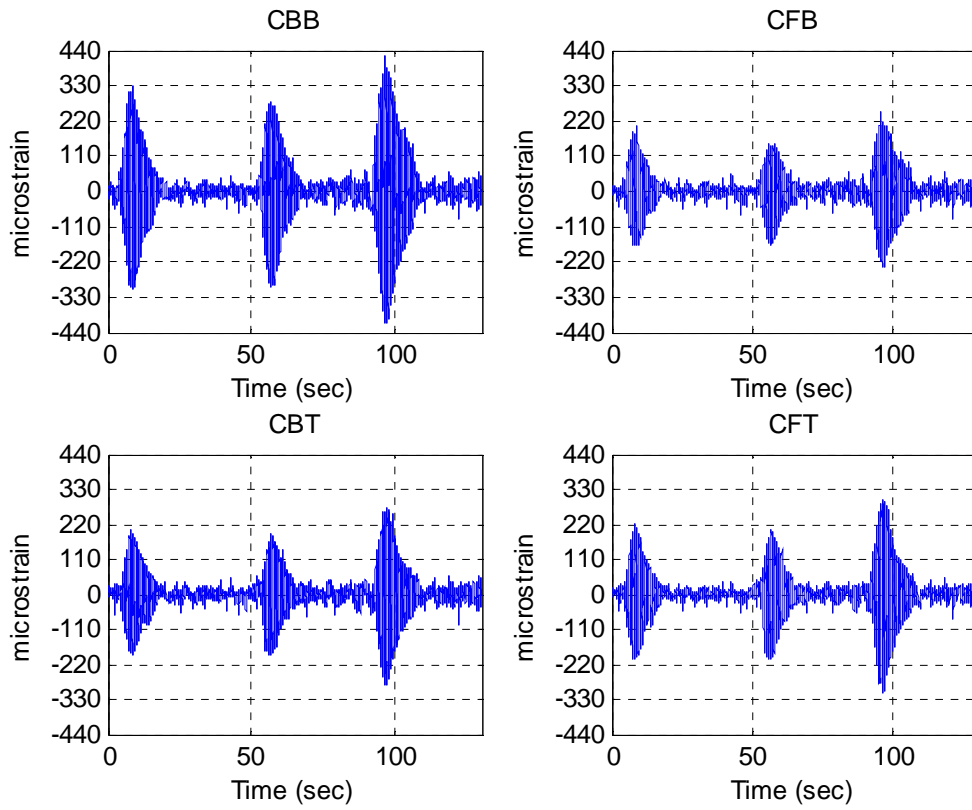
**Test M2**  
Data\I-A\I-A\_M2.txt

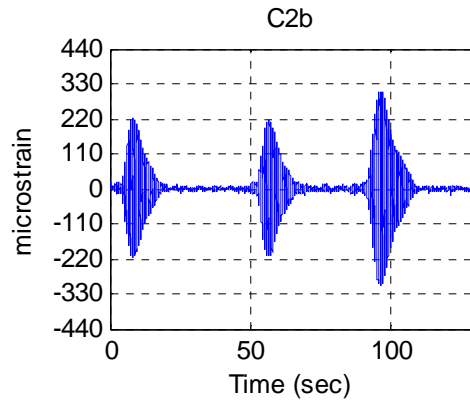
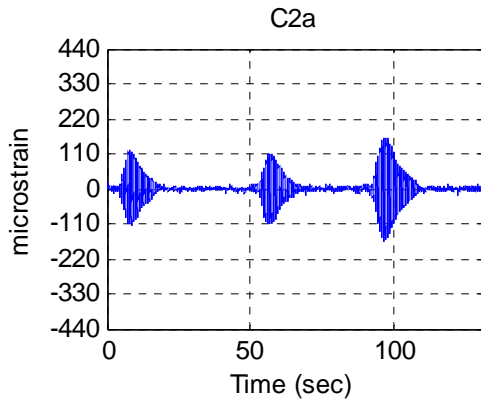
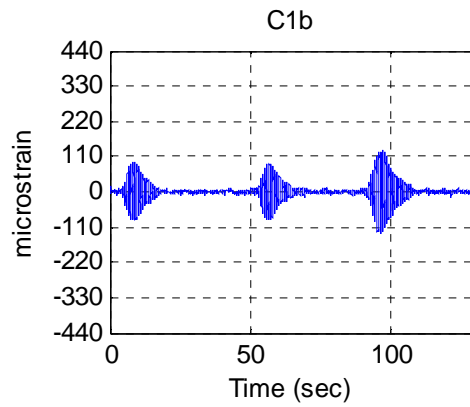
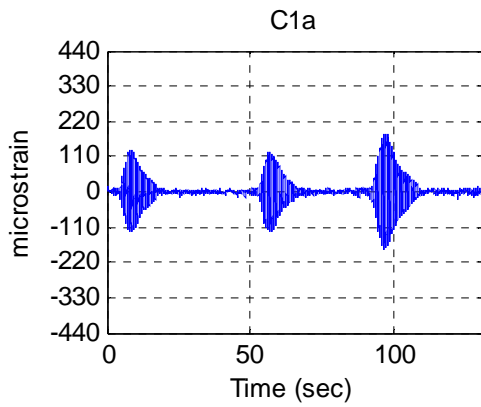
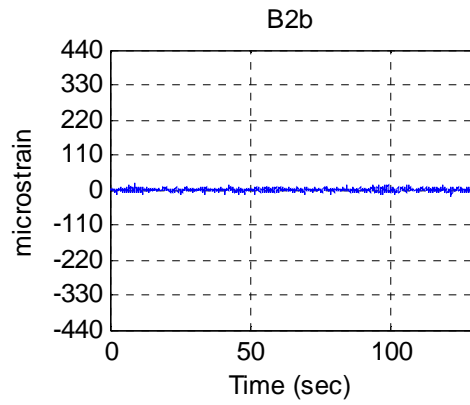
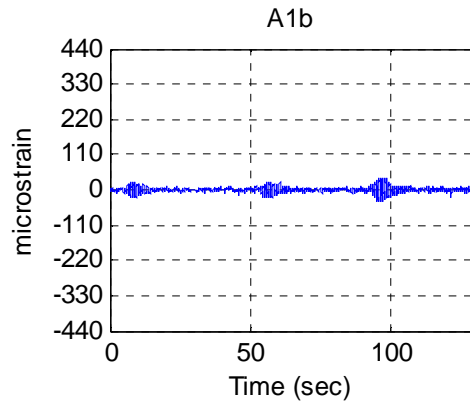
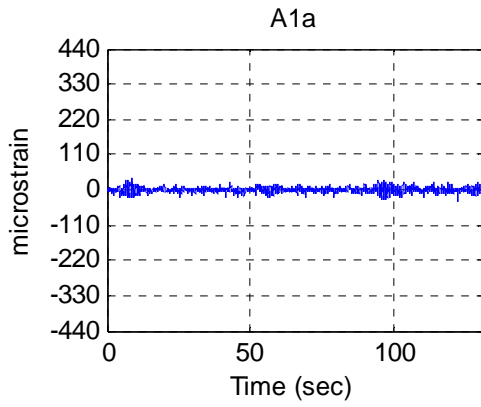


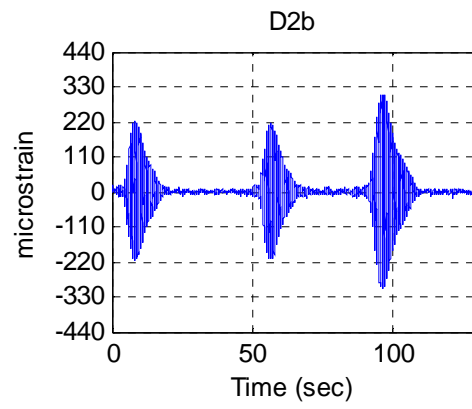
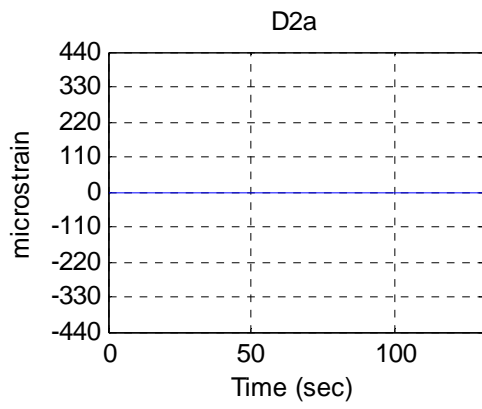
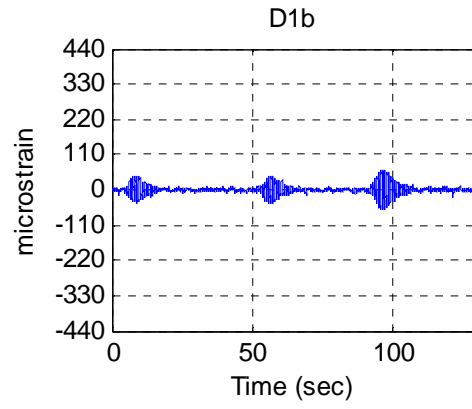
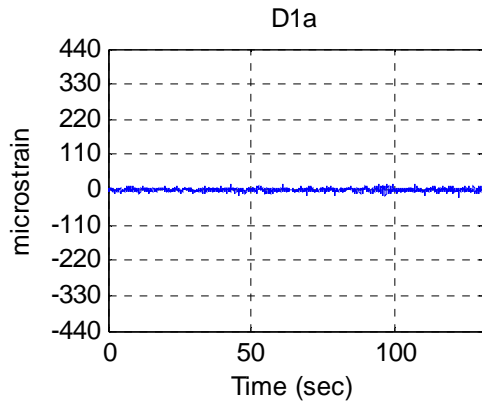


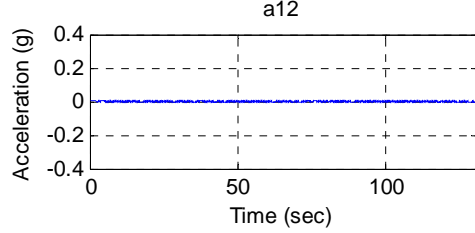
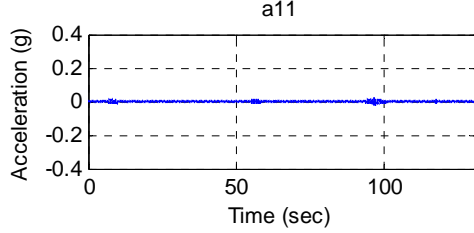
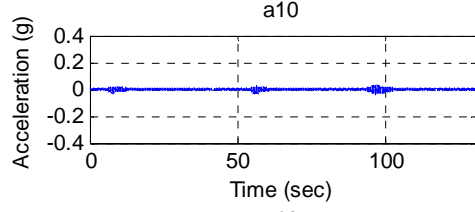
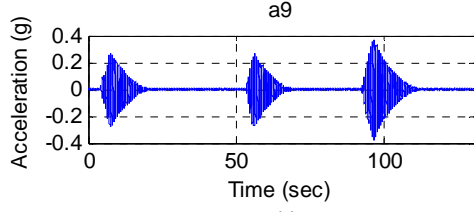
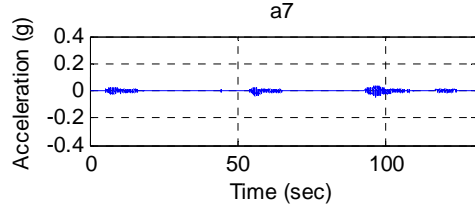
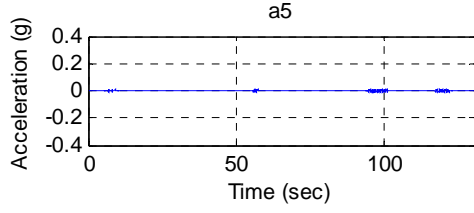
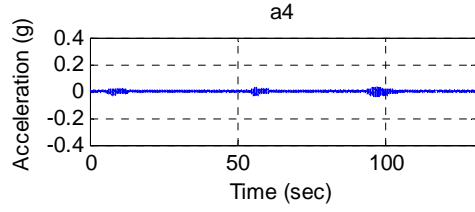
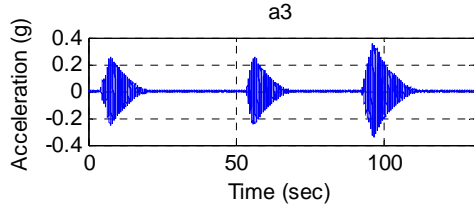
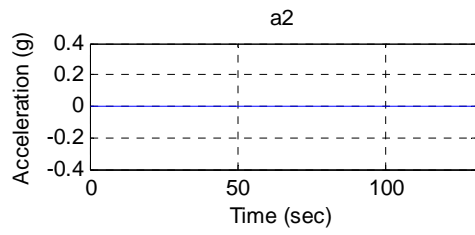
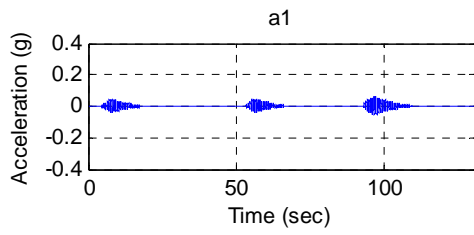


**Test M3**  
Data\I-A\I-A\_M3.txt

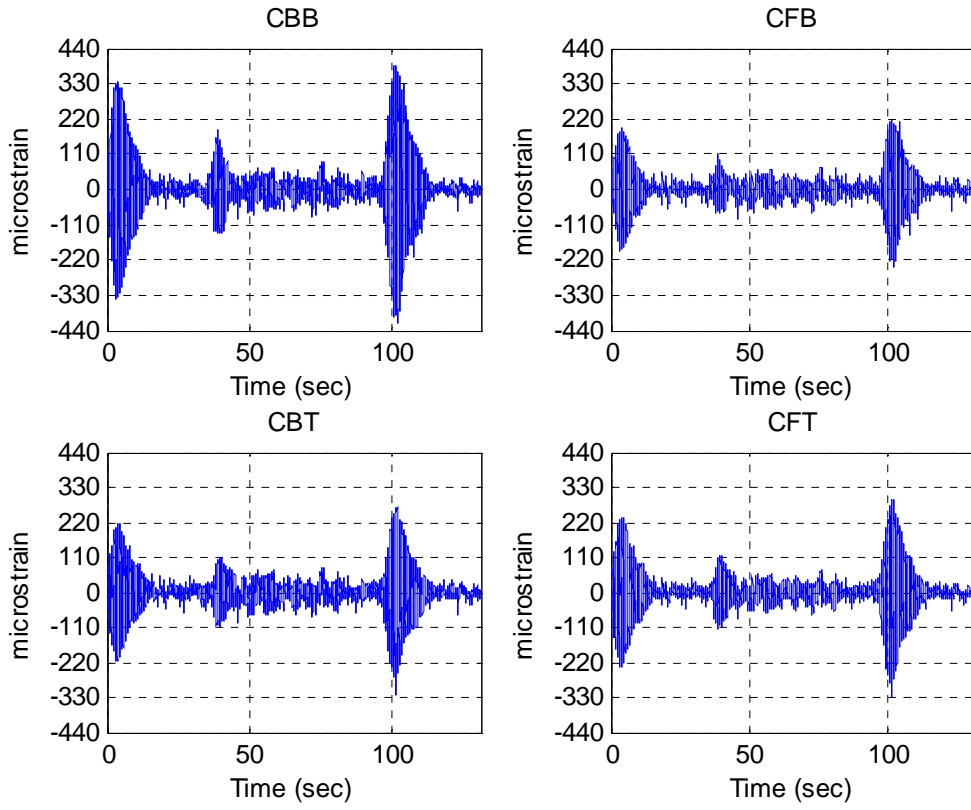


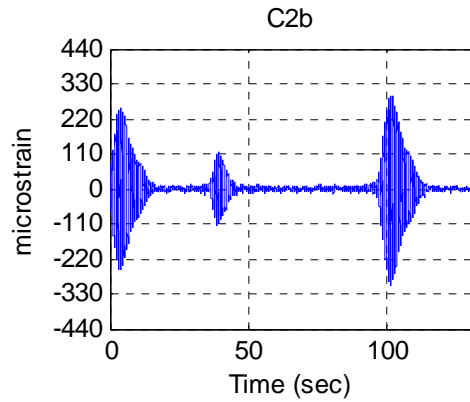
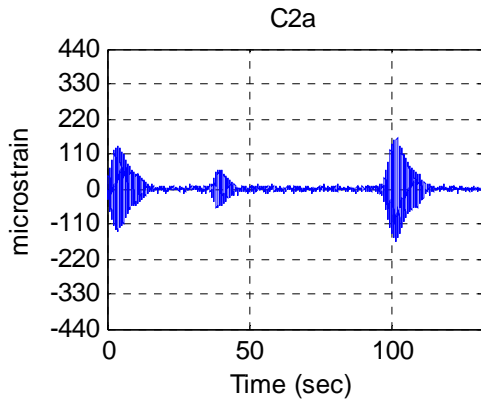
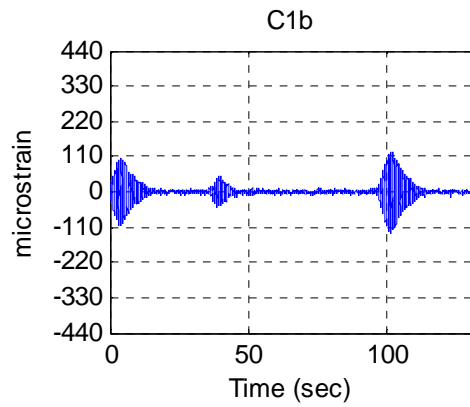
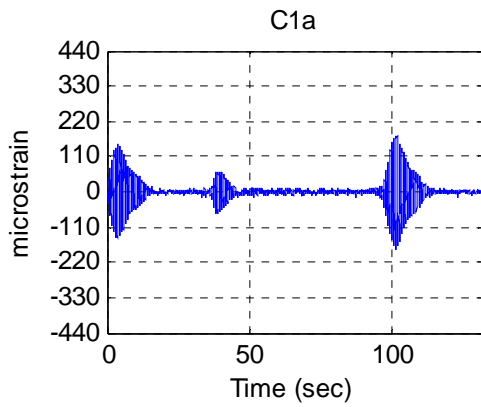
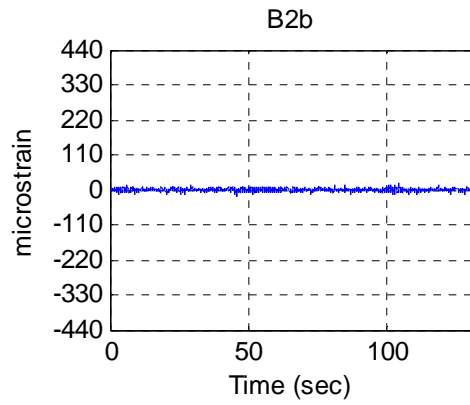
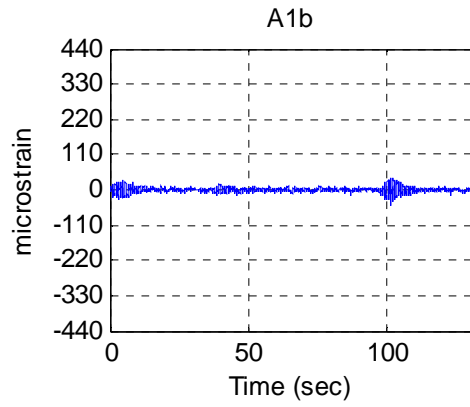
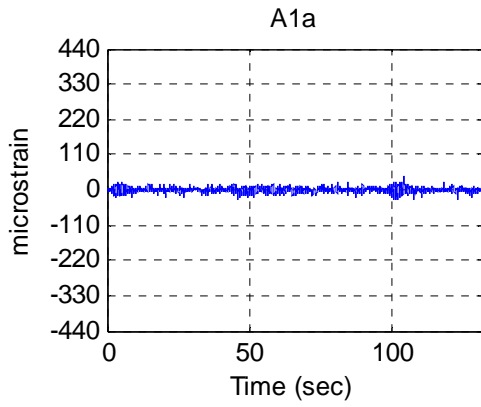


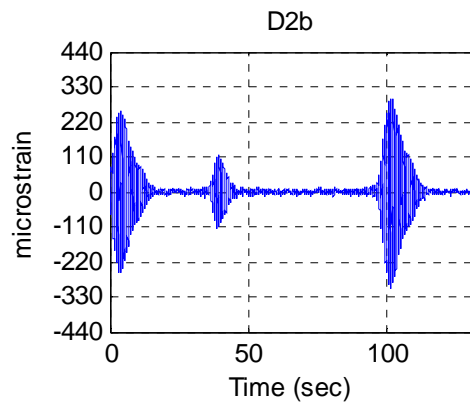
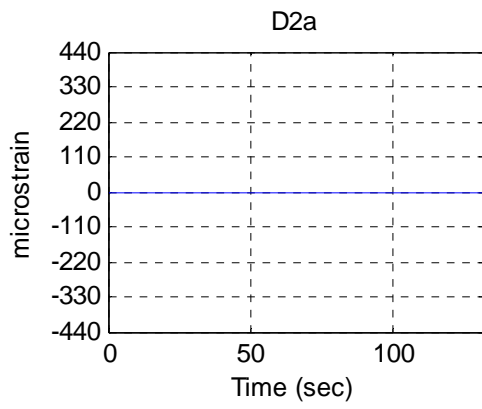
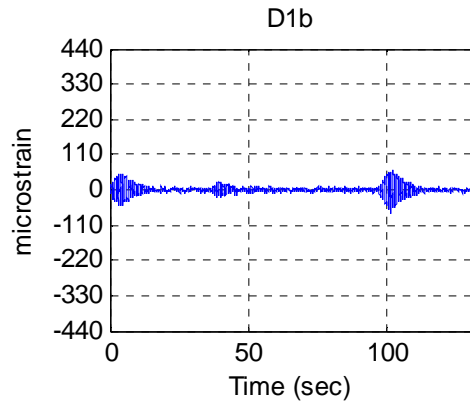
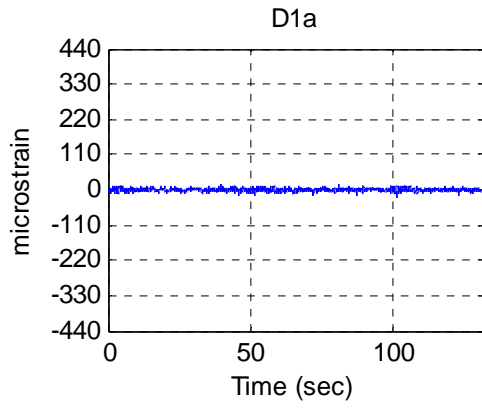


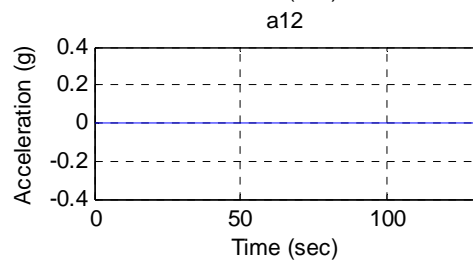
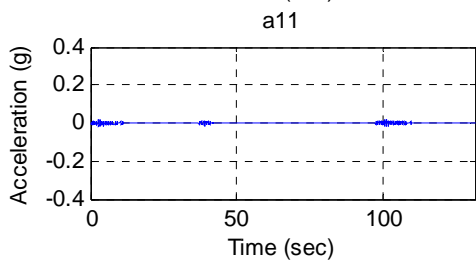
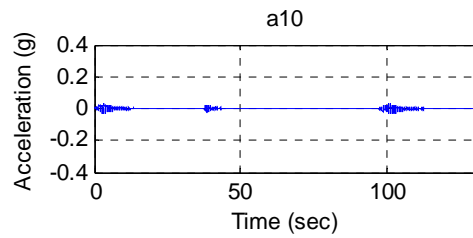
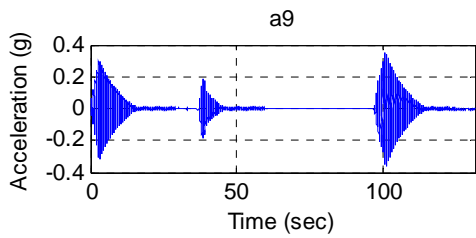
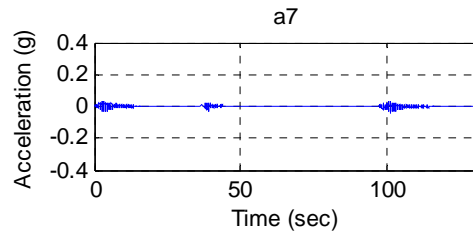
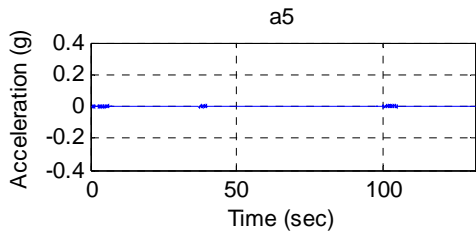
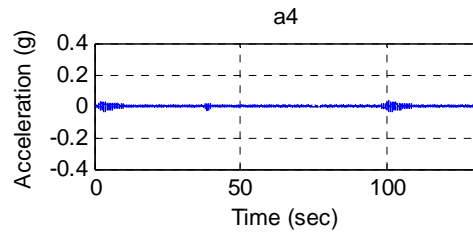
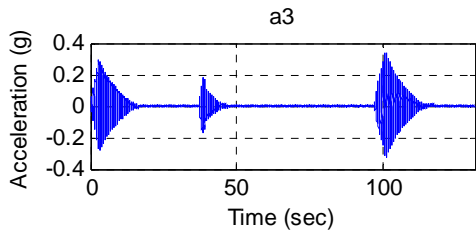
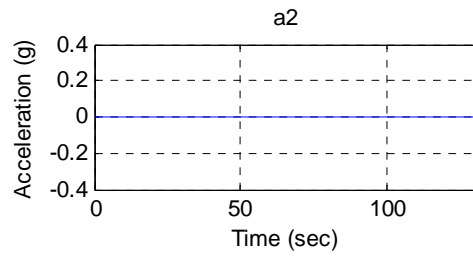
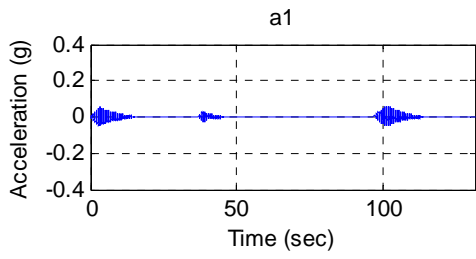


**Test M4**  
Data\I-A\I-A\_M4.txt







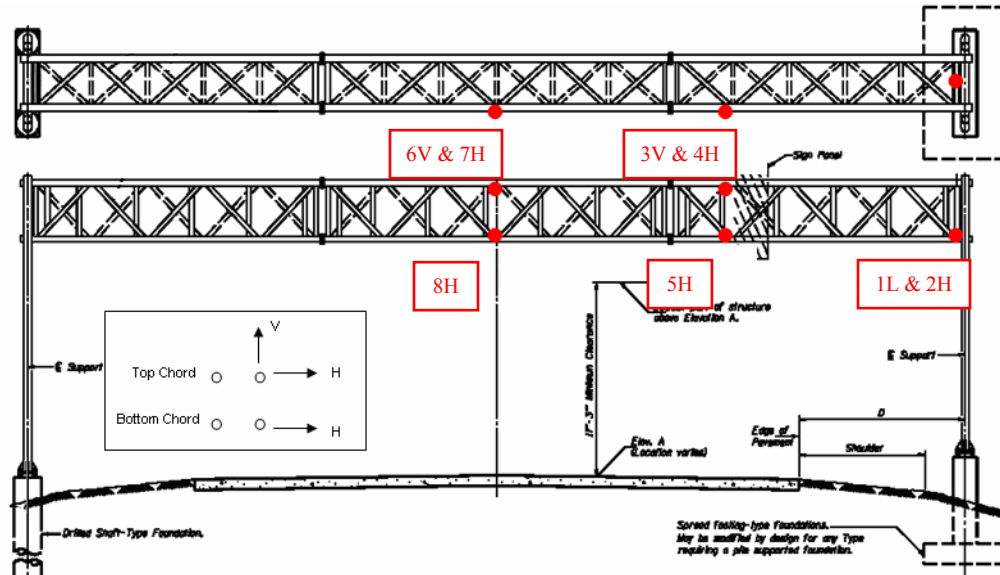


### A3.0 Type II-A Sign Structure Data

#### A3.1 Sensor names and locations

##### Accelerometers

The figure below shows the placement of the accelerometers on the Type II-A sign structure. The following table gives a detailed description of the sensor labels and locations.

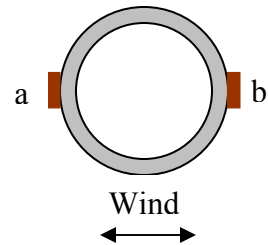
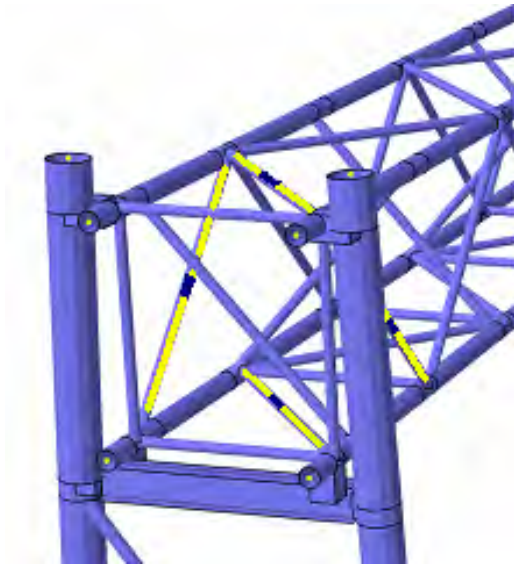


Accelerometer	Location	Measurement Direction
a1*	End – over support, bottom chord	Longitudinal
a2*	End – over support, bottom chord	Horizontal
a3*	Quarter-span, top chord	Vertical
a4	Quarter-span, top chord	Horizontal
a5*	Quarter-span, bottom chord	Horizontal
a6	Mid-span, top chord	Vertical
a7	Mid-span, top chord	Horizontal
a8	Mid-span, bottom chord	Horizontal

\*Bad accelerometers

##### Strain gages:

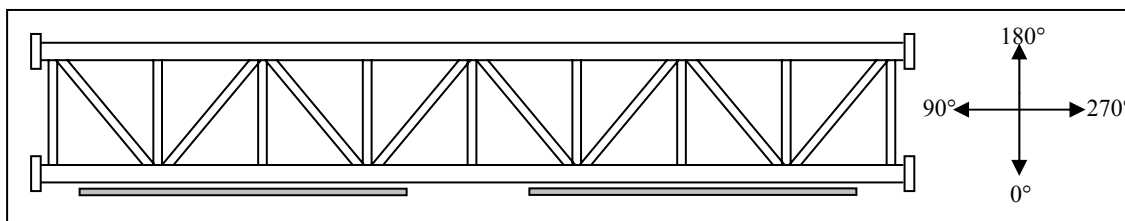
Twelve strain gages were installed on the II-A sign structure. Four gages were located on two chord members at the mid-span of the truss and eight on web members at one end of the truss. The locations of the strain gages at the end of the truss are indicated in the figure below. The table below details the locations and labeling of each gage.



Strain Gage	Location
C1a C1b	Bottom Chord – front plane
C2a C2b	Bottom Chord – back plane
H1a H1b	Horizontal Diagonal – top plane
HDa HDb	Horizontal Diagonal – bottom plane
V1a V1b	Vertical Diagonal – front plane
V2a V2b	Vertical Diagonal – back plane

*Anemometer*

The wind velocity and direction measured by the anemometer relative to the sign is shown in the figure below. Note that when the wind is blowing perpendicular to the face of the sign, the instrument will read a direction of 180 degrees.



### A3.2 Data Description

The data contained in the appendix files and plotted below is the filtered data acquired for the Type II-A sign structure. A link to a text file of each test is included with the plots of the data. To import the data into Excel follow the steps given below:

1. Click on the link to open a text file of the data
2. Click Edit → Select All
3. Click Edit → Copy
4. Open Excel
5. Once in Excel, click Edit → Paste

Test descriptions:

- W1 was recorded on a single day, March 31, 2005. The wind velocity ranged between 8 and 30 mph during data collection and primarily acted perpendicular to the face of the signs.
- TG1–TG13 are tests that were taken on April 11, 2005 during calm wind conditions to measure the response of the truss to truck gust excitation. Each record represents a single measured truck gust.
- M1-M4 were taken on August 26, 2005 prior to the deinstrumentation of the sign structure when the structure was subjected to both horizontal and vertical manual excitation.

### A3.3 Wind Data

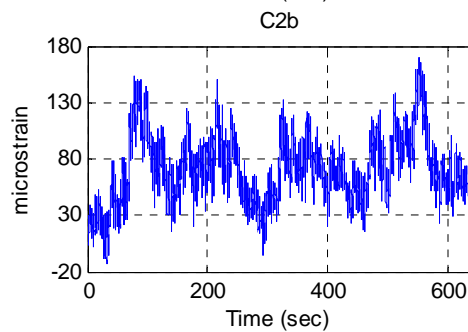
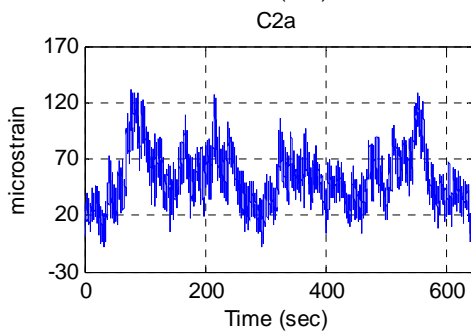
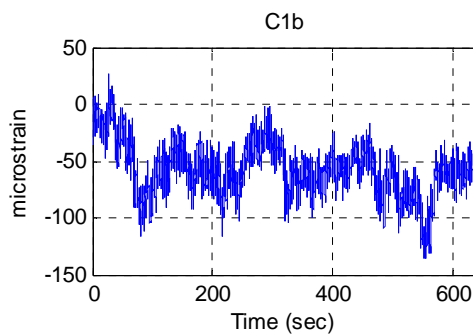
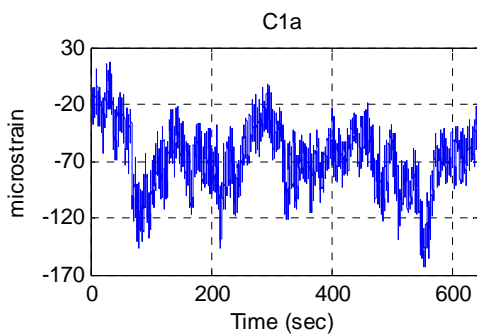
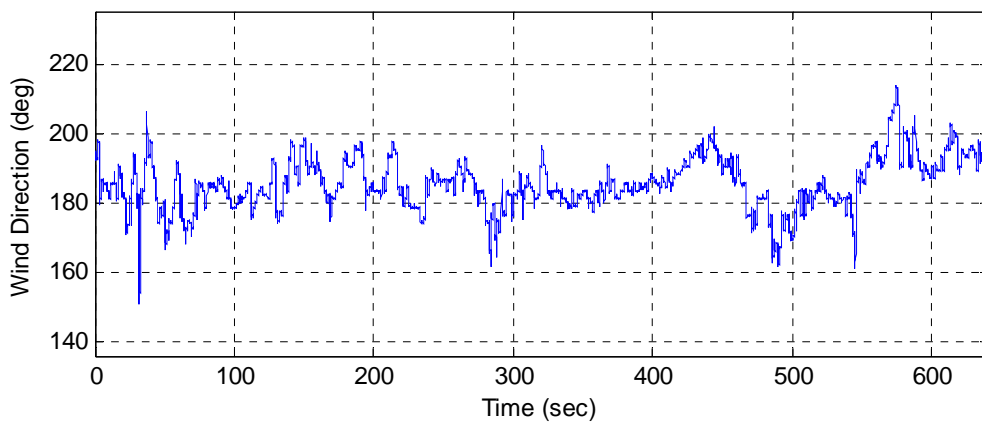
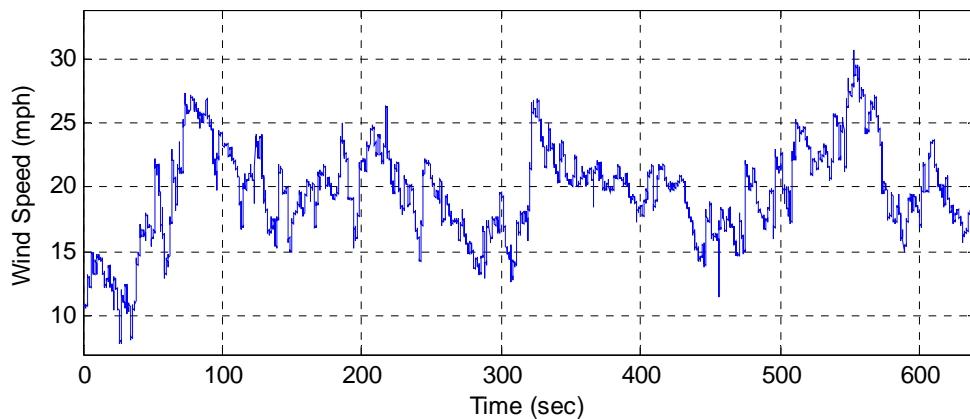
The data structure for the wind data is as follows:

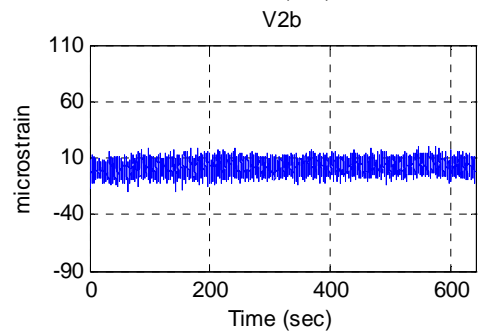
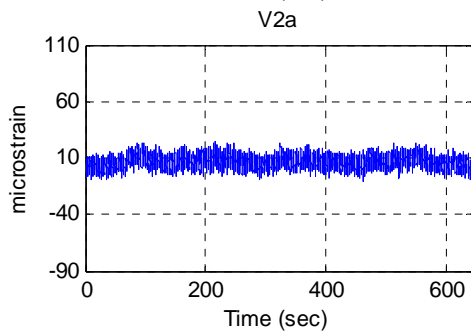
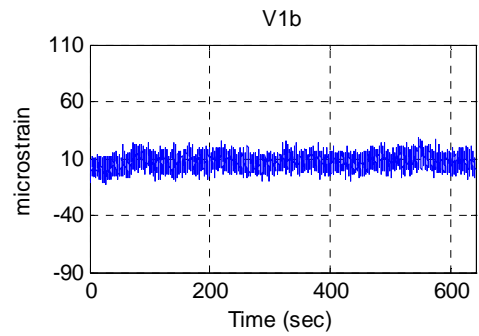
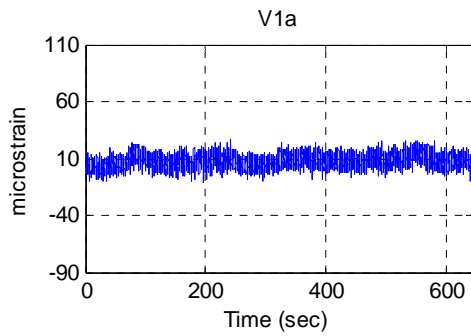
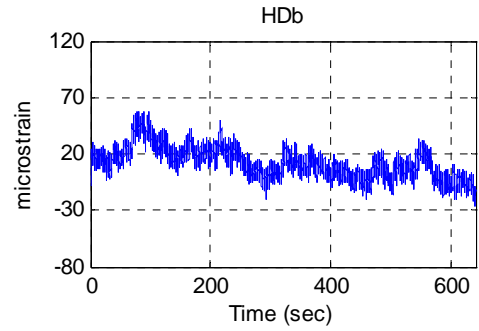
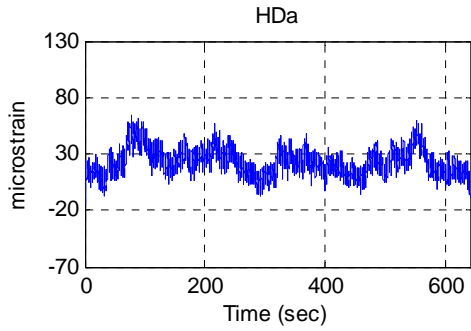
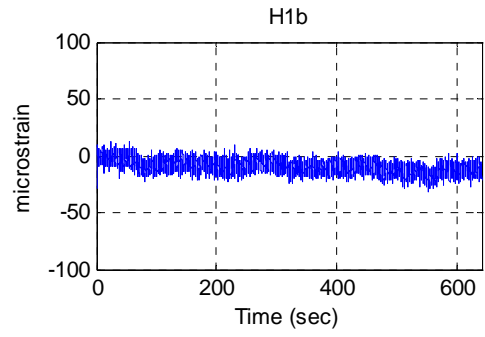
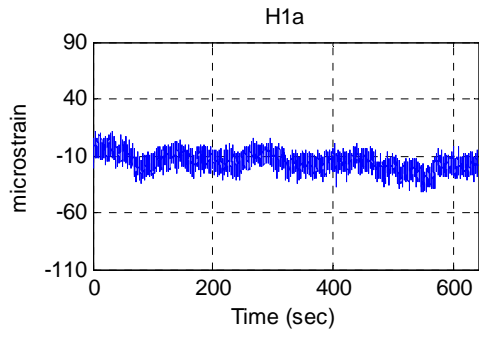
Time(sec), C1a, C1b, C2a, C2b, H1a, H1b, HDa, HDb, V1a, V1b, V2a, V2b, a4, a6, a7, a8, WS(mph), WD(deg)

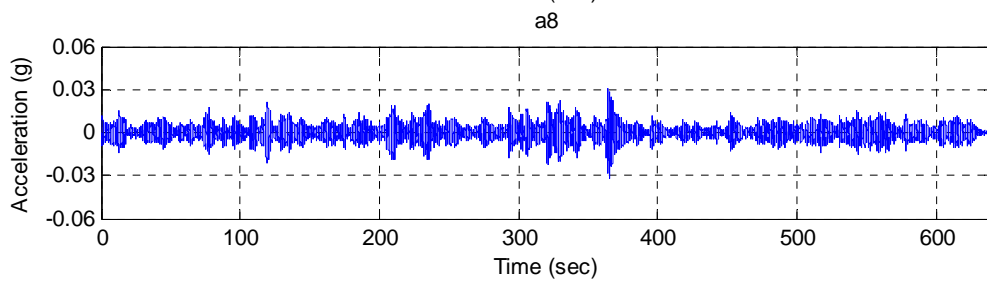
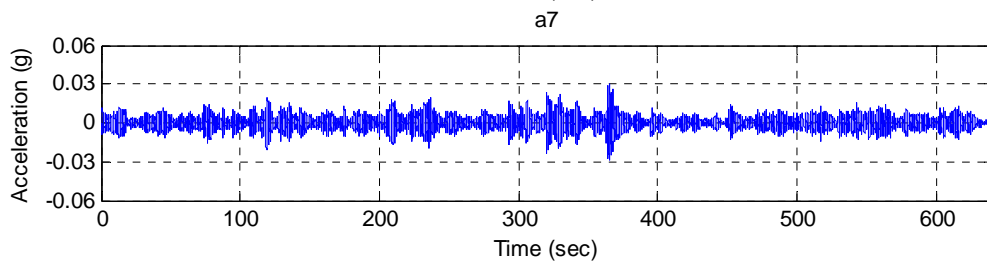
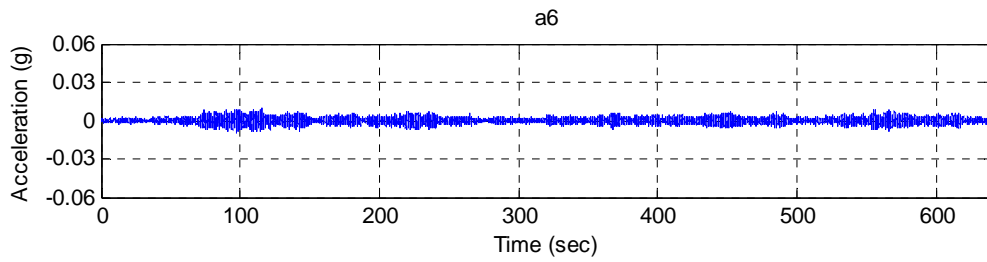
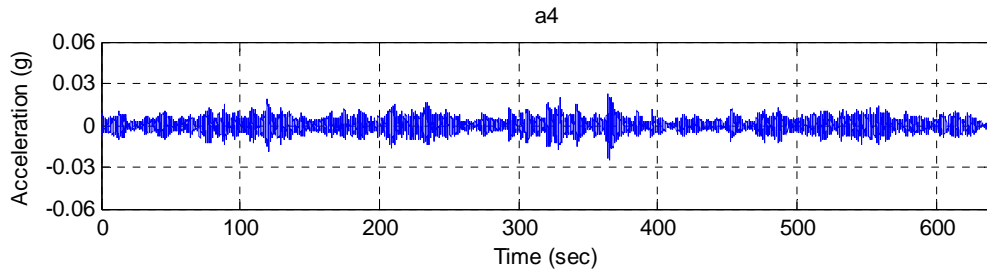
To determine the wind velocity acting perpendicular to the sign face the following calculation must be made:

$$WS_{\text{perpendicular}} = WS * \cos(WD)$$

**Test W1**  
Data\II-A\II-A W1.txt







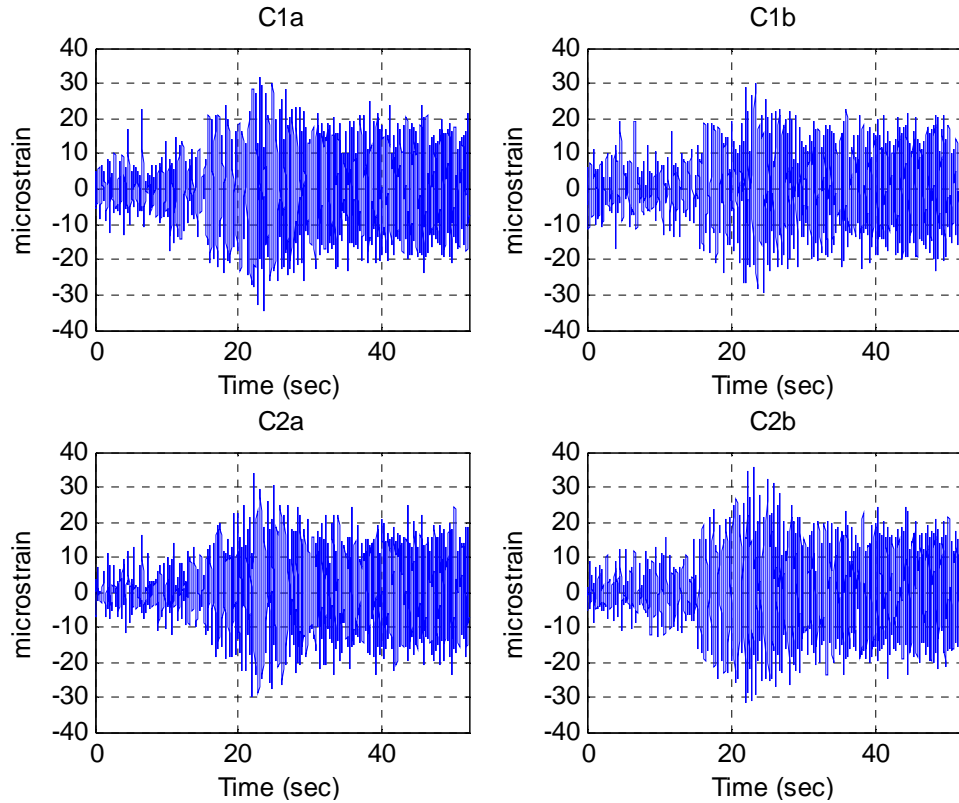
### A3.4 Truck Gust Data

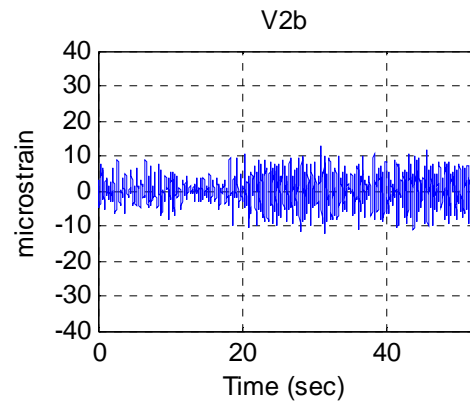
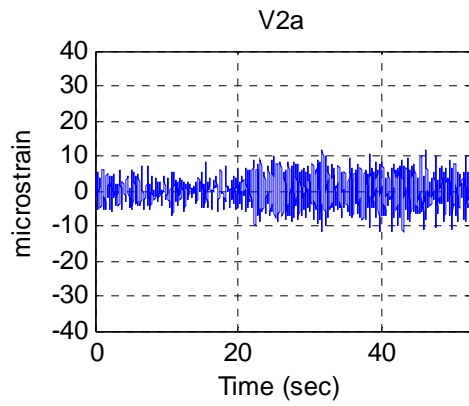
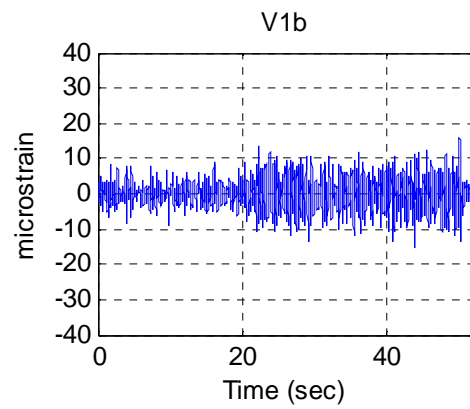
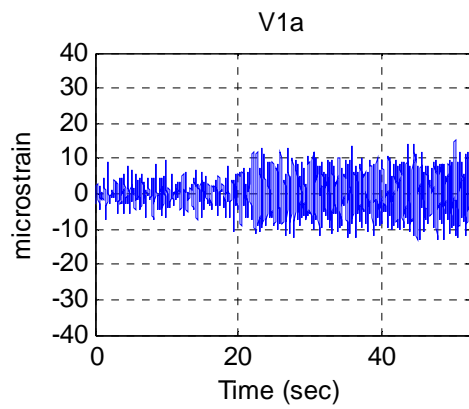
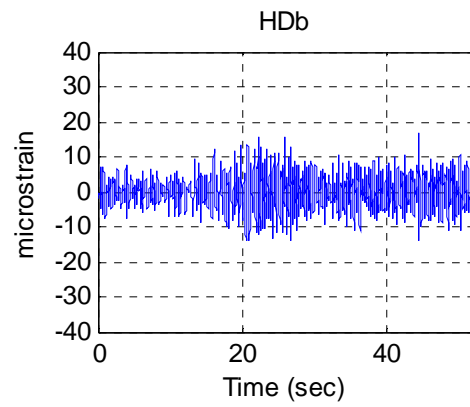
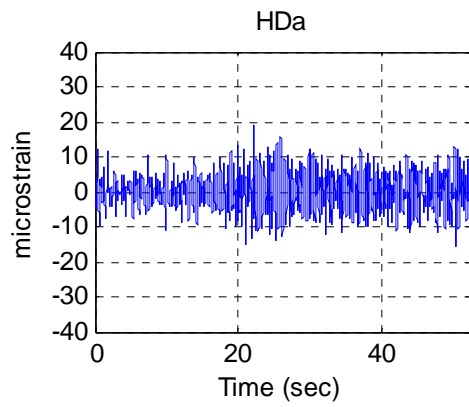
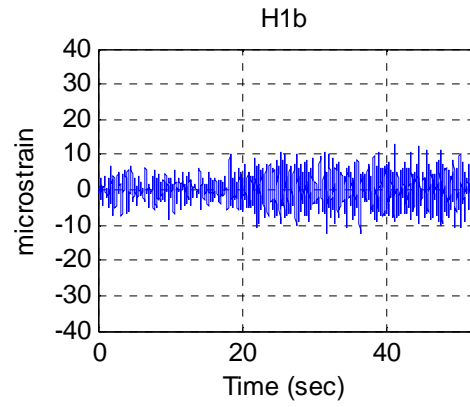
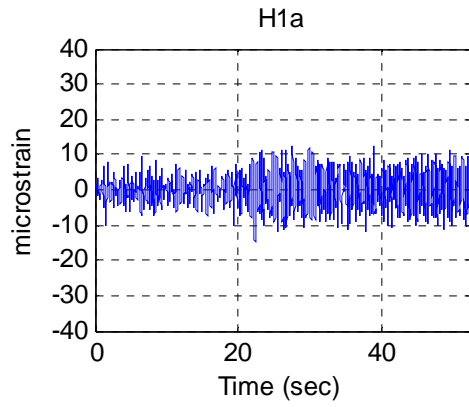
The data structure for the truck gust data is as follows:

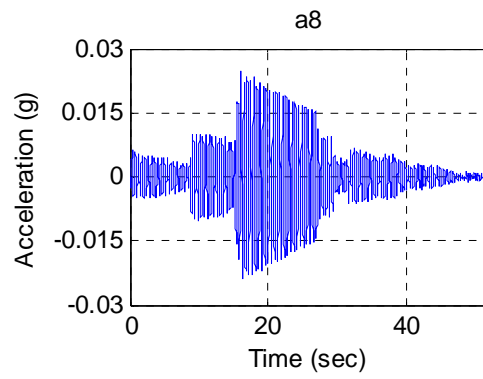
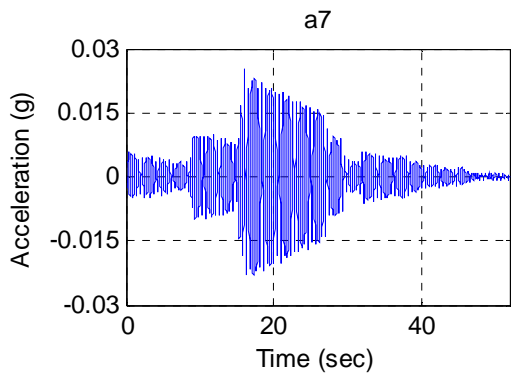
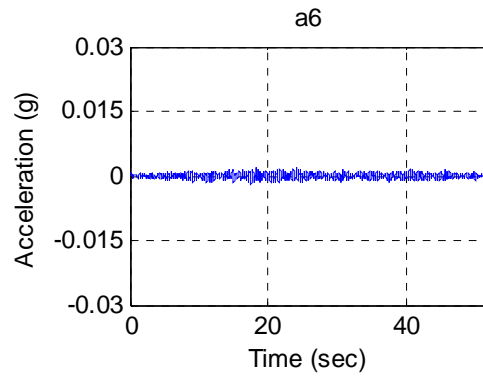
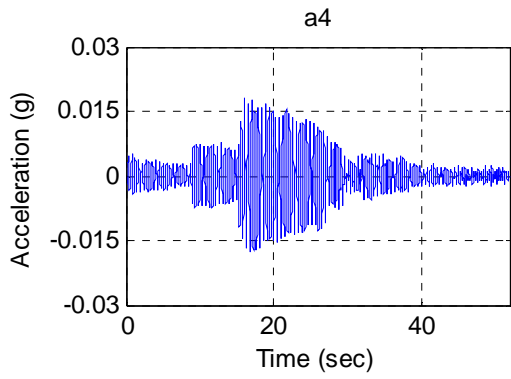
Time(sec), C1a, C1b, C2a, C2b, H1a, H1b, HDa, HDb, V1a, V1b, V2a, V2b, a4, a6, a7, a8.

#### Test TG1

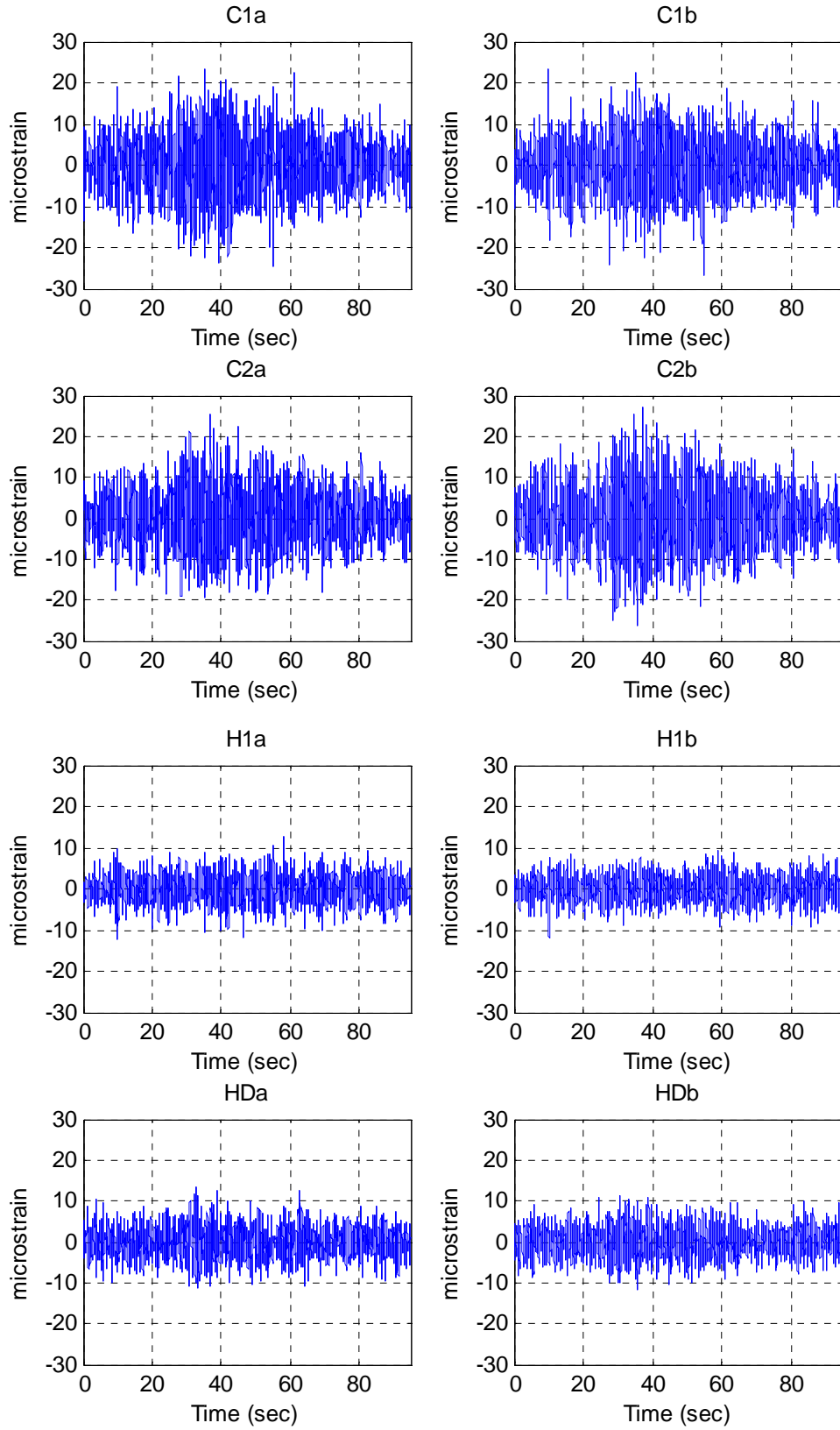
[Data\II-A\II-A\\_TG1.txt](#)

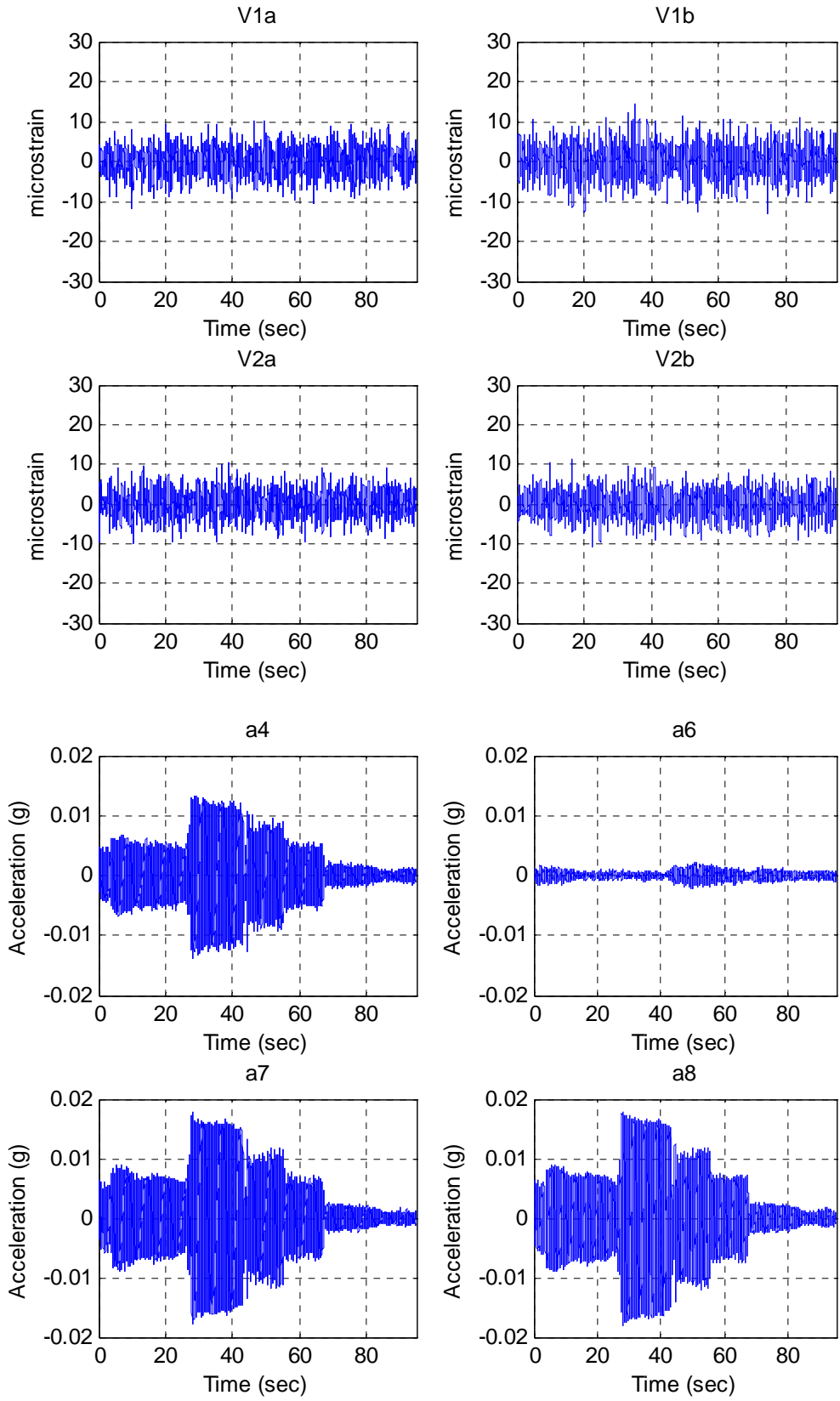




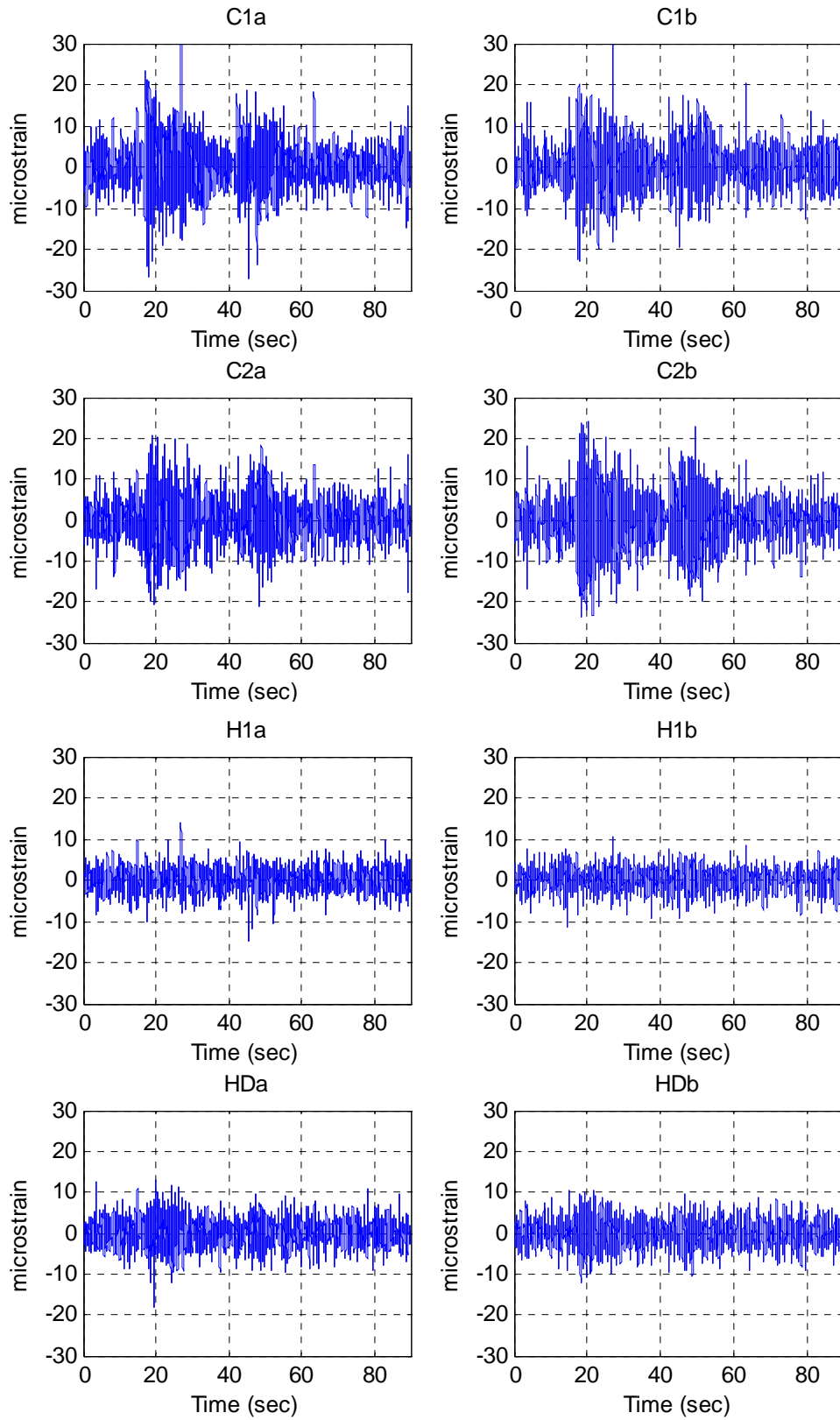


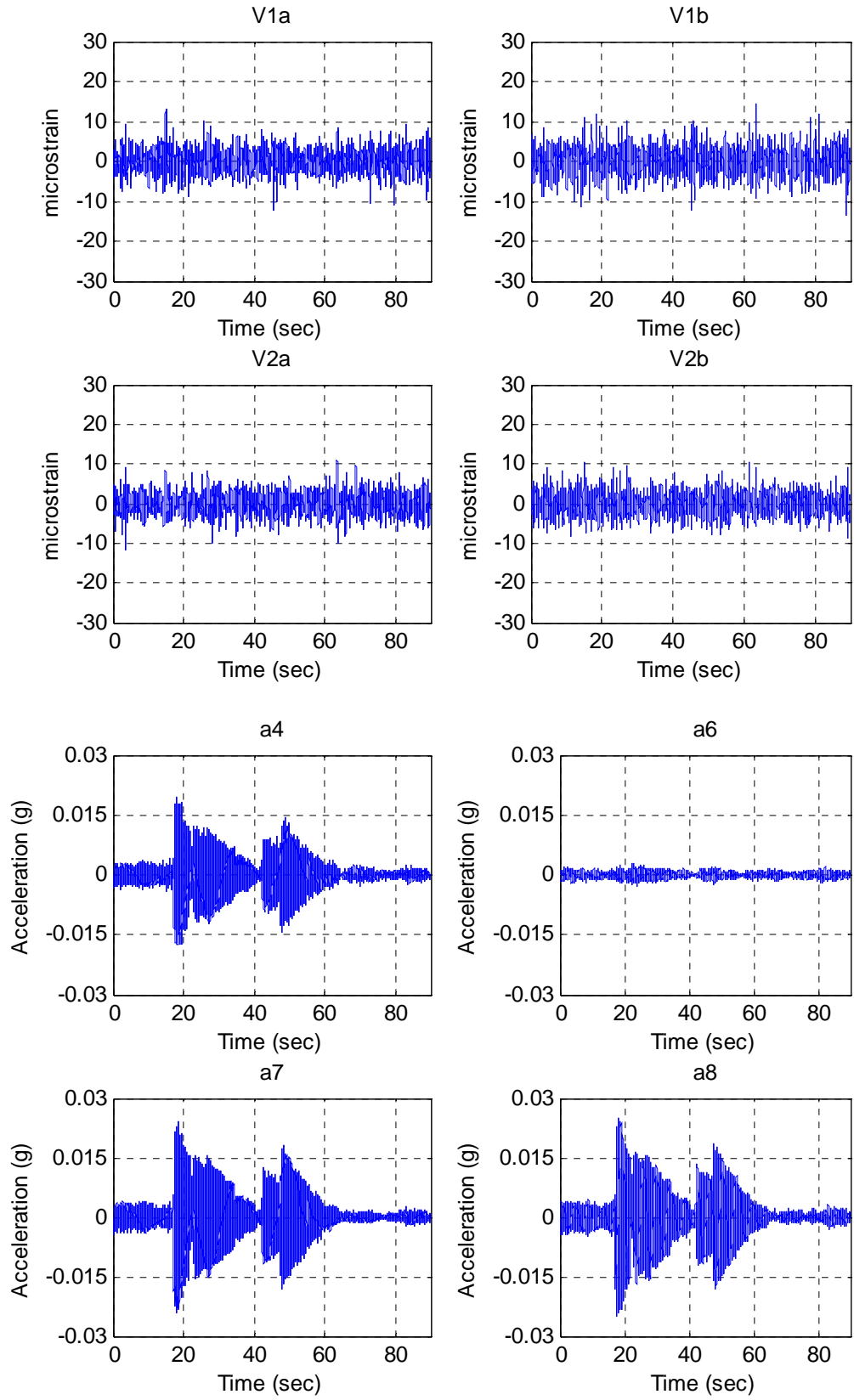
**Test TG2**  
Data\II-A\II-A\_TG2.txt



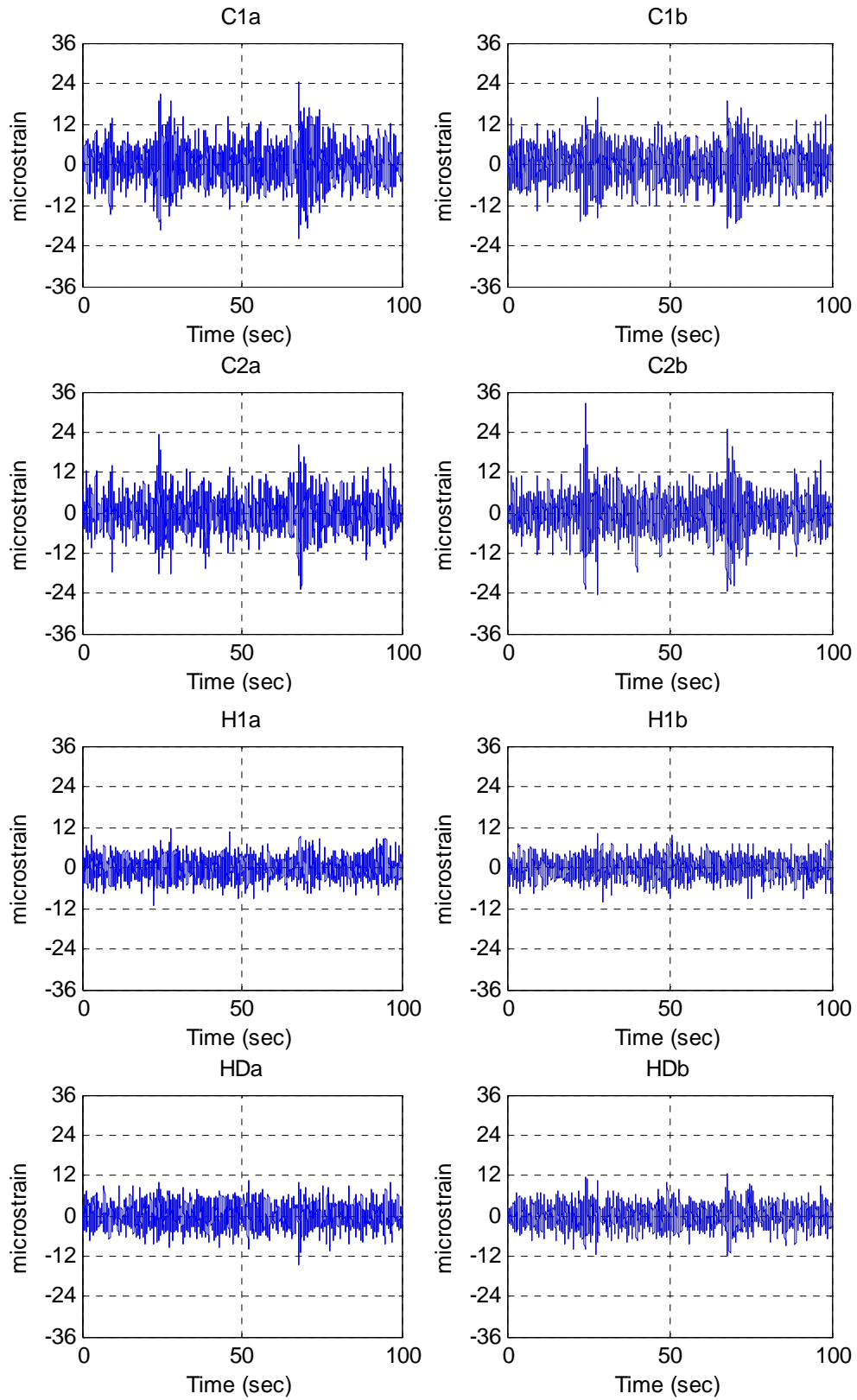


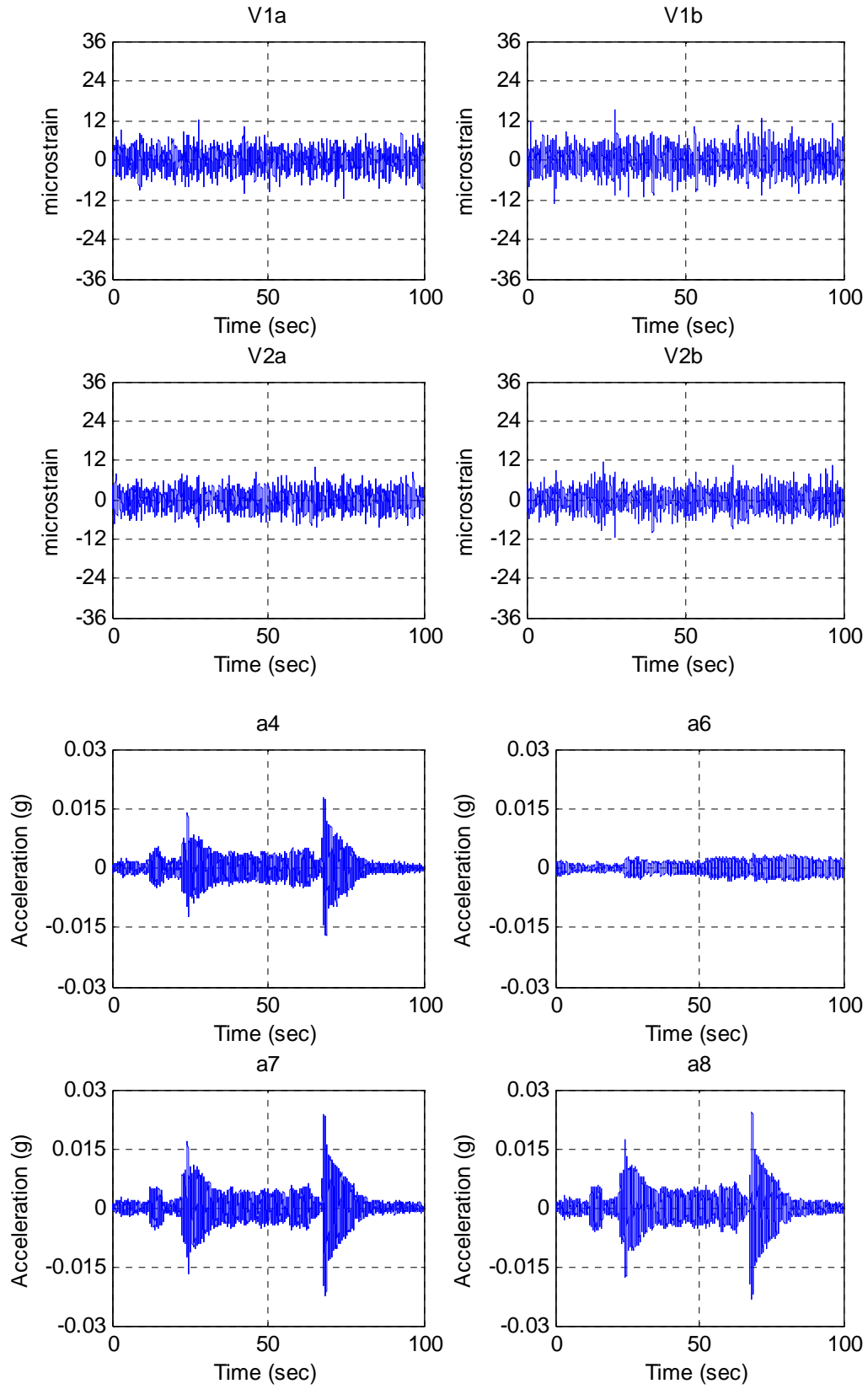
**Test TG3**  
Data\II-A\II-A\_TG3.txt



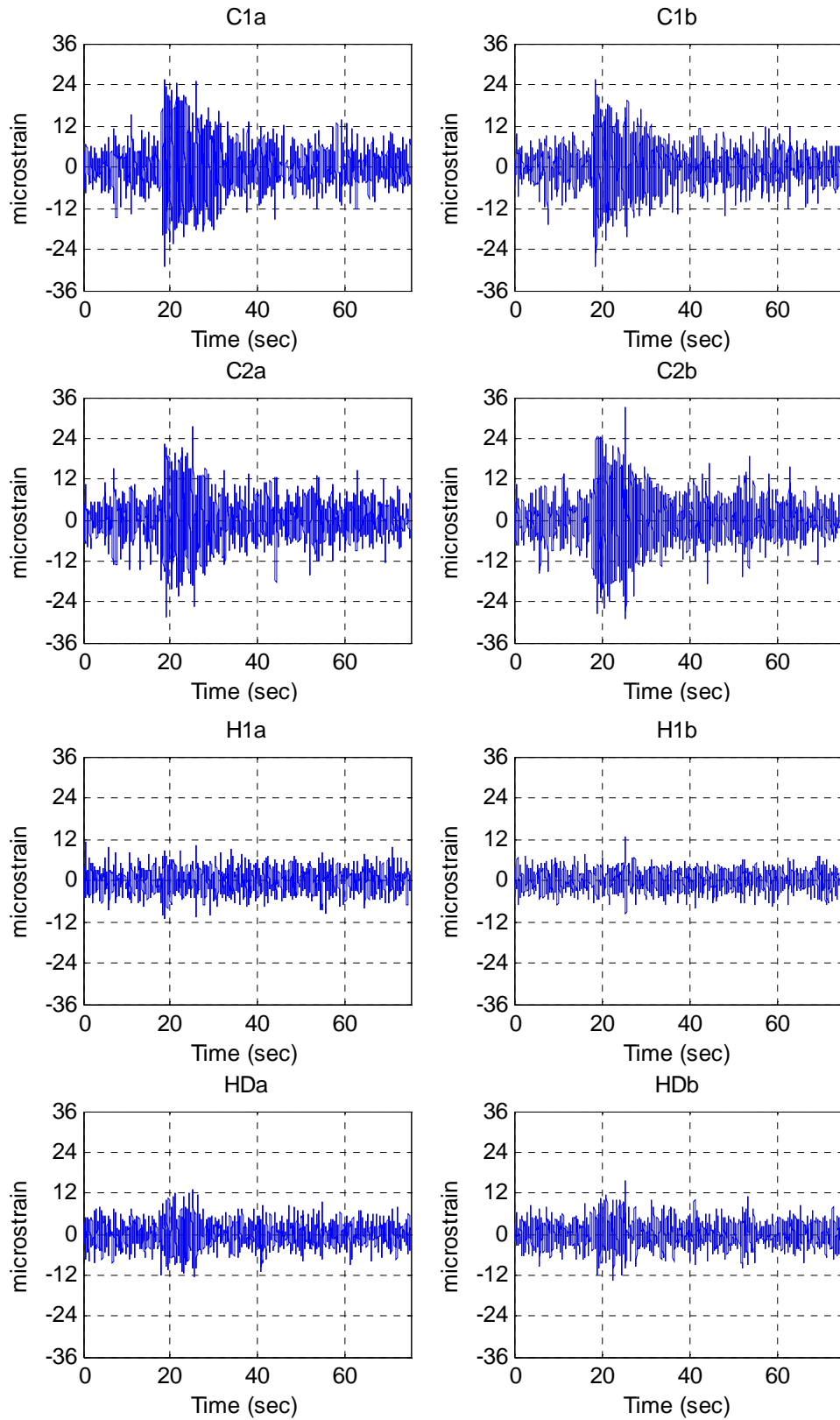


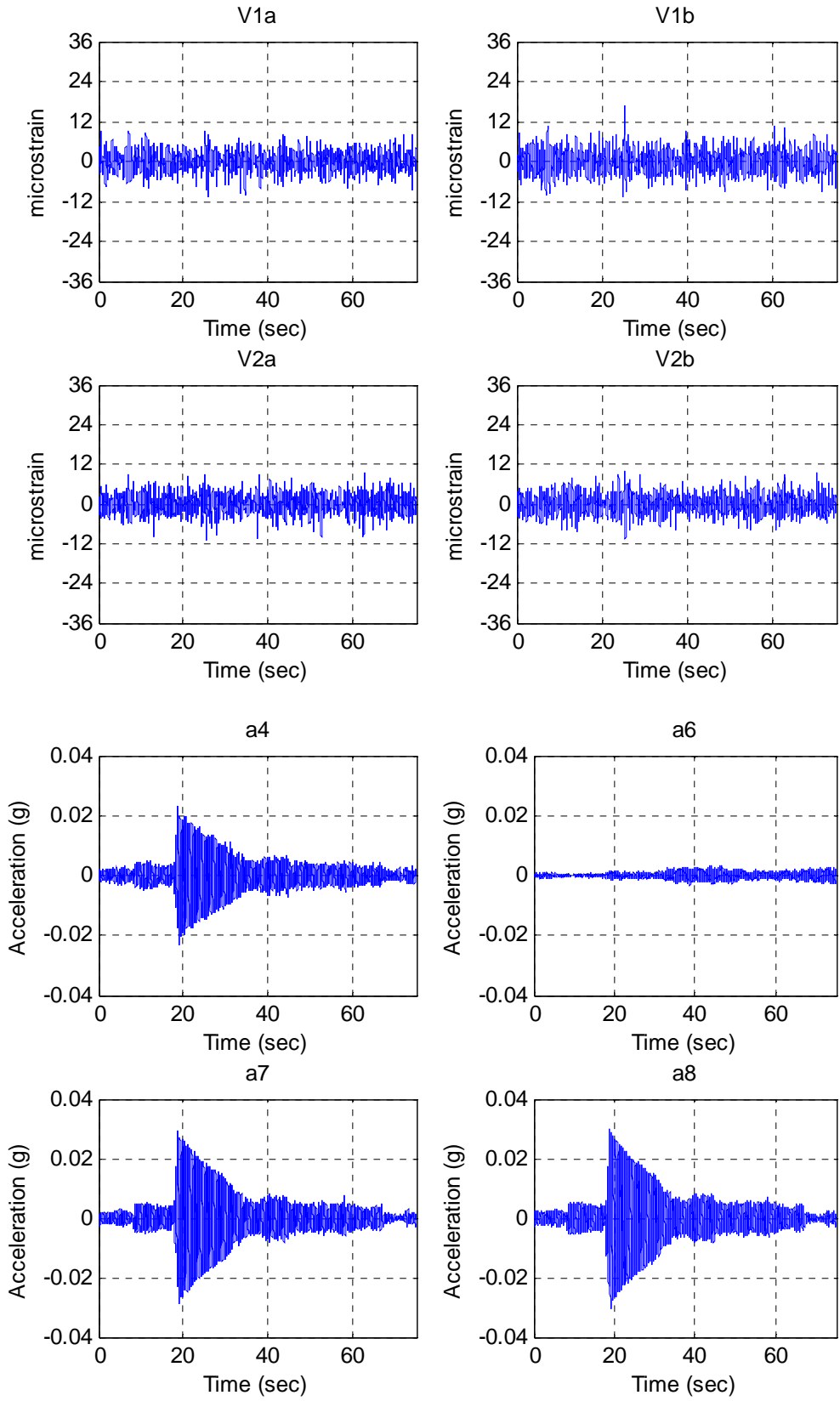
**Test TG4**  
Data\II-A\II-A\_TG4.txt



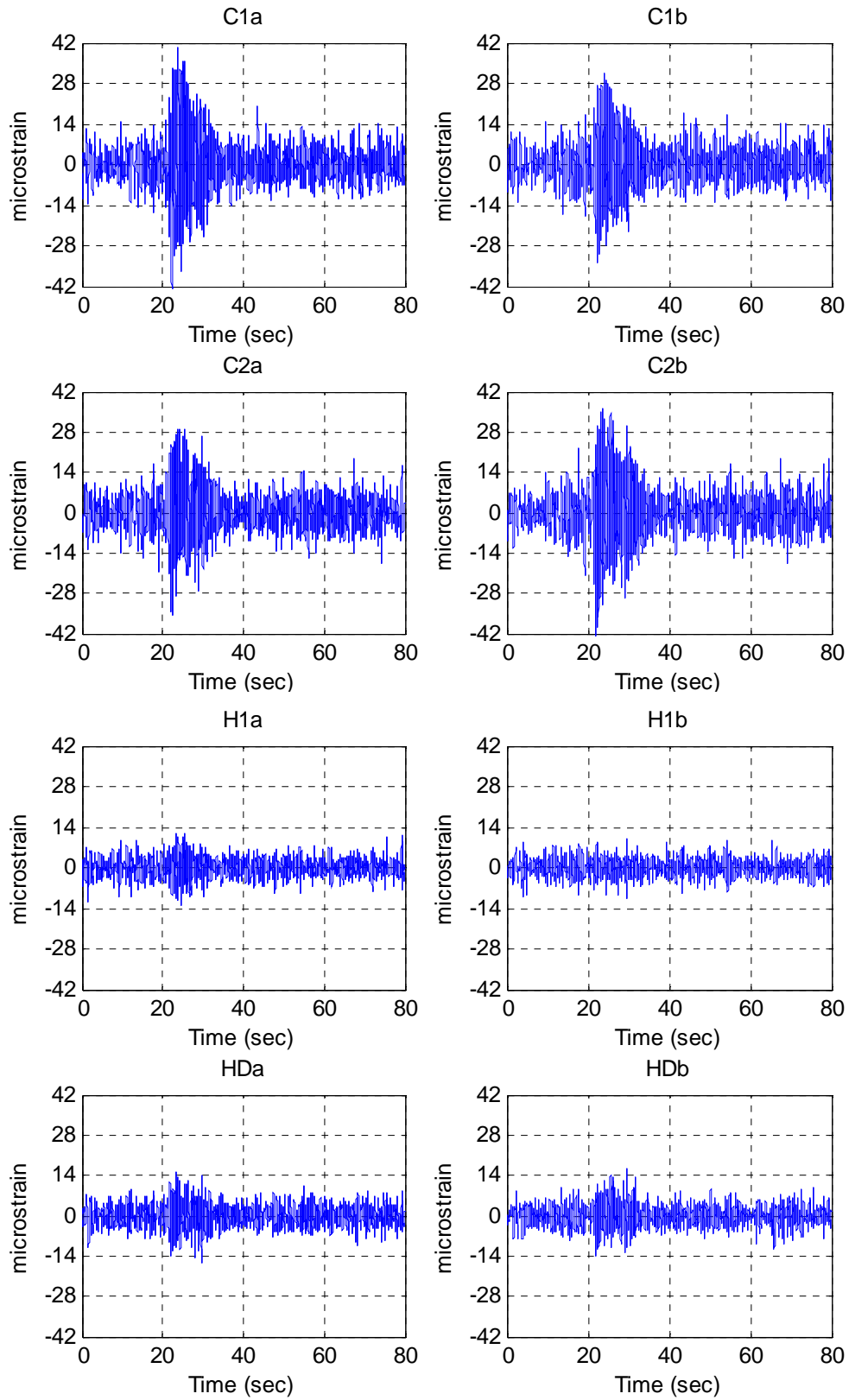


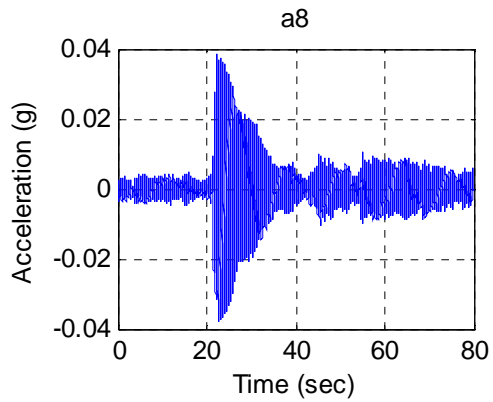
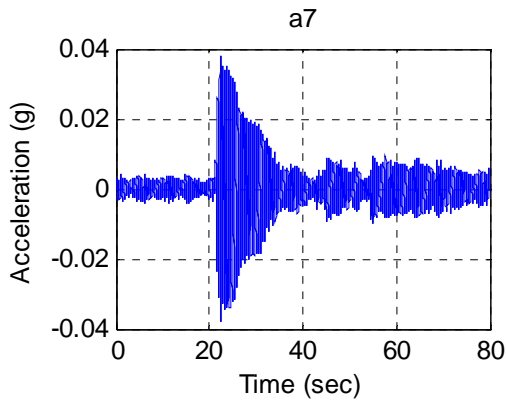
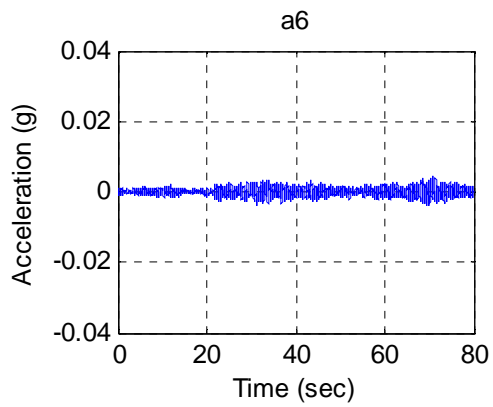
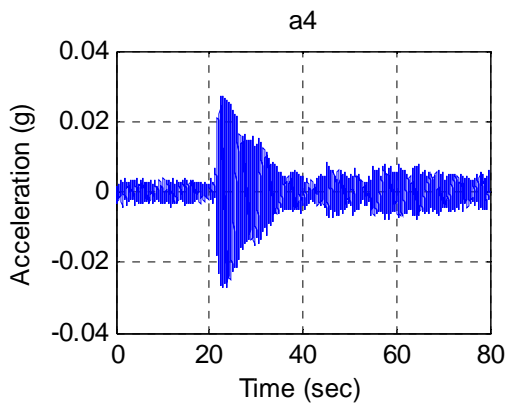
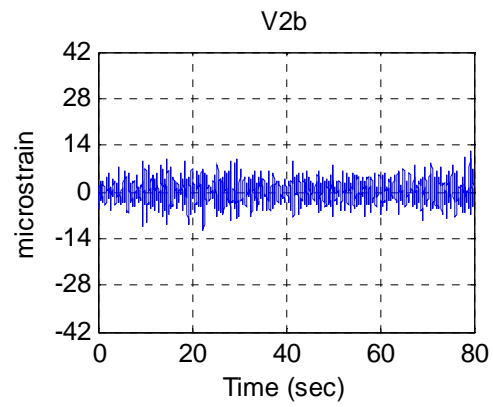
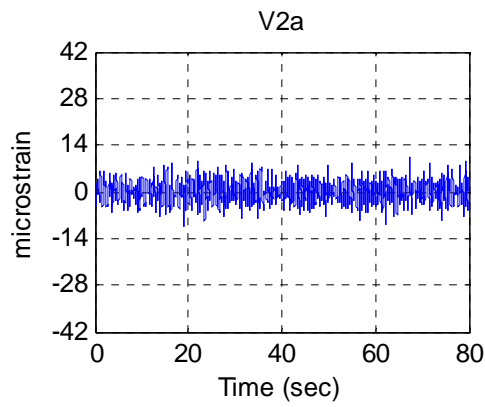
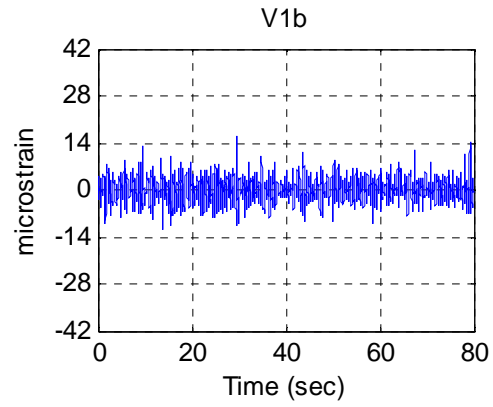
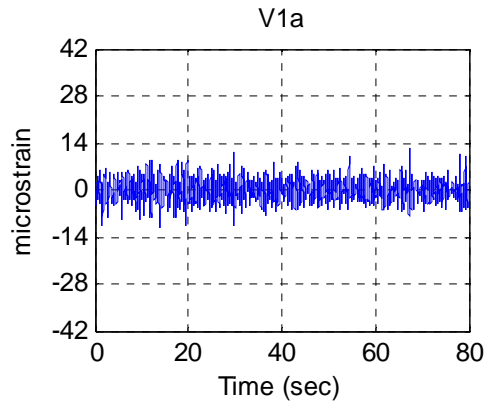
**Test TG5**  
Data\II-A\II-A\_TG5.txt



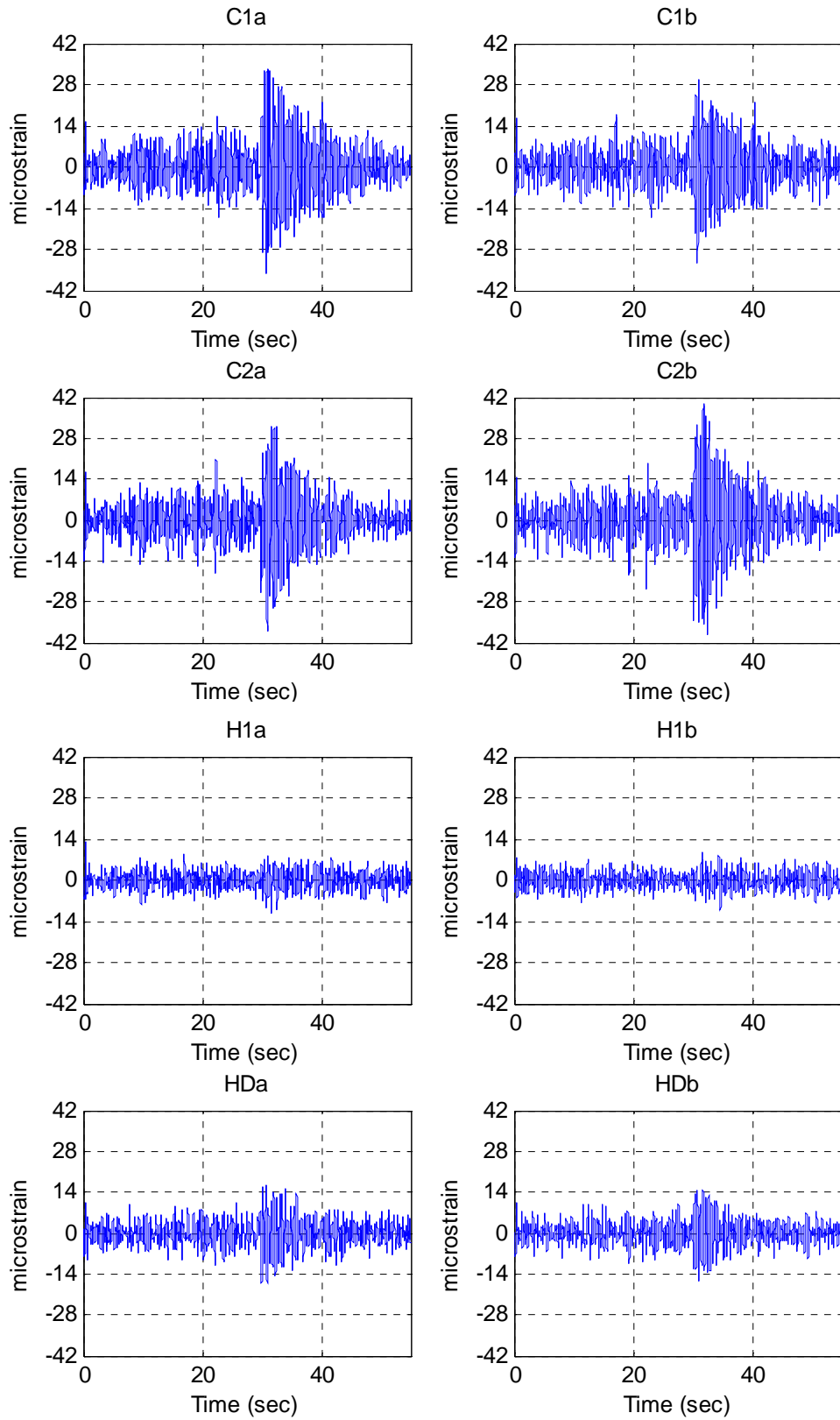


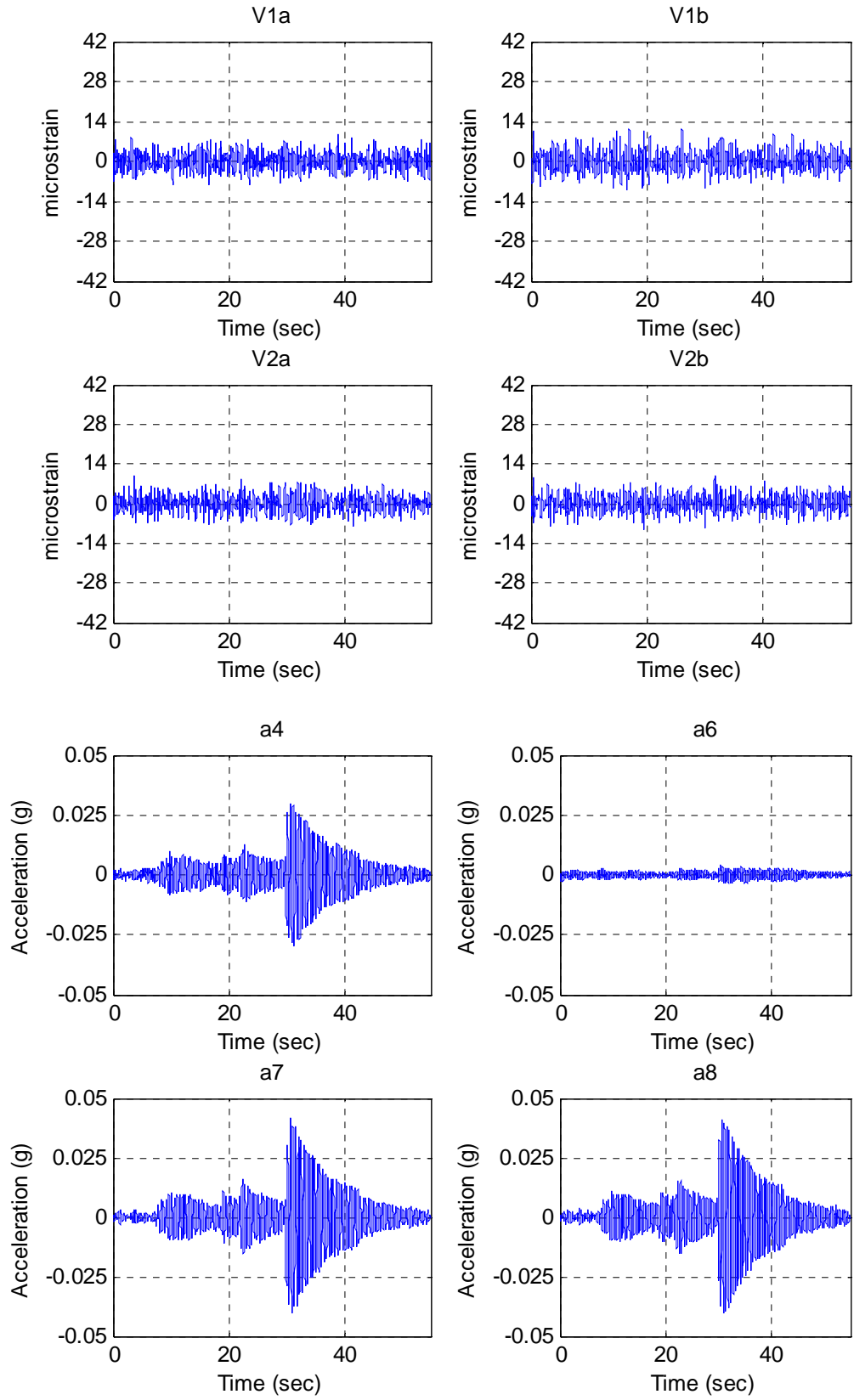
**Test TG6**  
Data\II-A\II-A\_TG6.txt



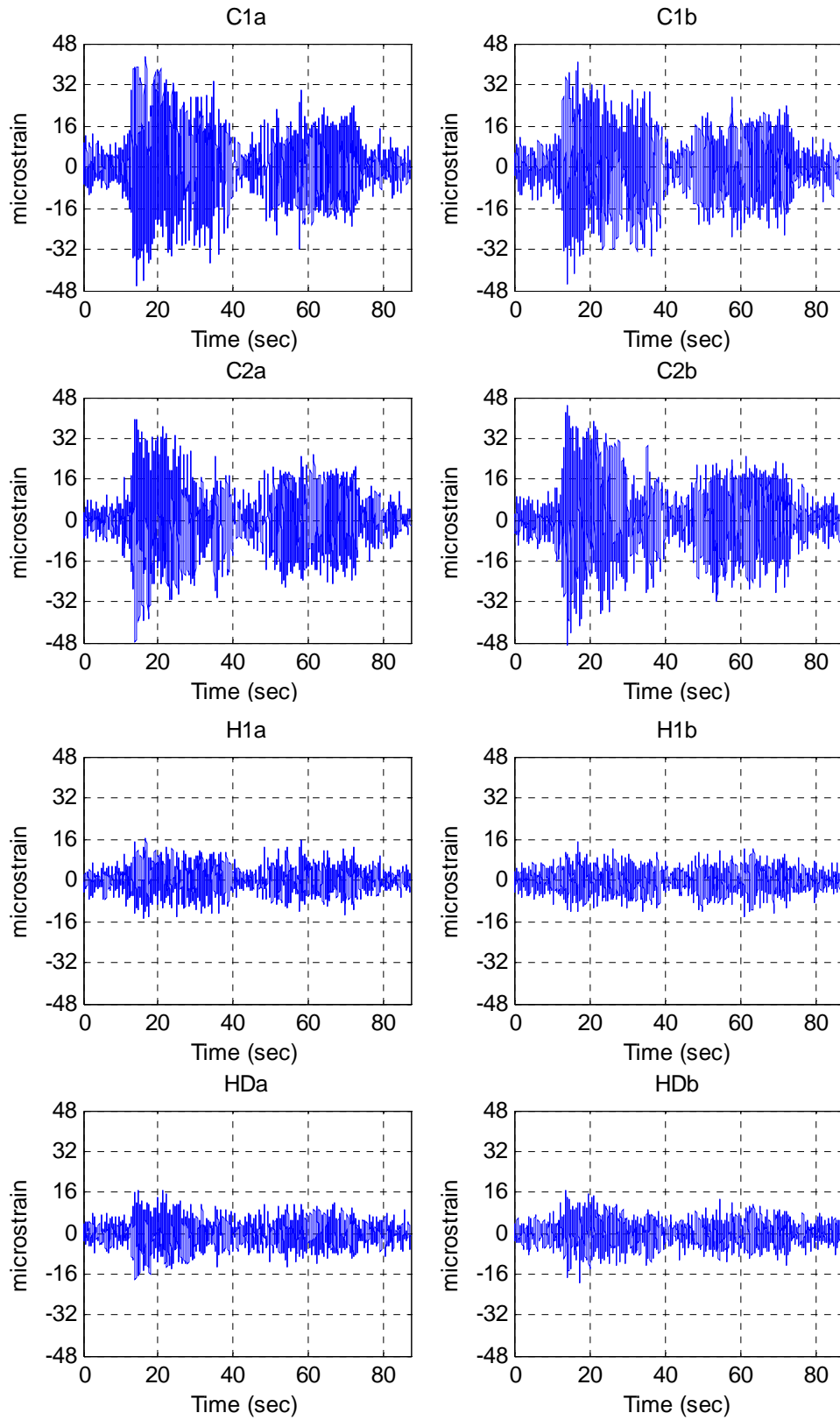


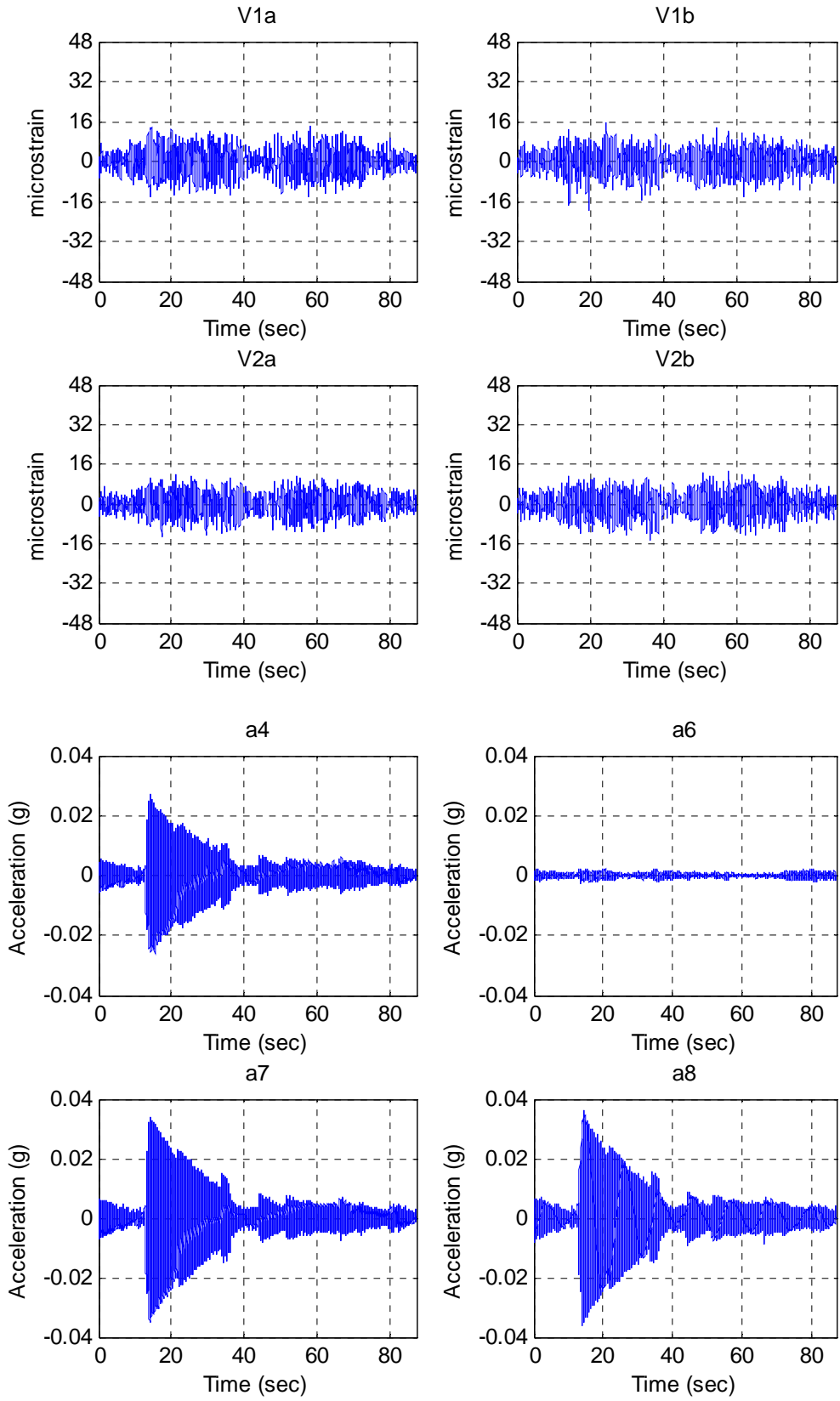
**Test TG7**  
**Data\II-A\II-A\_TG7.txt**



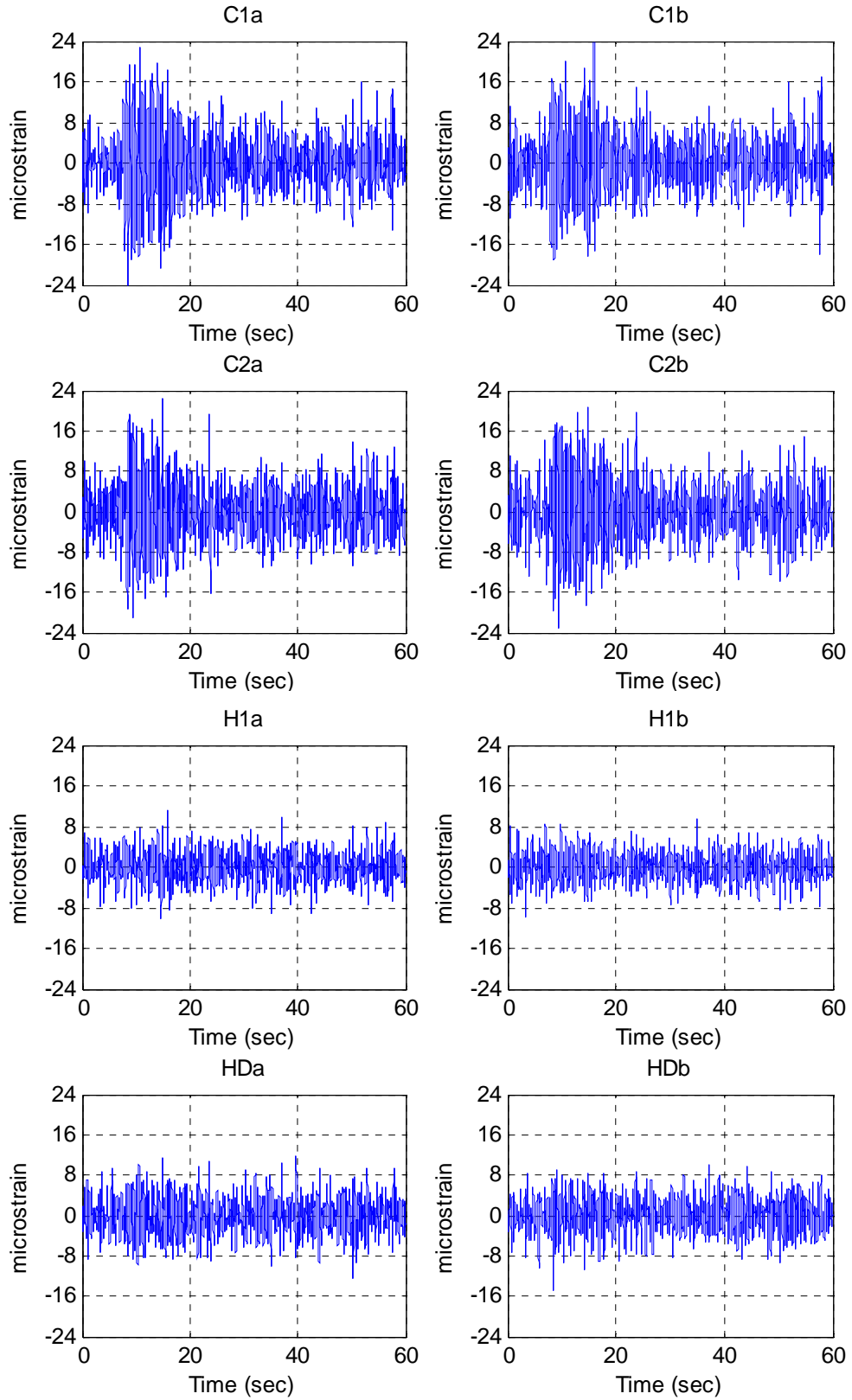


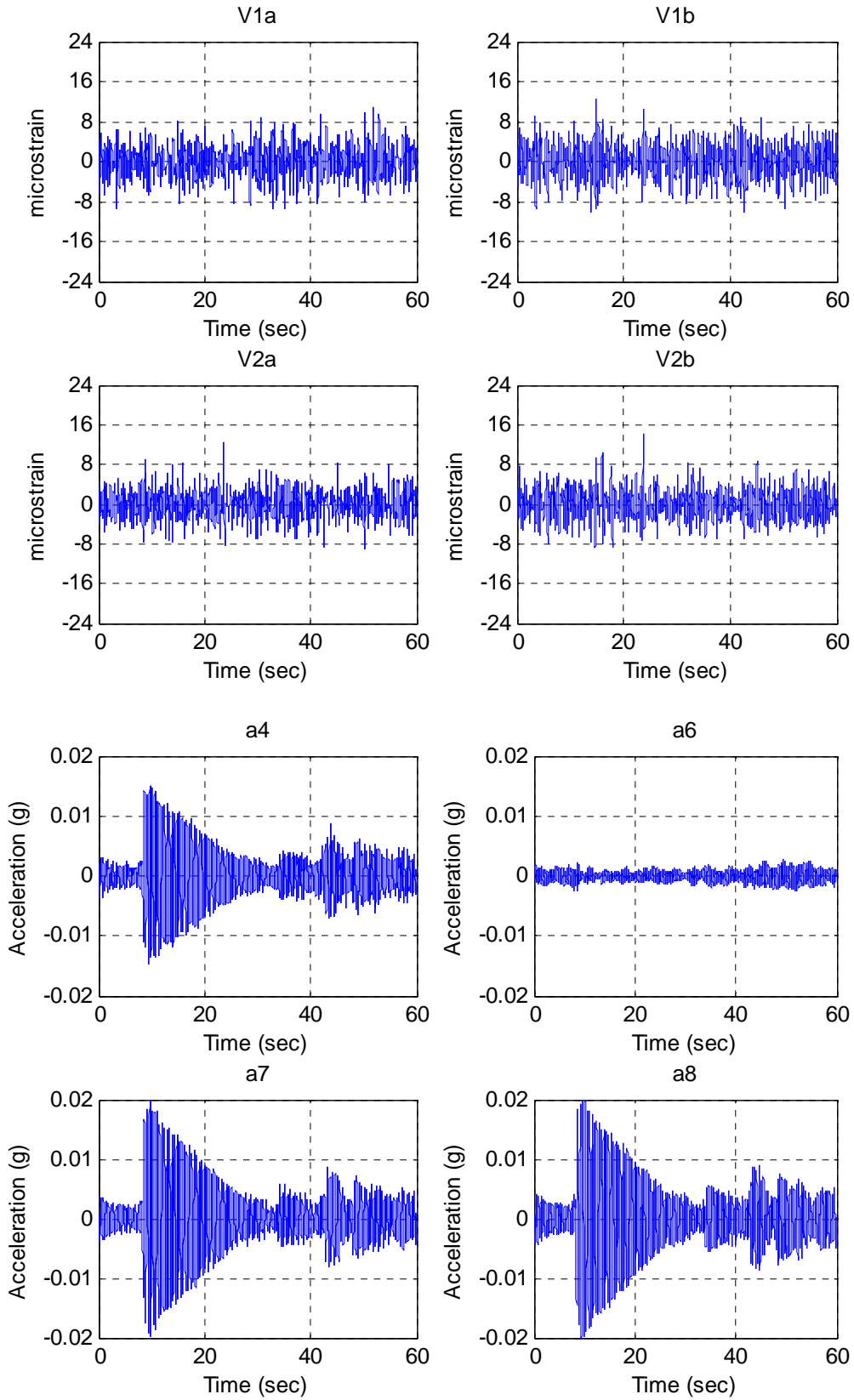
**Test TG8**  
Data\II-A\II-A\_TG8.txt



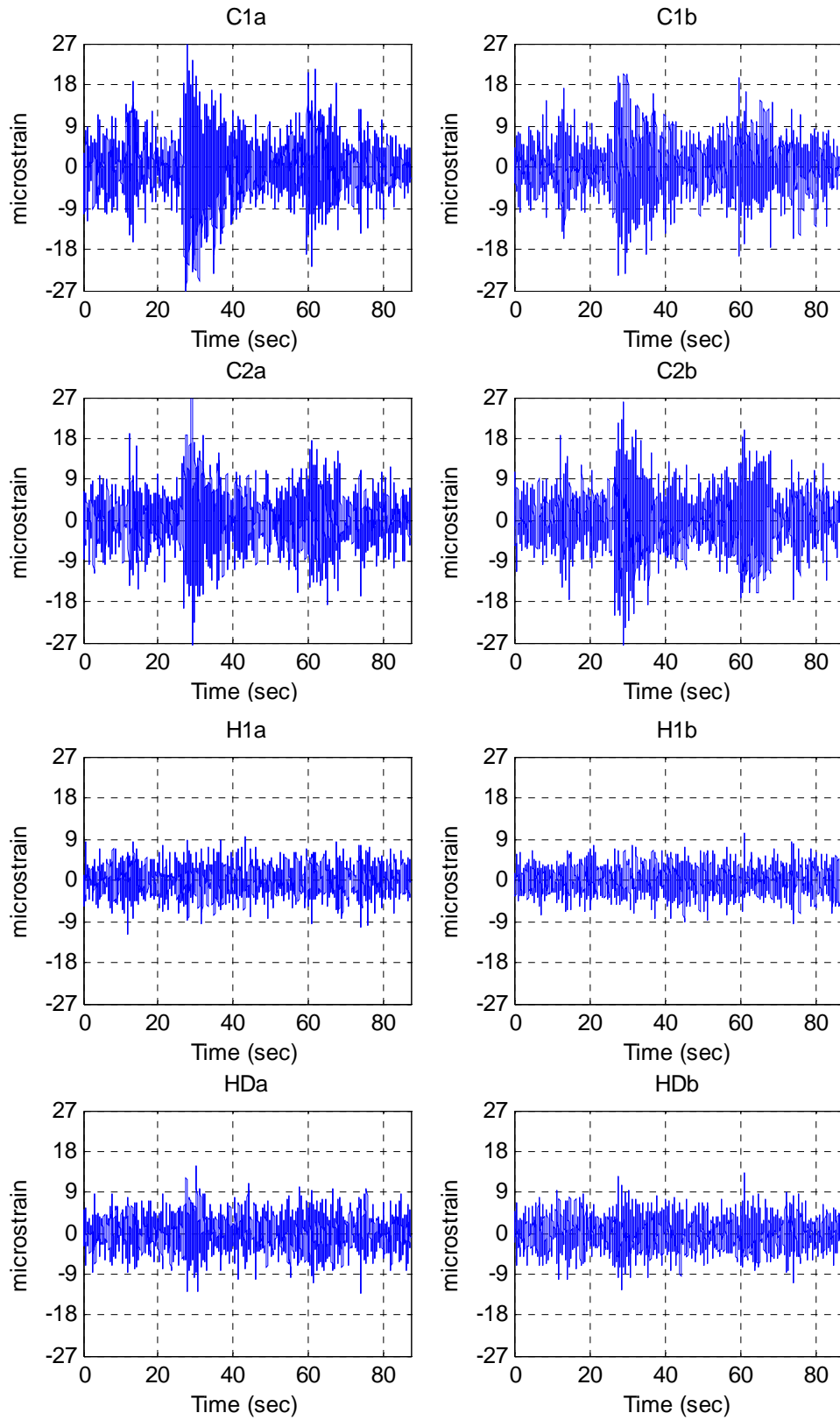


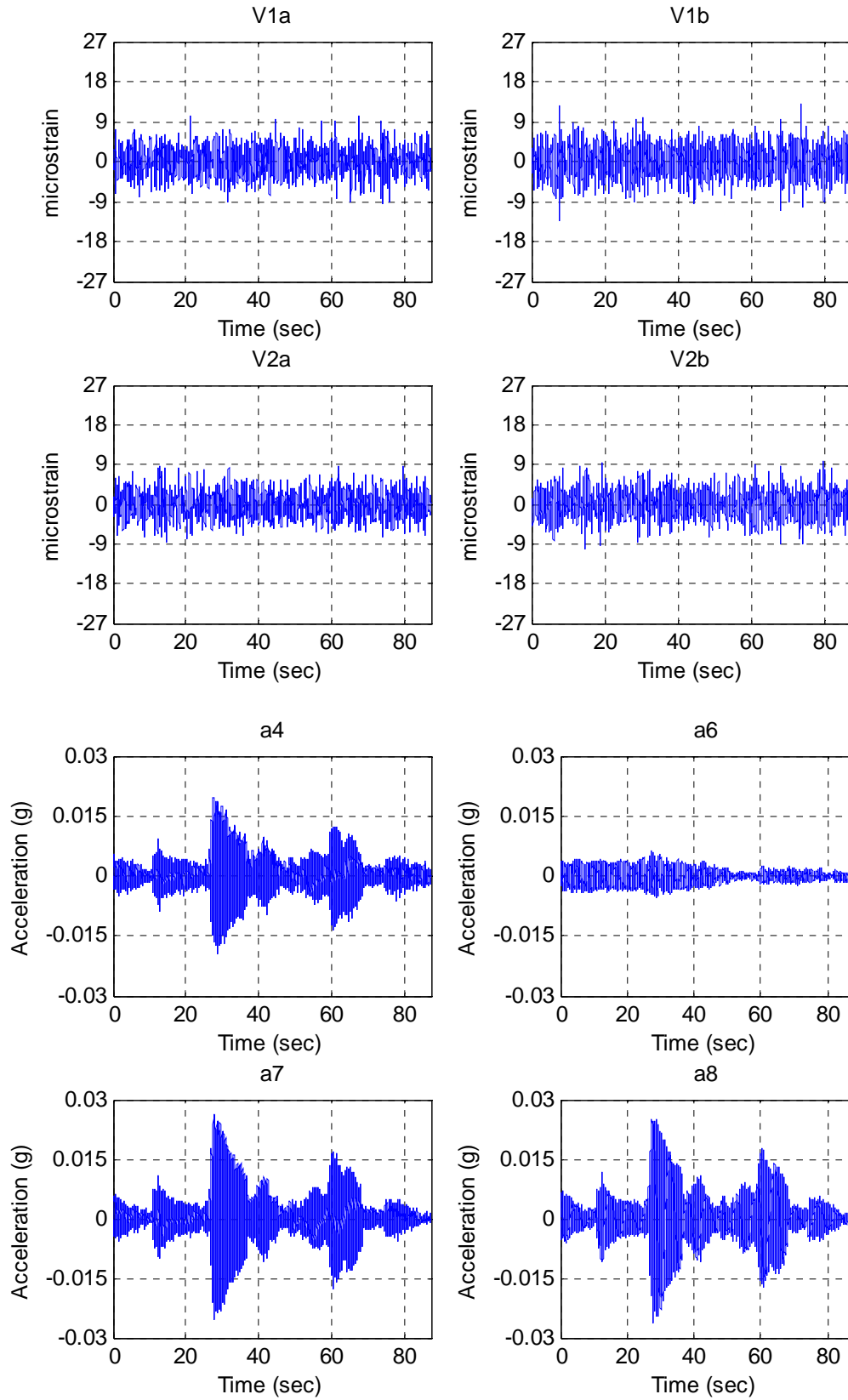
**Test TG9**  
Data\II-A\II-A\_TG9.txt



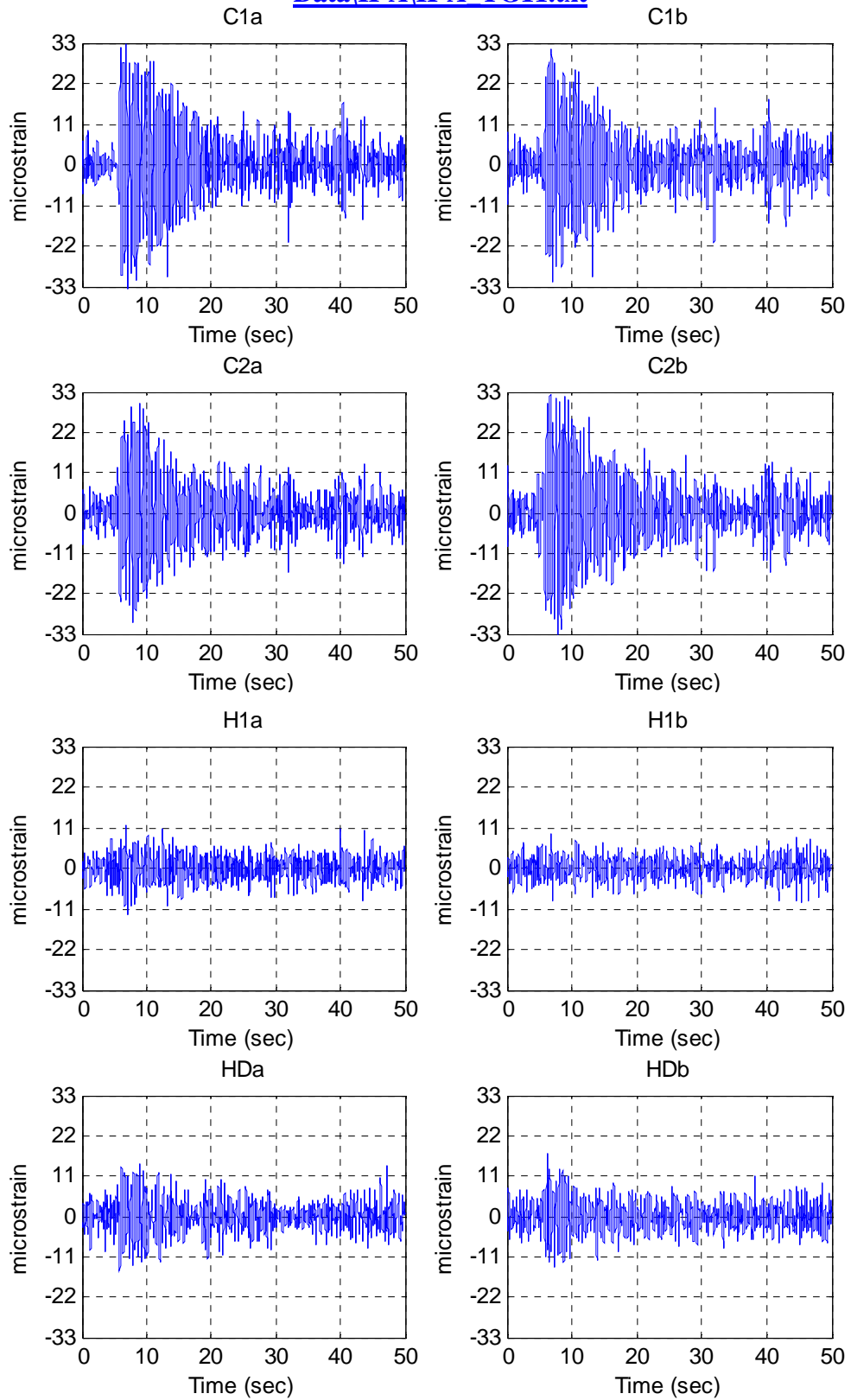


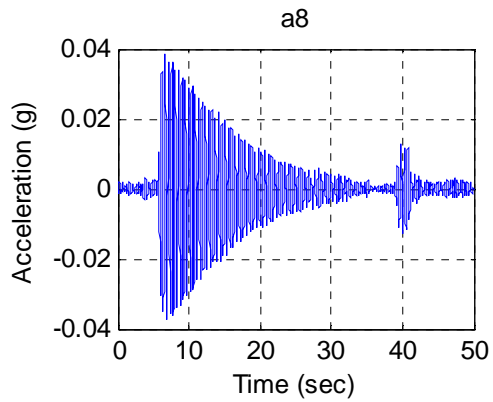
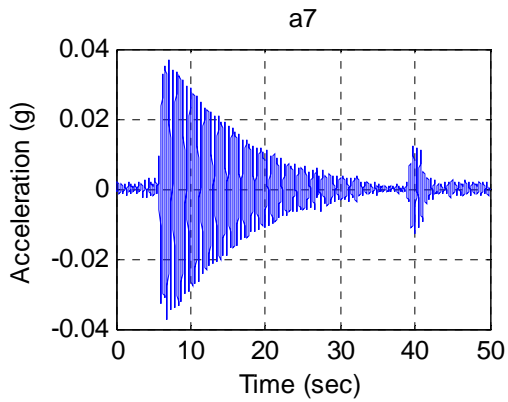
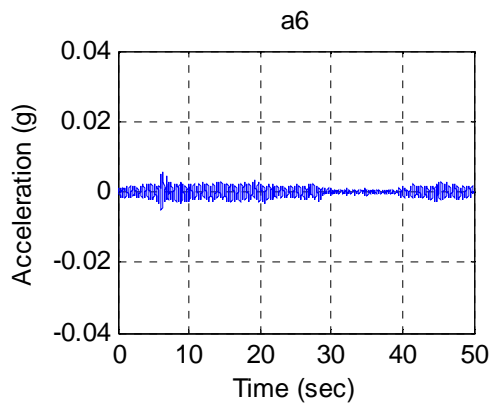
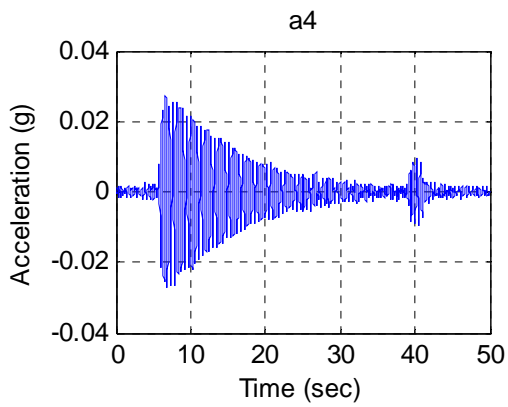
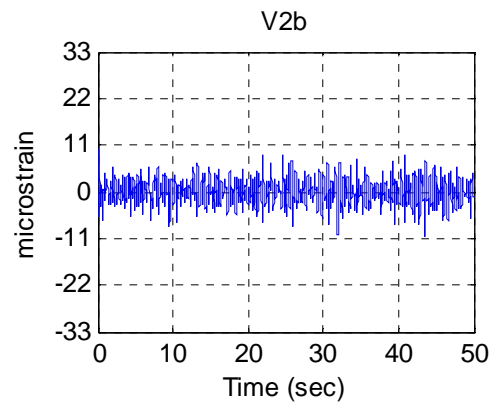
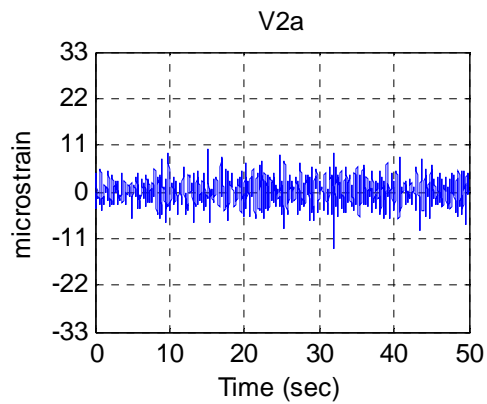
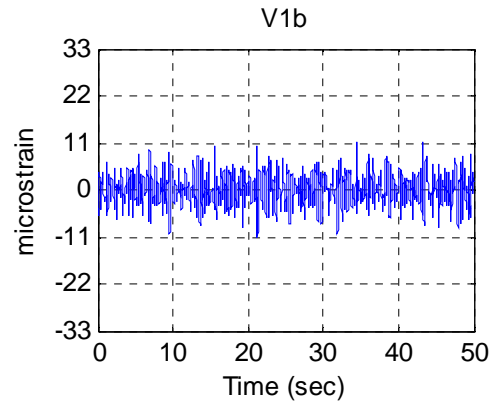
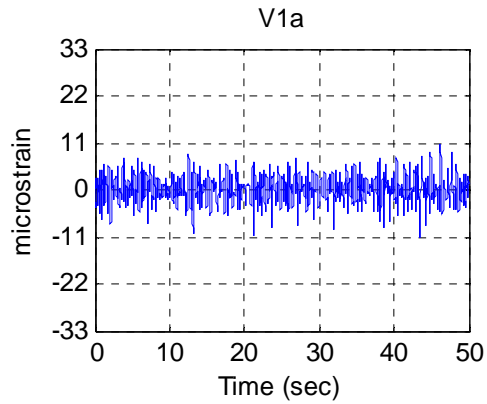
**Test TG10**  
**Data\II-A\II-A TG10.txt**



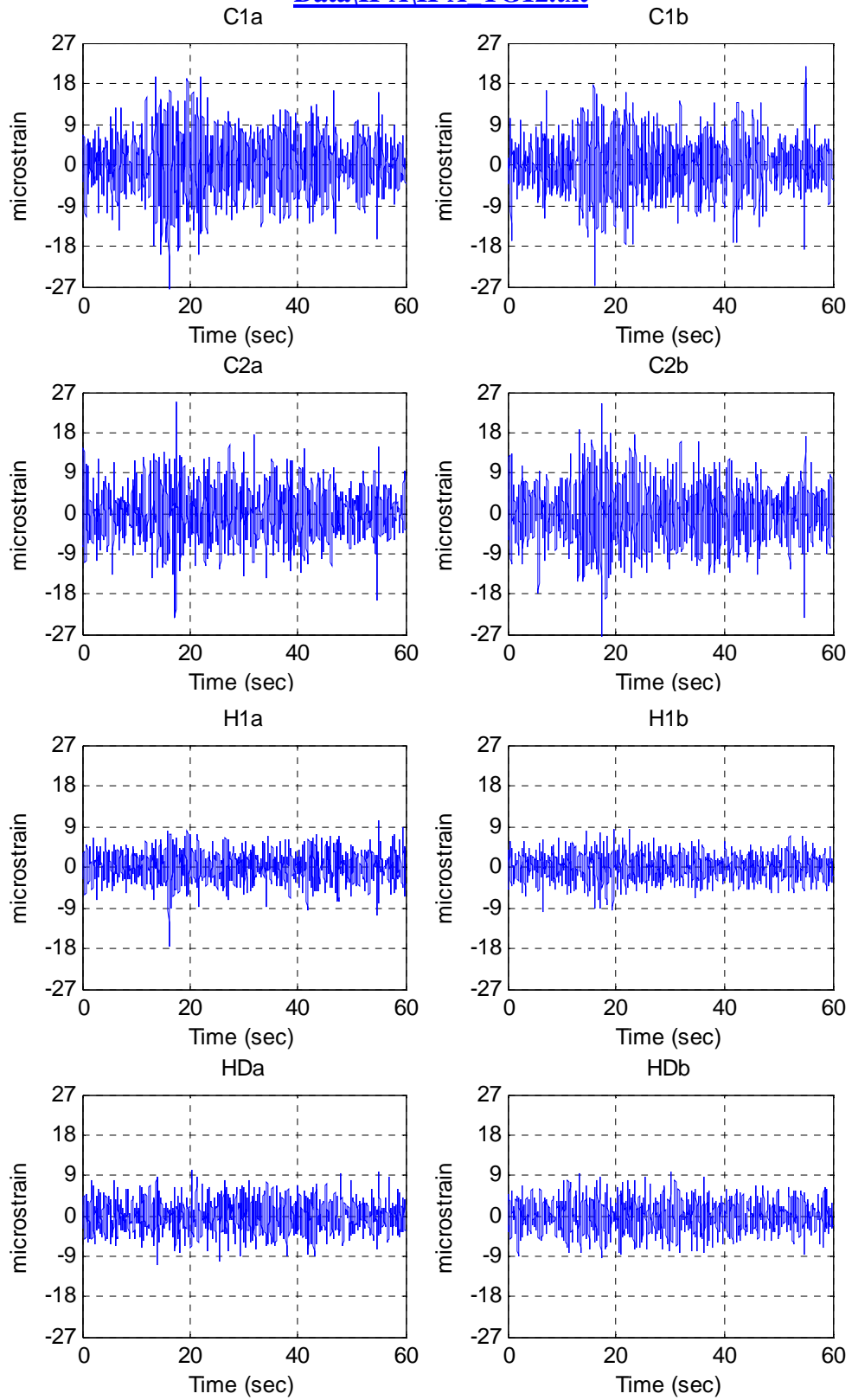


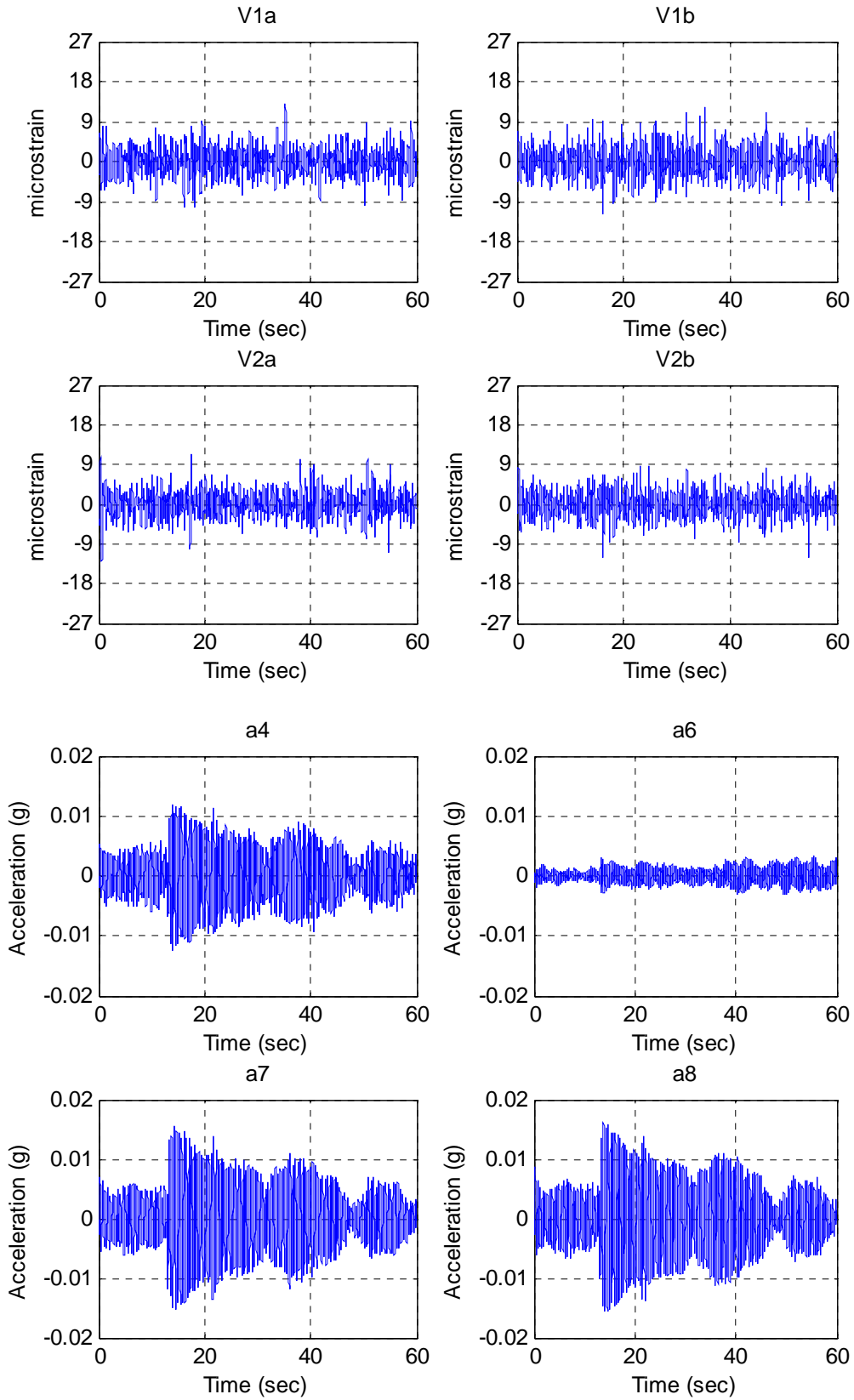
Test TG11  
[Data\II-A\II-A TG11.txt](#)



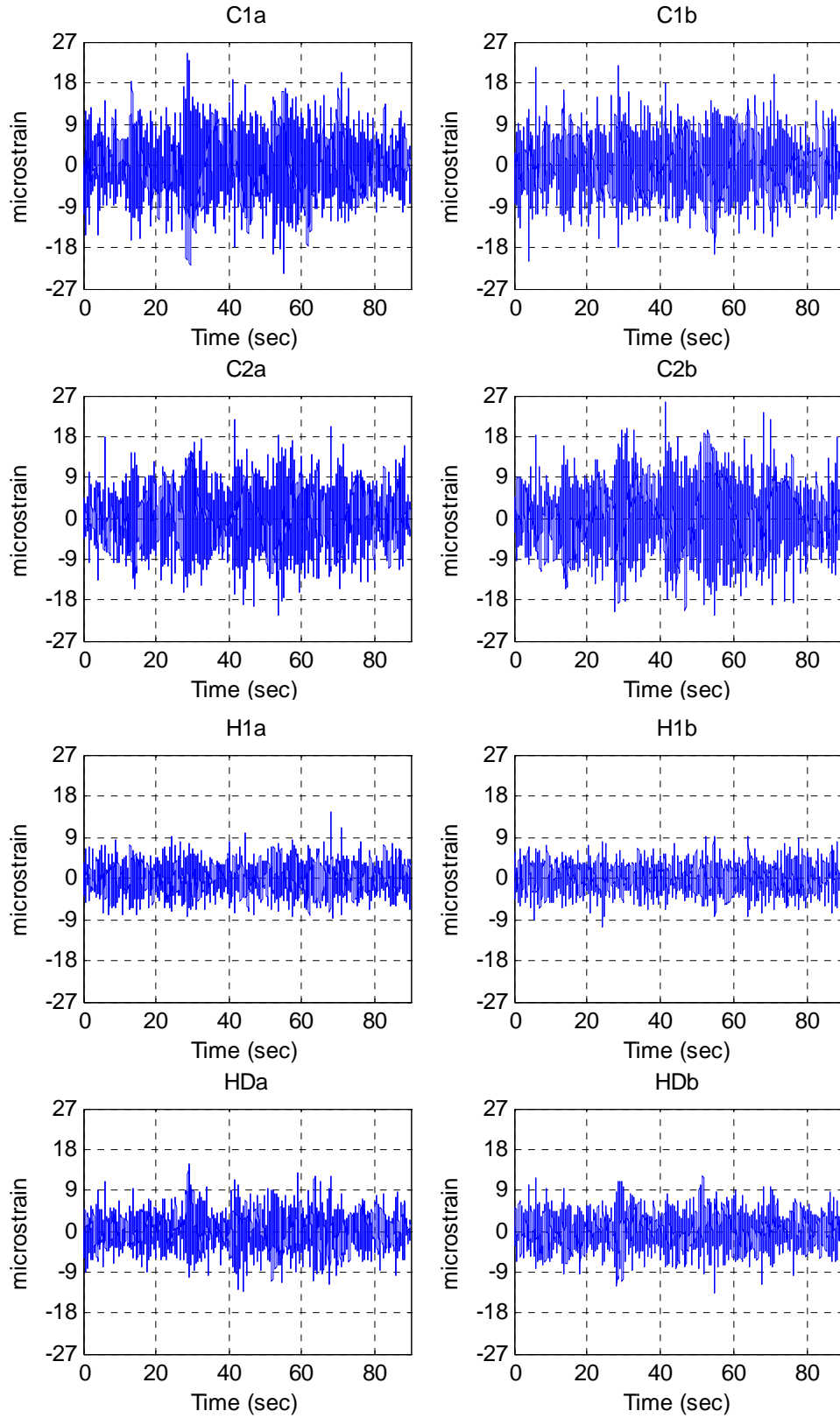


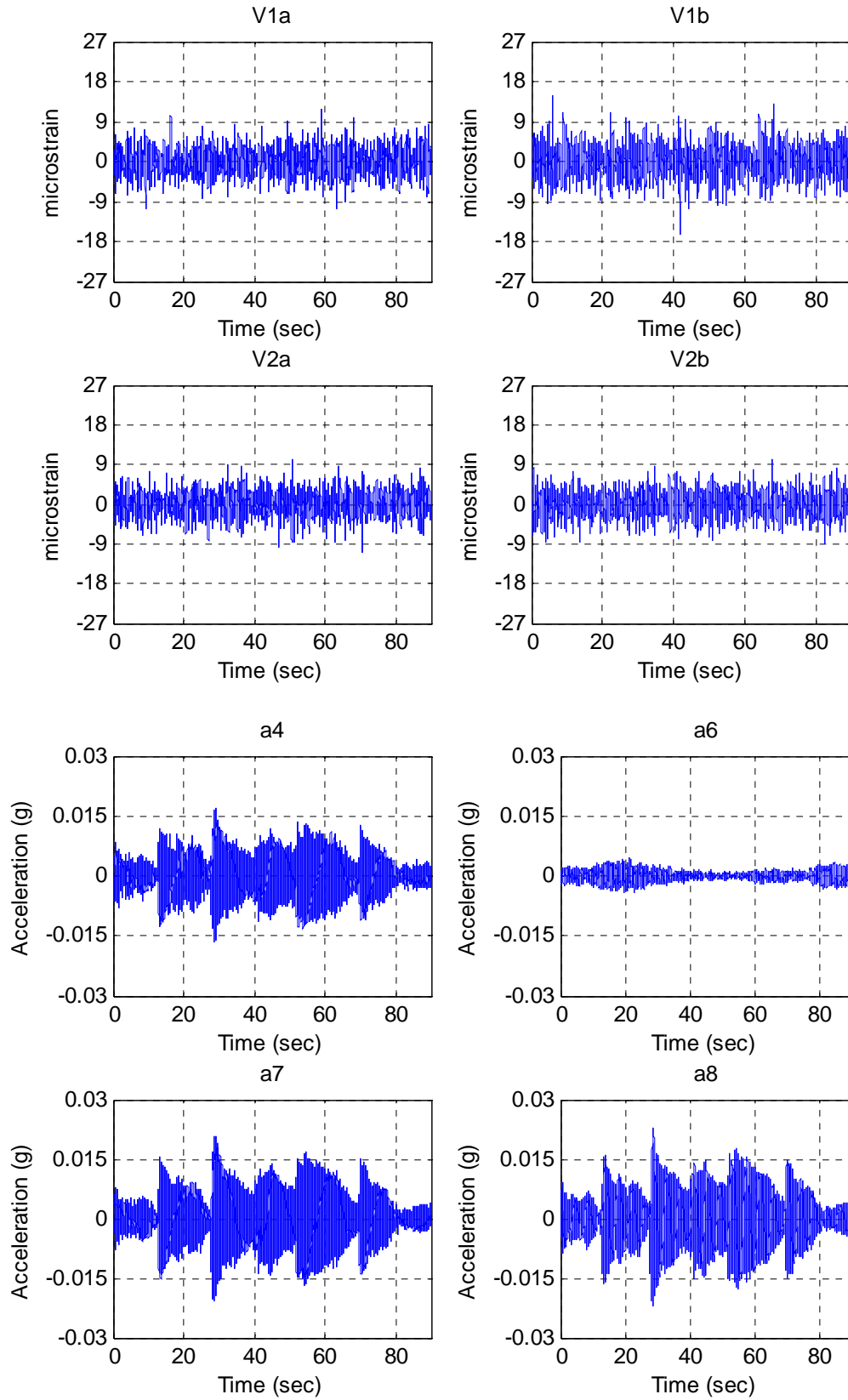
Test TG12  
Data\II-A\II-A TG12.txt





**Test TG13**  
**Data\II-A\II-A TG13.txt**





### A3.5 Manual Excitation Data

The data structure for the manual excitation data is as follows:

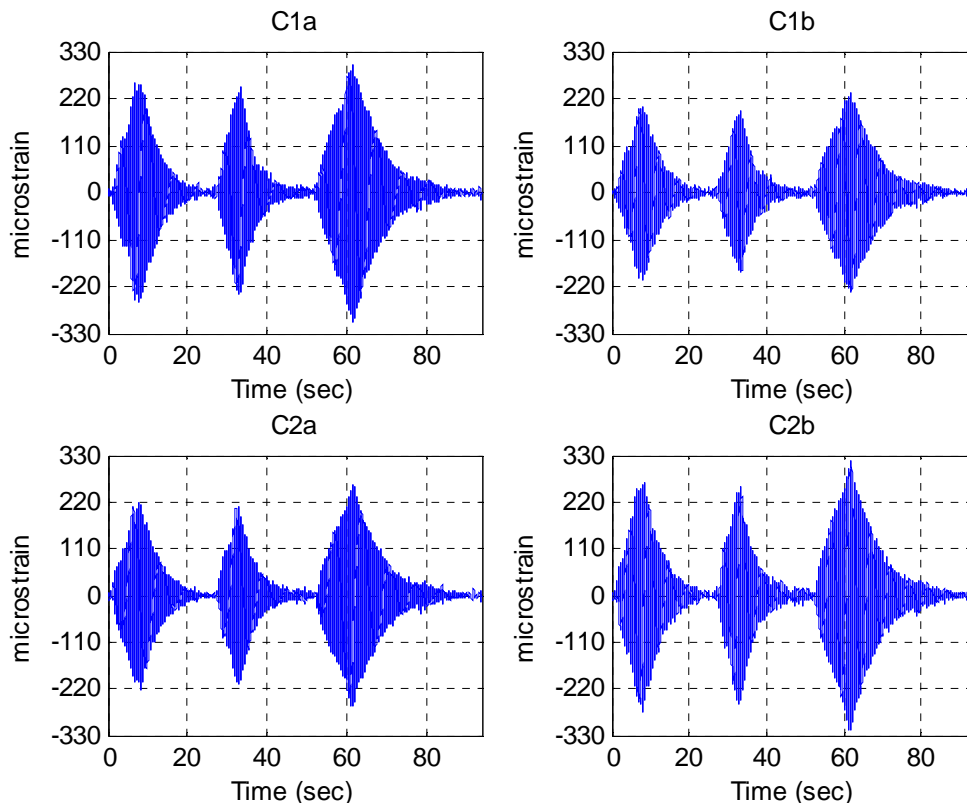
Time(sec), C1a, C1b, C2a, C2b, H1a, H1b, HDa, HDb, V1a, V1b, V2a, V2b, a4, a6, a7, a8.

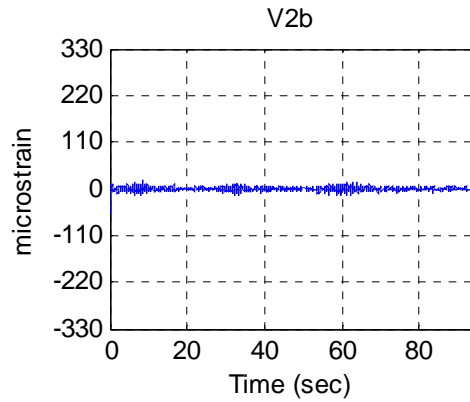
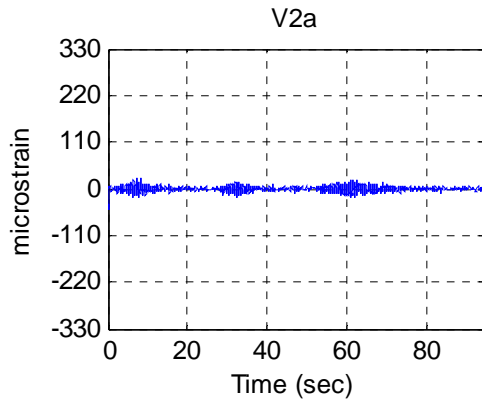
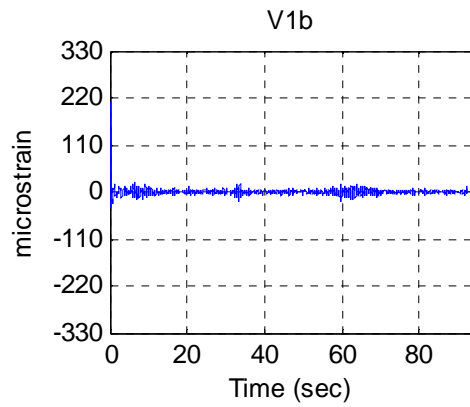
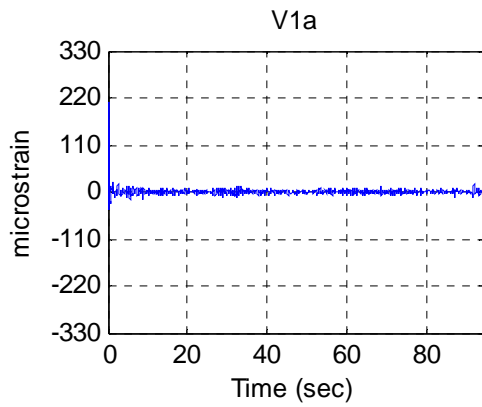
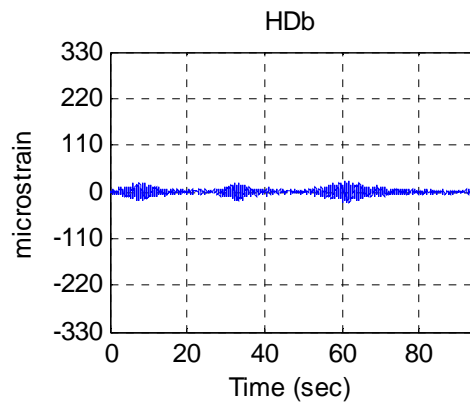
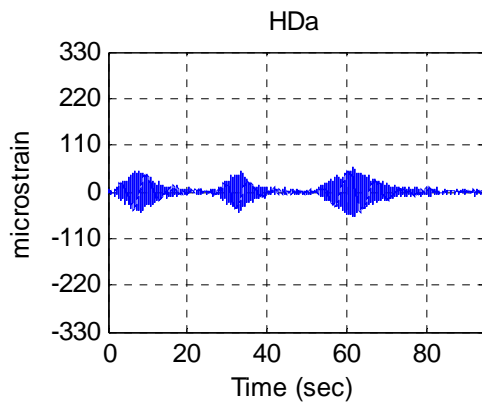
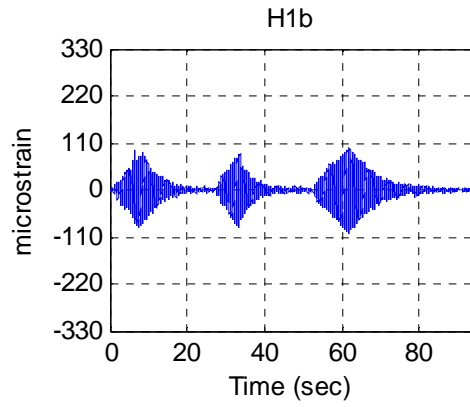
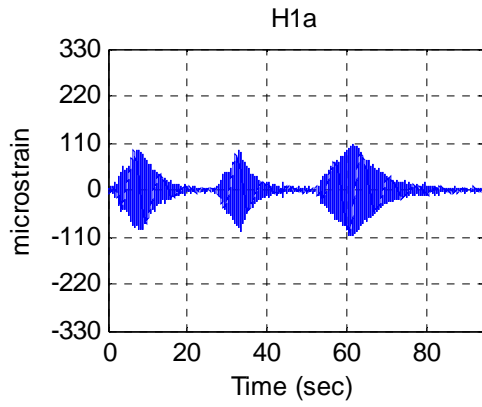
Test descriptions:

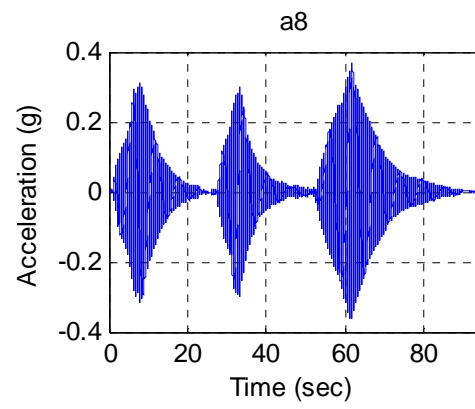
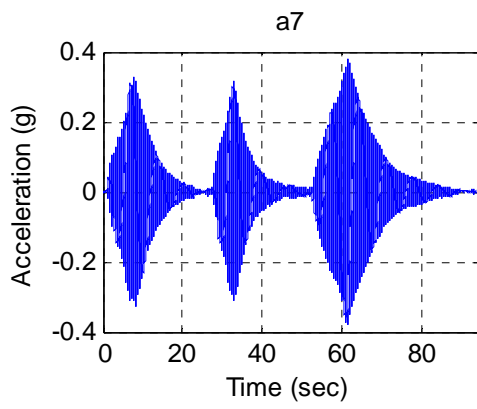
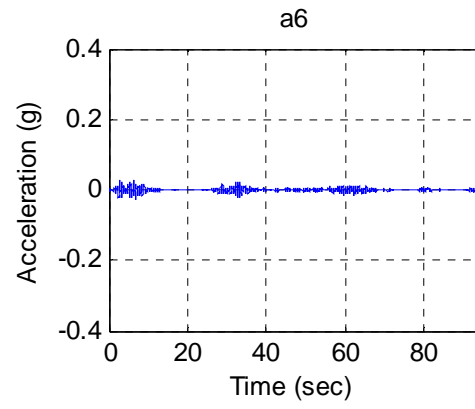
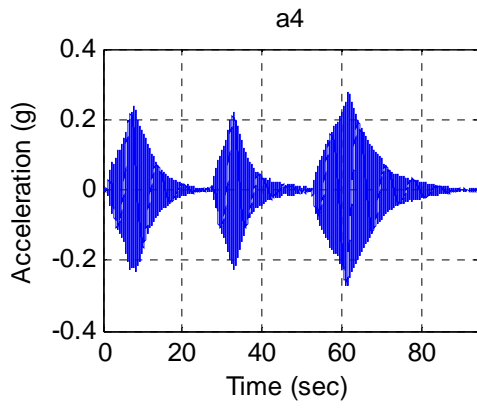
- M1 – horizontal excitation, damper engaged
- M2 – horizontal excitation, damper disengaged
- M3 – vertical excitation, damper engaged
- M4 – vertical excitation, damper disengaged

#### Test M1

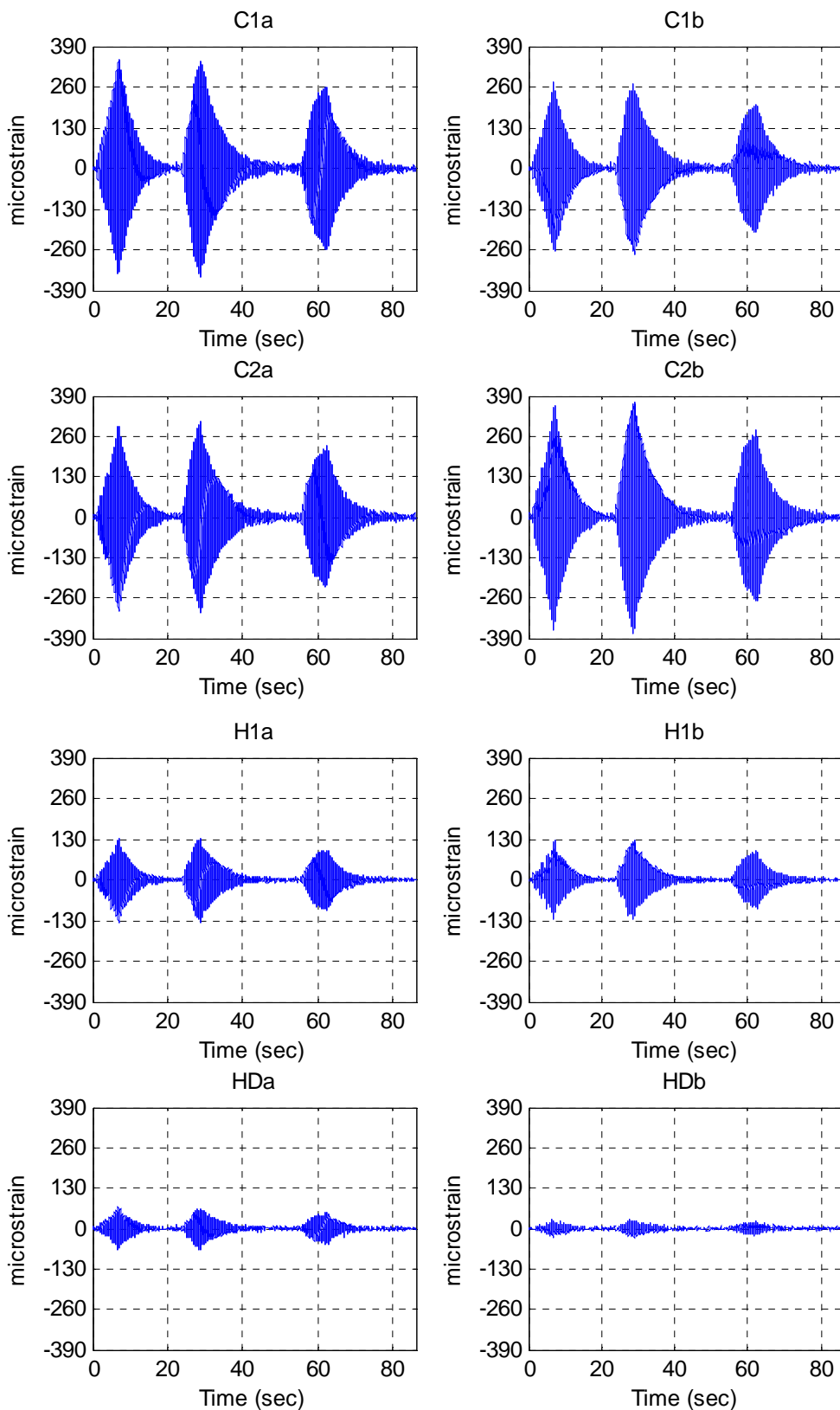
[Data\II-A\II-A\\_M1.txt](#)

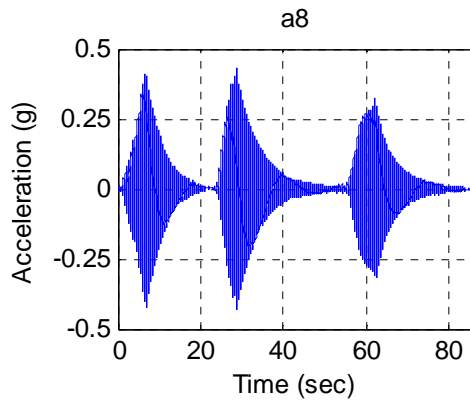
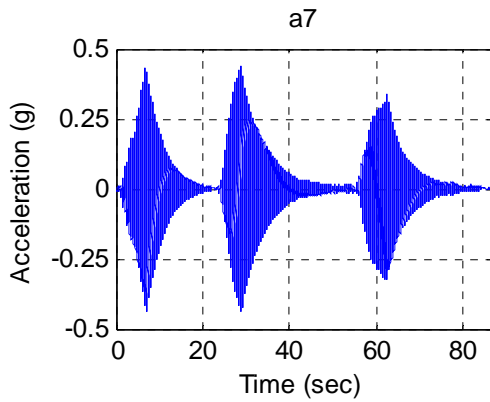
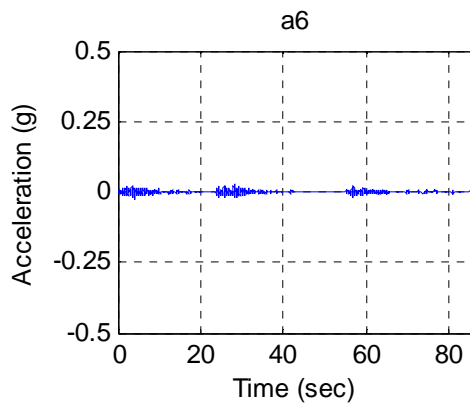
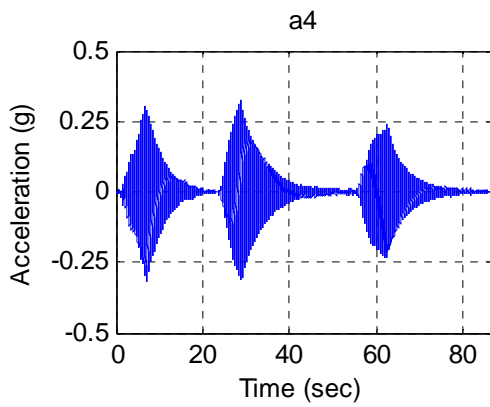
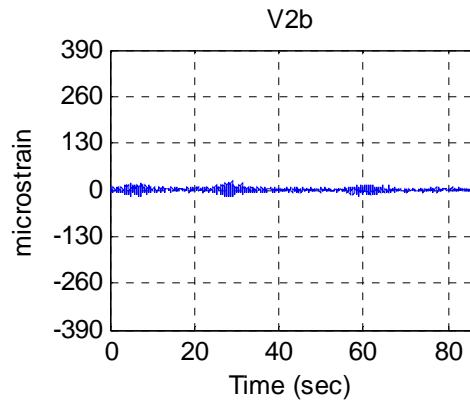
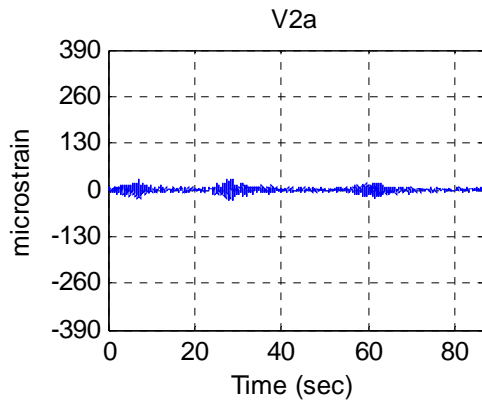
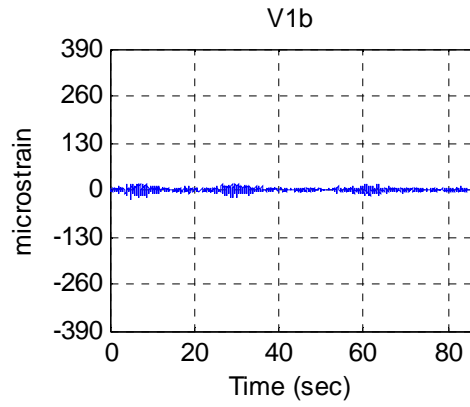
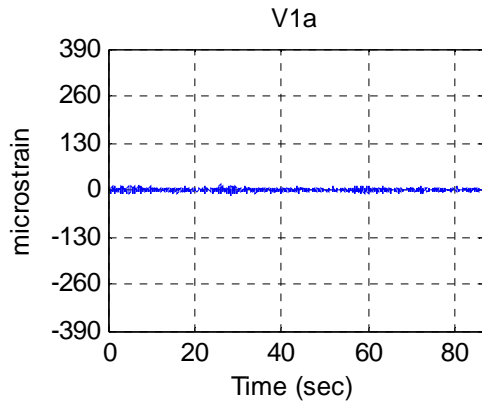




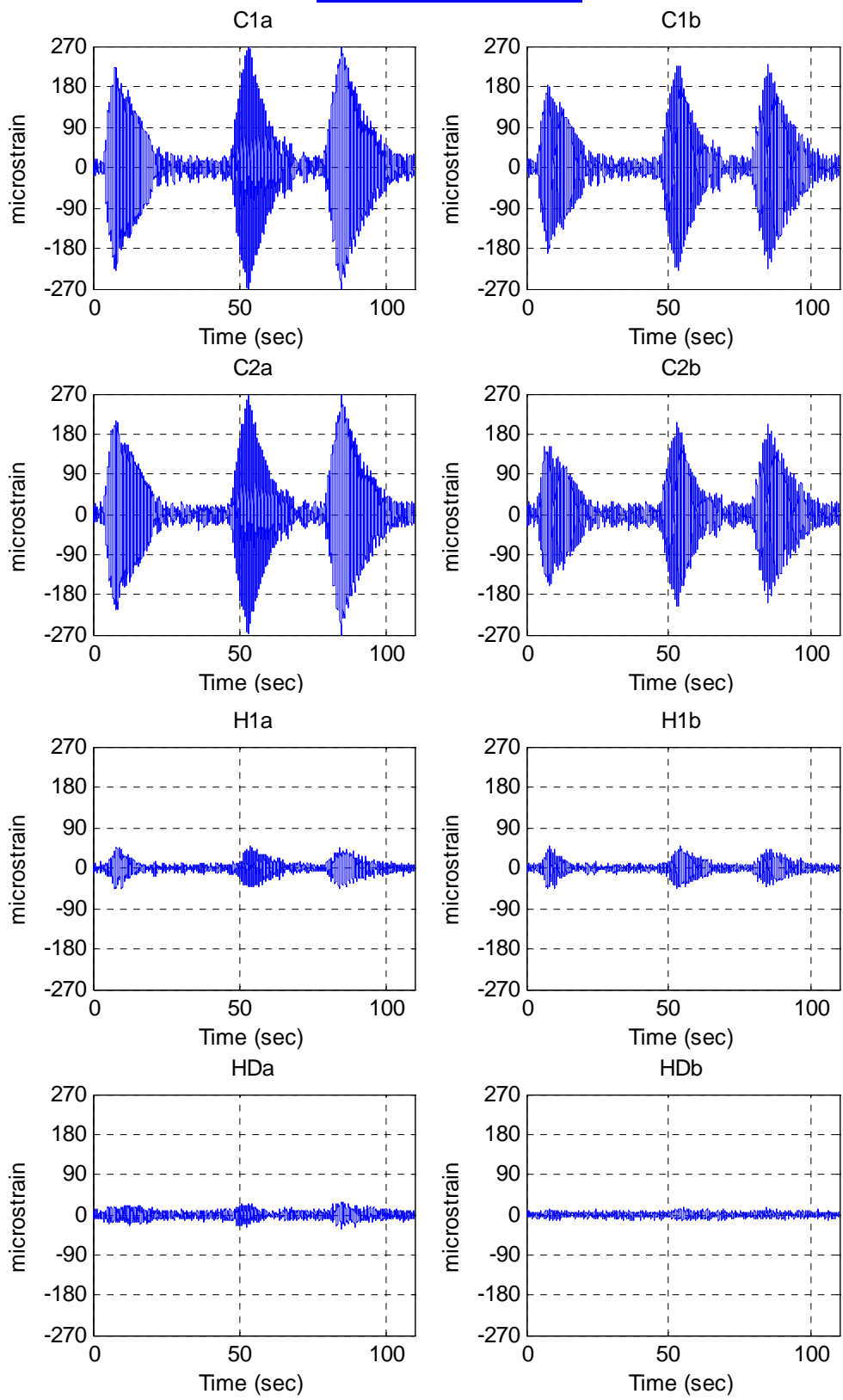


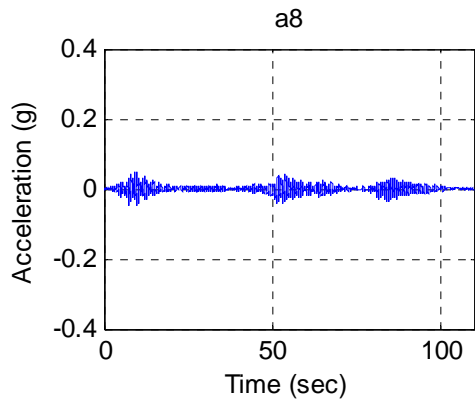
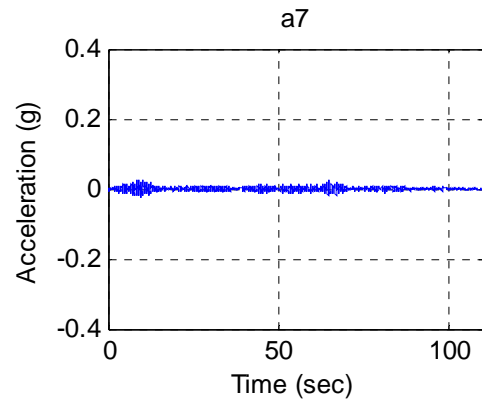
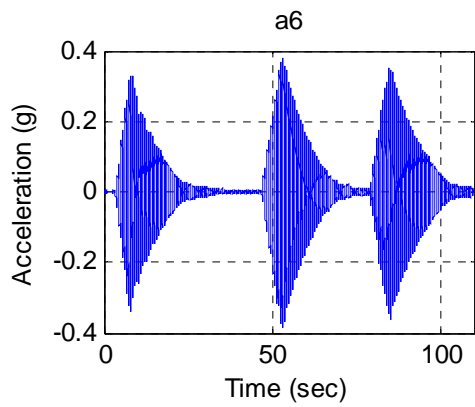
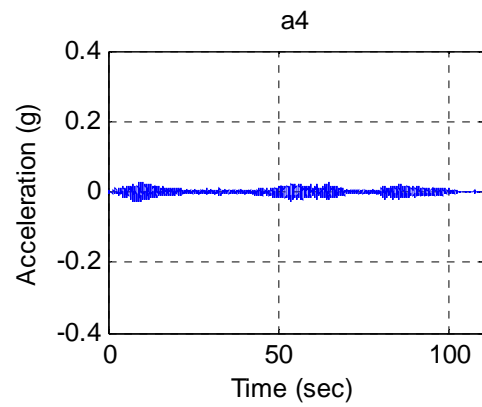
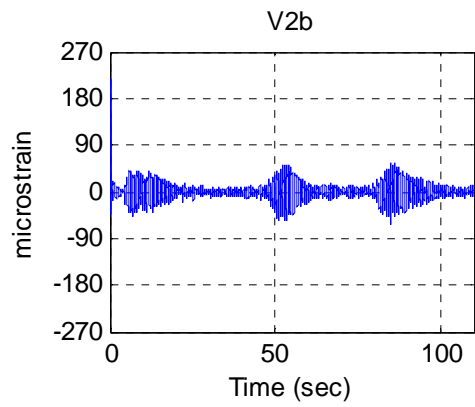
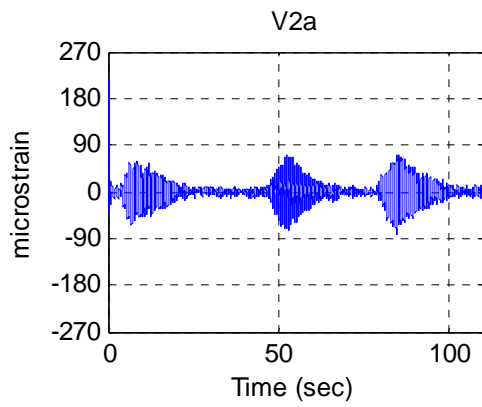
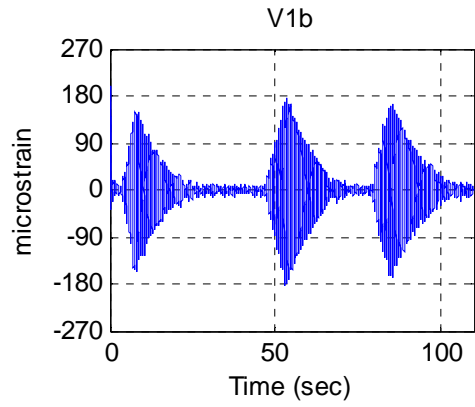
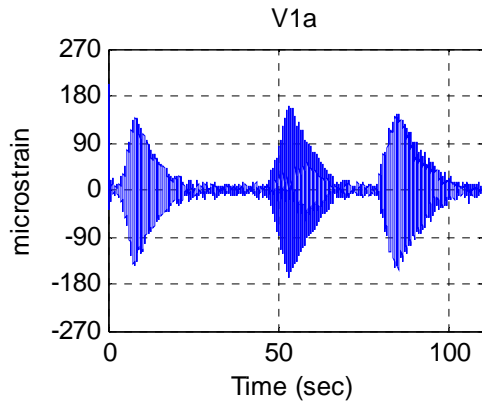
**Test M2**  
Data\II-A\II-A\_M2.txt



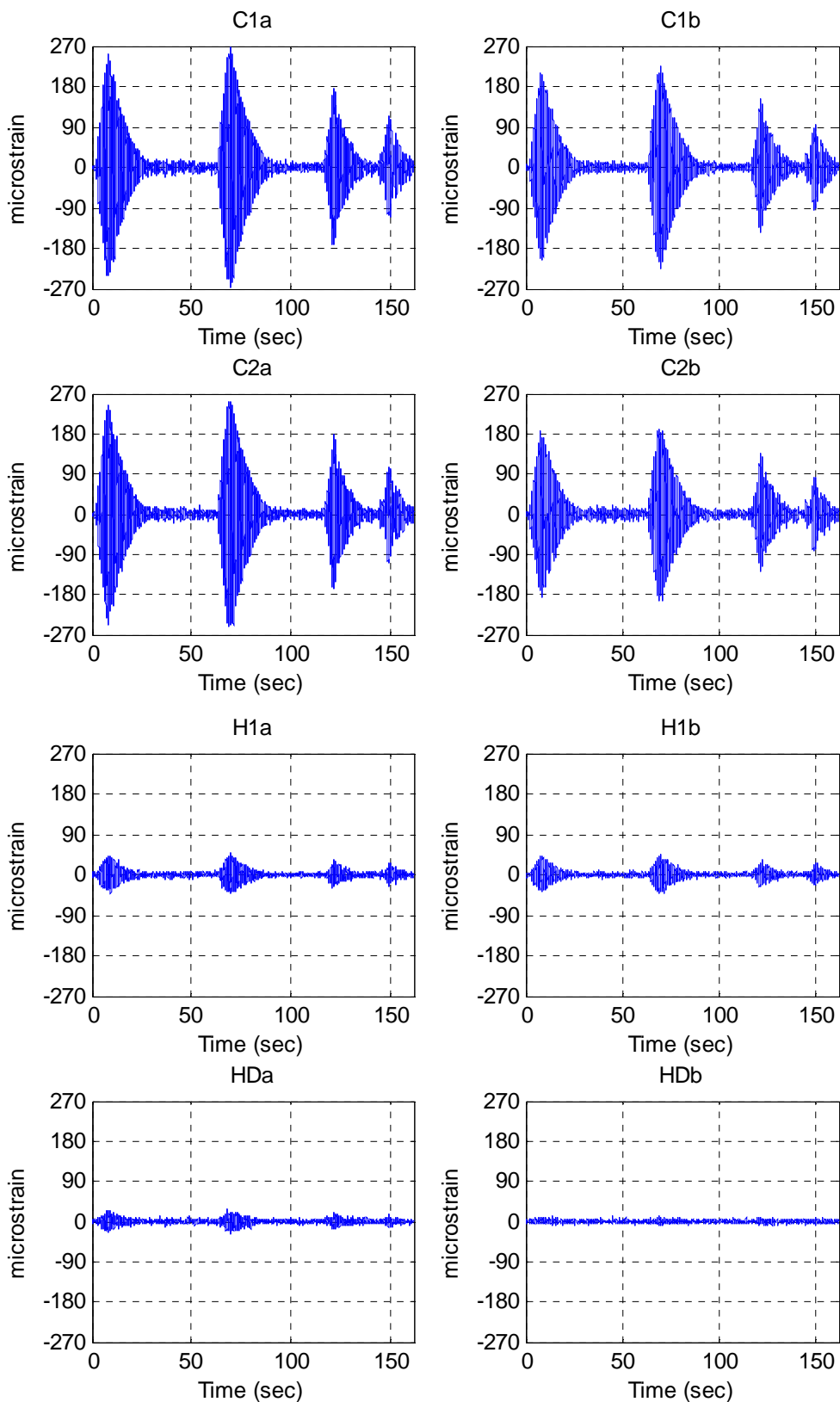


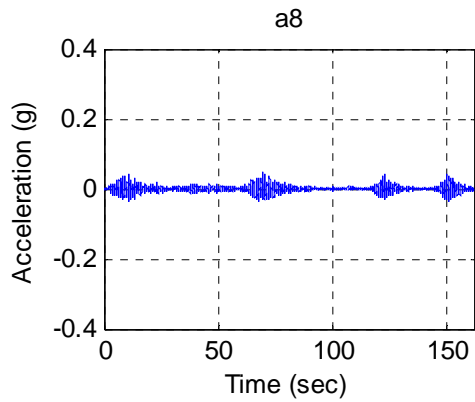
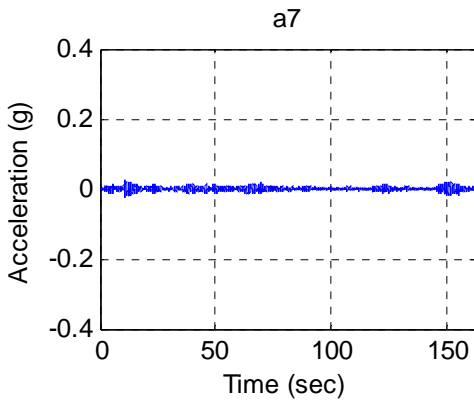
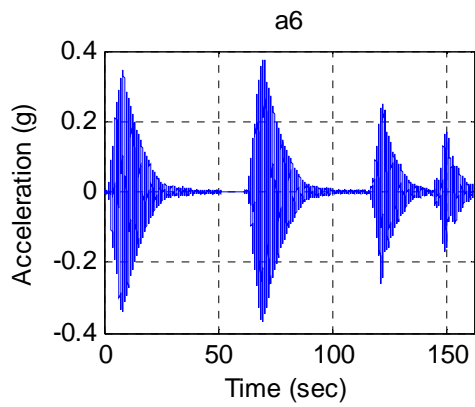
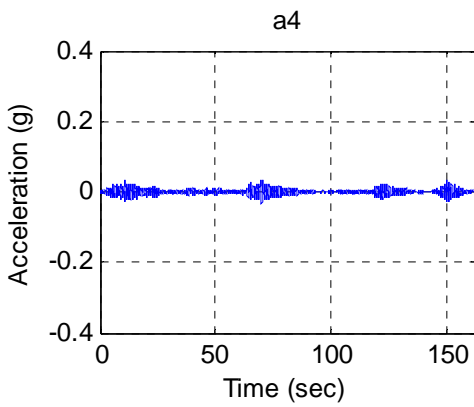
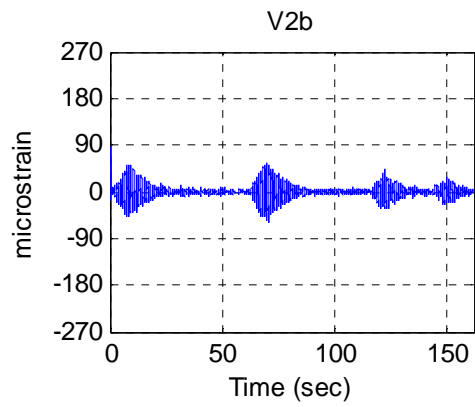
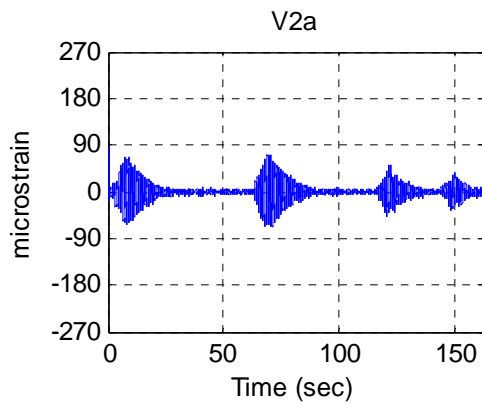
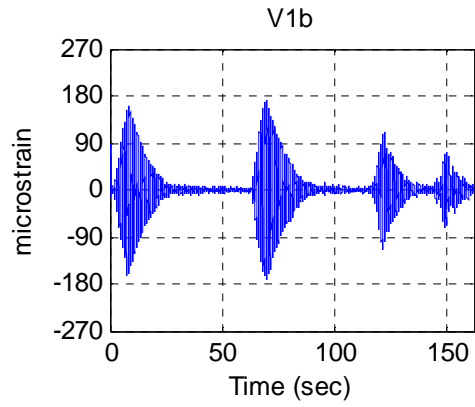
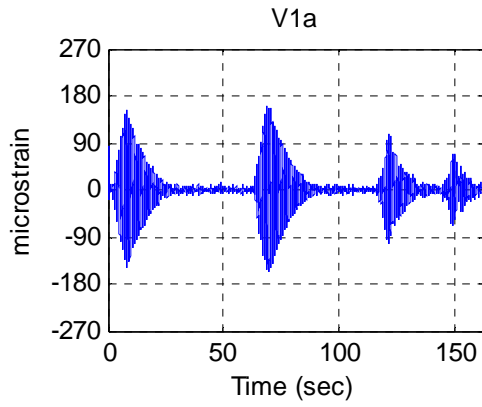
**Test M3**  
Data\II-A\II-A\_M3.txt





**Test M4**  
Data\II-A\II-A\_M4.txt



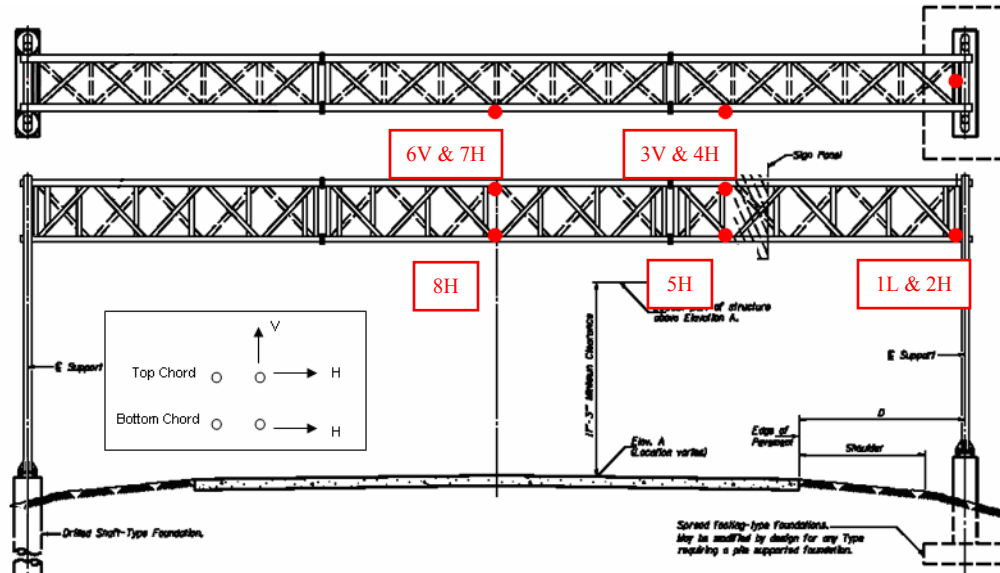


## A4.0 Type III-A Sign Structure Data

### A4.1 Sensor names and locations

#### Accelerometers

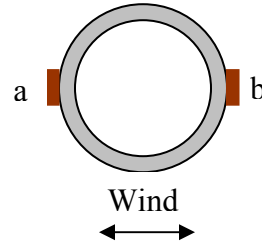
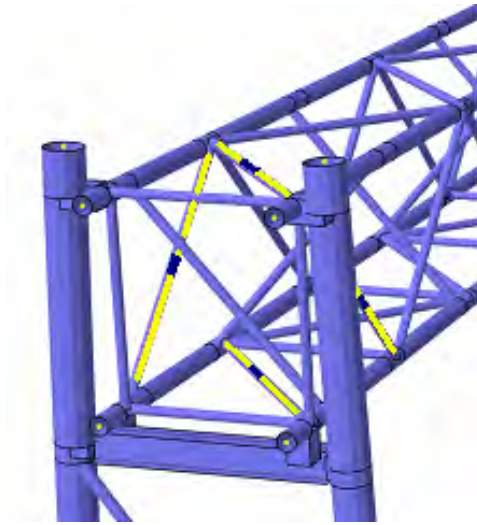
The figure below shows the placement of the accelerometers on the Type III-A sign structure. The following table gives a detailed description of the sensor labels and locations.



Accelerometer	Location	Measurement Direction
a1	End – over support, bottom chord	Longitudinal
a2	End – over support, bottom chord	Horizontal
a3	Quarter-span, top chord	Vertical
a4	Quarter-span, top chord	Horizontal
a5	Quarter-span, bottom chord	Horizontal
a6	Mid-span, top chord	Vertical
a7	Mid-span, top chord	Horizontal
a8	Mid-span, bottom chord	Horizontal

#### Strain gages

Twelve strain gages were installed on the III-A sign structure. Four gages were located on two chord members at the mid-span of the truss and eight on web members at one end of the truss. The locations of the strain gages at the end of the truss are indicated in the figure below. The table below details the locations and labeling of each gage.

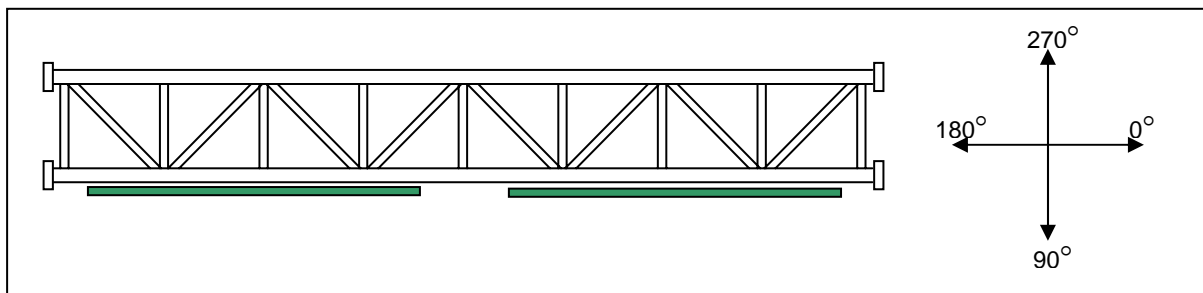


Strain Gage	Location
C1a C1b	Bottom Chord – front plane
C2a C2b	Bottom Chord – back plane
H1a H1b	Horizontal Diagonal – top plane
H2a* H2b	Horizontal Diagonal – bottom plane
V1a V1b	Vertical Diagonal – front plane
V2a V2b	Vertical Diagonal – back plane

\*This was a faulty gage

*Anemometer*

The wind velocity and direction measured by the anemometer relative to the sign is shown in the figure below.



## A4.2 Data Description

The data contained in the appendix files and plotted below is the filtered data acquired for the Type III-A sign structure. A link to a text file of each test is included with the plots of the data. To import the data into Excel follow the steps given below:

1. Click on the link to open a text file of the data
2. Click Edit → Select All
3. Click Edit → Copy
4. Open Excel
5. Once in Excel, click Edit → Paste

Test descriptions:

- W1-W10 are tests that were taken under strong wind conditions. Note that when the wind direction is equal to 90 degrees, the wind is blowing perpendicular to the sign face. This data was taken on November 3, 2005 when the wind was primarily blowing perpendicular to the sign face and ranged in speed from about 8 to 42 mph.
- TG1-TG10 are tests that were taken during calm conditions to record the response of the sign to truck gusts. Truck gust data was taken on two separate days. Tests TG1-TG6 were taken on May 31, 2005 and Tests TG7–TG10 were taken on June 10, 2005. The strain data acquired on these occasions was not satisfactory.
- M1-M4 are tests that were taken during calm conditions while the structure was manually excited in either the horizontal or vertical direction. These tests were taken on March 24, 2005.

## A4.3 Wind Data

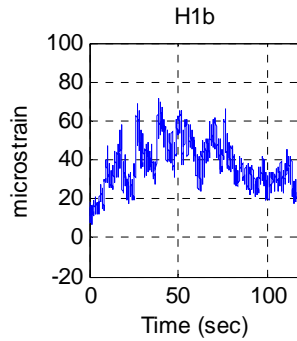
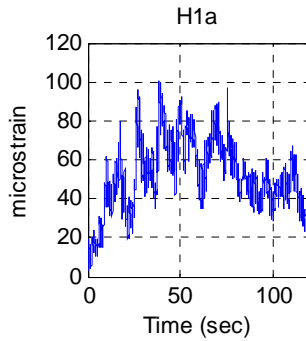
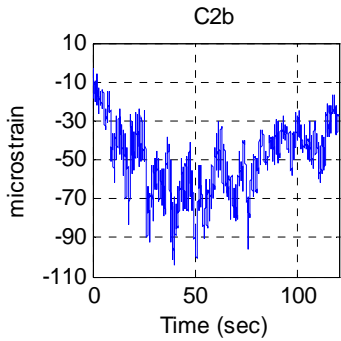
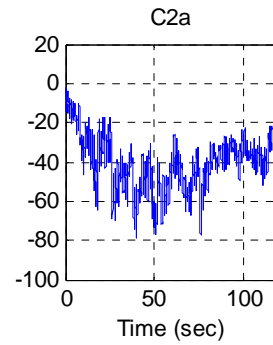
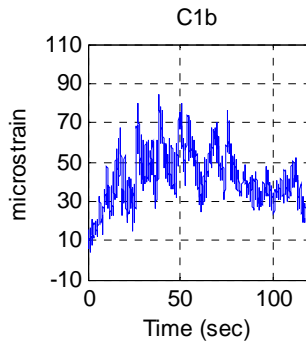
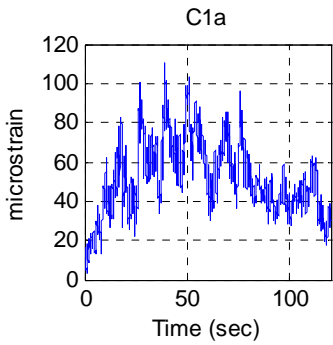
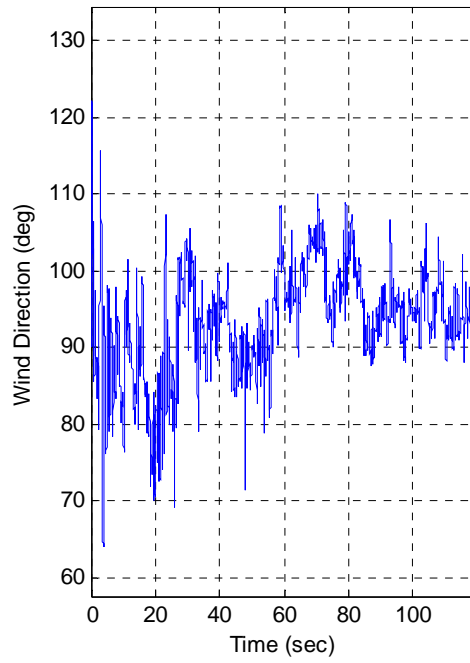
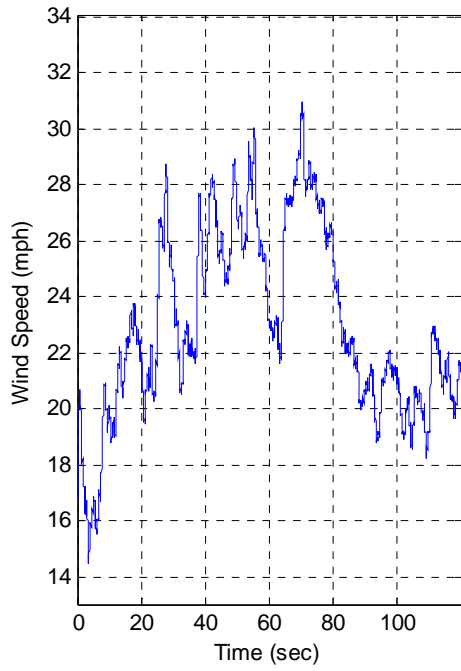
The data structure for the wind data is as follows:

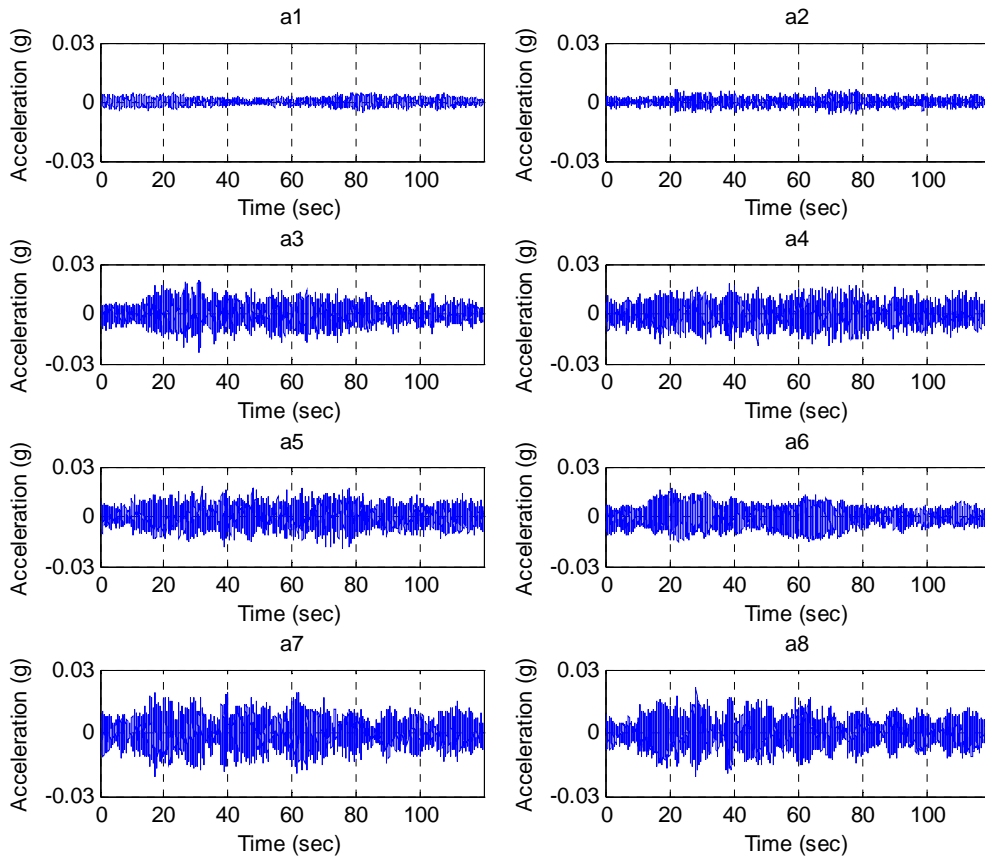
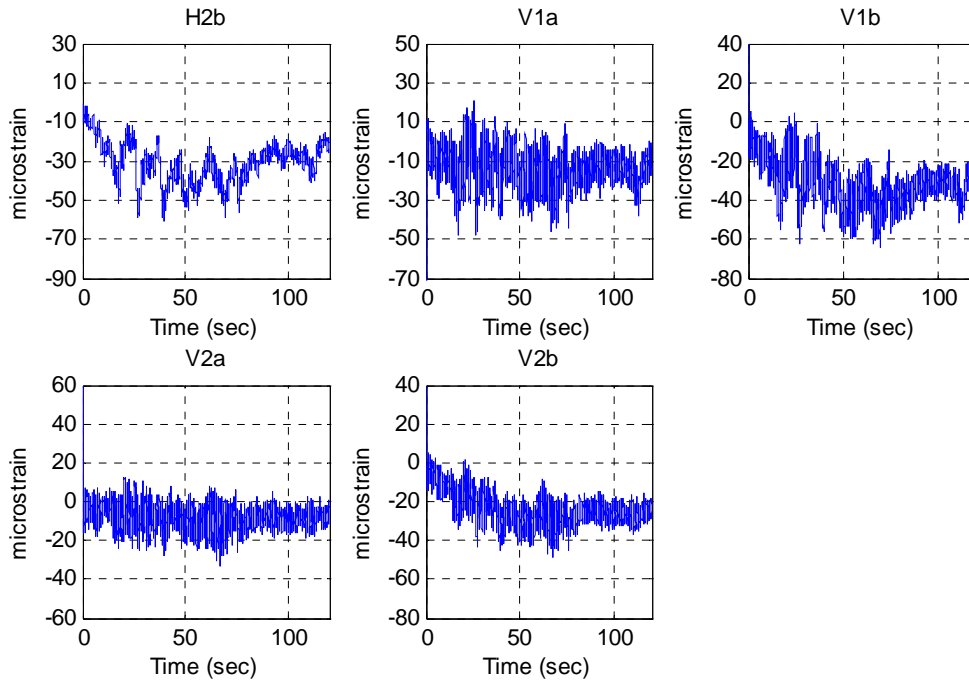
Time(sec), C1a, C1b, C2a, C2b, H1a, H1b, H2b, V1a, V1b, V2a, V2b, a1, a2, a3, a4, a5, a6, a7 a8 WS(mph), WD(deg)

To determine the wind velocity acting perpendicular to the sign face the following calculation must be made:

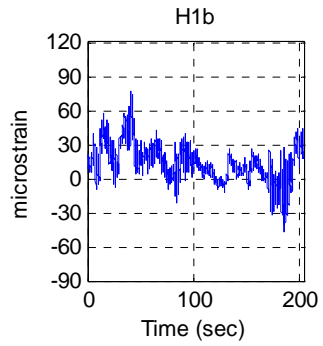
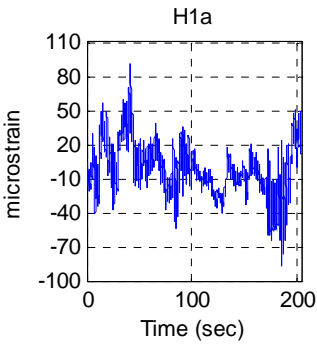
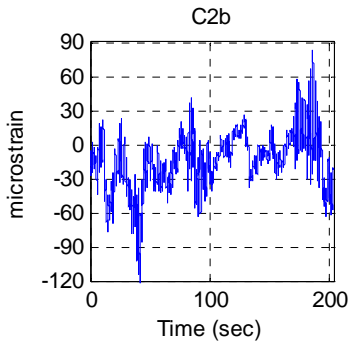
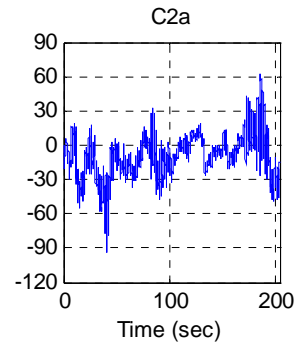
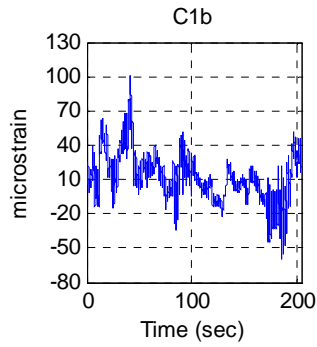
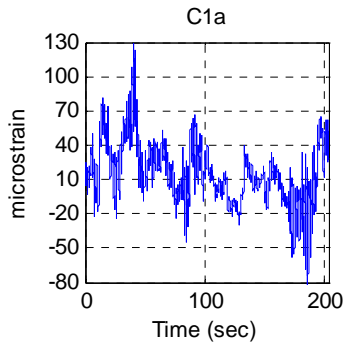
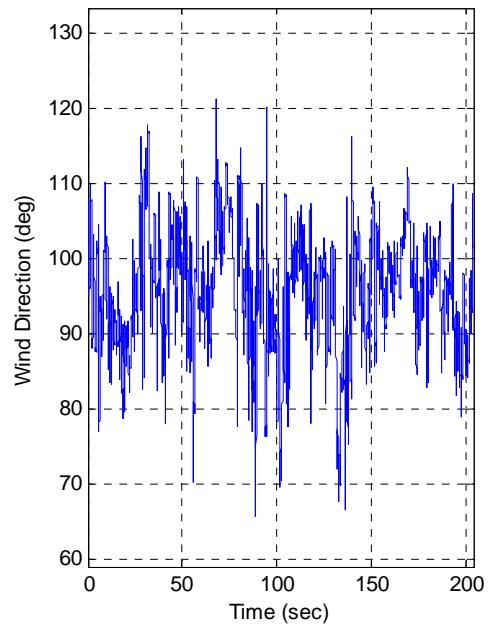
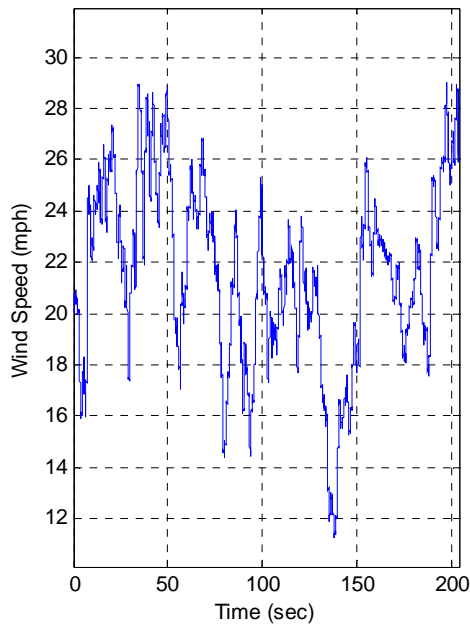
$$WS_{\text{perpendicular}} = WS * \sin(WD)$$

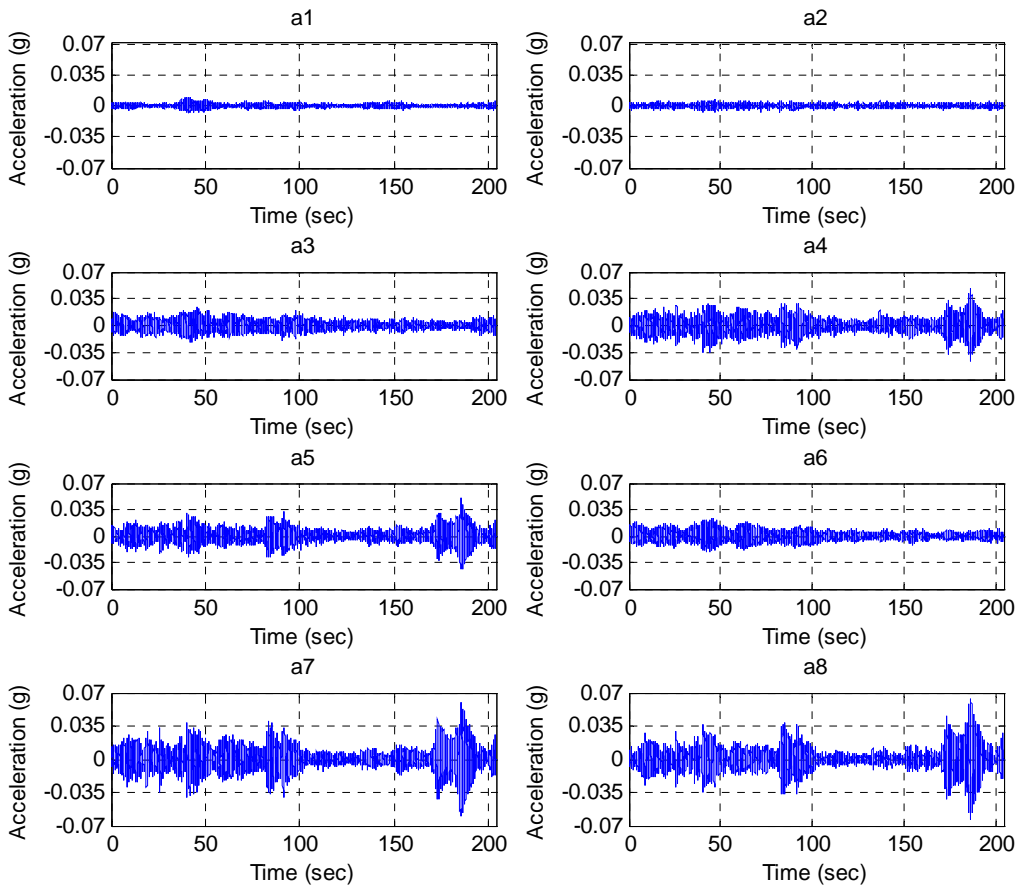
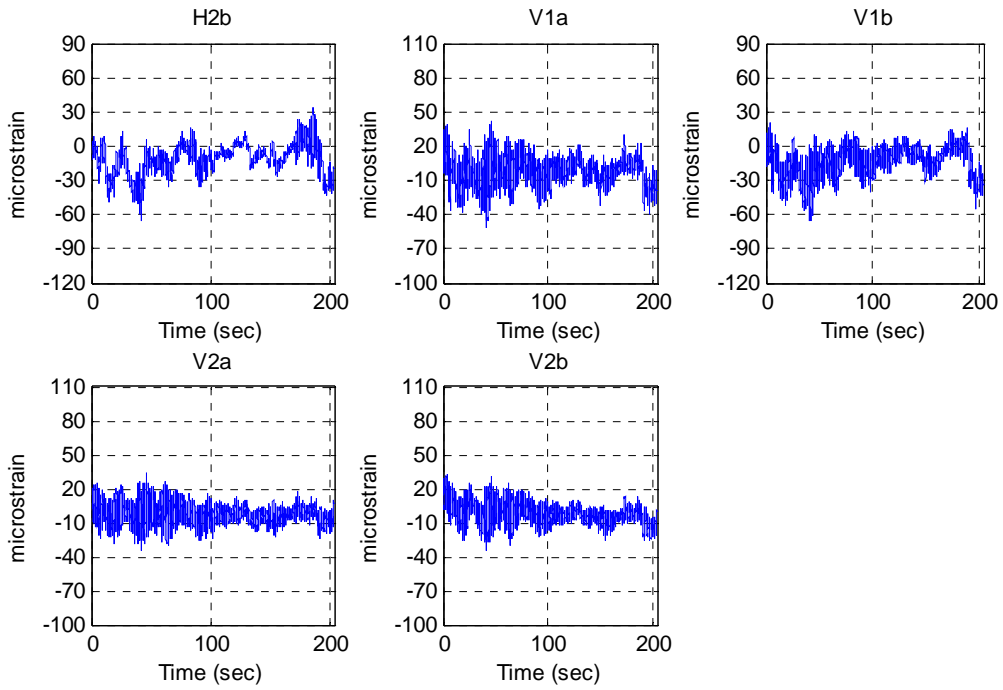
**Test W1**  
**Data\III-A\III-A W1.txt**



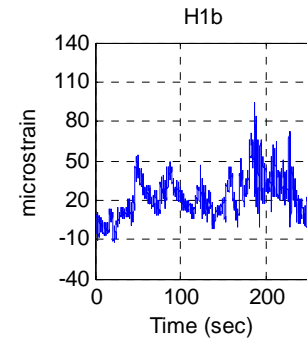
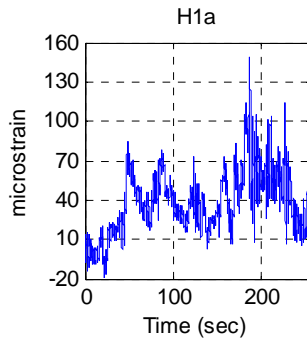
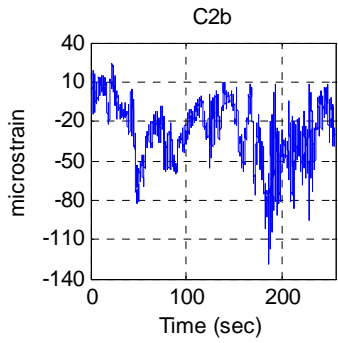
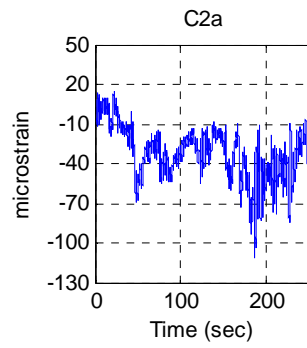
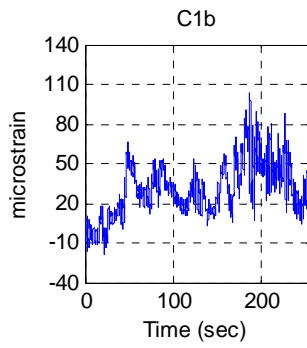
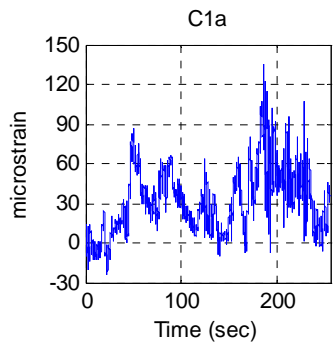
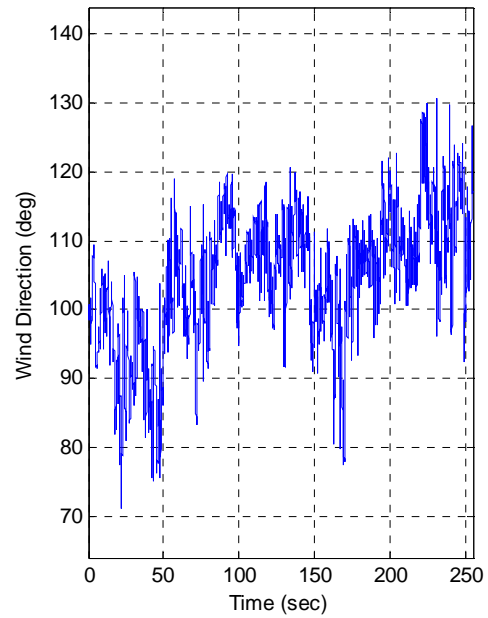
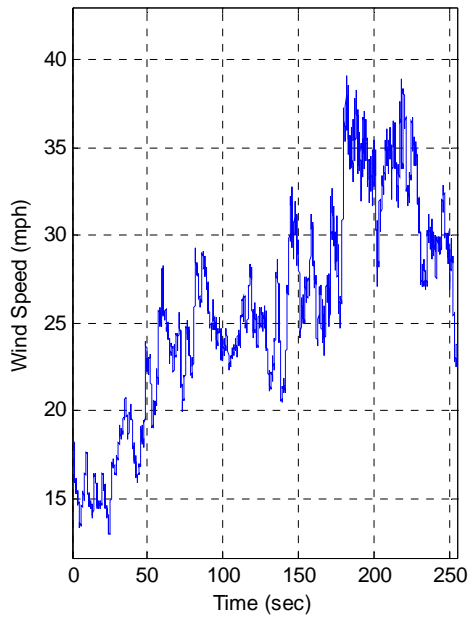


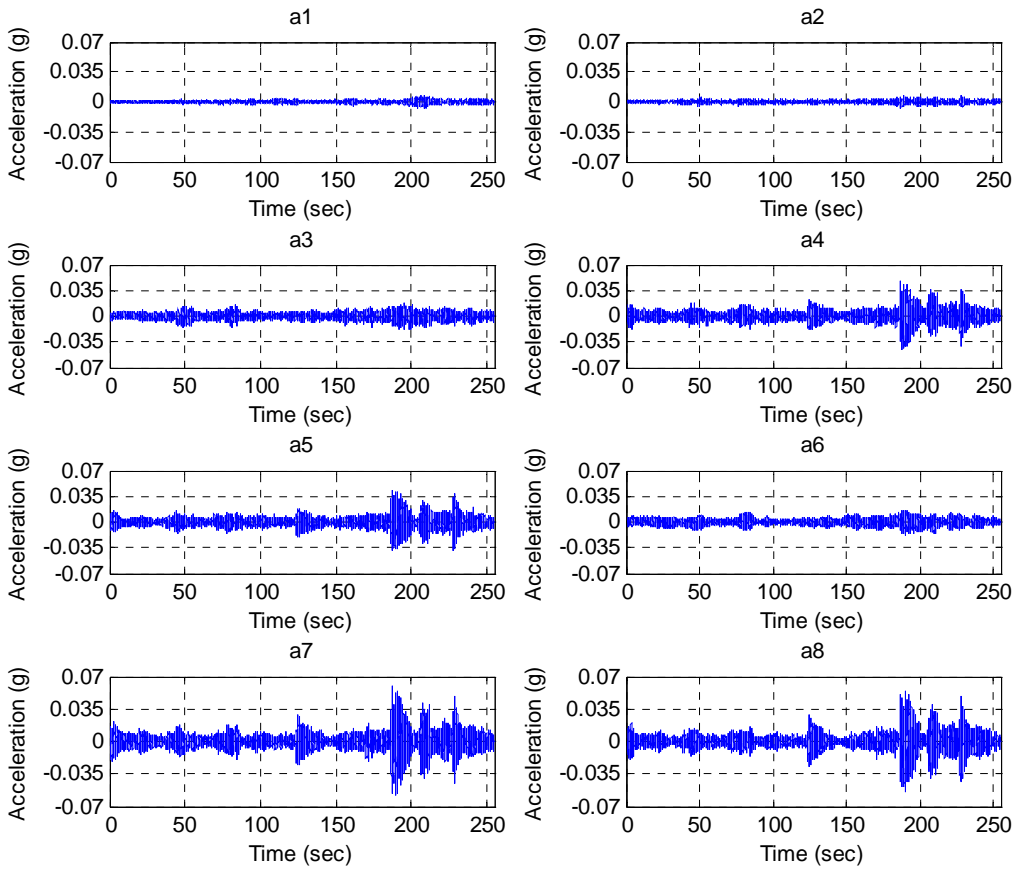
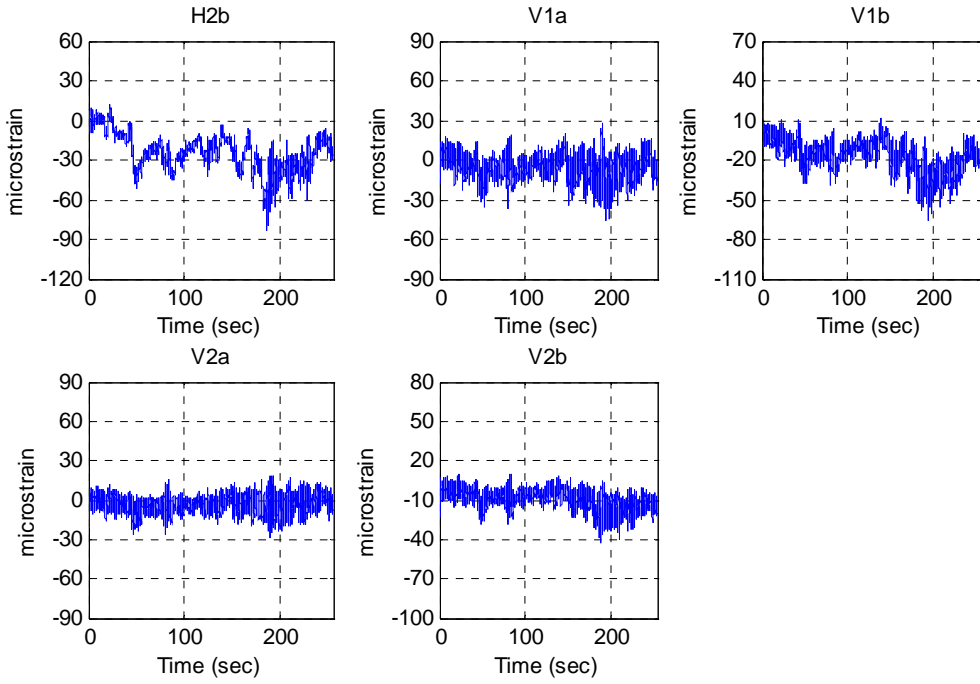
**Test W2**  
**Data\III-A\III-A W2.txt**



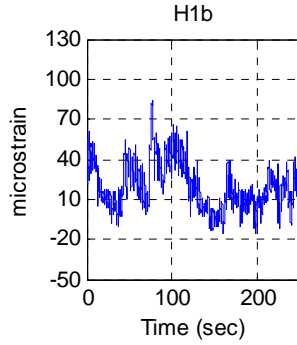
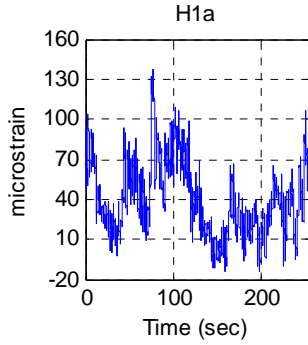
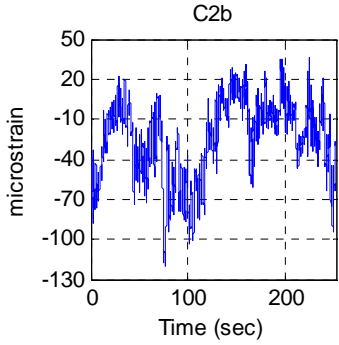
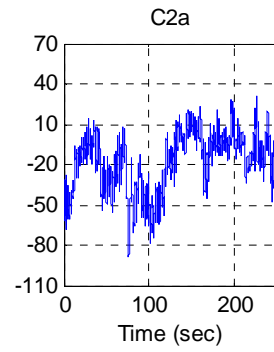
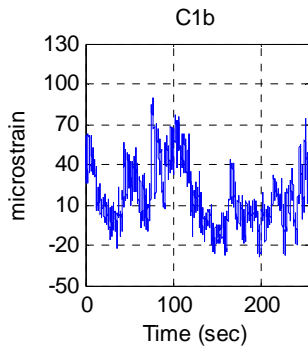
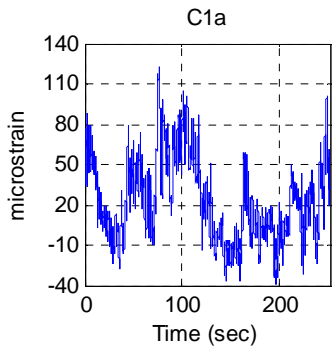
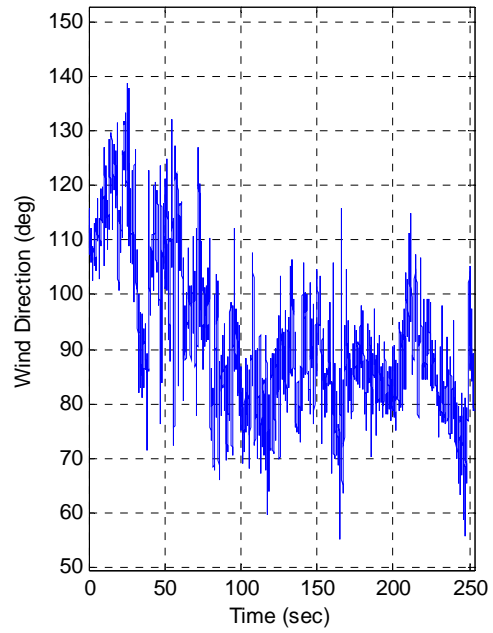
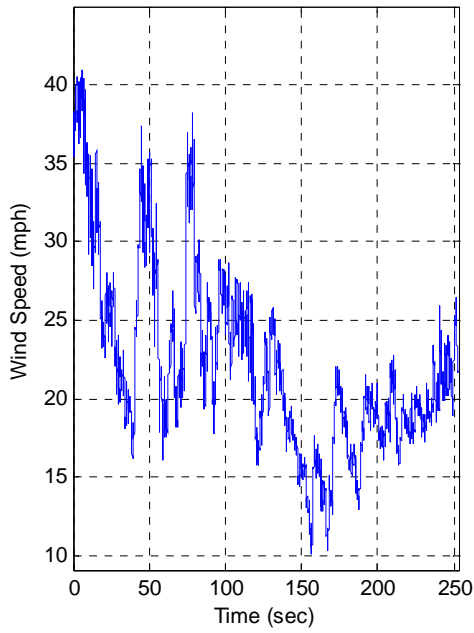


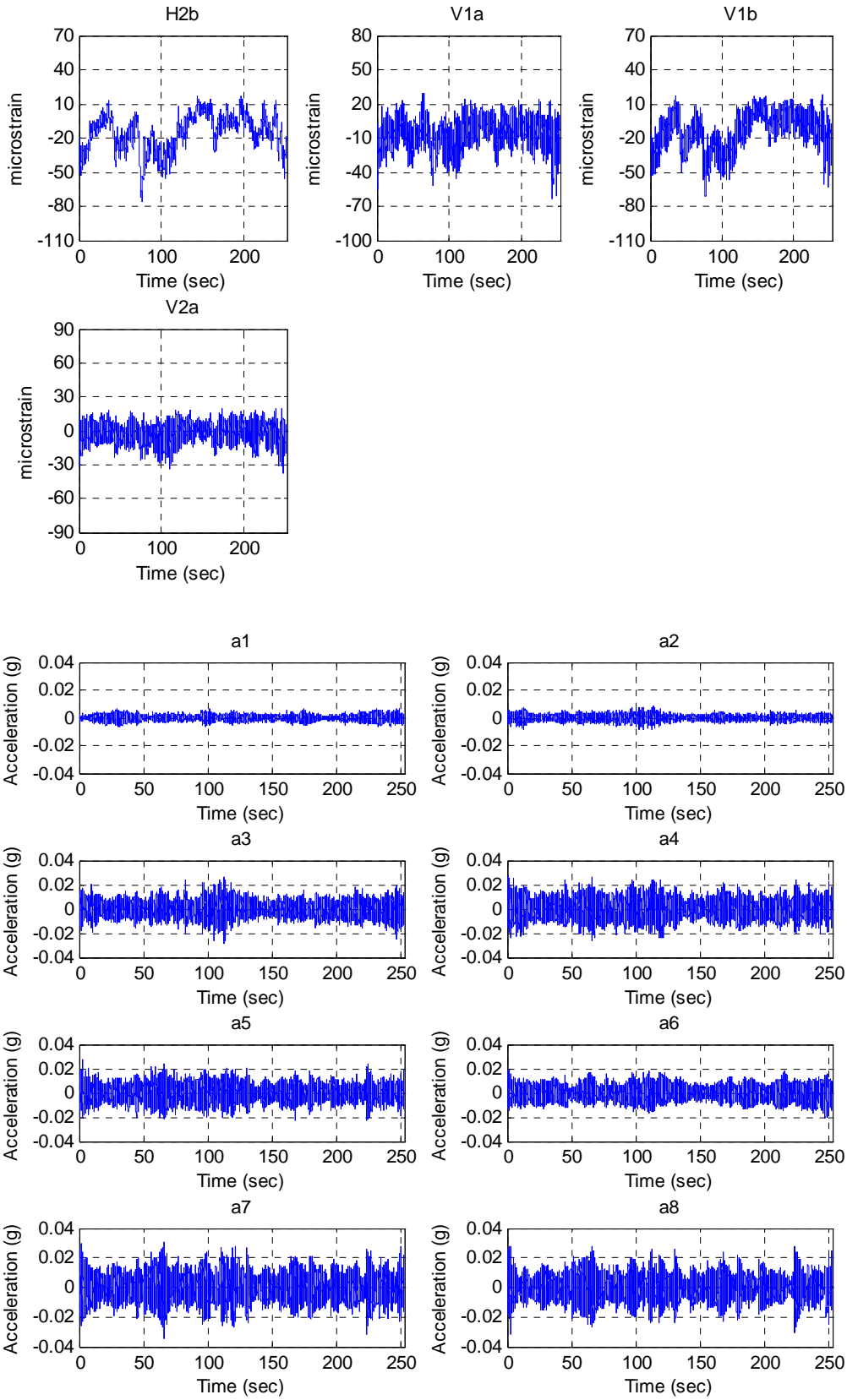
**Test W3**  
**Data\III-A\III-A W3.txt**



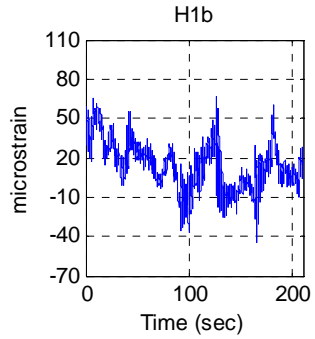
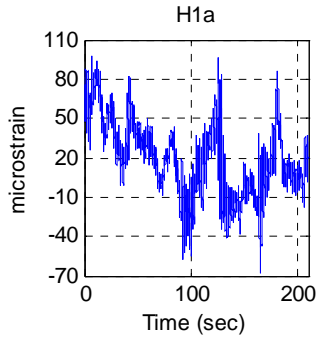
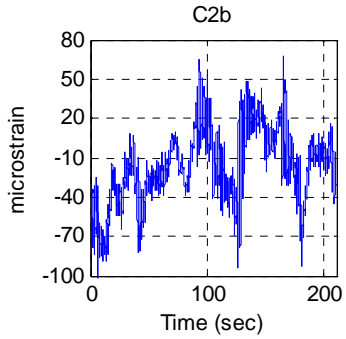
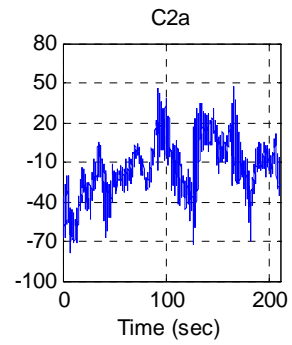
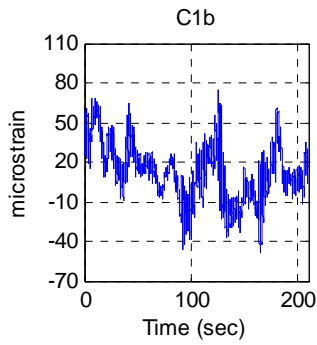
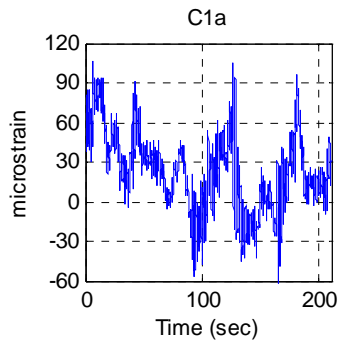
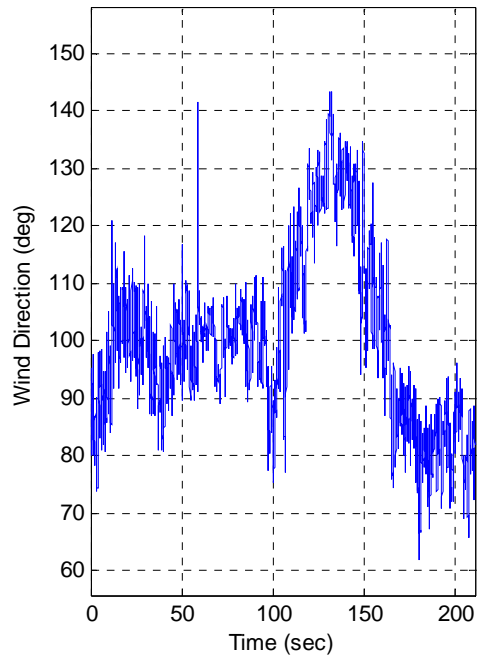
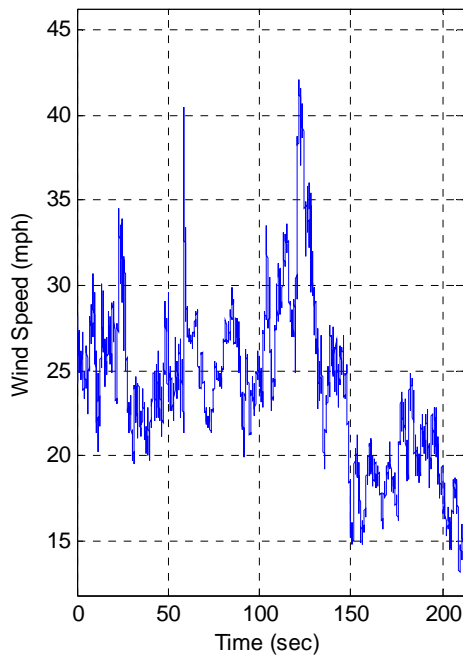


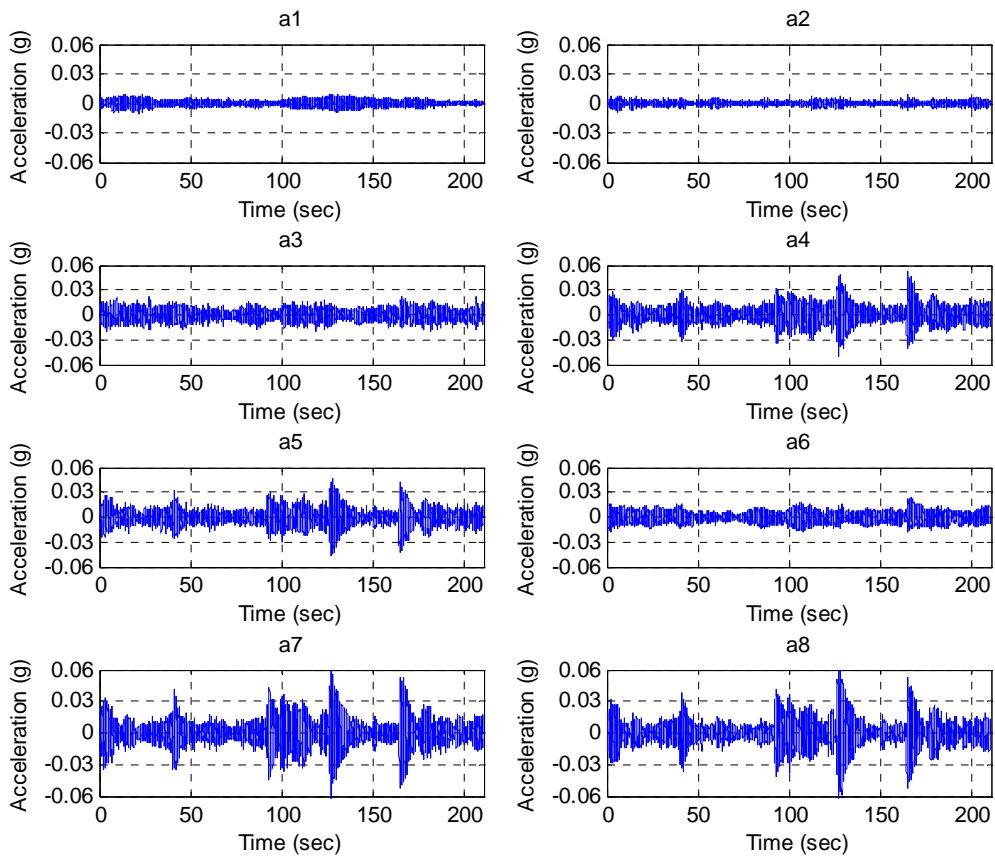
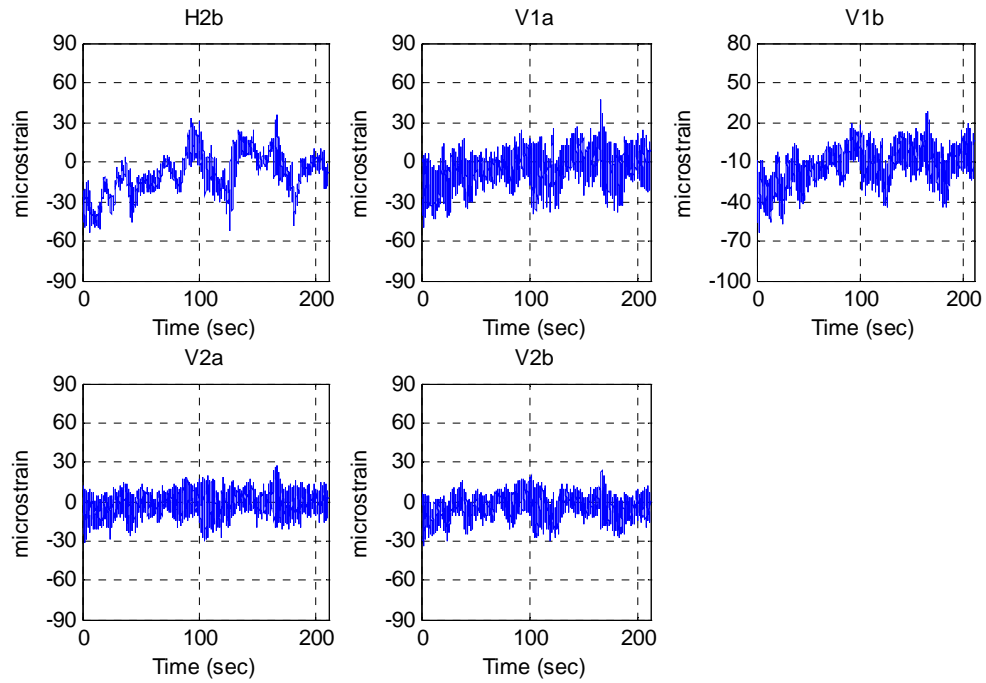
**Test W4**  
**Data\III-A\III-A W4.txt**



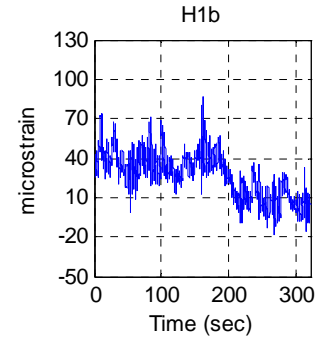
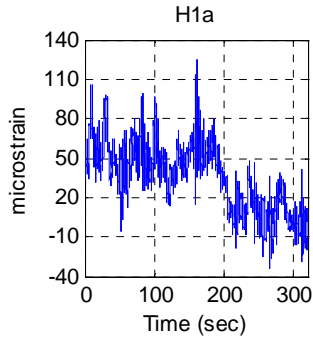
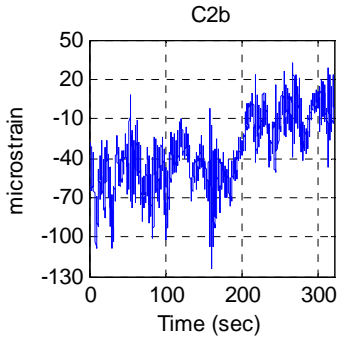
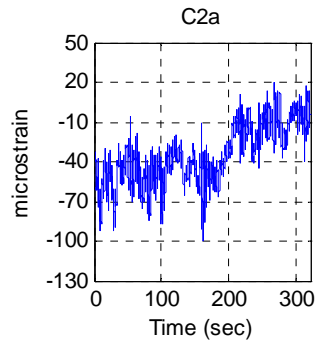
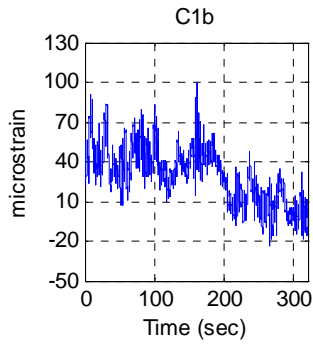
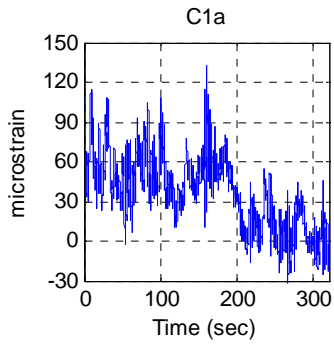
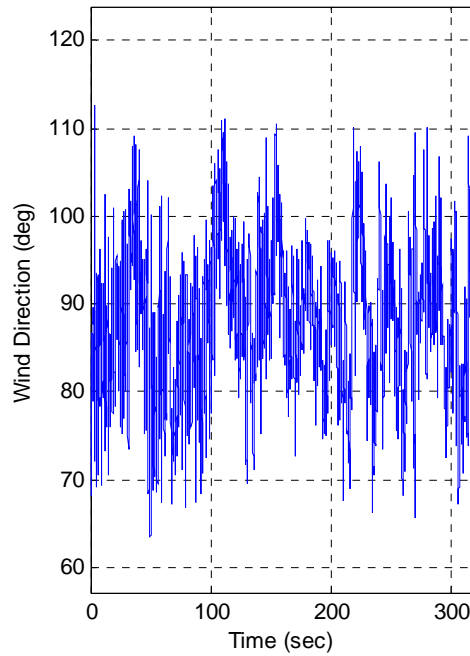
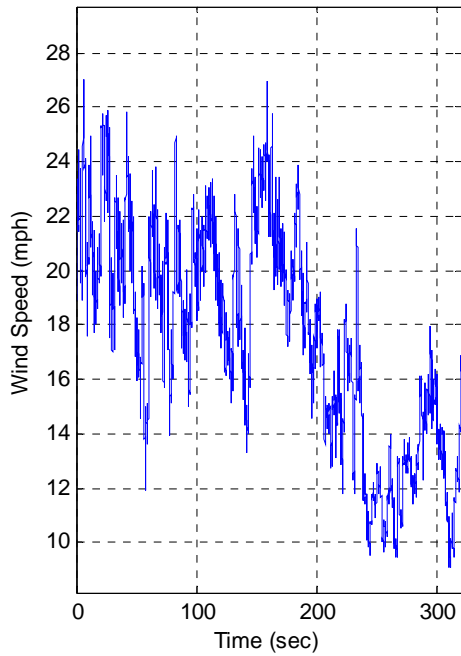


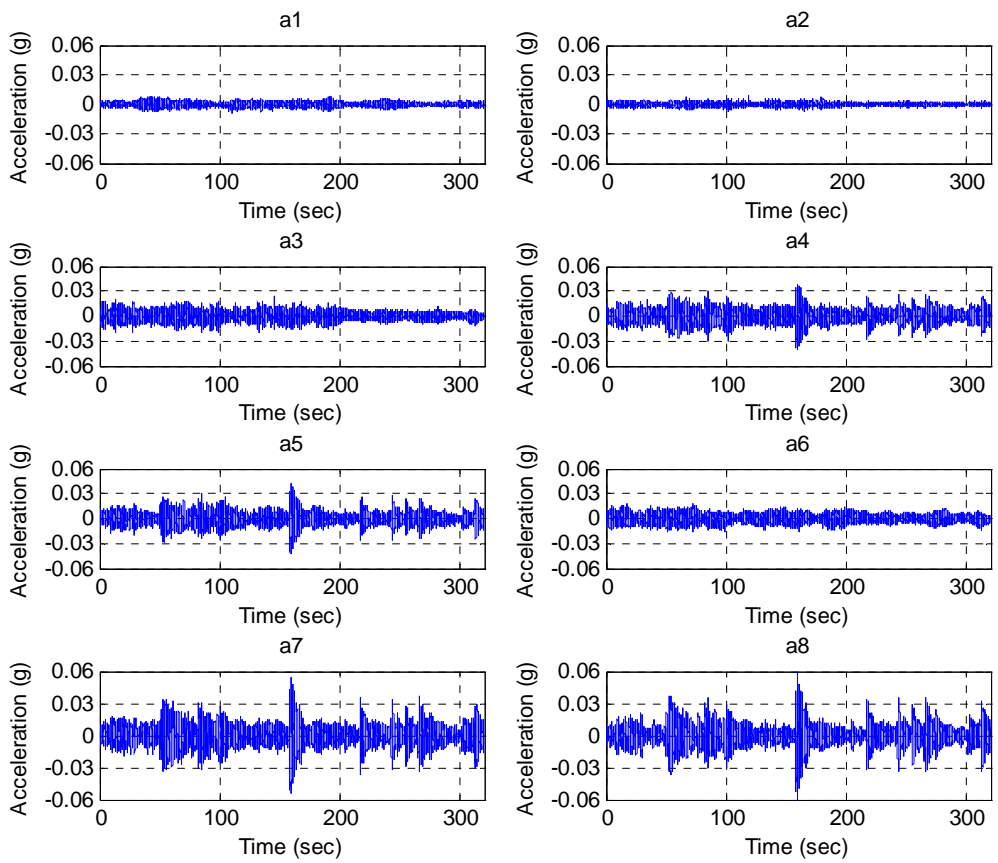
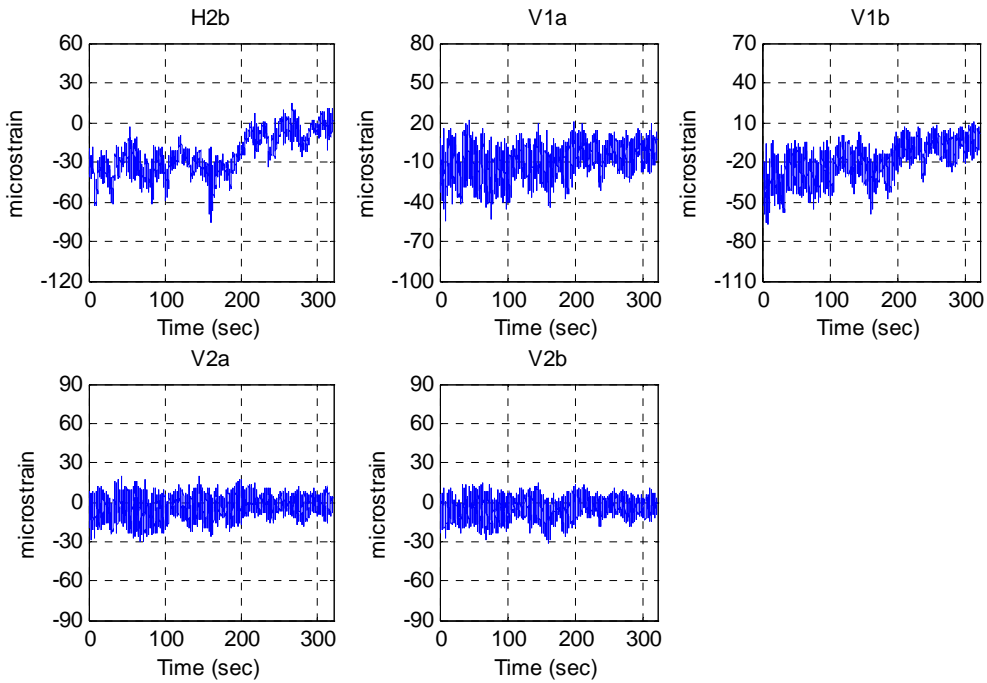
**Test W5**  
**Data\III-A\III-A W5.txt**



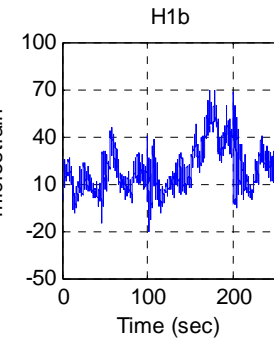
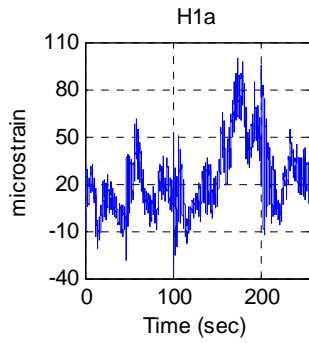
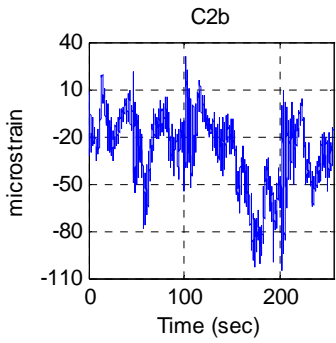
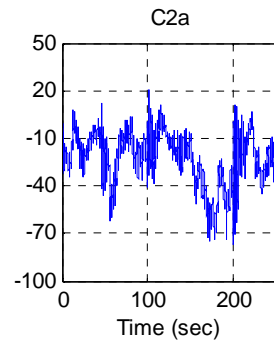
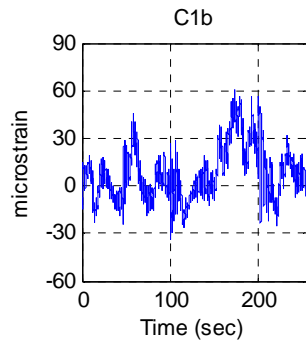
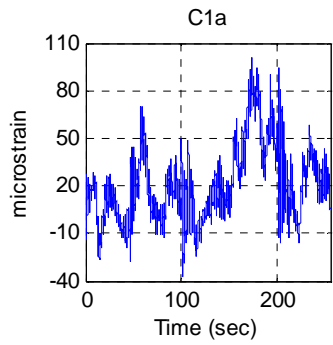
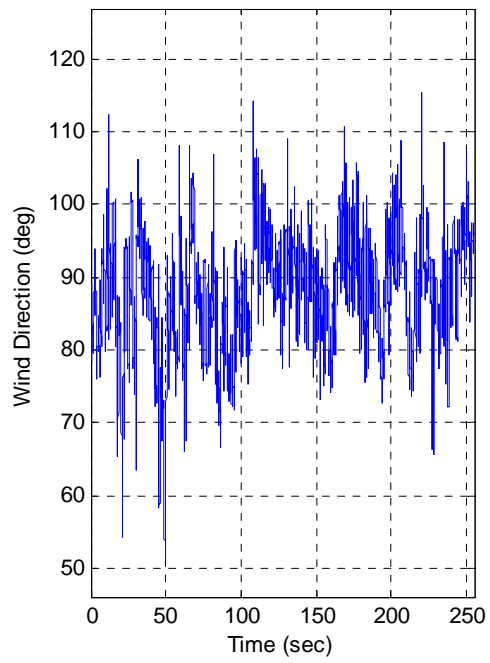
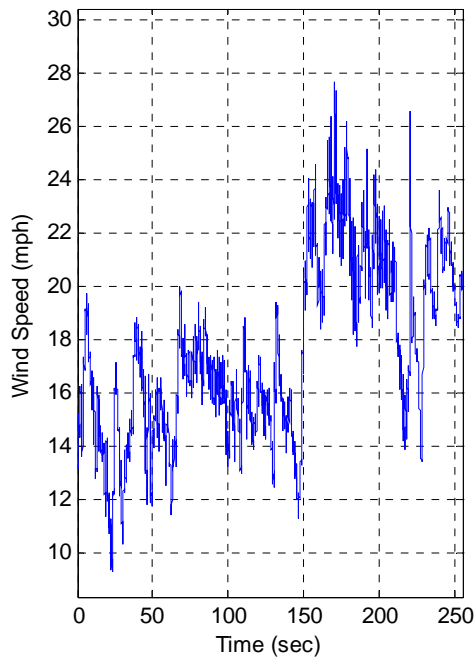


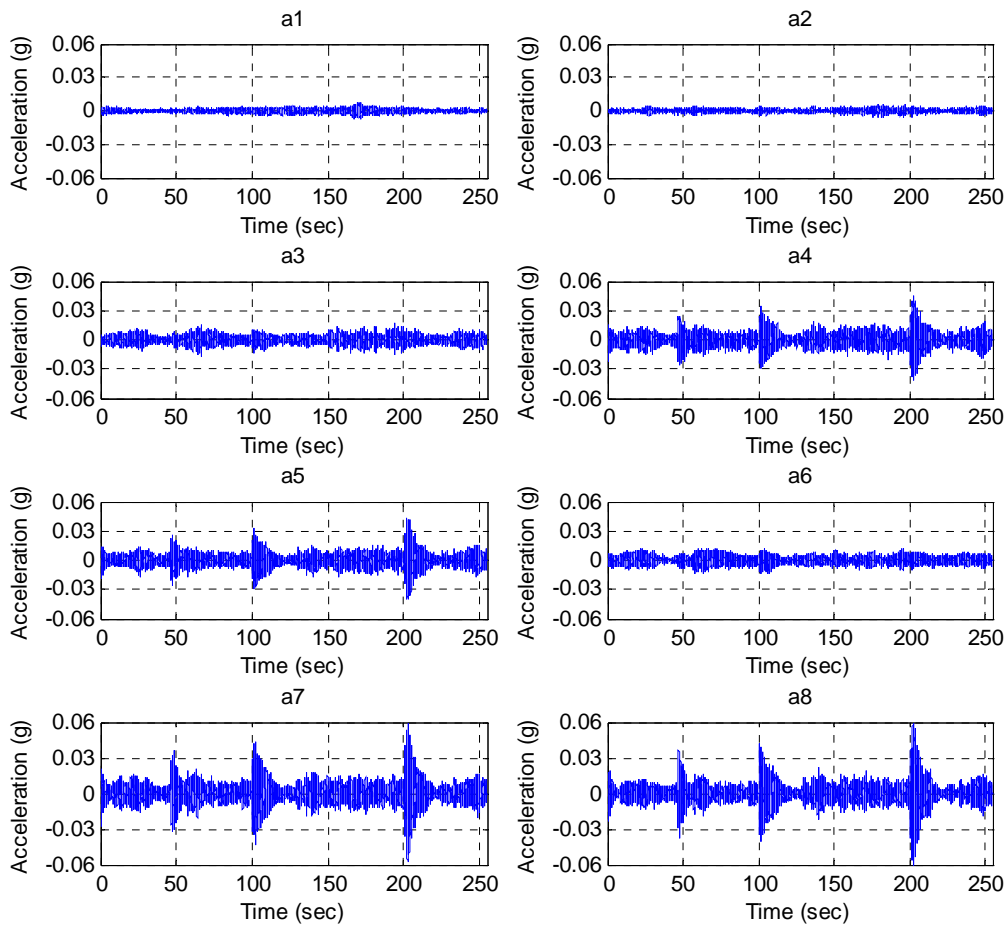
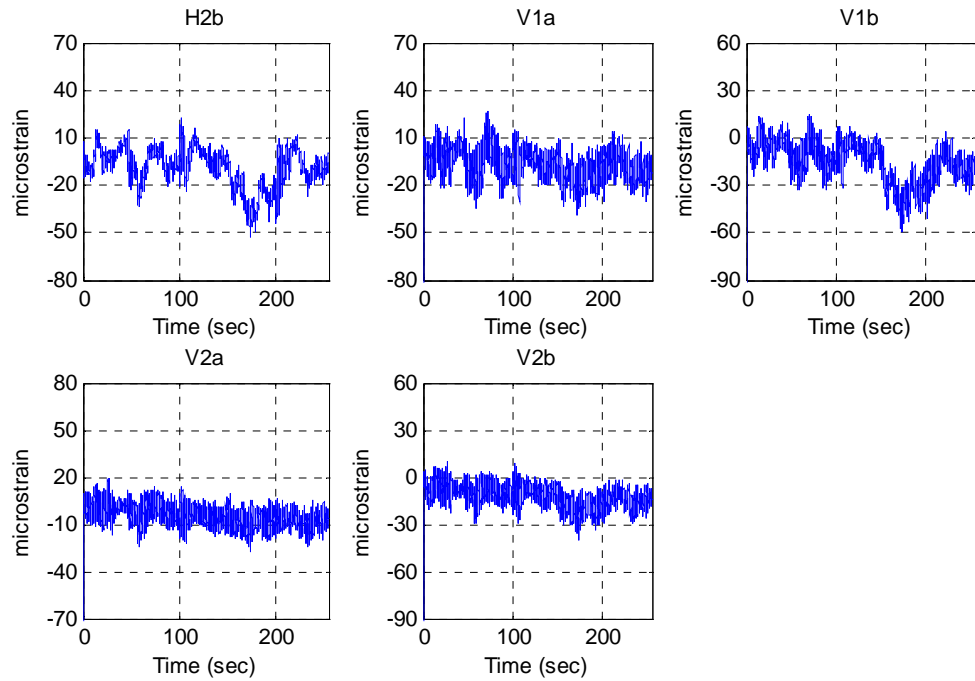
**Test W6**  
**Data\III-A\III-A W6.txt**



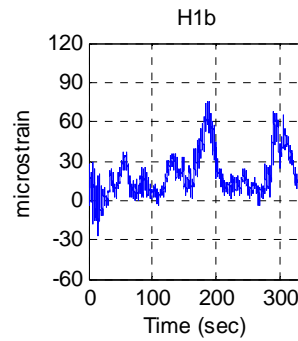
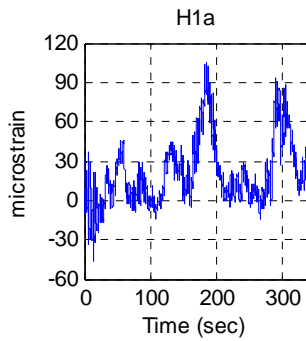
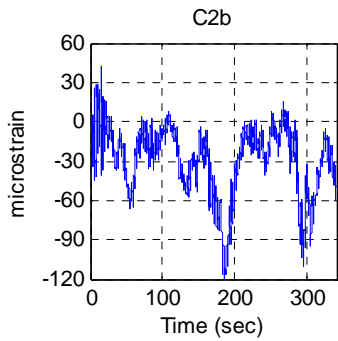
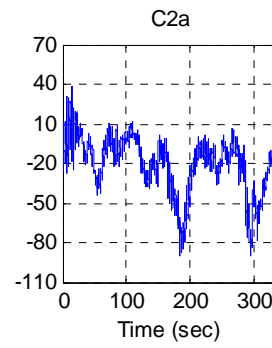
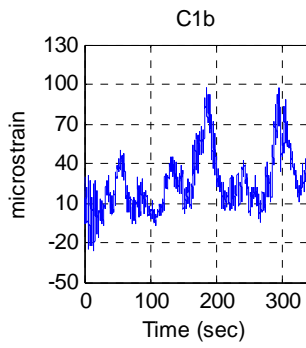
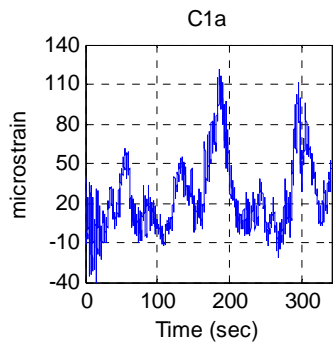
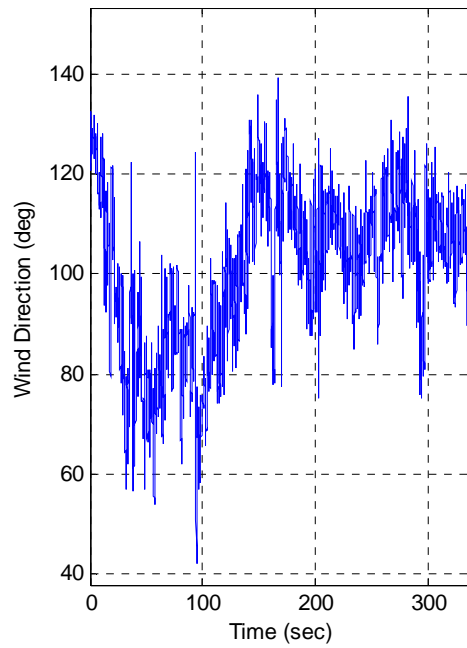
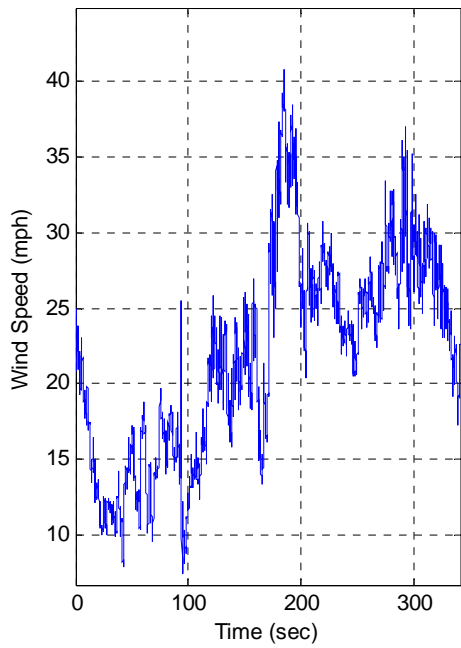


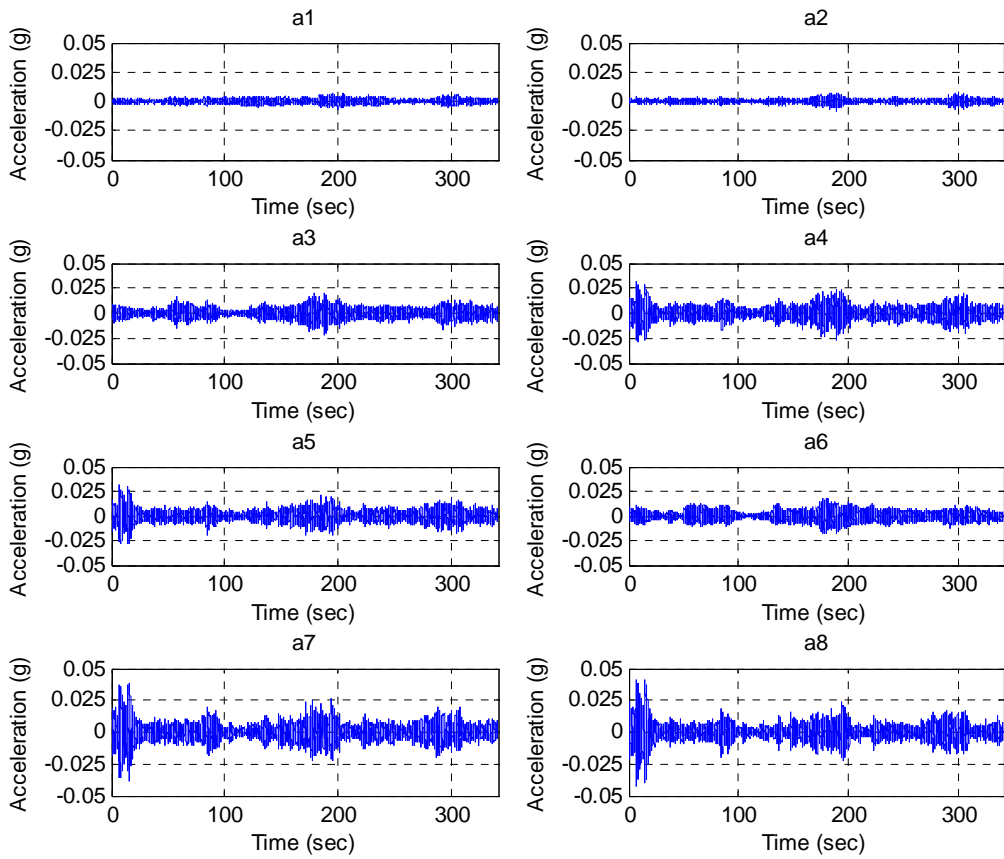
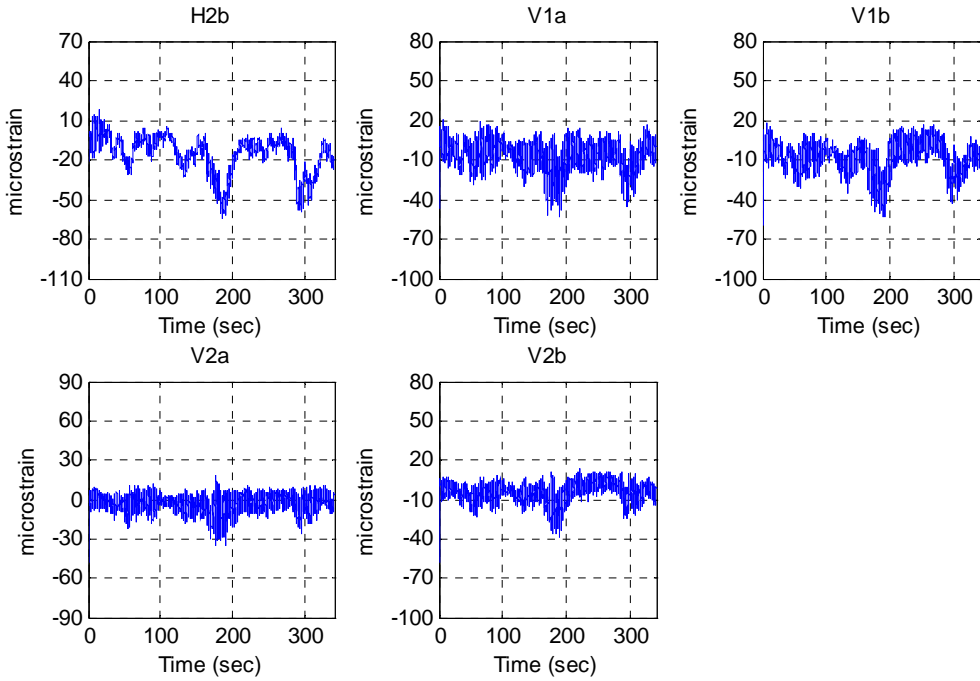
**Test W7**  
**Data\III-A\III-A W7.txt**



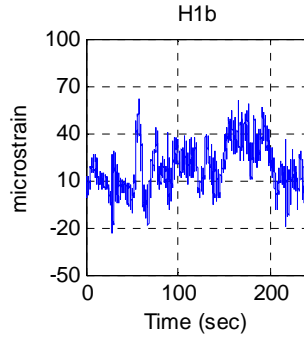
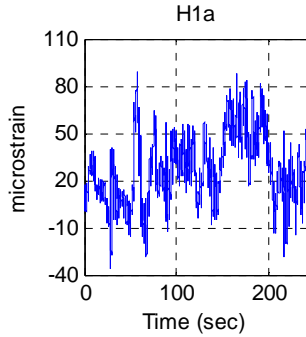
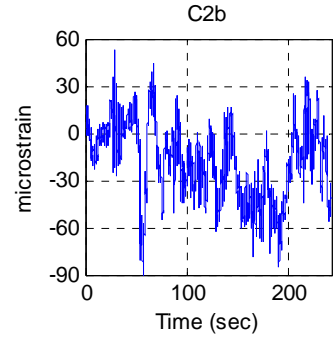
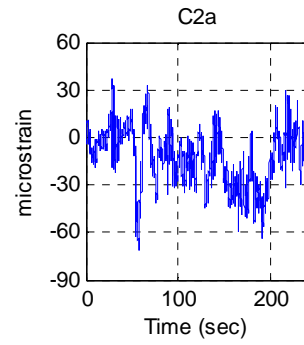
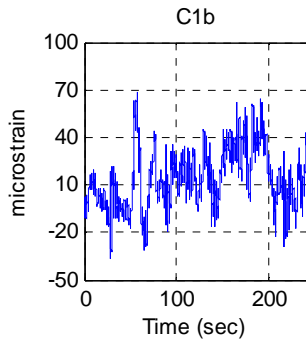
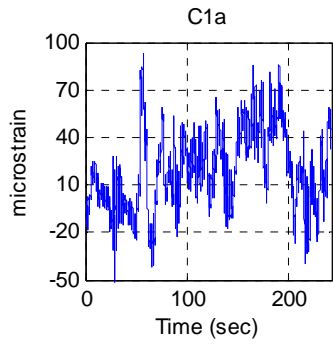
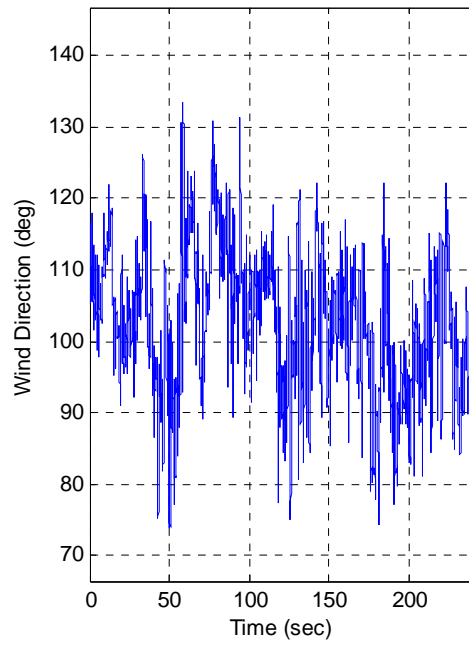
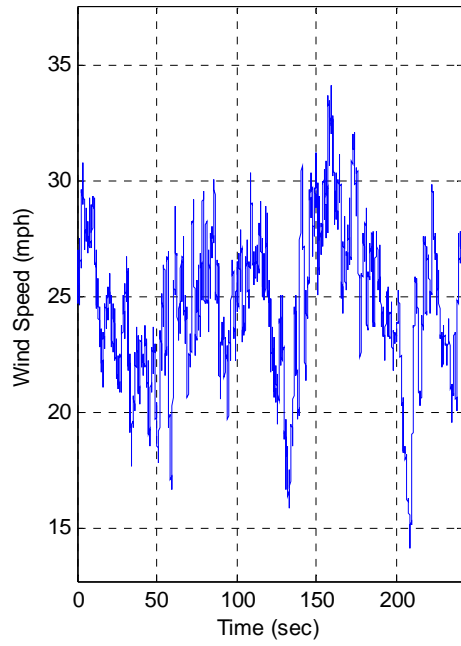


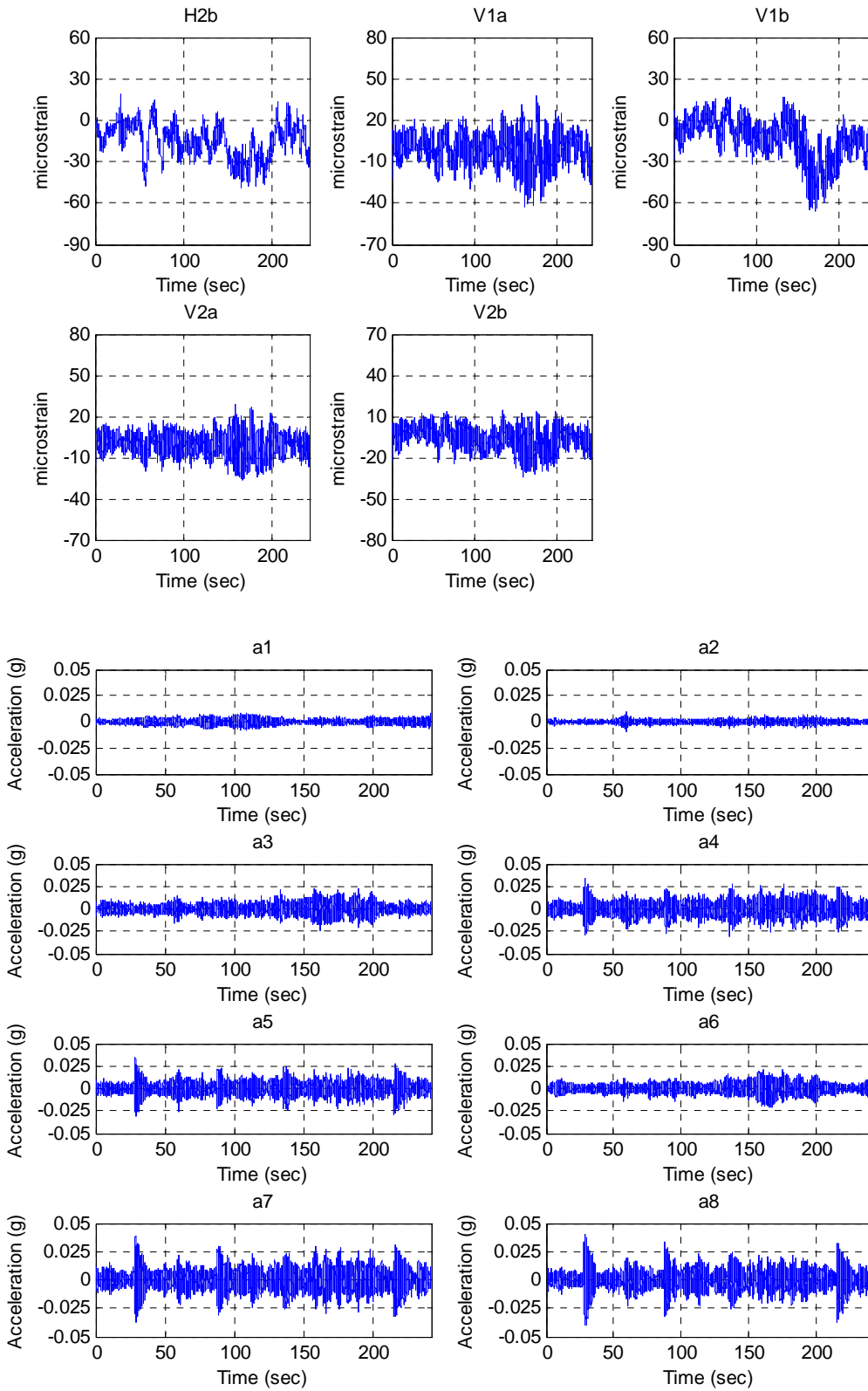
**Test W8**  
**Data\III-A\III-A W8.txt**



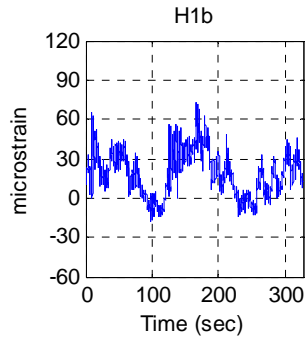
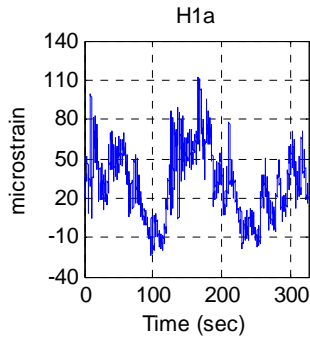
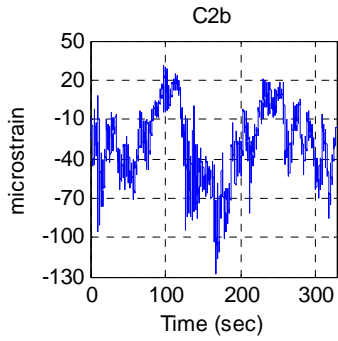
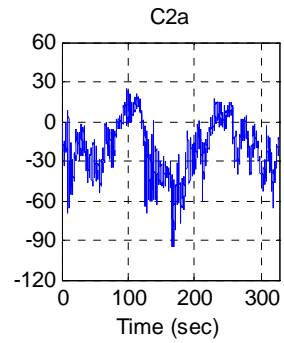
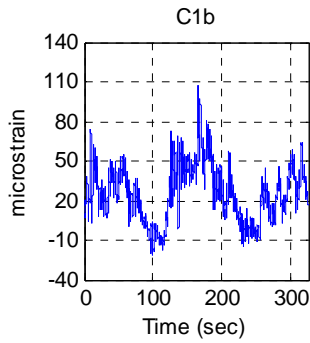
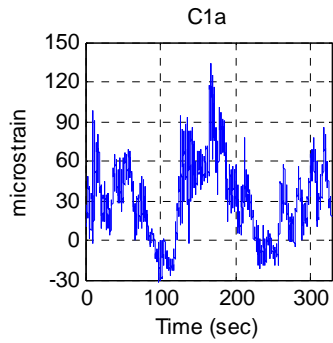
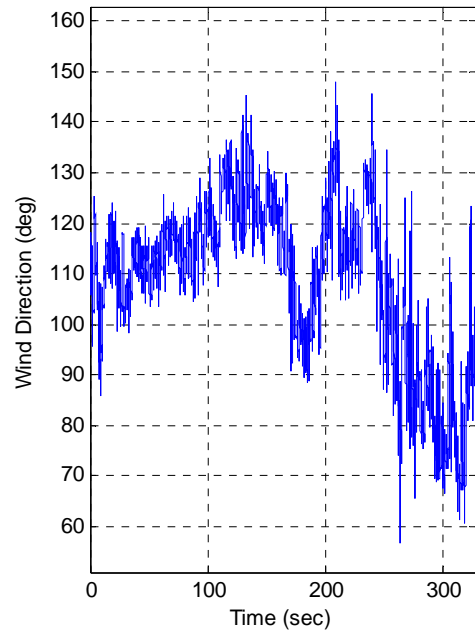
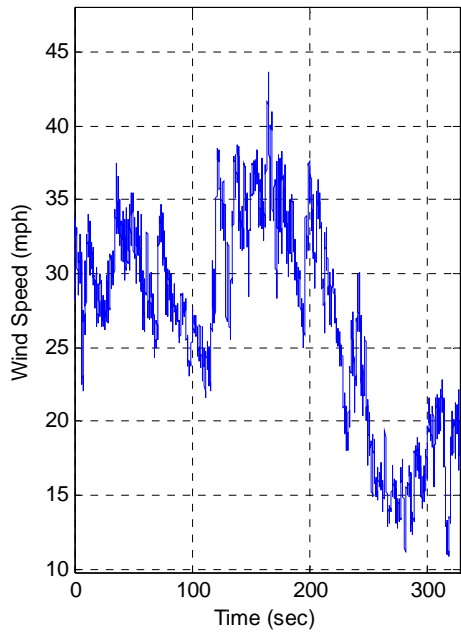


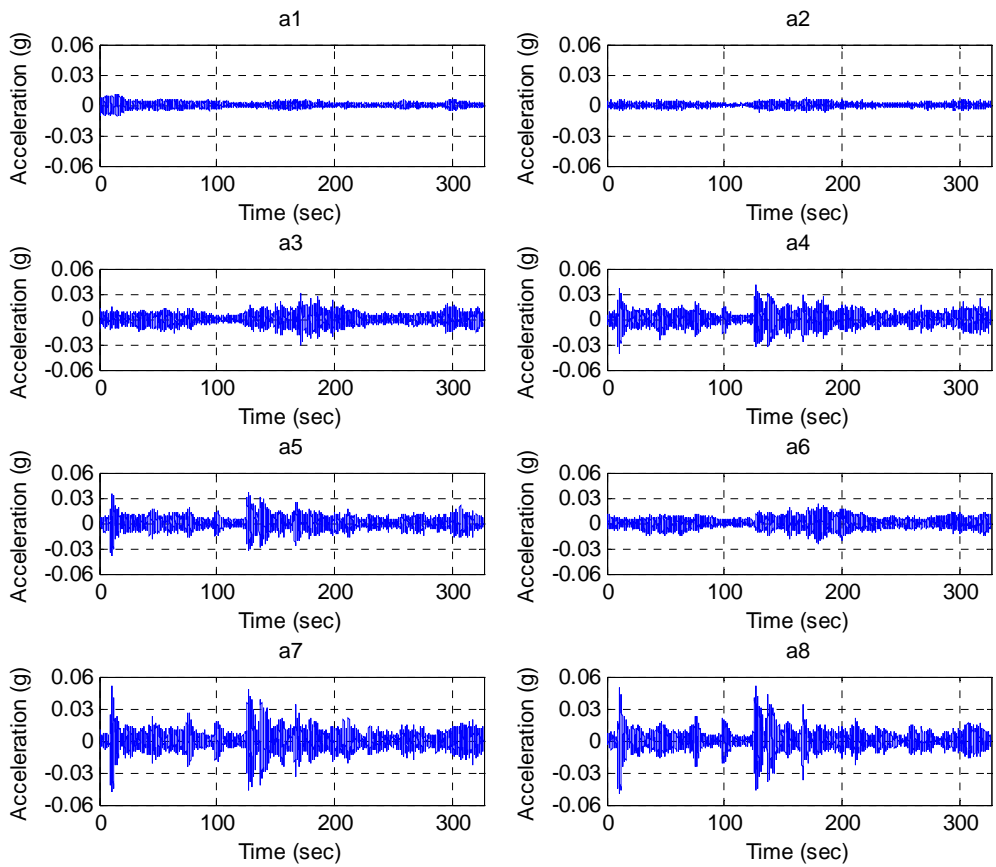
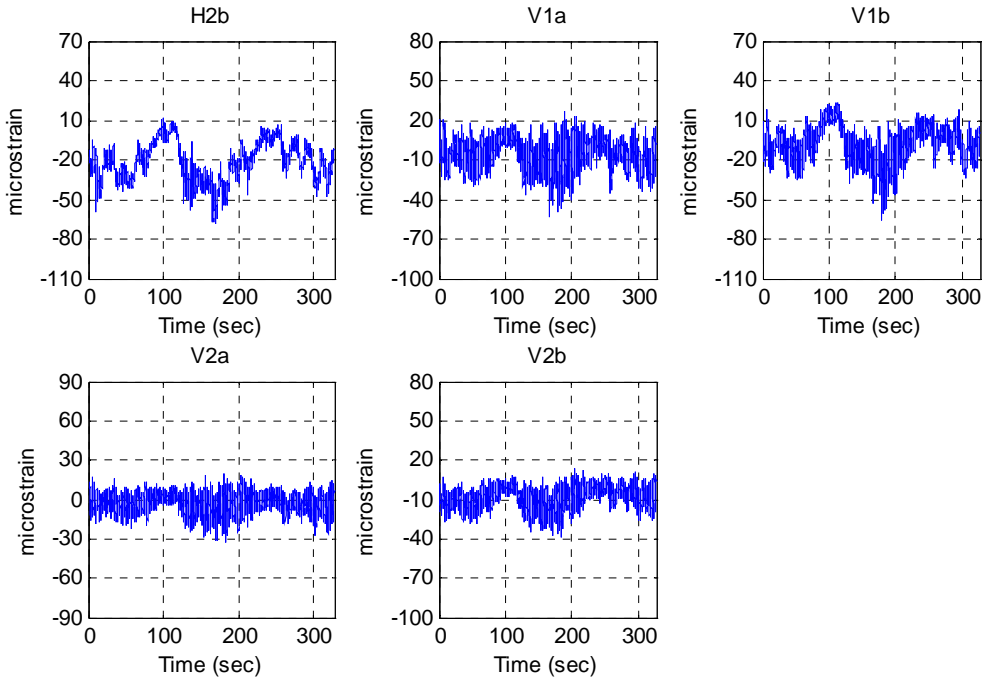
**Test W9**  
**Data\III-A\III-A W9.txt**





**Test W10**  
Data\III-A\III-A\_W10.txt





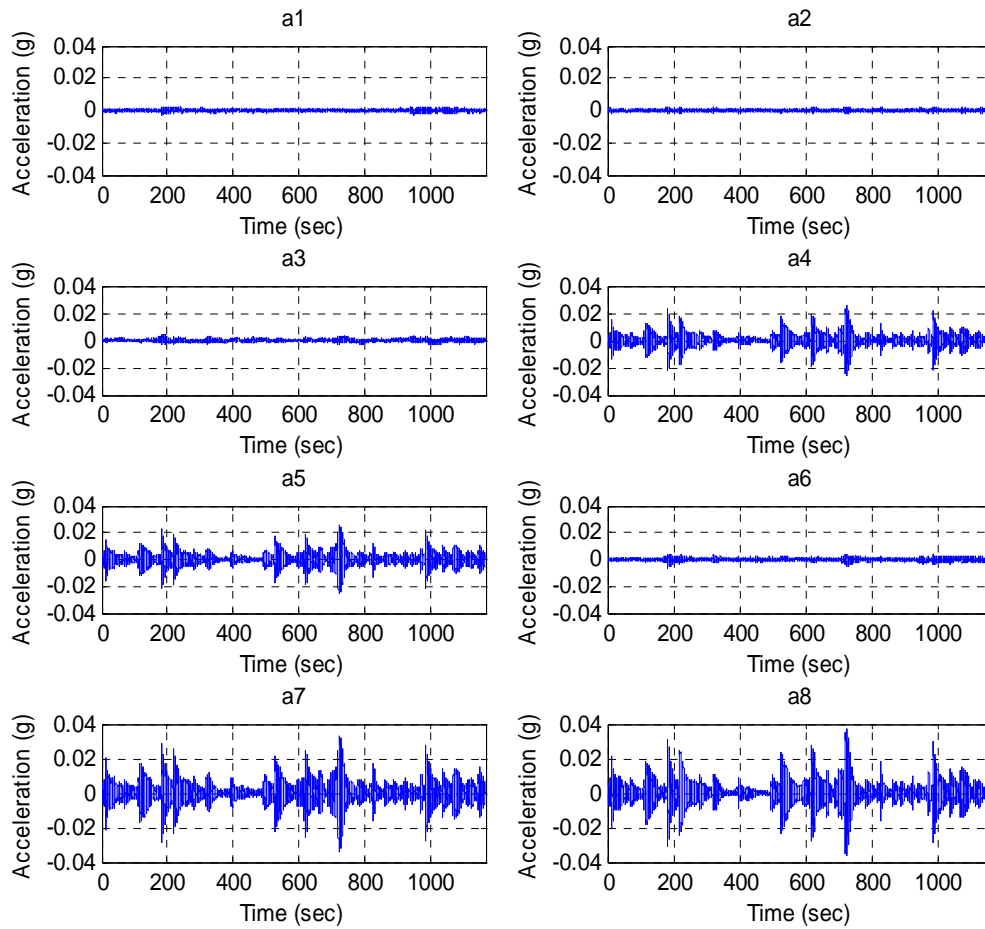
## A4.4 Truck Gust Data

The data structure for the truck gust data is as follows:

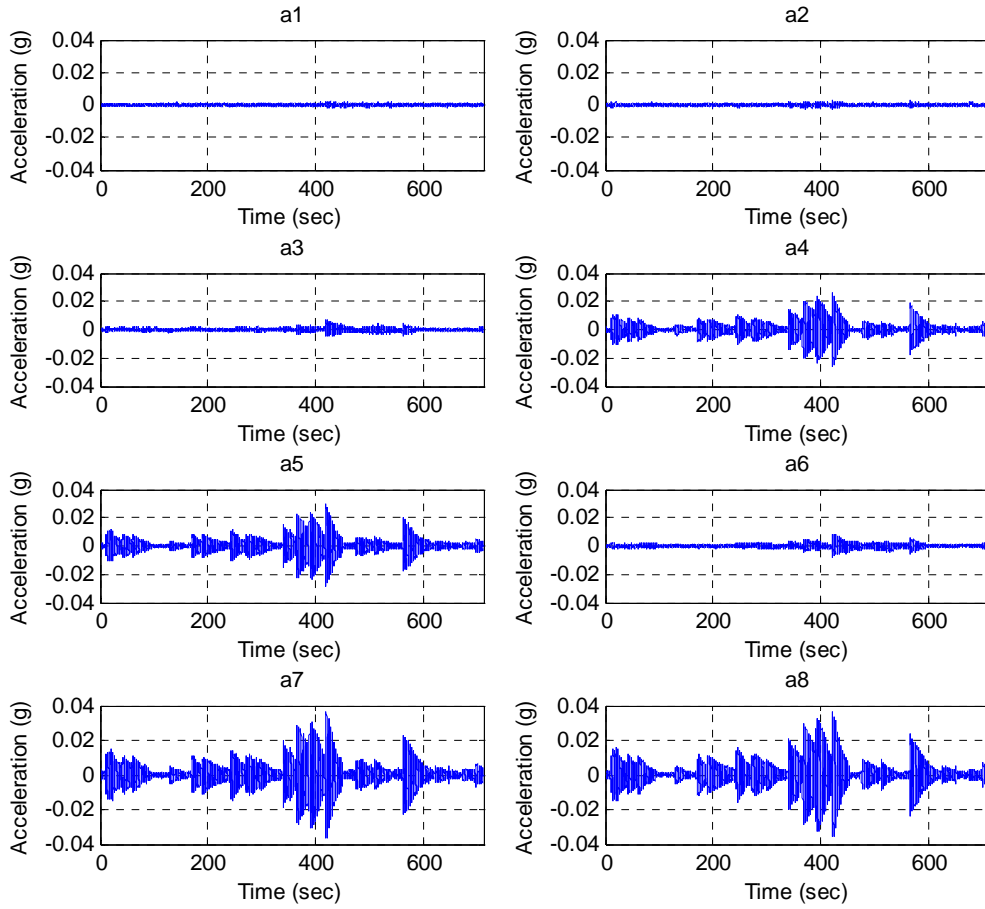
Time (sec), a1, a2, a3, a4, a5, a6, a7, a8

### Test TG1

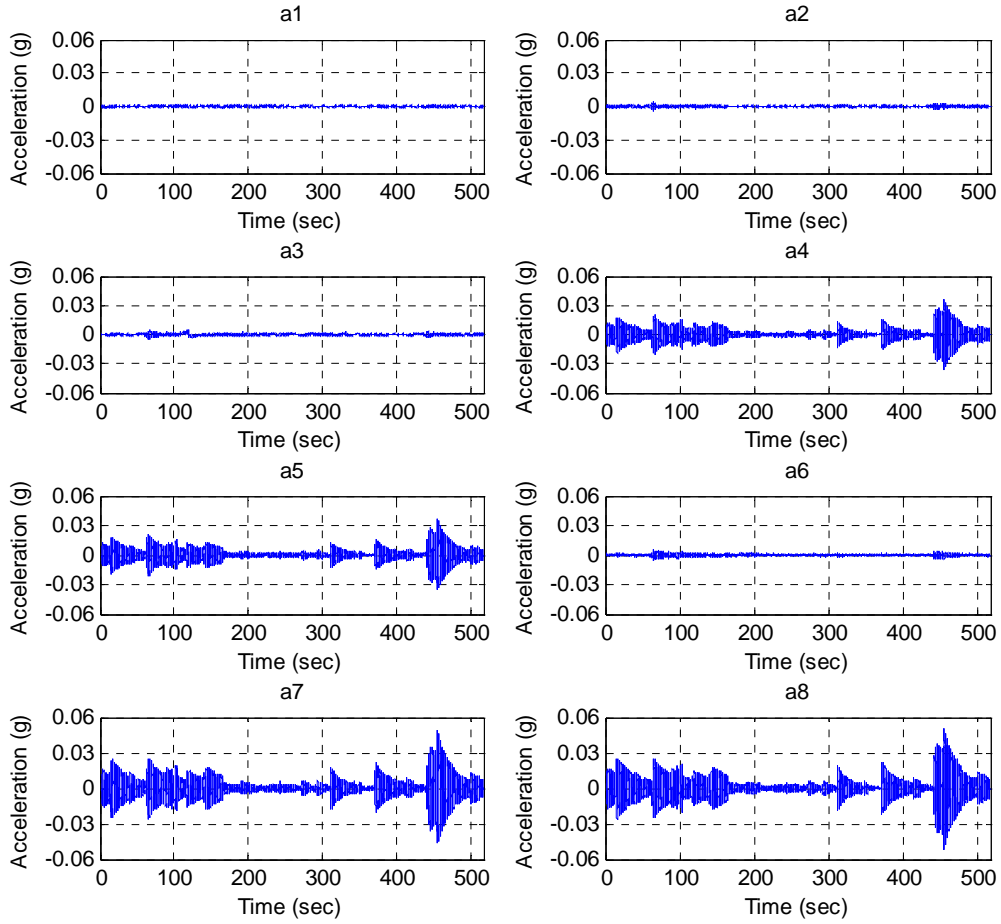
[Data\III-A\III-A TG1.txt](#)



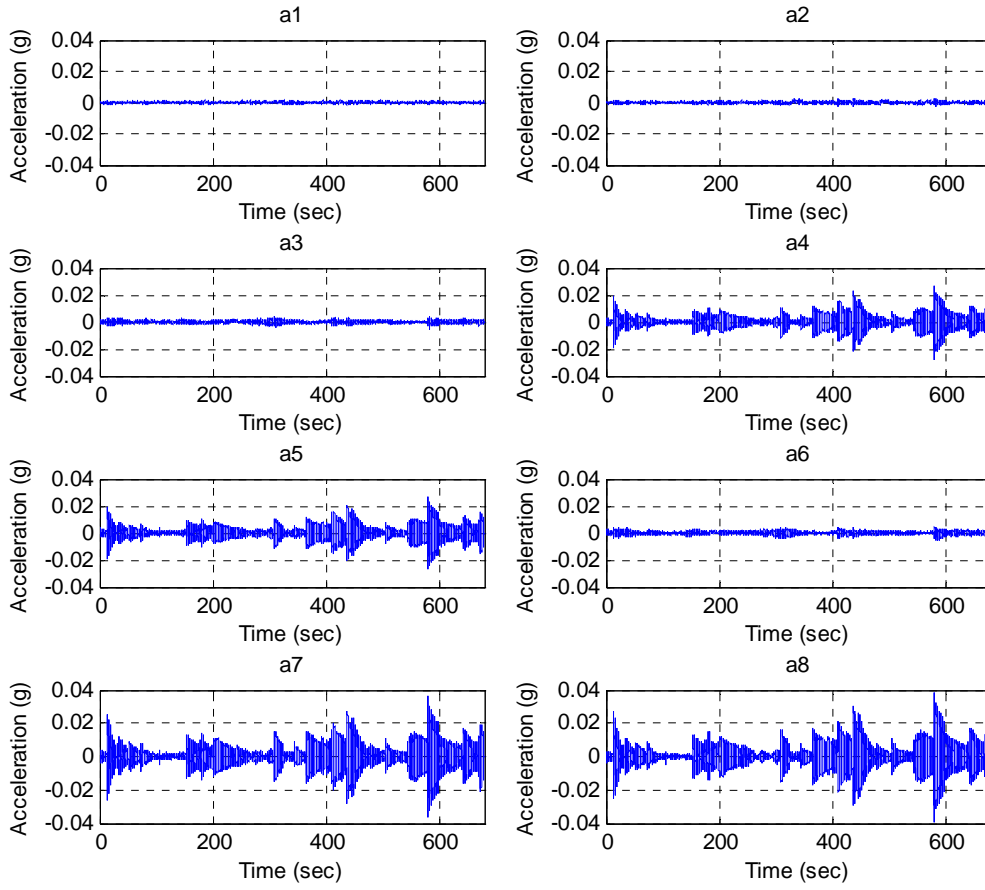
**Test TG2**  
Data\III-A\III-A TG2.txt



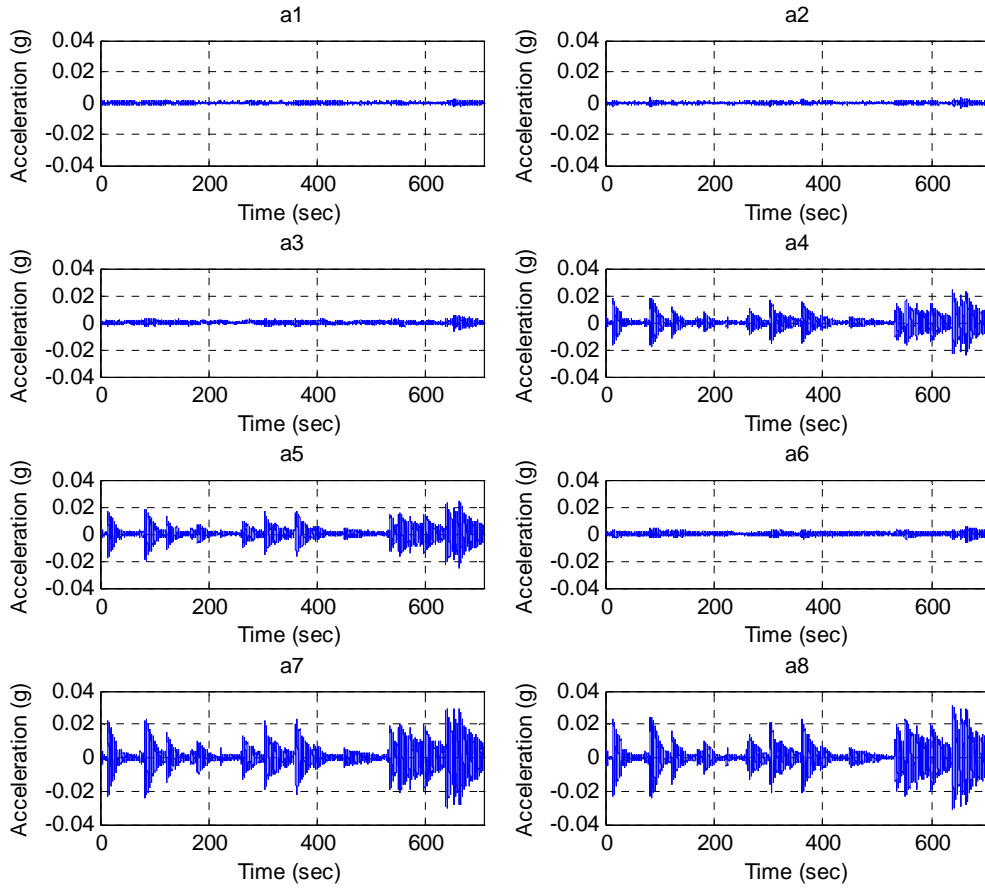
**Test TG3**  
Data\III-A\III-A TG3.txt



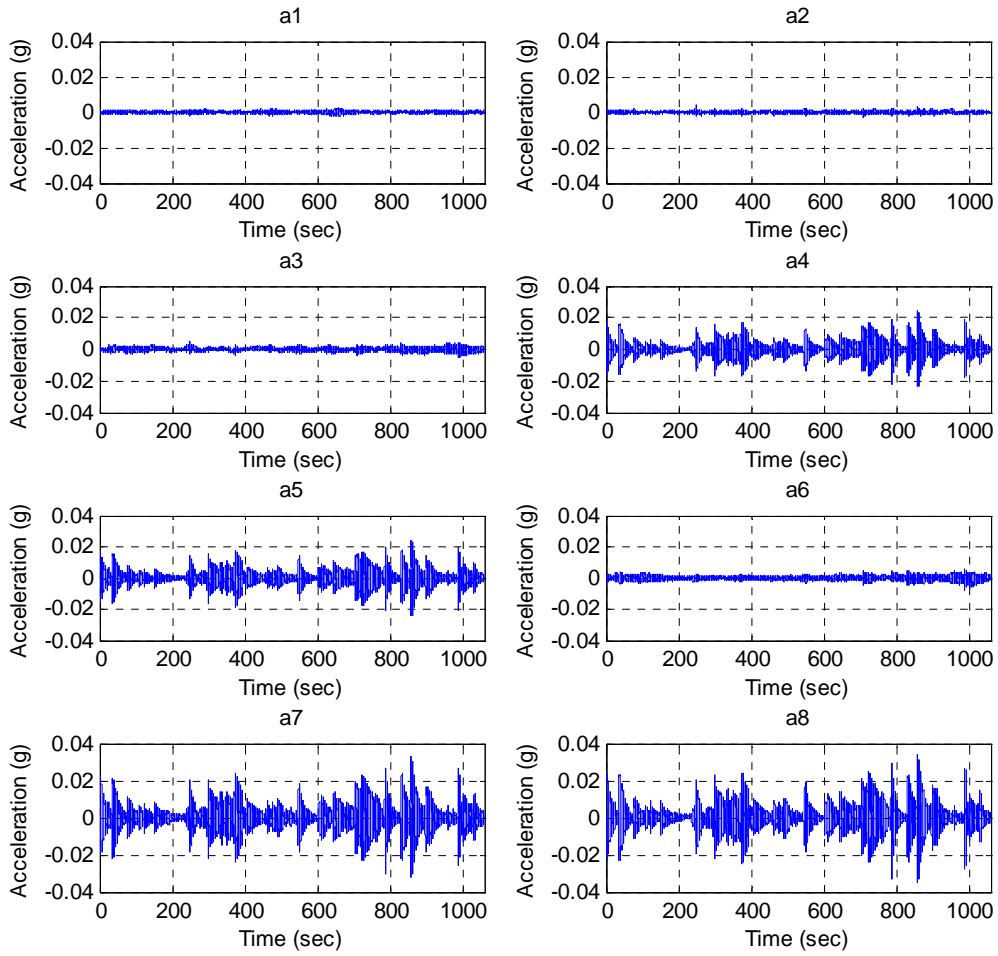
**Test TG4**  
Data\III-A\III-A TG4.txt



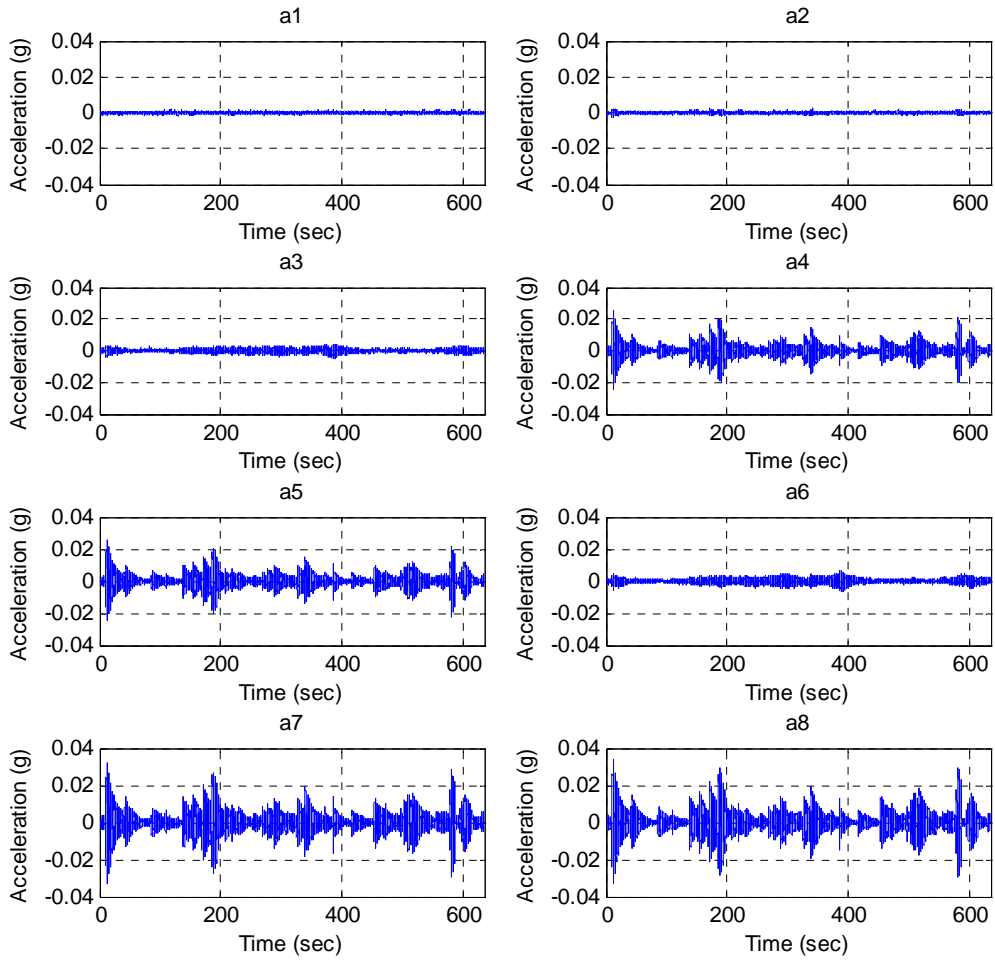
**Test TG5**  
Data\III-A\III-A TG5.txt



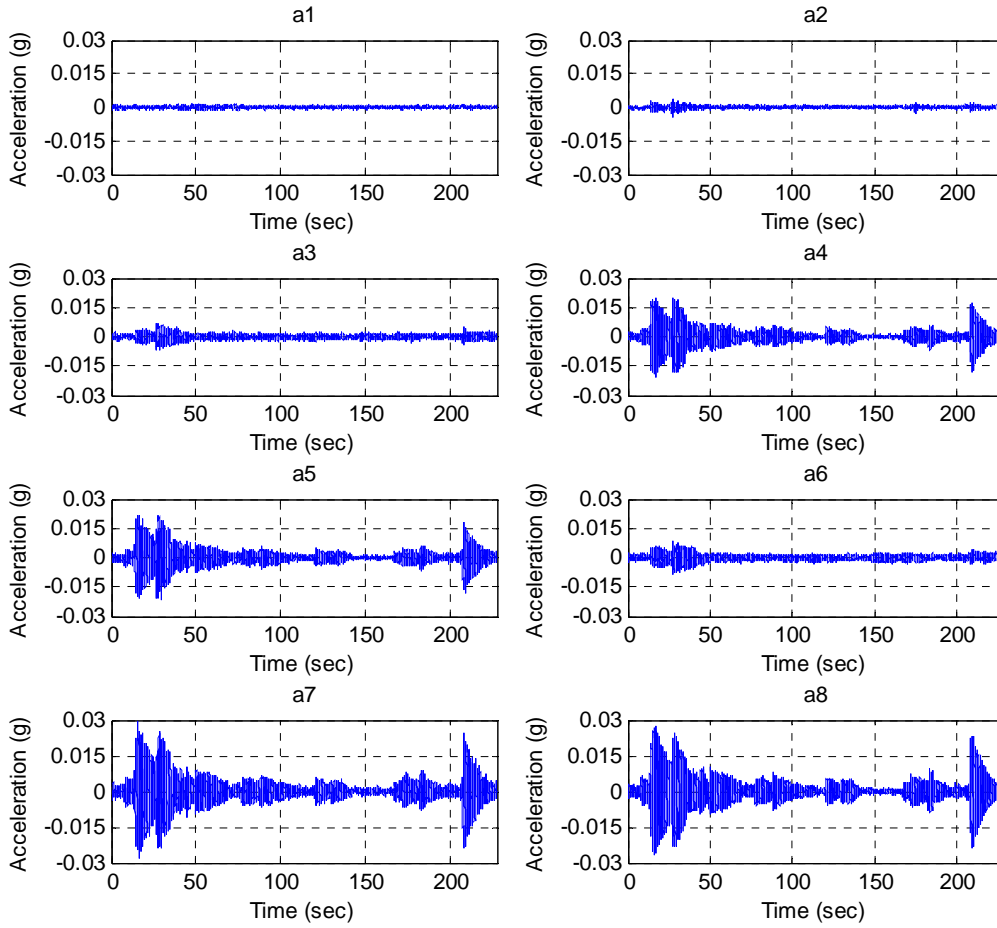
**Test TG6**  
Data\III-A\III-A TG6.txt



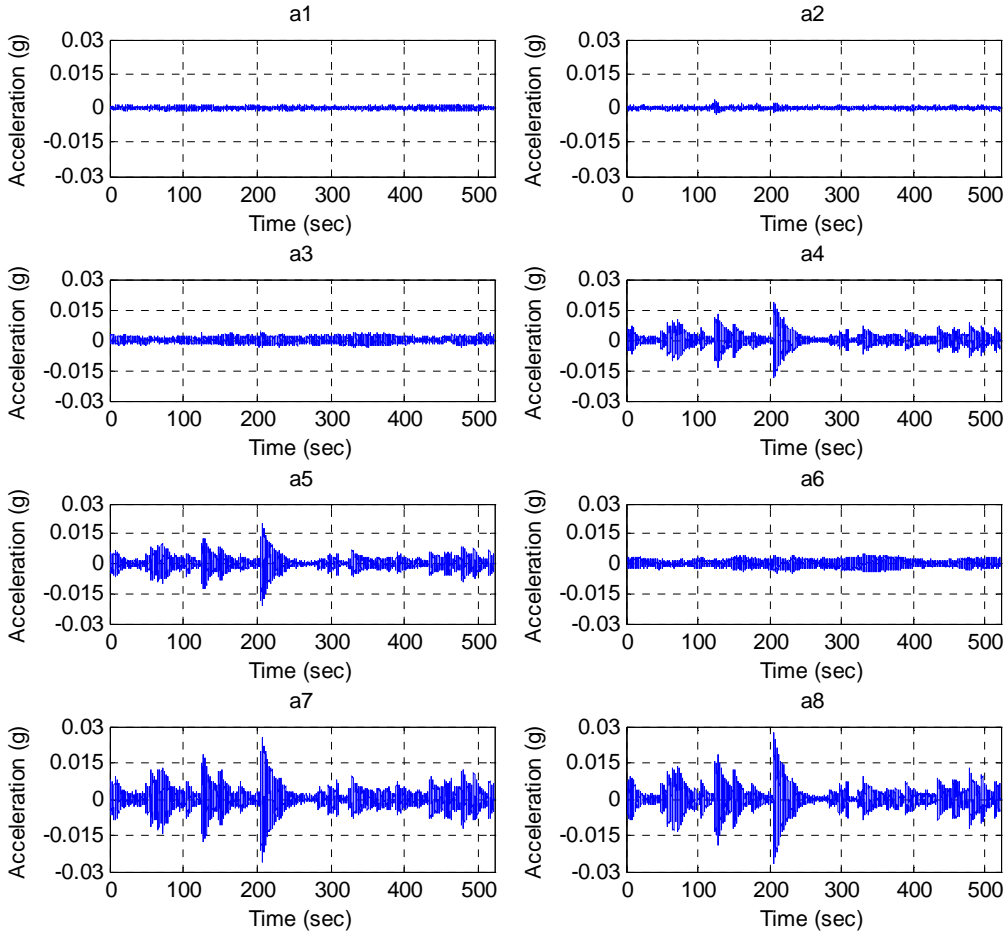
**Test TG7**  
Data\III-A\III-A TG7.txt



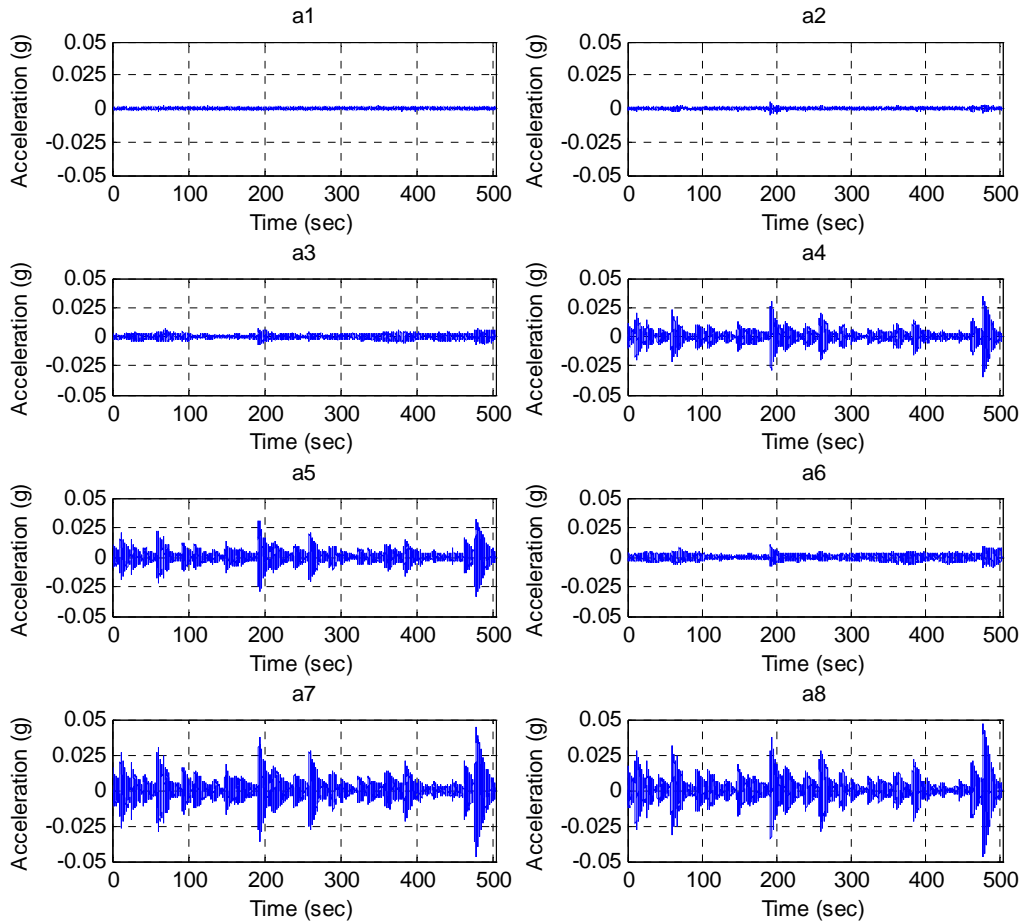
**Test TG8**  
Data\III-A\III-A TG8.txt



**Test TG9**  
Data\III-A\III-A TG9.txt



**Test TG10**  
**Data\III-A\III-A TG10.txt**



#### A4.5 Manual Excitation Data

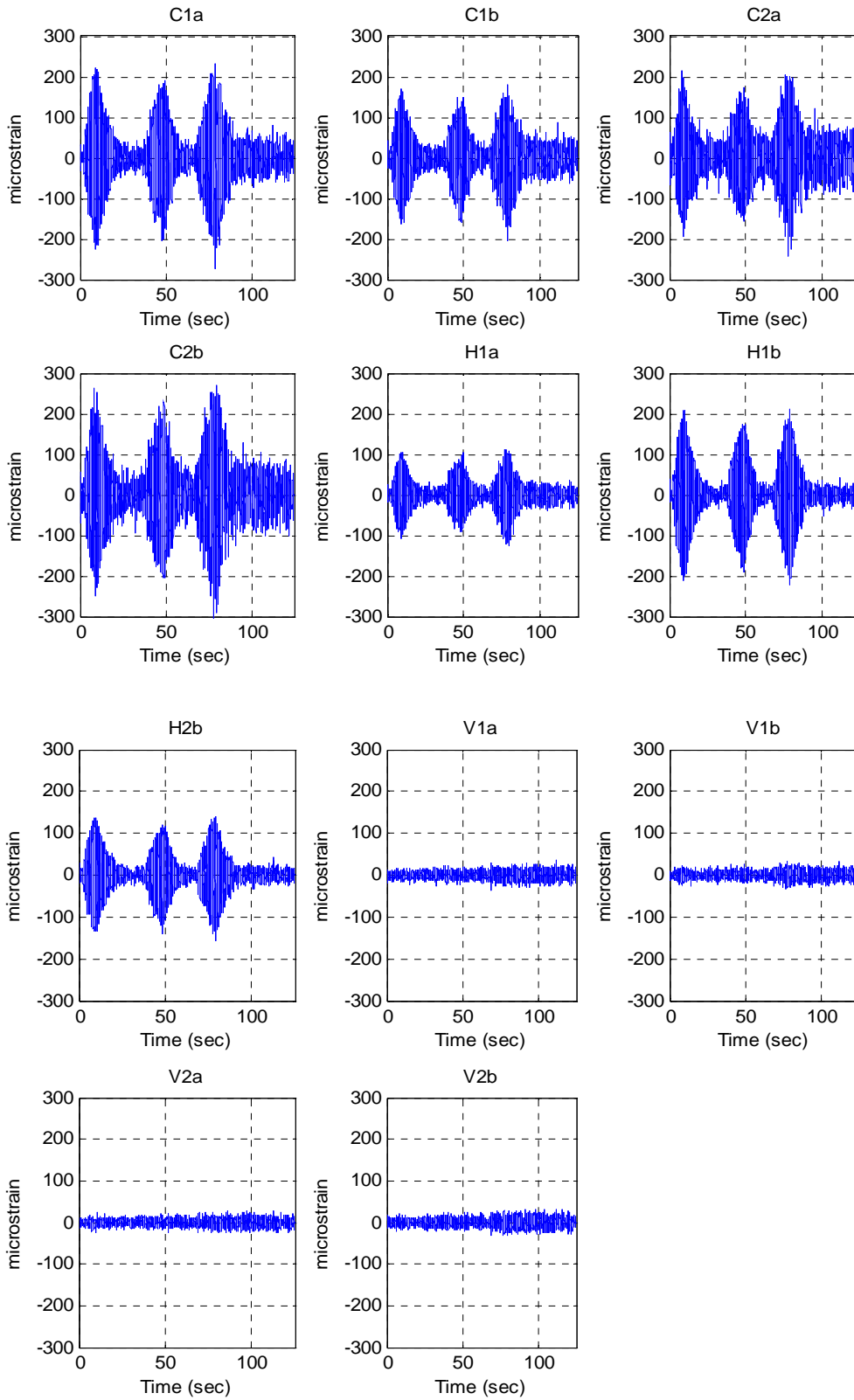
The data structure for the manual excitation data is as follows:

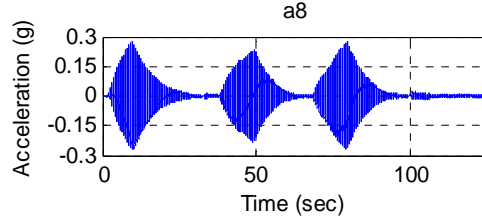
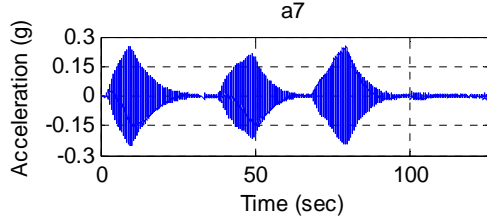
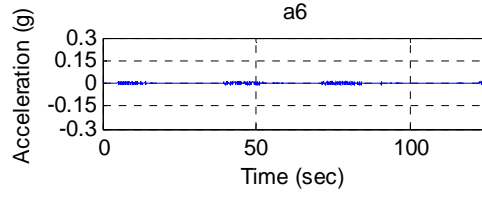
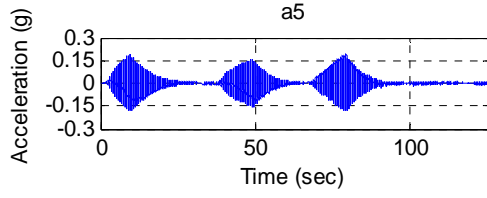
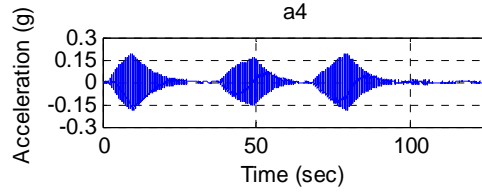
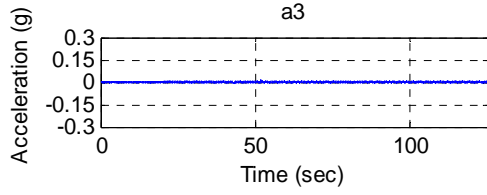
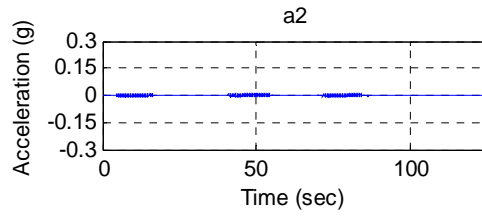
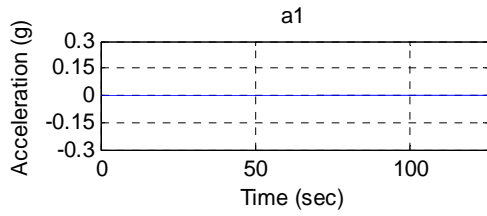
Time(sec), C1a, C1b, C2a, C2b, H1a, H1b, H2b, V1a, V1b, V2a, V2b, a1, a2, a3, a4, a5, a6, a7 a8

Test descriptions:

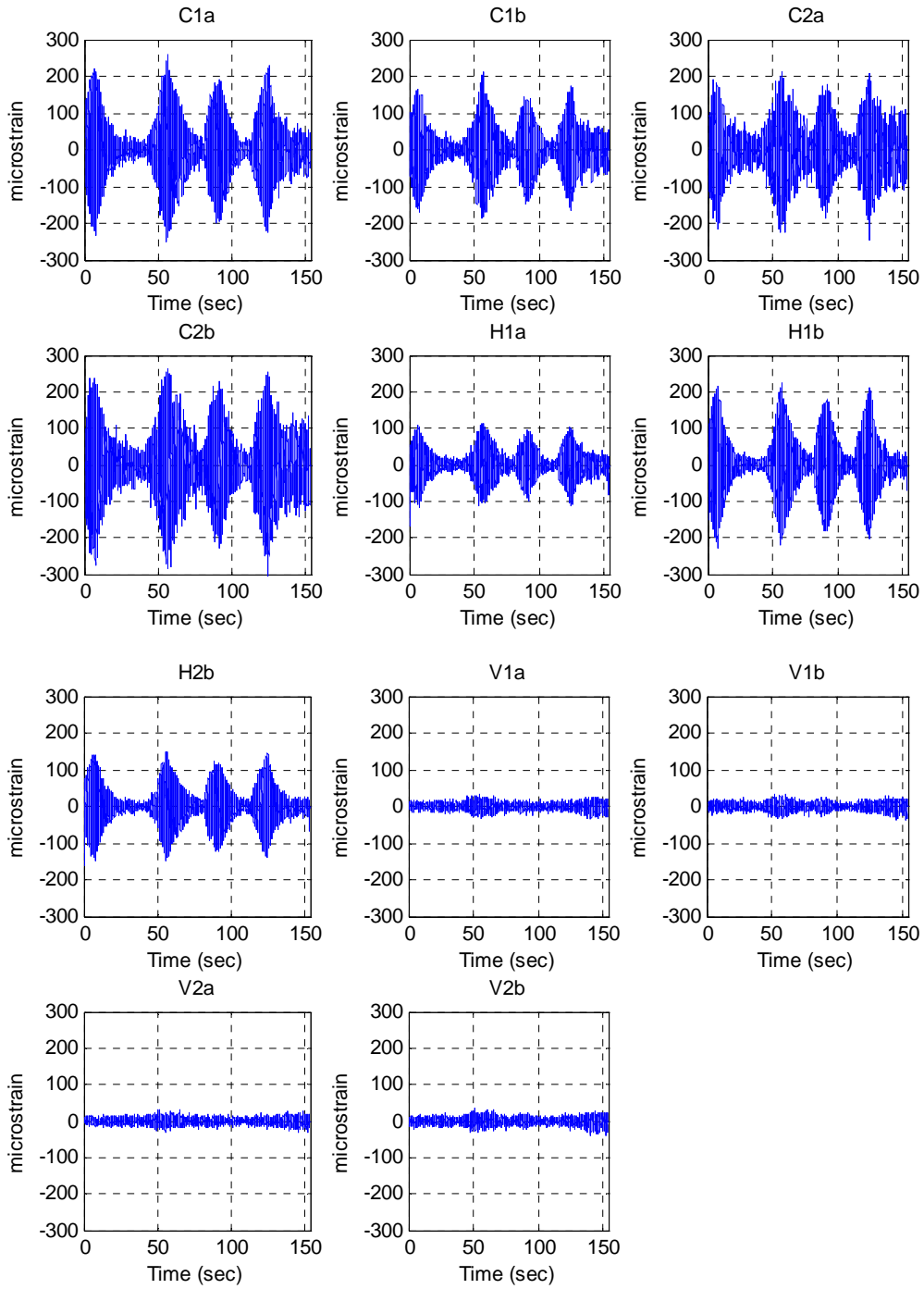
- M1 – horizontal excitation, damper disengaged
- M2 – horizontal excitation, damper engaged
- M3 – vertical excitation, damper disengaged
- M4 – vertical excitation, damper engaged

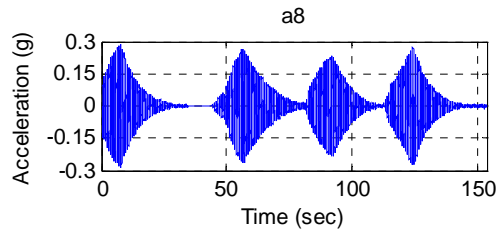
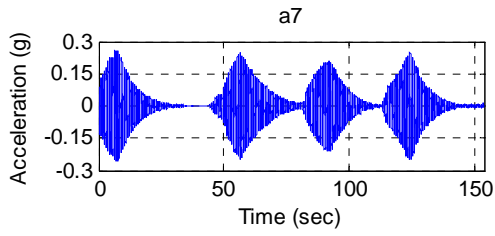
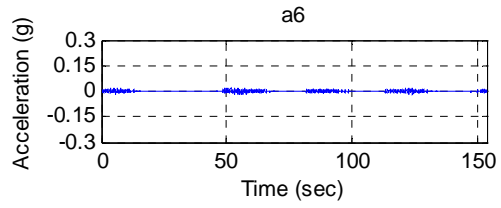
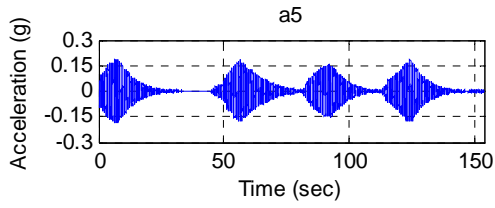
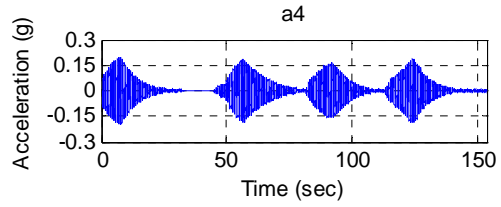
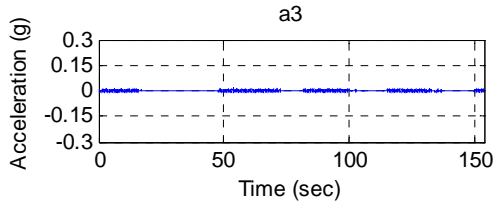
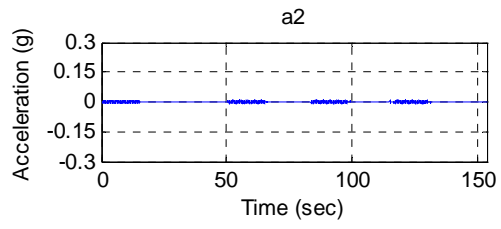
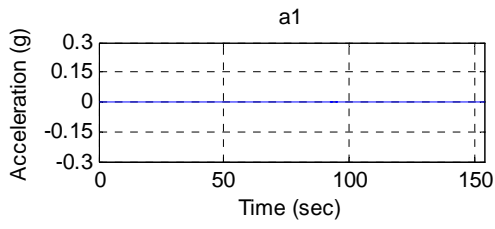
**Test M1**  
**Data\III-A\III-A M1.txt**



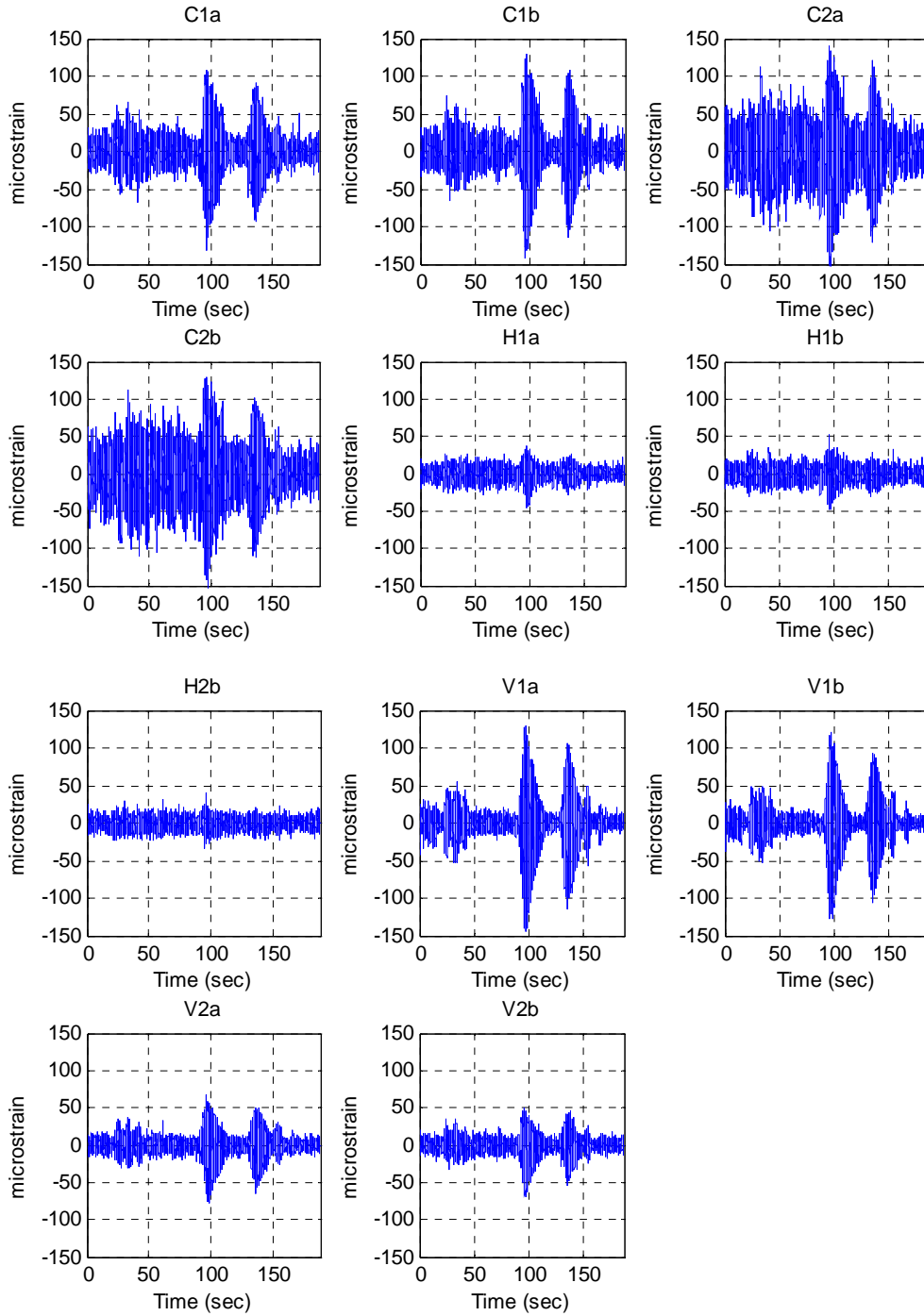


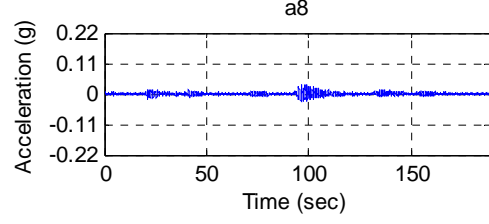
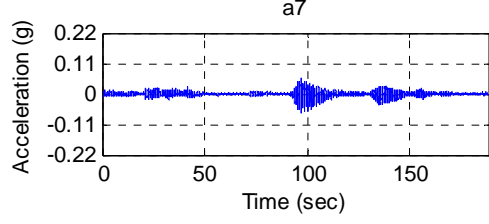
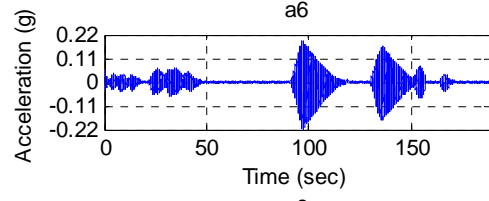
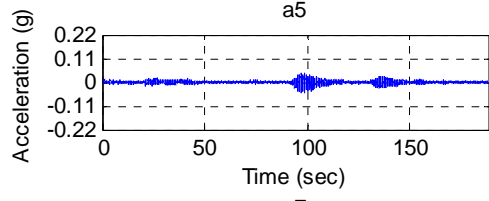
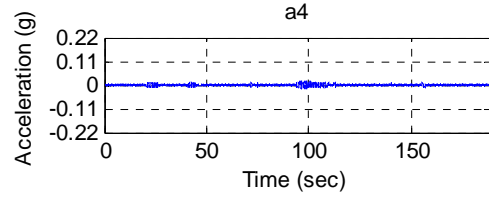
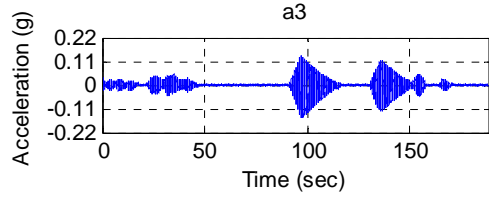
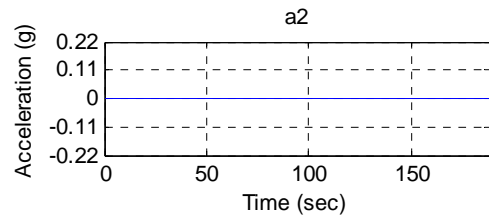
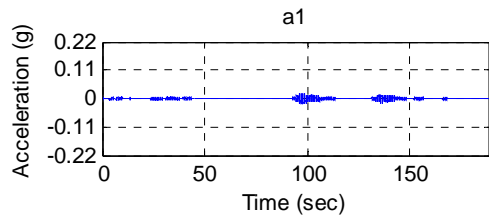
**Test M2**  
**Data\III-A\III-A M2.txt**





**Test M3**  
**Data\III-A\III-A M3.txt**





**Test M4**  
**Data\III-A\III-A M4.txt**

